Water Science and Technology Library

Prabhakar Shukla
Prachi Singh
Raj Mohan Singh *Editors*

Environmental Processes and Management

Tools and Practices for Groundwater

Springer

Water Science and Technology Library

Volume 120

The aim of the *Water Science and Technology Library* is to provide a forum for dissemination of the state-of-the-art of topics of current interest in the area of water science and technology. This is accomplished through publication of reference books and monographs, authored or edited. Occasionally also proceedings volumes are accepted for publication in the series. *Water Science and Technology Library* encompasses a wide range of topics dealing with science as well as socio-economic aspects of water, environment, and ecology. Both the water quantity and quality issues are relevant and are embraced by *Water Science and Technology Library*. The emphasis may be on either the scientific content, or techniques of solution, or both. There is increasing emphasis these days on processes and *Water Science and Technology Library* is committed to promoting this emphasis by publishing books emphasizing scientific discussions of physical, chemical, and/or biological aspects of water resources. Likewise, current or emerging solution techniques receive high priority. Interdisciplinary coverage is encouraged. Case studies contributing to our knowledge of water science and technology are also embraced by the series. Innovative ideas and novel techniques are of particular interest.

Comments or suggestions for future volumes are welcomed.

Vijay P. Singh, Department of Biological and Agricultural Engineering & Zachry Department of Civil and Environment Engineering, Texas A&M University, USA Email: vsingh@tamu.edu

All contributions to an edited volume should undergo standard peer review to ensure high scientific quality, while monographs should also be reviewed by at least two experts in the field.

Manuscripts that have undergone successful review should then be prepared according to the Publisher's guidelines manuscripts: https://www.springer.com/gp/authors-editors/book-authors-editors/book-manuscript-guidelines

Prabhakar Shukla · Prachi Singh · Raj Mohan Singh
Editors

Environmental Processes and Management

Tools and Practices for Groundwater

Springer

Editors
Prabhakar Shukla
UKRI GCRF Water Security
and Sustainable Development Hub
Indian Institute of Technology Delhi
New Delhi, India

Prachi Singh
Department of Civil Engineering
Madhav Institute of Technology
and Science
Gwalior, Madhya Pradesh, India

Raj Mohan Singh
Department of Civil Engineering
Motilal Nehru National Institute
of Technology
Prayagraj, Uttar Pradesh, India

ISSN 0921-092X ISSN 1872-4663 (electronic)
Water Science and Technology Library
ISBN 978-3-031-20207-0 ISBN 978-3-031-20208-7 (eBook)
https://doi.org/10.1007/978-3-031-20208-7

This Springer imprint is published by the registered company Springer Nature Switzerland AG
The registered company address is: Gewerbestrasse 11, 6330 Cham, Switzerland

Contents

Contributors

Pooja Agarwal Department of Civil Engineering, Indian Institute of Technology Roorkee, Roorkee, India

Vaseem Akram Economics and Business Environment Area, Indian Institute of Management Jammu, Jammu and Kashmir, Nawabad, Cantonment, Jammu, India

Mounika Aradala University of Soochow, New Taipei, China

Saima Aslam Department of Biotechnology, Baba Ghulam Shah Badshah University, Rajouri, Jammu and Kashmir, India

Shabana Aslam Department of Botany, S.P. College, Cluster University, Srinagar, Jammu and Kashmir, India

Abhishek Bhardwaj Department of Environmental Science, ASLS, Amity University Madhya Pradesh, Gwalior, Madhya Pradesh, India

Isha Burman Department of Environmental Science and Engineering, Indian Institute of Technology (ISM) Dhanbad, Dhanbad, India

Sumedha Chakma Department of Civil Engineering, Indian Institute of Technology (IIT) Delhi, Hauz Khas, New Delhi, India

Farzaneh Dadvar University of Toronto, Kensington Eye Institute, Toronto, Canada

Alka Dash Department of Geography, Central University of Haryana, Mahendragarh, India

Mridusmita Debnath ICAR Research Complex for Eastern Region, Patna, Bihar, India;
Civil Engineering Department, Indian Institute of Technology, Guwahati, Assam, India

M. D. Deepthi Nair Department of Child Neurology, Seattle Children's Research Institute, Seattle, USA

Kuldip Dwivedi Department of Environmental Science, ASLS, Amity University Madhya Pradesh, Gwalior, Madhya Pradesh, India

Swati Dwivedi Department of Urban Studies, Indira Gandhi National Open University, New Delhi, India

Farima Fakhri Department of Neuroscience, Kerman University of Medical Science, Kerman, Iran

Abhay Guleria Department of Civil Engineering, Indian Institute of Technology Delhi, Hauz Khas, New Delhi, India

Shashank Gupta Department of Civil Engineering, ITM University, Gwalior, Madhya Pradesh, India

Shahid Ul Islam Department of Civil Engineering, Baba Ghulam Shah Badshah University, Rajouri, Jammu and Kashmir, India;
Department of Civil Engineering, Indian Institute of Technology (IIT) Delhi, Hauz Khas, New Delhi, India

Pawan Jeet ICAR Research Complex for Eastern Region, Patna, Bihar, India

Nermeen Kolta Department of Internal Medicine, MM Jersey City Breathing Center, Jersey, USA

Praveen Kumar Motilal Nehru National Institute of Technology Allahabad, Prayagraj, India

Kayla Maclin Department of Mechanical and Civil Engineering, Alabama A&M University, Normal, AL, USA

Mallappa Madolli Department of Agricultural Engineering, College of Sericulture, Chintamani, University of Agricultural Sciences, Bengaluru, India

Rwitabrata Mallick Department of Environmental Science, ASLS, Amity University Madhya Pradesh, Gwalior, Madhya Pradesh, India

Muskan Mayank Department of Civil Engineering, National Institute of Technology, Srinagar (Garhwal), Uttarakhand, India

Devendra Mohan Department of Civil Engineering, Indian Institute of Technology Banaras Hindu University, Varanasi, Uttar Pradesh, India

Nirupama Nayudu Zhengzhou University, Zhengzhou, China

Akchhara Pandey Department of Pharmacology, Institute of Medical Sciences, BHU, Varanasi, UP, India

Shaghla Parveen National Institute of Urban Affairs, New Delhi, India

Epari Ritesh Patro Water, Energy and Environmental Engineering Research Unit, Faculty of Technology, University of Oulu, Oulu, Finland

Pooran Singh Patwal Independent Consultant (Hydrology and Natural Resource Management), Haridwar, India

Bishal Pokharel Department of Neurosurgery, Bhaktapur Cancer Hospital, Bhaktapur, Nepal

Bushra Praveen Department of Economics, IIT Indore, Indore, Madhya Pradesh, India

Pooja P. Preetha Department of Mechanical and Civil Engineering, Alabama A&M University, Normal, AL, USA

Swapnil Rai Department of Environmental Science, ASLS, Amity University Madhya Pradesh, Gwalior, Madhya Pradesh, India

Anusha Ramdoss PSG Institute of Medical Science and Research, Coimbatore, India

Shally Saini Hydrological Investigation Division, National Institute of Hydrology, Roorkee, Uttarakhand, India

Nitin Samaiya Department of Civil Engineering, Jaypee University of Engineering and Technology, Raghogarh, Guna, Madhya Pradesh, India

Pramod Kumar Sharma Department of Civil Engineering, Indian Institute of Technology Roorkee, Roorkee, India

Y. Shiva Shankar Indian Institute of Technology Hyderabad, Hyderabad, Telangana, India

A. K. Shukla Department of Civil Engineering, Motilal Nehru National Institute of Technology, Allahabad, India;
Department of Civil Engineering, Indian Institute of Technology Kanpur, Kanpur, India

Nidhi Shukla Department of Environmental Science, ASLS, Amity University Madhya Pradesh, Gwalior, Madhya Pradesh, India

Prabhakar Shukla GIS and Water Resources Management, Department of Civil Engineering, IIT Delhi, Delhi, India

Anil Kumar Singh ICAR Research Complex for Eastern Region, Patna, Bihar, India

R. Singh Department of Civil Engineering, Motilal Nehru National Institute of Technology, Allahabad, India;
Department of Civil Engineering, Indian Institute of Technology Delhi, New Delhi, India

R. P. Singh Department of Civil Engineering, Motilal Nehru National Institute of Technology, Allahabad, India

Raj Mohan Singh Motilal Nehru National Institute of Technology Allahabad, Prayagraj, India

Uttam Singh Department of Civil Engineering, Indian Institute of Technology Roorkee, Roorkee, India

Vijay Pratap Singh Department of Civil Engineering, Indian Institute of Technology Delhi, Hauz Khas, New Delhi, India

Tamanna Tazin Department of Internal Medicine, Greenville Community Shelter Clinic, Greenville, NC, USA

Rukhsana Miraj Uddin Women Medical College, Peshawar, Pakistan

Ashutosh Upadhyaya ICAR Research Complex for Eastern Region, Patna, Bihar, India

Jathot Veeranna Professor Jayashankar Telangana State Agricultural University, Hyderabad, Telangana, India

Poonam Yadav Department of Neurology, Apex Hospital, Jaipur, Rajasthan, India

Abbreviations

2D ERT	Two-dimensional electrical resistivity tomography
AARE	Average absolute relative error
ADE	Advection dispersion equation
AI	Artificial intelligence
ANN	Artificial neural network
ASTER	Advance spaceborne thermal emission and reflection radiometer
Avg.	Average
AWC	Available water content
AZURE	Auroral zone upwelling release experiment
BBB	Blood–brain barrier
BIS	Bureau of Indian Standards
BOD	Biochemical oxygen demand
BP	Back propagation
BTC	Breakthrough curve
Ca	Calcium
CA	Correlation analysis
CC	Climate change
CDP	City Development Plan
CGWB	Central Ground Water Board
CH_4	Methane
cm	Centimetres
CN2	Curve number
CO	Carbon monoxide
CO_2	Carbon dioxide
COD	Chemical oxygen demand
CPHEEO	Central Public Health & Environmental Engineering Organisation
CRU	Climatic Research Unit
CSE	Centre for Science and Environment
CSI	Composite Suitability Index
D50	Mean size particle
DAT	Dopamine transporter

DDT	Dichloro diphenyl trichloroethane
deg cel.	Degree Celsius
DEM	Digital elevation model
DO	Dissolved oxygen
DOC	Dissolved organic carbon
DW	Dug Well
EPA	Environmental Protection Agency
ERDAS	Earth Resources Data Analysis System
ERT	Electrical resistivity tomography
ESCO	Evaporation soil compensation factor
ESI	Evaporative Stress Index
ESRI	Environmental Systems Research Institute
ET	Evapotranspiration
FA	Factorial analysis
FADE	Fractional advection dispersion equation
FAO	Food and Agriculture Organization
FEM	Finite element method
FS	Fixed solids
GA	Genetic algorithm
GFMS	Global flood monitoring system
GIS	Geographical information system
GMS	Groundwater modeling system
GPS	Global Positioning System
GRACE	Gravity recovery and climate experiment
GVMC	Greater Visakhapatnam Municipal Corporation
GW	Groundwater
GWL	Groundwater level
GWMP	Geographic Water Management Potential
GWR	Groundwater recharge
GWRA	Ground Water Resources Assessment
H2S	Hydrogen sulfide
ham	Hectare meter
HI	Hazard Index
HQ	Head Quarter
HRU	Hydrologic response unit
HSPF	Hydrological Simulation Program—FORTRAN
IDW	Inverse distance weighting
IMA	Indian Medical Association
IMD	Indian Meteorological Department
INR	Indian rupee
IPCC	Intergovernmental Panel on Climate Change
IWMI	International Water Management Institute
IWRM	Integrated water resources management
K	Potassium
LMC	Lucknow Municipal Corporation

LPCD	Litre per capita per day
LPM	Litres per minute
LPPM	Low permeability porous media
LU	Land use
LULC	Land use/land cover
m	Metres
MADE	Macrodispersion experiment
Max.	Maximum
MBBR	Moving bed biofilm reactor
mbgl	Metres below ground level
MCM	Million cubic meters
ME	Model efficiency
Min.	Minimum
MK	Mann Kendall
M-K	Mann-Kendall
ML	Machine learning
ml	Millilitres
MLD	Million liters per day
mm	Millimeter
MOC	Method of characteristic
MODFLOW	Modular three-dimensional finite-difference groundwater flow model
MPN	Most probable number
MPWRD	Madhya Pradesh Water Resource Department
MRS	Magnetic resonance sounding
MSE	Mean squared error
MSW	Municipal solid waste
MT3DMS	Modular three-dimensional multispecies transport model
MT3D-USGS	Mass Transport in 3-Dimensions—U.S. Geological Survey
MVR	Water mover package
MZP	Mirzapur
Na	Sodium
NABARD	National Bank for Agriculture and Rural Development
NCAS	National Centre for Atmospheric Science
NE	North East
NIT	National Institute of Technology
NMR	Nuclear magnetic resonance
NO_3-N	Nitrate nitrogen
NRSC	National Remote Sensing Centre
NS	Nash Sutcliffe efficiency
NSE	Nash-Sutcliffe efficiency coefficient
NTU	Nephelometric turbidity unit
O&M	Operation and maintenance
OF	Objective function
OMP	Organic micro-pollutants

PCP	Precipitation
PD	Parkinson's disease
PMWin	Groundwater flow modeling software
PRM	Pre-monsoon
PTM	Post-monsoon
Q	Sen's slope estimate
R	Pearson r
R2	Coefficient of determination
RBF	Riverbank filtration
Rf	Rainfall
RMSE	Root mean square error
ROS	Reactive oxidation species
RS	Remote sensing
RWH	Rainwater harvesting
S	River meandering sinuosity value
sFADE	Spatial fractional advection dispersion equation
SFD	Shit flow diagrams
SGeMS	Stanford Geostatistical Modeling Software
SGI	Standardized Groundwater Level Index
SMDR	Soil moisture distribution and routing
SN	Substantia Nigra
SOMA	Switch Organic Micro-Pollutant Assessment Tool
SqKm	Square Kilometre
SRTM	Shuttle Radar Topography Mission
SS	Suspended solids
STP	Sewage treatment plants
Surface NMR	Surface nuclear magnetic resonance
SW	South West
SWAT	Soil and water assessment tool
T	Temperature
TCA	Tricarboxylic acid
TDS	Total dissolved solids
TIAA	Tucson International Airport Area
TNAU	Tamil Nadu Agricultural University
TR	Targeted risk
TS	Total solids
TSP	Travelling salesperson problem
TW	Tube well
U.P.	Uttar Pradesh
UNDRO	United Nations Disaster Relief Co-ordinator
USGS	United States Geological Survey
VI	Vulnerability Index
VLSI	Very large-scale integration
VOC	Volatile organic compound
VS	Volatile solids

WC	Water content
WHO	World Health Organization
WQ	Water quality
WRIS	Water Resources Information System

Symbols

Z	Mann Kendall test value
C	Dissolved-phase concentration
S	Sorbed concentration
a	Freundlich equilibrium sorption coefficient
t	Time
β	First-order sorption mass exchange rate between dissolved and sorbed phases
ξ	Frist-order mass transfer coefficient
C_{im}	Contaminant concentration in the immobile region
K_d	Linear sorption distribution coefficient
K_f	Freundlich equilibrium distribution sorption coefficient
K_l	Langmuir equilibrium constant
$\bar{S}$	Langmuir sorption capacity
α_L	Longitudinal dispersivity
α_{TV}	Traverse vertical dispersivity
θ_{im}	Porosity of the immobile region
ρ_b	Bulk density

Chapter 1
Non-invasive Subsurface Groundwater Exploration Techniques

Uttam Singh and Pramod Kumar Sharma

Abstract The present study focused on the different surface-based geophysical methods which are used to explore the subsurface aquifer characterizations including water availability. The principle of the Earth Resistivity Tomography (ERT) and different electrode array configurations like Schlumberger, Wenner, and dipole–dipole arrays is discussed in detail. Afterward, the surface nuclear magnetic resonance (surface NMR) technique is also described to measure the subsurface aquifer information like hydraulic conductivity and water content below the surface of the soil. The surface NMR hydraulic conductivity and decay time distribution curves complement the ERT results.

Abbreviations

ERT	Electrical resistivity tomography
2D ERT	Two-dimensional electrical resistivity tomography
Surface NMR	Surface nuclear magnetic resonance
NMR	Nuclear magnetic resonance
MRS	Magnetic resonance sounding
WC	Water content

U. Singh · P. K. Sharma (✉)
Department of Civil Engineering, Indian Institute of Technology Roorkee, Roorkee 247667, India
e-mail: pramod.sharma@ce.iitr.ac.in

U. Singh
e-mail: uttamsingh426@gmail.com; usingh@ce.iitr.ac.in

P. Shukla et al. (eds.), *Environmental Processes and Management*, Water Science and Technology Library 120, https://doi.org/10.1007/978-3-031-20208-7_1

1.1 Non-invasive Methods

Geophysical methods have been used to investigate subsurface groundwater for a long time. In this chapter, We discuss about non-invasive groundwater exploration methods

1. Electrical resistivity tomography (ERT)
2. Surface nuclear magnetic resonance (surface NMR)

ERT is based on electrical properties, and this method seems effective because it correlated with soil properties. These soil properties can be quantified through geo-electrical properties. The electrical conductivity of conducting materials such as electrolytes and metals has high values, and an insulating material such as air and plastic has nominal values, while soil materials have intermediated value of electrical conductivity.

The idea of groundwater exploration through nuclear magnetic resonance (NMR) was coined in the 1960s. However, in the 1980s, equipment was designed and used for surface geophysical investigation (Semenov et al. 1988; Legchenko et al. 1991). In the sandy aquifer, fractured limestone aquifer, clayey aquifer, and some unique geological settings under various conditions, extensive field surveys, and soil material testing have been carried out (Schirov et al. 1991; Goldman et al. 1994; Yaramanci et al. 2001; Vouillamoz et al. 2005).

1.1.1 Applications of the ERT and Surface NMR

- Mapping of the groundwater flow,
- Non-invasive detection of groundwater,
- Hydraulic conductivity estimation of the aquifer,
- Monitoring of the temporal changes in the aquifer properties,
- Estimation of the water content in the aquifer's vadose zone,
- Identification of the fractures and faults in the sedimentary rocks.

1.2 Principles of Electrical Resistivity Tomography

To determine the subsurface electrical resistivity distribution, ERT surveys are conducted. For the electrical resistivity surveys, four electrodes are a minimum requirement. Two electrodes are used to supply artificially created electric current to the ground, and the potential differences between the other two electrodes are measured. The distribution of potential differences will reveal the electrical characteristics and heterogeneity of the subsurface (Kearey et al. 2002). The distribution of the current flow lines distribution depends on the subsurface material. For example, if homogeneous soil material has electrical resistivity (R) within cross section (A) and length (L), then resistivity (ρ) of the sample body can be defined as:

$$\rho = R\left(\frac{A}{L}\right) \tag{1.1}$$

Ohm's law can be stated as for cylindrical body having R electrical resistivity, V the potential difference, and I current. Electrical characteristics of the subsurface are commonly described in the form of conductivity. The conductivity can be denoted by $\sigma\left(\mathrm{Sm}^{-1}\right)$ which is reciprocal to resistivity.

$$R = \frac{V}{I} \tag{1.2}$$

$$\sigma = \frac{1}{\rho} \tag{1.3}$$

The Earth's subsurface is assumed hemispherical, anisotropic, and homogeneous when the current electrode is inserted into the soil surface (Fig. 1.1) (Scollar et al. 1990; Reynolds 2011). The current density $J\left(\mathrm{Am}^{-2}\right)$ of the hemispherical subsurface can be calculated for all directions as given in Fig. 1.1.

$$J = \frac{I}{2\pi r^2} \tag{1.4}$$

where r is the radius, and $2\pi r$ are the surface of the hemisphere. Then, the potential (V) between the electrodes can be represented as follows:

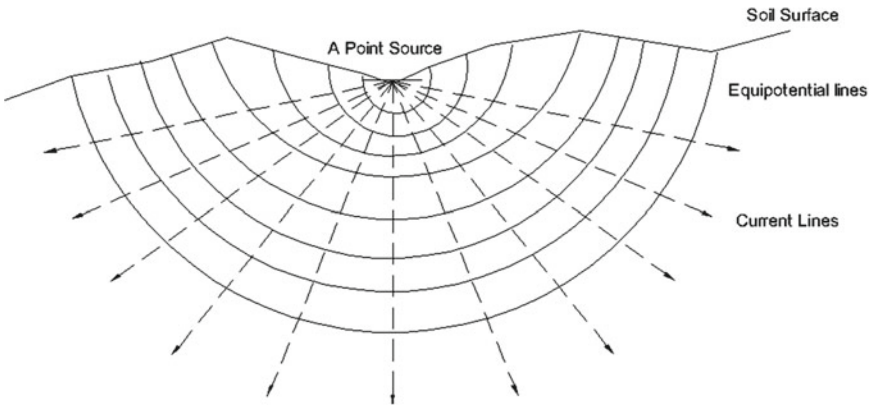

Fig. 1.1 Distribution of current flow in a homogeneous subsurface

$$V = \frac{\rho I}{2\pi r} \tag{1.5}$$

Different electrode array configurations can measure electrical resistivity. Some of the standard and widely used electrode configurations are given below.

1.2.1 Schlumberger Array Configuration

A minimum of four electrodes (A, B, M, and N) is considered for data collection. Electric current is penetrated into the ground through A, B the electrode, and developed potential is measured through M, N the electrode. The spacing between A, B and N, B electrodes is $n.a$, and similarly, spacing between M, N electrodes is a (Fig. 1.2).

Potential due to electrode A at the electrode $M = \frac{\rho I}{2\pi}.\frac{1}{r_1}$.

Potential due to electrode B at electrode $M = -\frac{\rho I}{2\pi}.\frac{1}{r_2}$.

Net potential at electrode M due to electrodes A and B

$$V_M = \frac{\rho I}{2\pi}\left(\frac{1}{r_1} - \frac{1}{r_2}\right) \tag{1.6}$$

Similarly, the net potential at electrode N due to B and A.

Where K is the geometric factor of subsurface, and each subsurface layer has a different resistivity, and observed resistivity is called apparent resistivity (ρ_a), which can be written as:

$$V_N = \frac{\rho I}{2\pi}\left(\frac{1}{r_3} - \frac{1}{r_4}\right) \tag{1.7}$$

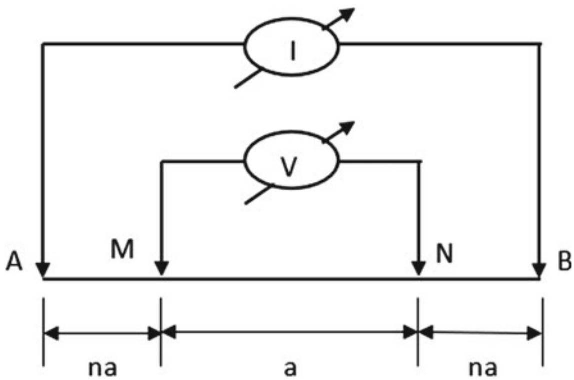

Fig. 1.2 Schematic diagram of the Schlumberger array configuration

The net potential difference between M and N

$$V_M - V_N = \frac{\rho I}{2\pi}\left(\frac{1}{r_1} - \frac{1}{r_2} - \frac{1}{r_3} + \frac{1}{r_4}\right) \tag{1.8a}$$

or

$$\Delta V = \frac{\rho I}{2\pi}\left(\frac{1}{r_1} - \frac{1}{r_2} - \frac{1}{r_3} + \frac{1}{r_4}\right) \tag{1.8b}$$

$$\rho = \frac{\Delta V}{I}.\left(\frac{2\pi}{\frac{1}{r_1} - \frac{1}{r_2} - \frac{1}{r_3} + \frac{1}{r_4}}\right) \tag{1.8c}$$

$$\rho = K\frac{\Delta V}{I} \tag{1.8d}$$

where K geometric factor of the subsurface and each subsurface layer has a different resistivity. Observed resistivity is called apparent resistivity (ρ_a) (Singh and Sharma 2022a), which can be written as:

$$\rho_a = K\frac{\Delta V}{I} \tag{1.9}$$

From Fig. 1.2,

$r_1 = r_2 = n.a$ and $r_2 = r_3 = (n+1)a$.

After substituting these values in Eq. 1.8c, the following equation can be written as:

$$\rho_a = \frac{\Delta V}{I}\left(\frac{2\pi}{\frac{1}{na} - \frac{1}{(n+1)a} - \frac{1}{(n+1)a} + \frac{1}{na}}\right) \tag{1.10a}$$

or

$$\rho_a = \frac{\Delta V}{I}an(n+1) \tag{1.10b}$$

1.2.2 Wenner Array Configuration

In this array configuration, a minimum of four electrodes are required, and each electrode has the same spacing as the other, i.e., a. Wenner array can be further classified into Wenner$-\alpha$, Wenner$-\beta$, and Wenner$-\gamma$. Wenner$-\alpha$ configuration is considered as a standard Wenner array (Fig. 1.3).

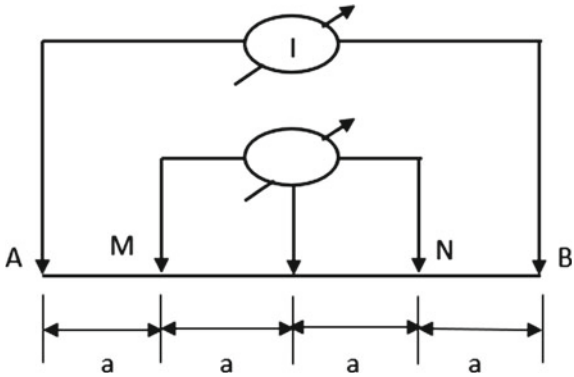

Fig. 1.3 Schematic diagram of the Wenner array configuration

From Fig. 1.3,
$r_1 = a, r_2 = 2a, r_3 = 2a$ and $r_4 = a$.
Substitute these values into Eq. 1.8c.

$$\rho_a = \frac{\Delta V}{I}\left(\frac{2\pi}{\frac{1}{a} - \frac{1}{2a} - \frac{1}{2a} + \frac{1}{a}}\right) \tag{1.11a}$$

$$\rho_a = \frac{\Delta V}{I}(2\pi a) \tag{1.11b}$$

1.2.3 Dipole–Dipole Array Configuration

The spacing between electrodes A, M, and N, B in the Dipole-dipole electrode configuration is a. While the spacing between electrodes M, N is $n.a$.

From Fig. 1.4,
$r_1 = a, r_2 = a(n + 1), r_3 = a(n + 1)$ and $r_4 = a$.

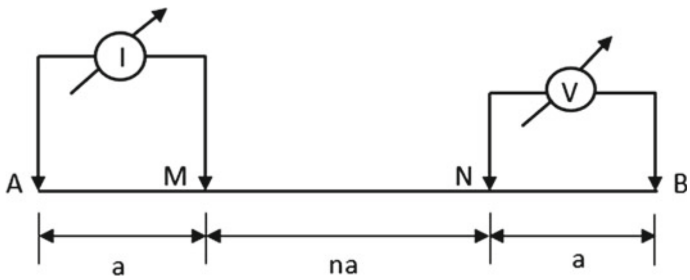

Fig. 1.4 Schematic diagram of the dipole–dipole array configuration

Substitute these values into Eq. 1.8c.

$$\rho_a = \frac{\Delta V}{I}\left(\frac{2\pi}{\frac{1}{a} - \frac{1}{a(n+1)} - \frac{1}{a(n+1)} + \frac{1}{a}}\right) \tag{1.12a}$$

$$\rho_a = \frac{\Delta V}{I}\frac{\pi a(n+1)}{n} \tag{1.12b}$$

1.2.4 2D Electrical Resistivity Tomography

Two-dimensional is a multi-electrode array configuration in which electrodes are inserted into the ground. All electrodes have a fixed distance from each other, and measurements should be recorded in each step. After measuring all these resistivity profile values at the initial spacing between electrodes, the spacing among the inter-electrodes is increased by factor $n = 2$, and the process is repeated till maximum spacing between inter-electrode is not reached (Singh and Sharma 2022b). Higher spacing between the inter-electrode gives a higher depth of investigation (Fig. 1.5).

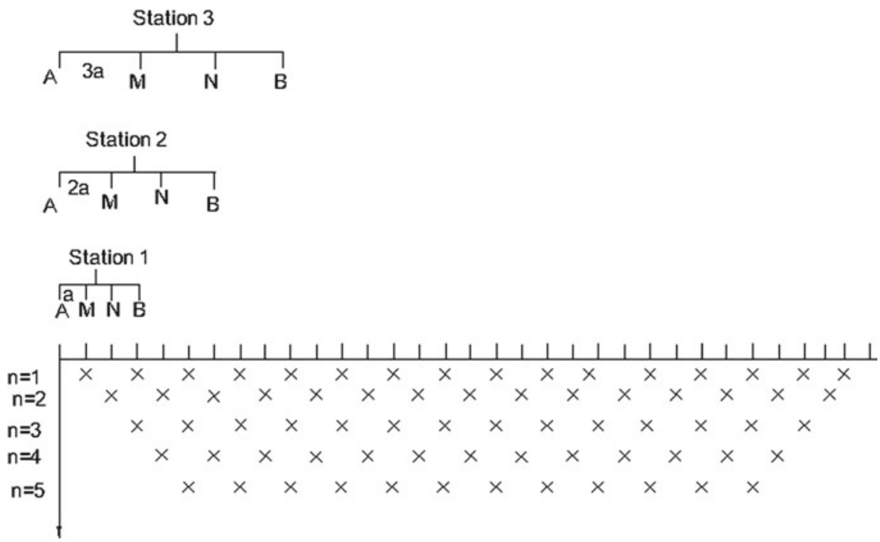

Fig. 1.5 Pseudo-section of 2D electrical resistivity survey

1.2.5 ERT Survey at Belra, Roorkee

At the study site, a 200 m long 2D ERT survey was conducted with a 5 m electrode spacing between each electrode, and forty electrodes were inserted into the ground. For better soil contact, the bottom two-thirds of each electrode is inserted into the ground. The field experiment was conducted by earth resistivity meter and geo-test software used to record the ERT data with different array configurations such as Schlumberger, Wenner, and dipole–dipole. Through ERT, data points were analyzed, and bad data points were removed from the data set. The inversion of analyzed 2D ERT data sets was carried out using RES2DINV software. The inversion of the Schlumberger array configuration shows that the top layer consisted of very high resistivity values beyond that entire subsurface can be divided into high, medium, and low water content zones (Fig. 1.6a). Similar to the Schlumberger array, Wenner array subsurface inversion can also be divided into the three subsurface zones (Fig. 1.6b). However, medium and low water content zone slightly differ from each other. Dipole–dipole array inversion results shows significantly different from the Schlumberger and Wenner array configurations (Fig. 1.6c). Dipole–dipole array configuration is the most susceptible to electromagnetic or environmental noise. Thus, it showed maximum error in the ERT inversion result, i.e., 2.3. The detailed subsurface ERT characterization at different depths along the survey line is given in Table 1.1.

1.3 The Principle of Surface NMR

The principle of surface NMR applications is the spin of water molecules' hydrogen proton (nuclei). The water molecules had angular momentum without physically rotating. The oscillating angular frequency, i.e., Larmor angular frequency (ω_L) of the hydrogen proton and the magnitude of the magnetic moment (μ_0), and equilibrium conditions are governed by the static Earth's magnetic field (B_0).

$$\vec{\mu}_0 = \frac{\gamma^2 \hbar \vec{B}_0}{3KT} \times \frac{N}{V} \tag{1.13a}$$

$$\omega_L = -\gamma B_0 \tag{1.13b}$$

where ω_L is the Larmor frequency, $\gamma = 0.267518\,\text{Hz/nT}$ is the hydrogen proton gyromagnetic ratio, and B_0 the magnetic field that is static. $\hbar$ is Planck's constant, K is Boltzmann's constant, and T is temperature, and N/V is the number of spins per unit volume.

When a secondary magnetic field (B_1) is applied, it has a Lamor frequency and is perpendicular to the stationary magnetic field (B_0). This phenomenon converts spinning magnetic moment into oscillating motion around B_0. During the excitation of the proton pulse, the spin's magnitude does not change, but the spin's orientation

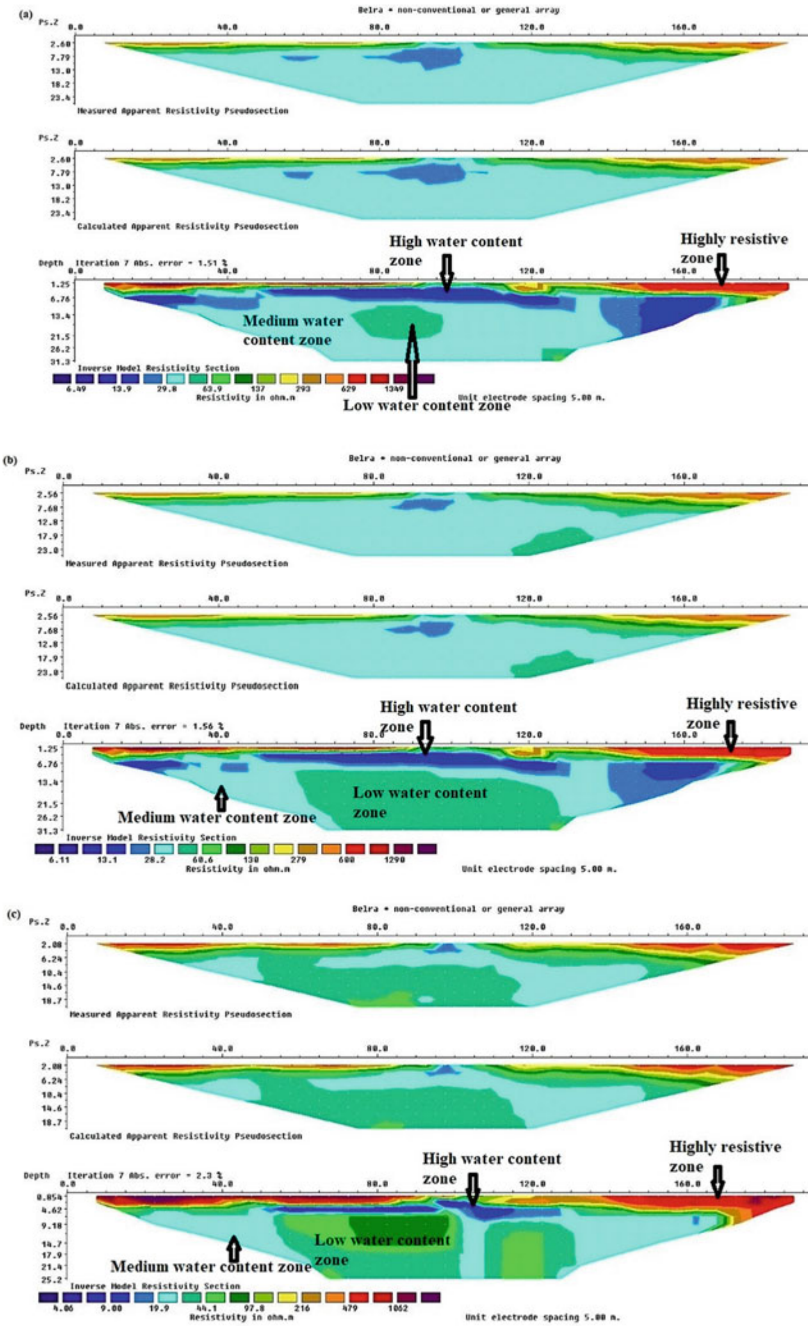

Fig. 1.6 **a** Subsurface ERT inversion of the 200 m survey line using Schlumberger array configuration, **b** Subsurface ERT inversion of the 200 m survey line using Wenner array configuration, **c** Subsurface ERT inversion of the 200 m survey line using dipole–dipole array configuration

Table 1.1 Probable the subsurface lithology by Schlumberger, Wenner, and dipole–dipole methods

S. No.	Survey length (m)	Survey depth (m)	Electrical resistivity (Ohm-m)	Probable lithology
Schlumberger array configuration				
1	0–40	0–5	1000	The mixture of sand and gravel
2	40–80		1000	
3	80–120		500	
4	120–160		630	
5	160–200		1000	
6	0–40	5–31.3	30	Clay with the high possibility of the water table
7	40–80		36	
8	80–120		36	
9	120–160		30	
10	160–200		25	
Wenner array configuration				
1	0–40	0–5	1000	The mixture of sand and gravel
2	40–80		1000	
3	80–120		500	
4	120–160		630	
5	160–200		1000	
6	0–40	5–31.3	30	Clay with the high possibility of the water table
7	40–80		70	
8	80–120		130	
9	120–160		120	
10	160–200		25	
Dipole–dipole array configuration				
1	0–40	0–5	1000	The mixture of sand and gravel
2	40–80		1000	
3	80–120		500	
4	120–160		630	
5	160–200		1000	
6	0–40	5–25.2	20	Clay with the high possibility of the water table
7	40–80		36	
8	80–120		97	
9	120–160		36	
10	160–200		25	

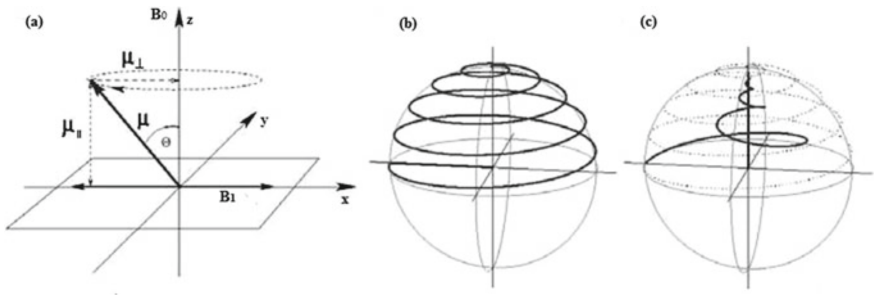

Fig. 1.7 Unit trajectory and processing components of spin magnetic moments during **a** excitation, **b** relaxation, and **c** 90° excitation angle

changes into the helix shape as described in Fig. 1.7. The harmonic functions of the B_1 are the components of the magnetization vectors parallel and perpendicular to the B_0. The pulse duration of hydrogen proton can be defined as follows:

$$\mu_T(\tau_p) = \mu_0 \sin\left(\frac{1}{2}\tau_p B_1(\vec{r})\right) \tag{1.14a}$$

$$\mu_{||}(\tau_p) = \mu_0 \cos\left(\frac{1}{2}\tau_p B_1(\vec{r})\right) \tag{1.14b}$$

The static magnetic field direction is the same as the z-axis. Bloch, 1946 stated that both magnetizations of perpendicular and parallel decay independently and individually from their respective magnitudes at decay time (τ_p). The parallel component decays exponentially and achieves equilibrium with the time constant (T_1). Perpendicular component decay to zero in-plane with the time constant (T_2). It was also observed that total magnetization during relaxation is not constant, but initial and final pulse cutoffs are μ_0. Magnitudes of magnetization during relaxation change with decreasing perpendicular decay and increasing parallel decay. Figure 1.7 shows the unit sphere of 90° excitation angle. Generally, $T_1 \geq T_2$, but in the case of a low static field, both can be considered to be equal.

The relaxation function can be described as follows:

$$\mu_\perp(t) = \mu_\perp(\tau_p)\mathrm{e}^{-\frac{1}{T_2}} \tag{1.15a}$$

$$\mu_{||}(t) = \mu_{||}(\tau_p)\left(1 - \mathrm{e}^{-\frac{1}{T_2}}\right) \tag{1.15b}$$

A geophysical method called surface nuclear magnetic resonance uses the groundwater's hydrogen proton's magnetic resonance sounding (MRS) phenomenon (Fig. 1.8). The perturbation of the spin system is caused by the transmitter coil pulse, which is emitted after the response signal has reached cutoff from the subsurface. Earth produced a static magnetic field with Larmor frequency (1.2–2.5 kHz). A

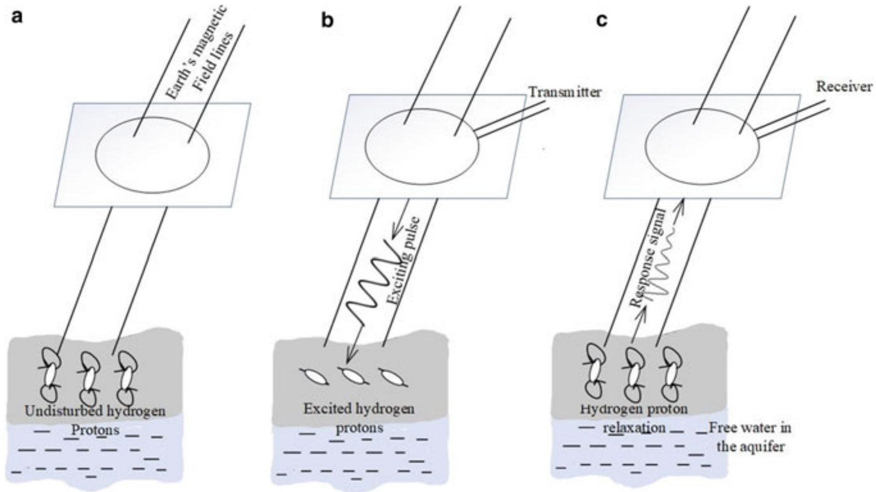

Fig. 1.8 Measurement sketch of magnetic resonance during **a** an undisturbed hydrogen proton, **b** an excited hydrogen protons, and **c** hydrogen proton relaxation

spin system develops the electromagnetic field of surface loops due to perturbation of the secondary magnetic field. Surface loops also record the data of response signals, and surface loops are usually the same size. For the one-dimensional investigation, the size and location of the transmitter and receiver loops coincide, and for two-dimensional investigations, both loops cannot be coincident and arbitrarily placed.

Governing equation of voltage response (V_R) depends on the pulse moment of the receiver loop (q), and signal capturing period (t) (Hertrich 2008).

$$V_R(q,t) = \omega\mu_0 \int_V d^3 r f(r) \sin\left(-\gamma \frac{q}{I_0}|B_1(r)|\right) \mathrm{e}^{-\frac{t}{T_2^*}} \times \frac{2}{I_0}|B_1(r)|\mathrm{e}^{i[\xi_T(r)+\xi_R(r)]} \times \left[\vec{b}_R(r).\vec{b}_T(r) + i\vec{b}_0.\vec{b}_R(r) \times \vec{b}_T(r)\right] \quad (1.16a)$$

where pulse moment can be defined as follows:

$$q = \tau_p I_0 \quad (1.16b)$$

The amplitude of the NMR response signal that the spin system emits is the first term in the voltage response equation. The energizing pulse consists of hydrogen nuclei and excitation angle, which is also known as the magnetization vector. The second term of this equation describes the receiver's sensitivity to the subsurface's signal. The surface NMR signals' vector nature was demonstrated by the third term of Eq. 1.16a. It displayed how the electromagnetic fields of the transmitter and receiver were oriented in relation to the static magnetic field.

This equation takes into account a portion of the total water content as water content. The water stored in the existing pores of the subsurface that does not contribute to the NMR signal is known as bound water. The bound water does not contribute because relaxation time is too short in this technique. So, we can say response signals are closely related to free water. The Kernel function is incorporated in Eq. 1.16a as given below (Eq. 1.17a):

$$V_R(q,t) = \omega\mu_0 \int_V d^3r f(r) K(q,t) \mathrm{e}^{-\frac{t}{T_2^*}} \tag{1.17a}$$

$$\begin{aligned} K(q,t) = \sin&\left(-\gamma \frac{q}{I_0} |B_1(r)|\right) \\ &\times \frac{2}{I_0} |B_1(r)| \mathrm{e}^{i[\xi_T(r)+\xi_R(r)]} \\ &\times \left[\vec{b}_R(r).\vec{b}_T(r) + i\vec{b}_0.\vec{b}_R(r) \times \vec{b}_T(r)\right] \end{aligned} \tag{1.17b}$$

The two-dimensional and three-dimensional forms of the above equation are the simplified form of this equation, and the Kernel function is also reduced. The above equation can be represented into the Cartesian dimension as follows:

$$V_R(q,t) = \int_0^\infty \int_{-\infty}^\infty \int_{-\infty}^\infty f(x,y,z) K_{3D}(x,y,z) \mathrm{e}^{-\frac{t}{T_2^*(x,y,z)}} \mathrm{d}x\mathrm{d}y\mathrm{d}z \tag{1.18a}$$

The 2D form of the above equation

$$V_R(q,t) = \int_0^\infty \int_{-\infty}^\infty f(x,z) K_{2D}(q;x,z) \mathrm{e}^{-\frac{t}{T_2^*(x,y)}} \mathrm{d}x\mathrm{d}z \tag{1.18b}$$

$$K_{2D}(q;x,z) = \int_{-\infty}^\infty K_{3D}(q;x,y,z)\mathrm{d}y; \ \frac{\partial f(y)}{\partial y} = 0 \tag{1.18c}$$

The 1D form of the above equation

$$V_R(q,t) = \int_0^\infty f(z) K_{1D}(q;z) \mathrm{e}^{-\frac{t}{T_2^*(z)}} \mathrm{d}z \tag{1.18d}$$

$$K_{1D}(q;z) = \int_{-\infty}^{\infty}\int_{-\infty}^{\infty} K_{3D}(q;x,y,z)\mathrm{d}x\mathrm{d}y; \quad \frac{\partial f(x)}{\partial x} = \frac{\partial f(y)}{\partial y} = 0 \tag{1.18e}$$

1.3.1 Surface NMR Survey at Belra, Roorkee

Site selection is an important step for the surface NMR experiment because a sufficient open space is required, and no potential noise source is available near the survey site. Noise sources will degrade the quality of the surface NMR data, and it will become a very difficult task to process noisy data. We selected a site between the Haridwar and Roorkee; it is a good site for the surface NMR and ERT field experimentation. Two reference loops (noise cancelation) of the same size and the main loop with a 30 m diameter were laid out on the ground. The spacing between the main loop and noise cancelation loop must be minimum 1.5 times of loop diameter. Before auto-tune, the system makes sure all connections are connected properly. After auto-tune, the Larmor frequency must be equal to the system frequency, and then, the system is ready for surface NMR data collection. Depending upon the site condition and electromagnetic noise or environmental noise level, the pulse moment (Fig. 1.9a) is set to record the surface NMR data. The recorded surface NMR data is processed on Vista Clara's software, and the high amplitude of noise level spikes is removed. After sufficient noise cancelation, NMR signals look in the exponential decay curve. The surface NMR data is ready for the inversion process.

Figure 1.9b shows the surface NMR signals decay matrix, hydraulic conductivity, water content distribution, and depth. The blue color of the water content distribution plot shows the mobile water content; however, the pink color shows the immobile water content of the subsurface.

1.4 Summary

ERT of the subsurface properties is a procedure where recorded data is inverted into the resistivity images. These images are used for the distribution of the hydrological parameters into the subsurface based on the petrophysical relationship. Establishing a site-specific, direct relationship between the hydrogeological properties is possible. The surface NMR method can accurately estimate the amount of mobile and immobile water as well as the hydraulic conductivity of the subsurface water and can directly detect it. Combining the surface NMR with the ERT method allows the direct assessment of the subsurface and data-enhanced understanding of the subsurface's geological, hydrogeological, and geophysical understanding.

A joint inversion with surface NMR can incorporate some of the method improvements still needed, such as the inversion archived from the ERT data. Understanding

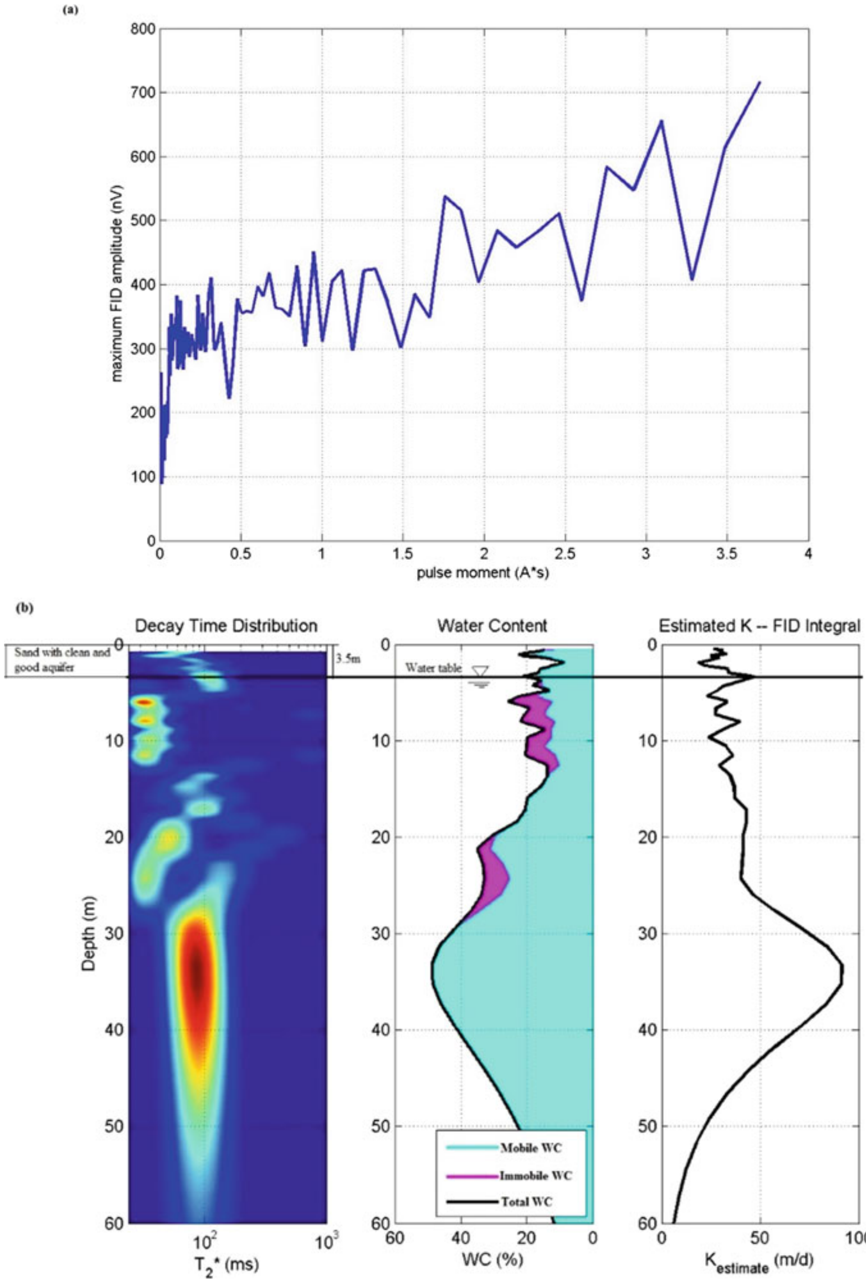

Fig. 1.9 **a** Pulse moment of the NMR signals during surface NMR data recording, **b** Distribution of hydraulic conductivity and water content by surface NMR along with the aquifer depth

the aquifer's geometry and the composition of its materials can be significantly improved through joint inversion study.

References

Bloch F (1946) Nuclear induction. Phys Rev 70(7–8):460. https://doi.org/10.1103/PhysRev.70.460

Goldman M, Rabinovich B, Rabinovich M, Gilad D, Gev I, Schirov M (1994) Application of the integrated NMR-TDEM method in groundwater exploration in Israel. J Appl Geophys 31(1–4):27–52. https://doi.org/10.1016/0926-9851(94)90045-0

Hertrich M (2008) Imaging of groundwater with nuclear magnetic resonance. Prog Nucl Magn Reson Spectrosc 53(4):227. https://www.alphageofisica.com.br/vistaclara/PAPERS/Hertrich2008review_www.alphageofisica.com.br.pdf

Kearey P, Brooks M, Hill I (2002) An introduction to geophysical exploration. vol 4. Wiley

Reynolds JM (2011) An introduction to applied and environmental geophysics. Wiley

Semenov A, Burshtein A, Pusep A, Schirov MD (1988) A device for measurement of underground mineral parameters (Russia). USSR Patent 1079063

Schirov M, Legchenko A, Creer G (1991) A new direct non-invasive groundwater detection technology for Australia. Explor Geophys 22(2:33–338. https://doi.org/10.1071/EG991333

Scollar I, Tabbagh A, Hesse A, Herzog I (1990) Archaeological prospecting and remote sensing

Singh U, Sharma PK (2022a) Study on geometric factor and sensitivity of subsurface for different electrical resistivity Tomography Arrays. Arab J Geosci 15(7):1–9. https://doi.org/10.1007/s12517-022-09844-3

Singh U, Sharma PK (2022b) Seasonal groundwater monitoring using surface NMR and 2D/3D ERT. Environ Earth Sci 81(7):1–17. https://doi.org/10.1007/s12665-022-10325-9

Vouillamoz JM, Descloitres M, Toe G, Legchenko A (2005) Characterization of crystalline basement aquifers with MRS: comparison with boreholes and pumping tests data in Burkina Faso. Near Surf Geophys 3(3):205–213. https://doi.org/10.3997/1873-0604.2005015

Yaramanci U, Lange G, Knödel K (2001) Surface NMR within a geophysical study of an aquifer at Haldensleben (Germany). Geophys Prospect 47(6):923–943. https://doi.org/10.1046/j.1365-2478.1999.00161.x

Chapter 2
Numerical Solution of Space Fractional Advection–Dispersion Equation and Application

Pramod Kumar Sharma, Muskan Mayank, and Pooja Agarwal

Abstract Generally, advection–dispersion and fractional advection–dispersion equations are used to model the transport of solute tracer in a porous medium. This study describes the numerical solution of both the general advection–dispersion equation and the space fractional advection–dispersion equation. The developed numerical model is used to simulate the observed data of chloride concentration obtained in the laboratory using soil column experiments. Different scenarios were used to estimate the transport parameters to simulate the concentration profiles through experiments.

Abbreviations

ADE	Advection–dispersion equation
FADE	Fractional advection–dispersion equation
sFADE	Spatial fractional advection–dispersion equation
BTC	Breakthrough curve
FEM	Finite element method
D50	Mean size particle
OF	Objective function
NSE	Nash–Sutcliffe efficiency coefficient
RMSE	Root mean square deviation

P. K. Sharma (✉) · P. Agarwal
Department of Civil Engineering, Indian Institute of Technology Roorkee, Roorkee 247667, India
e-mail: pramod.sharma@ce.iitr.ac.in

P. Agarwal
e-mail: pagarwal@ce.iitr.ac.in

M. Mayank
Department of Civil Engineering, National Institute of Technology, Srinagar (Garhwal), Uttarakhand, India
e-mail: muskan.mayank@nituk.ac.in

P. Shukla et al. (eds.), *Environmental Processes and Management*, Water Science and Technology Library 120, https://doi.org/10.1007/978-3-031-20208-7_2

2.1 Introduction

Advection is proportional to mean water velocity. Sternberg (2004) demonstrated that for a macroscopic condition, the experimentally determined dispersion coefficient behaves asymptotically through heterogeneous porous media. It is well understood, however, that this coefficient is spatially dependent and that it is not constant in heterogeneous porous media (Gelhar et al. 1992). Early breakthroughs and long tails characterize breakthrough curves in these cases. This is referred to as non-Fickian phenomenon. These anomalous dispersal characteristics cannot be explained by the traditional advection–dispersion equation (ADE) with constant coefficients. Benson et al. (2001) developed the spatial fractional advection–dispersion equation (sFADE) to address this issue.

Ben-Zvi et al. (2016) proposed a one-dimensional FEM solution by studying intro-differential advection–dispersion equations which have important applications for anomalous transport in highly disordered porous media. The formulation has been used to model the non-Fickian solute transport in porous media. Kundu (2018) studied the concentration distribution in suspension for turbulent flows using the fractional advection–diffusion equation. In addition, Sharma et al. (2020) conducted experiments in soil columns in the laboratory to investigate the non-Fickian behavior of solute transport through both homogeneous and heterogeneous porous media.

In the present study, we briefly discussed the advection–dispersion equation and the space fractional advection–dispersion equation. The sFADE model is then solved using the numerical explicit finite difference method. Chloride concentration profiles were obtained in the laboratory using soil column experiments. To investigate obtained concentration profiles at different lengths in the direction of flow, both the ADE and sFADE models were used. Different scenarios have been used to estimate transport parameters and simulated the concentration profiles.

2.2 Theoretical Concepts

2.2.1 Equations Influencing ADE

For reactive solutes with linear isotherm equilibrium adsorption, the equation can be written as (Bear and Cheng 2010):

$$R\frac{\partial C}{\partial t} + v\frac{\partial C}{\partial x} = D\frac{\partial^2 C}{\partial x^2} \tag{2.1}$$

For nomenclature explanations, refer the list of parameters.

2.2.2 Equations Influencing sFADE

Considering a linear isotherm equilibrium adsorption, the one-dimensional FADE for reactive solute can be expressed (Benson et al., 2000a, 2000b):

$$R\frac{\partial C}{\partial t}+v\frac{\partial C}{\partial x}=\left(\frac{1}{2}+\frac{\beta}{2}\right)D_f\frac{\partial^\alpha C}{\partial x^\alpha}+\left(\frac{1}{2}-\frac{\beta}{2}\right)D\frac{\partial^\alpha C}{\partial(-x)^\alpha} \tag{2.2}$$

For nomenclature explanations, refer the list of parameters.

The transition probability for $-1 \le \beta \le 0$ is skewed backward, whereas for $0 \le \beta \le 1$, the transition probability is skewed forward. For $\beta = 0$, the above equation can be expressed as:

$$R\frac{\partial C}{\partial t}+v\frac{\partial C}{\partial x}=\left(\frac{1}{2}\right)D_f\frac{\partial^\alpha C}{\partial x^\alpha}+\left(\frac{1}{2}\right)D\frac{\partial^\alpha C}{\partial(-x)^\alpha} \tag{2.3}$$

$$C(x,t)=C_0\left[1-F_\alpha\left(\frac{x-vt/R}{(\Re t)^{1/\alpha}}\right)\right] \tag{2.4a}$$

where $\Re = |\cos(\pi\alpha/2)|D_f/R$, $F_\alpha(y)$ is the probability function that is symmetric α-stable:

$$F_\alpha(y)=C(\alpha)+\frac{\text{sign}(1-\alpha)}{2}\int\limits_0^1 \exp\left(-y^{\frac{\alpha}{\alpha-1}}U_\alpha(\varphi)\right)\mathrm{d}\varphi \tag{2.4b}$$

where φ is the integration variable, sign$(1-\alpha)$ is -1, 0 and $+1$ for $\alpha > 1$, $\alpha = 1$ and $\alpha < 1$, respectively, and, $C(\alpha)$ and U_α can be expressed as:

$$C(\alpha)=\begin{cases}1 & \text{for}\,\alpha>1\\ 0.5 & \text{for}\,\alpha<1\end{cases} \tag{2.4c}$$

$$U_\alpha(\varphi)=\left(\frac{\sin(\pi\alpha\varphi/2)}{\cos(\pi\varphi/2)}\right)^{\left(\frac{\alpha}{1-\alpha}\right)} \tag{2.4d}$$

2.2.3 sFADE Equations and Its Numerical Solution

Derivation of a numerical scheme to solve sFADE is described in Meerschaert and Tadjeran 2004 and 2006, as:

$$\frac{\partial^{\alpha} C(x,t)}{\partial x^{\alpha}} = \lim \operatorname*{Lim}_{M_{+}\to\infty} \frac{1}{h_{+}^{\alpha}} \sum_{k=0}^{M_{+}} g_k C(x - kh, t) \tag{2.5a}$$

And,

$$\frac{\partial^{\alpha} C(x,t)}{\partial (-x)^{\alpha}} = \lim \operatorname*{Lim}_{M_{-}\to\infty} \frac{1}{h_{+}^{\alpha}} \sum_{k=0}^{M_{-}} g_k C(x + kh, t) \tag{2.5b}$$

The Grunwald weights g_k are defined as follows:

$$g_0 = 1 \tag{2.6a}$$

$$g_k = (-1)^k \frac{\alpha(\alpha-1)(\alpha-2)\ldots(\alpha-k+1)}{k!} \tag{2.6b}$$

$$\frac{\partial^{\alpha} C(x_i,t_n)}{\partial x^{\alpha}} = \frac{1}{h^{\alpha}} \sum_{k=0}^{M} g_k C(x_i - (k-1)h, t_n) \tag{2.7a}$$

Conversely, the right-sided fractional derivatives with the shifted Grunwald approximation

$$\frac{\partial^{\alpha} C(x_i,t_n)}{\partial (-x)^{\alpha}} = \frac{1}{h^{\alpha}} \sum_{k=0}^{M} g_k C(x_i + (k-1)h, t_n) \tag{2.7b}$$

The Grunwald weights are represented by g_k in these expressions.

$$\frac{C_i^{l+1} - C_i^l}{\Delta t} = -v \frac{C_{i+1}^l - C_{i-1}^l}{2h} + \frac{D_f}{2h^{\alpha}} \left(\sum_{k=0}^{M} g_k C_{i-k+1}^l + \sum_{k=0}^{M} g_k C_{i+k-1}^l \right) \tag{2.8}$$

In the internal points of the spatial domain, $(i = 1, \ldots, M-1)$, one has

$$C_i^{l+1} = \frac{D_f \Delta t}{2h^{\alpha}} \sum_{k=0}^{M} g_k C_{i-k+1}^l + \frac{D_f \Delta t}{2h^{\alpha}} \sum_{k=0}^{M} g_k C_{i+k-1}^l - \frac{v\Delta t}{2h} C_{i-1}^l + \frac{v\Delta t}{2h} C_{i-1}^l + C_i^l \tag{2.9}$$

The stability condition is $\left(\frac{v\Delta t}{h} + \frac{\alpha D_f \Delta t}{h^{\alpha}}\right) \leq 1.$

2.2.4 Experimental Procedure

On a 300 cm long horizontally placed soil column, a soil column experiment was carried out. Chloride was chosen as a non-reactive tracer for the experiment. The soil column is densely packed with sand of the mean particle size (D50). The value of the cumulative distribution's particle size diameter is at 50%. The calculated value of mean particle size (D50) for fine sand is 0.75 mm, D10 = 0.37 mm, D30 = 0.68 mm, D60 = 0.8 mm, Cc = 1.56 mm, Cu = 2.16. During the solute transport experiment, the soil column was gradually saturated with de-aired tap water from the soil column's inlet. As a result, the soil column's entrapped air was removed. A peristaltic pump was used to inject a common salt (NaCl) solution with an initial solute concentration of C0 = 60 mg/L. The total volumetric water content of the soil media within the column was estimated to be 0.34. The soil media's calculated dry bulk density was found to be 1.71 g/cm^3.

2.2.4.1 Goodness-of-Fit and Estimation of Parameters

The inverse problem method was used to estimate the mathematical model's parameters. An inverse model with the following objective function was created to obtain the parameters (Moradi and Mehdinejadiani 2020).

$$\mathrm{OF} = \frac{1}{N}\sum_{i=1}^{N}\left(C_i^{\mathrm{calc}} - C_i^{\mathrm{obs}}\right)^2 \tag{2.10}$$

The root mean square error, coefficient of determination, and Nash–Sutcliffe efficiency coefficients are all expressed below:

$$R^2 = \left[\frac{\sum_{i=1}^{N}\left(C_i^{\mathrm{obs}} - \overline{C}^{\mathrm{obs}}\right)\left(C_i^{\mathrm{calc}} - \overline{C}_i^{\mathrm{calc}}\right)}{\sqrt{\sum_{i=1}^{N}\left(C_i^{\mathrm{obs}} - \overline{C}^{\mathrm{obs}}\right)^2}\sqrt{\sum_{i=1}^{N}\left(C_i^{\mathrm{calc}} - \overline{C}^{\mathrm{calc}}\right)^2}}\right]^2 \tag{2.11}$$

$$\mathrm{RMSE} = \sqrt{\frac{1}{N}\sum_{i=1}^{N}\left(C_i^{\mathrm{obs}} - C_i^{\mathrm{calc}}\right)^2} \tag{2.12}$$

Nash–Sutcliffe efficiency coefficient (NSE) can be calculated by:

$$\mathrm{NSE} = 1 - \frac{\sum_{i=1}^{N}\left(C_i^{\mathrm{obs}} - C_i^{\mathrm{calc}}\right)^2}{\sum_{i=1}^{N}\left(C_i^{\mathrm{obs}} - \overline{C}^{\mathrm{obs}}\right)^2} \tag{2.13}$$

2.2.5 *Results and Discussion*

The results have been predicted for three cases. In the first case, we estimated the ADE as well as sFADE transport parameters at various points and used these estimates to simulate the observed chloride concentration profiles. Transport parameters were estimated at a distance of $x = 40$ cm in the second case, while in the third case, we estimated the values of transport parameters for observed breakthrough curves at upstream, i.e., at $x = 300$ cm, and used to simulate observed breakthrough curves at downstream distances.

2.2.5.1 Estimation of Transport Parameters of ADE and sFADE at Various Points

Table 2.1 shows the evaluated values of parameters for ADE along with sFADE, as well as the allied values of and NSE at various points in the flow direction. A constant value of pore velocity ($v = 2.12$ cm/min) was used in this simulation. The estimation of the predicted profile of concentrations at 40 cm using both the ADE and sFADE models is shown in Fig. 2.1a. Similarly, Fig. 2.1a–g shows simulations of observed concentration profiles at different points. These concentration profile simulation results show that the sFADE model outperforms the ADE model. The estimated results show that the coefficient of determination and NSE values for the ADE and sFADE models are nearly identical. The RMSE values, on the other hand, have varied. It demonstrates that the RMSE is lower for simulated results of observed concentration profiles at distances of 40 and 300 cm. Furthermore, for all distances, the estimated values of for the sFADE model are less than 2. This implies that the behavior of solute transport is non-Fickian.

Table 2.1 Estimated parameters for ADE and sFADE at variable distances

Distance (cm)	ADE				sFADE				
	D (cm^2/min)	R^2	RMSE	NSE	D_f cm$^\alpha$/min	α	R^2	RMSE	NSE
40	0.812	0.997	0.0339	0.994	0.982	1.861	0.996	0.030	0.995
80	1.365	0.996	0.0344	0.994	1.656	1.846	0.987	0.050	0.987
120	1.768	0.998	0.0322	0.995	2.012	1.824	0.990	0.045	0.990
160	2.051	0.997	0.0354	0.994	2.134	1.787	0.989	0.049	0.988
200	2.562	0.998	0.0426	0.990	2.765	1.756	0.988	0.050	0.987
250	2.893	0.998	0.0374	0.993	3.050	1.785	0.987	0.052	0.986
300	3.014	0.999	0.0347	0.994	3.126	1.864	0.997	0.025	0.997

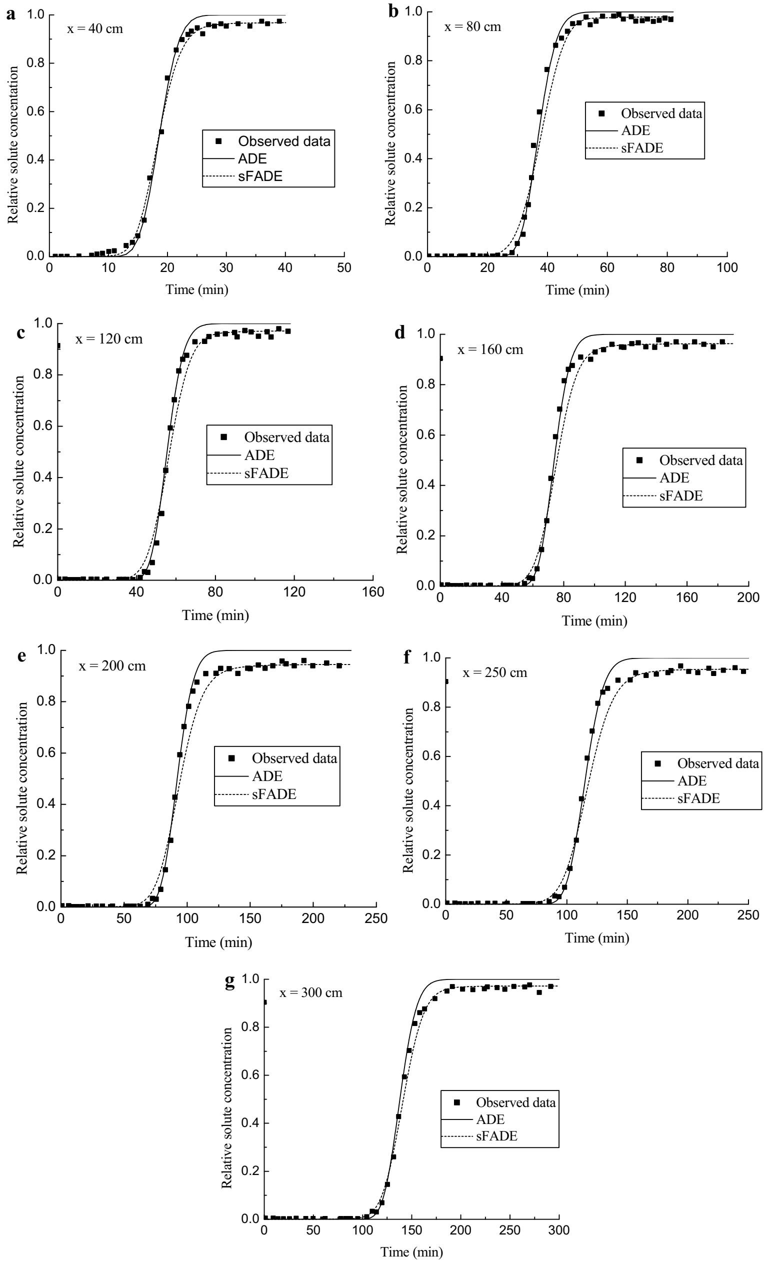

Fig. 2.1 **a** BTCs (at $x = 40$ cm) using ADE and sFADE, **b** BTCs of Cl^- (at $x = 80$ cm) using ADE and sFADE, **c** BTCs of Cl^- (at $x = 120$ cm) using ADE and sFADE, **d** BTCs of Cl^- (at $x = 160$ cm) using ADE and sFADE, **e** BTCs of Cl^- (at $x = 200$ cm) using ADE and sFADE, **f** BTCs of Cl^- (at $x = 250$ cm) using ADE and sFADE, **g** BTCs of Cl^- (at $x = 300$ cm) using ADE and sFADE

Table 2.2 Estimated parameters at 40 cm are used to simulate data at 80, 120, 200, 250 and 300 cms

Distance (cm)	ADE				sFADE				
	D (cm^2/min)	R^2	RMSE	NSE	D_f cm$^\alpha$/min	α	R^2	RMSE	NSE
40	0.812	0.997	0.034	0.994	0.983	1.86	0.996	0.030	0.995
80	0.812	0.995	0.041	0.991	0.983	1.86	0.997	0.027	0.996
120	0.812	0.998	0.040	0.992	0.983	1.86	0.999	0.015	0.999
160	0.812	0.993	0.053	0.986	0.983	1.86	0.995	0.033	0.995
200	0.812	0.991	0.064	0.978	0.983	1.86	0.996	0.036	0.993
250	0.812	0.987	0.069	0.975	0.983	1.86	0.993	0.043	0.990
300	0.812	0.989	0.063	0.980	0.983	1.86	0.995	0.034	0.994

2.2.5.2 Transport Parameters were Estimated at Distance of $x = 40$ cm. Simulation Done at Distances of $x = 80$, 120, 160, 200, 250 and 300 cm

In this case, the observed breakthrough curves at different points upstream in the flow direction were simulated using estimated transport parameters for the observed concentration profile at $x = 40$ cm (Table 2.2). The coefficient of determination and NSE have roughly the same value, as can be seen. The RMSE value, however, is lower in the sFADE model than in the ADE model, as shown in Table 2.2 and Fig. 2.2a–f.

2.2.5.3 Estimation of Transport Parameters for Observed Breakthrough Curves at Upstream ($x = 300$ cm) used for Simulation at Downstream Distances

In this case, the parameter values (i.e., D, D_f and α) are estimated at x = 300 cm in the flow direction and are shown in Table 2.3. These parameters have been used to estimate the obtained concentration profiles at variable points as shown in Fig. 2.3a–f. In this case, the values of the coefficient of determination are greater in the ADE model than in the sFADE model. Furthermore, the RMSE values for the ADE model are lower than those for the FADE model (Table 2.3).

2.2.5.4 Estimation of the Mean Values of Solute Transport Parameters

In this case, mean value of parameters, i.e., D, D_f and α for ADE and sFADE, has been utilized to estimate the obtained concentration profiles at various points as shown in Table 2.4. Simulated concentration profiles employing both ADE and sFADE models are shown in Fig. 2.4a–g. Values of RMSE indicate that the best simulation is obtained from sFADE model at distances of $x = 200$ cm, 250 cm, and 300 cm, respectively. When comparing the ADE model to the sFADE model, the

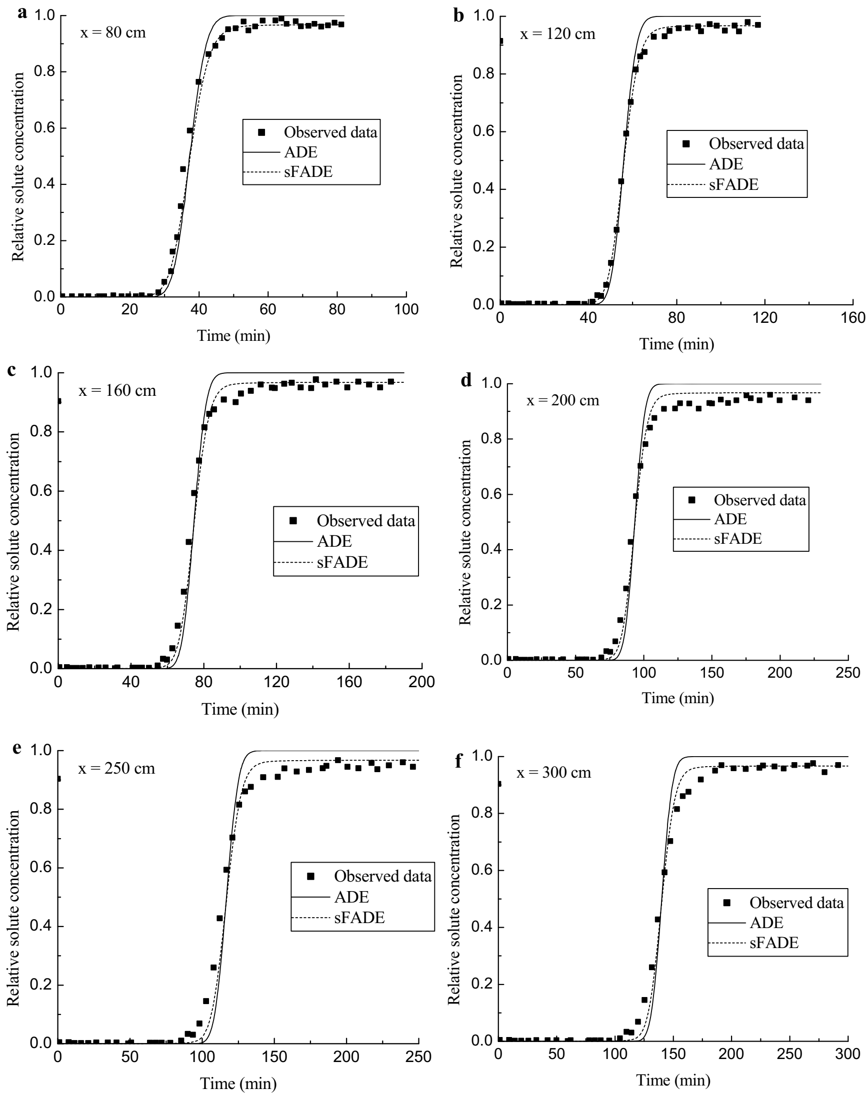

Fig. 2.2 **a** BTCs of Cl^- at $x = 80$ cm using estimated parameters of ADE and sFADE at $x = 40$ cm breakthrough curves, **b** The BTCs of Cl^- at $x = 120$ cm using estimated parameters of ADE and sFADE at $x = 40$ cm breakthrough curves, **c** BTCs of Cl^- at $x = 160$ cm using estimated parameters of ADE and sFADE at $x = 40$ cm breakthrough curves, **d** BTCs of Cl^- at $x = 200$ cm using estimated parameters of ADE and sFADE at $x = 40$ cm breakthrough curves, **e** BTCs of Cl^- at $x = 250$ cm using estimated parameters of ADE and sFADE at $x = 40$ cm breakthrough curves, **f** BTCs of Cl^- at $x = 300$ cm using estimated parameters of ADE and sFADE at $x = 40$ cm breakthrough curves

Table 2.3 Estimated parameters at 300 cm are used to simulate data at 250, 200, 160, 80 and 40 cms

Distance (cm)	ADE				sFADE				
	D (cm^2/min)	R^2	RMSE	NSE	D_f cm$^\alpha$/min	α	R^2	RMSE	NSE
40	3.014	0.976	0.070	0.974	3.126	1.864	0.964	0.095	0.952
80	3.014	0.990	0.047	0.989	3.126	1.864	0.982	0.066	0.978
120	3.014	0.990	0.050	0.987	3.126	1.864	0.984	0.059	0.982
160	3.014	0.995	0.038	0.992	3.126	1.864	0.987	0.052	0.986
200	3.014	0.998	0.043	0.990	3.126	1.864	0.992	0.039	0.992
250	3.014	0.998	0.037	0.993	3.126	1.864	0.993	0.039	0.992
300	3.014	0.999	0.035	0.994	3.126	1.864	0.997	0.025	0.997

RMSE value is lower (at x = 40, 80, 120 and 160 cm). This means that the ADE model provides better simulation at a few distances while the sFADE model provides better simulation at other distances.

2.2.5.5 Variation of RMSE and Coefficient of Determination

An attempt has been made to plot the variation of RMSE and coefficient of determination with distances in the flow direction. Four cases are selected; i.e., parameters are estimated at different distances (Case-A), estimated parameters at x = 40 cm

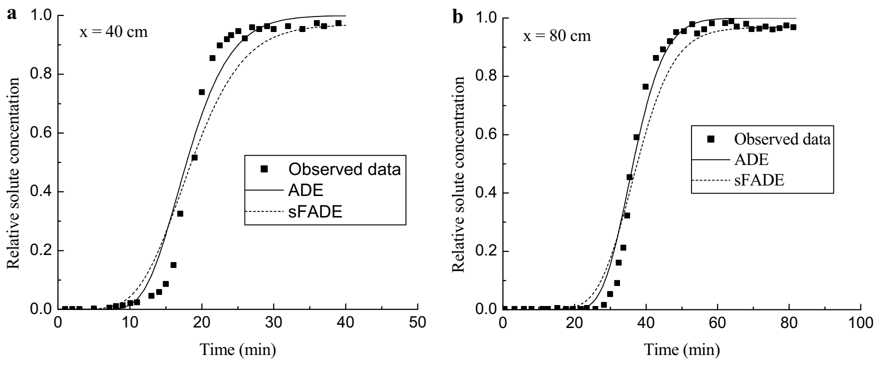

Fig. 2.3 **a** BTCs of Cl^- at x = 40 cm using estimated parameters of ADE and sFADE at x = 300 cm breakthrough curves, **b** BTCs of Cl^- at x = 80 cm using estimated parameters of ADE and sFADE at x = 300 cm breakthrough curves, **c** BTCs of Cl^- at x = 120 cm using estimated parameters of ADE and sFADE at x = 300 cm breakthrough curves, **d** BTCs of Cl^- at x = 160 cm using estimated parameters of ADE and sFADE at x = 300 cm breakthrough curves, **e** BTCs of Cl^- at x = 200 cm using estimated parameters of ADE and sFADE at x = 300 cm breakthrough curves, **f** BTCs of Cl^- at x = 250 cm using estimated parameters of ADE and sFADE at x = 300 cm breakthrough curves

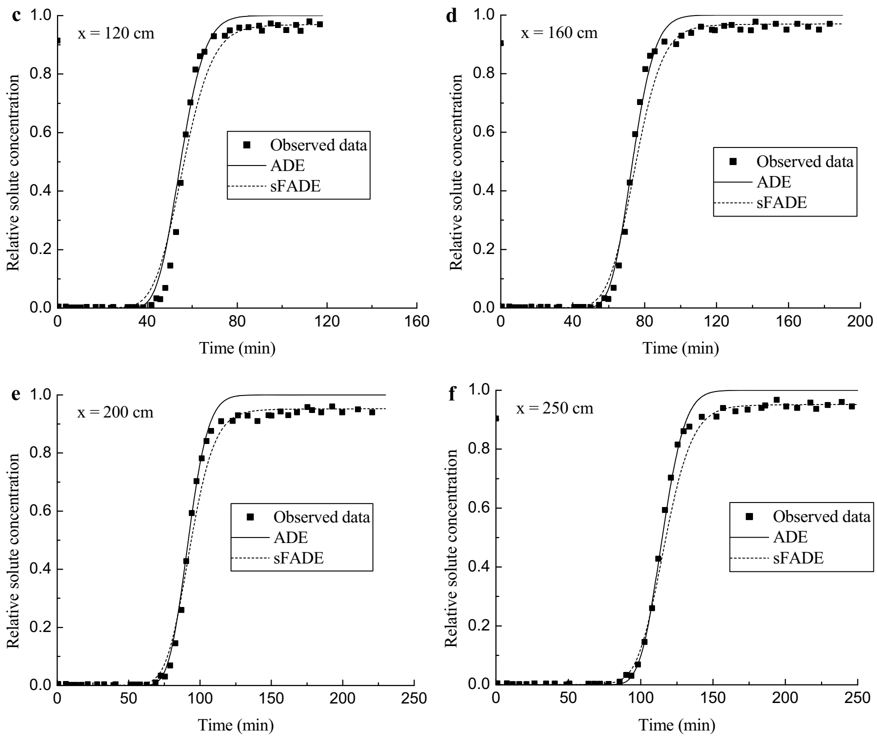

Fig. 2.3 (continued)

Table 2.4 Mean values of parameters are used to simulate data at different distances

Distance (cm)	ADE				sFADE				
	D (cm^2/min)	R^2	RMSE	NSE	D_f cm$^\alpha$/min	α	R^2	RMSE	NSE
40	2.066	0.987	0.051	0.986	2.464	1.818	0.969	0.089	0.958
80	2.066	0.994	0.037	0.993	2.464	1.818	0.984	0.062	0.980
120	2.066	0.996	0.036	0.993	2.464	1.818	0.985	0.057	0.983
160	2.066	0.997	0.036	0.993	2.464	1.818	0.988	0.050	0.988
200	2.066	0.998	0.044	0.990	2.464	1.818	0.991	0.040	0.991
250	2.066	0.997	0.043	0.990	2.464	1.818	0.991	0.043	0.990
300	2.066	0.998	0.039	0.992	2.464	1.818	0.998	0.022	0.998

have been used to determine the obtained concentration profiles at different points (Case-B), estimated parameters at $x = 300$ cm are used to simulate concentration profiles (Case-C), and mean values of parameters are used to simulate concentration profiles at various distances (Case-D). Figures 2.5 and 2.6 indicate the variation of coefficient of determination with distance for ADE as well as sFADE models.

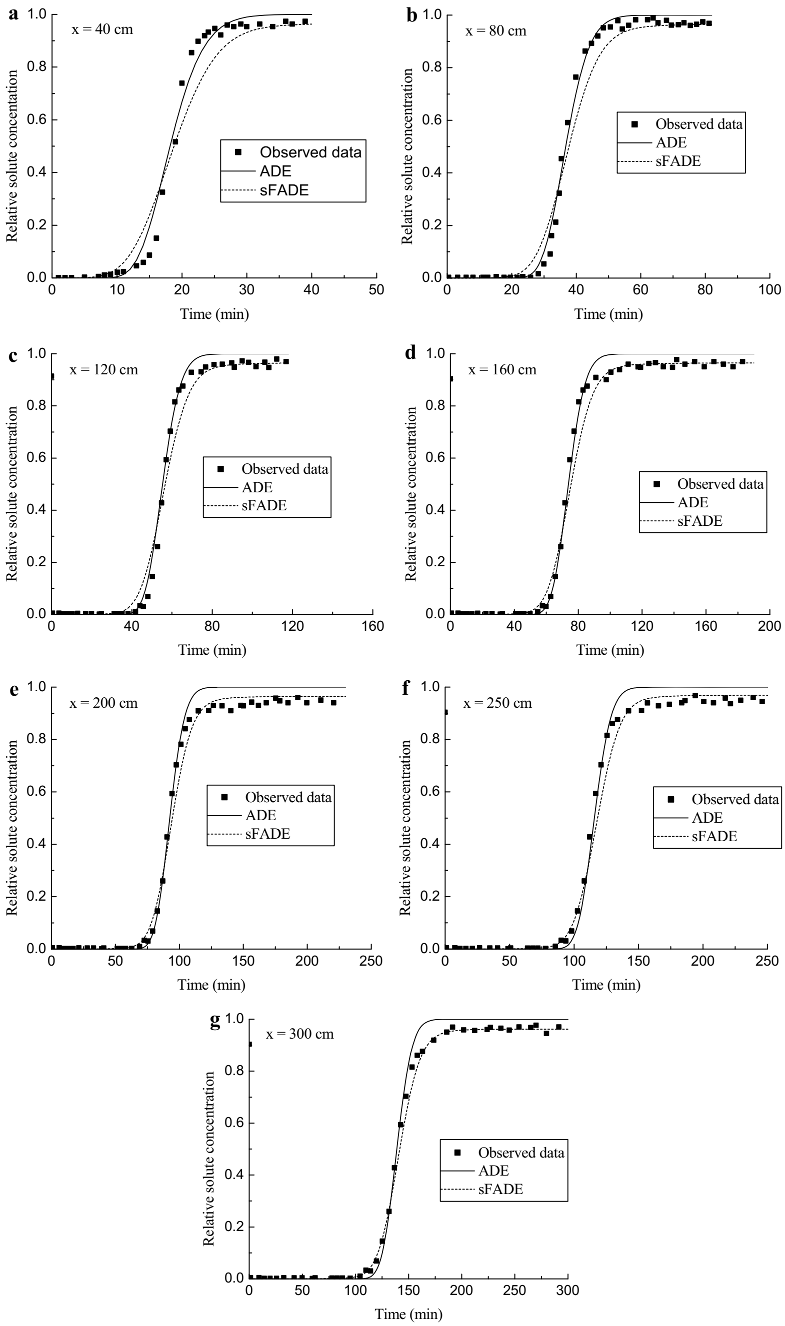
a
x = 40 cm
Observed data
ADE
sFADE
Relative solute concentration
Time (min)
b
x = 80 cm
Observed data
ADE
sFADE
Relative solute concentration
Time (min)
c
x = 120 cm
Observed data
ADE
sFADE
Relative solute concentration
Time (min)
d
x = 160 cm
Observed data
ADE
sFADE
Relative solute concentration
Time (min)
e
x = 200 cm
Observed data
ADE
sFADE
Relative solute concentration
Time (min)
f
x = 250 cm
Observed data
ADE
sFADE
Relative solute concentration
Time (min)
g
x = 300 cm
Observed data
ADE
sFADE
Relative solute concentration
Time (min)

◀**Fig. 2.4** **a** BTCs of Cl^- at $x = 40$ cm using mean value of parameters of ADE and sFADE, **b** BTCs of Chloride at $x = 80$ cm using the mean value of parameters of ADE and sFADE, **c** BTCs of Cl^- at $x = 120$ cm using mean value of parameters of ADE and sFADE, **d** BTCs of Cl^- at $x = 160$ cm using mean value of parameters of ADE and sFADE, **e** BTCs of Cl^- at $x = 200$ cm using mean value of parameters of ADE and sFADE, **f** BTCs of Cl^- at $x = 250$ cm using the mean value of parameters of ADE and sFADE, **g** BTCs of Cl^- at $x = 40$ cm using mean values of parameters of ADE and sFADE

The value of the coefficient of determination remains constant across all cases—A, B, C, and D. Figures 2.7 and 2.8 show the variation of RMSE with distance for various cases for both the ADE and the sFADE models. These findings show that the variation of RMSE at different distances is not uniform for both models.

Fig. 2.5 Variation of coefficient of determination with distance in the flow direction for ADE

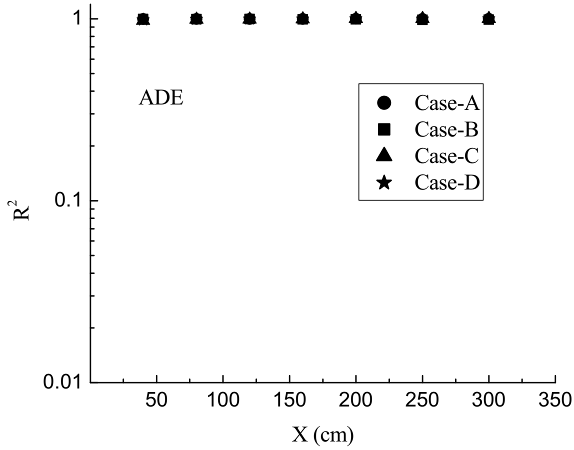

Fig. 2.6 Variation of coefficient of determination with distance in the flow direction for sFADE

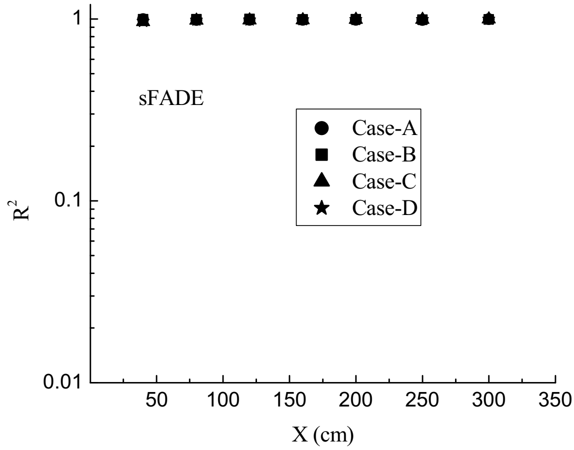

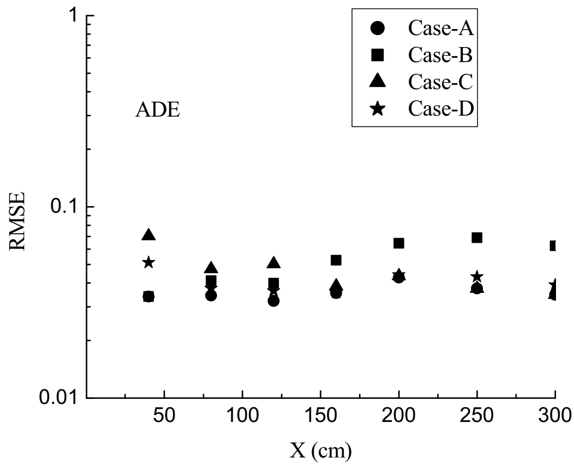

Fig. 2.7 Variation root mean square error (RMSE) with distance in the flow direction for ADE

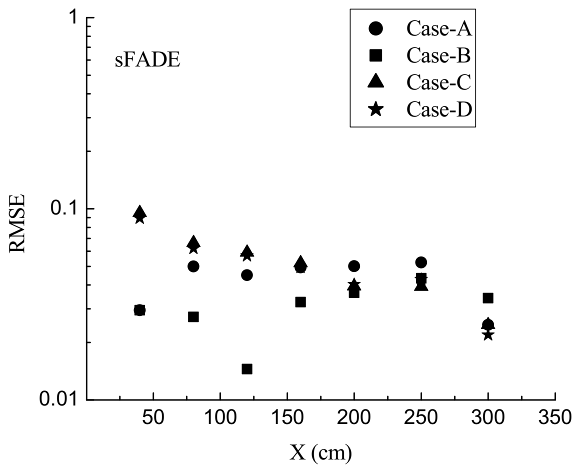

Fig. 2.8 Variation root mean square error (RMSE) with distance in the flow direction for sFADE

2.3 Summary

This study attempted to investigate the performance of the ADE and sFADE models. The solution of the sFADE equation was obtained using an explicit finite difference method. For both the ADE and sFADE models, transport parameters are estimated for various cases. The order of fractional differentiation () in the sFADE model is less than 2. It implies that solute transport is not Fickian in porous media. The determination coefficient and NSE for both the ADE and sFADE models are nearly constant across cases. The RMSE, on the other hand, varies with distance for both models. The RMSE value of the sFADE model is lower when compared to the ADE model. As a result, the non-Fickian transport model more accurately reproduces observed chloride breakthrough curves through porous media.

References

Bear J, Cheng AHD (2010) Modeling groundwater flow and contaminant transport. vol 23. Springer Science & Business Media

Benson DA, Wheatcraft SW, Meerschaert MM (2000a) The fractional-order governing equation of Lévy motion. Water Resour Res 36(6):1413–1423. https://doi.org/10.1029/2000WR900032

Benson DA, Wheatcraft SW, Meerschaert MM (2000b) Application of a fractional advection-dispersion equation. Water Resour Res 36(6):1403–1412. https://doi.org/10.1029/2000WR900031

Benson DA, Schumer R, Meerschaert MM, Wheatcraft SW (2001). Fractional dispersion, Lévy motion, and the MADE tracer tests. Transp Porous Media 42(1):211–240. https://doi.org/10.1023/A:1006733002131

Ben-Zvi R, Scher H, Jiang S, Berkowitz B (2016) One-dimensional finite element method solution of a class of integro-differential equations: application to non-Fickian transport in disordered media. Transp Porous Media 115(2):239–263

Gelhar LW, Welty C, Rehfeldt KR (1992) A critical review of data on field-scale dispersion in aquifers. Water Resour Res 28(7):1955–1974. https://doi.org/10.1029/92WR00607

Kundu S (2018) Suspension concentration distribution in turbulent flows: an analytical study using fractional advection–diffusion equation. Phys A 506:135–155

Meerschaert MM, Tadjeran C (2004) Finite difference approximations for fractional advection–dispersion flow equations. J Comput Appl Math 172(1):65–77. https://doi.org/10.1016/j.cam.2004.01.033

Meerschaert MM, Tadjeran C (2006) Finite difference approximations for two-sided space-fractional partial differential equations. Appl Numer Math 56(1):80–90. https://doi.org/10.1016/j.apnum.2005.02.008

Moradi G, Mehdinejadiani B (2020) An experimental study on scale dependency of fractional dispersion coefficient. Arab J Geosci 13:409

Sharma PK, Agarwal P, Mehdinejadiani B (2020) Study on non-Fickian behavior for solute transport through porous media. ISH J Hydraul Eng. https://doi.org/10.1080/09715010.2020.1727783

Sternberg SPK (2004) Dispersion measurements in highly heterogeneous laboratory scale porous media. Transp Porous Media 54:107–124. https://doi.org/10.1023/A:1025708313812

Chapter 3
Contaminant Transport Modeling for Homogeneous and Heterogeneous Porous Systems Using MODFLOW Models-Based Scripting Python Package

Abhay Guleria, Sumedha Chakma, and Vijay Pratap Singh

Abstract Contaminant transport modeling for soil column and heterogenous porous system poses a challenge when modeling approach involves non-linear and non-equilibrium sorption models and low permeability porous media (LPPM). Thus, in this chapter, contaminant transport modeling for soil column conditions via 1-D non-linear and non-equilibrium sorption models by means of MODFLOW models-based scripting Python package is presented. Further, contaminant plume evolution dynamics through homogeneous and heterogeneous porous systems, along with sensitivity analysis of flow and transport parameters, is conducted utilizing MT3D-USGS and MODFLOW 6 models. Results from 1-D modeling revealed sorption mass exchange rate as dominating parameter governing concentration at the outlet of soil column. Further, longitudinal dispersivity is observed to be affecting the peak value of concentration for non-equilibrium sorption model. The dominance of molecular diffusion and transverse dispersion on 2-D vertical transport through LPPM is observed from 2-D vertical transport modeling, whereas advection and mechanical dispersion are observed as governing mechanisms in the high hydraulic conductivity zone. Also, the difference in the simulation capabilities of two modeling (i.e., MT3D-USGS and MODFLOW 6) approaches is seen. Overall, this chapter highlighted the influence of sorption isotherm, LPPM, and modeling approach on the contaminant transport modeling.

Keywords Groundwater · Contaminant transport · Heterogeneity · MODFLOW 6 · FloPy

A. Guleria (✉) · S. Chakma · V. P. Singh
Department of Civil Engineering, Indian Institute of Technology Delhi, Hauz Khas, New Delhi 110016, India
e-mail: abhay_guleria@civil.iitd.ac.in

S. Chakma
e-mail: chakma@civil.iitd.ac.in

V. P. Singh
e-mail: ce1180173@iitd.ac.in

P. Shukla et al. (eds.), *Environmental Processes and Management*, Water Science and Technology Library 120, https://doi.org/10.1007/978-3-031-20208-7_3

Abbreviations

C_{im}	Contaminant concentration in the immobile region
K_d	Linear sorption distribution coefficient
K_f	Freundlich equilibrium distribution sorption coefficient
K_l	Langmuir equilibrium constant
$\overline{S}$	Langmuir sorption capacity
α_L	Longitudinal dispersivity
α_{TV}	Traverse vertical dispersivity
θ_{im}	Porosity of the immobile region
ρ_b	Bulk density
ANN	Artificial neural network
BTC	Breakthrough curve
GA	Genetic algorithm
GMS	Groundwater modeling system
GW	Groundwater
LPPM	Low permeability porous media
MADE	Macro dispersion experiment
MOC	Method of characteristic
MODFLOW	Modular three-dimensional finite-difference groundwater flow model
MT3DMS	Modular three-dimensional multispecies transport model
MT3D-USGS	Mass transport in 3-dimensions—U.S. geological survey
MVR	Water mover package
SGeMS	Stanford geostatistical modeling software
TDS	Total dissolved solid
TIAA	Tucson international airport area
C	Dissolved-phase concentration
S	Sorbed concentration
a	Freundlich equilibrium sorption coefficient
t	Time
β	First order sorption mass exchange rate between dissolved and sorbed phases
ξ	First order mass transfer coefficient

3.1 Introduction

Contaminant transport through saturated porous systems with multiple permeability regions is critical when planning remediation activities for any contaminated site (Chapman and Parker 2005; Guo and Brusseau 2017a). Low permeability porous media (LPPM) or aquitard regions behave as a sink during contaminant loading period and as a source, once the contaminating source is removed or isolated

(Chapman and Parker 2005; Rasa et al. 2011; Yang et al. 2017a, b; Guo and Brusseau 2017b). During flushing period or after contaminant source removal, immobile contaminants stored in the dissolved or sorbed phase in the LPPM either diffuse out of these zones due to concentration gradient or cause long plume tailing for a longer duration due to desorption (Brown et al. 2012; Brusseau et al. 2012). Connected networks of preferential flow pathways and mass transfer between high permeability channels and low permeability matrix were observed as governing factors controlling the transport behavior at Macrodispersion Experiment (MADE) site (Zheng et al. 2011). Transverse vertical dispersivity and length of silt/clay layer were found as governing factors of remediation during pump and treat operations while mimicking the field-scale conditions (Carey et al. 2015). Transverse mixing of the conservative contaminant was observed to be governed majorly by a difference in the hydraulic conductivity of matrix and high permeability lenses in comparison with actual pore scale dispersivity (Ballarini et al. 2014). It is observed that the non-ideal transport behavior for large heterogeneous system was mainly associated with mass-transfer mechanisms from dead-end regions, based on the observations of pump and treat operations at Tucson International Airport Area (TIAA) federal Superfund site (Guo and Brusseau 2017a, b). Furthermore, non-ideal mass-removal behavior was observed attributed solely to the back-diffusion from LPPM in the layered or highly heterogeneous subsurface system (Guo et al. 2019). Thus, it can be inferred that the contaminant transport in the presence of LPPM or aquitard regions is complex and needs attention while modeling using any mathematical model.

Several studies were carried out in 2-D and/or 3-D domains in the past that focused on contaminant transport behavior as well as identification of source using an inverse procedure. Singh et al. (2004) solved 2-D groundwater (GW) flow and transport equation using a method of characteristics (MOCs) and used the simulated concentration data to train and test the artificial neural network (ANN). The simulation-based ANN model was developed to identify the unknown pollution source; however, a study was limited to the synthetic case of homogenous aquifer conditions (Singh et al. 2004). A contaminant transport model-based ANN approach was developed too for a scenario in which concentration data for training is partially missing (Singh and Datta 2007). The 2-D GW flow and mass transport equation was solved by MOC. A single soil layer was assumed for an aquifer of size 732 m by 549 m, thus neglecting the impact of heterogeneity (Singh and Datta 2007). Also, a genetic algorithm (GA)-based simulation-optimizer was developed by Singh and Datta (2006) to determine the properties (release period, location, and magnitude of concentration) of unknown GW pollution sources for the simple case (two potential source points and six observation wells) to complex scenario (potential source assumed over some part of aquifer region). USGS-MOC method was used to generate the spatial and temporal concentration data for aquifer of size 1300 m by 800 m and further utilized the simulation data to compute the fitness function value (Singh and Datta 2006). In another study, Visual MODFLOW was used to assess the total dissolved solids (TDS) in the GW in and around dumpsite in Ranipet, Tamilnadu, India (Rao et al. 2011). Observed and model-simulated TDS values were compared to check the accuracy of a numerical model. Similarly, MODFLOW and MT3DMS modules were used via Visual MODFLOW 4.1 to simulate the TDS in the basaltic terrain of Bagalkot district, Karnataka, India (Rao et al. 2013). Calibration of numerical model was done using observed head data; however, a comparison between model simulations and field observations of TDS was not made (Rao et al. 2013). Different types of ANN models were developed based on the multilevel characterization of breakthrough curve data and highlighted the importance of data for the identification of unknown sources (Singh and Singh 2019). The GMS (version 7.1, 2011, Aquaveo) software was used to solve the GW flow and contaminant transport equations for a synthetic case study representing an aquifer of size 1300 m by 800 m (Singh and Singh 2019). Multilevel BTC characterization performed well as compared to conventional ANN models; however, study was limited to simplistic homogenous aquifer conditions and assumed single fixed lumped value of input parameters for simulations (Singh and Singh 2019).

A multi-layered GW flow and contaminant transport model was conceptualized in GMS v6.5 software to estimate the minimum value of required river flow to enhance the GW quality of the Cauvery river basin, Tamil Nadu (Vetrimurugan et al. 2017). The transport behavior of chloride and nitrate ions from July 2007 to June 2012 was simulated using MT3DMS and MOC-based models, and model calibration was done utilizing observed data (Zheng and Wang 1999; Vetrimurugan et al. 2017). The chloride and nitrate concentration was forecasted for September 2020, assuming various scenarios like water flowing in the river for 30 days in a year, 60 days in a year, and 90 days in a year (Vetrimurugan et al. 2017). Borah and Bhattacharjya (2015) used Groundwater modeling system (GMS 7.1, Aquaveo) software coupled with an ANN-based optimization model to identify the properties of contamination source assuming synthetic example mimicking confined aquifer conditions. Leichombam and Bhattacharjya (2019) implemented MODFLOW to solve GW flow and transport equations and coupled it with an optimization algorithm to determine the unknown locations and flux of contaminant sources. The developed neural network-based models performed well in determining the unknown contamination source, however, limited to simplistic homogeneous aquifer conditions (Singh et al. 2004; Singh and Datta 2007). It is observed that simplistic aquifer conditions, like isotropic, and homogeneous conditions, along with the single lumped value of parameters like porosity and dispersivity, were considered in these field-scale studies (Rao et al. 2011; Borah and Bhattacharjya 2015; Leichombam and Bhattacharjya 2019).

To incorporate the variable nature of flow and transport parameters in the mathematical model, several researchers have developed their in-house code rather than relying on open-source or commercial software. For example, in-house codes of single- and dual-porosity-based contaminant models were developed to simulate contaminant transport in the homogeneous and heterogeneous soil column (Gao et al. 2009; Sharma et al. 2016), and through the stratified porous system (Swami et al. 2016). Variant flow and transport parameters such as dispersion and mass-transfer coefficient were incorporated into the mathematical model to simulate non-Fickian transport behavior in heterogeneous porous systems (Gao et al. 2010; Swami et al. 2018; Guleria et al. 2019, 2020). A two-dimensional contaminant transport problem was solved by a dual porosity-based physical non-equilibrium model, and the impact of soil type on BTC was studied numerically (Guleria and Chakma 2022). However, it is observed that the above-mentioned studies were not implemented under field-scale conditions (Gao et al. 2009, 2010; Swami et al. 2016, 2018; Sharma et al. 2016; Guleria et al. 2019, 2020). There are few field-scale studies in which heterogeneity of the porous media was considered while developing GW flow and mass transport model. For example, MODFLOW was used to solve the steady-state GW flow equation for a petrochemical plant site of approximately 2 km^2 in Italy, and MODPATH was used to track the trajectory of contaminant plume by assuming different hydraulic conductivity zones (Elshall et al. 2020). A 2-layered aquifer system was considered, in which variation in the hydraulic conductivity (0.43−17.3 m/day) was assigned to the upper confined layer, while 0.01 m/day of hydraulic conductivity was assumed for the bottom confined layer (Elshall et al. 2020). Sathe and Mahanta (2019) assessed GW contamination due to arsenic in Assam, India, by representing porous systems using 2-D lithological and 3-D stratigraphy models, then applied MODFLOW-MT3DMS (3-D software) to simulate field-scale data. The heterogeneous porous system comprised several soil types such as clay, silt, sandy gravel, and boulder with gravel was considered in the modeling; however, model calibration was done by comparing the trend of observed and simulated GW level and ignoring the minimization of residual error (Sathe and Mahanta 2019). It is observed that studies in which MODFLOW-based open-source and/or commercial software was used ignored the variability in the GW flow and transport parameters (Rao et al. 2011; Borah and Bhattacharjya 2015; Leichombam and Bhattacharjya 2019). Most of the studies ignored the impact of LPPM such as silt or clay lenses, on the plume evolution dynamics in the adjoining aquifers (Gao et al. 2010; Rao et al. 2011; Borah and Bhattacharjya 2015; Sharma et al. 2016; Swami et al. 2018; Leichombam and Bhattacharjya 2019; Guleria et al. 2020). Therefore, in this study, the impacts of non-linear sorption processes, LPPM, and stagnant regions on the contaminant transport behavior in the aquifer are studied.

It can be concluded that the contaminant transport dynamics in the presence of immobile regions or LPPM are important to evaluate the risks of possible contaminant rebound during long late time periods. Thus, the main aim of this study is to enhance the understanding of the transport mechanisms in complex heterogeneous systems such as hydraulically coupled aquifers and low permeability porous media (LPPM). Thus, the focus of present chapter is to (i) conduct the contaminant transport simulations for 1-D saturated porous system and compare various non-equilibrium and non-linear sorption models, (ii) analyze the effect of flow and transport parameters on the contaminant plume evolution in the 2-D homogeneous and layered porous systems, and (iii) test the simulation capabilities of MT3D-USGS and MODFLOW 6 models to simulate the contaminant transport behavior in various type of porous systems (i.e., aquifer, aquifer with LPPM, aquifer-aquitard, and aquifer-aquitard with LPPM).

3.2 Methodology

3.2.1 Modeling Approach

The impact of flow and transport through LPPM is studied by developing specialized mathematical modeling approaches such as analytical, semi-analytical, and/or numerical models (Zhan 1998; Zhan et al. 2009; Yang et al. 2015, 2019; Rezaei et al. 2016). Forward and backward diffusive processes in aquitard were considered for an aquitard-aquifer porous system at a macro-scale (Yang et al. 2015). Yang et al. (2019) developed a 1-D analytical solution to analyze the effects of exponential depleting source and back-diffusion from LPPM on long tails in the contaminant breakthrough curves. In the study by Rezaei et al. (2016) and Zhan et al. (2009) for the single-species contaminant transport, flow and transport processes such as advection, vertical diffusion, linear sorption, and first-order irreversible decay were considered for the aquitard region too. However, analytical and semi-analytical solutions are limited to simplistic aquitard-aquifer and/or stratified porous systems. Therefore, graphical user interface-based software is used, developed, and updated to incorporate new challenges to simulate complex contaminant transport phenomena at field-scale conditions. One such popular software is ModelMUSE, which was developed by USGS to solve GW flow and transport problems (Winston 2009). Mescher (2018) used MODFLOW 2005 and MT3D-USGS via ModelMUSE platform to understand the contaminant transport behavior in and around Bordan site, Ontario, Canada. In the study by Mesher 2018, 3 packages of MODFLOW 2005 and five packages of MT3D-USGS models were used to compare the plume evolution of chloride (conservative) and carbon tetrachloride (reactive) contaminants (Mescher 2018). The implementation of the transfer of hydrologic processes among hydrologically connected units was done using water mover package (MVR) within MODFLOW 6 model (Morway et al. 2021). The water transfer between irrigation delivery ditch and multiple cropped areas representing "one-to-many" and runoff transfer from multiple fields routed toward sub-stream representing "many-to-one" connections were shown very well using MVR package (Morway et al. 2021).

In recent years, the Python language has gained acknowledgment in most computational works because of its open-source facility. In the contaminant transport modeling research field, there are few studies in which an open-source MODFLOW-based modeling approach is implemented. For example, Stanford Geostatistical Modeling Software (SGeMS) was utilized to generate the heterogeneous hydraulic conductivity field, and Python scripting package, FloPy, was used to run MODFLOW-based simulations from which flow and transport observed data was further used in parameter estimation (Kheirabadi 2018). A comparison of sequential and combined approaches to calibration was made using PEST++ via a Python programming environment (Kheirabadi 2018). The combined approach performed better than the sequential approach for estimating hydraulic conductivity and porosity, but was observed as time-consuming, complex in usage, and challenging for weight searching process in each run (Kheirabadi 2018). To determine hydraulic transmissivities via comparison model method for hypothetical aquifer conditions, Comunian and Giudici (2021) conducted simulations using FloPy environment. The Gaussian covariance distribution of transmissivity field was generated using Python package gstools (Müller and Schüler 2019), and further, MODFLOW 6 was used by means of FloPy platform to conduct simulations (Hughes et al. 2017; Langevin et al. 2017). White et al. (2021) developed Python scripting-based tools using FloPy to conduct high-dimensional and geostatistical-based analyses to derive environmental metrics. In another study, a new unstructured finite difference-based gridding approach was developed, and suitability was tested on single and multi-layered porous systems with 4-orders of magnitude variability in the distribution of hydraulic conductivity (Sbai 2020). The technique was ideal for MODFLOW-USG and MODFLOW 6 models and supported the update of the grid from conventional rectilinear to unstructured grids such as Quadtree/Octree Decomposition and Voronoi Tessellations (Sbai 2020). The developed gridding approach was not only confined to geometry-oriented workflow but considered the physics and feedback obtained from the GW flow model (Sbai 2020). Thus, by taking motivation from above-mentioned studies, in this work, an open-source Python scripting package (FloPy) is used to conduct simulations of GW flow and contaminant transport through saturated porous systems (Bakker et al. 2016, 2018). The scripts used in the present study are modified based on the tutorial on FloPy MT3DMS problem (Sudicky 1989; Bakker et al. 2018). Two types of problems were considered (i) 1-D reactive transport modeling through soil column using non-linear and non-equilibrium sorption models and (ii) 2-D vertical conservative transport modeling for homogeneous and heterogeneous aquifer conditions. A detailed description of model parameters and approach adopted is presented in subsequent sections.

3.3 Results and Discussion

3.3.1 Analyzing Non-linear and Non-equilibrium Sorption Isotherms Using 1-D Reactive Transport Modeling

One-dimensional contaminant transport behavior with non-linear (Langmuir and Freundlich) and non-equilibrium sorption isotherms are studied by conducting numerical simulations. The study used FloPy to solve 1-D advection-dispersive transport equation with non-linear equilibrium sorption and non-equilibrium sorption model (Bakker et al. 2016, 2018). The geometrical details mimic the soil column conditions and are based on the example presented in (Zheng and Wang 1999). In this sub-section, MT3DMS and MODFLOW 6 GWT models are used to carry out simulations via FloPy (Bakker et al. 2018); however, results from MODFLOW 6 are shown only. The main focus of these simulations is to analyze the impact of flow and transport parameters (velocity, sorption mass exchange rate, and longitudinal dispersivity) on reactive transport behavior. Non-equilibrium sorption via MT3DMS-based model is represented as:

$$\rho_b \frac{\partial S}{\partial t} = \beta\left(C - \frac{S}{K_d}\right) \tag{3.1}$$

where S is the sorbed concentration, C is the dissolved-phase concentration, β is the 1st order sorption mass exchange rate between dissolved and sorbed phases, ρ_b is the bulk density, t is the time, and K_d is linear sorption distribution coefficient.

Due to the inability of MODFLOW 6 to model non-equilibrium sorption, a model needs to be approximated by assigning an immobile domain. In this study for a 1-D problem, the value of distribution coefficient is 0.933, which is close to one; thus, the advantage of MODFLOW 6 to approximate non-equilibrium sorption via immobile domain was utilized. It was possible due to the assumption of not considering separate sorption, decay, and production within the immobile domain. The dissolved-phase contaminant mass transfer between the mobile and immobile domain region can be represented as:

$$\theta_{im} \frac{\partial C_{im}}{\partial t} = \xi(C - C_{im}) \tag{3.2}$$

where C_{im} is the contaminant concentration in the immobile region, θ_{im} is the porosity of the immobile region, and ξ is the 1st order mass-transfer coefficient. By assigning immobile domain porosity as bulk density and 1st order mass-transfer coefficient between mobile and immobile regions as 1st order mass-transfer rate for dissolved and sorbed phases, non-equilibrium sorption can be approximated.

Initially, contaminant transport behavior via non-linear sorption (i.e., Freundlich and Langmuir) isotherms are compared for two different down-gradient locations (8 and 16 cm). Secondly, non-equilibrium sorption model is used to simulate the contaminant transport behavior through saturated soil column. Numerical simulations are conducted for 1500 s in which the source is assumed to be present for up to 160 s. The detailed description, such as sorption distribution coefficient and dispersivity, is shown in Table 3.1.

3.3.1.1 Effect of Groundwater Velocity on the Contaminant Transport

The temporal variation of reactive contaminant for Freundlich and Langmuir isotherm model is shown in Fig. 3.1. An early breakthrough point is observed with an increase in velocity ($v = 0.10$ cm/s) for both the observation points (Fig. 3.1a). The peak concentration value is observed at ~ 250 s for $v = 0.10$ cm/s at an 8 cm down-gradient location, whereas for a 16 cm down-gradient location, peak value is observed at ~400 s, indicating the dominance of longitudinal dispersion over source boundary condition at a location away from source. For $v = 0.05$ cm/s at a 16 cm

Table 3.1 Input parameters used for simulation of 1-D column experiment base case

S. No.	Parameter	Value
1	Length	0.16 m (16 cm soil column)
2	Grid spacing	1.6E–03 m (0.16 cm)
3	Pulse duration	160 s
4	Total simulation time	1500 s
5	Dispersivity	0.016 m (1.6 cm)
6	Seepage velocity	1.0E−03 m/s (0.10 cm/s)
7	Porosity	0.32
8	Bulk density	1587 kg/m^3 (1.587 gm/cm^3)
9	Conc. of source fluid	1.0 (unitless)
10	Distribution coefficient	9.33E−04 m^3/kg (0.933 cm^3/gm)
11	Hydraulic conductivity	1.0E−05 m/s (0.001 cm/s)
12	Freundlich equilibrium sorption coefficient (K_f)	$0.3\left(\frac{\mu g}{g}\right) * \left(\frac{l}{mg}\right)^a$
13	Freundlich equilibrium sorption coefficient (a)	0.7 (unitless)
14	Langmuir equilibrium constant (K_l)	$100\left(\frac{l}{mg}\right)$
15	Langmuir sorption capacity ($\overline{S}$)	$0.003\left(\frac{\mu g}{g}\right)$
16	First-order mass-transfer rate between the dissolved aqueous and sorbed phases (β) of non-equilibrium sorption model	0.0/s (case 1)
		10^{-3}/s (case 2)
		10^{-1}/s (case 3)
		10.0 /s (case 4)

down-gradient location, the lowest value of peak concentration is observed at ~850 s among all four scenarios.

In the case of Langmuir sorption model, the rise and fall of breakthrough curve (BTC) is confined to a small-time duration, indicating an early achievement of Langmuir sorption capacity (Fig. 3.1b). A steep slope of rising portion and falling limb of BTC is observed for $v = 0.10$ cm/s as compared to $v = 0.05$ cm/s. The peak concentration of the BTC for the Langmuir model is higher than the Freundlich model for both the GW velocity. In case of Langmuir model, the tailing portion of BTC is smaller as compared to Freundlich model, indicating the attainment of maximum sorption capacity. A large difference in the rising and tailing portion of BTC for different sorption models indicated the significance of choosing the appropriate sorption isotherm as per in situ lab- or field-scale conditions.

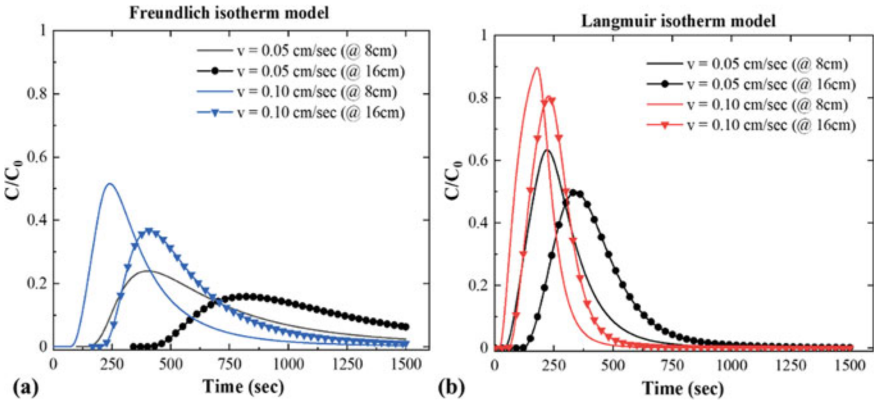

Fig. 3.1 BTC predicted at 8 and 16 cm down-gradient distances by implementing **a** Freundlich and **b** Langmuir isotherm model

3.3.1.2 Effect of Sorption Parameter on the Contaminant Transport Dynamics

The impact of non-equilibrium sorption parameter (β) on the BTC is studied at half- (8 cm) and full (16 cm) soil column length for GW velocity, $v = 0.05$ cm/s (Fig. 3.2). The value of $\beta = 0$ corresponds to a conservative contaminant where no sorption process exists, while a high value of β indicates that the non-equilibrium sorption process occurs at a faster rate so as reached equilibrium state. At 8 cm down-gradient location, the peak concentration value decreases as going from conservative to reactive contaminant ($\beta = 0$/s to $\beta = 10^{-3}$/s). The peak concentration value is observed at ~250 s for lower β values (0/s and 10^{-3}/s) at an 8 cm down-gradient location, while for higher β values (10^{-1}/s and 10/s), the peak value is observed at ~750 s. Also, the magnitude of concentration for higher values of sorption rate is found to be 3–4 times lower than that of lower sorption rate case. It is observed that the concentration value of contaminant decreases with an increase in β value at an 8 cm down-gradient location, showing the mass transfer from solution phase to sorbed phase by sorption processes. The peak value of 0.65 is observed at an 8 cm down-gradient location, while the peak value of 0.50 is observed at a 16 cm down-gradient location for the same value of $\beta = 0$, indicating the impact of longitudinal dispersion process on contaminant transport. Also, it is observed that with an increase in the value of β, the spreading of the BTC increases as observed from BTC at an 8 cm down-gradient location.

The magnitude of concentration ranging from 0.0001 to 0.1 is observed at a 16 cm down-gradient location for higher sorption rates ($\beta = 0.10\ \text{sec}^{-1}$ and $\beta = 10\,\text{sec}^{-1}$), indicating that the peak concentration is not reached yet after 1500 s. It is seen that for higher values of β (e.g., $\beta = 0.10\,\text{sec}^{-1}$ and $\beta = 10\,\text{sec}^{-1}$), the concentration value at both observation points dropped by ~ 5–8 times in comparison with lower values of β (e.g., $\beta = 0.0\ \text{sec}^{-1}$ and $\beta = 0.001\,\text{sec}^{-1}$). Thus, it can be stated that β

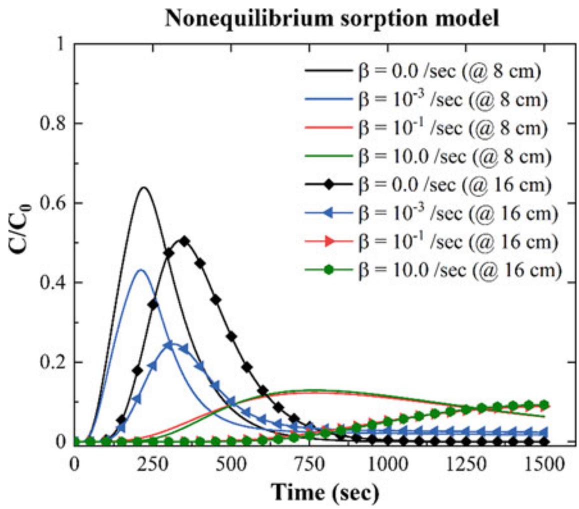

Fig. 3.2 BTC predicted at 8 and 16 cm down-gradient distance for various values of β of non-equilibrium sorption model at groundwater velocity = 0.05 cm/s

is the dominating parameter of non-equilibrium reactive transport model and governs the contaminant transport behavior even for small-scale soil column conditions.

3.3.1.3 Effect of Longitudinal Dispersivity on the BTC

In this sub-section, the effect of longitudinal dispersivity on the prediction of concentration for soil column conditions is shown. Figure 3.3 shows the predicted BTC at a 16 cm down-gradient location for longitudinal dispersivity, $\alpha_L = \frac{L}{10}$ and $\alpha_L = \frac{L}{3}$ via running simulations on MT3DMS (solid lines) and MODFLOW 6 (circles) in FloPy environment. The solid circles from MODFLOW 6 are presented for every 20th-time step. Also, the effect of the non-equilibrium exchange coefficient (β) for two different longitudinal dispersivity values is shown. The results for MODFLOW 6 are shown for every 20th-time step. As observed from BTCs, the results from MODFLOW 6 match well with the MT3DMS simulated BTC. The peak concentration value of 0.80 is observed for $\alpha_L = \frac{L}{10}$ as compared to 0.70 for $\alpha_L = \frac{L}{3}$, depicting the dominance of dispersion processes over advection which eventually causes the reduction in the peak concentration with an increase in longitudinal dispersivity value. The approximate time taken to reach peak value is found as 800 s for $\beta = 0.10$ and $\beta = 10.0$ at longitudinal dispersivity equal to 1/10th of domain length (Fig. 3.3a). However, for longitudinal dispersivity equal to 1/3rd of domain length, the time corresponding to peak concentration is observed to be ~ 550 s (Fig. 3.3b). It shows that the time to reach the peak concentration value and breakthrough time for $\alpha_L = \frac{L}{10}$ are higher than $\alpha_L = \frac{L}{3}$. Thus, it can be stated that with an increase in α_L, the effective dispersion coefficient increases, which causes the early breakthrough time. Overall, it can be observed that the longitudinal dispersivity affects the shape of BTC for higher

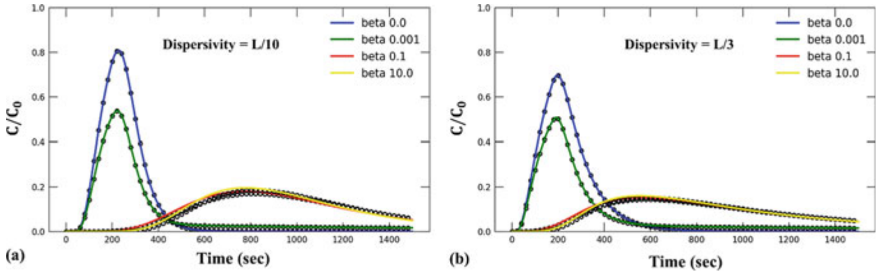

Fig. 3.3 BTC predicted at 16 cm down-gradient distances for **a** dispersivity = 1/10 of domain length and **b** dispersivity = 1/3 of domain length

values of non-equilibrium sorption exchange rate; thus, it needs to be taken care of when modeling the reactive transport behavior even for soil column conditions.

3.3.2 Analyzing the Contaminant Plume Evolution Dynamics for the Homogeneous and Heterogeneous Porous Systems Using 2-D Vertical Transport Model

Sudicky (1989) considered the synthetic field-scale problem to understand contaminant plume dynamics and one of the first problems in which a heterogeneous hydraulic conductivity field was assumed. A highly irregular flow field and a large variation in the longitudinal and transverse dispersivity were considered for testing the simulation capability of flow and transport code to solve real-world problems. By taking motivation from the study by Sudicky (1989), we have studied contaminant transport behavior for the homogeneous, simple layered, and heterogeneous porous system by implementing MT3D-USGS and MODFLOW 6 models in the FloPy environment (Bakker et al. 2016, 2018). Firstly, the impacts of flow and transport parameters such as longitudinal dispersivity, recharge rate, and vertical transverse dispersivity are studied for the homogeneous sand aquifer and simplistic layered porous systems. Then, contaminant plume evolution in various saturated porous systems is compared. Simulation capabilities of MT3D-USGS and MODFLOW 6 to model transport behavior in the layered and heterogeneous porous system are compared too.

A model domain of 250 m in width and 6.75 m on the left side was divided into 27 layers (Fig. 3.4). A steady-state flow in an unconfined aquifer was assumed to model the water table under the impact of recharge. The hydraulic conductivity in both the x- and z-directions was assumed to be equal for any porous media. The contaminant source was assumed to be present at the water table for the first five years of the simulation, and then, a source was removed, and plume evolution was studied for up to 20 years. An initial concentration equal to 0.0 was assumed throughout the domain. The detailed description of flow and transport parameters is shown in

Table 3.2. The XT3D solver was enabled in MODFLOW 6 to compare the simulations from MT3D-USGS and MODFLOW 6 (Bedekar et al. 2016; Hughes et al. 2017; Langevin et al. 2017; Provost et al. 2017).

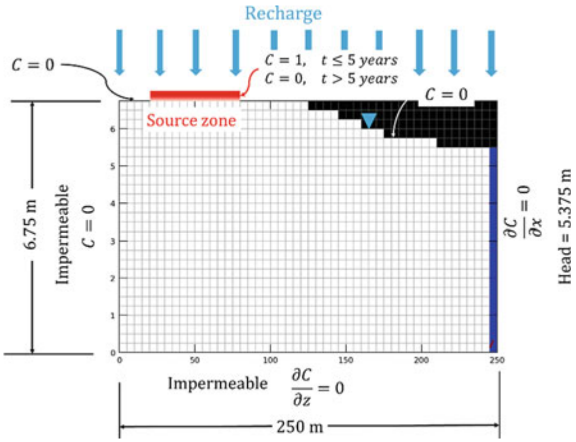

Fig. 3.4 Schematic of model domain used in the study [based on Zheng and Wang (1999)]

Table 3.2 Input parameters used for 2-D vertical transport base case

S. No.	Parameter	Value
1	Width	250 m
2	Depth	6.75 m (left)
3	Grid spacing in x-direction (horizontal)	$\Delta x = 5$ m
4	Grid spacing in z-direction (vertical)	$\Delta z = 0.25$ m
5	Applied recharge rate	10 cm/year (base case)
6	Pulse duration	5 year
7	Total simulation time	20 year
8	Longitudinal dispersivity	0.5 m
9	Traverse vertical dispersivity	0.005 m
10	Porosity	0.32
11	Bulk density	1587 kg/m^3 (1.587 gm/cm^3)
12	Conc. of source fluid	1.0 (unitless)
13	Distribution coefficient	0 m^3/kg (0 cm^3/gm)
14	Hydraulic conductivity (sand)	1.157E−5 m/s (1 m/day)
15	Hydraulic conductivity (clay or low permeability porous media, LPPM)	1.157E−8 m/s (0.001 m/day)
16	Molecular diffusion coefficient	1.34E−9 m^2/s (1.34 × 10^{-5} cm^2/s)

3.3.2.1 Effect of Longitudinal Dispersivity

Figure 3.5 shows the contaminant plume evolution in the homogeneous porous system after 5 and 15 years for different values of longitudinal dispersivity (α_L). Longitudinal dispersivity (α_L) is varied from 0.50 m to 50 m as shown in Fig. 3.5a, c, and e. Contaminant plume front was observed at ~ 100 m in the x-direction and ~2.5 m in the z-direction) away from source zone for $\alpha_L = 0.50$ m in 5th year (Fig. 3.5a), whereas for $\alpha_L = 50$ m, the plume front stretched along the x-direction and was observed near 200 m in the x-direction and ~5 m in the z-direction away from source zone (Fig. 3.5e). The maximum value of C/C_0 equal to 1 is observed near the water table in the source zone in 5th year. However, after source removal, the maximum value of C/C_0 decreases significantly, as observed at 15th-year time level. The contaminant plume shape varied significantly for different values of longitudinal dispersivity, as seen in Fig. 3.5b, d, and f. The peak concentration value of 0.50 is observed for $\alpha_L = 0.50$ m after 15 years in comparison with 0.15 value observed for $\alpha_L = 50$ m, indicating the effect of longitudinal dispersivity on the magnitude and shape of the contaminant plume.

Figure 3.6 shows the contaminant plume dynamics for a simplistic layered porous system in which one layer is kept with a hydraulic conductivity of 1.0 m/day while hydraulic conductivity of another layer is kept at 10^{-3} m/day. It is observed that the contaminant plume shape remains approximately the same for the homogeneous and layered porous system for $\alpha_L = 0.50$ m in 5th year (Figs. 3.5a and 3.6a). For $\alpha_L = 5$ m, the distribution of contaminant plume varied significantly when the plume front entered the LPPM zone. In the LPPM zone, the contour line of contaminant plume becomes perpendicular to bedding plane, indicating the dominance of transverse dispersion over other transport processes. More prominently, the impact of molecular diffusion on plume evolution is observed in the LPPM zone for all the

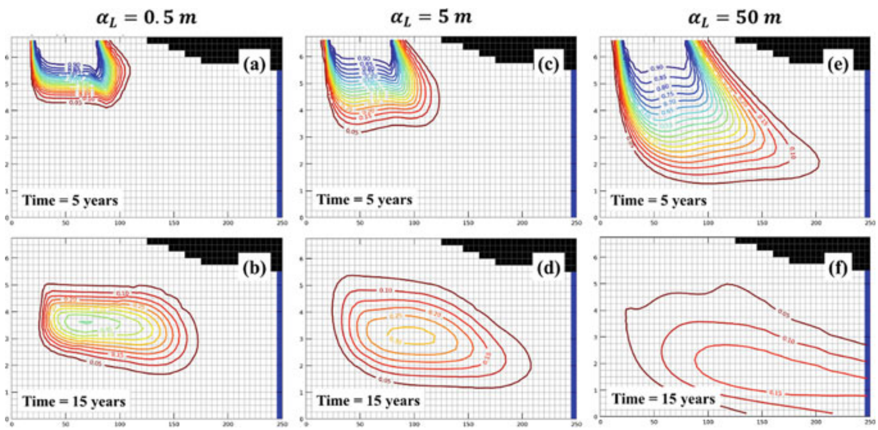

Fig. 3.5 Contaminant plume evolution in the homogeneous porous system for different longitudinal dispersivity values **a, b** $\alpha_L = 0.50$ m, **c, d** $\alpha_L = 5$ m, and **e, f** $\alpha_L = 50$ m

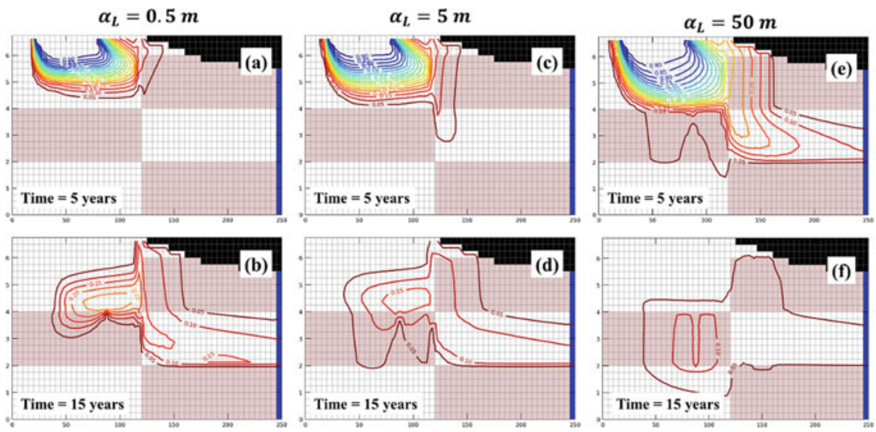

Fig. 3.6 Contaminant plume evolution in the layered porous system for different longitudinal dispersivity values **a, b** $\alpha_L = 0.50$ m, **c, d** $\alpha_L = 5$ m, and **e, f** $\alpha_L = 50$ m

values of longitudinal dispersivity. After source removal, in the 15th year, it is seen that the contaminant transport in the high hydraulic conductivity zone is governed by advection and mechanical dispersion, while contaminant transport in the LPPM zone is dominated by diffusion in the transverse direction. A decrease in the peak concentration value is observed with an increase in longitudinal dispersivity from $\alpha_L = 0.50$ m to $\alpha_L = 50$ m (Fig. 3.6b–f).

3.3.2.2 Effect of Recharge Rate

Recharge rate is one of the important parameters governing the dilution of contaminant plume. In this sub-section, the effects of three different values of recharge rates, viz. 10, 20 and 50 cm/year, on the contaminant transport behavior are analyzed in the presence and absence of contaminant source. The contaminant plume front in 5th year is observed at 120 m from left side of numerical domain for a 10 cm/year recharge rate (Fig. 3.7a), while for a 20 cm/year recharge rate, the plume front with 0.05 concentration contour line reaches at ~140 m distance after five years. For 50 cm/year of recharge rate, the plume front reaches 250 m distance in 5th year, showing an increase in migration rate of contaminant plume with an increase in recharge rate from 10 cm/year to 50 cm/year for a homogeneous porous system (Fig. 3.7c). After the source removal, the shape of contaminant plume is observed as different for different recharge rates. The contaminant plume in 10th year stretches from 25 to 125 m distance in the longitudinal direction for a 10 cm/year recharge rate; however, for a 20 cm/year recharge rate, the contaminant plume stretches from 25 to 225 m in the x-direction. A significant difference in the contaminant plume distribution is observed at 15th-year time level for different values of recharge rate. The peak concentration contour line of 0.50 is observed for a 10 cm/year recharge

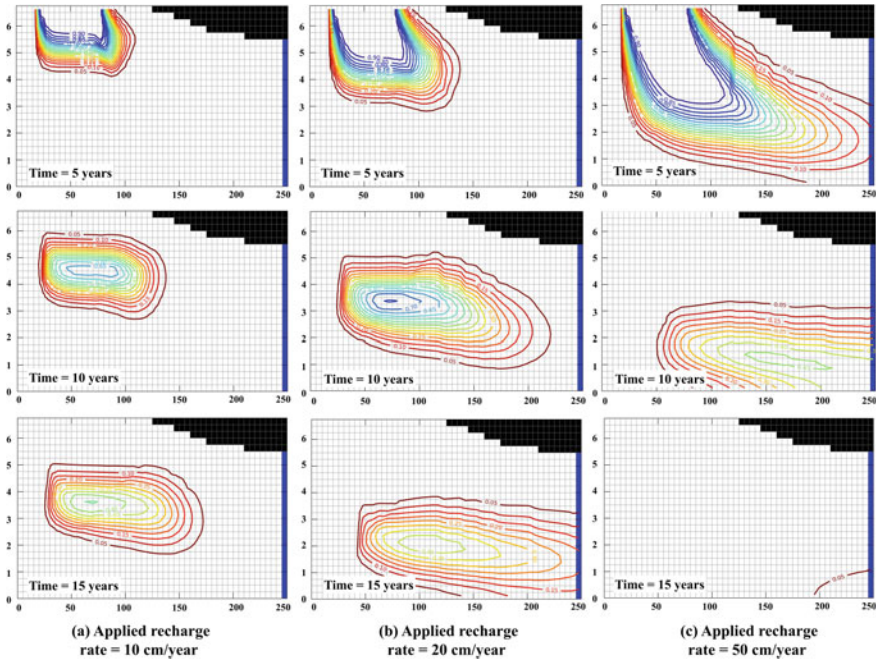

Fig. 3.7 Comparison of contaminant plume evolution with different recharge rates in the homogeneous porous system (MODFLOW 6)

rate, while for a 20 cm/year recharge rate, the peak contour line drops to 0.40, and plume moves to the right-bottom side of the domain. At 50 cm/year recharge rate, the contour line of 0.05 is observed at a right-bottom corner portion of the numerical domain depicting the complete dilution of contaminant plume at 15th year for 50 cm/year recharge rate. It is observed from Fig. 3.7 that the center of mass of plume moves diagonally, and dilution of contaminant plume becomes faster with an increase in applied recharge rate.

Figure 3.8 represents the contaminant plume evolution in the simplistic layered porous system for different values of applied recharge rates. The contaminant plume front at 5th year is observed at 140 m distance from left side of numerical domain for 10 cm/year recharge rate; however, for 20 cm/year recharge rate, the contaminant plume with 0.05 contour line is observed at 215 m. Similarly, highly non-uniform contaminant distribution is observed for a recharge rate of 50 cm/year in 5th year. It is interesting to see that the contaminant contour line becomes perpendicular to LPPM bedding plane at upper one-third portion of a numerical domain and then stretches along the x-direction when enters the aquifer region. The dominance of advection and dispersion processes increases with an increase in the applied recharge rate. However, in the LPPM zone, the impact of recharge rate is not as prominent as in the sand layer. It is observed that the contaminant plume distribution varied significantly for different recharge rates in 10th and 15th years during source unloading period.

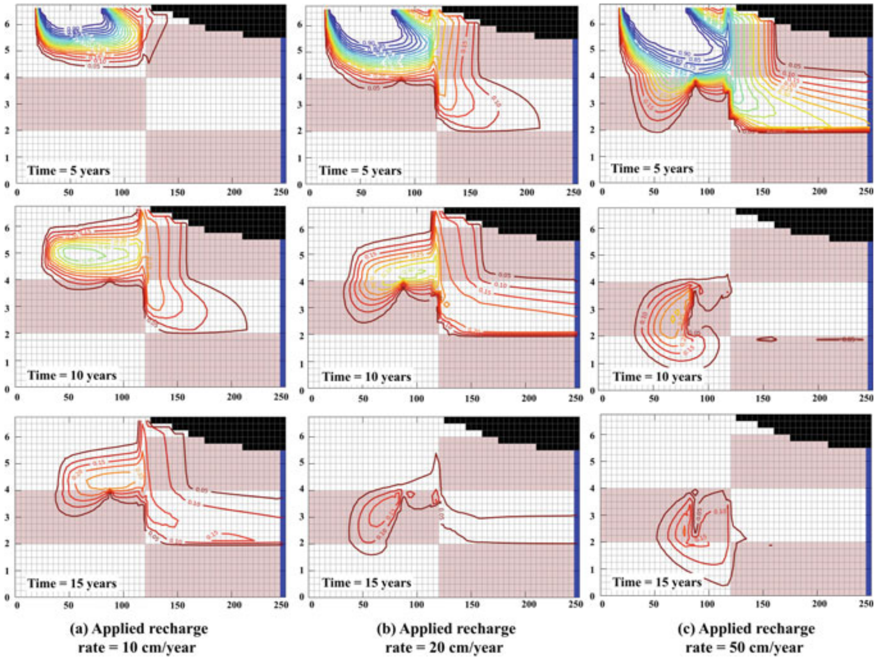

Fig. 3.8 Comparison of contaminant plume dynamics in the layered porous system with different recharge rates (MODFLOW 6)

The peak concentration contour line of 0.15 is observed in the LPPM regions for 20 and 50 cm/year recharge rates, whereas a negligible concentration value is observed in the sand (aquifer) layer. This shows the impact of back-diffusion at later transport times at higher recharge rates, which highlighted the significance of LPPM on contaminant distribution in the adjoining aquifer regions. Also, a significant difference in the plume evolution dynamics is observed for homogeneous and simplistic layered porous systems (Figs. 3.7 and 3.8).

3.3.2.3 Effect of Vertical Transverse Dispersivity

Figure 3.9 shows the contaminant plume evolution in the simplistic layered porous system for different values of α_{TV}/α_L, representing the impact of vertical transverse dispersivity on contaminant transport. The contaminant plume front representing 0.05 contour line reaches ~4.25 m from bottom of the numerical domain for $\frac{\alpha_{TV}}{\alpha_L} = 0.01$ in 5th year; however, for $\frac{\alpha_{TV}}{\alpha_L} = 0.10$, the plume front reaches at 3.5 m level. Thus, it can be stated that the spreading of contaminant plume along a vertical direction increases with an increase in α_{TV}/α_L ratio. After the source removal, the impact of diffusive process on the contaminant distribution in the LPPM zone is seen at 10th year (Fig. 3.9b) and 15th-year time level (Fig. 3.9c). For $\frac{\alpha_{TV}}{\alpha_L} = 0.01$, the effective hydrodynamic dispersion term in the transverse direction is dominated equally by molecular diffusion and mechanical dispersion term. The peak contour level of 0.45 is observed for $\frac{\alpha_{TV}}{\alpha_L} = 0.01$ in 10th year (Fig. 3.9b), while for $\frac{\alpha_{TV}}{\alpha_L} = 0.1$ ratio, the peak contour level drops to 0.25, showing the dilution of contaminant concentration at higher values of transverse dispersivity (Fig. 3.9e).

For $\frac{\alpha_{TV}}{\alpha_L} = 0.1$, the effective hydrodynamic dispersion term in the transverse direction is dominated by mechanical dispersion term. Also, it is observed that when contaminant plume front enters the LPPM zone at 10th year for $\frac{\alpha_{TV}}{\alpha_L} = 0.1$ value, then plume does not spread along the longitudinal direction, instead enters directly into LPPM zone (Fig. 3.9e). At the 15th-year time level, the peak concentration contour line of 0.25 is observed for $\frac{\alpha_{TV}}{\alpha_L} = 0.01$ with contour intervals at close distances;

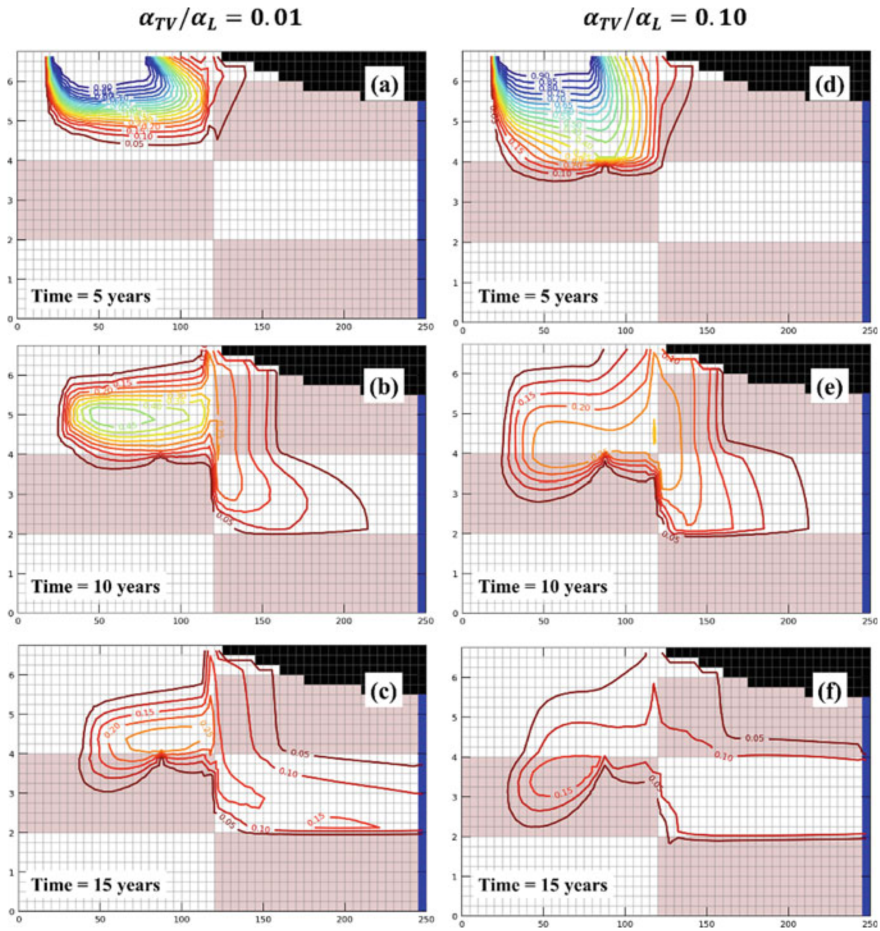

Fig. 3.9 Contaminant plume evolution in the layered porous system for the different ratio of transverse to longitudinal dispersivity **a**, **b**, and **c** $\frac{\alpha_{TV}}{\alpha_L} = 0.01$ and **d**, **e**, and **f** $\frac{\alpha_{TV}}{\alpha_L} = 0.10$

however, for $\frac{\alpha_{TV}}{\alpha_L} = 0.1$, the peak contour value drops to 0.15. It indicates that lumping of dispersion terms at higher values of vertical transverse dispersivity and plume evolution is dominated by advection and mechanical dispersion processes, which further lead to a decrease in the magnitude of contaminant concentration with an increase in α_{TV}/α_L ratio (Fig. 3.9f). Interestingly, the peak concentration contour is observed in the LPPM region, and very low concentration values are observed in the adjoining aquifer region, depicting the effect of back-diffusion from LPPM at very late transport times.

3.3.2.4 Comparison of Simulation Capabilities of MT3D-USGS and MODFLOW 6

In this sub-section, the impact of mathematical modeling choice on predicting contaminant concentration in the aquifer-aquitard system with LPPM is studied. The contaminant plume predicted via MT3D-USGS model for 5th, 10th, and 15th-year time level is shown in Fig. 3.10a, c, and e, while contaminant plume prediction using MODFLOW 6 in 5th, 10th, and 15th years is shown in Fig. 3.10b, d and f. It is observed that, during source loading period (at 5th year), the contaminant plume predicted by both the models is approximately the same (Fig. 3.10a and b). It may be due to the dominance of source concentration over GW flow and transport processes during early transport time. However, after the source isolation/removal, a significant difference in the contaminant plume distribution is observed in the 10th year and 15th year. The shape of contaminant plume lumps out when predicted via MT3D-USGS, while the MODFLOW 6 considers the GW flow and transport mechanisms at the microscale. It is observed that the contaminant plume shape predicted for 10th year (Fig. 3.10d) and 15th year (Fig. 3.10f) using MODFLOW 6 is highly asymmetrical, indicating that the GW flow and transport processes through LPPM are considered in the model. In contrast, MT3D-USGS lumps out the GW flow and transport processes through LPPM. The difference in the contaminant plume shape via different modeling frameworks highlights the impact of modeling choice. Based on the results highlighted above, it can be stated that MODFLOW 6-based modeling framework mimics the realistic contaminant transport scenario effectively as compared to MT3D-USGS model in FloPy.

3.3.2.5 Comparison of Contaminant Plume Evolution Dynamics for Homogeneous and Heterogeneous Porous Systems

Asymmetrical contaminant transport behavior is observed for a porous system comprising contrasting hydraulic conductivity regions, specifically after source removal/isolation. Based on observations obtained in previous simulations, in this sub-section, contaminant plume evolution is analyzed for different arrangements of saturated porous systems. Figure 3.11 shows the contaminant plume in 10th year for different types of saturated porous systems, viz. aquifer, aquifer with LPPM,

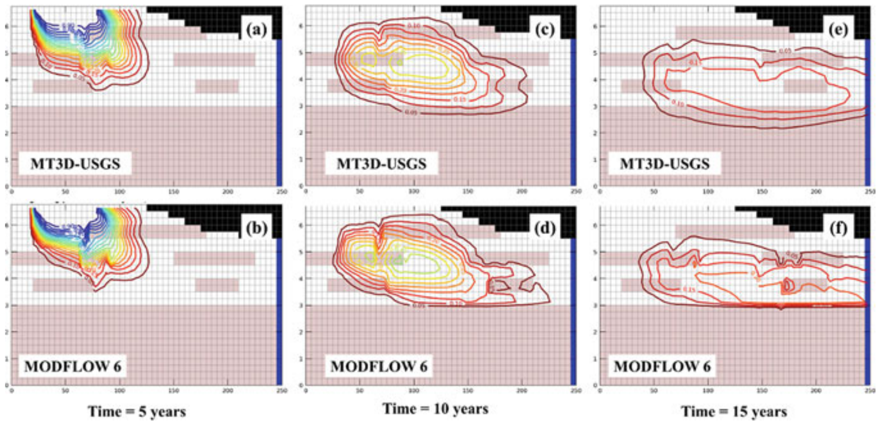

Fig. 3.10 Comparison of contaminant plume distribution in the aquifer-aquitard system with LPPM zone simulated via **a**, **c**, and **e** MT3D-USGS, and **b**, **d**, and **f** MODFLOW 6 models in FloPy environment

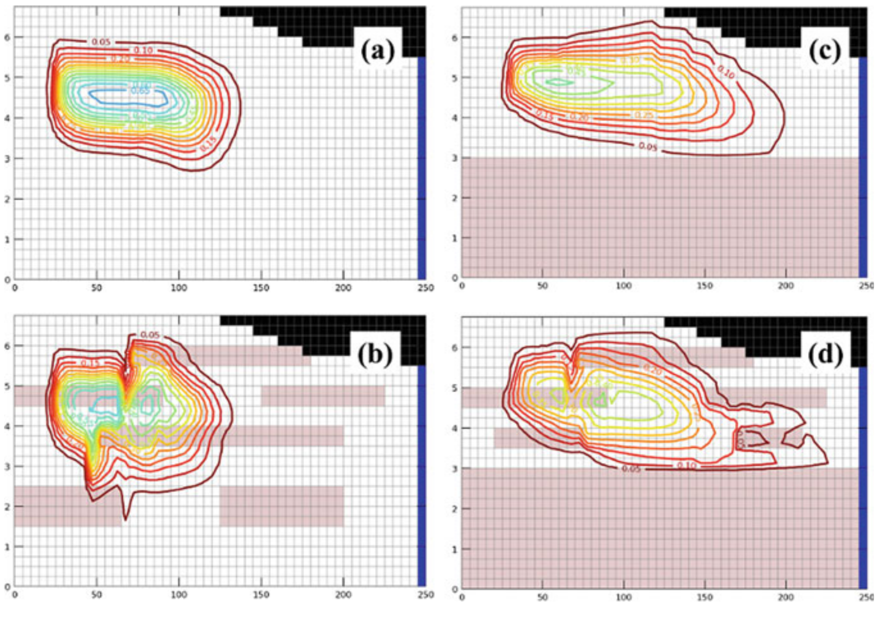

Fig. 3.11 Contaminant plume distribution after 10 years (source removal) in different types of porous system **a** aquifer, **b** aquifer with LPPM, **c** aquifer-aquitard, and **d** aquifer-aquitard with LPPM

aquifer-aquitard, and aquifer-aquitard with LPPM. The uniform distribution with a peak concentration contour of 0.65 is observed for aquifer-type porous systems (Fig. 3.11a). It is observed that the plume stretches along *x*-direction dominantly for aquifer system; however, for aquifer with LPPM, the plume stretches asymmetrically along *x*- and *z*-direction equally (Fig. 3.11b). Even the dominating effect of molecular diffusion and, subsequently, transverse dispersion on plume movement is seen for aquifers with LPPM, which is undermined in the case of homogeneous aquifer system. In the case of aquifer-aquitard system, the contaminant plume behaves same as aquifer system until the plume front reaches the aquitard layer. As plume front reaches the aquitard region, the contaminant plume gets elongated along the *x*-direction, showing that the aquitard layer does not allow the contaminant to penetrate, which might be due to very low flow velocities in aquitard layer (Fig. 3.11c). In the case of an aquifer-aquitard system with LPPM, a highly asymmetrical contaminant plume distribution is observed in the 10th year. The peak concentration contour level of 0.45 is observed, showing a decrease in contaminant movement in the aquifer-aquitard system with LPPM as compared to homogeneous aquifer system. The influence of molecular diffusion in the LPPM region is observed, while advective and dispersive fluxes dominate the contaminant transport in the high hydraulic conductivity (aquifer) region (Fig. 3.11d).

Figure 3.12 shows the contaminant plume in 15th year for different types of saturated porous systems. The overall transport behavior for various types of porous systems in 15th year is same as in the 10th year. The peak value of concentration decreases with an increase in time, which represents the dilution of concentration by dispersion processes. For aquifer-aquitard system, the peak concentration contour level of 0.25 is observed with contaminant plume stretched along the *x*-direction dominantly in comparison with *z*-direction after 15 years (Fig. 3.11c). The concentration contour level is observed as parallel to the aquitard layer and does not allow contaminant to penetrate. The zones of higher values of contaminant concentrations are observed in the high hydraulic conductivity regions even after ten years of source isolation/removal; however, small patches of high concentration values are observed in the LPPM regions. It shows that the LPPM regions act as a contaminant source at later transport times (Fig. 3.12b and d).

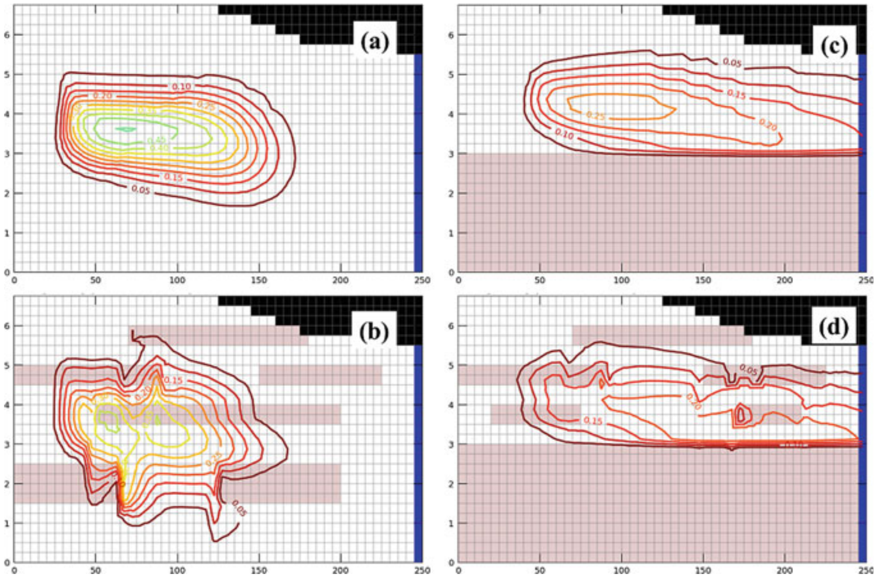

Fig. 3.12 Contaminant plume distribution after 15 years (source removal) in different types of porous system **a** aquifer, **b** aquifer with LPPM, **c** aquifer-aquitard, and **d** aquifer-aquitard with LPPM

3.4 Conclusion

This chapter presents the modeling of contaminant transport via 1-D non-linear and non-equilibrium sorption models. Secondly, a comparison of transport behavior for homogeneous and heterogeneous porous systems is presented, along with the sensitivity of model parameters. Finally, the simulation capabilities of MT3D-USGS and MODFLOW 6 models to simulate the contaminant transport behavior in various types of porous systems (i.e., aquifer, aquifer with LPPM, aquifer-aquitard, and aquifer-aquitard with LPPM) are highlighted. The results from non-equilibrium sorption model indicate that the concentration at a down-gradient location for soil column conditions decreases with an increase in sorption mass exchange rate, indicating it as dominating parameter of non-equilibrium reactive transport model. A significant impact of longitudinal dispersivity on the shape of BTC is seen for higher values of non-equilibrium sorption exchange rate. The results from 2-D vertical transport modeling depict the impact of LPPM on contaminant plume evolution. The dominance of molecular diffusion and, subsequently, transverse dispersion on contaminant transport behavior through LPPM is observed. At the same time, advection and mechanical dispersion processes are observed to be governing the transport behavior in the high hydraulic conductivity (aquifer) zone. Also, it is observed that the MODFLOW 6 considers the microscale processes through LPPM, whereas MT3D-USGS ignored these processes and lumped them into macro dispersion coefficient while modeling transport behavior in LPPM regions. The simulations depict the LPPM regions as source terms at later transport times after source isolation/removal and sink terms during the loading period. However, this chapter is limited to dissolved species transport problems in the saturated porous system. Flow and transport modeling of nonaqueous phase liquids (LNAPLs and DNAPLs) in unsaturated porous media can be conducted in FloPy environment to give a broader aspect to the applications of Python scripting-based package.

References

Bakker M, Post V, Langevin CD et al (2016) Scripting MODFLOW model development using python and FloPy. Groundwater 54:733–739. https://doi.org/10.1111/gwat.12413

Bakker M, White JT, Langevin CD, et al (2018) FloPy v3.2.9: U.S. geological survey software release. pp 12

Ballarini E, Bauer S, Eberhardt C, Beyer C (2014) Evaluation of the role of heterogeneities on transverse mixing in bench-scale tank experiments by numerical modeling. Groundwater 52:368–377. https://doi.org/10.1111/gwat.12066

Bedekar V, Morway E, Langevin C, Tonkin M (2016) MT3D-USGS version 1: A U.S. geological survey release of MT3DMS updated with new and expanded transport capabilities for use with MODFLOW

Borah T, Bhattacharjya RK (2015) Development of unknown pollution source identification models using GMS ANN–based simulation optimization methodology. J Hazardous, Toxic, Radioact Waste 19:04014034. https://doi.org/10.1061/(ASCE)HZ.2153-5515.0000242

Brown GH, Brooks MC, Wood AL et al (2012) Aquitard contaminant storage and flux resulting from dense nonaqueous phase liquid source zone dissolution and remediation. Water Resour Res 48:1–17. https://doi.org/10.1029/2011WR011141

Brusseau ML, Russo AE, Schnaar G (2012) Nonideal transport of contaminants in heterogeneous porous media: 9—impact of contact time on desorption and elution tailing. Chemosphere 89:287–292. https://doi.org/10.1016/j.chemosphere.2012.04.038

Carey GR, Chapman SW, Parker BL, McGregor R (2015) Application of an adapted version of MT3DMS for modeling back-diffusion remediation timeframes. Remediat J 25:55–79. https://doi.org/10.1002/rem.21440

Chapman SW, Parker BL (2005) Plume persistence due to aquitard back diffusion following dense nonaqueous phase liquid source removal or isolation. Water Resour Res 41:1–16. https://doi.org/10.1029/2005WR004224

Comunian A, Giudici M (2021) Improving the robustness of the comparison model method for the identification of hydraulic transmissivities. Comput Geosci 149:104705. https://doi.org/10.1016/j.cageo.2021.104705

Elshall AS, Ye M, Finkel M (2020) Evaluating two multi-model simulation–optimization approaches for managing groundwater contaminant plumes. J Hydrol 590:125427. https://doi.org/10.1016/j.jhydrol.2020.125427

Gao G, Feng S, Zhan H et al (2009) Evaluation of anomalous solute transport in a large heterogeneous soil column with mobile-immobile model. J Hydrol Eng 14:966–974. https://doi.org/10.1061/(ASCE)HE.1943-5584.0000071

Gao G, Zhan H, Feng S et al (2010) A new mobile-immobile model for reactive solute transport with scale-dependent dispersion. Water Resour Res 46:1–16. https://doi.org/10.1029/2009WR008707

Guleria A, Chakma S (2022) Mathematical modeling of contaminant transport in the subsurface environment. In: Gupta PK, Yadav B, Himanshu S (eds) Advances in remediation techniques for polluted soils and groundwater. Elsevier, First, pp 141–169

Guleria A, Swami D, Joshi N, Sharma A (2020) Application of temporal moments to interpret solute transport with time-dependent dispersion. Sādhanā 45:159. https://doi.org/10.1007/s12046-020-01402-5

Guleria A, Swami D, Sharma A, Sharma S (2019) Non-reactive solute transport modelling with time-dependent dispersion through stratified porous media. Sādhanā 44:81. https://doi.org/10.1007/s12046-019-1056-6

Guo Z, Brusseau ML (2017a) The impact of well-field configuration and permeability heterogeneity on contaminant mass removal and plume persistence. J Hazard Mater 333:109–115. https://doi.org/10.1016/j.jhazmat.2017.03.012

Guo Z, Brusseau ML (2017b) The impact of well-field configuration on contaminant mass removal and plume persistence for homogeneous versus layered systems. Hydrol Process 31:4748–4756. https://doi.org/10.1002/hyp.11393

Guo Z, Brusseau ML, Fogg GE (2019) Determining the long-term operational performance of pump and treat and the possibility of closure for a large TCE plume. J Hazard Mater 365:796–803. https://doi.org/10.1016/j.jhazmat.2018.11.057

Hughes JD, Langevin CD, Banta E (2017) Documentation for the MODFLOW 6 framework

Kheirabadi M (2018) Groundwater model parameter estimation with simultaneous and sequential use of hydraulic head and travel time measurements

Langevin CD, Hughes JD, Banta ER, et al (2017) Documentation for The MODFLOW 6 groundwater flow model

Leichombam S, Bhattacharjya RK (2019) New hybrid optimization methodology to identify pollution sources considering the source locations and source flux as unknown. J Hazardous, Toxic, Radioact Waste 23:04018037. https://doi.org/10.1061/(ASCE)HZ.2153-5515.0000431

Mescher L (2018) Evaluating the applicability of MODFLOW2005 plus MT3D-USGS: Borden Case Study

Morway ED, Langevin CD, Hughes JD (2021) Use of the MODFLOW 6 water mover package to represent natural and managed hydrologic connections. Groundwater 59:913–924. https://doi.org/10.1111/gwat.13117

Müller S, Schüler L (2019) GeoStat-Framework/GSTools: Reverberating Red v1.1.0

Provost AM, Langevin CD, Hughes JD (2017) Documentation for the " XT3D " option in the node property flow (NPF) package of MODFLOW 6

Rao GT, Rao VVSG, Ranganathan K et al (2011) Assessment of groundwater contamination from a hazardous dump site in Ranipet, Tamil Nadu, India. Hydrogeol J 19:1587–1598. https://doi.org/10.1007/s10040-011-0771-9

Rao GT, Rao VVSG, Surinaidu L et al (2013) Application of numerical modeling for groundwater flow and contaminant transport analysis in the basaltic terrain, Bagalkot, India. Arab J Geosci 6:1819–1833. https://doi.org/10.1007/s12517-011-0461-x

Rasa E, Chapman SW, Bekins BA et al (2011) Role of back diffusion and biodegradation reactions in sustaining an MTBE/TBA plume in alluvial media. J Contam Hydrol 126:235–247. https://doi.org/10.1016/j.jconhyd.2011.08.006

Rezaei A, Zare M, Zhan H (2016) Aquitard horizontal dispersion on reactive solute transport in an aquifer-aquitard system. Transp Porous Media 113:695–716. https://doi.org/10.1007/s11242-016-0719-6

Sathe SS, Mahanta C (2019) Groundwater flow and arsenic contamination transport modeling for a multi aquifer terrain: assessment and mitigation strategies. J Environ Manage 231:166–181. https://doi.org/10.1016/j.jenvman.2018.08.057

Sbai MA (2020) Unstructured gridding for MODFLOW from prior groundwater flow models: a new paradigm. Groundwater 58:gwat.13025. https://doi.org/10.1111/gwat.13025

Sharma PK, Shukla SK, Choudhary R, Swami D (2016) Modeling for solute transport in mobile–immobile soil column experiment. ISH J Hydraul Eng 22:204–211. https://doi.org/10.1080/09715010.2016.1155181
Singh P, Singh RM (2019) Identification of pollution sources using artificial neural network (ANN) and multilevel breakthrough curve (BTC) characterization. Environ Forensics 20:219–227. https://doi.org/10.1080/15275922.2019.1629548
Singh RM, Datta B (2007) Artificial neural network modeling for identification of unknown pollution sources in groundwater with partially missing concentration observation data. Water Resour Manag 21:557–572. https://doi.org/10.1007/s11269-006-9029-z
Singh RM, Datta B (2006) Identification of groundwater pollution sources using GA-based linked simulation optimization model. J Hydrol Eng 11:101–109. https://doi.org/10.1061/(ASCE)1084-0699(2006)11:2(101)
Singh RM, Datta B, Jain A (2004) Identification of unknown groundwater pollution sources using artificial neural networks. J Water Resour Plan Manag 130:506–514. https://doi.org/10.1061/(ASCE)0733-9496(2004)130:6(506)
Sudicky EA (1989) The Laplace Transform Galerkin Technique: a time-continuous finite element theory and application to mass transport in groundwater. Water Resour Res 25:1833–1846. https://doi.org/10.1029/WR025i008p01833
Swami D, Sharma PK, Ojha CSP et al (2018) Asymptotic behavior of mass transfer for solute transport through stratified porous medium. Transp Porous Media 124:699–721. https://doi.org/10.1007/s11242-018-1090-6
Swami D, Sharma PK, Ojha CSP (2016) Behavioral study of the mass transfer coefficient of nonreactive solute with velocity, distance, and dispersion. J Environ Eng 143:1–10. https://doi.org/10.1061/(ASCE)EE.1943-7870.0001164
Vetrimurugan E, Senthilkumar M, Elango L (2017) Solute transport modelling for assessing the duration of river flow to improve the groundwater quality in an intensively irrigated deltaic region. Int J Environ Sci Technol 14:1055–1070. https://doi.org/10.1007/s13762-016-1211-0
White JT, Hemmings B, Fienen MN, Knowling MJ (2021) Towards improved environmental modeling outcomes: enabling low-cost access to high-dimensional, geostatistical-based decision-support analyses. Environ Model Softw 139:105022. https://doi.org/10.1016/j.envsoft.2021.105022
Winston RB (2009) ModelMuse: a graphical user interface for MODFLOW-2005 and PHAST: U.S. geological survey techniques and methods 6–A29. US Geological Survey Reston, VA
Yang M, Annable MD, Jawitz JW (2017a) Forward and back diffusion through argillaceous formations. Water Resour Res 53:4514–4523. https://doi.org/10.1002/2016WR019874
Yang M, Annable MD, Jawitz JW (2017b) Field-scale forward and back diffusion through low-permeability zones. J Contam Hydrol 202:47–58. https://doi.org/10.1016/j.jconhyd.2017.05.001
Yang M, Annable MD, Jawitz JW (2015) Back diffusion from thin low permeability zones. Environ Sci Technol 49:415–422. https://doi.org/10.1021/es5045634
Yang M, McCurley KL, Annable MD, Jawitz JW (2019) Diffusion of solutes from depleting sources into and out of finite low-permeability zones. J Contam Hydrol 221:127–134. https://doi.org/10.1016/j.jconhyd.2019.01.005
Zhan H (1998) Transport of waste leakage in stratified formations. Adv Water Resour 22:159–168. https://doi.org/10.1016/S0309-1708(98)00001-3
Zhan H, Wen Z, Gao G (2009) An analytical solution of two-dimensional reactive solute transport in an aquifer-aquitard system. Water Resour Res 45:1–8. https://doi.org/10.1029/2008WR007479
Zheng C, Bianchi M, Gorelick SM (2011) Lessons learned from 25 years of research at the MADE site. Ground Water 49:649–662. https://doi.org/10.1111/j.1745-6584.2010.00753.x
Zheng C, Wang PP (1999) MT3DMS: a modular three-dimensional multispecies transport model for simulation of advection, dispersion, and chemical reactions of contaminants in groundwater systems

Chapter 4
Site Suitability Analysis for Identification of Riverbank Filtration (RBF) Sites: Case Study of the Alaknanda River Basin

Epari Ritesh Patro, Pooran Singh Patwal, and Mallappa Madolli

Abstract Demographic and geographic locations of various towns in the study area having proximity to the river like Alaknanda along with its tributaries Mandakini and Pindar make them suitable target locations to get the complications of water shortages. The rivers are malevolent when it comes to supply of water in balance in the times of crucial need as these rivers are basically glacier-fed rivers and their discharge varies with seasonal changes. Due to seasonal variation, only limited direct water abstraction is possible and it results into shortage of water for supply. The potential locations of alluvial deposits were identified by generating thematic GIS maps of land use, terrain, and geology, using a weightage factor. The sites thus identified were characterized using groundwater flow modeling for their optimal abstraction rate, travel time, and flow field of the induced bank filtrate. The purification capacity of the aquifer was estimated for the removal of organic micro-pollutants (OMP) using the SOMA tool and was correlated with the river meandering sinuosity (S). Along the 100 km river stretch, 8–9 locations were found suitable for indirect surface water abstraction. An S-value of around 1.4 resulted in the highest purification capacity and a bank filtrate portion of 44–100% in the abstracted water from 14 wells located 75 m from the riverbank under the defined conditions. The calculated removal of different OMP was 26–91%. Based on this study, potential riverbank filtration (RBF) sites were identified in seven large towns and cities Rishikesh, Ramnager, Haridwar, Dehradun, Roorkee, Kotdwar, and Haldwani having a total population of 1.23 million situated in the flood plains in the Himalayan area.

Keywords Himalaya · Riverbank filtration · Water quality · Groundwater · Modeling

---

E. R. Patro (✉)
Water, Energy and Environmental Engineering Research Unit, Faculty of Technology, University of Oulu, 90014 Oulu, Finland
e-mail: ritesh.patro@oulu.fi

P. S. Patwal
Independent Consultant (Hydrology and Natural Resource Management), Haridwar, India

M. Madolli
Department of Agricultural Engineering, College of Sericulture, Chintamani, University of Agricultural Sciences, Bengaluru, India

P. Shukla et al. (eds.), *Environmental Processes and Management*, Water Science and Technology Library 120, https://doi.org/10.1007/978-3-031-20208-7_4

Abbreviations

GIS	Geographical information system
SOMA	Switch organic micro-pollutant assessment tool
OMP	Organic micro-pollutants
S	River meandering sinuosity value
RBF	Riverbank filtration
DEM	Digital elevation model
LULC	Land use/land cover
ERDAS	Earth resources data analysis Ssystem
DOC	Dissolved organic carbon
VOC	Volatile organic compound
MLD	Million liters per day

4.1 GIS-Based Site Suitability Analysis

Based on the water quality index analysis of Alaknanda River in the study area from the chapter titled "Water Resource Estimation and Management: Case Study of the Alaknanda River Basin," it is clear that the water quality of the river is not fit for drinking purposes at the time of monsoon and non-monsoon due to presence of high turbidity and high coliform in river water. Also, existing water direct water production system in Srinagar is facing functional and operational problems. So for sustainable drinking water production for study area, we need suitable sites and sustainable technology. Riverbank filtration technology has been used since last decade in the mountain area for sustainable drinking water production. In this technology, the lowering of the water table of unconfined aquifer below the adjoining surface water table causes surface water movement through the permeable riverbed into the unconfined aquifer. This leads to the difference in water levels providing a natural path to this subterranean flow, which provides the raw water for drinking purposes.

But due to limited geology and geographical condition, there are always problems in suitable site selection. For suitable site selection, GIS and remote sensing are used. The selection of suitable location is based on a specific set of criteria and characteristics of the site and its condition, like land use/ land cover pattern of the area, slopes near the riverbank, water availability in the river (it should be Perennial River), development costs, geological condition of the site, and accessibility by roads.

4.1.1 Methodology for Suitable Site Identification

A methodology (Fig. 4.1) is adopted for the identification of the suitable sites for drinking water production and analysis of the purification and filtration capacity of the aquifer capacity of the river through induced river recharge. Following steps are considered as main part of the methodology.

(a) To create and digitize geological map of the area with the help of existing geological information and satellite data. The map will show the lithological and geological condition in the study area.
(b) To develop the drainage network pattern and watershed area map using the digital elevation model (DEM ASTER data, 30 m resolution) as well as a topographical map for carrying out a topographical analysis. The map will give you information about stream sources and its type
(c) To develop the contour map of the study area with the help of DEM 30 m resolution data for analysis of the river level and define the general model boundary of the study area.
(d) To develop the slope map of the study area with the help of DEM 30 data for reclassification of slope categories in different percentage.
(e) To convert all the vector layers in the raster layers and assign them a suitable weightage for selection of the suitable sites in the river stretch.

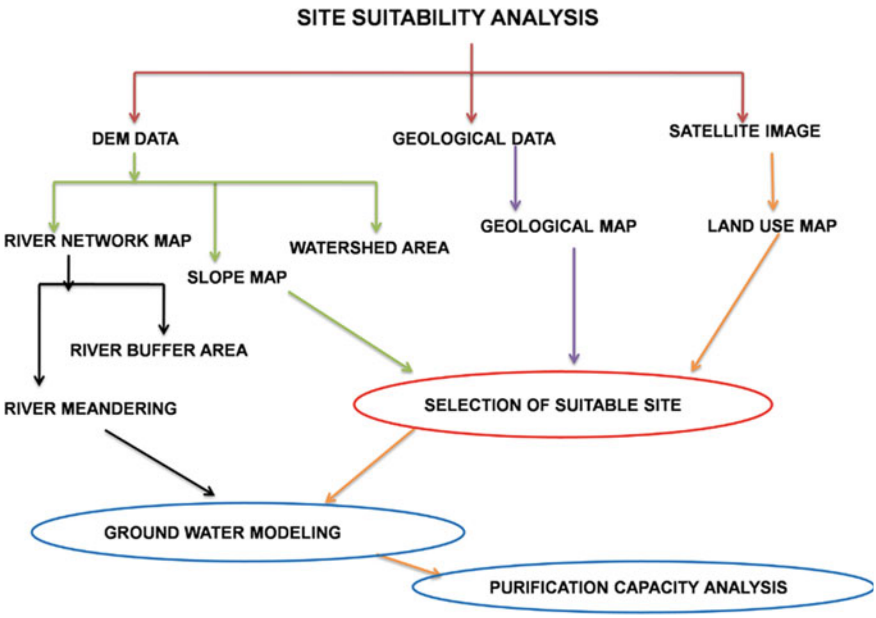

Fig. 4.1 Flow diagram for suitable site identification

(f) To categorize the sites on the basis of their suitability for indirect surface abstraction and river water purification and filtration capacity of aquifer on the basis of suitable slope, suitable geology, and suitable land use requirement in Arc GIS hydrology model.
(g) To identify the river meandering sinuosity of one suitable site which is coming under site suitability maps. This identification will be done with the help of visual identification and GIS domain.
(h) Mark the location of the imaginary wells in the selected site equal distance from the riverbank with equal discharge.
(i) To determine the hydraulic properties of the one suitable site, like travel time, percentage of bank filtration water and particle path of the indirect abstracted river water from alluvial deposits by using ground water flow modeling.
(j) Put all the calculated value of travel time and distance of well from riverbank in the SOMA tool for identification of purification capacity if the aquifer.

4.1.2 Data and Software

The ASTER (Aster Digital Elevation Model) digital elevation model, 30m data, is used for the watershed identification, stream network analysis, and slope identification of the study area. DEM data for the analysis of slope, stream network, and other thesis-related work is downloaded from the USGS website (http://earthexplorer.usgs.gov). Landsat Image is used to generate a classified LULC map. The process of classification is done by with the help of Arc GIS and ERDAS. The prepared LULC map is used in Arc GIS software as a layer for the calculation of the identification of suitable sites. Landsat MSS (Multispectral Scanner) data of the river stretch were downloaded from USGS website (http://earthexplorer.usgs.gov).

Geological information of the river stretch is extracted from the ground water prospects map of Uttarakhand. The map was prepared by the Uttarakhand Space application center under the guidance of the National remote sensing division of the Indian Space Research Organization, Department of Space, Govt of India in 2008 (Ground Water Prospects Map 2008). These maps were generated for the Rajiv Gandhi drinking water mission. The scale of the map was 1: 50,000. Information about the aquifer at the selected site is collected from the Uttarakhand state drinking water department. One well near the river was drilled in 2012; therefore, hydraulic conductivity, aquifer depth, and discharge of the well were collected and used for ground water flow modeling.

Arc GIS 10.2 software was used for DEM preparation, DEM hydro-processing and to prepare watershed, topology creation, slope, stream area network calculation and suitable site identification, etc. This software is also used for the digitization of geological map and converting to map in a form of raster image. The Earth Resources Data Analysis System (**ERDAS**) Imagine has been used for image processing like band composition, pan sharpening, and subset, file format transformation of the datasets, classification, re-projection, re-sampling, and LULC map creation by NDVI and other index calculation. **MODFLOW PMWIN 5** was used for the analysis of the subsurface river water and ground water flow near the riverbank. PMWIN is a groundwater simulation system, which is freely available in the public domain. This software was used for the calculation of subsurface water movement, travel time, water budgeting, and water abstraction capacity of the river aquifer.

The water quality prediction tool, **SOMA**—Switch Organic Micro-Pollutant Assessment Tool, helps to predict the removal performances of bank filtrate water systems for different organic micro-pollutants (OMPs). A simple Microsoft office excel spreadsheet was used for basic estimation of the removal of the different groups of OMPs, volatile organic compounds, and pesticides. The tool made by several excel worksheets that compute the removal of performance in riverbank filtrate water (or estimated range of effluent concentrations under given conditions) based on either a known travel time or production well distance from surface water sources (like river, lake, and infiltration basin). The tool was developed to estimate the preliminary removal of dissolved organic carbon (OMPs) and six selected groups of OMPs.

4.2 General Boundary Defining for Analysis

For the analysis of site suitability, we need some boundary for the preparation of thematic maps. Figure 4.2 shows the total catchment area of the Alaknanda River upstream from Srinagar (end point of study area) which is 10577 km^2. Out of total catchment area, Mandakini River has 1642 km^2, Pindar River has 1897 km^2, and study area has is 718 km^2. Out of 718 km^2 area, 63% area (around 457.95 km^2) is covered by the high mountains, which is not feasible for bank filtration. Only 260.05 km^2 area within the river stretch is selected for site suitability analysis on the basis of horizontal and vertical extend. Three general boundary conditions have been developed for suitable site analysis for riverbank water abstraction.

4.2.1 Defining Horizontal and Vertical Boundary

A buffer of 300 m from both side of riverbank is created and used for horizontal boundary because generally in mountain area floodplains do not extent more than 300 m from the river course (Patro et al. 2020). Horizontal boundary is used for checking the feasibility of the suitable sites. Elevation of 1000 m from upper and lower stretch of the study area is used for vertical boundary. Lower part elevation 510 m and upper part 775 m are noted from the field visit and DEM data. The main reason for selection of 1000 m elevation is from lower stretch; it is 490 m higher than the river surface level at and 225 m higher at upper river surface. In mountain areas, it is not possible to drill more than 200 m due to presence of hard rock. Longitudinal profile of river stretches in Fig. 4.3, which is developed by DEM data, is showing the exact overview of the elevation difference at lower and upper stretch. The overall

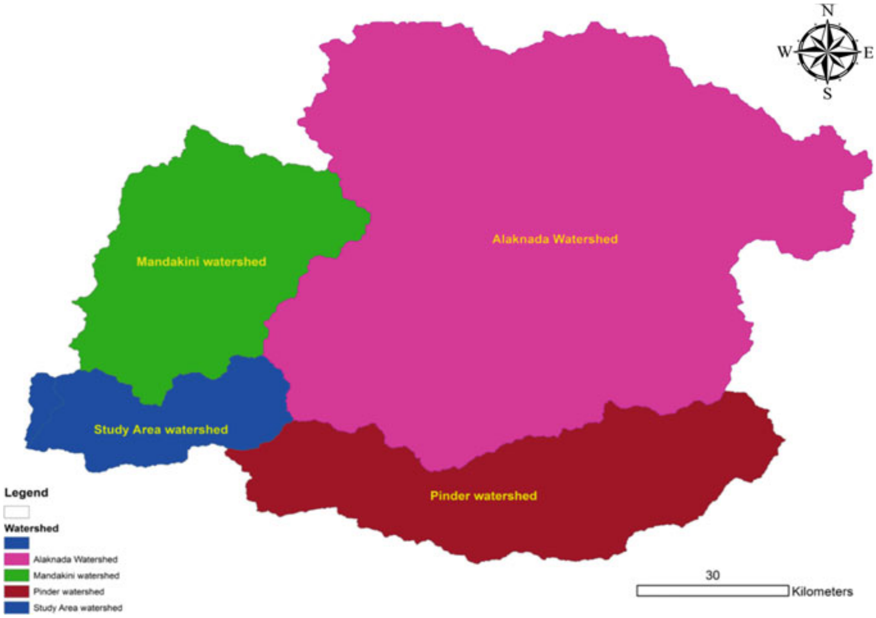

Fig. 4.2 Watershed area of Alaknanda river upstream from Srinagar

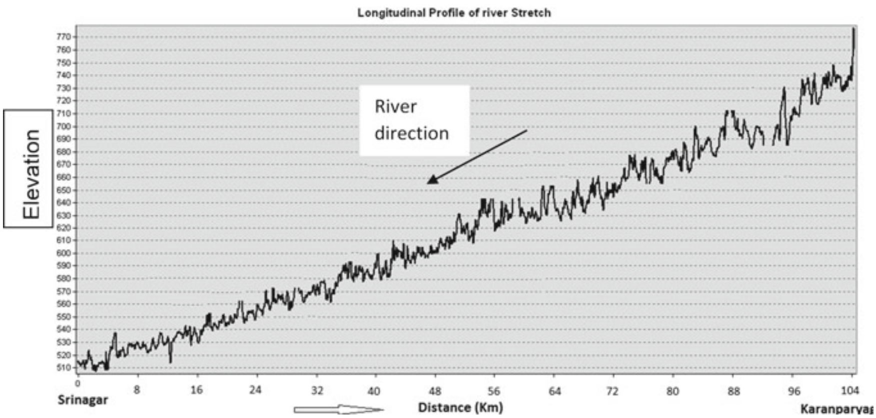

Fig. 4.3 Longitudinal profile of river stretch

slope of river stretch is 25% calculated on the basis of river profile map. Order 3 and order 4 stream are selected as a perennial river for analysis because most of the order 1 and order 2 streams are intermittent or rain-fed stream in mountain area (Patwal 2015). Mostly of the population habited near order 3 and order 4 streams and river water are more polluted near it.

4.3 Different Thematic Maps for Suitability Analysis

For analysis of site suitability map, a scoring and weighting system is applied in the model. The different thematic information is collected from different sources, like base line data was collected from field visits, land use land cover data was collected from Landsat 8 image data, slope map and stream network map were developed from ASTER DEM 30 m data, and geological information was collected from maps.

Following thematic maps are developed for the site suitability analysis of drinking water production well near the riverbank.

- Land use/Land cover map
- Slope map
- Geology map
- Stream network map.

4.3.1 Land Use/Land Cover

The land use/land cover map of the study area is prepared from the Landsat 8 satellite image which was acquired on Dec 2014 and analysis done in ERDAS imagine software. Out of the total area, 3.5% area comes under the agricultural and open land categories. From Fig. 4.4, it is clear that maximum agricultural land or open area exists near the riverbank due to easy availability of water from the river. Most of the area covered by forest land contributes 93.3% of the total area. These two types of land classification are suitable for well development near the river. But most of the suitable land (forest area) that comes under the high mountain region is unsuitable for well development near the river.

For the suitability analysis, image is classified in built-up area, agriculture land and open area, forest area, and river. In the study area, major land cover and use classes are water body or river area (3.7%), built-up areas (4.4%), agricultural and open land (8.8%), and forest land (83.1%) (Table 4.1). Land covered by forest, agriculture, and open lands account for about 91.9% which is highest suitable for well development near the riverbank.

Only 36.21% (260.05 km^2) area of the total catchment area (718 km^2) of study site is used for analysis of suitable site identification for river water purification and development of drinking water wells. Figure 4.5 shows the visual overview of land use land cover pattern of the study area under defined boundary.

4.3.2 Stream Network Map

For the preparation of stream map model, approach shown in Fig. 4.6 was prepared and run in the Arc GIS 10.2 software. Stream network map (Fig. 4.7) is created from

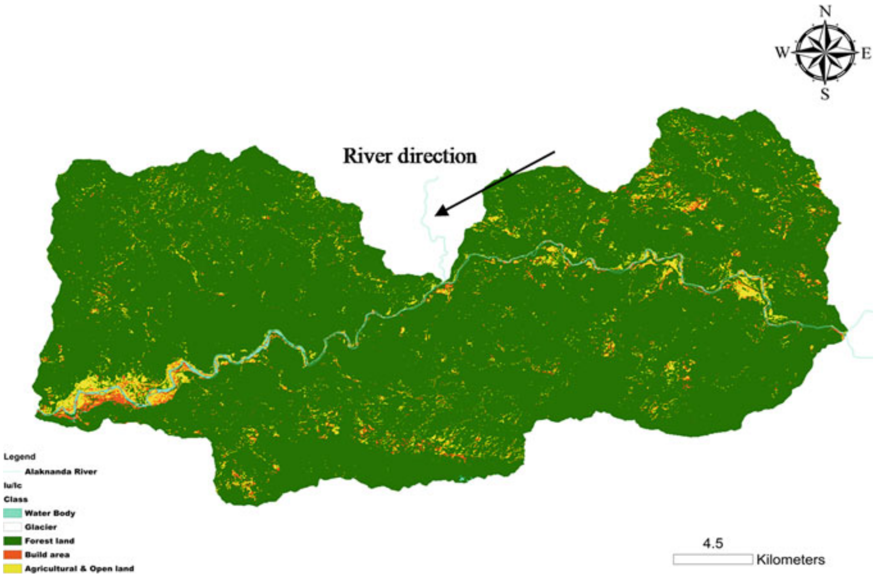

Fig. 4.4 Land use/land cover map of river stretch catchment

Table 4.1 Comparison of LU/LC area between study area and model defined boundary

Sl. No.	Land pattern	Model boundary area		Study area watershed	
		Area (km^2)	% Area	Area (km^2)	% Area
1	Agriculture and open land	22.82	8.8	25.41	3.5
2	Build area	11.44	4.4	14.14	2.0
3	Forest land	216.13	83.1	669.83	93.3
4	Water bodies	9.67	3.7	8.63	1.2
	Total area	260.05		718	

the 30 m resolution DEM data. After running model, stream order map of 1 to 4 is generated within the selected boundary. And 300 m buffer zones around the stream order 3 and 4 have been created for feasibility analysis of suitability map for drinking water abstraction. Most of the river stretch come under the order three and order four.

4.3.3 Geological Map

In order to find out the geological condition of the study area, geological map is created. Geological map was created by digitization of geological map of Uttarakhand prepared by Indian remote sensing department. Basically, five types of geological formation present in the study area are as follows: river terraces, intermediate

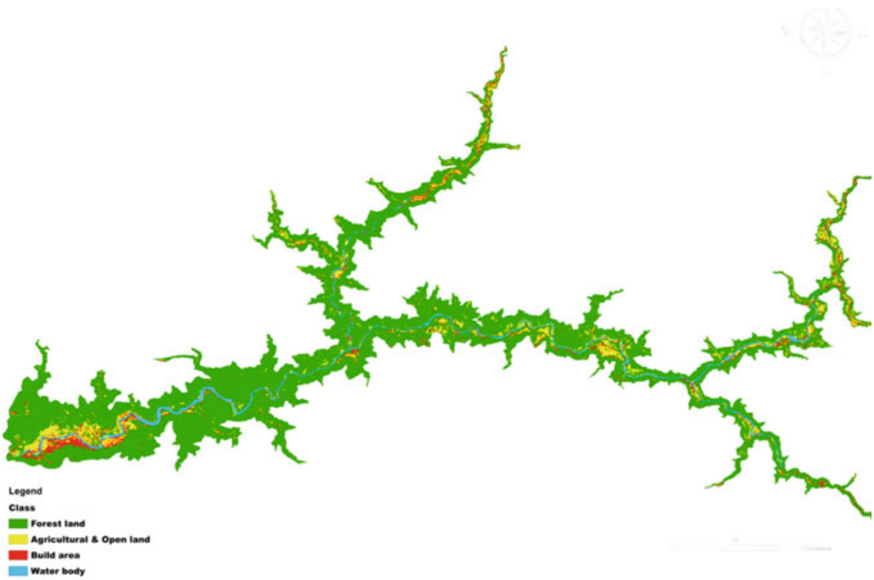

Fig. 4.5 Land use/land cover map of river stretch under defined boundary

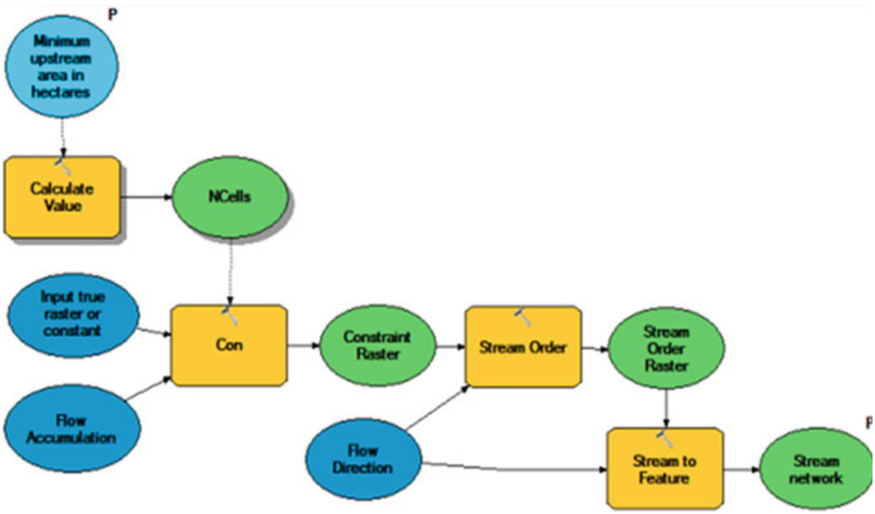

Fig. 4.6 Stream network model

valley, highly structured hills, fractured hills, and old landslide mass (Fig. 4.8). River terraces and intermontane valley are made by alluvial and sand material, which is good aquifer material for riverbank filtration. This geological formation has a high hydraulic conductivity in the mountain area.

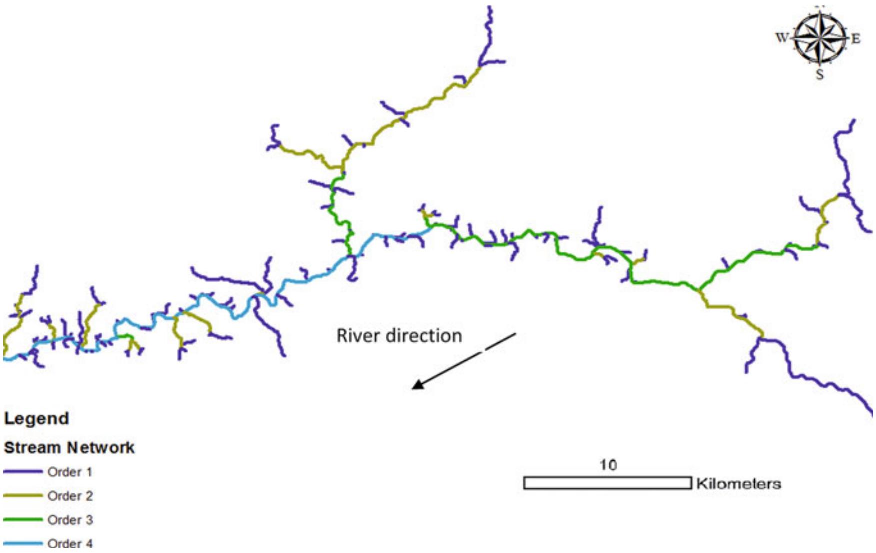

Fig. 4.7 Stream network map of the study area under defined boundary

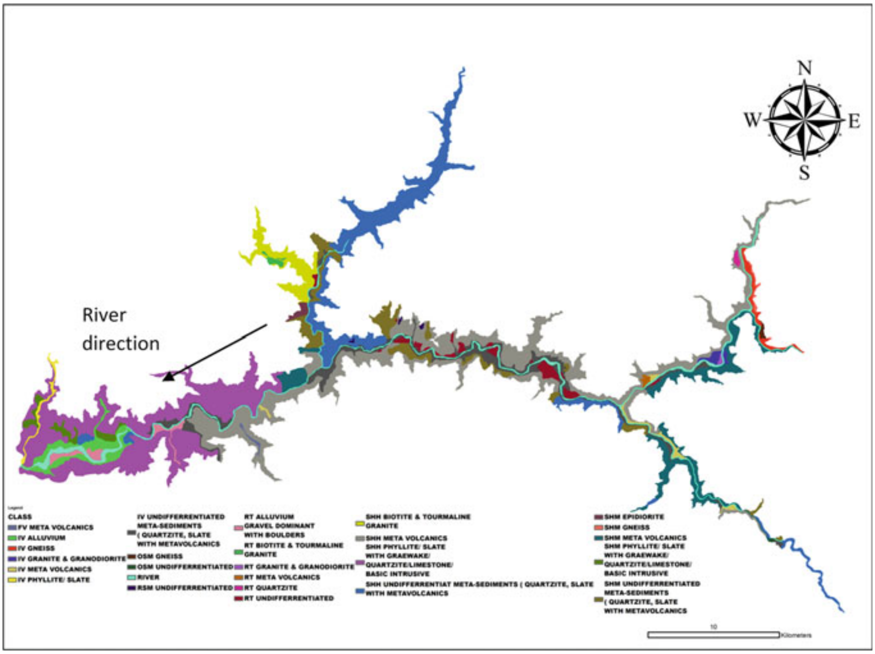

Fig. 4.8 Geological map of the river stretch under defined boundary

4.3.4 Slope Map

Slope is a very important parameter in mountain area for finding suitable sites for drinking water production near the riverbank. Steep slopes are disadvantageous for construction of well due to high velocity in river water which has a high capacity to damage the water production structure. Other main disadvantage of the steep slope is less deposition of alluvial soil near the riverbank. Table 4.2 shows the maximum percent (45%) of the area that comes under the higher slope (>20%).

In mountain areas where river has a high velocity due to high slope, they have deep gorges and cuts in rocks near the river courses and no sign of alluvial deposition. Steeper slopes also increase the construction costs, limit maximum floodplain areas, and contribute to erosion of riverbank. Figure 4.9 shows the maximum area that comes under higher slope more than 20%. The value of Slope less than 10° is considered as gentle slope (Rawat 2010) for construction activity. Slope value greater than 10° has been considered as unsuitable because river water has erosive nature.

4.4 Scoring and Ranking of Thematic Maps

For the site suitability, it is necessary to give some score to each of the category in each thematic map and ranking to each thematic map as per their suitability. Each category has not the equal weightage or usefulness for drinking water well development. The suitability scoring used in current study for each thematic map and their category at 3-point scale is given in Table 4.3. In the current study, higher weightage has been assigned to slope map and geological map. As slope has very important role in development of floodplain, also geology has an important role in well drilling and development and subsurface water movement in near riverbank.

The next important factor to consider in the development of the wells near river banks is the safety aspect, so as to avoid flooding and water contamination. The chances of damages to the wells are higher at the vicinity of the active flood area near the riverbank in the monsoon season. Large distance to the roads from the sites may involve some extra costs and also the accessibility is another important requirement, but it is not considered in this study because new road can change the

Table 4.2 Area of % of slope area in river stretch watershed under defined boundary

Sl. No.	Slope %	Area km^2	% of total area
1	5	23.28	8.95
2	10	34.84	13.4
3	15	40.54	15.59
4	20	42.76	16.44
5	>20	118.6	45.61
	Total	260.05	100

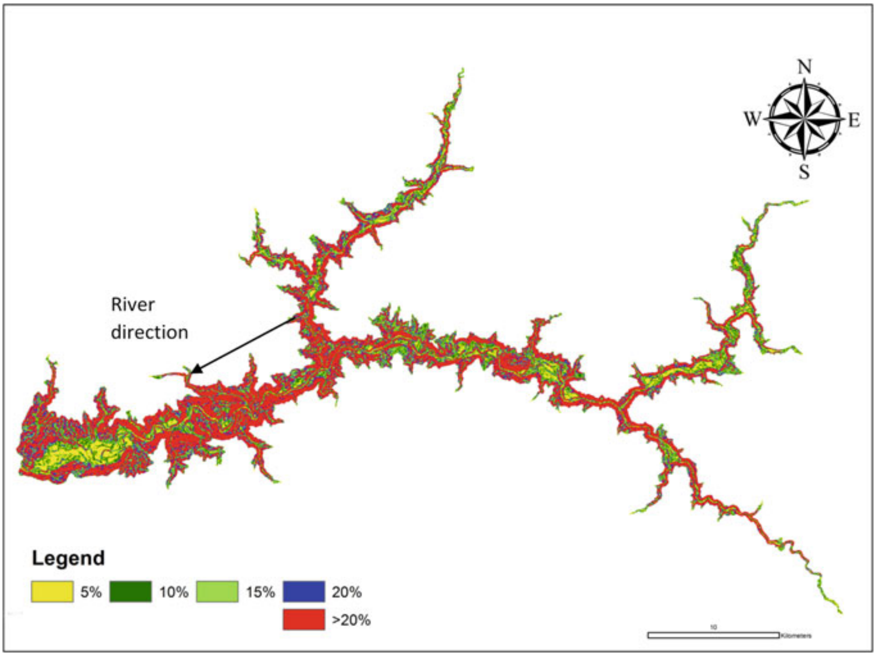

Fig. 4.9 Slope map of river stretch under defined boundary

situation and weightage assigned to the accessibility can change. Least priority has been given to land use/land cover pattern because of less land requirement for well development, and its influence by human activity can be changed if required.

4.5 Suitability Map with Weighting System

After digitization and reclassification of all thematic maps are converted in raster format, so that for each pixel, a value can be determined. All maps are then combined into a composite site suitability map by addition of all thematic maps with weight factor. In the current study, higher weightage has been assigned to slope map and geological map. The final output site suitable thematic raster map, which is prepared in Arc GIS 10.2 software, has particular suitability score which is based on following equation.

$$\text{Suitability score} = (\text{slope})^{*}40 + (\text{geology})^{*}40 + (\text{land use/land cover})^{*}10 + (\text{stream network})^{*}10 \tag{4.1}$$

The final site suitability thematic map in Fig. 4.10 indicates that area is divided into two different categories, suitable or unsuitable. The areas have been divided into

Table 4.3 Scoring value of thematic layers for site suitability analysis

Sl. No.	Thematic map	Class	Value
1	Geological map	River terrace with alluvium, gravel, and boulder	1
		Intermontane valley with alluvium, gravel, and boulder	1
		Old sided mass meta volcanic rock	Restricted
		Recently slide mass	Restricted
		High structural hills, Meta Volcanic rock	Restricted
2	Land use/Land cover map	Water	Restricted
		Forest	1
		Build area	Restricted
		Agricultural Land	1
		Open land	1
3	Slope map	5%	1
		10%	1
		15%	2
		20%	Restricted
		> 20%	Restricted
4	Stream network map	0rder 1	No data
		Order 2	No data
		Order 3	Restricted
		Order 4	Restricted

Note Value; 1 = Excellent, 2 = Good, Restricted = Unfit, No data = Unsuitable

suitable for higher value to unsuitable for lower value. Most of the area is unsuitable for development of drinking water well near the bank through riverbank filtration due to highest slope near the riverbank and unsuitable geological conditions.

4.6 Groundwater Flow Modeling

After selection of suitable site near the Alaknanda riverbank for indirect bank infiltrates abstractions with the help of GIS and remote sensing, one site was selected for ground water modeling. Drinking water scarcity is the basic factor for site selection. The main aim of groundwater modeling is to calculate the amount of river water which is abstracted for the 75 m away from the river course. For this purpose, a groundwater flow model has been constructed using mode flow software (PMWIN 5) for the area shown in Fig. 4.11. With the help of this software, an attempt is made

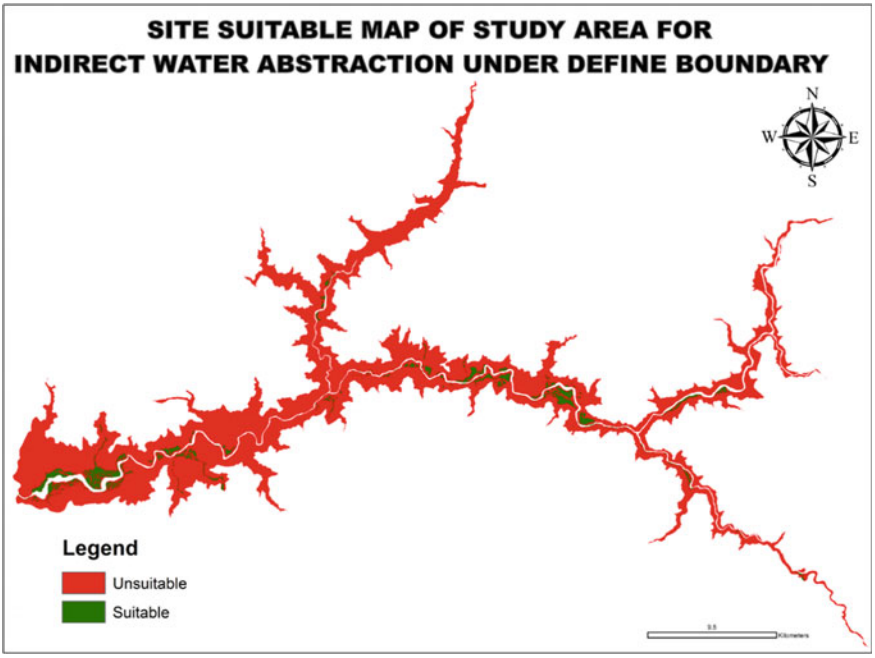

Fig. 4.10 Site suitability map for drinking water production

for subsurface water flow from river to 14 imaginary wells located 75 m away from the Alaknanda River course at Gaucher.

For the draw down, flow path, bank filtrate water quantity, groundwater quantity, and travel time for 14 imaginary production wells, a single-layered groundwater flow model is developed in steady state condition. The model has been developed for non-monsoon seasons. The following assumptions are considered for ground water model development.

I. Discharge rate of production wells is constant throughout the analysis
II. Unconfined aquifer and homogeneous material
III. Vertical hydraulic conductivity is one tenth of horizontal conductivity
IV. Steady state flow condition
V. Recharge rate to the aquifer, porosity, and horizontal hydraulic conductivity are constant for model area.
VI. Constant recharge from the rainwater and river water
VII. Water level in the river is assumed constant during the test.

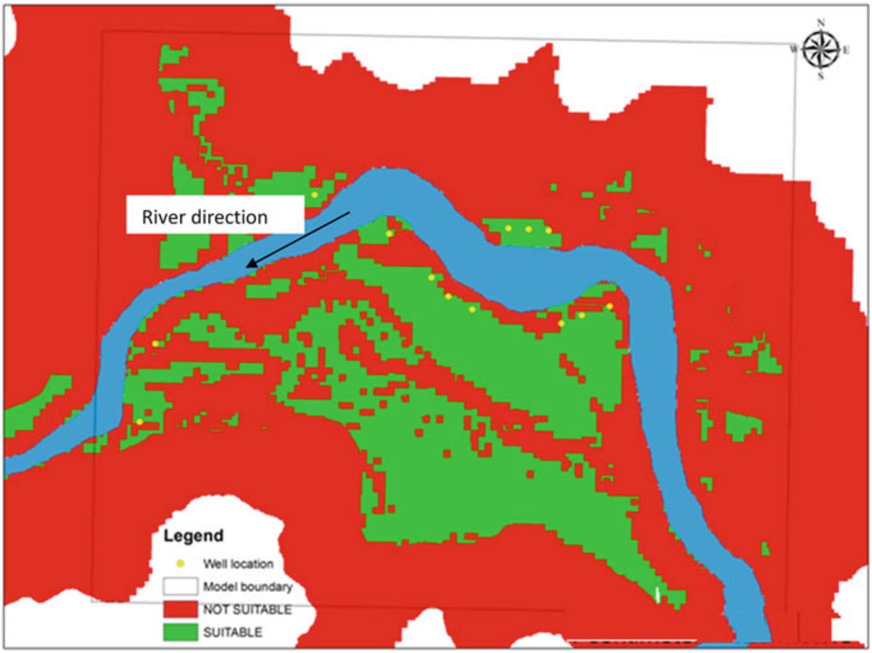

Fig. 4.11 Area for ground water model analysis

4.6.1 Area and Grid Formation for Model

The area is calculated in arc GIS domain, and according to the area, grids have been developed. The area for model domain is used 3000 × 2500 m divided in 100 rows, 120 columns; cell size 2.08 × 2.08 to 25 m × 25 m. River water level and surface elevation for modeling are calculated and measured by DEM data of the field visit. The thickness of the unconfined aquifer is 10.55 m determined with the help of borehole data (State drinking water department, Uttarakhand). Location of the wells is determined on the basis of river cross-sectional profile (Fig. 4.12).

4.6.2 Input Parameters for Modeling

The horizontal hydraulic conductivity of the riverbank material is assigned to the model as a value of 4.2×10^{-4} m/s obtained from the pumping test which was conducted by state drinking water department in 2012. Vertical hydraulic conductivity 4.2×10^{-5} m/s (ten time less than horizontal hydraulic conductivity) is used for model with 0.3 effective porosity. A recharge value of 3.96×10^{-8} m/s is assigned to the model based on a mean precipitation for the period 1965 to1986 for the study area.

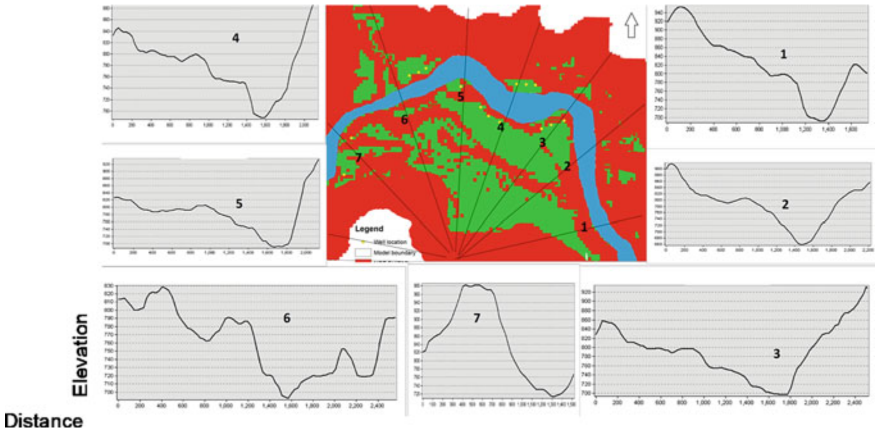

Fig. 4.12 Cross-sectional profile of selected site for ground water modeling (South to north direction)

The total selected river length for flow modeling is 4900 m with elevation difference of 20 m. For the simulation, river slope of 0.00408 is assigned.

Boundary conditions, like active, inactive, and constant head condition, are calculated on the basis of geological map and DEM map. Parameters required in steady state ground water modeling are given in Table 4.4. Based on the input data, the travel time and ratio of bank filtrate water are calculated in each of the 14 wells.

Table 4.4 Parameters required for Steady State Ground Water Simulation

Sl. No	Model parameter	Assigned value
1	Geometry	Area: 3000 × 2500 m; 100 rows, 120 columns; cell size: 2.08 × 2.08 to 25 × 25 m
2	Boundary conditions	River: assigned as constant head cells along western and northern boundary
		Wells: total discharge of 0.238 m^3/s at 0.017 m^3/s per well for 14 production well
		Rock: assigned as constant discharge cells
		Recharge: 3.96×10^{-8} m/s assigned to uppermost active cells
3	Hydraulic conductivity	Aquifer in floodplain area: $Kx = Ky = 4.2 \times 10^{-4}$ m/s; $Kz = 4.2 \times 10^{-5}$ m/s on the basis of pumping tests
4	Effective porosity	0.3
5	Simulation	Steady state, unconfined conditions

4.6.3 Drawdown

Yield capacity and efficiency of any production well can be calculated by the help of drawdown of water level in the well and also drawdown help to make sure that the water source is adequate and not being depleted. In groundwater flow model, contour line of subsurface water level without pumping water is called hydraulic head. It is called initial water level in the aquifer. After pumping 0.017 m^3/s water from each 14 wells, the drawdown is measured as shown in Fig. 4.13. The flow of old river water is observed from east to west, and flow direction of bank filtrate was observed from north to south or vice versa. The drawdown of group of wells in the same meandering site is influenced by each other because many drawdown lines are inter-link with each other.

Fig. 4.13 Drawdown of production wells

4.6.4 *Particle Transport*

Basically, the path lines are used in the MODFLOW for the trace particle analysis. With the help of particle transport, the ratio of young bank filtrate water (which takes less than 100 days to reach well for river) and mixture of both water (old bank filtrate water which takes more than 100 days to reach the well and ground water) is calculated for each well. The amount of ratio of water is measured by water budgeting of each single well. In Fig. 4.14, red color lines predict the path of the water which was abstracted from each well at the rate of 0.017 m^3/s. With the help of these path lines, the amount of water which comes from different sources, like river, ground, and surface recharge, can be calculated. After calculation of percentage of young and mix water (old river water + ground water) in the well discharge water, the travel time of well water is calculated for each well.

In Fig. 4.15, red arrow shows the different time steps (one arrow shows 30 days) taken by water to reach the well. Table 4.5 shows that the amount of water abstracted from different source forms different wells and its travel time. Discharge of the well 0.017 m^3/s is assumed constant during whole simulation for travel time. On the basis of travel time, organic matter removal capacity of the aquifer is calculated.

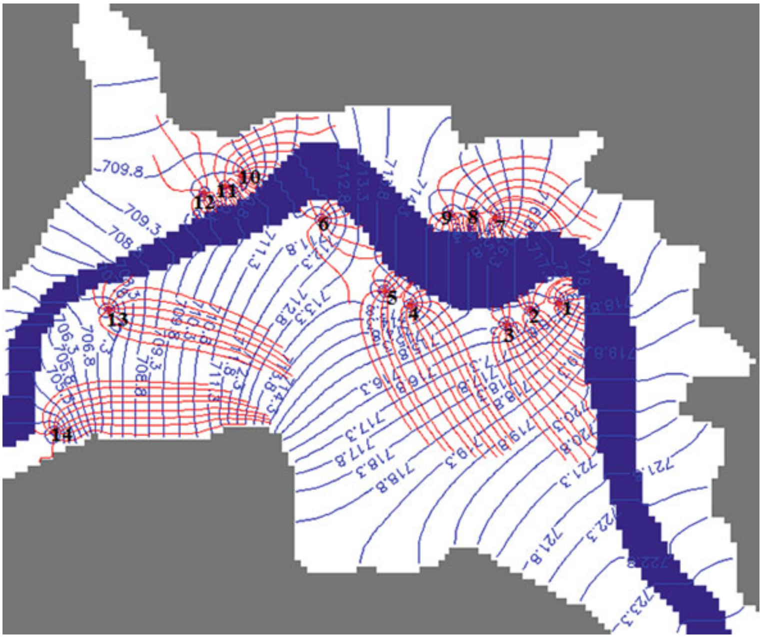

Fig. 4.14 Path line of subsurface and ground water in active zone

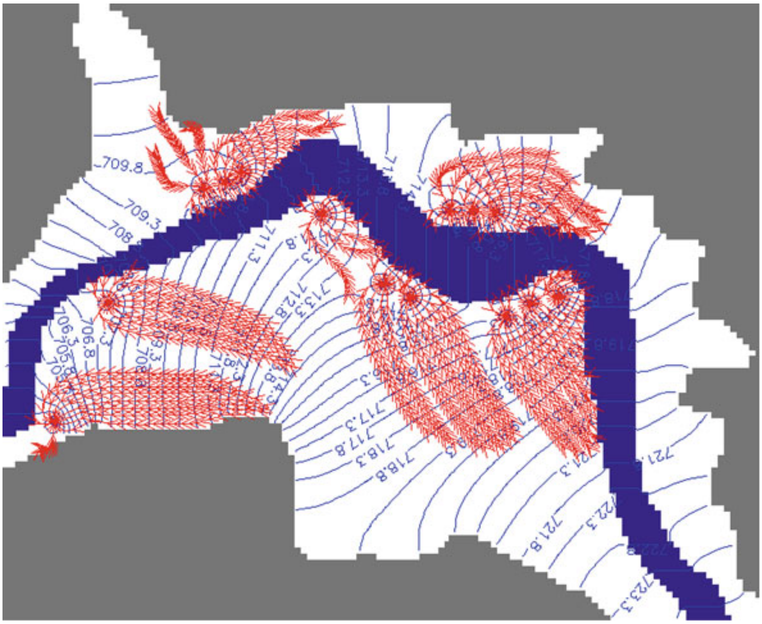

Fig. 4.15 Travel path and travel time of river water from river to wells

4.7 Riverbank Purification Capacity Analysis

The SOMA tool is used for analysis of organic micro-pollutant removal capacity of the riverbank aquifer material particular distance from the riverbank. Out of three input parameters, only two parameters, travel time and distance of well from riverbank, have been used for the purification analysis of riverbank material water. The third parameter influent concentration in the surface water source is not used in this analysis. Well distance 75 m from the riverbank is calculated from GIS domain and tried to make it fixed for all imaginary wells. Travel time for riverbank filtrate water put into SOMA tool. Figure 4.16 shows the outlook of the SOMA tool. In the given Table 4.6, the purification capacity or removal of organic micro-pollutant compound with respect travel time and distance of well from the riverbank are calculated. In Table 4.6, the output parameters or removable percentage of OMPs is noted that in both cases the young bank filtrate water and old bank filtrate water. It is noticed that in both cases removal efficiencies of dissolved organic carbon (DOC, 26–29%) and volatile organic compound (VOC, 93%) are same but for pesticides and pharmaceutical compound were different. This difference of removal of OMPs is based on different travel times.

Table 4.5 Recharge source and travel time of well water

Well	Discharge (m^3/s)	Young river water (m^3/s)	Old river water (m^3/s)	% Young river water	% Old river water + ground water	Travel time young river water (days)	Travel time old river water + ground water (Approx. in days)
1	0.017	0.0170	0.0000	100	0	30	0 0.0
2	0.017	0.0071	0.0099	42	58	25	140
3	0.017	0.0037	0.0133	22	78	30	280
4	0.017	0.0045	0.0125	26	74	26	645
5	0.017	0.0087	0.0083	51	49	20	630
6	0.017	0.0142	0.0028	84	16	35	225
7	0.017	0.0121	0.0049	71	29	14	750
8	0.017	0.0086	0.0084	50	50	12	700
9	0.017	0.0146	0.0024	86	14	22	400
10	0.017	0.0154	0.0016	91	9	22	150
11	0.017	0.0132	0.0038	77	23	18	375
12	0.017	0.0106	0.0064	62	38	20	700
13	0.017	0.0037	0.0133	22	78	60	650
14	0.017	0.0001	0.0170	1	99	61	625

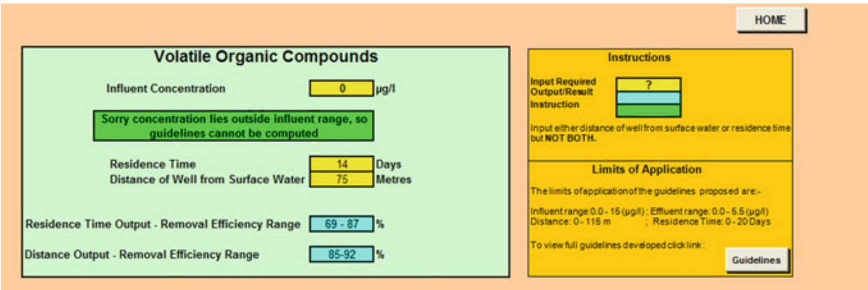

Fig. 4.16 Outlook of SOMA tool for analysis of organic micro-pollutant removal capacity

4.7.1 River Meandering and Its River Water Purification Capacity

After calculation of removal of OMPs in both type of filtered water in the well, the total average removal capacity is calculated for each river meanders on the basis of meandering zones. The total removable capacity of one well was compared with its

Table 4.6 Organic removable efficiency of aquifer material

Well	Removal of compound in river-filtrated water				Removal of compound in old river water + ground water				Total removal of compound in one production well			
	DOC %	VOC %	Pesticides %	Pharmaceuticals comp. %	DOC %	VOC %	Pesticides %	Pharmaceuticals comp. %	DOC %	VOC %	Pesticides %	Pharmaceuticals comp. %
1	28	93	76	51	29	93	86	94	28	93	76	51
2	28	93	76	51	29	93	86	94	28	93	82	76
3	28	93	76	51	29	93	86	94	28	93	83	85
4	28	93	76	51	29	93	86	94	28	93	83	83
5	27	93	76	51	29	93	86	94	28	93	81	72
6	28	93	76	51	29	93	86	94	28	93	78	58
7	24	78	76	51	29	93	86	94	25	82	79	63
8	23	78	76	51	29	93	86	94	26	85	81	72
9	27	93	76	51	29	93	86	94	27	93	77	57
10	27	93	76	51	29	93	86	94	27	93	77	55
11	26	93	76	51	29	93	86	94	26	93	78	61
12	26	93	76	51	29	93	86	94	27	93	80	67
13	29	93	86	65	29	93	86	94	29	93	86	88
14	29	93	86	65	29	93	86	94	29	93	86	94

river meander sinuosity value for visual identification of suitable sites in the mountain area.

$$\text{Average removal capacity} = \left(\begin{array}{l} \text{Sum of total removal capacity of all wells in a river meandering zone} \\ /\text{no of wells with the zone} \end{array} \right) \quad (4.2)$$

From the Deng and Singh (2002), it was found that the river which has 1.4−1.6 river sinuosity has a high self-purification capacity. For the analysis of organic micro-pollutant removal capacity of river meanders through riverbank aquifer deposition in mountain area, a correlation is established between sinuosity value and removable capacity. Figure 4.17 shows that for the calculation of removal capacity of the riverbank deposition, selected site is divided into five zones.

Table 4.7 shows that that river with sinuosity value (S) 1.28–1.45 has a higher removal capacity of organic micro-pollutant from river water. The higher removable value of OMPs from river water of river at 1.28–1.45 sinuosity reflects river-deposited good hydraulic material at the bank of river.

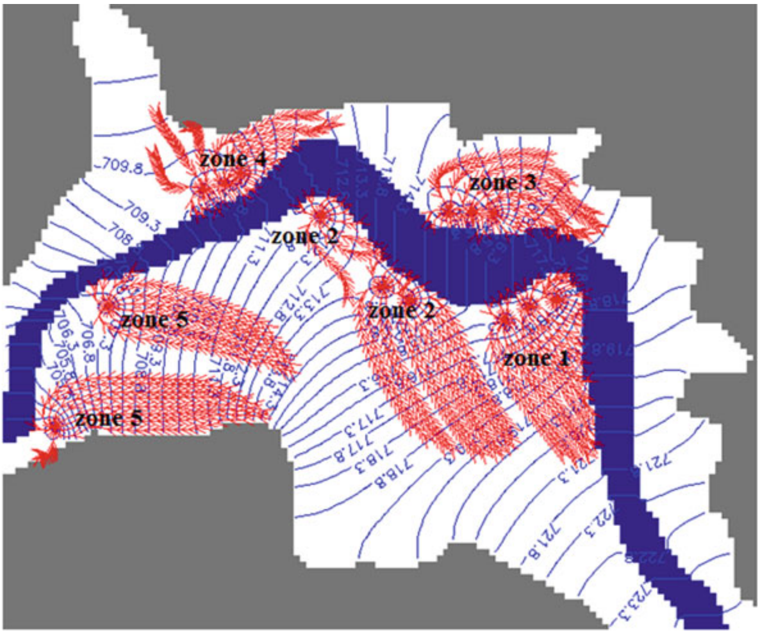

Fig. 4.17 Different river meandering zones

Table 4.7 Organic removable efficacy with river meandering

Sl. no	Zone	River sinuosity	Average purification capacity of one zone			
			DOC %	VOC %	Pesticides %	Pharmaceutical comp.%
1	1	1.45	28	93	81	71
2	2	1.28	28	93	81	71
3	3	1.60	26	86	79	64
4	4	1.07	27	93	79	61
5	5	1.20	24	62	57	60

Table 4.8 Water production capacity of river meanders

Sl. no	Zone	Discharge (m^3/s)	% Young river water	% Old river water + ground water	River sinuosity
1	1	0.017	54	46	1.45
2	2	0.017	53	47	1.28
3	3	0.017	69	31	1.6
4	4	0.017	76	24	1.07
5	5	0.017	11	89	1.2

4.7.2 Water Filtration Quantity

After calculation of water quality of bank filtrate water, a calculation is made for water production capacity of these meanders. Table 4.8 shows that low sinuosity value (S) has 1.07 high water production capacity of bank filtrate water. This type of analysis helps to water manager for finding the suitable site by visual inspection.

4.8 Discussion

For site suitability analysis for indirect surface water abstraction schemes, four types of thematic map are used in this study like Digital elevation model (DEM), Geological map, land use land cover map, and stream network map. With the help of DEM data watershed, stream network map and slope map are prepared and classified into different categories. Satellite image is used for preparation of land use land cover map of the area. Slope map is classified into 5, 10, 15, 20%, and more than 20% slope area. Land use land cover map was classified into 4 categories: water body, build area, forest land, and agricultural and open land. Stream network map is used for identification of river and its pattern. For the identification of suitable site, horizontal and vertical boundary are developed and defined in GIS domain for faster and accuracy of the output image. For vertical boundary, 1000 m elevation level and for horizontal boundary, 300 m vertical extent from both side of riverbank are used. After overlapping all the thematic maps together, weightage and scoring value are assigned to each layer and each category. Finally, suitability map was generated. In next, one location is selected from the generated site suitable map for ground water modeling. After putting all the required values in MODFLOW software travel time, path of particle and portion of bank filtrate amount are calculated for future analysis. Then, SOMA tool is used for purification capacity of the aquifer material. At the same time, river meandering sinuosity is calculated for the same selected site. The result for SOMA tool shows that the sinuosity value of 1.28–1.45 has the higher purification capacity and sinuosity 1.07 has a river water filtration capacity. During water modeling of the selected site, it is noticed that one site can produce 20 MLD water for drinking as well as agricultural purposes. This amount of water can meet the 130,000 people's drinking water demand. Figure 4.18 shows the systematic flow diagram for the site suitability analysis and its capacity analysis.

4.9 Conclusion

Most of the potential sites for water production near the river for indirect water abstraction in the river stretch are not approachable by road. Remote sensing and geographical system have a capability to get and analyze information within short time frame. During field visit, it was noticed that three indirect surface water abstraction schemes already existed within the river stretch come under the suitable sites generated by GIS domain. It indicates that the methodology which is adopted for site suitability analysis is fit for mountain area. Due to high slope and high hill structure, only few suitable sites are identified within the river stretch for indirect water abstraction. Ground water model shows that one suitable site has huge capacity of water production around 20 MLD and can meet the water demand of the area for long time. River meandering sinuosity is matched with the water purification capacity value (calculated by SOMA tool) which shows that sinuosity value of 1.4 has a highest purification capacity and sinuosity of 1.2 has the highest filtration capacity in the mountain area. This result will help the water managers and engineers to select a site for well development near the riverbank by visual survey.

After identification and analysis of all water resources within the 100 km river stretch under integrated water resource management, it is noticed that there is enough water available for meeting the local water demand. For integrated management of water resource, riverbank filtration technology should be implemented all over the mountain area to meet the local water demand. Proper sewage and sanitation facilities must be provided to all towns near the river stretch, and only after treatment of the sewage, it should be allowed to discharge into the river or domestic use. Unfit drinking water which has excess amount of nitrogen can be utilized for agricultural purposes. Most of the agricultural land exists near the towns and riverbanks in the study area. The agricultural water demand can be meet by domestic wastewater which has high nitrogen and phosphorus nutrient.

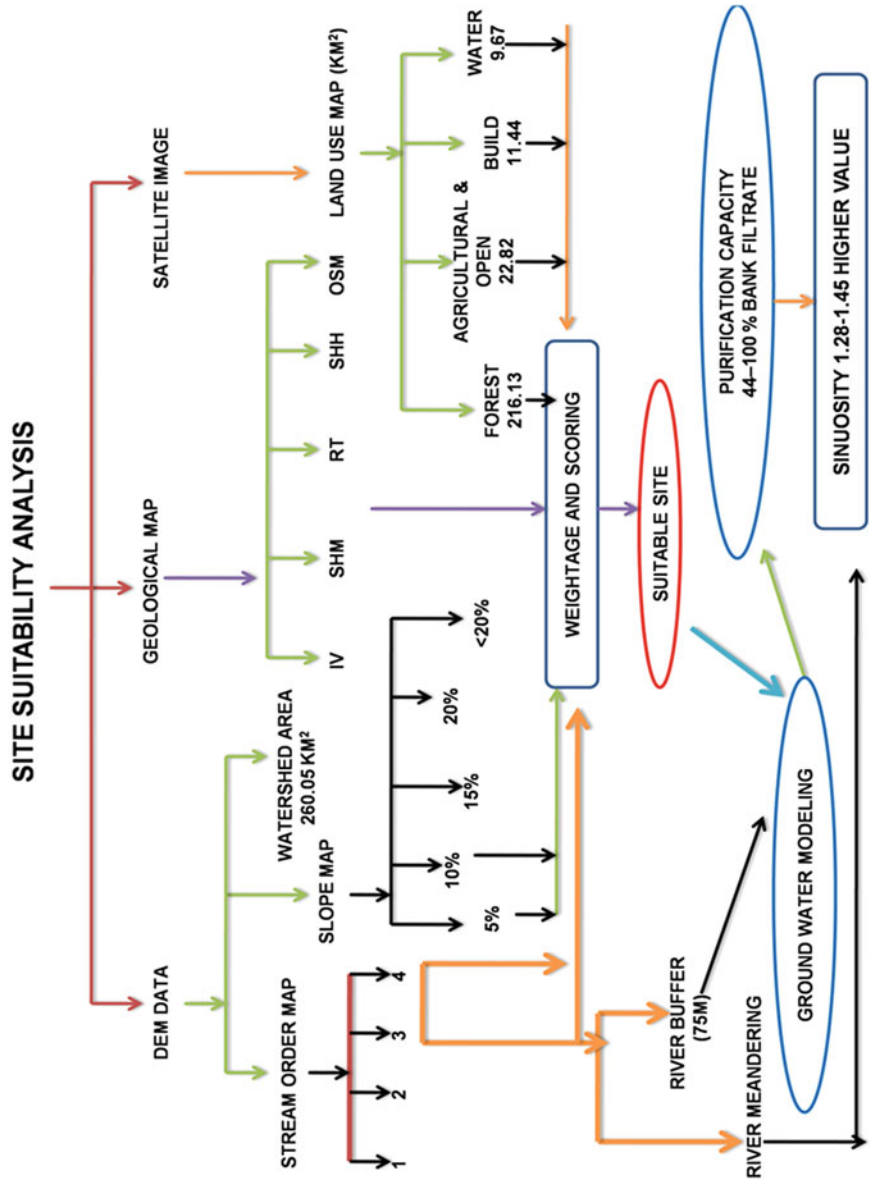

Fig. 4.18 Flow chart of site suitability analysis

References

Deng ZQ, Singh VP (2002) Optimum channel pattern for environmentally sound training and management of alluvial rivers. Ecol Model 154(1):61–74. https://doi.org/10.1016/S0304-3800(02)00053-4

Ground Water Prospects Map (2008) Uttarakhand Space Application Centre. NRSC (ISRO), Department of space, Government of India

Patro ER, Voltz TJ, Kumar A, Grischek T (2020) Micro-hydropower in drinking water gravity pipelines: a case study in Uttarakhand India. ISH J Hydraulic Eng 26(3):332–342. https://doi.org/10.1080/09715010.2018.1492977

Patwal PS (2015) Integrated water resources management of a river stretch using GIS & ground water flow modeling. M.Tech Thesis, Indian Institute of Technology Roorkee (IITR), India

Rawat JS (2010) Database management system for Khulgard watershed, Kumaun Lesser Himalaya, Uttarakhand, India. Curr Sci 98(10):1340–1348

Chapter 5
A Systematic Review on Groundwater Management: Opportunities and Challenges

Shaghla Parveen, Bushra Praveen, and Vaseem Akram

Abstract In both urban and rural settings, groundwater supports various aquatic habitats and plays a critical role in the economic growth and human well-being. Therefore, if properly assessed and sustainably used, groundwater has considerable importance to the development and well-being of people in underdeveloped nations. Although groundwater resource development potential is still discussed in the literature, there is still a lack of quantitative knowledge about these problems. The chapters goal is to draw attention to the key groundwater concerns and difficulties that developing nations face, as well as the existing and foreseeable potential for sustainable subterranean water governance. The purpose can be consummate through reviewing current groundwater resource information as well as current and upcoming groundwater management programs and efforts. Due to increased demand to fulfill human and agricultural requirements, groundwater resources in developing countries are increasingly at risk of contamination from urban spaces, manufacturing firms, farmlands, and excavation operations, as well as from inadequate hygiene standards and overexploitation. This paper will look at the importance of groundwater importance, groundwater challenges in developing countries, and a systematic review of drought management policy. Therefore, it is necessary to implement methods to corroborate with sustainable management and flourishment of groundwater reserves. These include developing groundwater monitoring systems, comprehending the connections between groundwater aquatic ecosystems, managing transboundary aquifers, addressing the repercussions of climate alterations on underground water, and determining how accelerated expulsion of subsoil waters will affect its retaining capacity.

S. Parveen (✉)
National Institute of Urban Affairs, New Delhi, India
e-mail: shaghlaparvn@gmail.com

B. Praveen
Department of Economics, IIT Indore, Indore, Madhya Pradesh, India

V. Akram
Economics and Business Environment Area, Indian Institute of Management Jammu, Jammu and Kashmir, Old University Campus, Canal Road, Nawabad, Cantonment, Jammu 180016, India

P. Shukla et al. (eds.), *Environmental Processes and Management*, Water Science and Technology Library 120, https://doi.org/10.1007/978-3-031-20208-7_5

Keywords Groundwater management and governance · Sustainability · Developing countries · Systematic review

Abbreviations

AI	Artificial intelligence
ML	Machine learning
ANN	Artificial neural network
FAO	Food and agriculture organization

5.1 Introduction

Groundwater is considerably a substantial freshwater body which is expected to threaten due to over-drafting. Nearly two million people utilize groundwater resources, causing a share of 33 percent water withdrawal. Therefore, over-drafting is noticeably one of the major causes of groundwater-level drop and directing toward crises. Figure 5.1 indicates the water that exists below the surface of the land is typically thought of as groundwater. More specifically, all cracks and pores beneath the surface of the earth are completely saturated by subsurface water. Thus, water that is more transiently held between soil granules close to the land surface is typically excluded from the concept of groundwater. An aquifer is a layer of gravel or stone in the earth that can produce groundwater. The world's total water resources ranged 46,000 km^3/year, with around 36,000 km^3/year of groundwater (Trenberth et al. 2007). The patchwork of climatic conditions and physiographic features determine how these resources are spread around the earth. At the continental level, America, with 45% freshwater globally, has the highest proportion at the continental level, accompanied by Asia with 28%, Europe 15.5%, and Africa 9%. America possesses 24,000 m^3 of resources per person/year, Europe contains 9300 m^3, Africa owns 5000 m^3, and Asia holds 3400.1 m^3 per year (FAO 2003).

The natural water cycle depends on groundwater, which is found almost everywhere beneath our feet. Groundwater contributes significantly to the flow of many streams and rivers as part of the water cycle, and it has a significant impact on the ecosystems of rivers and wetlands for both plants and animals. It creates the biggest accessible freshwater reserve on Earth. There are around 23,400,000 km^3 of groundwater on Earth, of which 10,530,000 km^3 are freshwater and 54% are saltwater (Gleick 1996).

Groundwater is a secret resource that is produced by rainwater that has seeped into the earth through continental surface waters (about 80%), oceans (20%) assisting waterways and retaining ecosystems. Therefore, throughout the summer or during

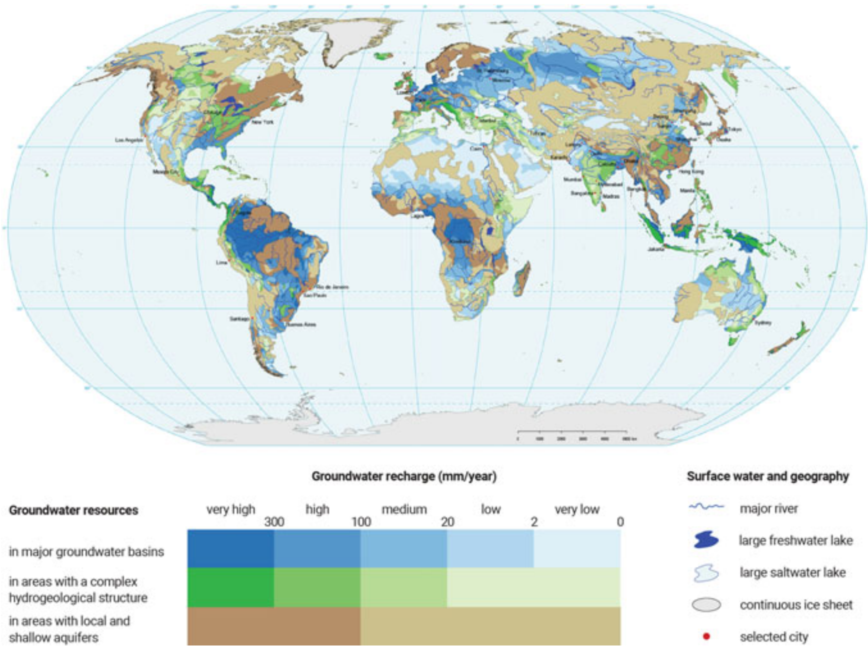

Fig. 5.1 Groundwater resources across the countries. *Source* Groundwater resources of the world Image Credit BGR/UNESCO (2008)

dry spells, groundwater serves as river's or lake's main supply of water. This review explained groundwater's significance, challenges, and possible solutions.

5.2 The Role of Groundwater

5.2.1 Importance

Only 0.2% of the freshwater on Earth is contained by lakes, streamlets, or rivers/rills; besides 70% is frozen; therefore, the statistics account for roughly 30% of all freshwater on Earth. Pragmatically, the water consumed for agriculture, industry, drinking purposes, domestic use, etc., comes from the groundwater resource.

Numerous crucial responsibilities for our environment and economy are carried out by groundwater. It sustains rivers, lakes, and wetlands in the ecosystem, particularly during the dry season with acute downpour.

5.3 Groundwater Management and Challenges

- Inadequate data and statistics for planning is one of the obstacles toward the governance and expansion of sustainable groundwater resources. For instance, it is not evident how far constructing wells can be placed apart from each other to avert leakage and how distant the extraction locations must be placed to restrict contamination. Thus, in order to conserve and develop groundwater resources for water supply, it is important to address the following practical issues: How much of the zonal space encompassing wells and springs needs to be protected from continuous pumping through various waterholes in order to prevent overexploitation of water reserves and an unwanted fall in the water level.
- Contamination of the groundwater. In both urban and rural regions, there are a growing number of documented cases of water-borne illnesses brought on by drinking tainted groundwater. This is linked to sanitary facilitie's poor placement, particularly pit latrines, whose contents seep into and mingle with groundwater. Urban area's crumbling solid waste disposal facilities and sewer systems, whose contents and leachates readily seep into groundwater and mix with it, are also to blame for groundwater pollution.
- Intricate geology fractures and worn zones that are present in intricate geological formations are where groundwater occurs. Due to the complicated geology, understanding the nature of groundwater occurrence and flow is highly challenging. As a consequence, this poses a significant obstacle in development of sustainable groundwater assets.

5.4 Climate Change and Groundwater

5.4.1 Impacts

Groundwater is frequently left out of the most recent assessments of how climate change ability influences water resources. This exclusion raises concerns, especially in developing nations where groundwater is heavily relied upon to supply the household, agricultural, and industrial water needs due to present practices and anticipated adjustments to climate change and rapid population expansion. Africa has already experienced climate change and variability, and this century is expected to see a significant rise in both (Taylor and Tindimugaya 2009).

5.5 Opportunities for Improving Groundwater Management

The developing countries have several active groundwater-based projects offering chances to enhance groundwater management. These may be divided into three categories: information management programs, capacity training programs, and frameworks for institution-formed cooperation and shareholder involvement.

There are several institutional coordination and stakeholder association structures that are essential for sustainable groundwater management. In addition to the African Union, the African Minister's Council on Water, specialized Africa Groundwater Commission, Regional Economic Communities, River Basin Organizations, member states (water ministries), and sub-national (basins, counties/districts, and local communities) organizations are among them.

The discourse of sustainable groundwater management gives a comprehensive clasp over the recent stature and the forecasting of the imperative resources. A number of automated models simulate differential techniques to stimulate the effective groundwater system**,** for instance MODFLOW (MacDonald et al. 2001).Various researches suggest that soft computing techniques are used to project groundwater contamination, such techniques are artificial neural network (ANN) and adaptive network-based fuzzy inference system. At some point, the literature review explains that in the process of predicting groundwater behavioral systems, physical and numerical techniques played their part; however, conventional techniques are convoluted to elaborate the results; therefore, AI is used to enhance the modeling technique and quality (Quadri 2017).

In the last many years, researchers inclined to machine learning (ML) and database methods and incorporated them in groundwater modeling (MacDonald et al. 2012). The subterranean water system has compounded features which remained unresolved in the conventional modeling. The acquisition of simulation and prediction techniques streamline a number of presumptions and undergo considerable groundwater unpredictability**.** A significant attribute of black-box models, for example ML, is that it does not need a thorough understanding of all the physical and mathematical operations to settle down nonlinear linkages among all the factors. Besides, linear stochastic and pre-processing methods demonstrated a propitious approach in level forecasting (Quadri 2017).

This research tries to bring a systematic review on ML techniques incorporated into modeling and forecasting of groundwater resources. This chapter also explores the appropriateness of ML models to envision the quality base aggregate groundwater. The extent of the review considers groundwater-level predictability through artificial intelligence (AI) and soft computing procedures amalgamated into various studies**.** Moreover, this review chapter fashioned upon earlier research articles corresponding to ML and deep learning techniques in the arena of hydrology, water resources, and groundwater (Nijsten et al. 2018). This attempt helps in bridging a research gap for systematic meta-analysis ML modeling in groundwater. ML modeling in groundwater contemplates spatiotemporal scale, meteorological studies, sample division, input factors. The modeling ensembles results of predicament indices, resolution-based spatiotemporal scale, and forecast time. Accordingly, a collective and sturdy collation of the ML model's presentation in observance and prediction of groundwater attributes can be exacting. A coherent meta-analysis assembles this study with a pooled summary of various studies and sequels (GRAC 2013). The present chapter fulfills the research gap with a notion of CEBC protocol to coordinate an orderly review of the environment (Agency 2011). In the words of CEBC, a systematized review is a methodological synthesis of resolving the queries in an unbiased mode with precision (Quadri 2017). We intended to resolve the notion of the accuracy of ML modeling for prediction of groundwater resources. Therefore, using meta-analysis, the performance of ML techniques in groundwater studies can be studied well.

5.6 Conclusions and Recommendations

The groundwater systems confer gradual response to the changes occurring in the biome (climate and human) as compared to the subsurface water systems. However, climatic alterations possess a considerable impact on groundwater through changes in groundwater recharge, storage, and use.

Other factors like increased water demand, transformation in land use land cover, and variations in temperature and downpour act as contributing keys to the changes in groundwater complexities. Despite being a resource that is crucial to both socioeconomic development and ecosystem, groundwater mechanism has endured unacknowledged and unsupervised. Groundwater supplies are becoming widely contaminated, and groundwater's crucial environmental functions are being ignored. The organizational structure and the development of institutional capacity for groundwater appear to have serious flaws. To meet this challenge, it will be necessary to have a much greater knowledge of how groundwater contributes to the goals set by state coordination committees for its management and integration structures that facilitate local actions.

The chapter also suggests groundwater observance projects to understand storage and discharge systems which will help in preserving aquatic ecosystems. A thorough appraisal of interactions between various aquifers (including transboundary aquifers) would eventually increase capacity of pumping water from the subterranean waters.

References

Adelana SMA, MacDonald AM (2008) Groundwater research issues in Africa. In: Adelana SMA, MacDonald AM (eds) Applied groundwater studies in Africa. IAH Selected Papers on Hydrogeology, vol 13. Balkema, Leiden, The Netherlands

Akbar TA, Hassan QK, Ishaq S, Batool M, Butt HJ, Jabbar H (2019) Investigative spatial distribution and modelling of existing and future urban land changes and its impact on urbanization and economy. Remote Sens 11(2):105

Environment Agency (2011) Groundwater protection: policy and practice (GP3), part 2—technical framework. Environment Agency, Bristol, UK

FAO (2003) Review of world water resources by country. FAO, Rome. ftp://ftp.fao.org/agl/aglw/docs/wr23e.pdf

Gleick PH (1996) Water resources. In: Schneider SH (ed) Encyclopedia of climate and weather, vol 2. Oxford University Press, New York, pp 817–823

GRAC (2013) Groundwater monitoring in the SADC Region: overview on the current state of national monitoring networks and their future challenges. IGRAC, Delft, The Netherlands, pp 19

MacDonald AM, Calow RC, Nicol A, Hope B, Robins NS (2001) Ethiopia: water security and drought. BGS technical report WC/ 01/02, BGS, Keyworth, UK

MacDonald AM, Bonsor HC, Dochartaigh B, Taylor RG (2012) Quantitative maps of groundwater resources in Africa. Environ Res Lett 7:024009, 7. https://doi.org/10.1088/1748-9326/7/2/024009

Nijsten G-J, Christelis G, Villholth KG, Braune E, Gaye CB (2018) Transboundary aquifers of Africa: review of the current state of knowledge and progress towards sustainable development and man- agement. J Hydrol. https://doi.org/10.1016/j.ejrh.2018.03.004

ORASECOM (2000) Agreement between the governments of the Republic of Botswana, the Kingdom of Lesotho, the Republic of Namibia, and the Republic of South Africa on the Establishment of the Orange-Senqu River Commission. ORASECOM, Gauteng, South Africa

ORASECOM (2017) ORASECOM resolution on nesting the Stampriet Transboundary Aquifer System (STAS) Multi-Country Cooperation Mechanism (MCCM) in ORASECOM. ORASECOM, Gauteng, South Africa

Quadri E (2017) The Mubian sandstone aquifer system: a case of coop-eration in the making. World Water Congress XVI, International Water Resources Association (IWRA), Cancun, Mexico

Taylor RG, Tindimugaya C (2009) Groundwater and climate change: Proceedings of the Kampala Conference, June 2008, IAHS Publ. 334. IAHS, Wallingford, UK

Trenberth KE, Smith L, Qian T, Dai A, Fasullo J (2007) Estimates of the global water budget and its annual cycle using observational and model data. J Hydrometorol 8:758–769

Chapter 6
Chemicals in the Water: A Serious Concern for the Humans and Aquatic Life

Rwitabrata Mallick, Swapnil Rai, Kuldip Dwivedi, Nidhi Shukla, Abhishek Bhardwaj, and Shashank Gupta

Abstract Water is an essential element for life without which the life cannot sustain on the earth. The earth's major part is covered with water which carry maximum biodiversity. The humans, animals and plants of the terrestrial ecosystem depend on freshwater sources which are less than 3% of the total water available on the earth while marine water sources have saline water available in oceans, seas and saline lakes. Both these sources are suffering from contamination by different chemicals. The majority of chemical contamination in water is due to human activities. Human population growth is directly proportional to the degradation of the environment which means mismanaged human activities are causing different types of environmental problems. Out of all environmental problems, contamination of water and degradation of water quality is a big problem for the water resources. It is evident that water has high levels of harmful chemicals like heavy metals, pesticides and volatile organic compounds. These chemicals are now getting accumulated in the plants, humans and animals. In humans, these chemicals get deposited in the tissues and are responsible for the different types of life-threatening diseases. The studies on different water sources including poles and glaciers have shown the presence of different harmful chemicals, and even at some places these are found in high concentration. The people from different parts of the world are suffering from

R. Mallick · S. Rai (✉) · K. Dwivedi · N. Shukla · A. Bhardwaj
Department of Environmental Science, ASLS, Amity University Madhya Pradesh, Gwalior 474005, Madhya Pradesh, India
e-mail: srai@gwa.amity.edu

R. Mallick
e-mail: rmallick@gwa.amity.edu

K. Dwivedi
e-mail: kdwivedi@gwa.amity.edu

N. Shukla
e-mail: nshukla@gwa.amity.edu

A. Bhardwaj
e-mail: akbhadwaj@gwa.amity.edu

S. Gupta
Department of Civil Engineering, ITM University, Gwalior, India

P. Shukla et al. (eds.), *Environmental Processes and Management*, Water Science and Technology Library 120, https://doi.org/10.1007/978-3-031-20208-7_6

various diseases like arsenic poisoning, fluorosis, itai–itai, mercury poisoning, liver failure, nervous system failure and many more. Some of these chemicals are carcinogenic and mutagenic too which is responsible for the different types of cancer and mutation in the body. Therefore, the proper treatment of waste, awareness of people and following the standard guidelines strictly are only the way to reduce the chance of contamination of different water sources by chemicals.

Keywords Water · Diseases · Pesticides · Heavy metals · Degradation · Environment

6.1 Introduction

Humans are the dominant species among all present on the planet. We are trying to control and rule the nature by modifying the natural ecosystems, overexploiting the natural resources and generating huge amounts of waste of all forms. The economic disparities between the nations as well as in the society are also responsible for environmental degradation. The contamination in the air, water and soil is causing many problems for all types of ecosystems including the extinction of species from the earth. The increasing concentration of carbon dioxide in the air is responsible for global warming and climate change that also results from the melting of ice from the cryosphere. The melting of ice from the poles is causing the emission of different gases trapped in the polar reason. All types of water are suffering contamination by chemicals and other types of waste products generated by human activities.

Water contamination can be defined as the changes in the composition of water due to the dumping of waste to an extent which makes it unfit for human uses like drinking/domestic purposes and to support biotic communities, such as fish. The contamination of water also impacts aquatic flora and fauna that survive in the aquatic ecosystem with the effect on individual species or whole populations and biological communities.

The rivers, ponds and lakes are the source of freshwater, facing several problems. The rivers are dying, and lakes are facing the problem of the accelerated rate of eutrophication. Oceans and seas are now acting as dumping grounds for different types of harmful waste especially radioactive waste. The waste from human settlements, agricultural practices, petroleum drilling, landfills, industrial sources, construction sites and mining sites is being dumped into the water bodies which carry different types of hazardous and toxic chemicals to water sources especially rivers, ponds and lakes (Agrawal et al. 2010). Water contaminants are a major threat and cause of global concern which are responsible for detrimental diseases and 14,000 deaths every day (Daniel 2006). Overexploitation of water resources along with other resources and unplanned rapid industrialization is responsible for the fall in the quality of water in most cities with its contamination with many toxicants which are harmful to the health of humans (Jadon et al. 2016).

Excess chemicals in the water bodies reduce the dissolved oxygen in the water which results in the death of the aquatic animals. The major rivers of India like the Ganges and Yamuna are worse polluted with high levels of toxic chemicals in the water. The Yamuna is considered almost a dead river within the Delhi stretch because of DO below 4 ppm. There are reports which show the occurrence of different harmful chemicals like OCPs, VOCs and PAH in the waters of different rivers in India.

Oceans and seas are also facing a similar problem as they are covering a large area of the earth's surface. Most of the world's big cities are situated in the coastal region, and sea routes are also being used to transport goods from one part to the other part of the world. Sometimes, accidents and oil spills also take place which also add harmful chemicals into the marine system. The oceans also receive many harmful chemicals through waste from coastal cities and surface run-off which leads to marine pollution. The oceans are the major sink for CO_2 which is responsible for the acidity of oceans and affects the coral reefs and molluscs. Oil spills are also responsible for the death of many marine animals and birds as it hinders the gaseous exchange in the water.

Groundwater is another source of fresh water on which the majority of the human population is dependent to fulfil their demand. With unplanned construction in the urban areas, overexploitation of groundwater and depletion of recharging points, the groundwater table is depleting rapidly. The quality of groundwater is also diminishing due to landfill sites and open dumping sites of waste which causes the seepage of leachate to the groundwater. The leachate contains different types of toxic chemicals depending on the types of waste on dumping sites. The leachate is highly toxic and contaminates the groundwater badly and causes harmful effects on humans and animals.

6.2 Major Chemicals Toxicants of Water Environment

There are many chemicals' toxicants of the water environment that alter the properties of water as well as get accumulate in humans, animals and plants (Alam et al. 2021). These toxic chemicals disrupt the functioning of important organs of humans and animals as well as disrupt the important process in the plants (Tilwankar et al. 2019a, b). Here, the details of different chemical toxicants of water are given.

6.2.1 Heavy Metals

Heavy metals are the elements that have specific density more than 5 g/cm^3 (Järup 2003) and are important for the metabolic activities of plants and animals in small quantity. It becomes toxic even in low quantity when goes beyond the threshold limit.

The major sources of heavy metals in water bodies are industries, synthetic pesticides, agro-chemicals, run-off water, industrial and domestic waste water, mining

Table 6.1 Effects of heavy metal on humans

Pollutant	Effects on humans	WHO permissible limit (ppm)
Cadmium	Lung problems like cancer, defects of bone, high B.P., kidney disease, gastrointestinal problems, etc	0.06
Lead (Pb)	Infant encephalopathy, mental problems of children, congenial paralysis, kidney and liver diseases	0.1
Copper (Cu)	Damage of liver and kidney, intestinal irritation	0.1
Chromium (Cr)	Nervous system damage, fatigue and irritability	0.05
Zinc (Zn)	Zn fumes may cause corrosive effect on skin, stomach pain, diarrhoea and nausea	15
Mercury (Hg)	Damage to nervous system, protoplasm poisoning, tremors, acrodynia, gingivitis	0.01
Manganese (Mn)	Damage of CNS, insomnia, memory loss	0.26
Arsenic (As)	Bronchitis, vitamin A deficiency, dermatitis	0.02
Fluoride (F)	Dental and skeletal fluorosis	1.5

and natural process like weathering of rock and magma. The main heavy metals are lead (Pb), Ni (Nickel), Zn (Zinc), As (Arsenic), Cu (Copper), Cr (Chromium) and Hg (Mercury) that have many consequences on humans and other living organisms (Lambert et al. 2000). These chemicals got the entry in the environment through the different routes and persist for longer period of time by the process of bio-accumulation and bio-magnification. These chemicals get accumulated in human body through ingestion, inhalation and through the skin and when the levels of these heavy metals increase inside the body, become toxic and risky for the health of humans (Suruchi et al. 2011). The heavy metals once get high concentration in different components of environment, and they pose threat to humans, animals and vegetation. As these chemicals are having role in different metabolic activities if is in trace amount but metals like Pb, Hg, Cu, Cd, As and Cr are toxic in low concentration and affects metabolism of animals and plants including humans. The accumulation of heavy metals in environment is a matter of great concern as there is a contamination of food we eat, the water we drink and the air we breathe (Tilwankar et al. 2018) (Table 6.1).

6.3 Pesticides

The chemicals used to control the different pests, weeds and other disease-causing agents of agriculture and society are called pesticides. These pesticides are belonged to different category depending on its uses for a particular disease-causing agent like insecticides, weedicides, herbicides, fungicide, rodenticide, molluscicides and nematicides for insects, weeds, herbs, fungi, rodents, mollusc and nematodes, respectively (USEPA 2014).

The pesticides are developed to kill the insects-pests in general and are designed to kill only target organism avoiding non-target organisms under standard application methodologies. One of the characteristics of these chemicals is susceptibility to certain toxins which mean a chemical toxic to one living being may also cause poisoning to other forms of life. A large dose of these chemicals is required to harm humans than the target organisms but these are toxic to humans. The doses used in a formulation to kill pests are affecting humans by causing disruption of functioning of hormones, disturbance of metabolic activities and effects on reproductive performance (Munkittrick et al. 2005; Cocco 2002; Massad et al. 2002).

The pesticides act as xenohormones (mimicking the action of endogenous hormones) or otherwise interfere with endocrine processes; hence, they have been collectively categorized as endocrine disruptors (Straube et al. 2003). The development of pesticides increased during World War II to increase the production of food and develop potential chemicals as warfare agents (Gupta et al. 2007). The discovery of insecticidal properties of DDT in 1939 marked growth in synthetic pesticides without the concern about its harmful risk and toxicity to the human health, environment and ecosystem (Unsworth 2010). The aquatic life also gets affected due to these chemicals as these tend to accumulate in the different body tissues of the animals and affect their metabolic activities (Table 6.2).

6.4 Radioactive Waste

The radioactive pollutants are the chemical with an unbalanced number of protons and neutrons resulting in unstable atoms that can emit ionizing radiation like caesium, plutonium and uranium. The radioactive waste is generated by nuclear power plants, mining, industrial, medical and scientific processes and has detrimental impacts on all biological forms. The groundwater is more prevalent for radioactive compounds than surface water as radioactive elements are naturally found in the rocks. A good number of radioactive elements like 3H, 14C, 40K, 210Pb, 210Po, 222Rn, 226Ra, 228Ra, 232Th and 234, 235, 238U are found in the surface and sub-surface water. Uranium, thorium, actinium and radium are the radiotoxic elements of the aquatic system.

Major sources of radioactive waste are nuclear power plants and the research laboratories where research on radioactive substances is being carried out. Cobalt 60, Iridium-192, Caesium-137 and Strontium-90 are the radioisotopes produced by atomic power plants, and 40K and 7Be are the common radioactive elements occurred in wastewater sludge. 40K also occurs in the marine environment while Uranium is also found naturally in oceans as uranyl carbonate ion. The marine environment contamination of radioactive material is due to accidents of nuclear submarines,

Table 6.2 Summary of the different classes of pesticides, their properties and impacts

Types of Pesticides	Physical and Chemical Properties	Exposition	Toxicokinetics	Toxicodynamics
Organophosphorus pesticides	These chemicals are phosphorus containing organic compounds, soluble in organic solvents. Their properties vary according to size and structure	Lungs, conjunctiva, gastrointestinal system	Fast absorption and metabolized by P450-isozyme in Oxon form. Highly toxic	Makes bond with the serine residue at the acetylcholinesterase active site
Carbamate pesticides	Derivatives of ester Melting point ranges from 50 to 150 °C with low vapour pressure and poor volatility	Skin, lungs and gastrointestinal system	Absorbed by organisms with the exception the blood–brain barrier	Carbamylation at active site of Acetylcholinesterase
Organochlorine compounds	Fat-soluble compounds, persistent in the components of environment, fat soluble and semi-volatile	Fatty tissues of body	Approx. 10% of applied dose absorption by organism but accumulate due to lipid solubility	Disrupt the endocrine system and affect the child growth and also cause cancer
Pyrethrin and pyrethroid	Water insoluble, low henry law constant, low vapour pressure, have acid moiety, central ester bond, large octanol water coefficient	Gastrointestinal tracts, skin and lungs	Shows hydrolysis/oxidation by P450 isozymes and fast distribution in the target organisms after absorption	Affects sodium channel, muscular system
Triazines	Persistence in soil depends upon the alkyl chain length, melting point ranges from 133 to 177 °C	Respiratory system, gastrointestinal system, eyes and nose	Dealkylation makes conjunction with glutathione	Not reported yet

(continued)

Table 6.2 (continued)

Types of Pesticides	Physical and Chemical Properties	Exposition	Toxicokinetics	Toxicodynamics
Phenoxy derivatives	Aliphatic carboxylic acid found attached to chloride/methyl substituted aromatic ring, absorption coefficient varies from 76 to 315 L kg^{-1}	Lungs and digestive system	Not stored in target due to fat insolubility, fast dissociation or hydrolyse	Irritation in the respiratory tracts, digestive system, eyes, skin and mucous membrane Damage of cell membrane, uncoupling of phosphorylation
Dipyridyl derivatives	It is a dipyridylium quaternary ammonium, non-volatile with a vapour pressure <0.013 mPa and water soluble	Gastrointestinal system, lungs skin and eyes	Free radicals are produced by biotransformation with liquid peroxidation and cell injury	Due to lipid peroxidation cause tissue damage in liver, lungs and kidney
Glycine derivatives	Sold as iso-propylamine/ammonium salt, have no effect on AChE	Skin and Digestive System	Production of amino-methyl phosphonic acid due to action of glyphosate oxidoreductase	Damage of DNA and uncoupling of electron transport chain
Dithiocarbamates	Zineb and Maneb are identical in structure	Slowly absorb through oral and dermal contact	Formation of ethylene thiourea from dithiocarbamates due to biotransformation	Inhibition of acetaldehyde dehydrogenase, impacts thyroid hormones and thyroid cancer

Ref: Bernardes et al. 2015 *(Source:* https://www.intechopen.com/chapters/48406) dumping of nuclear waste in the deep ocean and nuclear disasters like Colorado, Fukushima and the Chernobyl nuclear disaster.

The permissible limit for the radioactive substance in drinking water should be 0.1 micro sievert/ year as per the guidelines of World Health Organisation (WHO). The United States Environmental Protection Agency (USEPA) guidelines also called as radionuclides rule are as follows:

- 30 μg/litre for uranium
- 4 millirems/year for gross beta emitters
- 5 picocuries/litre for combined radium
- 15 picocuries/litre for gross alpha emitter

The radioactive chemicals/isotopes have harmful impacts on environment and can cause a risk to human health. These chemicals enter into humans through inhalation, polluted water and foodstuff which leads to harmful diseases. In aquatic systems, these chemicals are equally harmful to humans (Madhav and Ritu 2021).

6.5 Conclusion and Recommendation

The chemical contaminants of water are a matter of concern for the proper functioning of the metabolic activities of living organisms. There are many chemical elements that are required in minor amounts for the proper functioning of the cell but beyond the threshold limit, harmful for the functioning of the body. World water is highly contaminated with different chemical toxicants which are deadly for all forms of life. The apocentric view of humans is also responsible for the deterioration of the water environment. The aquatic animals are under threat due to the dumping of chemical waste and humans get indirect exposure to these elements through drinking water as well as agricultural products. There is a need of the hour to increase awareness among the mass for the conservation of water resources from chemical toxicants. There should be proper execution of prevailing policy and guidelines for the dumping of waste in the water bodies.

References

Agrawal A, Pandey R, Sharma B (2010) Water pollution with special reference to pesticide contamination in India. J Water Resour Prot 2(5):432–448. https://doi.org/10.4236/jwarp.2010.25050

Alam Sadre, Rai S, Singh GK (2021) A review on pesticides in Yamuna river and its impact on vegetables grown nearby areas. Plant Arch 21 (Supplement 1):1791–1797

Bernardes FF, Pazin M, Pereira Cristina L, Dorta DJ (2015) Impacts of pesticides on environmental and human health: In: Toxicology studies: cell drugs & environment. https://doi.org/10.5772/59710. https://www.intechopen.com/chapters/48406

Cocco P (2002) On the rumors about the silent spring. Review of the scientific evidence linking occupational and environmental pesticide exposure to endocrine disrupting health effects. Cadernos Saúde Pública 18(2):379–402

Daniel PH (2006) Investing in tomorrow's liquid Gold, 19 April 2006. http://finance.yahoo.com/columnist/article/trenddesk/pp3748

Gupta PK (2007) Toxicity of herbicides. In: Gupta RC (ed) Veterinary toxicology: basic and clinic principles. Elsvier, USA, pp 567–586

Jadon NK, Sharma H, Rai S, Pandey A (2016) Quality and risk assessment of drinking water of Gwalior city, India. Int J Sci Res Growth 1(2):76–81

Järup L (2003) Hazards of heavy metal contamination. Br Med Bull 68(1):167–182

Lambert M, Leven BA, Green RM (2000) Environmental science and technology briefs for citizens. Kanas State University, Manhattan

Madhav S, Misra Ritu (2021) Radioactive pollution in water: A global concern for human health. Down to Earth: https://www.downtoearth.org.in/blog/water/radioactive-pollution-in-water-a-global-concern-for-human-health-80637

Massad C, Entezami F, Massade L, Benahmed M, Olivennes F, Barouki R, Hamamah S (2002) How can chemical compounds alter human fertility? Eur J Obstetrics Gynecol Reproductive Biol 100(2):127–137

Munkittrick KR, Servos MR, Parrott JL, Martin V, Carey JH, Flett PA, Potashnik G, Porath A (2005) Dibromochloropropane (DBCP): a 17-year reassessment of testicular function and reproductive performance. J Occupational Environ Med 37(11):1287–1292

Straube E, Straube S, Straube W (2003) Hormonal disruption in humans. In: Pimental D, Cook JL, Baumann P, Jackmang JA, Stevenson D (ed) Encyclopedia of pest managaement, College Station

Suruchi, Khanna P (2011) Assessment of heavy metal contamination in different vegetables grown in and around urban areas. Res J Environ Toxicol 5:162–179

Tilwankar V, Rai S, Bajpai SP (2018) A review on contamination profile of heavy metals and their role in the environment. Plant Arch 18(2):1239–1247

Tilwankar V, Rai S, Bajpai SP (2019a) The trend of Heavy metals in soil and vegetables from industrial areas of Bhopal. Indian J Environ Prot 39(4):359–263

Tilwankar V, Rai S, Bajpai SP (2019b) Seasonal profile of heavy metals in the water samples of Bhopal Industrial area. Indian J Environ Prot 39(8):758–762

USEPA (United States of Environmental Protection Agency). About pesticides. U.S. EPA. http://www.epa.gov/pesticides/about/index.htm. 27 Aug 2014

Unsworth (2010) History of pesticides use. International Union of pure and applied chemistry (IUPAC). http://agrochemicals.iupac.org/index.php?option=com_sobi2Task=sobi2Details&catid=3&sobi2ld=31

WHO/FAO (2007) Joint FAO/WHO Food Standard Programme Codex Alimentarius Commission 13th Session. Report of the Thirty-Eight Session of the Codex Committee on Food Hygiene, Houston, United States of America, ALINORM 07/ 30/13

Chapter 7
Potential Impacts of Climatic Changes and Human Activity on Water Quality

Nidhi Shukla, Shashank Gupta, and Swapnil Rai

Abstract The term "climate change" refers to the changes in weather patterns brought on by an increase in the atmospheric concentration of gases that absorb heat. In response to human activity, CO_2 levels in the atmosphere have steadily increased, with the associated "greenhouse" effect possibly altering future climate on both global and regional scales. The greenhouse effect's climatic and hydrological consequences have been studied for some time, but researches on water quality have just lately begun. The quality of water may be influenced in a number of ways. Securing access to high-quality water for its numerous purposes becomes more challenging and pertinent as a result of climate change's impact on long-standing, conventional methods of managing water resources and disruptions to the hydrologic cycle. Higher water temperatures may hasten biological metabolic processes while also affecting stratification, sediment nutrient release, and ice conditions in water bodies. Changes in precipitation volume and distribution will affect runoff conditions. Changes in runoff will affect nutrient loads from non-point sources as well as the residence duration of water system. All of the aforementioned elements may have a substantial impact on the eutrophication of standing waters. Higher CO_2 levels in the atmosphere may have a direct influence on the inorganic carbon system of waters' chemical equilibrium processes. Groundwater is a vital resource, which is used for a range of human activities as well as maintaining natural flows in rivers and other ecosystems. However, a number of human activities are rapidly deteriorating these limited resources, and a variety of natural (geogenic) water quality issues limit its use in some areas.

Keywords Climate change · Water quality · Human activities · Water contamination · Groundwater

N. Shukla (✉) · S. Rai
Department of Environmental Science, Amity University Madhya Pradesh, Gwalior, Madhya Pradesh, India
e-mail: nshukla@gwa.amity.edu

S. Gupta
Department of Civil Engineering, ITM University, Gwalior, Madhya Pradesh, India

P. Shukla et al. (eds.), *Environmental Processes and Management*, Water Science and Technology Library 120, https://doi.org/10.1007/978-3-031-20208-7_7

7.1 Introduction

Climate change is disrupting ecosystems and daily life. It is described as changes in weather patterns induced by rising gas concentrations in the atmosphere that absorb heat. The devastating effects on water resources, which have recently become increasingly important due to water shortages in many parts of the world, are one of the catastrophes of this event. The impact of the climate change on temperature and precipitation on runoff volume, as well as the transit and dilution of pollutants, might all be affected (Luo et al. 2013; Barrow et al. 1996). A rise in temperature directly affects the rate of chemical processes, which is frequently followed by a decline in water quality and modifications to the aquatic ecosystem. Increasing flow rates may have an impact on the rate of sedimentation, altering the geomorphology and structure of the rivers and jeopardizing the availability of drinking water. According to climate change predictions, droughts will become more severe and floods will be more damaging, leading to unmanageable water inflow coming from various urban areas towards riverine bodies (Rehana and Mujumdar 2011; Whitehead et al. 2009). Low flow rates raise the possibility of a potentially hazardous algal bloom by limiting the amount of oxygen that the algae can get. Increasing water velocity, decreasing water detention time, and lowering dissolved oxygen levels are all variables in rivers and lakes. As a result of the increased soluble organic matter and colour, flows from upstream areas may have an influence on the quality of water resources, particularly rivers. Despite the fact that climate change's implications on water supplies have gotten a lot of attention, current estimates are frequently understated and little knowledge about the repercussions in water quality brought on by climate change (Marzouni et al. 2014).

For the whole ecosystem and human civilization, water is the most significant resource, and its availability must be managed in a fair, stable, and productive manner (Gain et al. 2016). But, presently this natural resource is becoming more and more scarce and contaminated for human civilization worldwide (Mishra et al. 2021). A growing global population and climate change are making the world's water availability worse. More than 1.1 billion people throughout the world are unable to have clean potable water, and almost 2.5 billion are unable to access the basic sanitary facilities (AWDO 2016). A consistent and hygienic supply of drinking water is crucial for the human survival on this planet in order to maintain good health. Areas with less rainfall are highly exposed to severe climatic variation and changes in land-use pattern. Increasing human demand undermines the capacity to supply appropriate water supplies and the functioning of ecosystem services. Water pollution has become a global problem with the enhancement of economical and anthropogenic activities (Chellaney et al. 2011). Groundwater is one of the most extensively distributed and valuable natural resources for municipal, agricultural, industrial, and environmental applications. The impact of groundwater withdrawals on water levels in surrounding wells or wetlands, the migration of pollutants or saltwater towards wells, and the lowering of flow in neighbouring streams must all be considered when studying groundwater systems (Lapwortha et al. 2022). Numerous of these uses place stress on water resources, which is probably made worse by climate change. Climate change is the statistical variation in weather patterns that occurs over an extended period of time. Both natural and man-made processes have been recognized as climate change causative agents. These factors are called climate forcing or forcing mechanisms (Perera 2018). Natural factors leading to climate change are biotic processes, variation in solar radiation received by earth, plate tectonic, and volcanic eruption. The anthropogenic forcing mechanism leading to climate change is caused by human influences. One of the most serious factors contributing to climate change is the increase in atmospheric CO_2 levels owing to emissions from fossil fuel burning and industrial activity (Gornall et al. 2010). Other human factors include land use, faulty agricultural practices, ozone depletion, deforestation, and over-exploitation of available resources. The ecosystem suffers the effects of climate change, including unpredictable weather, altered ecosystems, and risks to human health and civilization. Climate change is also influencing the water quality of both inland and coastal water resources. Water resources are very essential for the normal functioning of the ecosystem. Human survival depends largely on water resources. Climate change influences water resources because of its impact on precipitation quality, variability, timing shape, and intensity. Climate change has its projected effect on the physical and economic status of water reservoirs. Water resources are being impacted by significant climatic changes, including increased evaporation, increased rainfall, less snowfall, higher water temperatures, earlier and shorter runoff seasons, and a reduction in the quality of both inland and coastal water reserves (Hakeem et al. 2020). Quality of water could suffer in areas experiencing increased rainfall. Higher precipitation has a detrimental impact on water infrastructure since sewage systems and water treatment plants are overburden as a result of the increased volume of water.

7.2 Water Contamination

Whenever rainfall is heavy, the runoff into lakes, rivers, streams increases with a high amount of trash, nutrients, animal faeces, and other types of contaminations and pollutants. This turns water supplies harmful and unusable, and a proper remedial process of water treatment is required (Cui et al. 2020). In many areas, high losses of water like evaporation create water scarcity. In the summer season as the temperature rises, this water scarcity occurs which leads to lower water content in the soil which ultimately results in severe conditions of drought. As a result of climate change, droughts will become more frequent and severe, providing significant management problems for water resource users (Delpla et al. 2009). Especially in India where most of its development depends on agriculture is particularly vulnerable to this situation because here the agricultural sector is largely dependent on natural water precipitation. Freshwater resources near beaches are threatened by the rising sea levels. As the water level rises in the sea, the chances of moving salt into freshwater also rise (Li et al. 2020). This situation creates a problem with the supply of drinking water, and the managers either need to find other sources of freshwater or desalination, i.e. removal of salt from the water is required on a high scale. The use of freshwater from river streams for household or industrial purposes will lead to saltwater moving further upstream (Cosgrove and Louck 2015). Droughts can deplete freshwater supplies in the river, making coastal water resources more saline. Even the water infrastructure built in coastal cities like sewer systems, water supply systems, water treatment facilities are at risk with the rise of sea levels and the surges that may create in storm conditions may damage them (Xia et al. 2014). The high water temperatures also decrease dissolved oxygen (DO), increase the pH of increasing, resulting in more acidic water. Decreased DO solubility is associated with increased assimilation of DO in the biodegradation of organic matter by microorganisms. The principal sources of organic matter in the water bodies are dead and decaying organic matter, runoff water from the agricultural lands, and soil leaching. Degrading and dissolved organic matter affects the water quality and aquatic ecosystem through its influence on acidity, trace metal transport, light absorbance, photochemistry, energy, and nutrient supply. Water quality and the aquatic environment are impacted by degrading and dissolved organic matter due to their effects on pH, photochemistry, energy, and nutrition availability. Many potential factors like air, temperature, and increase in rainfall intensity, atmospheric CO_2 increase, and decline in acid deposition change the amount of dissolved organic matter available in water bodies. Significant hydrological changes, an increase in water temperature, and an increase in pollution load may all be consequences of climate change either chemical or microbiological. Weather seasonality affects the quality of water bodies, which has a substantial impact on their nutrient patterns (Mujere and Moyce 2017). Even the temperature rises of the environment results in degradation of water quality of ponds and rivers with increased thermal stability and changed mixing patterns, which results in a reduction of oxygen concentration and the phosphorus release is increased from the sediments. A warmer temperature will have indirect consequences on water bodies, such as increasing the amount of nutrients in groundwater and surface water, which will negate the effects of measures that reduce external nutrient loading. The release of nitrogen, phosphorus, and carbon as well as the mineralization of soil organic matter will all be accelerated by rising temperatures (Prathumratana et al. 2008). Additionally, higher runoff and erosion due to increased precipitation intensity accelerate the transmission of pollutants, especially during a drought period. Higher ammonium concentrations may be detected in rivers that have less diluting capability as a result of droughts. Due to the decreasing oxygen levels in the bottom waters, it is anticipated that the release of phosphorus from bottom sediments in stratified lakes will rise. These habitats are affected by climate change in a variety of ways: temperature, ice, wind, and precipitation changes (Kiedrzynska et al. 2015). The amount of phosphorus loading in the water bodies is determined by the discharge carried by heavy rainfalls. Climate change will likely lead to a rise in phosphorus loading exports, which is controlled by discharges following significant rainfall, which will have an effect on lakes. In the limnetic zone, phosphorus loading increases due to the death and decomposition of organisms by microbes. But nitrogen content in water bodies is not dependent upon stream flow. It is anticipated that the nitrogen concentration would change as the temperature increased. Higher denitrification as a result of temperature change leads to increased nitrogen losses in soil and surface water upstream.

As water temperature changes, precipitation intensity increases, and extended periods of low flows occur, several types of water pollution, such as increased flow of sediments, nutrients, dissolved organic matter, pathogens, pesticides, salt, and thermal pollution, are likely to rise. The increased flow of sediment and dissolved organic matter and nutrients will assist algal blooms, bacterial biomass, fungus, and plant materials. Eutrophication is defined as excessive plant and algal development and is brought on by an increase in the availability of one or more factors that limit growth, such as nutrients, sunshine, and carbon dioxide (Alexandra et al. 2020). By releasing nutrient-limiting substances from both point and non-point sources, like nitrogen and phosphorus, man-made activities have accelerated eutrophication's rate and range. These types of point and non-point discharge caused due to runoffs from agricultural fields are mixed with several pollutants like chemical fertilizers and pesticides, industrial and sewage disposal (Xia et al. 2020). Freshwater resources, aquaculture, and water amusement parks, all suffer as a result of eutrophication. This affects the quality of drinking water like foul-smelling, increase in phytoplankton and blooms of noxiousness, and reduction of water clarity. The growth and development of organisms in the littoral zones are hampered by the algal blooms, which reduce light penetration in water bodies. Additionally, during the day time, high rates of photosynthesis brought on by eutrophication can deplete dissolved inorganic carbon and increase pH to dangerous levels. By diminishing chemosensory abilities, increased pH can render blind species that depend on detecting dissolved chemicals for survival. When dense algal blooms die, microbial decomposition reduces the amount of dissolved oxygen, creating a hypoxic or anoxic "dead zone" where the majority of species cannot survive. Hypoxia and anoxia caused by eutrophication continue to be a threat to commercial and recreational fisheries all over the world. Some algal blooms also act as potential harmful agents because they produce toxic substances like microcystin and anatoxin-a. Toxic cyanobacteria like *Microcystis, Anabaena, Oscillatoria,* and *Cylindrospermopsis* with their inherent superior efficiency they tend to dominate freshwater systems enriched with nutrients under certain physico-chemical conditions (Miruka et al. 2021). Toxic cyanobacterial blooms have poisoned wildlife, farm animals, and even people. This bacterium is also responsible for many off-flavoured compounds like methylisoborneol and geosmin that are found in drinking water systems. They are also affecting the aquaculture-raised fishes, due to which state and regional economies face large financial loss. Modern-day agricultural system relies on the use of excessive chemical fertilizers and pesticides for increasing crop productivity and resistance to insect pests. The runoff from agricultural fields and eroding soils can carry pesticides into aquatic environments. The residues of pesticides have been detected in rain, river, ground, and drinking water; also among these, the surface water resources act as significant receptors of pollution created by various pesticides. The fate of pesticides in water bodies is influenced by climate drivers like change in rainfall seasonality, intensity, and increased air temperature. The physico-chemical interactions between aquatic organisms and pesticides depend upon the climatic condition and quality of water bodies. Variations in soil water content have been found to alter the structure of the soil's organic matter, which interferes with the pesticides' ability to diffuse and become trapped in the soil. With the increase in industrialization, the discharge of industrial waste containing metals has also increased during the past few decades. Seasonal variations influence the concentration of these metals in river bodies. Metals are known to interact with the suspended particulate matter of the water and get adsorbed on them. The mobilization of trace elements in soils and water can benefit greatly from these organic and inorganic collisions (Kaur and Sinha 2019).

The heavy flow of sediments and nutrients caused by the events of heavy rainfall will also be an additional overload to the sewer systems and wastewater treatment plants. Areas such as semi-arid areas facing drought situations will have a problem of low flows in streams of water. As low flows become more typical, contaminant diluting capabilities will be reduced, resulting in higher pollutant concentrations, including illness. Areas with overall decreased runoff lead to increasing evapotranspiration which ultimately increases the salination of the groundwater. This increase in salination may also be a cause of lower levels of water in streams which increases estuaries. More evapotranspiration also leads to lower infiltration and reduction of groundwater recharge. This will minimize subsurface salt mobilization, perhaps counteracting the effect of lower salt dilution in estuaries. Storm water drainage and sewage disposal are also some of the negative effects of rising sea levels in coastal areas. While in the aquifers present in coastal areas, saline water intrusion into fresh groundwater will become more widespread, posing a hazard to groundwater resources. An increase in the rate of precipitation and its intensity leads to lower water quality because high runoff will result in soil erosion and transport high number of pathogens and other dissolved pollutants like chemical fertilizers and pesticides to the surface water and groundwater; this, in turn, leads to mobilization of adsorbed pollutants such as heavy metals and phosphorus. Another reason for highly intensive precipitation leading to more pollutants could be because of suspended solids whose presence will increase in lakes and reservoirs due to soil fluvial erosion (Alam et al. 2021). This change in quality and increase of microorganisms can deteriorate human health and also the ecosystem.

In recent time, one of the highly contentious issues pertaining to river water quality has been Ganga River's contamination. The river has grown significantly contaminated as a result of unchecked household sewage discharge without treatment, excessive industrial pollution discharge, agricultural runoff, and other issues. The Ganga Action Plan (GAP) was created in 1986 with the objective of improving the water quality to that of a "Bathing Class". Individual companies are required to employ centralized monitoring systems and several sewage treatments plants, as well as common effluent treatment plants in places with enterprises are created under GAP. The pulp and paper industries, as well as the tannery, sugar, and distillery sectors, are the biggest polluters of the Ganga River. The primary pollutants produced by these industries include solids, total nitrogen (TN), chromium, sulphide, sulphate, and chloride, as well as biochemical oxygen demand (BOD), chemical oxygen demand (COD), and sulphate and chloride. Furthermore, because agricultural land makes up a large amount of the river's catchment area, nutrient contamination (nitrogen N and phosphorus P) becomes an issue (Santy et al. 2020).

7.3 Conclusion and Perspective

Climate change is a challenging phenomenon nowadays worldwide leading to irrational weather changes. Water quality is being impacted by the climate change phenomena, and the deterioration of drinking water quality is increasing the danger of extreme climatic events having a negative impact on health. Due to rising temperature (in the water, air, and soil), as well as heavy precipitation, certain water quality metrics, such as dissolved organic matter, micro-pollutants, and pathogens, are prone to concentration increases.

The waste arising from industries, emissions from the transport sector (surface, air, water) municipal sewage sludge, and agriculture runoff needs to be reduced and managed in such a way as to minimize global warming phenomena. Changing the scenario of climate leading to a drastic change in weather cycles demands the urgent attention of the planners, technologists, and social workers for the benefit and welfare the humanity. In order to identify health concerns, take corrective and ameliorative measures; we needed tools for water quality monitoring, predicting models, and decision support system immediately. These alarming situations require and force society to adopt sustainable development practices in the different field of industry, agriculture, and transport sector to control future global warming and climatic challenges and to compensate for the damages caused until now.

Global change has a direct impact on the chemical processes occurring in sediment and the water column, and because higher temperatures hasten biological processes, climate warming is a direct result of this impact. Nitrification and denitrification, for example, are biological reactions that are intimately tied to temperature. Climate change-related changes in hydrology have an indirect impact on physico-chemical water quality. Increased and more intense precipitation is projected to enhance nutrient runoff from agricultural fields into surface waterways.

Several aspects of climate change affect the distribution and mobility of hazardous chemicals in freshwater systems (e.g. temperature increases, fluctuations in rainfall and runoff).

Hazardous substance loading may increase as a result of sewage overflows, as well as increased pesticide use and runoff as a result of heavy rains, while higher temperatures accelerate the degradation of some pesticides and organic pollutants, potentially lowering their concentrations in rivers and lakes. As a result, the overall impact of climate change on dangerous compounds remains unknown.

According to widely recognized climate change projections, the summer will witness an increase in droughts and flash floods, which will result in unchecked outflow from metropolitan areas into receiving water courses and estuaries. In rivers and lakes, reduced flow and lower velocities lead to prolonged water residence times, which increase the danger of harmful algal blooms, and lowers dissolved oxygen levels. In order to prevent dangerous by-products from entering public water sources, water treatment facilities may need to intervene when dissolved organic carbon and colour levels in upland streams increase. Drought periods will cease when storms wash minerals out of the urban and rural areas and cause acid pulses in acidified highland catchments. Freshwater quality will be significantly impacted by policy responses to climate change, such as the adoption of biofuels or emission restrictions.

References

Alam S, Borthakur A, Ravi S, Gebremichael M, Mohantya SK (2021) Managed aquifer recharge implementation criteria to achieve water sustainability. Sci Total Environ 768:144992

Alexandra M, Heléne Ö, Viklander MM (2020) The pollution conveyed by urban runoff: a review of sources. Sci Total Environ 709:136125

Asian Water Development Outlook (AWDO) (2016) Strengthening water security in Asia and the Pacific. Accessed on 27 Aug 2018. Available online: https://www.adb.org/publications/asian-water-development-outlook-2016

Barrow E, Hulme M, Semenov M (1996) Effect of using different methods in the construction of climate change scenarios: examples from Europe. Clim Res 7(3):195–211

Chellaney B (2011) Water: Asia's new battleground. Georgetown University Press, Washington, DC, USA

Cosgrove WJ, Louck DP (2015) Water management: current and future challenges and research directions. Water Resour Res pp 4823–4839

Cui Y, Liao Z, Wei Y, Xu X, Song Y, Liu H (2020) The response of groundwater level to climate change and human activities in Baotou City, China. Water 12:1078

Delpla I, Jung AV, Baures E, Clement M, Thomas O (2009) Impacts of climate change on surface water quality in relation to drinking water production. Environ Int 35:1225–1233

Gain AK, Giupponi C, Wada Y (2016) Measuring global water security towards sustainable development goals. Environ Res Lett 11(124015):1–13

Gornall J, Betts R, Burke E, Clark R, Camp J, Willett K, Wiltshire A (2010) Implications of climate change for agricultural productivity in the early twenty-first century. Philos Trans R Soc Lond B Biol Sci 365(1554):2973–2989

Hakeem KR, Bhat RA, Qadri H (2020) Concerns and threats of contamination on aquatic ecosystems. Bioremediat Biotechnol, pp 1–26

Kaur T, Sinha AK (2019) Pesticides in agricultural run offs affecting water resources: a study of Punjab (India). Agric Sci 10:1381–1395

Kiedrzynska E, Kiedrzy´nski M, Zalewski M (2015) Sustainable floodplain management for flood prevention and water quality improvement. Nat Hazards 76:955–977

Lapwortha DJ, Boving TB, Kreamerc KDK, Smedleye PL (2022) Groundwater quality: global threats, opportunities and realising the potential of groundwater. Sci Total Environ 811:152471

Li X, Zhang L, O'Connor PJ, Yan J, Wang B, Liu DL, Wang P, Wang Z, Wan L, Li Y (2020) Ecosystem services under climate change impact water infrastructure in a highly forested basin. Water 12:2825

Luo Y, Ficklin D, Liu X, Zhang M (2013) Assessment of climate change impacts on hydrology and water quality with a watershed modeling approach. Sci Total Environ 450–451:72–82

Marzouni MB, Akhoundalib M, Moazed H, Jaafarzadeh N, Ahadian J, Hasoonizadeh H (2014) Evaluation of Karun river water quality scenarios using simulation model results. J Adv Biol Biomed Res 2(2):339–358

Miruka JB, Getabu A, Sitoki L, James O, Mwamburi J, George O, Chrisphine N, Odoli C (2021) Water quality, phytoplankton composition and microcystin concentrations in Kisumu Bay (Kenya) of Lake Victoria after a prolonged water hyacinth infestation period. 26(4). https://doi.org/10.1111/lre.12380

Mishra BK, Kumar P, Saraswat C, Chakraborty S, Gautam A (2021) Water security in a changing environment: concept, challenges and solutions. Water 13(490):1–21

Mujere N, Moyce W (2017) Climate change impacts on surface water quality. https://doi.org/10.4018/978-1-5225-1607-1.ch012

Perera F (2018) Pollution from fossil-fuel combustion is the leading environmental threat to global pediatric health and equity: solutions exist. Int J Environ Res Public Health 15(16):1–17

Prathumratana L, Sthiannopkao S, Kim KW (2008) The relationship of climatic and hydrological parameters to surface water quality in the lower Mekong River. Environ Int 34(860):1–6

Rehana S, Mujumdar PP (2011) River water quality response under hypothetical climate change scenarios in Tunga-Bhadra river, India. Hydrol Process 25(22):3373–3386

Santy S, Mujumdar P, Bala G (2020) Potential impacts of climate and land use change on the water quality of Ganga river around the industrialized Kanpur Region. Sci Rep 10:9107. https://doi.org/10.1038/s41598-020-66171-x1

Whitehead PG, Wilby RL, Battarbee RW, Kernan M, Wade AJ (2009) A review of the potential impacts of climate change on surface water quality. Hydrol Sci 54(3):101–123

Xia XH, Wu Q, Mou XL, Lai YJ (2014) Potential impacts of climate change on the water quality of different water bodies. J Environ Inform, pp 1–14

Xia Y, Zhang M, Tsang DC, Geng N, Lu D, Zhu L, Igalavithana AD, Dissanayake PD, Rinklebe J, Yang X, Ok YS (2020) Recent advances in control technologies for non-point source pollution with nitrogen and phosphorous from agricultural runoff: current practices and future prospects. Appl Biol Chem 63(8):1–13

Chapter 8
Groundwater Vulnerability Assessment Using Drastic Method: A Case Study of Bhilwara District, Rajasthan

Shally Saini

Abstract Globally, groundwater (GW) is a significant source of fresh water utilized in home, commercial, industrial, and other applications, as well as in ecosystem support. As a result, Rajasthan, a desert state in India, has experienced groundwater quality issues caused by both man-made contaminants and naturally occurring hazardous minerals. With a land size of 10,445.1 square kilometers, the Bhilwara district is situated in southern Rajasthan. Since groundwater contamination will directly influence human health, it is important to evaluate how it is affected by the availability of minerals, the rise in anthropogenic activities, and the number of mining companies. The DRASTIC model, based on a geographic information system (GIS), was used in this study to create a susceptibility vulnerability map of the groundwater system. Adding Land Use (LU) maps from the research area has further upgraded the DRASTIC maps. Using a technique called hotspot mapping, it is possible to forecast how many significant hotspots will be present in the area under study and to find the sources of contamination. The water quality index and overlay approach were also used to understand the state of vulnerability better. The results showed that the index value has seven subclasses and spans from 100 to 205. The DRASTIC and DRASTIC–LU maps were linked with the nitrate concentration map for validation. It was discovered that the Sahara, Mandal, and Raipur blocks are particularly susceptible to the rapid increase in nitrate concentration. The highest percentages of TA, TDS, and NO_{3-} (100%) are found in the entire dataset.

Keywords Groundwater vulnerability · DRASTIC · Rajasthan · Land use

8.1 Introduction

To raise awareness of the condition of groundwater, the word vulnerability was first used in France in 1960 (Vrba and Zoporozec 1994). Across several segments of the globe, groundwater is an important resource of drinking water. A significant health

S. Saini (✉)
Hydrological Investigation Division, National Institute of Hydrology, Roorkee, Uttarakhand 247667, India
e-mail: sainishally64@gmail.com

P. Shukla et al. (eds.), *Environmental Processes and Management*, Water Science and Technology Library 120, https://doi.org/10.1007/978-3-031-20208-7_8

risk will result from GW becoming polluted. All around the world, especially in rural areas, emerging nations, numerous megacities, and industrialized regions, it is a vital source of water supply. Through farming, industrialization, garbage disposal, sewage, and the leaching of pesticides and fertilizers, it has succeeded in getting more and more contaminated every day. According to Rao and Mamatha (2004), biological, organic, and inorganic processes are responsible for contaminating 70% of the nation's surface water resources.

India has 3.287 million km^2 of land area and surpassed one billion people in population in 2000. The amount of precipitation that falls on average each year is roughly 4000 km^3, of which 700 km^3 directly evaporates, 1150 km^3 flows by way of superficial water, and the residual 3000 km^3 infiltrates into the soil, of which 2150 km^3 is used to compensate for the soil's lack of moisture, 1650 km^3. The other 500 km^3 is utilized only to fill the groundwater reservoir (Singh et al. 1997).

690 km^3 of India's yearly water resources are surface water, while the remaining 450 km^3 are groundwater. Together, these 1140 km^3 of water resources can be used annually. Approximately 84% of the overall water used in the nation is castoff for irrigation, followed by roughly 4.4% for drinking water and community use, 4% for commerce, 3.6% for the creation of new energy sources, and the remaining 4% for other services. By 2025, the country would require approximately 1050 km^3 of water yearly due to the rising demand for water needed to cultivate supplementary sustenance ounces for the expanding inhabitants, which is anticipated to grasp up to 1.25 billion people by that time. Year 2000 saw a 750 km^3 annual water requirement for India.

Ajmer, Rajsamand, Bundi, and Chittorgarh are to the north, west, east, and south, respectively, of Bhilwara, which has a population of 20,13,789 (Hydrogeological Atlas in Rajasthan, Bhilwara District 2001). Several mining companies are currently operating in the area, which has been reported to contain a range of minerals, including lead, zinc, soapstone, China clay, feldspar, quartz, garnet, silver, beryllium, mica, asbestos, barite, agate, and kyanite (district survey) disclosed in 2017 Since there are many minerals available and mining and anthropogenic activities are expanding daily, it is crucial to establish the impact on water quality because groundwater pollution directly affects human health. People should take precautions because, according to WHO (1998), water-borne diseases are the primary cause of most illnesses affecting humans. It is also impossible to exaggerate how crucial it is to safeguard water supplies and give people access to high-quality water that will meet their needs after seeing this scene. The appropriate steps must be taken in order to appropriately plan, develop, conserve, and manage the existing water resources.

8.1.1 Scope of the Work

According to earlier studies, the Bhilwara district has not yet had its risk assessed, despite the fact that the entire region is undergoing tremendous economic growth and advancement. Due to extensive urbanization and mining operations, the possibility of groundwater contamination has dramatically increased in this region. The fact that the aquifer is the only substantial source of water supply for all kinds of needs in the examined area contributes to the development of a sufficient understanding of the aquifer's health and groundwater quality. With a focus on the DRASTIC model, the current work will review the methods already in use for assessing groundwater vulnerability before using them to determine the susceptibility of groundwater in the Bhilwara district.

8.1.2 Objectives

The prime objective of current investigation is to evaluate the groundwater vulnerability of Bhilwara district, Rajasthan, India, using DRASTIC method. The specific objectives are as follows:

- To evaluate the susceptibility of groundwater to contamination using DRASTIC model for Bhilwara district.
- To explore comparison between DRASTIC and modified DRASTIC model after integrating Land Use attribute.
- To explore the water quality (WQ) status of the region by estimating the violations in standards and calculating WQ Index to interpret the pollution scenario of the region through overlaying of various thematic maps.

8.2 Study Area

8.2.1 General Depiction

Bhilwara, the southernmost district of Rajasthan, is encircled by other districts in all four directions. It has a topographical area of 10,445.1 km^2, located between the latitudes of 25° 00′ 38.87″ and 25° 57′ 53.70″ N and 74° 00′ 31.67″ and 75° 27′ 46.25″ E. Overall, it has 11, 1753 towns and villages. With lows as low as 7.3 °C in January and highs as 46 °C in June, January is the district's coldest month. August has the greatest relative humidity of any month (79.30%). April has the lowest relative humidity of any month (18.71%). August is the month with the most days with rain (17.43 days). December had the fewest days with precipitation (0.57 days). The difference in precipitation between the wettest and the extremely dry month is 245 mm (10 in.).

8.2.2 Topography

This district is rectangular in shape with undulating plains where western portion is broader than the eastern one. The hills that are in the southeastern and western direction follow a trend from northeast to southwest. Banas River enters the Bhilwara district, flows from west to east, and exits from South West (SW) to North East (NE).

8.2.3 Geological Setup

Out of the four Supergroups, the Bhilwara Supergroup occupies the most land. Along the major boundary fault, a few conglomerates and shale, sandstone, and limestone make up the Vindhyan Supergroup. The Proterozoic-aged Delhi Supergroup comprises two groups, Gogunda (a larger group than Kumbhalgarh Group) and its equal, the Alwar Group. West of the district is where the Paleoproterozoic Aravalli Supergroup is exposed. It is represented by the Dovda Group and characterized by metamorphic rocks that underwent amphibolite metamorphism under the influence of greenschist facies. The Sandmata Complex, Hindoli Group, Mangalwar Group, Jahazpur Group, and Pur-Banera Group all comprise the Bhilwara Supergroup. The location map of study area is shown in Fig. 8.1.

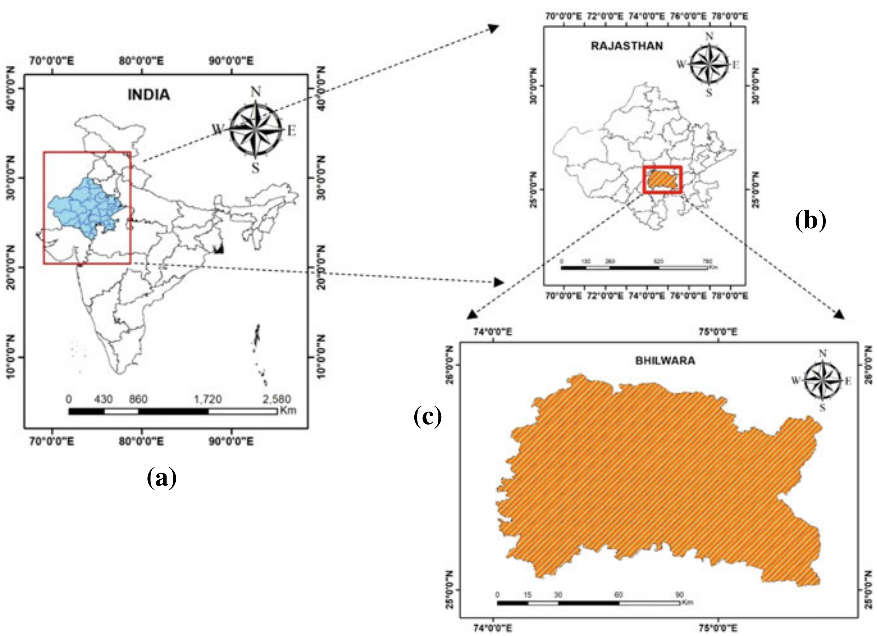

Fig. 8.1 Location map of study area: **a** India, **b** Rajasthan, and **c** Bhilwara

8.2.4 Hydrogeology

The literature of the Bhilwara region revealed the existence of two aquifer systems, the first phreatic in nature and the other non-homogeneous and distributed isostatically throughout the territory. Weathered gneisses make up the top layer of the substratum in the center. Most likely, the northernmost section is coated in weathered gneiss beneath a thin layer of alluvium. Major formations that include water include gneisses and schist. Muscovite schist develops foliation, and irregular joints are invaded by granite, pegmatite, and quartz veins due to temperature and pressure changes. The contact between these intrusive and schists creates a beneficial conduit for groundwater circulation.

8.3 Methodology

8.3.1 Introduction

The assumptions on which the DRASTIC method is based are:

1. GW pollution follows at the surface of the ground.
2. Contaminants are brought into groundwater by rainwater.
3. It has the freedom of movement to water.
4. The mapping zone assessed by means of DRASTIC should be 0.4 km^2 or more than this (Aller et al. 1987).

8.3.2 Procedure

- The final vulnerability map, which is known as a DRASTIC map, is the combinations of initial letters of all seven parameters that have been created in different steps of the procedure given below:
- The extent to the hydrological parameters such as water table, recharge, and type of aquifer media, soil type, local topography, rainfall statistics, and hydraulic conductivity are taken into account while making a map for each attribute. Combining these parameters in the spatial database will produce the DRASTIC INDEX map. Further reclassification of the DRASTIC INDEX map will have the vulnerability map of the area. Arc GIS 10.1 software creates these single maps and the overall vulnerability map.
- DRASTIC index number is determined by augmenting every single constraint rating by its assigned weightage and then combining it together, which is ranked on a scale of 1–10. The highest number, like 10, indicates an increased rating of contamination potential of the constraint.

- DRASTIC vulnerability index is calculated by a linear sequence of each parameter with a specific symbol for each, which is shown below.
- DRASTIC vulnerability index (VI), Eq. (8.1):

$$\text{DVI} = D_r D_w + R_r R_w + A_r A_w + S_r S_w + T_r T_w + I_r I_w + C_r C_w \quad (8.1)$$

D_r Ratings to the depth to water table,
D_w Weights given to the depth to water table,
R_r Ratings for scales of aquifer recharge,
R_w Weights for aquifer recharge,
A_r Ratings designated to aquifer media,
A_w Weights designated to aquifer media,
S_r Ratings for the soil media,
S_w Weights for the soil media,
T_r Ratings for topography,
T_w Weights designated to topography,
I_r Ratings assigned to vadose zone,
I_w Weights allotted to vadose zone,
C_r Ratings for rates of hydraulic conductivity,
C_w Weights given to hydraulic conductivity.

- Using original DRASTIC parameters with their rating and assigned weight, the DI equation to calculate DRASTIC Index will become Eq. (8.2):

$$D_I = D_r * 5 + R_r * 4 + Ar * 3 + Sr * 2 + Tr * 1 + Ir * 5 + Cr * 3 \quad (8.2)$$

- Finally, the DRASTIC vulnerability map is categorized as per the area prone to contaminant. Now, the extension of the DRASTIC vulnerability map is DRASTIC—LU map in which all the previous parameters used in DRASTIC map will be same; only the new parameter Land Use will be added to the modified DRASTIC map ($D + R + A + S + T + I + C + \text{LU}$).
- Now the modified equation will become to calculate DRASTIC–LU Index is: DI Eq. (8.3)

$$-\text{LU} = D_r * 5 + R_r * 4 + A_r * 3 + S_r * 2 + T_r * 1 + I_r * 5 + C_r * 3 + \text{LU} * 5 \quad (8.3)$$

The overall summary of methodology is shown in Fig. 8.2

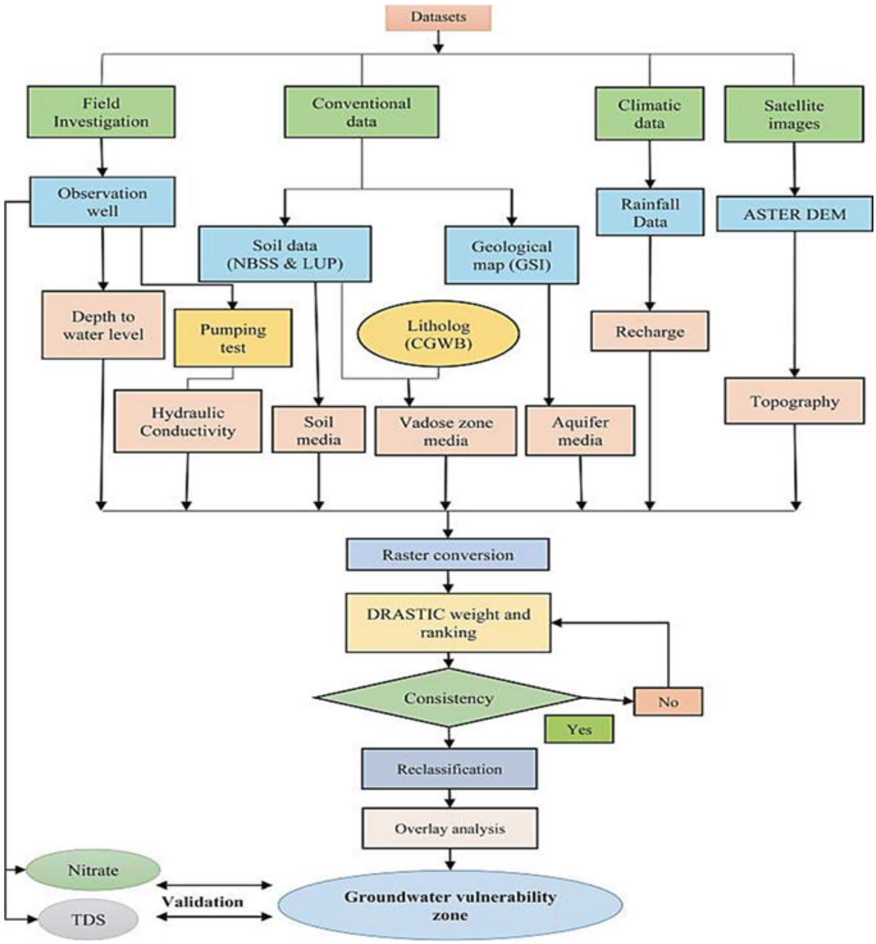

Fig. 8.2 Flowchart representing the methodology

8.3.3 Preparing Layer Maps

8.3.3.1 Depth to Water Table

It displays the distance among the ground surface to the water table. There is a decreasing likelihood of contamination with depth. Nearly 80 wells were sampled to gauge the groundwater level. The groundwater table stretches between 1 and 350 m below the surface. The data has been tabulated using depth and location as input parameters in the ArcGIS 10.1 spatial analyst tool to interpolate using an IDW approach and reclassify it according to the reclassified algorithm.

8.3.3.2 Net Recharge

There are some parameters that can be used to test a vulnerability, such as net recharge. To test the vulnerability, knowing how much water runs deep down into the ground during a rain event is necessary. As a result, more precipitation will cause a higher net recharge. A key parameter in determining recharge is rainfall. Data for the year 2019 has been taken from IMD for the Bhilwara district with five rainfall gauge stations. The amount of rain from these gauges has been used to calculate net recharge with interpolation using IDW in ArcGIS 10.1.

8.3.3.3 Aquifer Media

The capacity of an aquifer's formations to store water is indicated by their degree of consolidation or consolidation. The aquifer with the largest water storage capacity will be the best one. When creating the aquifer media map, the inputs utilized to reclassify the map include the study area's lithology (Aller et al. 1987).

8.3.3.4 Soil Media

The amount of water infiltration that occurs below the unsaturated layer is determined by the soil media. Many organic materials are found in soil, which increases the likelihood of biological activity there. Data from the National Bureau of Soil Survey and Land Use Planning was utilized to create this map, which was then divided into three groups using digital technology (loamy, clay loamy, and loamy).

8.3.3.5 Topography

The study area topography depicts the slope variance. Along with flow rate, steep slope, gentle slope, heavy runoff, and low runoff are also impacted. An elevation map has been produced using ASTER DEM as an input parameter. Aquifer media have been divided into four classes by examining the local lithology and utilizing the reclassification tool in Arc GIS.

8.3.3.6 Impact of Vadose Zone

The vadose zone is the region from the ground surface to the upper part of the water table and lies in the unsaturation zone through which water percolates into the water table. The material permeability substantially impacts the vadose area recharge rate and pollutant migration.

8.3.4 Violation

A cumulative density graph between concentration and %file was created. A cumulative density graph of water quality parameters was plotted between concentration and percentage. The values that were discovered following the crossing must be deducted from one hundred ($X - 100$), and the outcome reveals that values over the standard are %age violations. When creating a thematic map to illustrate which area has been exhibited more % violation and which area has less, the value of each parameter's station was entered into the formula below. The greater the %age of parameters that are violated, the more clearly those parameters are over their normal range and have an adverse effect on human health.

$$\text{Violation} = \{(\text{Parameter value} - \text{Standard value})/\text{Parameter value}\} * 100$$

8.3.5 Mapping of Hotspots

The hotspot map indicates that how much a source of contamination is present in this area. This map is prepared using the input data from Google Earth, CGWB report, and state pollution control board (SPCB).

8.3.6 Overlay Analysis

8.3.6.1 Overlay of Vulnerability Map with % Violation Parameter Map

To compare the vulnerability map with individual %age violation parameter, overlay method was used where %age violation parameter was overlaid over vulnerability map in Arc GIS.

8.3.6.2 Overlay of Hotspot Map with % Violation Parameter Map

In order to compare the hotspot map with the % violation parameter, an overlay method was used. To do this, the hotspot map and vulnerability map were both added to Arc GIS. Reducing the transparency helped to make both maps transparent, which led to sharpening the features of the overlaid map and making the features of both maps visible together.

8.3.7 *Calculation of Water Quality Index*

The assessed rates of the physicochemical constraints have been used to create the WQI. Ten variables were chosen because of their significance to water quality. pH, TDS, TH, Ca, Mg, Na, K, Cl, NO_2, HCO_3, and SO_4 were among them. The Guidelines BIS: 10,500 Indian standards for drinking water were the drinking water standard used in this investigation.

There are four steps in calculating the water quality: -

- All of the ten constraints have been given a weight (wi), which ranges from 1 to 5, based on its significance in the overall characteristic of the water. The most significant weight was 5.00, and the least effective was 2. Due to their considerable importance in determining water quality, calcium, magnesium, and total hardness were given the highest weight of 5, and potassium and sulfate were given the minimum weight of 2. Additional constraints for instance pH, TDS, HCO_3, Na, and Cl were given weights ranging from 1 to 5.
- The relative weight (Wi) of the chemical constraints was computed by applying the subsequent equivalence.

$$Wi = wi / \sum Wi$$

- In accordance with the recommendations of the World Health Organization, a quality rating scale (Qi) for each constraint is calculated by dividing its concentration in each water sample by its equivalent standard. The Indian Standard BIS (2012) is used if the WHO standard is unavailable, and the result is augmented by 100.

$$\text{Qi} = (\text{Concentration}/\text{standard}) * 100$$

- Next, the sub-indices (SI) have been computed to calculate the WQI: SI = Relative weight (Wi)* Quality rating scale Qi

$$\text{WQI} = \sum \text{SI}$$

8.4 Results and Discussions

8.4.1 Evaluation of Vulnerability

8.4.1.1 DRASTIC Model

DRASTIC parameter input data was entered in vector form in Arc GIS 10.1 software. The map was prepared and modified by assigned ratings and weights to all seven constraints extending from 1 to 10 (Aller et al. 1987).

8.4.1.2 Depth to the Water Table

The distance from the surface to the water table is the primary component of what is known as the depth to the water table. In addition, it is involved in a wide variety of chemical and biological processes, which in turn have an impact on the amount of time it takes for contamination to reach the groundwater table (leaching, oxidation, and sorption). If the water table is located very close to the earth's surface, then the likelihood of it being contaminated is increased. Final map generated (Fig. 8.6a) according to (Aller et al. 1987) assign highest weight "5" to depth to water table and rating was classified into seven classes (1, 2, 3, 5, 7, 9, 10) to determine vulnerability by using DRASTIC model generally shallowest water table remark in southern, northern, and western while deepest water observed in eastern part of Bhilwara district generally shallowest water table remark in eastern part of Bhilwara district generally shallowest water table remark.

8.4.1.3 Net Recharge

The precipitation is a highly essential source for groundwater recharge because it enables polluted water to rise precipitously to the water level and then move straight to reach the aquifer. As a result, the possibility of contaminants reaching the water table increases proportionately with the magnitude of the recharge. The net recharge value was computed using the average annual rainfall that was collected from seven rain gauge stations in the Bhilwara district. These stations were located in Bhilwara, Asind, Jahazpur, Kotri, Mandalgarh, and Raipura. The yearly rainfall averaged between 430 and 730 mm. The second final layer was produced after net recharging was given a weight of 4, divided into five groups based on rating (1, 3, 6, 8, 9), and class, respectively (Fig. 8.6b). The region to the southeast and northeast had the lowest rating ranking, which encompassed five blocks: Shahpura, Jahazpur, Kotri, Mandalgarh, and Beejoliya blocks. The region to the southwest had the highest rating, which was noticed in the smaller area that covered the Raipur block.

8.4.1.4 Aquifer Media

The aquifer media deal with the geology and lithology of the research area; corresponding to Aller et al. in 1987, the aquifer media are assigned weight “3” in the DRASTIC model. The likelihood of contamination increases when pre-existing rocks possess high permeability and porosity. In this location, different aquifer formations were documented. Sand and gravel, which have high porosity and high permeability and are more susceptible to contamination, were assigned an “8” rating (Aller et al. 1987) and covered the majority of the Raipur, Sahara, Mandalgarh, Kotri, and Banera blocks, followed by sandstone, which covered a portion of the Beejoliya block, and Dolomite bearing aquifer, which was observed in the Mandalgarh block. Moreover, schist and gneiss are less susceptible to contamination; they were rated “3” due to their low permeability and porosity; they covered most of the study region and generated the final third parameter layer (Fig. 8.6c).

8.4.1.5 Soil Media

The soil medium is responsible for a significant amount of the movement of water deep within aquifers where it is found. In the DRASTIC model, which was developed in 1987 by Aller et al., the weight “2” was given to the soil medium. In addition, the attenuation activities of percolation, biodegradation, sorption, and volatilization may be particularly substantial in regions of the soil when the soil zone is quite thick. The soil media organization has separated soil into two categories, namely loamy and clay loamy, and it was given ratings of five and three for both of these categories (Aller et al. 1987). The majority of the research area is comprised of loamy soil. However, the part that is situated in the north-northeast corner of the study area was composed of clay loam (Fig. 8.6d). To put it another way, loamy soil is more prone to contamination, whereas clay loam is the soil type least prone to contamination.

8.4.1.6 Topography

Topography implies to the slope of the area, how gentle and steep it is. If the site is gentle, then the water will stagnate there for a long time; the chances of pollutant infiltration will be more, and it will be more vulnerable to contamination while in mountainous region because of steep slope where the water does not stop for long, more runoff generation thus reported to less susceptible to contamination. The topography was assigned weight “1” in DRASTIC model according to Aller et al. in 1987. It reflects topography does not play a significant character to assess the vulnerability of any area and it was categorized accordingly into five classes based on rating (10, 9, 5, 3, 1); therefore, the highest rating “10” covered maximum blocks of the study zone while moderate and lowest rating covered some minor area in southeastern and northeastern direction (Fig. 8.6e).

8.4.1.7 Impact of Vadose Zone

Vadose zone always rests above the water table. The below lying formation affects water percolation reaches the aquifer and it has assigned weightage "5" while rating (Aller et al. 1987) accordingly in three classes (3, 4, 6). The material below the normal soil horizon and above the water table attenuates differently depending on the kind of vadose zone media. According to geological profile of this area, vadose zone consists of amphibolite, sandstone, shale, granite, dolomite, gneiss, quartzite, phyllite, schist, and calc-silicates. Formation like sandstone and dolomite was assigned highest rating "6," and it has more vulnerable to contamination and majorly covered three blocks of southwestern part (Sahara, Mandal, and Raipur); subsequently, the metamorphic rocks were assigned rating "4" and it covers maximum blocks (Beejoliya, Mandalgarh, Jahazpur, Kotri, Shahpura, Bhilwara, Banera, Hurda, Asind) of the study area while Shales has lowest rating and covered minor area of Hurda, Shahpura, Banera, Kotri, and Jahazpur block which indicates the low tendency to retain water inside and become less vulnerable to contamination (Fig. 8.6f).

8.4.1.8 Hydraulic Conductivity

Hydraulic conductivity concerns with the ease with which the water transmitted. The groundwater flow affects the flow of contaminants (Aller et al. in 1987) which weight assigned "3" to this parameter in DRASTIC model. It reclassifies rating into three classes: (a) "1" (<0.002), (b) "1" lies in range between 0.2 and 0.5, and (c) "2" lies in range between 0.5 and 2.0. Highest rating display in the maximum portion of the study zone shielded Sahara, Raipur, Bhilwara, Mandal, Asind, Banera, Beejoliya, Mandalgarh, and Kotri, whereas lowest rating "1" assigned to some part of northeastern region covered majorly three blocks (Sahara, Jahazpur, and Kotri) and has low hydraulic conductivity, which means the area is less prone to pollution while the rest area has high value of hydraulic conductivity which is more vulnerable to contamination (Fig. 8.6g).

8.4.1.9 DRASTIC Index

DRASTIC map was created by integrating seven different raster maps together. The finished product is referred to as the vulnerability map. According to the findings, the value can range anywhere from 100 to 205, and it is broken down into seven different subclasses: low vulnerability zone, moderate vulnerability zone, moderate to elevated vulnerability zone (VZ), high VZ, very VZ, and completely VZ. The map that was constructed using color codes can be found in Table 8.2, and it reveals that the majority of the Beejoliya block and a small portion of the Jahazpur block are located in a low vulnerability zone (100–119). This indicates that the location in question is located in a region that has a high slope, hilly terrain, non-porous and non-permeable soil, limited infiltration of water, and an impervious surface. The blocks

Table 8.1 Color codes DRASTIC index

Classes	Index ranges	Color codes
1	Less than 79	Violet
2	80–99	Indigo
3	100–119	Blue
4	120–139	Dark green
5	140–159	Light green
6	160–179	Yellow
7	180–199	Orange
8	200 and above	Red

Source Aller et al. (1987)

Table 8.2 WQI scales

Water quality	WQI Ramakrishnaiah (2009)	WQI Mohanty (2004)
Excellent	<50	<50
Good	50–100	50–100
Poor	100–200	100–200
Very poor	200–300	200–300
Unsuitable	>300	>300

of Asind, Hurda, Banera, Shahpura, Kotri, Mandalgarh, and Jahazpur are located in an area with a moderate to high vulnerability; the value of this zone ranges from 120 to 179. Very high vulnerability zones include Mandal, Bhilwara, and a portion of Raipur and Sahara; their values range from 180 to 199. Completely vulnerable zones include the majority of the Raipur block and a little sector of Sahara; their values range from 180 to 199 (200 and above), as shown in Table 8.1. It is a sign that the location is located in a region with a gentle slope and a plain terrain, maximum opportunities for water infiltration, porous rock and soil with high permeability and porosity, and a surface that is pervious (Fig. 8.6h).

8.4.1.10 DRASTIC–Land Use (LU) Model

Integrating the LU map into the DRASTIC map resulted in certain changes being made to it. Natural Breaks (Jenks) categorization strategies were evaluated by Ersoy and Gultekin (2013) and determined to be appropriate for use in dividing the ranges for the DRASTIC–LU model. The index value can range from 100 to 250 and is divided into five different classes. The areas of Bhilwara, Asind, and a portion of Banera are classified as belonging to a very high vulnerability zone, with an index value that ranges from 163 to 214. On the other hand, the majority of Asind, Banera, Shahpura, Kotri, and Jahazpur are classified as belonging to a high vulnerability zone (144–163). The plain terrain and mild slope in that location, both of which have maximum potential for seepage of water inside the aquifer, as well as the rocks that are present in the research area, are two of the possible reasons why extremely high vulnerability to high vulnerability exists in the area. It has the ability to hold onto water, in contrast to loamy soil, which helps more contaminants to become ingrained in the ground. It is clear from examining the similarities and differences between the DRASTIC model and the DRASTIC–LU model that the DRASTIC–LU model is superior to the DRASTIC model. This is because there are more anthropogenic activities being included as a parameter, each of which plays an essential part in the poisoning of groundwater. Regarding the land use category, agriculture was carried out across the entirety of the research region. When compared with the DRASTIC map, which reveals the high vulnerability formed in the southwestern portion of the region, the DRASTIC–LU map shows that the impact of agricultural operations can be seen quite clearly (Fig. 8.6j).

8.4.2 Validation

8.4.2.1 Drastic

In order to validate the DRASTIC map, it was combined with the nitrate concentration map. It was discovered that nine water samples fall into the low to moderate vulnerability zone, with concentrations ranging from 1.69 to 70 mg/L encompassing the eastern portion of the district. Eight samples of water with a medium concentration of nitrate (70–120 mg/L) fall in a zone of high vulnerability, covering Kotri, Banera, and Hurda, while eight samples of water with a high concentration of nitrate (120–283 mg/L) fall in a zone of extreme vulnerability, covering Raipur block and a portion of the Sahara block (Fig. 8.3).

8.4.2.2 DRASTIC–LU

The nitrate values in the study area vary from 1.69 and 283 mg/L, respectively, and it can be seen from the spatial distribution of the parameters when DRASTIC–LU map integrated with nitrate concentration map; Raipur, Sahara, and some part of Mandal are completely vulnerable area in which concentration of nitrate is getting very high (120–283 mg/L). The agricultural contaminants mix up with the recharge water and further contaminate the groundwater. The nine lowest nitrate concentration samples generally fall in the eastern part of the district which belongs low to moderate vulnerability zone, and chance of contamination was less likely (Fig. 8.4).

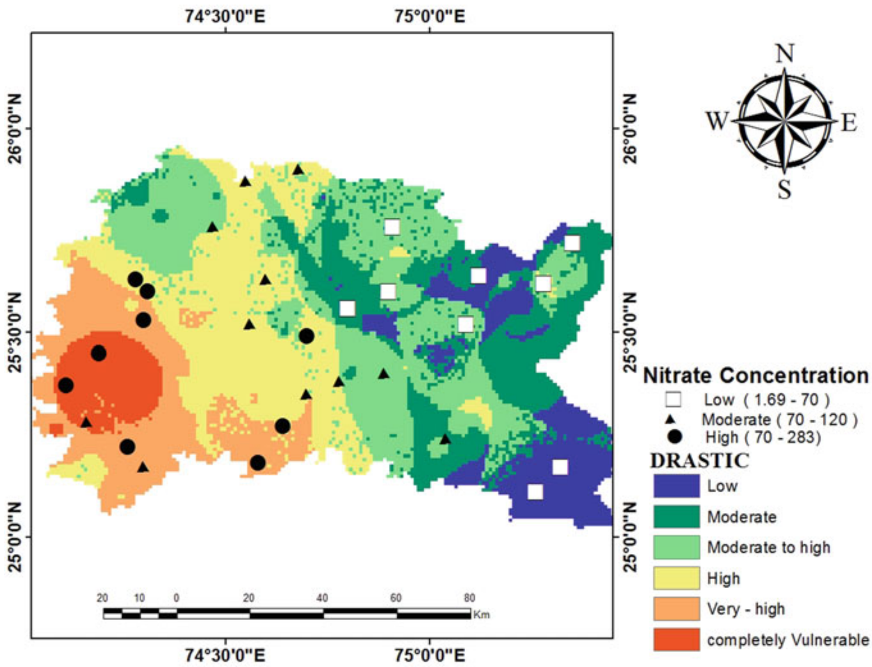

Fig. 8.3 Nitrate distribution over DRASTIC vulnerability map

8.4.3 Evaluation of %Age Violation W.R.T Drinking Water Standard

8.4.3.1 % Violation on the Basis of the Overall Dataset

Percentage violation is generated for those stations whose value is above its standard. NO_3^-, TA, and TDS show that 100% violation which means 100% values are above than its standard. TDS % and NO_3^-% violation evidently draw attention to the impact of anthropogenetic undertakings in the groundwater quality. The value that was found after the calcium intersection shows that 78% values are less than standard and 22% value is higher than standard because of some geochemical process like dissolution, leaching, and precipitation of calcium bearing rocks and mineral (sandstone, limestone, calcite, and dolomite) which further help to uplift the calcium concentration and responsible for causing hardness in groundwater. Magnesium graph shows 20% values are less than standard and 80% values lie above standard, it shows highest %age violation, and along with hardness, its deficiency also causes loss of appetite, fatigue, and weakness while its exorbitance causes gastrointestinal problems, such as diarrhea, nausea, or cramping. Sodium %age violation graph is taken out; it shows 40% values lie below standard and 60% lies above while chloride shows 55% values lie below standard and 45% lies above standard; it shows no harmful effect on human

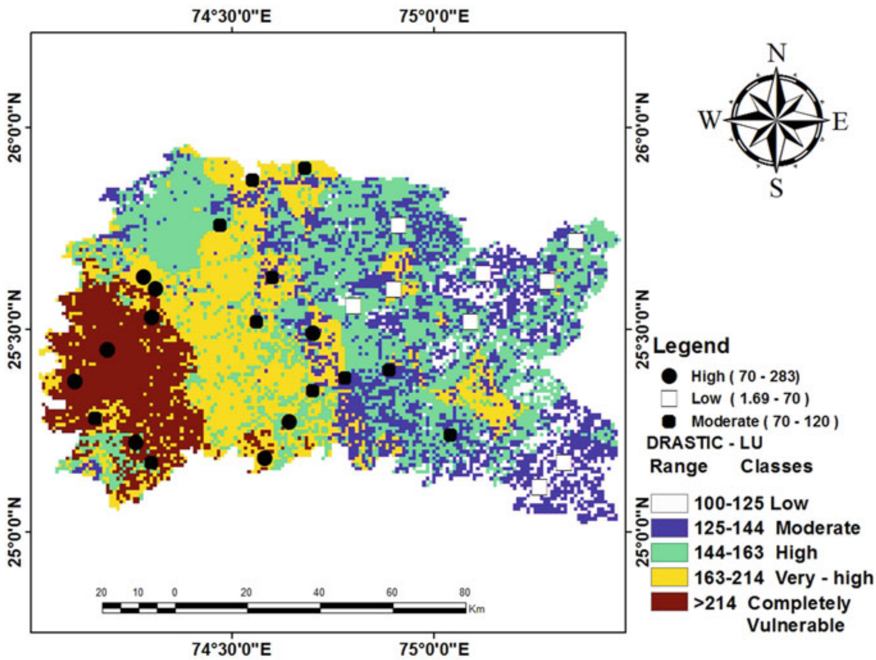

Fig. 8.4 Nitrate distribution over DRASTIC–LU vulnerability map

but causes salty taste if present in high quantity; sulfate shows 62% values are less than standard and 38% values lie above standard; its concentration increases due to leaching Glauber's salt or Epson salt; and its high concentration causes objectionable taste and causing unwanted laxative effect. The high concentration of iron is very toxic; its %age violation value is 42%. Industrial activities happening in the surrounding region were the reason of having such high value of violation while TH shows 56% %age violation.

8.4.3.2 Spatial Representation of % Violation

The violation %ages are calculated for every station, and the spatial representations are made using the kriging method in ArcGIS 10.1, suggesting that the highest violation is found in this location, while the lowest violation is located in this location. Moreover, the TDS, Cl (chloride), NO_3 (nitrate), and SO_4 (sulfate) parameters play an important role from the viewpoint of anthropogenic activities, where TDS and sulfate (Fig. 8.7b, c) are generally higher in Sahara, Bhilwara, and Jahazpur which indicates a greater level of anthropogenic activities. The highest %age violation of chloride has been observed in the northeastern and southwestern directions, mainly in the Shahpura, Jahazpur, Bhilwara, Sahara, and Raipur blocks; therefore, Beejoliya, Banera, Asind, and Hurda areas have a much lower %age violation, indicating that these areas are less affected by anthropogenic activity. Figure 8.7d shows moderate to high %age violations in the southern direction, covering Bhilwara, Sahara, Raipur, Mandal, Asind, and some parts of Banera. A geological activity has caused the presence of Ca^{++} , Mg^{++} , Na^{+} , TH, Fe^{++} , and TA in groundwater. Calcium shows (Fig. 8.7i) the highest %age in eastern part of the area and covered Jahazpur, Shahpura, and Bhilwara blocks, while Magnesium shows (Fig. 8.7f) the lowest value of %age violation in Mandal, Asind, and Hurda blocks. Sodium and TH show the high value of %age violation in such areas, viz. Bhilwara, Kotri, Shahpura, and Jahazpur. In the district, only Shahpura, Kotri, and Jahazpur showed more than 1% violation in iron, while TA showed % violation in just three places (Shahpura, Kotri, and Jahazpur).

8.4.4 Overlay

8.4.4.1 LU Map and DRASTIC Map Overlay with Hotspot Map

Even less experienced users may understand the idea of overlaying data layers. Additionally, as the majority of data currently comes in a digital format, the data need might be seen as modest. Information on hydrogeology is either already known or might be inferred using pertinent data. Consequently, these approaches produce generally accurate answers for vast regions with a complicated geological structure. Finally, water resource managers may quickly understand the outcome of this strategy and use it to inform their decision-making. Important contamination hotspots may be seen on the vulnerability map even with only a cursory visual examination. The inherent subjectivity in determining the rating scales and the weighting factors is perhaps the most significant and evident drawback of these systems noted by scientists and professionals.

When the LU and DRASTIC maps are superimposed on top of the hotspot map (Fig. 8.5), it can be seen that the western segment of the region is home to the majority of the region mining and agricultural activity. This is one of the primary contributors to the district's high level of vulnerability. It has been observed that the maximum number of hotspots can be found in the Bhilwara block and the Hurda block, both located close to vulnerable districts. As a result, there is a possibility that the water in this region will be exposed to a higher level of danger and will be more likely to become polluted. The Bhilwara block has the highest rate of urbanization, which has a variety of negative effects on the urban settlement and takes the lead to an expansion in the amount of surface water and groundwater that is polluted. As a result of the fact that groundwater can be a source of contamination, these locations must be inspected regularly.

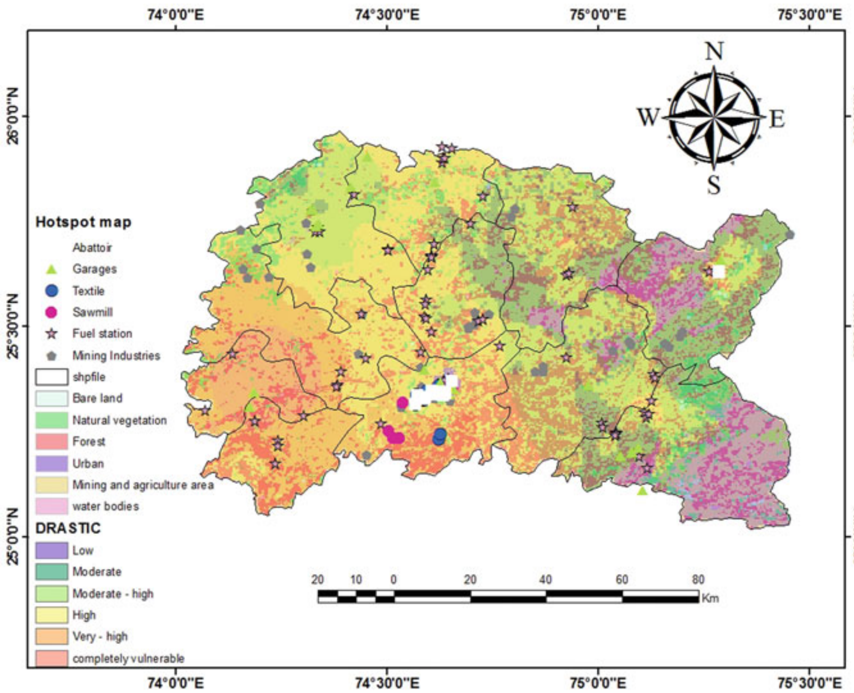

Fig. 8.5 DRASTIC, LU, and hotspot overlay map

8.4.4.2 Overlay Violation Parameter with DRASTIC Vulnerability Map

Sub-regional and regional size vulnerability maps are often used. They are often not used for assessments that are site-specific, especially zones that are less than a few tens of square kilometers. To accurately determine groundwater susceptibility, several methods have been devised. The majority of these methods rely on analytical tools to link land use with groundwater pollution. Process-based simulations, statistical techniques, and overlay and index approaches are the three different categories of assessment methodologies. Numerical modeling is a component of process-based techniques, which are helpful at the local level but not the regional one. Statistical methods demand a considerable amount of site-specific data and entail linking real water quality data to geographical characteristics. By assigning a numerical index, overlay and index methods stress the inclusion of different zonal maps. In the GIS, both processes are easy to apply, particularly when using a zonal measure. As a result, these techniques are the most often used for vulnerability estimates.

A process typically changes in many directions is known as percentage violation. Based on the analysis of the collected data, it was discovered that the value of TA and TDS indicates the highest value of % violation. In contrast, the value of pH shows the lowest value of % violation. When the vulnerability map was overlaid

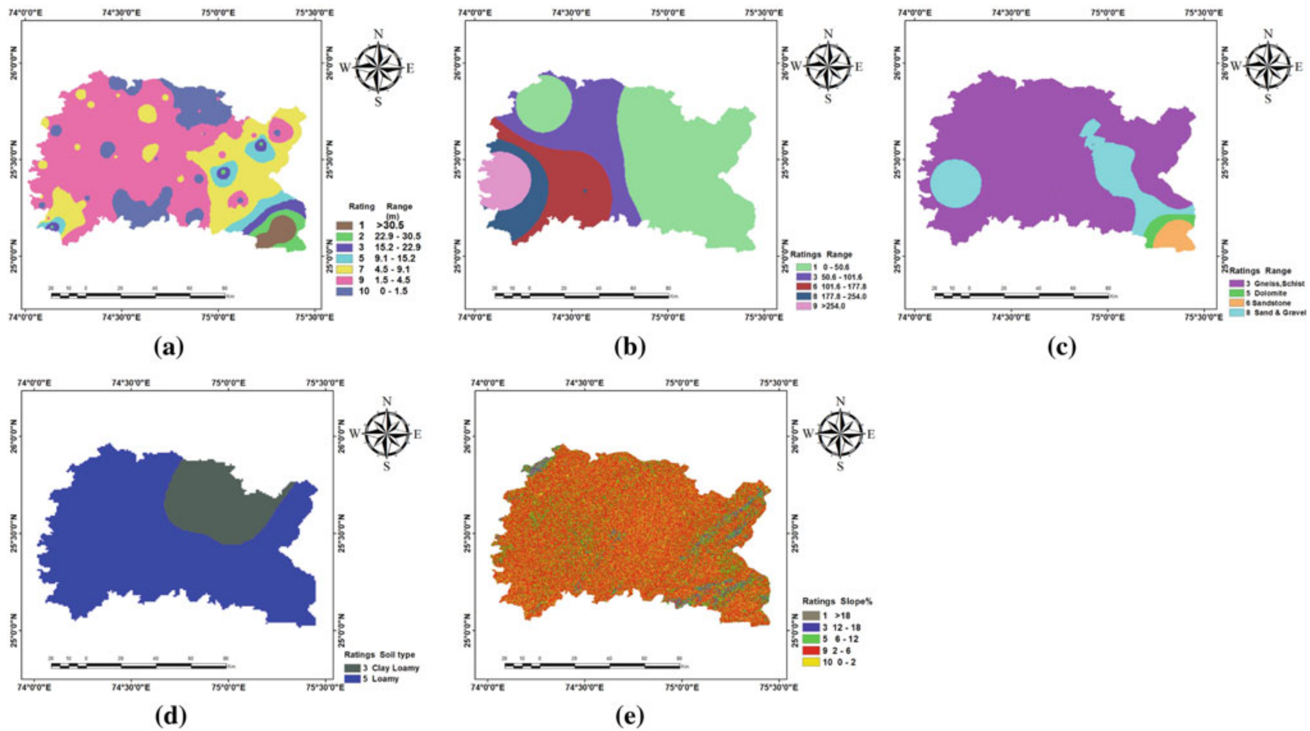

Fig. 8.6 Input maps for DRASTIC MODEL **a** Depth to water table **b** Recharge **c** Aquifer media **d** Soil Media **e** Topography **f** Impact of vadose zone **g** Hydraulic Conductivity **h** DRASTIC Vulnerability map i LU map **j** DRASTIC—LU map

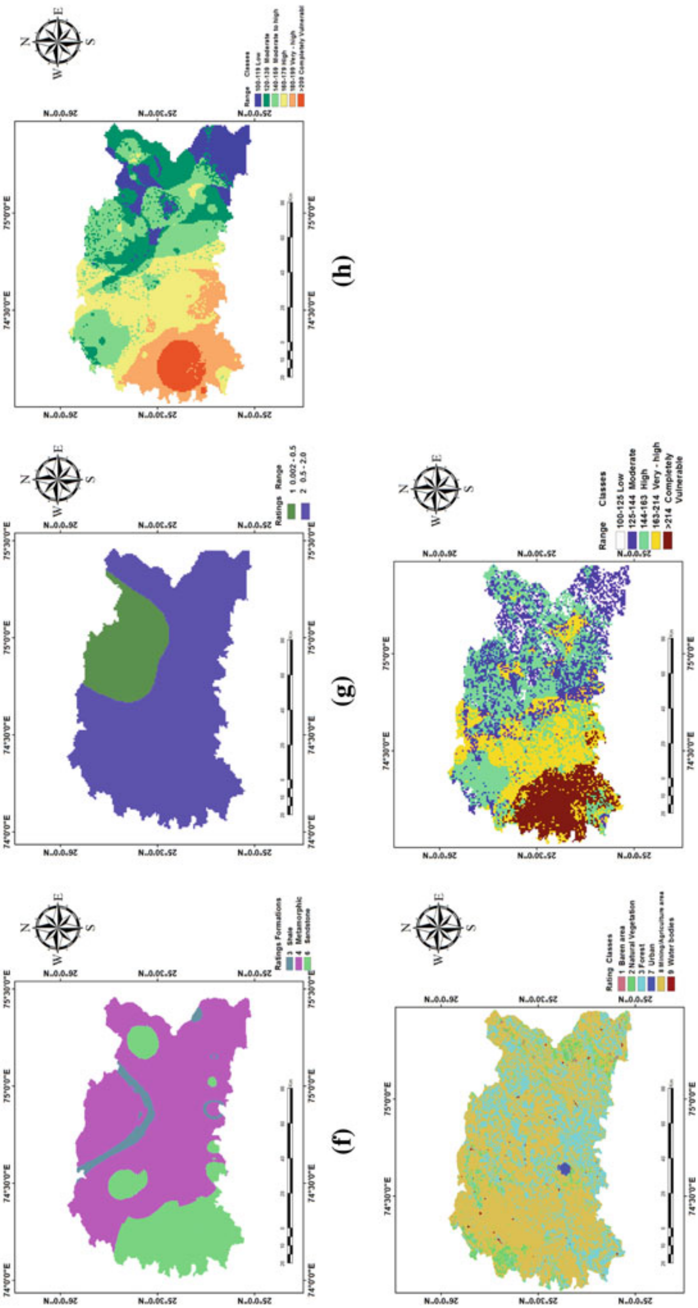

Fig. 8.6 (continued)

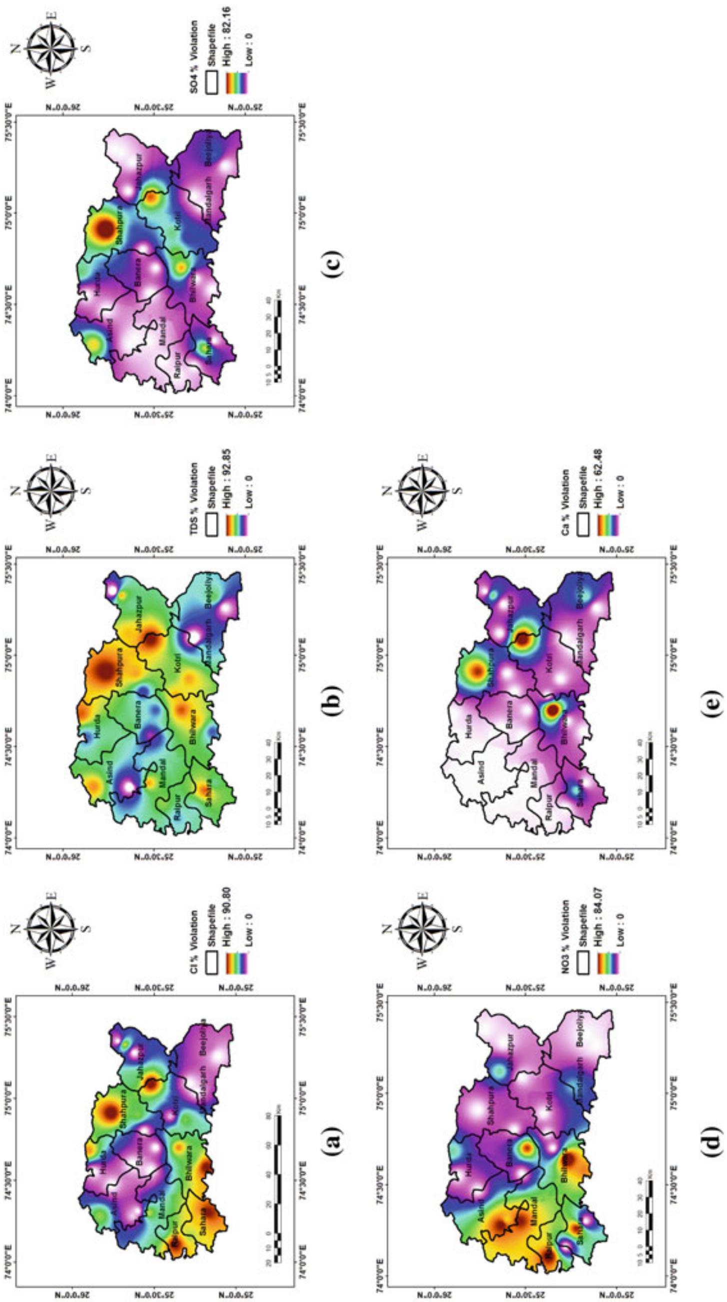

Fig. 8.7 % Violation maps of **a** Cl^- **b** TDS **c** SO_4^{--} **d** NO_3^- **e** Ca^+ **f** Mg^{++} **g** Na^+ **h** Fe^{++} **i** TA **j** TH

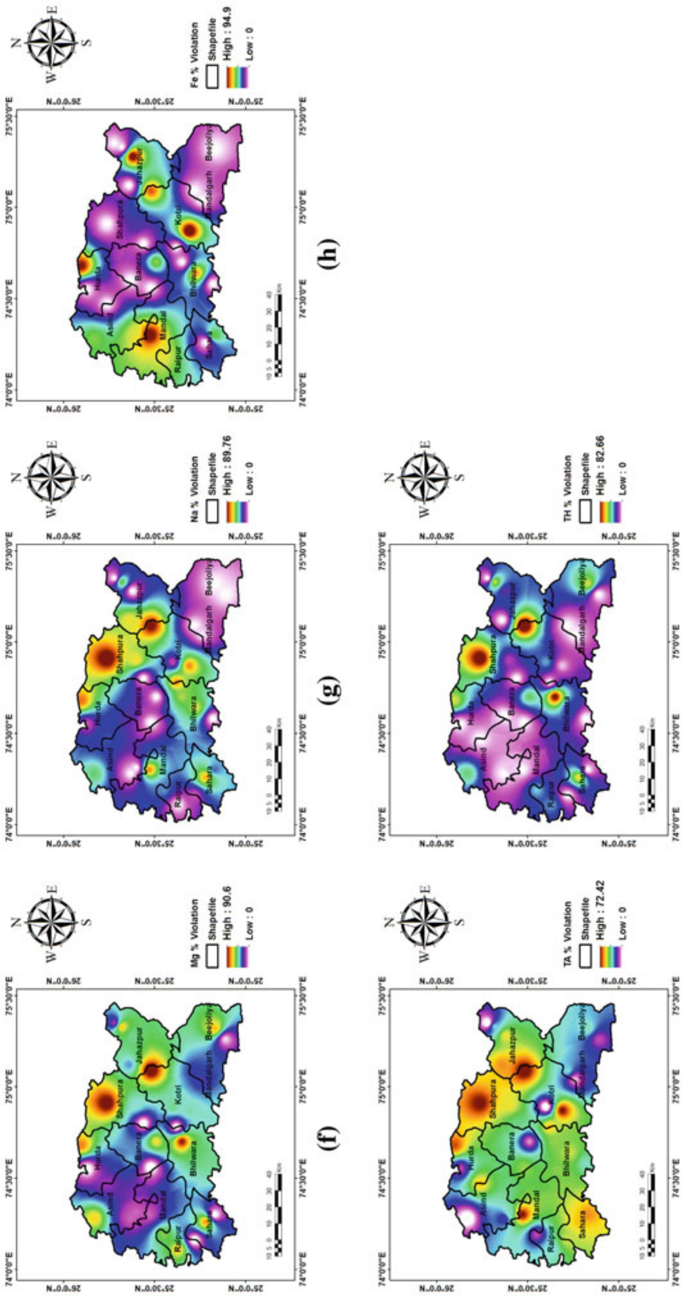

Fig. 8.7 (continued)

with each violating parameter individually, it was discovered that the Ca % violation (Fig. 8.6a) was greater in the northeastern part, which covered Jahazpur, Shahpura, and Bhilwara, all of which belong to the moderate vulnerability zone. Likewise, the Mg % violation was greater in the east and the west, with high concentrations being observed in Bhilwara, Banera, Beejoliya, Kotri, and Jahazpur; it was discovered that the district as a whole had a greater %age of violations. It was observed from the layered map that the violation % of Na (Fig. 8.6c) was higher toward the southern and northern parts of the Bhilwara area, whereas the Cl concentration elevated in the northeastern and southwestern parts, which resulted in the water having a salty taste in that particular region. A higher %age of total alkalinity being violated was discovered in zones rated as moderately vulnerable to extremely highly vulnerable or entirely vulnerable, indicating that these zones are very susceptible to industrial and chemical contamination. Similarly, TDS exhibits the highest trend toward northern, southern, covered Sahara, and Raipur blocks. Higher violations were recorded in the corners in all four directions for Fe. However, the SO_4 overlaid map with vulnerability represented the relatively small area coverage of the northeastern region and the Bhilwara block. Nitrate concentrations are rising in the southwest region, which is classified as extremely sensitive to vulnerable. The zone of moderate to high vulnerability contains the whole hardness value at its highest.

8.4.4.3 Overlay Violation Parameter with Hotspot Map

The soil medium is responsible for a significant amount of the movement of water deep within aquifers, where it is found. In the DRASTIC model, which was developed in 1987 by Aller et al., the weight “2” was given to the soil medium. In addition, the mitigation practices of percolation, biodegradation, sorption, and volatilization may be particularly significant in regions of the soil when the soil zone is quite thick. The soil media organization has separated soil into two categories, namely loamy and clay loamy, and it was given ratings of five and three for both of these categories (Aller et al. 1987). The majority of the research area is comprised of loamy soil, but the part that is located in the north-northeast corner of the study area was comprised of clay loam (Fig. 8.6d). To put it another way, loamy soil is more prone to contamination, whereas clay loam is the soil type that is least prone to contamination. The findings are shown in Figs. 8.9 and 8.10.

8.4.5 Water Quality Index (WQI)

The weighted arithmetic WQI approach that was established for groundwater constraints characterizes the overall excellence of water depending on the extent of purity for any deliberate purpose. This approach was established for the purpose of groundwater parameters. This approach was developed specifically for analyzing groundwater properties. The values of the individual samples for the water quality index as well as the types of water that are contained in each sample are documented in Table 8.3, which can be located further down the page. It is a mathematical equation that summarizes a set of data relevant to water quality into language that can be understood by the average person (excellent, good, poor, etc.) The WQI for the Bhilwara district extends from 92 to 791, which shows that the water quality in this region is both poor and unsuitable for consumption or use. The quality of the groundwater samples was evaluated as follows: Ten % were classified as "good," eighteen % were rated as "poor," and seventy-two % were assessed as "unsuitable."

You can view the work that was completed in the past for certain aspects of the water quality index on this page (Saini et al. 2020, Multivariant Statistical Analysis of Bhilwara, Bhilwara district, Rajasthan; Internship report). Corresponding to the extent that was developed by Ramakrishnaiah et al. (2009) and Mohanty (2004), the following is how the water quality index value is broken down: According to this classification, the vast majority of the water quality tests that were taken in the Bhilwara region fall under the category of improper water type. Near Guwardi Dam, the readings on the water quality index are among their highest, followed by Bholi.

Table 8.3 Water quality classification

Location	WQI	Type
Sharda dream city colony	341.82	Unsuitable
Gathila Kheda	198.18	Poor
Sangam University	245.58	Unsuitable
Patel Nagar	595.72	Unsuitable
Dantajati	236.81	Unsuitable
Pansal	340	Unsuitable
Sangam University	264.00	Unsuitable
Kanoli Chuaraha	277.83	Unsuitable
Atoon	251.13	Unsuitable
Sameliya	555.00	Unsuitable
Thagon Ka Kheda	160.74	Poor
Harni Mahadev	92.06	Good
Kumhariya	177.98	Poor
Bholi	791.89	Unsuitable
Hajari Kheda	550.98	Unsuitable
Mandapiya Station	398.56	Unsuitable
Borda	274.20	Unsuitable
Biliya	183.77	Poor
Guwardi	527.79	Unsuitable
Swarup Ganj	446.79	Unsuitable
Kanya Kheri	93.78	Good
Near Guwardi Dam	638.00	Unsuitable

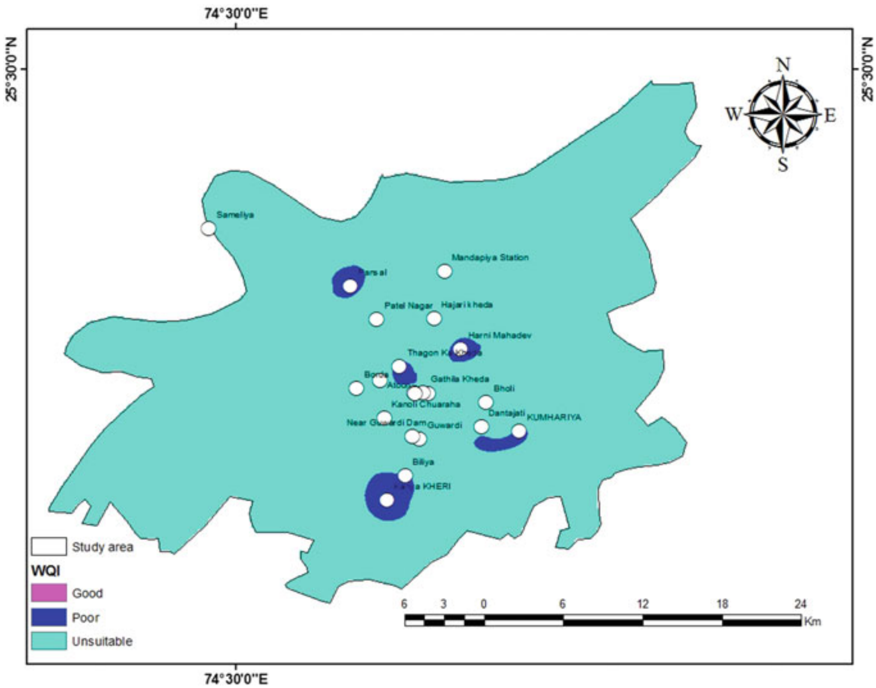

Fig. 8.8 Spatial representation of WQI

The values are at their absolute minimum close to Harni Mahadev. The high value of WQI in the region around Bholi and Guwardi Dam (Fig. 8.8) could be attributable to the presence of heavy metals (chromium, lead, zinc, and iron) in the open wells of the surrounding villages, or it could be the result of agricultural practices. Both of these explanations are plausible. When compared, the water at Harni Mahadev has a higher quality than the water at Kanya Kheri. In accordance with the findings, each and every well had a WQI that was higher than 90, and the results demonstrated that the water quality varied depending on the location of the wells. The quality of the water is established on the scale as suggested in Table 8.2.

8.5 Conclusions

In developing nations urban centers with fast population growth, the vulnerability assessment of the groundwater is an important area of research. Due to the declining groundwater level and rising pollution, which constitute a major danger to the ecosystem, groundwater vulnerability is a pressing problem everywhere in the globe. Numerous studies have been conducted to evaluate the groundwater sensitivity using various techniques in order to detect this risk. Process-based approaches, statistical

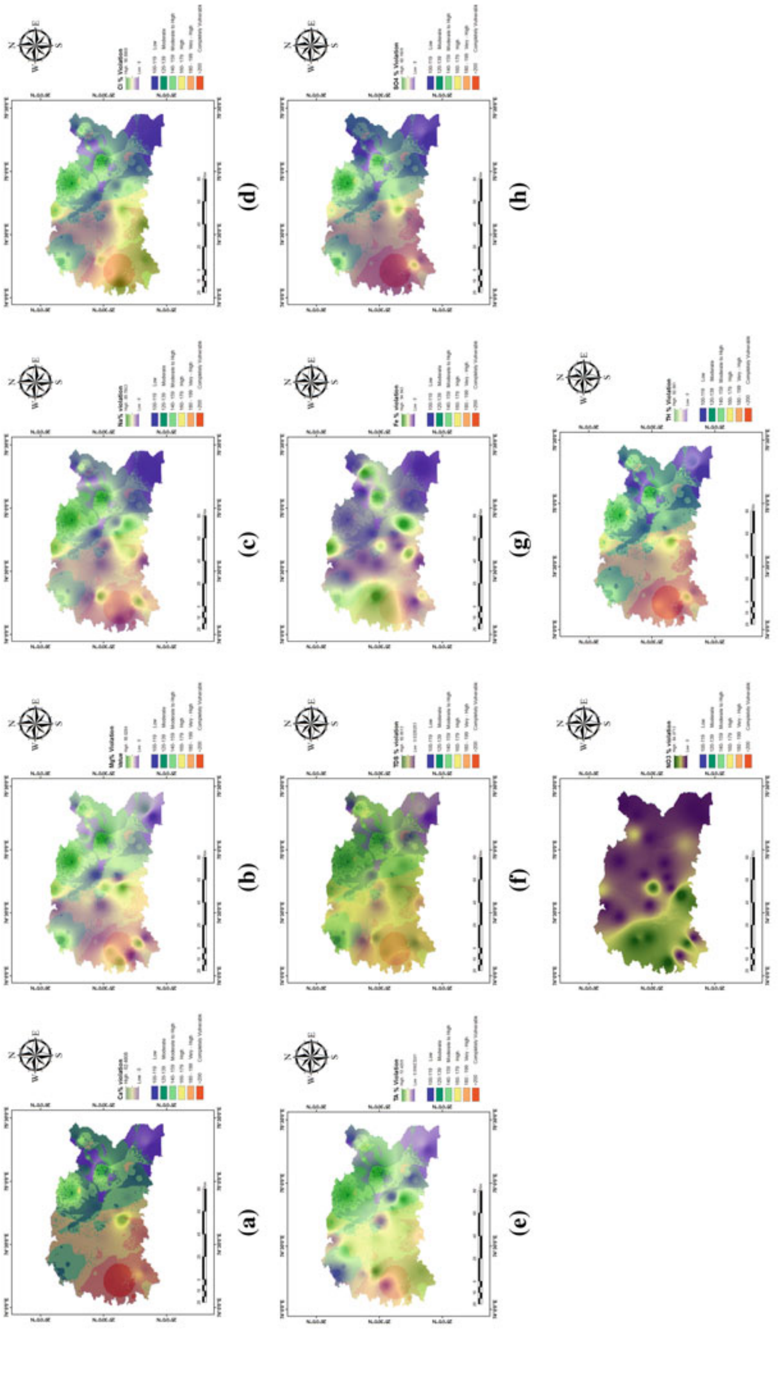

Fig. 8.9 Overlay Vulnerability map with **a** Ca^{+} % violation **b** Mg^{++} % violation **c** Na^{+} % violation **d** Cl^{--} % violation **e** TA % violation **f** TDS % violation **g** Fe^{++} % violation **h** % SO_4^{--} violation **i** TDS %violation **j** NO_3^{-} % violation **h** TH % violation

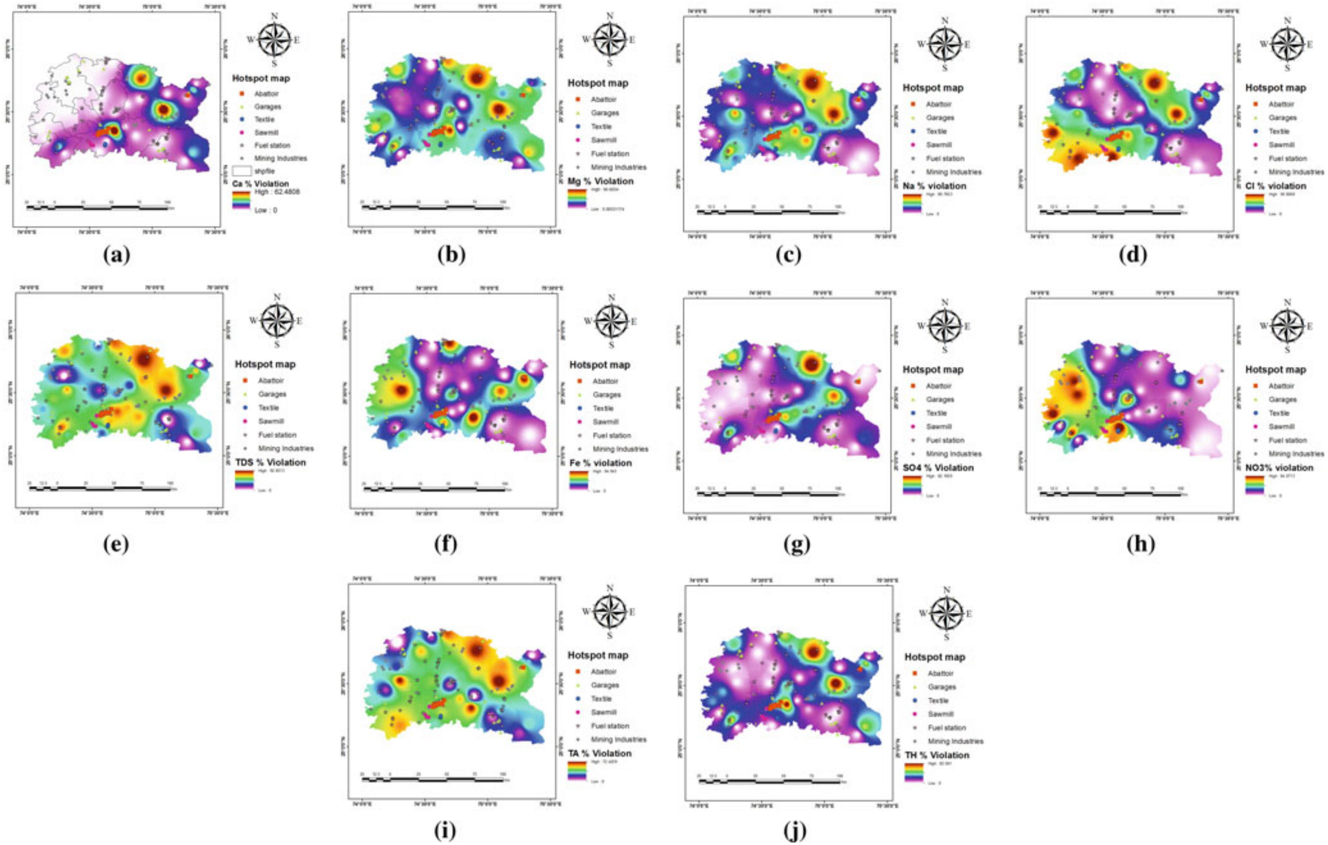

Fig. 8.10 Overlay Hotspot map with **a** Ca^{++} % violation **b** Mg^{++} % violation **c** Na^{+} % violation **d** Cl^{--} % violation **e** TDS % violation **f** Fe^{++} % violation **g** SO_4^{--} % violation **h** NO_3^{-} % violation **i** TH% violation

methods, and overlay and index methods are often used in this context. One overlay and index approach for assessing vulnerability is the DRASTIC method. The goal of this research project was to develop the DRASTIC vulnerability map by thoroughly examining the depth to the water table, net recharge, aquifer types, soil profile, topography, and hydraulic conductivity. After analyzing the information from a rigorous field study, the following conclusions have been made:

1. According to the vulnerability map result, the value ranges from 100 to 205 and is classified into six subclasses. The resulted map revealed that the major northeastern and minor north-southern parts are in the low vulnerability zone (100–119), the moderate vulnerability zone (120–139), the moderate to high vulnerability zone (140–159), the high vulnerability zone (160–179), and the very high vulnerability zone (180–199), while the Raipur and Sahara are in the super vulnerable zone (>200).
2. The DRASTIC–LU map illustrates that 15–20% of the district area is in the southwestern part, which is a high vulnerability zone. Low vulnerability has been reported in the northeastern part of the district.
3. It was discovered when the DRASTIC–LU map was validated with the nitrate concentration map. Bhilwara, Sahara, and a portion of Raipur are completely vulnerable areas, with index values ranging from >214, while the majority of Mandal, Banera, and Hurda are in the high-vulnerable zone, with nitrate concentrations extending from 120 to 283 mg/L. Low to moderate vulnerability index values ranging from 100 to 144 reported in Shahpura, Beejoliya, Jahazpur, Mandalgarh, and Kotri in the Bhilwara district indicate low contamination, with nitrate concentrations ranging from 1.69 to 70 mg/L.
4. The Bhilwara block is the block with the most contamination sources out of the 12 blocks shown on the hotspot map. This block's water is highly vulnerable to contamination and at risk. Total soluble solids (TDS), chloride (Cl), nitrate (nitrate), and sulfate (SO_4) characteristics all play a very important role from the perspective of anthropogenic activities. TDS and sulfate are typically more evident in Sahara, Bhilwara, and Jahazpur, signaling that more anthropogenic activities are actually happening in these blocks. Chloride exhibits the highest %age violation in the northeastern and southwestern directions, mostly covering the Shahpura, Jahazpur, Bhilwara, Sahara, and Raipur block. As a result, the low %age violation discovered in Beejoliya, Banera, Asind, and Hurda indicates that these areas are less impacted by anthropogenic activity. In the southern direction, which includes Bhilwara, Sahara, Raipur, Mandal, Asind, and a portion of Banera, nitrate displays moderate to high %age violations. Due to geogenic processes, groundwater contains Ca++ , Mg++ , Na+ , TH, Fe++ , and TA. Magnesium exhibits the lowest amount of %age violation, while calcium exhibits the greatest, covering the Jahazpur, Shahpura, and Bhilwara blocks in the eastern portion of the area. In certain locations, specifically Bhilwara, Kotri, Shahpura, and Jahazpur, sodium and TH exhibit a significant %age of violations. In such common blocks as Mandal, Bhilwara, Kotri, and Jahazpur, iron exhibits the maximum %age violation value.

5. Data analysis revealed that pH exhibits the least amount of % violation, while the values of TA and TDS show the highest %ages of violation. When the vulnerability map was overlaid with each violating parameter separately, it became clear that Ca% violation surpassed toward the northeastern half, covering Jahazpur, Shahpura, and Bhilwara, and Mg exceeds toward the east and west, with high concentrations found in Bhilwara, Banera, Beejoliya, Kotri, Jahazpur, and Shahpura. The overlaid map showed that the Na violation %age was higher in the southern and northern parts of the Bhilwara area, while the Cl concentration was higher in the northeastern and southwestern parts, causing the water in that area to have a salty taste. In zones that were moderately to extremely vulnerable or entirely vulnerable, there was a higher %age of total alkalinity violations, indicating that there was significant chemical and industrial pollution in these areas. Similar to TDS, the covered Sahara and Raipur blocks in the north and south exhibit the highest trends. While SO4 overlayed map with vulnerability depicts the modest area coverage of the northeastern region and Bhilwara block, higher violation was recorded in the corners of all four directions for Fe. Nitrate concentration is rising in the southwest, a region that is extremely vulnerable to entirely vulnerable.
6. By overlaying the hotspot map with the violation parameter map, it was noticed that there were four similar blocks, namely Bhilwara, Sahara, Shahpura, and Jahazpura, where the concentration of each parameter was extremely high. Sahara is in a very high vulnerability zone, Shahpura is in a low vulnerability zone, Jahazpura is in a moderate vulnerability zone, and Bhilwara is one of the blocks in the Bhilwara district where the majority of the hotspots are located (Abattior, Garages, textile, sawmill, fuel station, mining industries).
7. The majority of Bhilwara water quality samples fell into the category of inappropriate water, according to the WQI. The greatest WQI values are found near Guwardi Dam, followed by Bholi, while the lowest values are found at Harni Mahadev. The presence of heavy metals (chromium, lead, zinc, and iron) in open wells in the villages or possible agricultural practices seem to be responsible for the high value of WQI near Bholi and Guwardi Dam. Water quality is best at Harni Mahadev and then at Kanya Kheri. The findings showed that all wells had WQI values above 90 and that water quality varied depending on where it was found. It is abundantly obvious that the water in this region is highly contaminated or dangerous because the value of % violation is similarly high and belongs to a high-vulnerable area. As a result, the region has to be examined, and the sources of contamination need to be addressed.

References

Aller L, Bennett T, Lehr JH, Petty RJ, Hackett G (1987) DRASTIC: a standardized system for evaluation groundwater pollution potential using hydrogeologic setting. EPA-600/2-87-035. Environmental Protection Agency, Ada, Oklahoma: U.S

BIS (2012) Indian standard drinking water specification. Bureau of Indian Standards, New Delhi

Ersoy FA, Gültekin F (2013) DRASTIC-based methodology for assessing groundwater vulnerability in the Gümüşhacıköy and Merzifon basin (Amasya, Turkey). Earth Sci Res J Res. SJ 17(1):33–40

Hydrogeological Atlas of Rajasthan Bhilwara District (2001)

Mohanty SK (2004) Water quality index of four religious ponds and its seasonal variation in the temple city, Bhuvaneshwar. In: Kumar A (ed) Water pollution, APH Publishing Corporation, New Delhi, pp 211–218

Ramakrishnaiah CR, Sadashivaiah C, Ranganna G (2009) Assessment of water quality index for the groundwater in Tumkur Taluk, Karnataka State, India. E-J Chem 6(2):523–530. https://doi.org/10.1155/2009/757424

Rao SM, Mamatha P (2004) Water quality in sustainable water management. Current Sci 87(7):942–947. https://www.jstor.org/stable/24109398

Saini et al (2020) Multivariant statistical analysis of Bhilwara, Bhilwara district, Rajasthan; Internship report

Singh RP, Malhotra SK, Srivastava SS (1997) Technical feasibility of groundwater availability and utilization on compact area basis in white, grey and dark blocks as on 31.3.97 of district Haridwar. Groundwater Department Uttar Pradesh, Division Roorkee

Vrba J, Zaporozec A (1994) Guidebook on mapping groundwater vulnerability. In: International association of hydrogeologists, international contributions to hydrogeology, vol 16, Verlag Heinz, Hanover, Germany

World Health Organization (1998) The world health report: 1998: life in the 21st century : a vision for all : report of the director-general. World Health Organization. https://apps.who.int/iris/handle/10665/42065

Chapter 9
Exploring the Sustainable Water Management and Human Well Being Nexus in Indian Context

Y. Shiva Shankar, Nitin Samaiya, and Devendra Mohan

Abstract Present research outlines need for wholesome approach for sustainable replenishment of water resources with participatory decentralized services as replacement to conventional centralized systems. Work highlights the variables that have been influencing the effective management of water resources with strong emphasis on ecologically unsound practices. Paper also attempts to draw attention of policymakers presenting various dimensions of the sustainable water management and human well being nexus relevant to water stressed nation like India through case study of Raghogarh, Guna District, Madhya Pradesh, India. The results obtained from the study project the necessity of closed cycle water management strategies operated in decentralized mode with community participation. The lowering groundwater tables augmented with rainwater harvesting and utilizing the clays for effective defluoridation form the feasible solutions for rural water supply in Raghogarh. Cumulative measures regulating the water supply and improving the wastewater collection are the key challenges for improved health and sanitation in the region. Jaypee University of Engineering and Technology (JUET) of the study area has been adopting energy intensive decentralized closed loop water management systems. Replacing the moving bed biofilm reactor adopted for secondary treatment with aerobic ponds/lagoons and restricting the utilization of household demineralization units for treated water enhance the energy savings in management. The work highlights need for strategic planning on regional scale considering the various primary and secondary concerns of the region for sustainable replenishment of the water.

Keywords Sustainable water management · Groundwater recharge · Wastewater reuse · Energy efficiency · Rural water supply · Decentralization

Y. Shiva Shankar
Indian Institute of Technology Hyderabad, Hyderabad, Telangana 502285, India

N. Samaiya
Department of Civil Engineering, Jaypee University of Engineering and Technology, Raghogarh, Guna, Madhya Pradesh 473226, India

D. Mohan (✉)
Department of Civil Engineering, Indian Institute of Technology Banaras Hindu University, Varanasi, Uttar Pradesh 221005, India
e-mail: devendra.civil.iitbhu@gmail.com

P. Shukla et al. (eds.), *Environmental Processes and Management*, Water Science and Technology Library 120, https://doi.org/10.1007/978-3-031-20208-7_9

9.1 Introduction

Replenishment of the water resources has emerged as one of the biggest challenges posed due to changes in hydrologic cycle attributed by climate change. Changing hydrologic scenarios have been influencing sectors such as agriculture, hydropower generation, livestock production, forestry, fisheries, navigation and recreational activities. These issues have been predicted to be much higher for developing densely populated nation such as India with predominant rural population. These changing dynamics have been altering rural demographics forcing migrations toward non-agrarian sectors of urban areas for sustaining livelihoods. These developments in longer run could have serious implications to food security, economic development and haphazard urban areas. These issues coupled with pollution of water bodies, over-exploitation of groundwater, changes in landuse pattern and faulty agricultural practices have been threatening the well being of humans as whole (Hans 2018; Lohani et al. 2016; WBG 2016; Cronin et al. 2014; Misra 2014; MSPI 2013; Kumar et al. 2005; Kumar et al. 2013; NAAS 2013; NWM 2011; Biswas 1991).

Report by Niti Aayog, a national advisory body for providing strategic policy vision (2019), has highlighted certain findings, alarming the policymakers for suitable addressal:

- **Economic development** in the future could be affected due to changing scenarios of actual water demand against available resources.
- **Food security** arising out of the water shortage in perennial river basins (such as Ganges) affecting large populations and food production in the country.
- **Increasing deaths** due to insufficient water, sanitation and hygienic surroundings.
- **Desertification** and **land degradation** due to inadequate availability of water.
- **Groundwater under potential threat** due to the over-exploitation for irrigation and water supply.
- **Contamination of surface and groundwater bodies** due to various natural and anthropogenic factors.
- **Lack of complete safe access** to water supplies in majority of rural areas, highlighting disparity between urban and rural livelihoods (inequitable sharing of resources).

9.1.1 Water Policy Needs for Sustainable Management

With due consideration to foster the industrial progress achieved post-liberalization reforms and sustain the agricultural growth, Indian water policy has been updated periodically. Proactive initiatives have been taken in due course by the various governments: recognizing ‘right to water,’ safeguarding water as an economic entity, encouraging water savings in irrigation, expanding duties of water resources ministry, proposals for interlinking rivers, water augmenting schemes, pollution abatement measures, adaptation of digital tools in planning and seeking international cooperation. But, the major concern despite all these proactive measures has been imbalances arising out of consumption patterns, widening gap between initiatives and outcomes. These issues have been exerting the need for sustainable water management strategy balancing the urban, rural, industrial and agricultural needs (Chandran et al. 2021; Niti Aayog 2019; Punjabi et al. 2018; Mukherjee et al. 2015).

Sustainable water management aims at developing framework addressing technical, legal, environmental, social and financial constraints. Global organizations such as the United Nations Organization, UNESCO, World Bank, Global Environmental Facility and Organization for Economic Co-operation and Development (OECD) have been partnering with regional stakeholders for promoting the same. Conventional water management mainly deals with infrastructural requirement for diversion, utilization and storage of potential water supplies, replenishment of existing resources by planned rainwater harvesting structures, etc. (UNESCO 2021; Bhattacharya 2015; Biswas 1991; Jain and Kumar 2014; Keshari 2007; Loucks 2000; Megdal et al. 2017; Marlow et al. 2013; Poff et al. 2016; Singh et al. 2017; Howarth and Monasterolo 2016).

The following aspects studied by various researchers could be possibly adopted at regional scale in addition to conventional water management methods for reducing financial burden on local bodies and minimizing negative impacts of wastewater disposal:

- Decentralization (Fischer and Ali 2019; Moore 2017) of systems against centralized processing approaches for water supply and wastewater management systems with community participation.
- Water foot print (Hoekstra 2017) estimates: benefits of augmenting blue (available water resources) with gray water (wastewater) and green water (rainwater).
- Governance: Araral and Ratra (2016) have compared water governance in populated nations such as India and China with reference to various parameters. The work has underlined the need for suitable linkages in exerting control with technical approach from top to bottom in political system as in case of China for devising and implementing suitable development plans for water conservation. Wescoat et al. (2019) and Dhanya and Renoy (2017) explained the need for considering the regional dimensions (including technical, geographic, political, social and cultural aspects) and challenges at grass root level in formulating a national strategy.

9.2 Study Area and Rationale for the Study

Study area in the present work is Raghogarh municipal area extended at 75 km^2 with population of 62,163 (as per 2011 census) with prominent industries, institutions and townships. Layout of the municipal area with available water resources is shown in Fig. 9.1 Jaypee University of Engineering and Technology (JUET) existing in the study area was established by Jaiprakash Sewa Sansthan in an area of 125 acres, with population more than 3000 within the campus. Layout of the campus with rainwater harvesting system was shown in Fig. 9.2; Table 9.1 draws the comparison between JUET and Raghogarh area showcasing the existing scenario and issues in water supply and wastewater disposal. The table compares the diverse conditions in both the areas; Raghogarh municipal area was seen as facing shortages of water supply with qualitative issues for available groundwater source and haphazard wastewater collection affecting the health and sanitation in the area. JUET on other hand was observed to implementing energy intensive closed loop approach in water management.

The main rationale behind the need of the study is water resource development which is seen as the framework for water-related issues in many regions of the country that is unsustainable in the current scenario due to the fluctuations in the rainfall and insufficient understanding of the future implications on the water storage in the proposed storage structures (Hamish et al. 2021; Zang et al. 2021). In the study area, the proposed diversion project in future from the existing Gopi sagar dam (explained in Table 9.1) was seen as solution without addressing the ground level concerns. Addressing the existing concerns prior to the commissioning of the proposed project ensures the sustainability of the system. Figure 9.3 shows the outline for the proposed research, and the research attempts to analyze the concerns in water management with suitable solutions for Raghogarh municipal area and JUET that are highly relevant for the national scenario. The paper presents need for the wholesome approach for India addressing the primary concerns (basic issues involved in treatment and supply in rural areas) and secondary concerns (energy efficiency and economics) for planning sustainable water management framework.

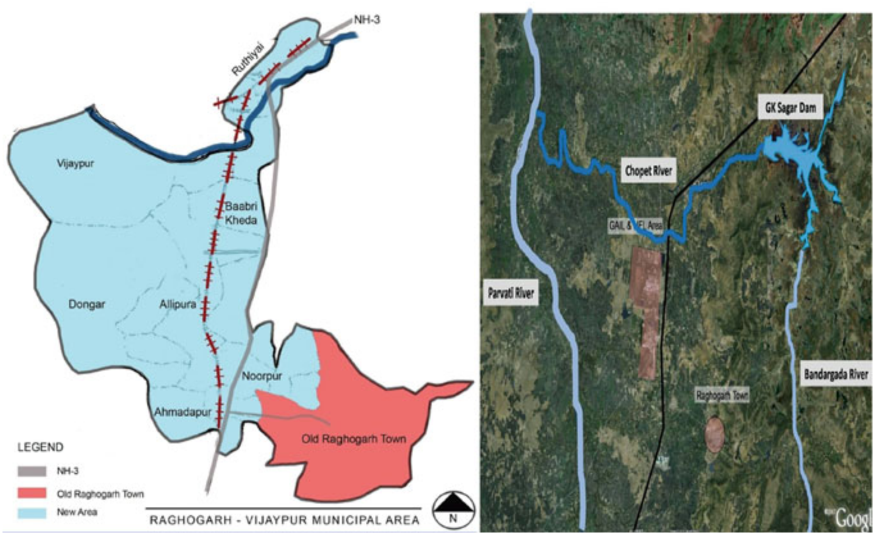

Fig. 9.1 Raghogarh municipal area (left) and existing surface water resources (right). *Source* City Development Plan, Raghogarh

Fig. 9.2 Layout of the campus and the existing rainwater harvesting system

9.3 Preliminary Studies

Preliminary studies have been conducted to understand the bigger picture and suitable variables that needed further investigations. These investigations have been undertaken in three steps: data collection, water quality investigations and informal survey. No major issues have been observed at JUET primarily due to the systematic water supply and suitable awareness among all the stakeholders. In case of Raghogarh municipal area from the previous studies of Srivastava and Ramanthan (2018) and MPWRD (2021), groundwater quality analysis has been undertaken for parameters mentioned in Table 9.2.

Table 9.1 Existing water supply and wastewater management scenario in the Raghogarh municipal area and JUET

Parameter	Raghogarh municipal area (City Development Plan for Raghogarh and ADB 2021; MPWRD 2021)	JUET
Source(s)	Groundwater (137 hand pumps and 47 tube wells) (direct supply) Surface water resources, i.e., back water from Gopi Krishna Sagar Dam (with water treatment plant of 5 MLD based on sand filtration)	Gopi Krishna Sagar Dam (30 km away from the campus) (complete treatment with unit operations/processes such as lime treatment sedimentation cum coagulation, filtration, adsorption and disinfection)
Supply versus demand	Inadequate (less than 50% of actual demand)	Adequate
Proposed solution for water crisis	State government with loan funding from Asian Development Bank (ADB) has proposed to construct of 17 MLD water treatment plant on Gopi Krishna Sagar Dam targeting 100% supply in municipal area and alternative to depleting groundwater table	Not applicable
Sewerage system	Chaotic without underground sewerage system with certain unsewered areas affecting the surrounding hygienic and polluting nearby water bodies	Systematic Storm water: harvested in lake of 10,000 cubic meter capacity Domestic sewage is suitably processed by screening, comminuting, skimming tank, equalization basin, moving bed biofilm reactor (MBBR), filtration through sand and carbon filters and UV disinfection for reuse in gardening

9.3.1 Groundwater Quality

Multiple samples were collected covering total municipal area (37 samples from 18 locations). Samples were taken from open dug wells (DW), tube wells (TW) and hand pumps being used for drinking purpose and/irrigation. In order to relate the samples collected with population distribution and geographic area, first eight groundwater samples (shown in Fig. 9.4) were collected from Raghogarh town and ninth sample shown corresponds to treated municipal supply (surface water). The remaining samples were collected from different locations indicated as TW for tube well/hand pump and DW for dug well. Collected samples were processed in

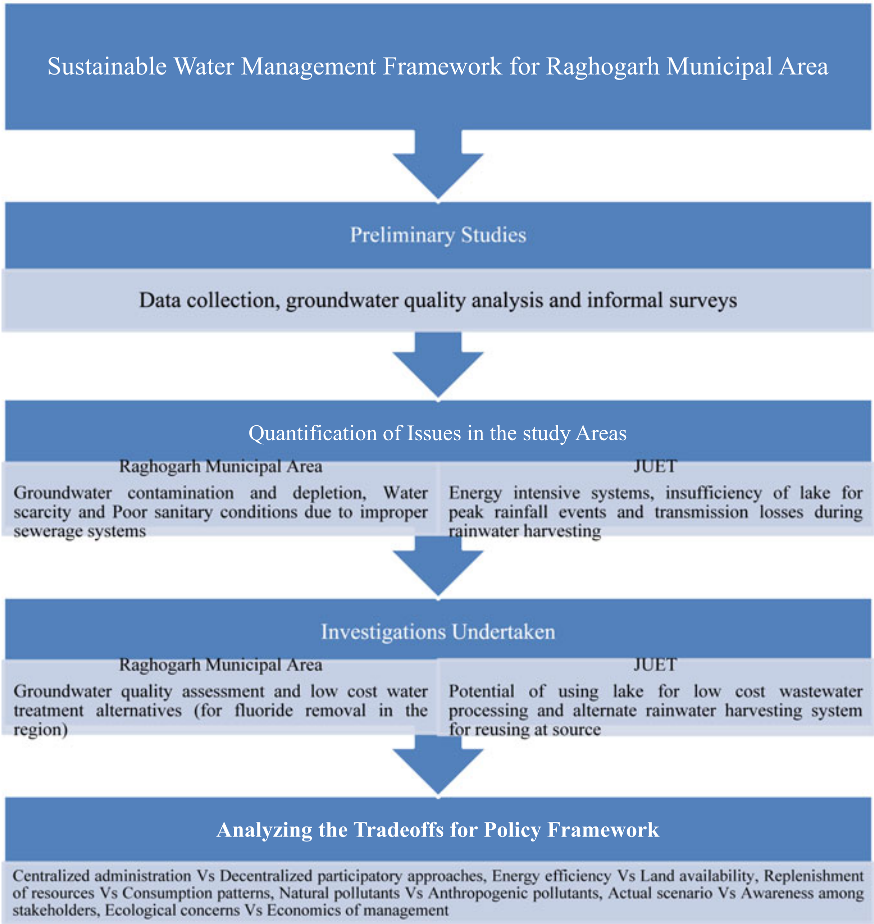

Fig. 9.3 Outline for the proposed research

accordance with Indian standards IS 3025 (Part 1) (BIS 1987) and subsequently analyzed.

Results obtained were shown in Fig. 9.4; the figure also depicts the conformance of the samples as per Indian standards for drinking purpose and consideration of source in absence of alternate source.

The following inferences could be drawn from the results:

- Groundwater quality with respect to the analyzed parameters has presented grim picture of the actual scenario. As per Indian standard drinking water quality standards (BIS 2012a) except the pH and chlorides, all other parameters in most of the areas were found to be in the undesirable range. In certain areas, the samples were found to be highly objectionable for drinking purpose and even consideration as source for water supply.

Table 9.2 Water quality parameters analyzed

S. No	Parameter	Reference	Method/instrument
1	pH	IS: 3025 (Part 11)-1983	Electrometric method (BIS 1983)
2	Total dissolved solids (mg/L)	IS: 3025 (Part 15)-1984	(BIS 2003)
3	Fluoride (mg/L)	IS: 3025 (Part 60)-2008	Electrochemical probe method (Wensar Ion Selective Electrode) (BIS 2008)
4	Chloride (mg/L)	IS: 3025 (Part 32)-1988	Argentometric titration method (BIS 1988)
5	Total hardness (mg/L as $CaCO_3$)	IS: 3025 (Part 21)-1983	EDTA method (BIS 2009)

- Variability in the samples within a region was found to be high, for example, in groundwater samples of Sadha colony, Ramnagar village and Daurana (in samples of DW and TW). Hardness was commonly found to be high in majority of the groundwater samples. Variability has been noticed due to geological and local to regional influences like improper sewerage system (particularly open sewers nearby hand pumps) that resulted in higher concentrations of chloride. Higher TDS contents in certain regions corresponded well with elevated hardness and also combined with chlorides in a few samples.
- As per the aforementioned discussion, parameter of greater concern was found to be fluoride distribution and its content. The geogenic fluoride concentration in almost all the samples was found to be much higher than the permissible limit (i.e., 1.5 mg/L) according to Indian drinking water standards (BIS 2012b). Sample collected from Shivrampur region has shown abnormally high TDS content (above 5000 mg/L), but tube well water was not being used for drinking; hence, the further investigations have not been considered in the present work.
- Findings of Srivastava and Ramanathan (2018) for Guna district have also shown conformance with study highlighting the variability from 'poor to worse' in the water quality of samples obtained from various tube wells, which are being used for domestic purpose. Presence of higher concentrations of nitrates has also been observed due to the fertilizer industry in the study area. Depleting groundwater table resulting in increased intrusion of some geogenic as well as higher concentrations of manmade pollutants was projected as possible reason for groundwater contamination.

9.3.2 *Results of Informal Survey*

An informal survey has been conducted in the study areas for understanding the extent of awareness regarding the water-related issues among the consumers and

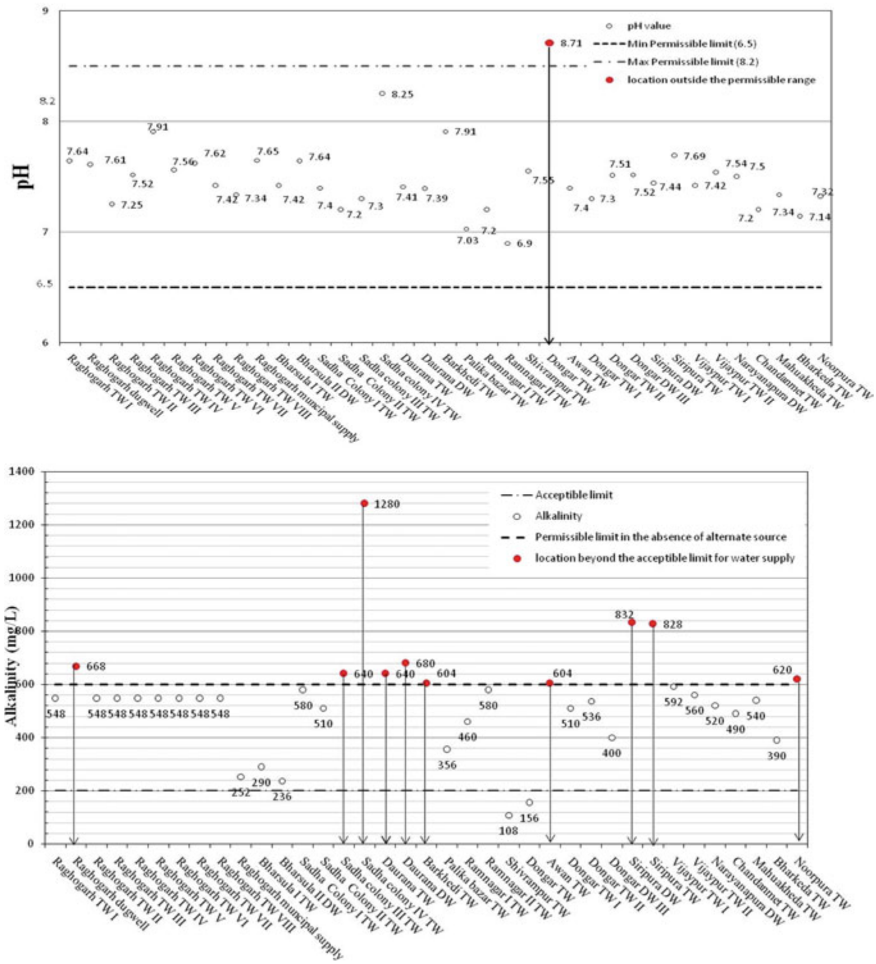

Fig. 9.4 Groundwater quality in various regions of Raghogarh municipal area

local bodies. The interactions (informally) were held with two broader categories of the stakeholders, i.e., public servants (associated with Raghogarh municipality) and consumers in different villages. The responses are presented in a nut shell in Table 9.3, and corresponding remarks from their observations have also been discussed.

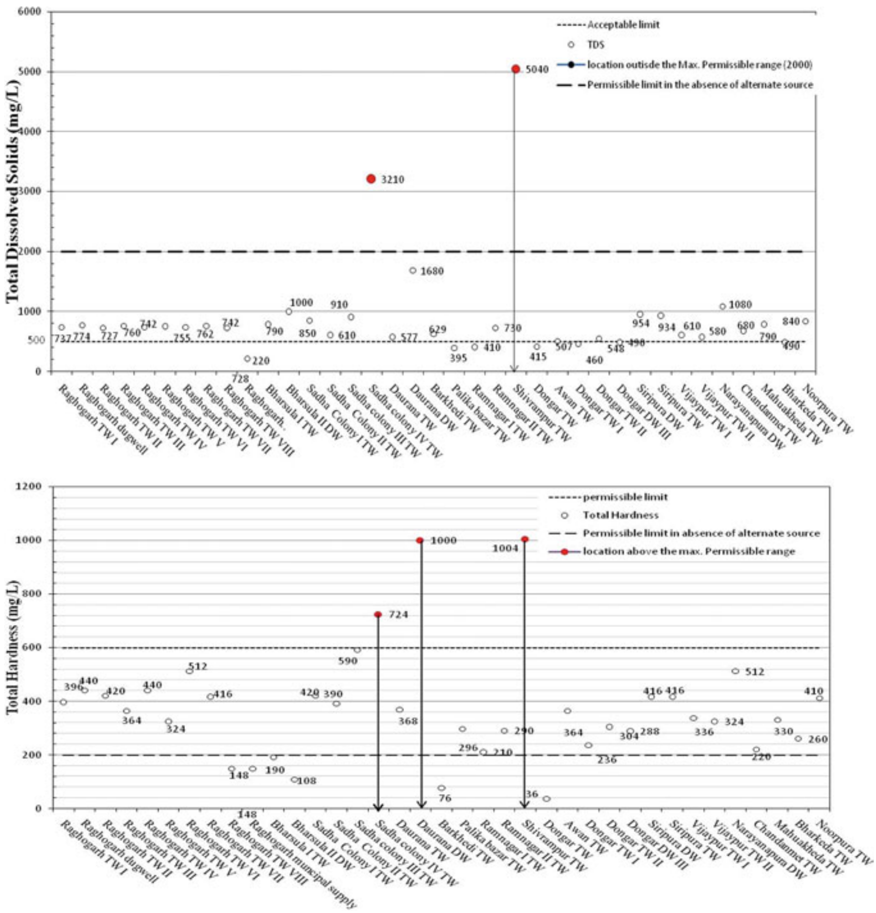

Fig. 9.4 (continued)

9.4 Investigations Undertaken

9.4.1 Defluoridation Potential of Local Clays

To study the applicability of local clays for fluoride removal, standard fluoride solutions were prepared and the efficacy of fluoride removal was studied for varying fluoride concentration, contact time, adsorbent dosage and pH in batch mode of operation with constant agitation rate of 100 RPM. Local clays provide benefit of low cost and ease of recycling with suitable processing. The following are characteristics of clay: specific gravity of 2.8, coefficient of uniformity—8.8, coefficient of curvature—1.05, liquid limit—41%, plastic limit—23% and shrinkage limit—19%. Potters clay was obtained from nearby Raghogarh area and then washed with

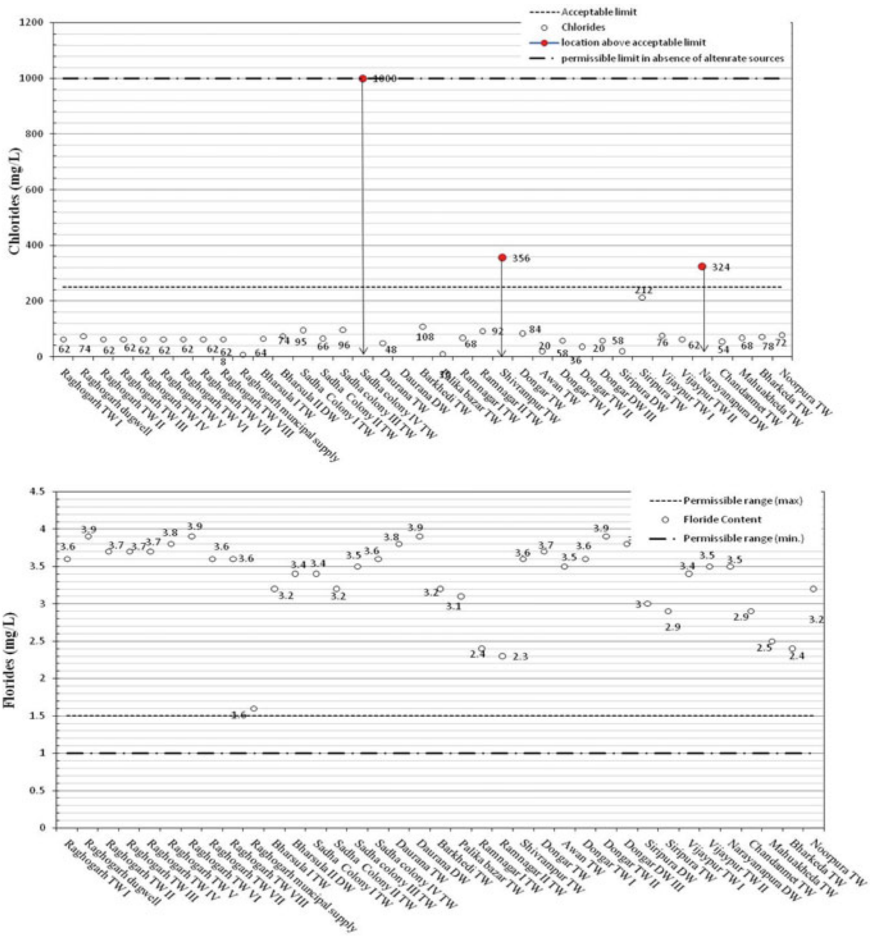

Fig. 9.4 (continued)

distilled water twice and, subsequently, oven-dried for two days. Chemical analysis of the clay indicated the presence of flowing oxides: SiO_2—78.6%, Al_2O_3—8.06%, Fe_2O_3—7.65% and loss on ignition—4.87%. These tests were conducted as per IS 1727-1967 (BIS 1967), to understand the potential of the material for fluoride uptake.

Results of batch studies conducted at varying conditions were shown in Fig. 9.5. The results have proved that locally available clay could be used as potential adsorbent for defluoridation (up to 60%) for the fluoride concentration of 4 mg/L without any pretreatment. Another advantage observed in the work was lesser influence of pH and contact time. The adsorbent could be adopted at normal pH of groundwater.

Table 9.3 Results of informal survey regarding water supply

Stakeholders	Broad topics of discussion	Issues highlighted	Remarks
Public servants	– Status of existing water supply – Contaminants – Health impacts	– Decreasing groundwater levels – Presence of contaminants in certain blocks – No clarity about direct health issues The solution that has been highlighted for all the abovementioned problems was the sanctioned 17 MLD water treatment plant with 100% coverage	The officials were aware of the problems in certain blocks, but overall magnitude of the problems in the study area was not clear
Consumers		– Need for more number of tube wells for fulfilling existing demands – No idea (some of them have expressed the concerns related to the hardness causing salty taste) – No awareness on health-related concerns	Public at large was not even aware of the qualitative and quantitative issues. People expressed satisfaction with the available water supplies

9.4.2 Alternate Rainwater Harvesting System for JUET

One of the feasible alternatives for water quality issues and transmission losses in the present mode of rainwater harvesting is by providing harvesting structures nearby the source of generation for immediate reuse. Present work has also examined the scope for such arrangement with proposed multiple reservoirs at different locations in the campus. Water requirements of respective units were calculated in accordance with IS 1172 (BIS 1993b), and rain harvesting potential was assessed using rational method using the following equation given below.

$$Q = \frac{\text{CIA}}{360}$$

where Q = Quantity of runoff, $\frac{\text{m}^3}{\text{s}}$, C = Coefficient of runoff (the values of C were varied as follows: $C = 0.9$ for roof top areas, $C = 0.7$ for roads, open and garden areas = 0.3), I = Intensity of rainfall (mm/h), A = Area in hectares (MOUD 2013).

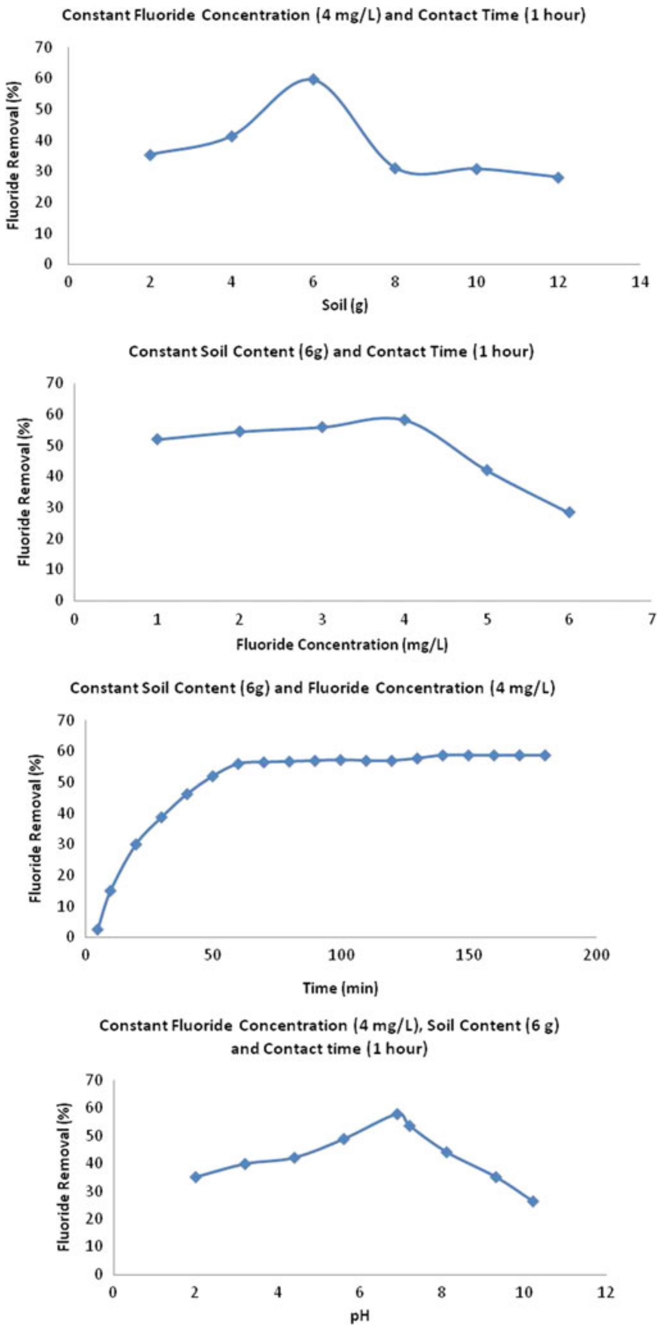

Fig. 9.5 Defluoridation using local clay at varying conditions

Landuse pattern and roof top areas of various buildings are shown in the Fig. 9.6a. After calculations based on rational method, the rainwater harvesting potential annually of the campus is shown in Fig. 9.6b. From the figure, it could be concluded that actual harvesting potential of the campus is much higher than the existing capacity of the lake (without losses). Harvested rainwater could well be utilized near the source itself for its potential reuse, reducing the costs associated with transmission, treatment and distribution in the existing scheme. Feasible locations for reservoirs have also been identified through an understanding of the storm water path from point of origin to drain. Reservoir locations have been finalized after study of contour plan of the campus so as to facilitate easy capture of rainwater from single or multiple buildings. Layout showing the reservoir locations is presented in Fig. 9.6c, and details of the reservoirs indicating the buildings from which storm water can be beneficially collected and put to effective reuse were shown in Table 9.4. Additionally, it could also result in significant savings in the present mode of water supply from source that is far away from the institute. Reservoirs could be equipped with conventional filtration type of chambers for immediate processing for reuse.

9.4.3 Feasibility Studies for Multiple Aerobic Lagoons

With alternate rainwater harvesting system in place (as proposed in the study), existing lake can be developed as multiple ponds in series for low-cost treatment of domestic wastewater. Multiple aerobic systems in series are proposed and designed: aerobic lagoon—(30*15*0.9) m (2), contact basin—(25*20*1) m and maturation lagoon—(30*20*1) m. Design of these treatment systems was done as per Manual of Sewerage and Sewage Treatment, GOI (MOUD 2013). Design parameters such as oxygen requirements for the aerobic ponds have been calibrated on basis of a series of trials in aeration apparatus by properly correlating air transfer mechanically with respect to contact time in the device. The abovementioned parameters have been simulated in aeration studies apparatus by KC Engineers, for evaluating actual performance of respective units. Though the performance in simulated aeration apparatus could vary with actual performance in the external environment, the studies could provide valuable information for understanding the oxygen transfer efficiency of the proposed system.

Integrated sample has been collected on hourly basis for 24 h for obtaining a representative sample. Samples were obtained before and after biological treatment (MBBR) and compared with results obtained from aeration studies for multiple aerobic lagoons. The collected sample was analyzed immediately for the parameters such as dissolved oxygen (DO), biochemical oxygen demand (BOD), chemical oxygen demand (COD), total solids (suspended and dissolved) and chloride with respect to IS: 3025 (BIS 2012b; BIS 1993a; BIS 2006; BIS 2003; BIS 1988).

Table 9.5 shows the comparison of wastewater analysis results between the existing MBBR with the proposed treatment system (i.e., aerobic lagoon, contact basin and maturation lagoon in series). The results reveal clearly that the alternate

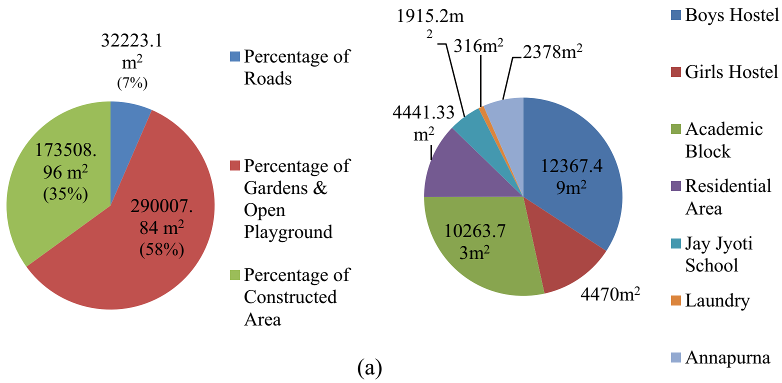

(a)

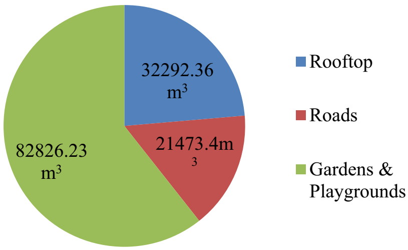

(b)

(c)

Fig. 9.6 **a** Delineation of the landuse in campus, **b** annual rainwater harvesting potential and **c** layout showing various locations of reservoirs and building for immediate reuse

Table 9.4 Reservoir and their associated buildings for storm water collection

Building name	Reservoir	Reservoir capacity (m^3)
Boys Hostel (1–6)	R1	34.3
Boys Hostel (7–9) Annapurna Mess	R2	38.55
Boys Hostel (10–16)	R3	34.3
Boys Hostel (17–21)	R4	25.47
Girls Hostel	R5	40.23
Academic Block-I	R6	25.2
Academic Block-II	R7	31.62
Academic Block-III	R8	35.55
Residential Area-I	R9	13.83
Residential Area-II	R10	12.43
Residential Area-III	R11	5.64
Residential Area-IV	R12	7.12
Residential Area-V	R13	8.03
Residential Area-VI	R14	6.73
Jay Jyoti School	R15	17.23
Laundry	R16	2.84

treatment has been adequate to maintain the effluent standards similar to that of MBBR technology. Adaptation of such systems shall result in energy efficiency for closed loop systems. The study has examined the benefits of only using the lake as a substitute to the existing MBBR for achieving energy efficiency; the other preliminary and primary treatment systems such as equalization, screening and comminuting could be continued as existing in the present scenario. Moreover, there will be direct saving in terms of reduction of costs incurred for installation of equipment, operational and maintenance costs as compared to MBBR system. In addition to its simplicity in operation, the proposed system could also augment groundwater against for declining groundwater levels in the region.

9.5 Tradeoffs for Policy Framework

Tradeoffs between the following variables need to be analyzed clearly in devising suitable water management framework relevant to broader national context. These approaches draw the comparison between the present systems at national scale causing negative impacts on human well being in form or other with proposed modified systems augmenting sustainable water supplies.

Table 9.5 Performance of the proposed treatment systems in comparison to existing MBBR

Parameter	BOD (mg/L)	COD (mg/L)	DO (mg/L)	pH	Chlorides (mg/L)	Total suspended solids (mg/L)	Total dissolved solids (mg/L)
Influent wastewater characteristics	140	320	0	7.1	120	60	120
Proposed system: aerobic pond	45	280	3.9	7.3	70	20	98
Contact basin	34	258	4	7.5	65	0	95
Maturation pond	26	245	4.1	7.6	65	0	95
Existing system: MBBR	18	210	4.2	7.8	60	0	90

9.5.1 Centralized Administration Versus Decentralized Participatory Approaches

Water supply systems could be either centralized or decentralized, but decentralized system offers wider advantages due to the reduction in transmission costs and associated environmental burdens in processing. The study urges the need for participatory decentralized approach with due involvement of all the stakeholders against the centralized administration. In case of JUET, the stakeholders in the university feel sense of responsibility and pride, in sharing the information on the existing system. This pragmatic approach could be really useful to focus on diverse areas in conserving environment. In adopting local materials for water treatment, the continuity of the system in rural areas depends on the resource availability and its reclamation. Hence, it becomes imperative to involve public with suitable incentives for providing the raw material and reusing the processed exhausted material. As a whole, decentralized participatory approaches could assist easy installation and handling of the system within the available resources. Additionally, other issues such as water harvesting could also be well dealt in conjunction by suitably educating the stakeholders.

9.5.2 Energy Efficiency Versus Land Availability

Adoption of closed cycle approach employing wastewater treatment and reuse could reduce the burden on existing water resources to cater to the ever-increasing demands. Decentralized treatment can be classified further as ‘with source separation’ and ‘without source separation.’ In the source separation-based treatment systems, such as urine diversion toilets and composting toilets, the gray water and night soil are separated at the source, for more effective treatment of wastewater along with relatively easier reuse. These systems provide multiple benefits through compost preparation from anaerobic digestion of night soil along with processing of urine containing natural nutrients as a fertilizer for plant growth. Treatment systems such as upflow anaerobic sludge blanket, constructed wetlands and stabilization basins including aerated ponds employing natural treatment systems such as duckweeds, water hyacinth and algae can be beneficially employed for low-cost wastewater treatment contributing to sustainability (Al-Jayyosi 2003; Arceivala and Asolekar 2007; Bernal 2018; Randall and Naidoo 2018). These systems can be instrumental in achieving higher water use efficiency even in urban areas by optimizing the water requirements for various purposes. Meteorological conditions in majority of the areas in the country are favorable for adaptation of such decentralized aerobic systems, that can result in potential savings in the treatment costs.

9.5.3 Replenishment of Resources Versus Consumption Patterns

It is highly necessary to have suitable balance between these variables in present era of changing hydrologic scenarios. Possible ways of replenishment such as rainwater harvesting, wastewater reuse and optimizing the consumption patterns need to be well explored. The work puts forward certain issues for beneficial and optimal utilization of available resources and also for augmenting the supplies with artificial recharge. In addition to the aspects mentioned here, another important fact noticed during the course of study was increasing application of domestic demineralization systems (such as Reverse Osmosis system (RO)) at household level. Use of RO-based systems generates large amount of reject water, after treatment, and it constitutes wastewater again increasing the load on existing sewage treatment facilities. The National Green Tribunal (a statutory body for speedy dealing of environmental issues) has issued notification banning RO purifiers at locations having TDS in water less than 500 mg/L and instructed the ministry of environment and forest to notify guidelines accordingly (The Hindu 2020). As a matter of fact, there is need to address this issue as in case of JUET campus the water being supplied in the campus is being treated to the level of tertiary treatment, and therefore, it does not require any further processing. Moreover, the RO users need to be educated properly about its adverse health effects of consuming excessively polished effluents.

9.5.4 Natural Pollutants Versus Anthropogenic Pollutants

Groundwater quality in the study has been influenced by both natural and manmade contaminants. Increasing entry of geogenic pollutants has been one of the major problems in many regions of the country. Therefore, it has become imperative to focus on preventing the entry of manmade pollutants from unsewered areas along with other factors. Geogenic pollutants such as fluoride increase with rock-water interaction, and therefore, replenishment or augmenting the existing water resources could dilute such contaminants significantly.

9.5.5 Actual Scenario Versus Awareness Among Stakeholders

The biggest challenge in transforming the existing patterns toward healthy and sustainable lifestyles is the social acceptance. As pointed previously, consumers of polluted water have been in denial to accept the actual scenario. This aspect needs to be carefully addressed through proper education of the exposed public. Awareness about the future consequences encourages people to adopt necessary measures for ensuring a sustainability of the system.

9.5.6 Ecological Concerns Versus Economics of Management

This aspect needs a brainstorming discussion urgently at national and global platforms. There is an immediate need to understand that ecological variables have significant influence on economic development of every nation. Hydrologic component in a country like India has strong influence on well being of its population. Hence, there is an immediate need to devise strategies for short-term as well as long-term benefits with due importance to ecological variables with economic savings through alternate technologies and use of renewable resources, as discussed in study.

9.6 Concluding Remarks

In the present era of anthropogenic intervention with natural systems, educating the human conscience on futuristic consequences and their relevance to human well being remains vital. Encouraging the decentralized participatory approaches with community participation provides the necessary solution in that direction. Devising national policy framework adopting closed loop approaches considering the regional concerns is of prime importance. The present work outlines various aspects that could aid in devising an appropriate strategy. This wholesome approach offers ecological benefits such as reducing the carbon foot print of the systems, exploration of low-cost alternatives and more importantly restoration of nature systems. These initiatives in longer run could reduce the water stress at national level in addition to overcoming diverse challenges of nation due to anomalies in distribution of water resources, development patterns and regional issues.

The following are the major outcomes from the study area:

- Groundwater quality in the Raghogarh municipal area projects a grim picture of its suitability for consumption in most of the areas. Fluoride remains major pollutant of concern throughout the study area, and other parameters such as high dissolved solids, total hardness and chlorides were observed due to geological and local to regional influences like improper sewerage system (particularly open sewers nearby hand pumps).
- Defluoridation using the local clays proves to be low-cost suitable option with removal up to 60% for fluoride concentration of 4 mg/L. The process can be further enhanced with suitable pretreatment and reusing the exhausted adsorbent.
- Proposed alternate rainwater harvesting system provides multiple advantages, i.e., converting the existing lake into low biological wastewater processing unit and reusing the rainwater nearby the source minimizing the transmission losses. A total quantity of 32,292.36 m^3 from rooftop and 104,299.63 m^3 from open areas can be harvested in the campus. Feasibility studies conducted with domestic wastewater on aerobic ponds/lagoons in the series have yielded identical results to the existing moving bed biofilm reactor. With availability of lake with storage potential of 10,000 m^3, ponds/lagoons are beneficial for economical processing of the wastewater.

Acknowledgements The authors express heartfelt regards to management of Jaypee University of Engineering and Technology for providing necessary data. Authors are also thankful to Dr. P. K. Singh and Dr. Sunil Srivastava, Faculty, JUET for providing support in sample analysis. The authors also thank undergraduate students Sukalp Jain, Ashutosh Yadav, Sanjay Yadav and Kanha Garg for their assistance at various points of time.

References

Al-Jayyousi OR (2003) Greywater reuse: towards sustainable water management. Desal 156(1–3):181–192. https://doi.org/10.1016/S0011-9164(03)00340-0

Araral E, Ratra S (2016) Water governance in India and China: comparison of water law, policy and administration. Wat Po 18:14–31. https://doi.org/10.2166/wp.2016.102

Arceivala SJ, Asolekar SR (eds) (2007) Wastewater treatment for pollution control and reuse. Mcgraw Hill Education Pvt Ltd, New Delhi, India, ISBN 978-0-07-062099-5

Asian Development Bank (ADB) (2021) Details available online at https://www.adb.org/projects/42486-018/main

Bernal D (2018) A conceptual model for decentralized municipal wastewater management. Wat Pract Tech 13(1):134–143. https://doi.org/10.2166/wpt.2018.022

Bhattacharya S (2015) Traditional water harvesting structures and sustainable water management in India: a socio-hydrological review. Int Lett Nat Sci 37:30–38. https://doi.org/10.18052/www.scipress.com/ILNS.37.30

Biswas AK (1991) Water for sustainable development in the 21st century. GeoJ 24:341–345. https://doi.org/10.1007/BF00578255
Bureau of Indian Standards (BIS) (1967) Methods of test for pozzolanic materials. IS: 1727
Bureau of Indian Standards (BIS) (1983) Methods of sampling and test (physical and chemical) for water and wastewater. IS: 3025 (PART-11) pH
Bureau of Indian Standards (BIS) (1987) Methods of sampling and test (physical and chemical) for water and wastewater. IS: 3025 (PART-1) Sampling
Bureau of Indian Standards (BIS) (1988) Methods of sampling and test (physical and chemical) for water and wastewater. IS: 3025 (PART-32) Chloride
Bureau of Indian Standards (BIS) (1993a) Methods of sampling and test (physical and chemical) for water and wastewater. IS:3025 (PART-44) Biochemical oxygen demand
Bureau of Indian Standards (BIS) (1993b) Code of basic requirements for water supply, drainge and sanitation. IS: 1172
Bureau of Indian Standards (BIS) (2003) Methods of sampling and test (physical and chemical) for water and wastewater. IS: 3025 (PART-16-17) Total solids, Total suspended solids and Total dissolved solids
Bureau of Indian Standards (BIS) (2006) Methods of sampling and test (physical and chemical) for water and wastewater. IS: 3025 (PART-58) Chemical oxygen demand
Bureau of Indian Standards (BIS) (2008) Methods of sampling and test (physical and chemical) for water and wastewater. IS: 3025 (PART-60) Fluoride
Bureau of Indian Standards (BIS) (2009) Methods of sampling and test (physical and chemical) for water and wastewater. IS: 3025 (PART-21) Hardness
Bureau of Indian Standards (BIS) (2012a) Indian standard drinking water specification. IS: 10500
Bureau of Indian Standards (BIS) (2012b) Methods of sampling and test (physical and chemical) for water and wastewater. IS: 3025 (PART-38) Dissolved oxygen
Central Public Health & Environmental Engineering Organization (CPHEEO) (1999) Manual on water supply and treatment, Ministry of urban development, GOI.
Central Water Comission CWC (2017) Available online at http://www.cwc.nic.in/main/webpages/statistics.html#1
Chandran S, Thiruchelve SR, Dhanasekarapandian M (2021) Integrated urban water resources management strategy for a smart city in India. Wat Sup 21(2):736–749. https://doi.org/10.2166/ws.2020.325
Cronin AA, Prakash A, Priya S, Coates S (2014) Water in India: situation and prospects. Water Pol 16:425–441
Dhanya V, Renoy G (2017) Water governance and public participation: what matters? Cur Sci 112(4):686
Fischer HW, Ali SS (2019) Reshaping the public domain: decentralization, the Mahatma Gandhi national rural employment guarantee act (MGNREGA) and trajectories of local democracy in rural India. World Dev 120:147–158. https://doi.org/10.1016/j.worlddev.2018.09.013
Hamish H, Philip S, Vera N (2021) Using community data to improve rural water infrastructure in India. Proc Ins Civil Eng Civil Eng 174(6):3–10. https://doi.org/10.1680/jcien.20.00058
Hans BV (2018) Water management in agriculture: issues and strategies in India. Int J Dev Sus 7(2):578–588
Hoekstra AY (2017) Water footprint assessment: evolvement of a new research field. Wat Res Manage 31:3061–3081. https://doi.org/10.1007/s11269-017-1618-5
Howath C, Monasterolo I (2016) Understanding barriers to decision making in the UK energy-food-water nexus: the added value of interdisciplinary approaches. Env Sci Pol 61:53–60
Indian Meteorological Department IMD (2017) Available online at http://www.imd.gov.in/
Jain SK, Kumar P (2014) Environmental flows in India: towards sustainable water management. Hyd Sci J 59(3–4):751–769. https://doi.org/10.1080/02626667.2014.896996
Keshari AK (2007) Water resources scenario of India: emerging challenges and management options. National Training Course on Farm land and water management, Central Soil Salinity Research Institute, Karnal, Haryana, March, pp 16–25

Kumar M, Kumar PP (2013) Climate change, water resources and food production: some highlights from India's standpoint. Int Res J Env Sci 2(1):79–87

Kumar R, Singh RD, Sharma KD (2005) Water resources of India. Cur Sci 89(5):794–811

Lohani B, Siddiqi Y, Kilroy G (2016) Economic growth and climate proofing Asia through sustainable water resources management. In: Biswas AK, Tortajada C (eds) Water security, climate change and sustainable development, Springer Nature, Switzerland, pp 83–105

Loucks DP (2000) Sustainable water resources management. Wat Int 25(1):3–10. https://doi.org/10.1080/02508060008686793

Marlow DR, Moglia M, Cook S, Beale DJ (2013) Towards sustainable urban water management: a critical reassessment. Wat Res 47(20):7150–7161. https://doi.org/10.1016/j.watres.2013.07.046

Megdal SB, Eden S, Shamir E (2017) Water governance, stakeholder engagement, and sustainable water resources management. Wat 9(3):190–197. https://doi.org/10.3390/w9030190

Ministry of Statistics and Programme Implementation (MSPI) (2013) Statistics related to climate change—India. Available online at https://mospi.nic.in/mospi_new/upload/climate_change_29nov13.pdf

Ministry of Urban Development (MOUD) (2013) Manual on sewerage and sewage treatment. Available online at http://moud.gov.in/Manual%20on%20Sewerage

Misra AK (2014) Climate change and challenges of water and food security. Int J Sus Built Env 3:153–165. https://doi.org/10.1016/j.ijsbe.2014.04.006

Moore SM (2017) The dilemma of autonomy: decentralization and water politics at the subnational level. Wat Int 42(2):222–239. https://doi.org/10.1080/02508060.2017.1276038

MPWRD (2021) Madhya Pradesh water resources department. Available online at http://www.mpwrd.gov.in/water-quality

Mukherjee A, Saha D, Harvey CF, Taylor RG, Ahmed KM, Bhanj SM (2015) Groundwater systems of the Indian sub-continent. J Hyd Reg Stud 4:1–14. https://doi.org/10.1016/j.ejrh.2015.03.005

National Academy of Agricultural Sciences (NAAS) (2013) Climate resilient agriculture in India. Policy Paper 65. Available online at http://naasindia.org/Policy%20Papers/Policy%2065.pdf

National Water Mission (NWM) (2011) National action plan on climate change comprehensive mission document, vol 1. Available online at http://wrmin.nic.in/writereaddata/nwm16606419934.pdf

Niti Aayog (2019) Composite water management index. Available Online at https://niti.gov.in/sites/default/files/2019-08/CWMI-2.0-latest.pdf

Poff NL, Brown CM, Grantham TE, Matthews JH, Palmer MA, Spence CM, Wilby RL, Haasnoot M, Mendoza GF, Dominique KC, Baeza A (2016) Sustainable water management under future uncertainty with eco-engineering decision scaling. Nat Clim Change 6(1):25–34. https://doi.org/10.1038/nclimate2765

Punjabi B, Johnson CK (2019) The politics of rural–urban water conflict in India: untapping the power of institutional reform. World Dev 120:182–192. https://doi.org/10.1016/j.worlddev.2018.03.021

Randall DG, Naidoo V (2018) Urine: the liquid gold of wastewater. J Env Chem Eng 6(2):2627–2635. https://doi.org/10.1016/j.jece.2018.04.012

Satvat PS, Nayak SC, Shukla SP (2004) Rainwater treatment technology: a viable solution for green water in the new millennium. In: Proceedings of workshop on environmental pollution: perspectives and practices, institute of engineering and technology, Lucknow, pp 111–117

Singh LK, Jha MK, Chowdary VM (2017) Multi-criteria analysis and GIS modeling for identifying prospective water harvesting and artificial recharge sites for sustainable water supply. J Cle Prod 142(4):1436–1456. https://doi.org/10.1016/j.jclepro.2016.11.163

Srivastava SK, Ramanathan AL (2018) Geochemical assessment of fluoride enrichment and nitrate contamination in groundwater in hard-rock aquifer by using graphical and statistical methods. J Earth Sys Sci 127:104. https://doi.org/10.1007/s12040-018-1006-4

The Hindu (2020) Available online at https://www.thehindu.com/news/national/ngt-asks-govt-to-ban-ro-purifiers-that-demineralises-water/article32075468.ece. Date of publication 14th July 2020

UNESCO (2021) A qualitative framework to evaluate the extent of integrated urban water management in Indian cities and applying the framework to Delhi. National institute of urban affairs and United Nations educational, scientific and cultural organization. Available at https://en.unesco.org/news/indian-cities-aiming-sustainable-water-management

Wescoat JL Jr, Shah RP, Singh R, Murty JVR (2019) Habitations, villages, and gram panchayats: local drinking water planning in rural India with a Pune district case study. J Wat San Hyg Dev 9(3):522–530. https://doi.org/10.2166/washdev.2019.196

World Bank Group (WBG) (2016) High and dry-climate change, water, and the economy. International Bank for Reconstruction and Development/The World Bank, Washington, DC

Zang J, Kumar M, Werner D (2021) Real-world sustainability analysis of an innovative decentralized water system with rainwater harvesting and wastewater reclamation. J Env Mgmnt 280:111639. https://doi.org/10.1016/j.jenvman.2020.111639

Chapter 10
Linkages of Surface Water with Groundwater for Water Resource Management in Water Deficit Region of India

Pawan Jeet, Mridusmita Debnath, Jathot Veeranna, Ashutosh Upadhyaya, and Anil Kumar Singh

Abstract Groundwater contributes 98.5% of the remaining fresh water available for use is stored in groundwater and only 0.98% of fresh water is available at surface, viz. rivers, lakes, ponds, and so on. However, over time, aberrations in rainfall patterns and overuse of aquifers resulted in groundwater recharge (GWR) depletion and water level has fallen in most parts of India resulting in severe drought like situations in several parts of the country. This can be resolved mainly through linking surface water with groundwater resources for GWR. It is reported that by considering 60% and 30% of surface runoff combined with river bed recharge and natural recharge through rainfall, the net GWR varied from 0.33 to 1.66 m and 0.16 to 1.06 m above mean sea level, respectively. In plain dryland conditions and hills and plateau regions, GWR rates are approximately 11–18 and 11–16% of average annual rainfall. Through water harvesting structures, the total GWR is about 38.53% of total GWR. Therefore, assessment of GWR potential is essential to develop linkages of surface water to groundwater for integrated water resource management.

Keywords Groundwater · Surface water · Water resource · GWR · India

10.1 Introduction

Water is required to safeguard food security, feed livestock, conserve biodiversity and environment, and industrial uses. Rising population, excess water resource use, underground salty water, insufficient canal water supply for irrigation, and frequent

P. Jeet · M. Debnath (✉) · A. Upadhyaya · A. K. Singh
ICAR Research Complex for Eastern Region, Patna, Bihar 800014, India
e-mail: mridu.ars590@gmail.com

M. Debnath
Civil Engineering Department, Indian Institute of Technology, Guwahati, Assam 781039, India

J. Veeranna
Professor Jayashankar Telangana State Agricultural University, Hyderabad, Telangana 500030, India

P. Shukla et al. (eds.), *Environmental Processes and Management*, Water Science and Technology Library 120, https://doi.org/10.1007/978-3-031-20208-7_10

aridity are the significant reasons for critical water shortage. The ever-increasing difference between availability and utilization of surface and groundwater is causing severe water shortages in many regions. Worldwide water demand has been rising annually at around 1% over the decades on account of the socio-economic rise and changes in consumption patterns. Water demand for domestic and industrial sector is increasing rapidly than that of agricultural water demand, although agriculture will continue to be the most prominent water consumer. Globally, demand for water in agricultural and energy production will probably increase by about 60 and 80% by 2025 (Water 2018). Groundwater and surface water are two interlinked parts, and impacts on any of the components will affect the other (Abdelhalim et al. 2020). The failure of monsoonal rainfall in particular areas leads to a decline in groundwater and surface water availability, which has impacted the water availability for agriculture, industries, drinking water supply, flora, and fauna. Globally, groundwater extraction for irrigation has been recognized as the primary driver of groundwater depletion. Even as the country's population is increasing and the demand of water resources is also increasing, resource accessibility of the country continues to be limited.

Rainwater is the basis of surface and groundwater availability. Generally, rainfall above the interception, surface storage, and infiltration flows as overland flow and reaches the outlets as surface runoff. Runoff potential at a location on the ground surface mainly depends on the intensity and duration of the rainfall, infiltration rate, and vegetative cover. In contrast, the amount of surface runoff reaching the outlet depends upon the length and characteristics of the surface over which the water flows. However, urbanization leads to impermeabilization, affecting the direct infiltration of rainfall underground. It also lowers evaporation thereby increasing and accelerating surface runoff. Further, radical changes to the surface water movement pathway also occur, which in turn can change direct groundwater recharge or discharge.

Groundwater recharge (GWR) is when infiltrated water travels across the vadose zone and joins to the underground water table. The amount of water reaching to the water table under specific geo-hydrologic and orographic conditions can be expressed as the groundwater recharge potential. The response of different pockets in a watershed to hydrologic variables is not the same as it depends on the land use, soil characteristics, and groundwater situation. These pockets are defined as Hydrologic Response Unit (HRU). Similar HRUs have the same runoff potential to a given amount of rainfall. The potentiality of rainwater harvesting of a catchment can be expressed as the part of runoff potential that reaches to the outlet of HRU. Different HRUs in the watershed may have additional groundwater recharge potential. It assumes its importance in the augmentation of groundwater storage, conservation of surface runoff in subsurface aquifers, and prevention of evaporation losses from surface water bodies by diverting a part of groundwater (Upadhyaya et al. 2007).

Rainwater harvesting (RWH) and GWR are essential activities to augment the depleting groundwater resources, particularly in water deficit regions. Rainwater harvesting is practiced in these places for groundwater recharge and supplemental irrigation through lined and unlined ponds. In many other regions, which have medium rainfalls but experience medium to high evaporation, availability of water limits the recharge. Hard rock poses a constraint for groundwater recharge in several regions of India (Kumar et al. 2006). Essential aspects in deciding the location and size of the RWH and GWR structures are assessing aquifers surface runoff potential and rechargeability. Usually, the area of RWH structures is found by multiple factors, though based on less than intuitive, and includes compromising interests (Mohtar et al. 2006). For the appropriate design of RWH and GWR structures, understanding the spatial and temporal variability in rainfall-runoff and GWR is essential. Though the tools are available for assessing the RWH and GWR potential, these do not account for variability within the watershed. Glendenning and Vervoort (2010) reported that the average daily potential recharge from RWH structures river catchment in the Rajasthan state of India is much more than the actual recharge reaching the groundwater. So far, these water imbalances have been balanced by water storage techniques such as constructing water harvesting bodies to accumulate surplus monsoonal water for use in the drier period of year. In contrast, other parts of the country, there are limited scopes for designing water storage structure. In this part, groundwater resources were previously overexploited, limiting the scope for exploring water to satisfy the demands of different sectors. In some regions, the problem is checking expansion and the rate of exploitation of surface and groundwater resources. Although early hydrological research has given importance to linkages between groundwater and surface water (Chen et al. 2018; Duque et al. 2020), they have long been comprehended and managed separately. However, with growing demand for water and increasing uncertainties in water supply due to climate change, the need to work surface and groundwater as a no-separate entity has drawn attention (Ross 2018; Zeinali et al. 2020). Thus, many countries adopt new legal models for sustainable water use (e.g., Luo et al. 2020). This river interlinking and linking of surface and groundwater resources can be a possible way to resolve the country's water crisis (Jeet et al. 2020). Therefore, there is a need to develop a tool that can account for the variability in rainfall-runoff and GWR potential for evaluating the feasibility of HRU for water harvesting and groundwater recharge.

10.2 Surface and Groundwater Potential Along with Its Availability

10.2.1 Hydrologic Response Unit and Surface Runoff Potential

Rainfall in excess to the interception, surface storage, and infiltration flows as overland flow and reaches to the outlets as surface runoff. Runoff potential at a point on the earth's surface depends on the intensity and duration of the rainfall, infiltration rate, and vegetative cover. In contrast, the amount of surface runoff reaching at the outlet depends upon the length and characteristics of the surface over which the water flows.

An afforested area has a higher infiltration rate and less surface runoff than an urbanized area with a comparatively less infiltration rate and more surface runoff (Ahirwar and Shukla 2018). Flügel (1995) delineated HRUs by using Geographic Information System (GIS) and reported that the interflow is the governing flow process through the slope and the most critical contributor to GWR and river runoff. Several physical hydrological models are used for estimating the surface runoff at the outlet of the basin. Soil and Water Assessment Tool (SWAT), a one such model, is a continuous time, semi-distributed, river basin model. The SWAT model mainly estimates surface runoff and GWR. Abeysingha et al. (2015), Sisay et al. (2017) have drawn much interest over the last two decades due to its easy handling of wide range of basin-based problems at specified spatial and temporal scales. Singh et al. reported that SWAT model estimates were somewhat better than the Hydrological Simulation Program—FORTRAN (HSPF) model mainly due to perfect simulation of low stream flows by SWAT model. Thampi et al. (2010) reported that SWAT model performed practically well in the river basin at both small and large scale for simulating overland flow. The model consistently under-predicted streamflow with relatively higher discharge rates at a larger scale than at a smaller scale. He also found more significant uncertainty in SWAT simulation estimates for the larger watershed. The hydrologic response of any river basin is appropriately assessed by using lumped, semi-distributed, and spatially distributed hydrological models (Watts 2010). Several researchers in India and elsewhere have used SWAT model for studies. Pandey et al. (2008) found that the head reach of the Betwa catchment is more liable to severe drought than the tail reach. Suryavanshi et al. (2017) reported an rising tendency of groundwater storage and surface runoff in the Betwa basin. Similar results were also reported for the Gomati river basin of India (Abeysingha et al. 2016). Gitau and Chaubey (2010) used various techniques-based input to calculate runoff using SWAT model. SWAT-CUP is a calibration and uncertainty quantification model developed by Abbaspour et al. (2007) to interface with the SWAT model tool for estimating surface runoff, ET, and streamflow components. Sequential Uncertainty Fitting (SUFI-2) is a tool in SWAT-CUP used to assess the uncertainty and sensitivity in streamflow estimation. The parameter's uncertainty is considered one of the sources of uncertainties in modeling. The level of uncertainty is estimated by a parameter called as the *p*-factor. The percentage of observed data is associated with the 95% prediction uncertainty (95PPU). The *p*-factor ranged from 0.64 to 0.84 for calibration and 0.65–0.79 for validation. They used SUFI-2 algorithm of SWAT-CUP with multiple sets of parameter values for calibration and validation. They stated that the parameter uncertainty was not the single source of uncertainty but the structural uncertainty of model was also important for the basin. Uniyal et al. (2015) used SWAT model to simulate stream flow in an east India river basin and evaluate optimization methods' performance to quantify uncertainties. They used SUFI-2, ParaSol, and GLUE optimization methods for the evaluation of model and sensitivity analysis. They found that the model performance using ParaSol and SUFI-2 for simulating the daily stream flow was reasonably good. Based on the evaluation, they also reported that SUFI-2 was able to estimate the uncertainty in complex models like SWAT. Sahoo et al. (2006) used SWAT model to predict streamflow and identify uncertainty and sensitive parameters in the Mahi river basin. They used SWAT-CUP for performing the uncertainty and sensitivity analysis. From statistical analysis, they found that four out of five gauging points resulted in good NSE and R^2. Singh et al. (2013) used SWAT model for prediction of the stream flow in the Tungabhadra catchment of India. They utilized SUFI-2 and GLUE algorithms of SWAT-CUP which works on multiple parameter values. They reported that the difference between simulated and observed discharge was not significant at 95% level of certainty.

Climate change influences various hydro-meteorological components such as precipitation and streamflow, which would impact agricultural productivity in a significant manner, water resource management, and the country's overall economy (Palizdan et al. 2015). The irregularity in monsoonal rainfall has severely affected the water resources in river. The resulting diminishing surface and groundwater has decreased the water availability for flora and fauna of the region and increased famine and drought.

10.2.2 Modeling of Groundwater Recharge Potential and Availability

Water table in developing countries may rise because of the increase in groundwater infiltration rate due to urbanization processes. More generally, heavy abstraction shadows the significant changes in the recharge processes. Piezometric levels decline because of overexploitation of groundwater locally. Thus, it can have additional consequences for groundwater quality with contaminated groundwater being abstracted from deep semi-confined aquifers (Foster and Lawrence 1995). Groundwater modeling is used to predict and evaluate the response of an aquifer to imposed stresses. With predictive capability, groundwater models are a handy tool for planning, designing, and managing groundwater resources. The amount of water reaching the water table under specific geo-hydrologic and orographic conditions can be termed the groundwater recharge potential. The GWR can be estimated with the help of hydrologic model such as SWAT and groundwater models such as MODFLOW (Wang et al. 2008) individually. Later, these two model are integrated as SWAT–MODFLOW model (Yi and Sophocleous 2011). In many other regions other than, arid and semi-arid regions, which have medium rainfalls but experience medium to high evaporation, the availability of water limits the recharge. GWR in dry upland places showed approximately 11–18% of average annual rainfall, and hard rock poses a constraint for GWR in several regions of India and abroad (Gates et al. 2011; Kumar et al. 2008). Head to middle reach of the Betwa basin received more rainfall than that of the middle to tail reach of the catchment (Singhai et al. 2019). However, the groundwater table elevation is more in the head reach than the tail reach of the basin. So, groundwater resource development in the basin is also quite poor. This is possible mainly due to lack of construction of percolation tanks, check dams, and farm ponds structures in the basin. In recent year, the groundwater level in the upper Betwa basin is declining with 65.83% of the total basin area under moderate groundwater recharge zone (Avtar et al. 2010) and the construction of percolation tanks, check dams and farm ponds in the basin may improve this (Nayak et al. 2015). Chung et al. (2006) used SWAT model to estimate a shallow GWR at the watershed scale and reported that the annual recharge ranged from 125 to 191 mm, depending on the selected pedo-transfer functions. Planning of water storage at the river basin scale should be considered for both surface and subsurface water storage. Gontia and Patil (2012) estimated GWR at the Jamka small river watershed of Gujarat, India, using water table fluctuation method. They found that the natural GWR varied from 11 to 16% of average rainfall annually. The total GWR was estimated to be 390.29 ha m, out of total 38.53% GWR through water harvesting structures. This study also revealed that the water harvesting structures were essential in elevating the GWR. Modeling surface runoff, soil moisture, lateral runoff, and GWR announced a higher water deficit in small watersheds. Kumar et al. (2008) delineated possible locations for water harvesting using remote sensing (RS) and GIS in Bakhar watershed of Mirzapur district of Uttar Pradesh using the thematic maps and geomorphological properties of areas. They also suggested the sites for water harvesting and GWR structures in the watershed. Lee and Chung (2006) used SWAT model to estimate a shallow GWR in the watershed. The watershed was dominated with the mixed-forest and agricultural land. The annual recharge in watershed was estimated to be 125–191 mm, depending on the selected pedo-transfer functions such as soil hydraulic conductivity. The result indicated that it is challenging to identify a unique and spatially consistent soil hydraulic conductivity, which is important for modeling groundwater recharge at the watershed. Ouessar et al. (2009) reported that more accurate estimation of GWR would require a ponding and the transmission loss from the stream. In-depth investigation of the movement of water in the vadose zone is needed to better understand the flow as well as recharge processes. Saraf et al. (2004) identified the GWR zones in Dwarkeshwar watershed in Bankura district of West Bengal and Kethan watershed in Vidisha districts of Madhya Pradesh and reported that the degree of difference between the simulated and surveyed drainage networks was also more in GWR areas. The basis of GWR zone recognition was that recharge through rainwater was not entirely flowing as surface runoff. Weerasinghe et al. (2011) developed a model Geographic Water Management Potential (GWMP) for the Sao-Francisco and Nile catchments, which differed in various conditions. They reported that the model may represent potential water harvesting and recharge places for on-farm water management, dams, and soil moisture storage.

10.3 Integration of Surface Water and Groundwater

Integration or conjunctive use of surface and groundwater is more common for two main reasons: (i) to increase the supply of irrigation water and (ii) to improve the groundwater quality. Simultaneous use of groundwater and surface water to meet crop water demand adjoins the advantages of groundwater storage with the surface water storage system. It assists as best measures for efficient water management. Tube wells irrigated areas enhanced irrigation systems' productivity, extended the culturable command areas, and helped prevent waterlogging. Excessive withdrawal of groundwater, declining water level, and well failure are visibly occurring in dry regions or water deficit regions.

A natural resource index was developed using a principal component analysis (PCA) regression tool considering numerous parameters such as rainfall, frequency of drought, and available water. Further, the degraded wastelands, rainfed regions, groundwater availability, etc., are also taken into account. PCA is a tool for grouping geomorphic parameters of a catchment in hydrologic modeling, evaluating and supervising water quality (Gajbhiye et al. 2015), and developing a water sustainability index (Ali 2008). Further, estimation of ecological water level range for lake ecosystems as well as considering water level fluctuations parameters and evapotranspiration index for investigating surface moisture status was developed by Aqua/MODIS model. Spatial water resource vulnerability index was developed using Technique for Order Preference by Similarity to Ideal Solution (TOPSIS) model. Runoff-denoted drought index was developed using statistical distribution for water resource management. The researcher has developed various indices for characterization of spatial problem. For example, a composite hydrological drought index was developed for irrigated areas, index for groundwater quality, soil moisture deficit index, and evapotranspiration deficit. A multimetric index was created for river biological conditions and a index for watershed sustainability (Chandniha et al. 2014). Most hydrologic indexes are based on a single variable, such as precipitation or runoff, soil moisture, or groundwater recharge. Alawneh et al. (2011) worked in the Wadi Bayer Jordan's deserted areas having deficient rainfall and limited water resources. They observed that the GWR strategy is a long-term solution because of harsh climatic conditions and high evaporation rate in areas. They used a homemade spread sheet model and an HEC-HMS model to estimate the surface runoff and the PMWIN model for GWR modeling. They found that the groundwater table will rise from 0.33 to 1.5 m and 0.11 to 0.90 m for 30-day and 15-day retention periods, respectively. Anderson et al. (2011) assessed the value of the drought index and compared it with the evaporative stress index (ESI). They reported that ESI is a function of ET, surface runoff, and soil moisture. Further, evaporative fluxes were likely to be joined to rainfall intensity only over longer period. Kumar and Kumar (2010) developed a composite suitability index (CSI) for water harvesting and GWR structure for Lower Sanjai watershed of Kolhan division in Jharkhand. CSI for each composite unit is calculated by multiplying weightage with each parameter's rank and summing up all the parameters' values. Based on CSI value, they suggested suitable structures for water harvesting and GWR. Snedden and Swenson (2012) developed a hydrologic index for coastal side reference monitoring system across coastal Louisiana and used it to evaluate wetland condition in coastal area.

10.4 Conclusions

There are various parts of India, where groundwater levels are depleting rapidly and need planners' attention to develop some control measures. A suitable and economical water resource management technology should be adopted to maintain balance between availability and withdrawal of surface and groundwater. Assessment of GWR potential is required in order to develop linkages of surface water to groundwater for integrated water resource management techniques. SWAT model can be effectively used for generating water management scenarios for watersheds. An integrated approach is required to manage surface and groundwater resources and link them for groundwater recharge. Further, artificial GWR information must be necessary to comprehend the interaction between groundwater and surface water resources needed to plan and implement water harvesting schemes. Models helped in visualizing the spatial variability in GWR and water availability.

References

Abbaspour KC, Vejdani M, Haghighat S, Yang J (2007) SWAT-CUP calibration and uncertainty programs for SWAT. In: MODSIM 2007 international congress on modelling and simulation, modelling and simulation society of Australia and New Zealand, pp 1596–1602

Abdelhalim A, Sefelnasr A, Ismail E (2020) Response of the interaction between surface water and groundwater to climate change and proposed megastructure. J Afr Earth Sc 162:103723

Abeysingha N, Singh M, Sehgal V, Khanna M, Pathak H (2016) Analysis of trends in streamflow and its linkages with rainfall and anthropogenic factors in Gomti River basin of North India. Theoret Appl Climatol 123(3–4):785–799

Abeysingha NS, Singh M, Sehgal VK, Khanna M, Pathak H, Jayakody P, Srinivasan R (2015) Assessment of water yield and evapotranspiration over 1985 to 2010 in the Gomti River basin in India using the SWAT model. Current Sci 2202–2212

Ahirwar S, Shukla J (2018) Assessment of groundwater vulnerability in upper Betwa river watershed using GIS based DRASTIC model. J Geol Soc India 91(3):334–340

Alawneh B, Al-Salihi A, Rimawi O, Abed A (2011) Modeling of groundwater recharge by rainwater harvesting-Wadi Bayer (Case Study). Jordan J Civil Eng 5(2):191–209

Ali HM (2008) Development of Arab water sustainability index using principal component analysis. In: The 3rd international conference on water resources and arid environments. Citeseer

Anderson MC, Hain C, Wardlow B, Pimstein A, Mecikalski JR, Kustas WP (2011) Evaluation of drought indices based on thermal remote sensing of evapotranspiration over the continental United States. J Climate 24(8):2025–2044

Avtar R, Singh C, Shashtri S, Singh A, Mukherjee S (2010) Identification and analysis of groundwater potential zones in Ken-Betwa river linking area using remote sensing and geographic information system. Geocarto Int 25(5):379–396

Chandniha SK, Kansal M, Anvesh G (2014) Watershed sustainability index assessment of a watershed in Chhattisgarh, India. Curr World Environ 9(2):403

Chen I-T, Chang L-C, Chang F-J (2018) Exploring the spatio-temporal interrelation between groundwater and surface water by using the self-organizing maps. J Hydrol 556:131–142

Chung E-S, Lee KS, Shin M-J (2006) Characteristics of water quantity and quality of the anyangcheon using SWAT model and calculation result of EMC. J Korean Soc Water Environ 22(4):648–657

Duque C, Russoniello CJ, Rosenberry DO (2020) History and evolution of seepage meters for quantifying flow between groundwater and surface water: Part 2–marine settings and submarine groundwater discharge. Earth Sci Rev 204:103168

Flügel WA (1995) Delineating hydrological response units by geographical information system analyses for regional hydrological modelling using PRMS/MMS in the drainage basin of the River Bröl, Germany. Hydrol Process 9(3–4):423–436

Foster S, Lawrence A (1995) Groundwater quality in Asia: an overview of trends and concerns. Water Res J 97–110

Gajbhiye S, Sharma S, Tignath S (2015) Development of a geomorphological erosion index for Shakkar watershed. J Geol Soc India 86(3):361–370

Gates JB, Scanlon BR, Mu X, Zhang L (2011) Impacts of soil conservation on groundwater recharge in the semi-arid Loess Plateau, China. Hydrogeol J 19(4):865–875

Gitau MW, Chaubey I (2010) Regionalization of SWAT model parameters for use in ungauged watersheds. Water 2(4):849–871

Glendenning C, Vervoort R (2010) Hydrological impacts of rainwater harvesting (RWH) in a case study catchment: the Arvari River, Rajasthan, India. Part 1: field-scale impacts. Agric Water Manag 98(2):331–342

Gontia NK, Patil PY (2012) Assessment of groundwater recharge through rainfall and water harvesting structures in Jamka microwatershed using remote sensing and GIS. J Indian Soc Remote Sens 40(4):639–648

Jeet P, Kumar A, Sundaram PK (2020) Interlinking of river: issues and challenges. Hydrology

Kumar B, Kumar U (2010) Integrated approach using RS and GIS techniques for mapping of ground water prospects in Lower Sanjai Watershed, Jharkhand. Int J Geomatics Geosci 1(3):587

Kumar M, Ramanathan A, Rao MS, Kumar B (2006) Identification and evaluation of hydrogeochemical processes in the groundwater environment of Delhi, India. Environ Geol 50(7):1025–1039

Kumar MG, Agarwal A, Bali R (2008) Delineation of potential sites for water harvesting structures using remote sensing and GIS. J Indian Soc Remote Sens 36(4):323–334

Lee D, Chung I (2006) Estimation of ground water recharge using SWAT model. In: AGU fall meeting abstracts, pp H41B–0393

Luo P, Sun Y, Wang S, Wang S, Lyu J, Zhou M, Nakagami K, Takara K, Nover D (2020) Historical assessment and future sustainability challenges of Egyptian water resources management. J Clean Prod 263:121154

Mohtar RH, Zhai T, Choi J-Y, Bruggeman A, Ouessar M, Abdelli F, Engel BA (2006) Web-based GIS-hydrologic modeling for siting water harvesting reservoirs. In: 14th International soil conservation organization conference. Water management and soil conservation in semi-arid environments. Marrakech, Morocco, May 2006, pp 14–19

Nayak T, Gupta S, Galkate R (2015) GIS based mapping of groundwater fluctuations in Bina basin. Aquat Procedia 4:1469–1476

Ouessar M, Bruggeman A, Abdelli F, Mohtar R, Gabriels D, Cornelis W (2009) Modelling water-harvesting systems in the arid South of Tunisia using SWAT. Hydrol Earth Syst Sci 13(10):2003–2021

Palizdan N, Falamarzi Y, Huang YF, Lee TS, Ghazali AH (2015) Temporal precipitation trend analysis at the Langat River basin, Selangor, Malaysia. J Earth Syst Sci 124(8):1623–1638

Pandey R, Mishra S, Singh R, Ramasastri K (2008) Streamflow drought severity analysis of Betwa river system (India). Water Resour Manag 22(8):1127–1141

Ross A (2018) Speeding the transition towards integrated groundwater and surface water management in Australia. J Hydrol 567:e1–e10

Sahoo G, Ray C, De Carlo E (2006) Use of neural network to predict flash flood and attendant water qualities of a mountainous stream on Oahu, Hawaii. J Hydrol 327(3–4):525–538

Saraf A, Choudhury P, Roy B, Sarma B, Vijay S, Choudhury S (2004) GIS based surface hydrological modelling in identification of groundwater recharge zones. Int J Remote Sens 25(24):5759–5770

Singh V, Bankar N, Salunkhe SS, Bera AK, Sharma J (2013) Hydrological stream flow modelling on Tungabhadra catchment: parameterization and uncertainty analysis using SWAT CUP. Current Sci 1187–1199

Singhai A, Das S, Kadam AK, Shukla J, Bundela D, Kalashetty M (2019) GIS-based multi-criteria approach for identification of rainwater harvesting zones in upper Betwa sub-basin of Madhya Pradesh, India. Environ Dev Sustain 21(2):777–797

Sisay E, Halefom A, Khare D, Singh L, Worku T (2017) Hydrological modelling of ungauged urban watershed using SWAT model. Modeling Earth Syst Environ 3(2):693–702

Snedden GA, Swenson EM (2012) Hydrologic index development and application to selected coast-wide reference monitoring system sites and coastal wetlands planning, protection and restoration act projects. US Department of the Interior, US Geological Survey

Suryavanshi S, Pandey A, Chaube UC (2017) Hydrological simulation of the Betwa River basin (India) using the SWAT model. Hydrol Sci J 62(6):960–978

Thampi SG, Raneesh KY, Surya T (2010) Influence of scale on SWAT model calibration for streamflow in a river basin in the humid tropics. Water Resour Manag 24(15):4567–4578

Uniyal B, Jha MK, Verma AK (2015) Assessing climate change impact on water balance components of a river basin using SWAT model. Water Resour Manag 29(13):4767–4785

Upadhyaya A, Singh A, Bhatnagar P, Sikka A (2007) Prospects of artificial ground water recharge in India

Wang S, Shao J, Song X, Zhang Y, Huo Z, Zhou X (2008) Application of MODFLOW and geographic information system to groundwater flow simulation in North China Plain. China Environ Geol 55(7):1449–1462

Water U (2018) 2018 UN World water development report, nature-based solutions for water

Watts G (2010) Water for people: climate change and water availability. Wiley-Blackwell, Chichester, UK

Weerasinghe H, Schneider U, Loew A (2011) Water harvest-and storage-location assessment model using GIS and remote sensing. Hydrol Earth Syst Sci Discuss 8(2):3353–3381

Yi L, Sophocleous M (2011) Two-way coupling of unsaturated-saturated flow by integrating the SWAT and MODFLOW models with application in an irrigation district in arid region of West China. 干旱区科学 3(3):164–173

Zeinali M, Azari A, Heidari MM (2020) Multiobjective optimization for water resource management in low-flow areas based on a coupled surface water–groundwater model. J Water Resour Plan Manag 146(5):04020020

Chapter 11
Water Resource Management—A Sustainable Approach Towards Ground Water Conservation

Rwitabrata Mallick, Swapnil Rai, Kuldip Dwivedi, Nidhi Shukla, and Abhishek Bhardwaj

Abstract A sustainable approach towards water resource management involves land, water and biodiversity in a specific designated area for ecological and sustainable socio-economic purpose towards ground water conservation in hilly areas. The present study shows concept and implementation of watershed management towards developing ground water conservation strategy to minimize the scarcity of water for the local people of Kurseong hill area. Present study finds out the significance and applicability of combined watershed management in and around various tea gardens in Kurseong. Local inhabitants depending on rainfed agriculture are at risk as they are highly vulnerable to changes in seasonal climatic patterns and disturbed water cycle. The people depend on natural jhoras for drinking water supply, household activities and irrigation, but in recent times most of them become seasonal or extinct. 12-month rainfall data has been collected from selected 13 locations of the research area which shows productivity is adversely affected by non-availability of adequate ground water for drinking, household activities and irrigation at critical stages of crop growth. Therefore, the solution is an integrated sustainable approach through watershed management towards conservation of ground water in the study area.

Keywords Water harvesting · Watershed management · Sustainable · Rainfall · Kurseong

R. Mallick · S. Rai (✉) · K. Dwivedi · N. Shukla · A. Bhardwaj
Department of Environmental Science, ASLS, Amity University Madhya Pradesh, Gwalior, Madhya Pradesh, India
e-mail: srai@gwa.amity.edu

R. Mallick
e-mail: rmallick@gwa.amity.edu

K. Dwivedi
e-mail: kdwivedi@gwa.amity.edu

N. Shukla
e-mail: nshukla@gwa.amity.edu

A. Bhardwaj
e-mail: abhardwaj@gwa.amity.edu

P. Shukla et al. (eds.), *Environmental Processes and Management*, Water Science and Technology Library 120, https://doi.org/10.1007/978-3-031-20208-7_11

11.1 Introduction

A watershed is the area of a particular land where the total amount of water that drains off from that region goes into the same place; it might be a stream, a lake or a river (Agarwal and Garg 2002). This water is significant as it is used for drinking purpose, agricultural activities, manufacturing purpose, etc. It also can help in recreational and entertainment activities and function as habitat for various flora and fauna (Al-Rashed et al. 2002). As a result, watershed management towards conservation of ground water resource has become need of the hour especially in hilly areas. Watershed is also an example of a biophysical, hydrological and ecological unit in terms of energy and materials. For that reason, it can also be a suitable and sustainable socio-economic approach towards ground water conservation. Watersheds can be of variable quantitative measures as per the requirement is concerned (Anonymous 1999).

Integrated approach of watershed management is "An adaptive, comprehensive, integrated multi-resource management planning process that seeks to balance healthy ecological, economic, and cultural/social conditions within a watershed. It serves to integrate planning for land and water; it takes into account both ground and surface water flow, recognizing and planning for the interaction of water, plants, animals, and human land use found within the physical boundaries of a watershed" (Anonymous 2003).

Objective of the study is as follows:

- Analysis of the yearly rainfall pattern to understand quantity of precipitation
- Study the present condition of water resources
- Assessment of water resource scarcity issue in the hill area
- Identify the scope of watershed management towards ground water conservation.

11.2 Materials and Methods

11.2.1 Components of Watershed Management

1. Land Resource Management:

In broad sense, the land management interventions activities like structural, productive, vegetative and protective measures.

Several vegetative measures are taken towards establishing watershed management, like adoption of contour farming, controlling soil loss, grassland development, strip cropping, etc. All these practices are primarily done on the hill faces. On the other hand, vegetation development in the barren land is done as a common practice towards vegetative measures for land management (Anonymous 2008a). These practices further involve processes like grassland management, vegetative cover development, mulching, agroforestry, plant cover, vegetative hedges, etc. In case the slope of the hill face is more than carrying capacity, methods like check dam, terracing, bunding, etc., are applied mostly in cases where vegetative measures are insignificant (Anonymous 2008b).

As a part of water resource management, several landslide and mudslide control structures are prepared which also include runoff collection structures and gully plugging structures (Basu and Starkel 2000). Once adopted properly as per the geomorphological characteristics of the land area, this type of water conservation process will become highly successful and implementable (Basu 2001).

2. Water Management under Watershed Management:

Under watershed management task, the ground water management is one of the very important components. For the overall development of the area, it is very important to develop a good and favourable water potential through watershed management. Main source of ground water in watershed is happened to be rainfall; however, the incoming ground water from surrounding areas also shares to some extent. A large portion of rainwater is lost either due to flowing away (runoff) from the area or by some other means.

In order to manage the rainwater, it is very essential to check the outflowing rainwater. It could be done by constructing the structures like pond, reservoirs, etc., in the area. Also, the rain-dependent farming systems can be practised for better utilization of rainwater which is also considered as a measure for ground water management (Das 2006b). Apart from conserving the rainwater, their judicious use either for crop production or other farm operations also plays very significant role in water management (De 2004).

As far as the water management regarding irrigation point of view is concerned, the selection of most suitable irrigation method depending on the crop, soil, land topography, availability of water in the area, etc., is very important. Those irrigation methods should always be at priority, which have better water use efficiency, lesser loss of ground water, etc. Similarly, the choice on cropping system, crop variety, crop duration, etc., based on the water availability can also be very effective in water management (De and Kulirani 2007).

Overall, various interventions followed for water management are outlined below:

(a) Rainwater harvesting
(b) Ground water recharge
(c) Maintenance of water balance
(d) Preventing water pollution
(e) Economic use of water.

In watershed, the ground water conservation by rainwater harvesting is most significant as compared to the other means. The harvested rainwater can be retained for the duration of its need by designing and constructing the suitable structures in light of the same (Jansky and Uitto 2006).

The rainwater harvesting can be in the form of profile ground water conservation or surface water storage. The water conserved in the topsoil profile is the profile ground water conservation. Using the practices of tillage operations such as conservation tillage, zero tillage, mulch tillage, etc., it can be achieved.

Depending on the moisture content in the topsoil profile, a suitable crop can be taken successfully (Koppen et al. 2008). Also, if the quantum of rainwater is very high, then a part of that gets percolate to the lower soil profile and joins to the water table. This happening is called ground water recharge. There have been formulated several water harvesting techniques, worldwide.

However, few simple and cost-effective rainwater-harvesting structures are listed as under:

(a) Percolation pits/tanks
(b) Farm ponds
(c) Bunds and terraces
(d) Reservoirs
(e) Community tanks
(f) Water spreading.

3. Biomass Management:

In a watershed, the task of biomass management can be achieved by following intervention areas:

(a) Preservation of ecosystem
(b) Regeneration of biomass
(c) Conservation and management of forest resource
(d) Enhancement and development of social forestry and strategic approach towards protection of plants
(e) Enhancement in faunal productivity
(f) Activities visioning financial potential and generation of employment
(g) Schemes related to sanitation and health services
(h) Better standard of living of people
(i) Eco-friendly lifestyle of people
(j) Formation of learning community.

11.2.2 Watershed Management Practices

A watershed may involve a host of problems related to soil, water, society, etc., and constraints in between. To remove all the associated problems mere should be need-based objectives. For achieving the target, various practices need to follow in the watershed (Mallick 2008).

Amongst them, the most common practices are listed as under:

1. Management purpose
2. Increasing infiltration rate
3. Increasing field capacity

4. Controlling soil abrasion
5. Method and accomplishment.

The practices to be used for watershed management should be decided on the basis of the management objectives, exactly. Otherwise, the expected result may not be possible to get achieve. For example, if there is need of enhancing the ground water potential in the watershed, then priority must be given for those practices, which augment the ground water recharge, effectively. A little deflection in selection of practices may cause in-conducive result (Mallick 2009).

The task of increasing infiltration rate is to enhance the soil moisture status and accordingly to grow the crop depending on available soil moisture. On the other hand, the enhancement in infiltration rate causes reduction in level of runoff yield from the watershed, which in turn to affect the net available water for reservoir storage or satisfying the demand of other's need (Mallick and Sanyal 2009). The practices to enhance the infiltration rate are the tillage practices, cropping system, addition of organic materials, etc.

The tillage practices make the topsoil surface in loose condition; as a result, when rainfall takes place, a large amount of that gets entered into the soil. The crops enhance the infiltration rate in significant way. In cropped field, there is development of surface roughness, which obstructs the overland flow. Because of this reason, the rainwater gets more time to retain over the land surface; as a result, a huge amount of water gets infiltrated into the soil. The organic matter in the soil improves the soil texture, favourable to enhance the infiltration rate (Nandy 2004).

The status of ground water holding capacity of the soil falling in the watershed plays very important role to develop overall effects on watershed behaviour, either that is in respect of increasing the runoff amount, soil erosion/soil loss or making the soil properties better for good crop yield. The water holding capacity of soil can be improved by adding organic matters in the soil (Randhawa 1963).

The management of watershed with severe soil erosion problem requires very attentive measures to check the erosion, immediately. The practices to be used for erosion control depend very much on the erosion intensity, soil features and cropping practices, mainly. If erosion intensity is not very high and land slope is in mild range, then agronomical measures could be significant to check the soil erosion. On the other hand, when erosion rate and slope steepness of the area are very high, agronomical measures are not effective to check the erosion.

For this situation, the mechanical measures such as bunding and terracing are highly significant in controlling land erosion. Similarly, for gully erosion control a host of practices/methods have been devised such as drop structures, check dams and gabions which can be suitably used for watershed management.

In watershed, if there is stream bank erosion problem, then it can be tackled by using various methods such as spurs, gabions and agronomical measures depending on the bank situation and stream flow rate.

The watershed management measures can be grouped under following two main categories:

1. In terms of purpose
2. Method and accomplishment.

In first category of management measures, the land use and treatment measures are considered which are effective to increase the infiltration rate and water holding capacity of the soil and also prevent the soil erosion from watershed. Under this group, all the biological and mechanical methods employed for erosion control are included.

In second category, those measures are included, which are planned primarily for the management of water flow. The flood water retarding structures, stream/channel improvement to make their carrying capacity sufficient, minor floodways, sediment detention in watershed, etc., are counted for watershed management work.

In brief, the various control measures adopted for watershed management work are listed as under:

1. Vegetative Measures (Agronomical Applications):
   (a) Timber cropping
   (b) Grazing farming
   (c) Fecundating the crop land
   (d) Pampas farming, etc.
2. Engineering Measures (Structural Applications):
   (a) Gorge plugging
   (b) Digressions
   (c) Loughs
   (d) Tarns
   (e) Bilge works
   (f) Deluge protection
   (g) Ground water recharging structures
   (h) Banking.

The 13 locations are denoted numerically in the graphical representations. These are as follows:

Number	Location
1	Gulma Tea Estate
2	Bagdogra
3	Kolabari
4	Kalijhora
5	Bamonpokhari
6	Panighata
7	Khairbani

(continued)

(continued)

Number	Location
8	Long View
9	Pankhabari
10	Jungpana Tea Estate
11	Phulaguri
12	Bittong Cinchona Division
13	Dow Hill

11.3 Result and Discussion

Table 11.1 provides an idea of precipitation in various months beginning from May 2020 to April 2021. Locations are part of Kurseong sub-division as a part of the present study.

According to the data obtained (Fig. 11.1), July received the maximum downpour. May, June, August and September receive relatively higher rainfall. Proper water management plan is required to conserve water (Ray 2005). Climate of Kurseong is happened to be very pleasant; neither chilling winter of eastern Himalaya nor scorching sunlight of bed of Bengal can disturb the weather. Only the monsoon is very dangerous and definitely against the prevailing beauty of the area. It is never ending precipitation at the time of monsoon, especially from the month of June end to early September.

Table 11.1 Month-wise precipitation in the study area

Month	No. of rainy days	Amount of rainfall in mm
May 2020	31	531.6
June 2020	30	971.8
July 2020	31	1639.7
August 2020	31	794.6
September 2020	30	756.5
October 2020	26	123.2
November 2020	13	31.4
December 2020	19	26.9
January 2021	14	31.5
February 2021	9	14.3
March 2021	9	3.6
April 2021	18	140.5

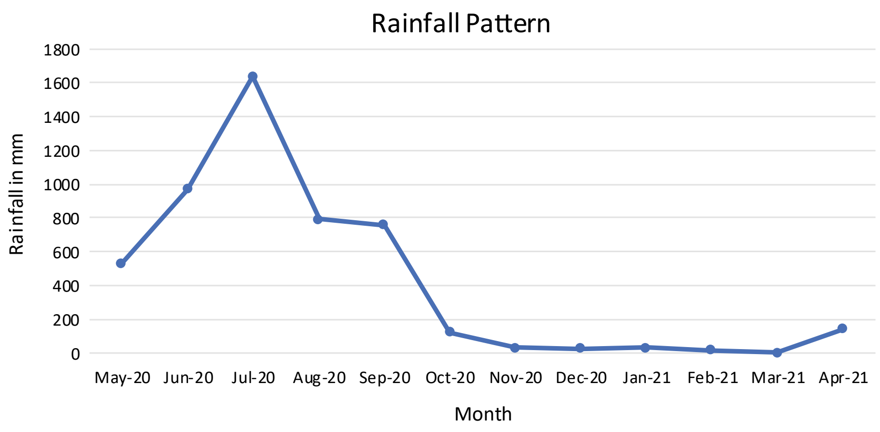

Fig. 11.1 Month wise rainfall mm

11.3.1 Watershed Management

On the basis of exhaustive field study and continuous analysis of data to understand the issue of watershed in the study area, it was found that the main hindrance behind scarcity of water is happened to be the non-availability of domestic water supply during dry period of summer. This is further enhanced by less productivity and scarcity of irrigational water. Watershed management is the only possible effective solution to the situation (Vajpeyi 1998).

Watershed management helps in reducing load of contamination and ground water replenishment. As the process is approach initiated by the local people, sustainable socio-economic development is the key of the approach (Waibel and Zilberman 2007). Through the implementation of integrated water resource management, over-exploitation of natural resources is also reduced. The approach also helps in better crop production and enhancement in land use and land capability. As it is quite evident that watershed areas need good quantity of annual rainfall, it is very much area specific, and the process needs huge investment (Watson 2004). But once the process is initiated and implemented, water conservation will become effective and significant to reduce water scarcity in the area.

11.4 Conclusion

Watershed management is evidently happened to be more comprehensive ground water resource conservation strategy. In watershed management, modifiable and integrated management strategies are being implemented to keep a balance between physical, social and biological components within the landscape. Advanced technologies have influenced very significantly to fulfil the approach. Watershed management is the overall knowledge based on relevant characteristics of a watershed which is primarily focused on sustainable disbursement of its resources and the method of generating and applicability of plans, strategies, policies and opportunities towards sustaining and enhancing watershed functions. Proper implementation of watershed management is only possible and applicable depending on the ground water quality and availability in the region. The approach will lead towards conservation of enough quantity of rainwater as possible at the area where it downpours both at farmlands and common property resources. The integrated practice will help in challenging out excess water with a limited and controllable pace and diverting it to pre-structured storage vacant areas and storing it there for future use especially during the dry season. This process will not only help in water conservation but also increase the socio-economic potential significantly. There is still enough scope for improvement in ground water conservation through watershed management strategies and research.

There is no doubt that watershed development helps to balance the regeneration, conservation and utilization of land resource and water resource within a watershed area by humans. Proper integrated watershed management can lead towards better agricultural yields and potential enhancement in the supply of drinking water.

Present study suggests that the impact of watersheds is relatively more focused towards biological and physical achievements and less on social aspects. There are specific positive trends towards enhancement of water level, better soil regeneration capability, land use, cropping methodology and livestock production because of water management approach. But social achievements are not given sufficient weightage in case of watershed development programme. So, it can be concluded that there should be an integrated approach towards water conservation in the study area so that each and every component is addressed and sustainable development can be achieved at the end.

References

Agarwal SC, Garg KP (2002) Text book on remote sensing. In: Natural resource monitoring and management, Wheeler Publication

Al-Rashed M, Singh VP, Sherif MM (2002) Water resources development and management. In: Proceedings of the international conference on water resources management in arid regions, vol 4, A.A. Balkema, Netherlands

Anonymous (1999) Inter-sectoral water allocation, planning, and management—page 13 by World Bank Staff, World Bank Group, World Bank. South Asia Regional Office. Rural Development Sector Unit, India. Ministry of Water Resources, World Bank—Technology and Engineering

Anonymous (2003) Water resources sector strategy: strategic directions for world bank engagement. World Bank Publications

Anonymous (2008a) Annual report. Divisional Forest Office, Kurseong, West Bengal

Anonymous (2008b) Database. Block Development Office, Kurseong

Basu SR, Starkel L (2000) Rains, Landslides and floods in the Darjeeling Himalaya. INCA, New Delhi

Basu SR (2001) Urbanization and environmental catastrophe in the Darjeeling Himalayas. Impact of Man on Environment: Some Cases of Concern, pp 1–21

Briscoe J, Malik RPS (2007) Handbook of water resources in India: development, management, and strategies, World Bank - Business and Economics, p 46
Das K (2006a) Water resource management of Mahanadi River Basin, Kurseong Block, District Darjeeling, IISWBM
Das M (2006b) Natural resource management of Mahananda River Basin, Kurseong Block, Darjeeling District, IISWBM
De SK (2004) Morphology of Braiding in the lower part of the river Balasan. Indian J Landscape Syst Ecolog Stud 27(2):39–42
De UK, Kulirani F (2007) Issues on national resource management: with special reference to North-East, Regency Publications
Jansky L, Uitto JJ (2006) Enhancing participation and governance in water resource management: conventional approaches and information technology, ISBN: 9280811207, United Nations University Press
Koppen BCP, Giordano M, Butterworth J (2008) Community-based water law and water resource management reform in developing Technology and Engineering, EAN: 9780195685619 Oxford University Press.
Mallick R (2008) An approach towards natural resource management in Kurseong Hill Area. Banabithi, Wild Life Issue, Forest Department, Govt. of West Bengal, pp 18–22
Mallick R (2009) Eco-tourism in Kurseong Hill Areas. Wildly Ours, Volume LI, No.: 9 &10, Director of Information, Department of Information & Cultural Affairs, Govt. Of West Bengal, pp 42–47
Mallick R, Sanyal P (2009) Water resource management in Kurseong Hill Area. J Int 13(4):440–450
Nandy DR (2004) Need for management and conservation of water resources. Indian J Landscape Syst Ecolog Stud 27(3):19–24
Randhawa MS (1963) Natural resources of India: a brief statement
Ray UN (2005) People's Participation in Watershed Management. Kanishka Publishers
Vajpeyi KD (1998) Water resource management. Praeger Publishers, A Comparative Perspective
Waibel H, Zilberman D (2007) International research on natural resource management: advances in impact. Food and Agriculture Organization of the United Nations, Nature
Watson N (2004) Integrated river basin management: a case for collaboration. Int J River Bas Manage 2(3):1–15

Chapter 12
Evaluation of Hydrogeological Models and Big Data for Quantifying Groundwater Use in Regional River Systems

Pooja P. Preetha and Kayla Maclin

Abstract The balanced utilization of water resources is necessary to manage the global water cycle. Hydrogeological models capturing complex interactions of all the spheres of the earth are indispensable for effective strategy formation by a better knowledge of the temporal water cycle patterns with due consideration of environmental changes. In large watersheds, groundwater management and its influences on the surface water systems and the hydrological processes are significant. To account for the interactions of groundwater and to ascertain their consequences on the hydrological responses in large watersheds, integrated models are implemented. This chapter explores the combined use of process-based hydrological models and finite element method to improve groundwater management in regional watersheds comprising multiple cities. The study aims to modify basin-scale hydrogeological model, SWAT-FEM to simulate groundwater use in interconnected regional river systems by combining them with big data-based methodical approaches of statistical and mathematical modeling. Such studies are essential to quantify the significant impact of contaminant transport on groundwater use and other groundwater responses in the natural and anthropogenic conditions in river basins. The negative impacts of anthropogenic activities suggested seasonal reduction of groundwater use in the summer months and a significant rise in the winter months. The annual mean groundwater use in the Chennai basin was predicted as 3.18 mm which is well within the safe groundwater abstraction rate of 4.9 mm. The study results would help reinforce and monitor the extremity of groundwater fluctuations prevalent in the study areas through the combined model systems.

Keywords Hydrogeological modeling · Big data · Remote sensing · Groundwater use · SWAT-FEM

P. P. Preetha (✉) · K. Maclin
Department of Mechanical and Civil Engineering, Alabama A&M University, Normal, AL 35782, USA
e-mail: pooja.preetha@aamu.edu

K. Maclin
e-mail: kmaclin2@bulldogs.aamu.edu

P. Shukla et al. (eds.), *Environmental Processes and Management*, Water Science and Technology Library 120, https://doi.org/10.1007/978-3-031-20208-7_12

12.1 Introduction

The balanced utilization of water resources are necessary to manage the global water cycle. Hydrogeological models capturing complex interactions of all the spheres of the earth are indispensable for effective strategy formation by a better knowledge of the temporal water cycle patterns with due consideration of environmental changes (Al-Hamdan et al. 2018a, b). In large watersheds, groundwater management and its influences on the surface water systems and the hydrological processes are significant which can be quantified by evaluating the groundwater use (Preetha et al. 2019, 2021a). Groundwater use is the ideal amount of groundwater that can be extracted from an aquifer annually for irrigation, industrial, and domestic needs. It is also referred to as groundwater withdrawal. It is principally governed by hydrogeological parameters such as intensity of rainfall, soil, and aquifer conditions, and socio-economic variables such as population and lifestyle (Mays 2001). Many shreds of literature explored ways to estimate groundwater use using field methods, hydrological models, statistical analysis, and data-enhanced techniques (Huo et al. 2016; Li et al. 2008; Freeze and Harlan 1969). One of the popular process-based basin-scale models is Soil and Water Assessment Tool (SWAT). It performs steady-state analysis on different spatial and temporal resolutions and allows simulation of water balance components that are continuous with space and time (Arnold et al. 2012; Lin et al. 2013; Preetha and Al-Hamdan 2019, 2022a). Ehtiat et al. (2016) validated the application of SWAT for the estimation of the spatiotemporal groundwater responses and found that the auto-calibration of groundwater functionalities assumed basin-wise recharge as unknown parameters. Some uncertainties are associated with predictions of these groundwater responses derived from the outcomes of the surface water model, SWAT. It was corroborated by studies by Dripps (2003) and Simunek et al. (2005). To add, the hydrologic process of base flow is modeled using an empirical equation called Hooghoudt's equation in SWAT (Neitsch et al. 2005). However, the equation lacks dynamics in environmental modeling both spatially and temporally. Therefore, it is regarded that the physically based and numerical representation of the hydrologic processes is superior to the empirical methods for predicting groundwater recharges in hydrological models like SWAT (Kim et al. 2008).

In efforts to account for the groundwater use and management comprehensively, SWAT model has been coupled with several non-empirical models in the last 20 years. A huge number of studies explored the advantages of connecting SWAT to MODFLOW for multi-scale data and response assessment (Sophocleous and Perkins 2000; Kim et al. 2008; Guzman et al. 2017; Bailey et al. 2016). A study by Chung et al. (2010) and Lin et al. (2013) predicted groundwater recharge and storage using SWAT-MODFLOW model in a multi-aquifer system. A few studies applied the integrated models for evaluating the distribution of water availability in managed watersheds subjected to heavy fertilizer use (Narula and Gosian 2013; Galbiati et al. 2006). Studies were also carried out to combine SWAT with groundwater tools like MODFLOW and optimization tools with numerical and statistical approaches for quantifying groundwater resources in watersheds with significant lateral inflows of salty water (Preetha and Johns 2022). Bailey et al. (2016) modeled the enhanced internal mapping between hydrologically significant units in SWAT and finite-difference pixels in MODFLOW which progressively simulated the hydrological components on time steps defined by the model user. Nonetheless, due to the loose coupling of the models, the groundwater processes are completely addressed, but the land surface processes including stream flow and solute transport were not addressed completely. Under these circumstances, tight coupling for better integration is recommended in the watershed scale specifically in areas where groundwater is close to the ground surface, which is highly complex. The data availability owing to climate, land use land cover, and geological features is detrimental in estimating the model performance for the various components of groundwater systems (Bradford et al. 2002; Dripps 2003).

An alternative to the complex coupling processes in hydrological modeling is data fusion into the existing surface water models like SWAT to improve the groundwater recharge and other constituent predictions and to obtain high-resolution groundwater recharge data for geo-visual mapping. Some studies attempted to use modified versions of land surface models including Noah-MP (Cai et al. 2014; Niu et al. 2011; Yang and Niu 2003) FLUXNET (Baldocchi et al. 2001), WRF-Hydro (Gochis et al. 2015; Dugger et al. 2017), remote sensing modules (Murray et al. 2011; Preetha and Al-Hamdan 2020a, b, 2022b), hyper-resolution (Wood et al. 2011), and multi-parameterization (Clark et al. 2011) to advance the ground-based measurements and elevate the reliability in groundwater recharge estimation within land surface models. For instance, the Noah-MP model employed important geophysical characteristics such as dynamic water tables and the presence of an unconfined aquifer for groundwater storage. Likewise, the WRF-Hydro model served as a substitute for complex data modeling by embedding conceptual functions based on channel infiltration and base flow that significantly reduced the stream flow errors and improved the hydrological responses of interconnected systems. Despite the large-scale usability of models like Noah-MP and WRF-Hydro, there prevail calibration uncertainties in the models which are likely due to input biases in the structural attributes of the models employed (Lespinas et al. 2017). Hence, the current chapter recalls the need for regional hydrogeological models that provides a complete representation of the spatio-dynamic and time-dynamic groundwater processes. Preetha et al. (2021a) developed a process-based hydrological model combined with finite element method called SWAT-FEM that can bridge the gaps and provide realistic estimates of groundwater systems. In efforts to advance the groundwater use quantification in river basins of the southern coastal plains of India, we employ a manageable combination of SWAT-FEM modeling and big data using historical and remotely sensed data and data products. We also reinvestigate the performance capabilities of satellite remotely sensed data on impacting the groundwater use estimates in the coastal aquifer system.

12.2 Study Area

12.2.1 Hydrogeological Characteristics

Chennai, a large city in India, has a plain topography and a westward coastal zone. Although the groundwater availability in India exceeds the groundwater demand, the spatiotemporal mismatch in the availability and demand has resulted in the fall in water table fluctuations, well damages, and saltwater intrusion in coastal areas (Joseph et al. 2021). In Chennai, groundwater has become a vital source of water for domestic and agricultural activities (Jagadeshan et al. 2015; Sivaraman and Thillaigovidarajan 2016). In addition, excessive groundwater pumping in this region has led to reduced base flow contribution and formation of the sand bars. It could profoundly impact the ongoing and future water demands and water availability in the state of Tamil Nadu, Andhra Pradesh, and Karnataka (Sivaraman and Thillaigovidarajan 2016; Jagadeshan et al. 2015). Therefore, it is important to quantify the interconnections between surface water and groundwater in the Chennai basin, an area of extensive agricultural irrigation to shallow and deep aquifer regimes. Altogether, they signify the need for assessing spatiotemporal estimates of groundwater components, groundwater use, and their interdependence in Chennai rivers. This is a pioneer study in Chennai basin that comprehensively assessed groundwater use and its trends both in space and time. In this chapter, Chennai basin is classified into four sub-watersheds, namely Arainayar, Coovum, Adayar, and Kosthalayar (Fig. 12.1).

Adayar is the primary sub-basin that forms an area of 827 km^2 and 40 km in length. The river transcends through the three main tanks of Pillapakkam, Kallampadu, and Kavanur. These other tanks include Chembarambakkam, Sriperumpudur, and Pillapakkam and 100 minor tanks with 23 observation wells. This is a seasonal sub-basin, and it carries heavy discharges during the northeast monsoon period from October to December. Arainayar sub-basin flows for 65.20 km in Andhra Pradesh and covers an area of 1426.234 km^2. This non-perennial river extends to 66.40 km in Tamil Nadu, and the complete length of the river is 131 km. The two anicuts encompassing this sub-basin are Annappanaicken Kuppam and Lakshmi Puram with ten multi-sized observation wells.

Coovum is another sub-basin that has a length of 65 km and covers an area of 464 km^2. Coovum sub-basin starts at Thiruvallur district of Tamil Nadu and enters Chennai city in a length of 17.98 km. The major anicut in this sub-basin is Kesavaram anicut which flows through Old Bengaluru channel with twelve observation wells in this sub-basin. Kosthalayar sub-basin extends to an area of 3684 km^2 and has a length of 155 km. The major tributaries of the sub-basin are Nagari and Nandi rivers. The sub-basin flows into Kesavaram anicut which falls at the 38th km extent of 694 km^2 in Kosthalayar area. The main reservoir in this sub-basin is Poondi reservoir with eighteen observation wells (Preetha et al. 2021b).

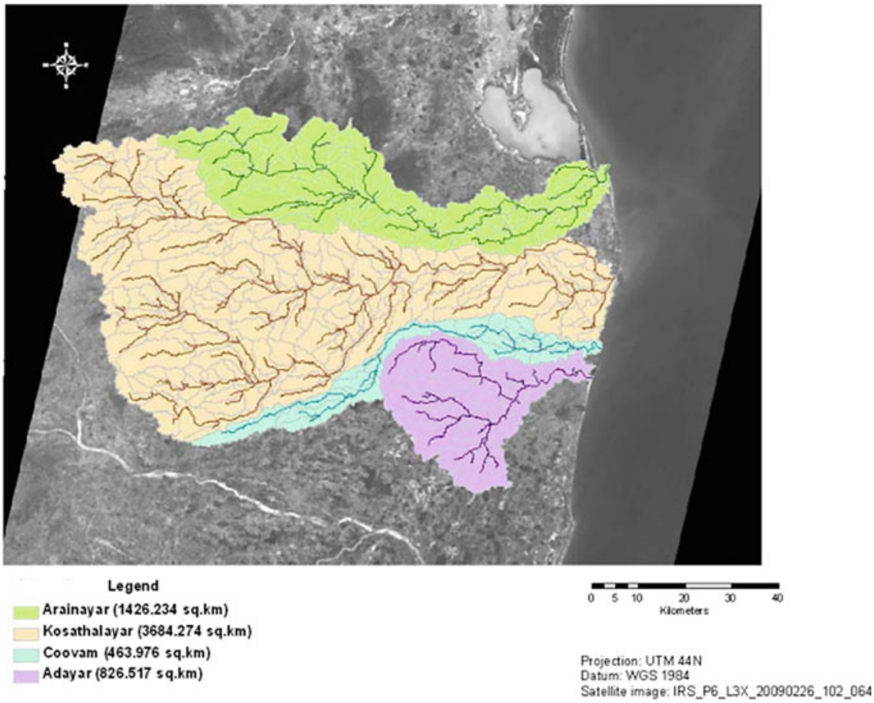

Fig. 12.1 Study area

12.2.2 Groundwater Resources

The western and southern parts of the Chennai basin are comprised of igneous and metamorphic rocks which covers 40% of the river basin. The rest of the area falling in eastern and northern sectors comprises of sedimentary formations. Rainfall and hydrogeological conditions prevailing in Arainayar, Coovum, and Kosthalayar sub-basins of the Chennai basin attribute to the groundwater use in this area which is contained by unconfined, leaky, and confined aquifers. The groundwater safe yield was estimated as 27.0 million galloon per day, while the present yield is estimated as 160 L/min.

The Groundwater Estimation Committee Norms estimated the groundwater potential of Chennai basin as 1119 million cubic meters (MCM) annually with the groundwater level fluctuations varying from 8 to 29 m spatially. The total annual groundwater potential was slightly higher considering the infiltration from the wells (1120 MCM). Therefore, the accountable balance of groundwater potential in the study area is approximated as 350.57 MCM. However, the decline in groundwater levels is likely to occur in encompassing small streams and water bodies due to exorbitant utilization of groundwater resources. The Krishna River and Veeranam tank are the major sources of water import and export to the Chennai basin. The water transfer occurs through Redhills and Chembarambakkam lakes from Poondi reservoir which is supplied to Chennai city after wastewater and drinking water treatment. After treatment following the regulations of Veeranam Water Supply Project, water is pumped to 235.66 km and transmitted to Chennai city (Sridhar and Thanthoni 2004).

12.3 Materials and Methods

The study outcomes are achieved through the following tasks: (i) big data collection: data collection using historical data sources and geoprocessing remotely sensed data for hydrological variables and responses, (ii) implementation and validation of the modified SWAT-FEM with big data to predict the groundwater responses, and (iii) estimation of groundwater use based on the modified SWAT-FEM at the multi-spatial and multi-temporal levels (Fig. 12.2).

12.3.1 Big Data Collection

The data collection process of the study comprised of two methods. One was to collect the historical groundwater data using field sampling, laboratory experiments, and various agencies. The second method of data collection was retrieved from online data portals that provide remotely sensed hydrogeological data.

12.3.1.1 Historical Data

The historical hydrogeological data for the study included the stream flows and base flow contribution between 1994 and 2000. They were consolidated from Central Ground Water Board (CGWB), Monthly Runoff Simulation (MRS) model, and the

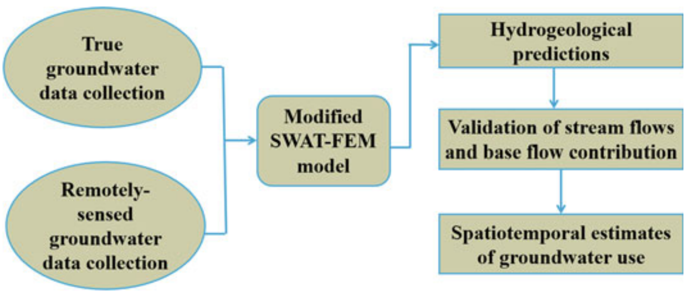

Fig. 12.2 Flowchart of the study

Global Flood Monitoring System (GFMS). The climatological data for the SWAT-FEM modeling in the study were daily precipitation, maximum air temperature, and minimum air temperatures that were used to simulate the monthly hydrological processes (IMD 2018). The solar radiation, wind speed, and relative humidity are the important climatological variables that were simulated using the statistical weather generator (WXGEN) of the study model.

12.3.1.2 Data from Remote Sensing

The remotely sensed hydrogeological data are land use land cover, topographical feature derived from digital elevation model (DEM), soil, groundwater storage, and water flux equivalents. They were obtained for each pixel from the processed satellite data for the Chennai basin. They were masked for the study area from the online databases for the entire modeling period, 1986–2010. The slope and topographic features for the study were obtained from a DEM of Shuttle Radar Topography Mission (SRTM) with a 90 m resolution (CGIARCSI 2019). The land use land cover data were obtained from National Remote Sensing Centre (NRSC) and International Water Management Institute (IWMI) at 56 m resolution and 500 m resolution, respectively (NRSC 2018; IWMI 2018). The soil data were obtained from two different organizations including the Tamil Nadu Agricultural University (TNAU), Coimbatore, and from Food and Agriculture Organization, United Nations, FAO, with a resolution of 1:50,000 and 1:10,000,000, respectively (TNAU 2018). The groundwater storage product was derived from the Gravity Recovery and Climate Experiment (GRACE) with a spatial resolution of 500 × 500 km for every month. The remotely sensed datasets were generated by the overlay of the processed data for every hydrologic response unit (HRU) in the basin. The main steps are:

1. Feeding in the raw data from remote sensing portals to ArcMap
2. Identify the coordinates of the basin
3. Masking the remote sensing data to match the basin map
4. Spatiotemporal joining of the remote sensing data to each sub-unit/sub-basin/HRU map.

12.3.2 Hydrogeological Modeling Using SWAT-FEM Model

The SWAT-FEM was employed for hydrogeological modeling of the study area. First, the hydrologic model was classified. Then, the process of watershed delineation was carried out to form 298 sub-units. The next step was the overlay of soil type attributes, slope features, and land cover characteristics to form 4282 HRUs. The implementation of land use land cover data derived from remote sensing from two sources elevated the number of HRUs in Chennai basin from 2382 to 4282 (Preetha and Al-Hamdan 2019). The next step involved incorporating the meteorological data into the SWAT-FEM. The base model was simulated with the existing management practices for the year 2010. Then, the model was refitted and simulated for the periods 1986 to 2010. Thus, the application of spatiotemporally progressive remotely sensed data in the modified SWAT-FEM resulted in accounting for the temporal changes in groundwater predictions within the HRUs of the Chennai basin. Besides, the inclusion of monthly groundwater storage estimates from remote sensing as a SWAT-FEM input resulted in temporally dynamic simulations of groundwater responses in the Chennai basin.

The SWAT-FEM was calibrated and validated using observed daily stream flow data at two stations from the United States Geological Survey (USGS) between 1986 and 2010. Two methods of calibration, such as auto-calibration and manual calibration, were deployed in the study to ensure handy and unwavering results while dealing with multiple temporal observations from the monitoring stations. The parameters evaporation soil compensation factor (ESCO), available water content (AWC), and curve number (CN_2) were susceptible to stream flows.

12.3.3 Quantifying Groundwater Use

The groundwater responses in this study were predicted using the outputs of the SWAT-FEM such as base flow, groundwater discharge, groundwater tables, and groundwater recharge. The estimates of groundwater use in anthropogenic conditions for sub-units/sub-basins/HRUs of Chennai basin were estimated using SWAT-FEM. We estimated groundwater use (mm) as the difference between base flow (mm) and groundwater discharge (mm). The SWAT-FEM predicted groundwater use estimates annually and monthly for the sub-basins of the study area which was classified into 298 sub-units and 4282 HRUs.

$$\text{Groundwater use} = \text{Base flow} - \text{Groundwater discharge} \tag{12.1}$$

12.4 Results and Discussion

12.4.1 True Groundwater Trends

12.4.1.1 Irrigation Statistics

The different modes of applied irrigation and seasonal agriculture are the dominant activities in the three districts of the study site. Figure 12.3 shows the irrigation sources and crops grown for the years of 2005 and 2006 at the three districts of Kancheepuram, Thiruvallur, and Vellore.

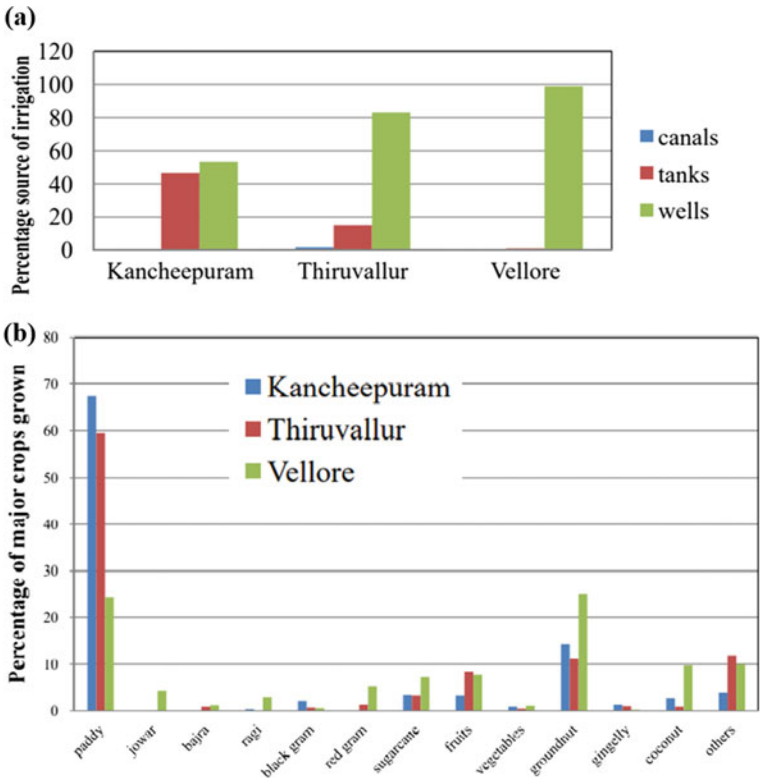

Fig. 12.3 **a** Major irrigation sources, and **b** major crops encompassing the Chennai basin

In cases where surface water is unavailable in hot summers, groundwater is generally used for annual crops where water is supplied constantly. The information regarding thirteen crop varieties and sources of irrigation prevailing in the districts of the study basin are shown in Fig. 12.3a. The proportion of well irrigation in Chennai basin is 50% in Kancheepuram district, 80% in Thiruvallur district, and 95% in Vellore district, while that of tank irrigation is 40% in Kancheepuram district and 20% in Thiruvallur district. The climate of the study area is appropriate for the large quantity irrigation of the crops such as groundnut, sugarcane, and fruits and medium-quantity cultivation of rice and sugarcane. The districts of Kancheepuram and Thiruvallur have rice as the prime cultivated crop cultivated for 60% of the area. On the other hand, Vellore district has groundnuts cultivated for an aerial extent of 25%. The study is important to quantify the sensitivity of crops such as rice, sugarcane, and banana to water-intensive irrigation, droughts, and wildfire scenarios. They were considered as the main contributor of the anthropogenic activity of irrigation for SWAT-FEM modeling in Chennai basin.

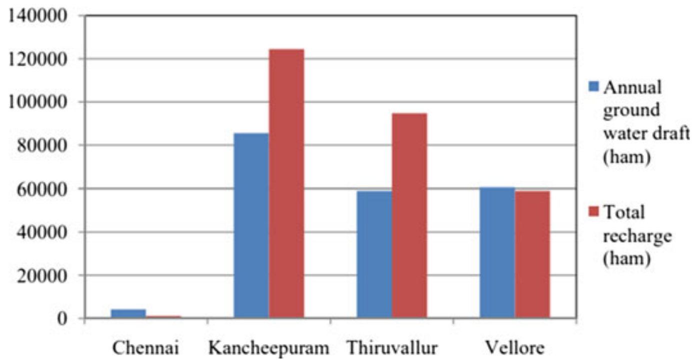

Fig. 12.4 Annual estimates of groundwater draft and total recharge in hectare meter (ham) for districts encompassing the Chennai basin

12.4.1.2 Water Draft Statistics

An overall reduction in groundwater drafts was observed in the districts of Tamil Nadu. The main causes of elevated groundwater recharge are found to be due to rainfall intensity, water conservation practices, and canal seepage. Figure 12.4 illustrates the annual estimates of groundwater statistics in the four study area districts. The study area experienced 72% average increase in groundwater draft compared to groundwater recharge.

12.4.2 Hydrogeological Predictions Using SWAT-FEM

Figure 12.5 compares monthly estimates of simulated and observed stream flows at the four sub-basin outlets, depicting that the SWAT-FEM is a good performer in predicting stream flows (coefficient of determination, R^2 of 0.8144) from 1994 through 2000. A remarkable finding revealed in Fig. 12.5 was that the SWAT-FEM performed better than the standalone MRS model over 93% of temporal conditions in the watershed which comprises of low stream flows and medium stream flows. It is noteworthy that the finite element model (FEM) component has reasonably compensated for the deficiency of SWAT in the representation of the stream flow depths which would help advance the groundwater predictions as well. This is relevant because of the huge stress faced during the low flow periods for water supply in the area where the study model may be preferred for better simulations. The results showed the temporal variation of stream flows at the spatial segment of the sub-basin outlets. Hence, the values of groundwater recharge and groundwater discharge from the basin into the streams/rivers were progressively analyzed with changes in time and space using the SWAT-FEM, unlike the SWAT and MRS models. The results showed that the closeness of observed flow depths to MRS and SWAT-FEM was

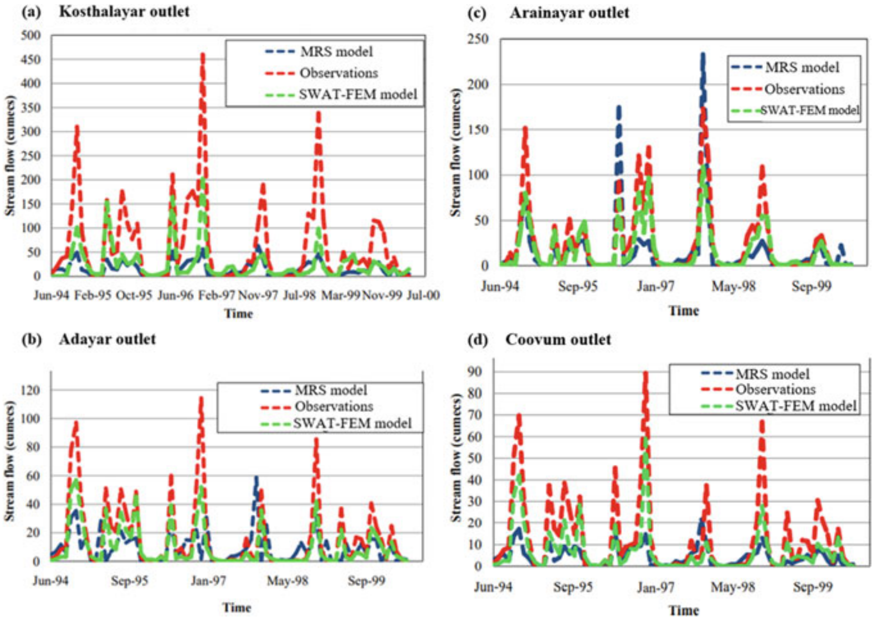

Fig. 12.5 Stream flow predictions from the MRS model simulations, observations, and SWAT-FEM for the four sub-basin outlets of Chennai basin

0.59, and 0.79, respectively. Both MRS and SWAT-FEM underestimated the higher stream flow fluctuations. It may be due to the lack of parametric calibration of the models for the different stratum of soils. Nevertheless, the SWAT-FEM performed well for the Chennai basin in stream flows compared to other hydrological models such as the MRS model. The validation results suggested strength in reliability and precision for SWAT-FEM predictions in the Chennai basin (Nash Sutcliffe efficiency, NS: 0.56–0.80; R^2: 0.61–0.83).

12.4.3 SWAT-FEM-Based Groundwater Predictions

Figure 12.6 depicts the seasonal, annual, and annual average variation of the groundwater responses and groundwater use in the Chennai basin between 1986 and 2010. The annual groundwater discharge to the mainstream ranged between 318 and 616 mm, the annual base flow from the basin was between 304 and 564 mm, and the annual groundwater use in the Chennai basin was between −1.7 and 59 mm. The results indicated comparable trends of annual groundwater discharge and base flow generated by SWAT-FEM in the basin. The groundwater use predictions for the summer months (January to May) were relatively lesser compared to the winter months (June to December). This could be attributed to the less groundwater demand in the summer months due to the available groundwater storage from the winter months. In the wettest month of November, higher groundwater discharge and relatively high base flows were predicted which resulted in a higher groundwater use (1.68–10.1 mm). It follows that more groundwater draft prevailed in the anthropogenic conditions for the Chennai basin where intense irrigation, domestic enhancements, and industrialization exist. Also, flow seasonality was highly pronounced due to watershed management, despite the contribution from precipitation and aquifers that can ensure a stable flow regime in the watershed. One of the major sources of irrigation in the Chennai basin comes from the Chembarambakkam reservoir which lies in the Adayar sub-basin. It was built in 1978 and has an annual irrigation requirement of 1,200,000,000 cumecs of water. In and around Chembarambakkam reservoir with multiple ponds, the dominant land use land cover is agriculture, comprising 45% of the total watershed area. The groundwater drafts were found to be more severe in this region due to the application of irrigation management from ponds (Butler et al. 2005; Cannon and Johnson 2004). This is also attributed to the increases in percolation that elevated the groundwater use estimates in the Adayar outlet to 58.56 mm. Therefore, the SWAT-FEM simulations can assess the groundwater responses and their eventual reactions water systems across the basin. Such predictions facilitate decisions on the efficacy of various management practices in plausibly enhancing the water budget in a river system. All these can further be used in risk assessment and decision analysis to explore the different natural and anthropogenic practices that can increase the sustained and healthy interaction of groundwater systems with the other environmental spheres.

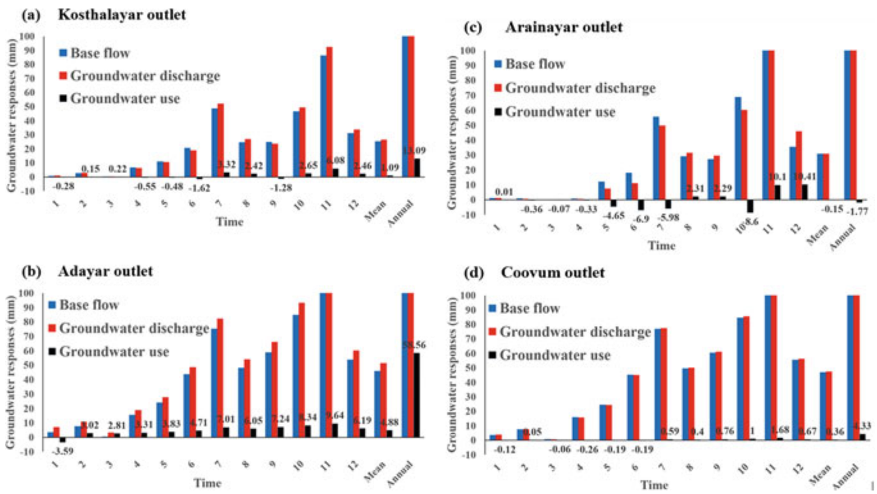

Fig. 12.6 Multi-temporal variation of the groundwater responses and groundwater use in the Chennai basin, between 1986 and 2010

12.4.4 Variation of Spatiotemporal Groundwater Use

Figure 12.7 depicts the predicted groundwater use (mm) for the Chennai basin for multi-temporal scales of seasons, years, and yearly average. The water levels indicated that the groundwater flow is progressing toward the mainstream, which is flowing from west to east direction. Hence, the water levels were after the topography of the basin. Low groundwater use (−5 to 0 mm) was observed for about 60% of the spatial extent of the Arainayar sub-basin in summer (Fig. 12.7). However, the groundwater use increased to 72% of the sub-basin with the incoming winter months (−10 to 6 mm). The mean yearly results suggested a much higher groundwater use in the Arainayar basin was due to the elevated percolation rates in these areas. Rainfall and hydrogeological conditions prevailing in the basin were primarily responsible for the groundwater use in this area.

Slightly lower values of groundwater use were observed in summer (2.42 mm), and a much higher deviation was found in winter (4.81 mm) when compared to the annual average groundwater use in the Chennai basin (3.18 mm). High groundwater extraction was seen in the winter months in which the monthly trend of groundwater demand escalated closely to the surface water demands. It was substantiated by studies by Sivaraman and Thillaigovidarajan (2016) and Paul and Elango (2018). The spatially averaged annual groundwater use predicted by SWAT-FEM (3.18 mm) depicted the managed/anthropogenic watershed conditions with alternate agricultural water use, three reservoirs, and irrigational contribution from ponds and shallow groundwater. Nevertheless, the predicted groundwater use from the SWAT-FEM with the ongoing management practices was found to be lower than the safe abstraction rate of 4.9 mm (Sivaraman and Thillaigovidarajan 2016). However, these predictions might alter due to uncertainties prevailing in real hydrological and geological conditions as well as in the scientific assessments. For instance, the total water potential observations for the year 2003 were 2431 MCM which can easily suffice the Chennai water goals. However, the hydrological systems do not always really adhere to these surveyed, analyzed, and documented estimates which ultimately led to the water crisis in Chennai from 2003 to 2006 (Paul and Elango 2018). Thus, the spatial and temporal predictions of the groundwater responses modeled using the SWAT-FEM can be quite useful for more accurate assessments of the various hydrogeological processes showcasing the real watershed conditions. They serve as better representations of groundwater contribution to surface water and surface water contribution to groundwater across the basin. Their thorough testing and verification under a multitude of environmental scenarios could lead to exemplary assessments of the interaction between various groundwater systems.

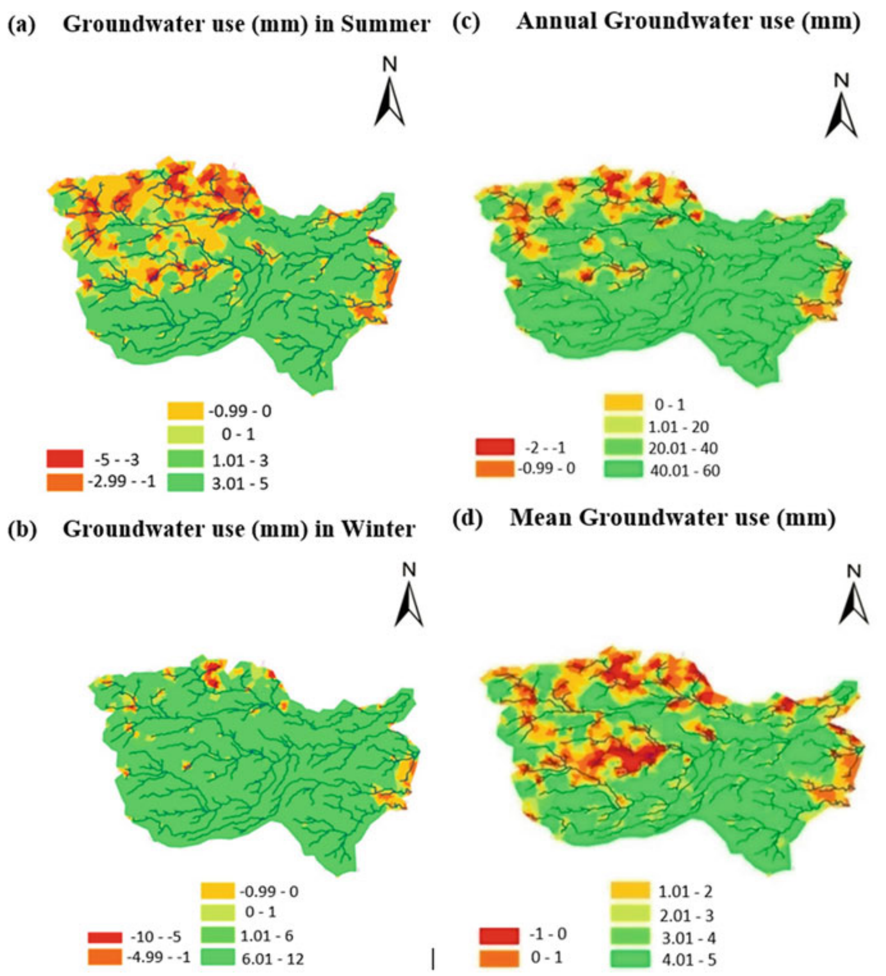

Fig. 12.7 Spatial predictions of groundwater use (mm), averaged from 1986 to 2010 in Chennai basin for multi-temporal conditions **a** summer, **b** winter, **c** annual, and **d** mean

12.5 Conclusions

The interactions of the interconnected water systems and their influences on the hydrogeological processes are significant in agricultural and coastal watersheds. To account for the spatiotemporal subsurface interactions and to ascertain their impacts on the hydrogeological processes in watersheds, a process-based hydrogeological model, SWAT-FEM, was implemented with the aid of big data. The SWAT-FEM simulations used in the study would be quite useful to assess the hydrogeological processes and their eventual impacts on the surface and groundwater systems across regional river basins. The estimated stream flows and groundwater uses under management practices can provide useful insights for water-quality modelers and managers. Such predictions facilitate decisions on the efficacy of various management practices in plausibly enhancing the water budget in a river system. All these can further be used in risk assessment and decision analysis to explore the different natural and anthropogenic practices that can increase the sustained and healthy interaction of interconnected water systems. The application of the modified SWAT-FEM with big data at multi-spatial scales (sub-basins, sub-units, HRU) and multi-temporal scales (years, months) was carried out as an initiative to understand the spatiotemporal interactions of various groundwater responses and to apply it to other comparable basins. This chapter contributed to developing and implementing novel conceptual modeling methods that provide radically new approaches to the estimation of groundwater responses in a multitude of river basins through the collaborative synthesis of data and model outcomes.

Funding The data assimilation and processing scenarios were partially supported by the NSF grant OIA-2019561. The hydrogeological modeling framework was partially supported by the NSF supplementary grant OIA-A20-0472-S006.

References

Al-Hamdan AZ, Preetha PP, Al-Hamdan MZ, Crosson WL, Albashaireh RN (2018a) Reconnoitering the linkage between cardiovascular disease mortality and long-term exposures to outdoor environmental factors in the USA using remotely-sensed data. J Environ Sci Health, Part A 809–818. https://reference.medscape.com/medline/abstract/29517416

Al-Hamdan AZ, Preetha PP, Albashaireh RN, Al-Hamdan MZ, Crosson WL (2018b) Investigating the effects of environmental factors on autism spectrum disorder in the USA using remotely sensed data. Environ Sci Pollut Res 25(8):7924–7936. https://pubmed.ncbi.nlm.nih.gov/29299867/

Arnold JG, Kiniry JR, Srinivasan R, Williams JR, Haney EB, Neitsch SL (2012) Input/output documentation. Soil Water Assess Tool. https://swat.tamu.edu/media/69296/swat-io-documentation-2012.pdf

Bailey RT, Wible TC, Arabi M, Records RM, Ditty J (2016) Assessing regional-scale spatiotemporal patterns of groundwater–surface water interactions using a coupled SWAT-MODFLOW model. Hydrol Process 30(23):4420–4433. https://doi.org/10.1002/hyp.10933

Baldocchi D, Falge E, Gu L, Olson R, Hollinger D, Running S, Anthoni P, Bernhofer C, Davis K, Evans R, Fuentes J, Goldstein A, Katul G, Law B, Lee X, Malhi Y, Meyers T, Munger W, Oechel W, Paw UKT, Pilegaard K, Schmid HP, Valentini R, Verma S, Vesala T, Wilson K, Wofsy (2001) FLUXNET: a new tool to study the temporal and spatial variability of ecosystem-scale carbon dioxide, water vapor, and energy flux densities. Bull Am Meteorol Soc 82(11):2415–2434. https://doi.org/10.1175/1520-0477(2001)082%3c2415:FANTTS%3e2.3.CO;2

Bradford RB, Ragab R, Crooks SM, Bouraoui F, Peters E (2002) Simplicity versus complexity in modelling groundwater recharge in Chalk catchments. Hydrol Earth Syst Sci 6(5):927–937. https://doi.org/10.5194/hess-6-927-2002

Butler JJ Jr, Zlotnik VA, Tsou MS (2005) Drawdown and stream depletion produced by pumping in the vicinity of a partially penetrating stream. Groundwater 39(5):651–659. https://doi.org/10.1111/j.1745-6584.2001.tb02354.x

Cai X, Yang ZL, David CH, Niu GY, Rodell M (2014) Hydrological evaluation of the Noah-MP land surface model for the Mississippi River Basin. J Geophys Res Atmos 119(1):23–38. https://doi.org/10.1002/2013JD020792

Cannon MR, Johnson DR (2004) Estimated water use in Montana in 2000. U.S. Geological Survey. Scientific Investigation Report 2004–5223. https://doi.org/10.3133/sir20045223

CGIARCSI (2019) SRTM 90m DEM. SRTM 90m digital elevation database v4.1: consortium for spatial information (CGIARCSI). http://www.cgiar-csi.org/data/srtm-90m-digital-elevation-database-v4-1

Chung IM, Kim NW, Lee J, Sophocleous M, Lee J (2010) Assessing distributed groundwater recharge rate using integrated surface water-groundwater modeling: application to Mihocheon watershed, South Korea. Hydrogeol J 18:1253–1264. https://doi.org/10.1007/s10040-010-0593-1

Clark MP, Kavetski D, Fenicia F (2011) Pursuing the method of multiple working hypotheses for hydrological modeling. Water Resourc Res 47(9) https://doi.org/10.1029/2010WR009827

Dripps WR (2003) The spatial and temporal variability of groundwater recharge within the trout lake basin of northern Wisconsin. Department of Geology and Geophysics, University of Wisconsin–Madison. https://www.proquest.com/openview/473fac4c60a2c3a554f817740bdcdae2/1?pq-origsite=gscholar&cbl=18750&diss=y

Dugger A, Gochis DJ, Yu W, Barlage M, Yang Y, McCreight J, Karsten L, Rafieeinasab A, Sampson K (2017) Learning from the national water model: regional improvements in streamflow prediction through experimental parameter and physics updates to the WRF-Hydro Community Model 6A.3. In: 31st conference on hydrology, Seattle, WA. American Meteorological Society. https://ams.confex.com/ams/97Annual/webprogram/Paper314352.html

Ehtiat M, Mousavi SJ, Vaghefi SA, Ghaheri A (2016) Analysis of recharge conceptualization in inverse groundwater modeling. Hydrol Sci J 61(15):2789–2801. https://doi.org/10.1080/02626667.2016.1151978

Freeze RA, Harlan RL (1969) Blueprint for a physically-based, digitally-simulated hydrologic response model. J Hydrol 9(3):237–258. https://doi.org/10.1016/0022-1694(69)90020-1

Galbiati L, Bouraoui F, Elorza FJ, Bidoglio G (2006) Modeling diffuse pollution loading into a Mediterranean lagoon: development and application of an integrated surface-subsurface model tool. Ecol Model 193(1–2):4–18. https://doi.org/10.1016/j.ecolmodel.2005.07.036

Gochis DJ, Yu W, Yates DN (2015) The WRF-hydro model technical description and user's guide, version 1.0. NCAR Tech Doc 120. https://www.ral.ucar.edu/projects/wrf_hydro

Guzman SM, Paz JO, Tagert MLM (2017) The use of NARX neural networks to forecast daily groundwater levels. Water Resour Manage 31:1591–1603. https://doi.org/10.1007/s11269-017-1598-5

Huo A, Dang J, Song J, Chen XH, Mao H (2016) Simulation modeling for water governance in basins based on surface water and groundwater. Agric Water Manag 174:22–29. https://doi.org/10.1016/j.agwat.2016.02.027

Indian Meteorological Department (2018) Meteorological centre: season's rainfall. IMD: season's rainfall 1986–2010 Meteorological Centre, Tamil Nadu

IWMI (2018) Land products. In: International water management institute (IWMI): global irrigated area mapping (GIAM) database. http://www.iwmi.cgiar.org/

Jagadeshan G, Anandasabari K, Poornavel S (2015) Groundwater quality of Kosasthalaiyar River Basin, Thiruvallur District, Tamil Nadu, India. Int J Innov Res Sci Eng Technol 4(3):1164–1170 https://www.researchgate.net/publication/276207510_Groundwater_Quality_of_Kosasthalaiyar_River_Basin_Thiruvallur_District_Tamil_Nadu_India

Joseph N, Preetha PP, Narasimhan B (2021) Assessment of environmental flow requirements using a coupled surface water-groundwater model and a flow health tool: a case study of Son river in the Ganga basin. Ecol Ind 121:107110. https://doi.org/10.1016/j.ecolind.2020.107110

Kim NW, Chung IM, Won YS, Arnold JG (2008) Development and application of the integrated SWAT-MODFLOW model. J Hydrol 356(1–2):1–16. https://doi.org/10.1016/j.jhydrol.2008.02.024

Lespinas F, Dastoor A, Fortin V (2017) Performance of the dynamically dimensioned search algorithm: influence of parameter initialization strategy when calibrating a physically based hydrological model. Hydrol Res 49(4):971–988. https://doi.org/10.2166/nh.2017.139

Li Q, Unger A, Sudicky E, Kassenaar D, Wexler E, Shikaze S (2008) Simulating the multi-seasonal response of a large-scale watershed with a 3D physically-based hydrologic model. J Hydrol 357(3–4):317–336. https://doi.org/10.1016/j.jhydrol.2008.05.024

Lin H, Ke K, Tan Y, Wu S, Hsu G, Chen P, Fang S (2013) Estimating pumping rates and identifying potential recharge zones for groundwater management in multi-aquifers system. Water Resour Manage 27:3293–3306. https://doi.org/10.1007/s11269-013-0347-7

Mays L (2001) Water resources engineering, 1st Edn. John Wiley and Sons https://www.public.asu.edu/~lwmays/preface.pdf

Murray S, Foster P, Prentice I (2011) Evaluation of global continental hydrology as simulated by the land-surface processes and exchanges dynamic global vegetation model. Hydrol Earth Syst Sci 15(1):91–105. https://www.researchgate.net/publication/307777123_Evaluation_of_global_continental_hydrology_as_simulated_by_the_Landsurface_Processes_and_eXchanges_Dynamic_Global_Vegetation_Model

Narula KK, Gosian AK (2013) Modeling hydrology, groundwater recharge and non-point nitrate loadings in the Himalayan Upper Yamuna basin. Sci Total Environ 468–469:S102–S116. https://doi.org/10.1016/j.scitotenv.2013.01.022

Neitsch SL, Arnold JG, Kiniry JR, Williams JR (2005) Soil and water assessment tool theoretical documentation. https://swat.tamu.edu/media/1292/swat2005theory.pdf

Niu G, Yang Z, Mitchell KE, Chen F, Ek M, Barlage M, Kumar A, Manning K, Niyogi D, Rosero E, Tewari M, Xia Y (2011) The community Noah land surface model with multiparameterization options (Noah-MP): 1. Model description and evaluation with local-scale measurements. J Geophys Res 116(D12). https://doi.org/10.1029/2010JD015139

NRSC (2018) Geophysical products/land products. Natural Remote Sensing Centre, Indian Space Research Organization. https://nrsc.gov.in/Geophysical_Products

Paul N, Elango L (2018) Predicting future water supply-demand gap with a new reservoir, desalination plant and waste water reuse by water evaluation and planning model for Chennai megacity, India. Groundw Sustain Dev 7:8–19. https://doi.org/10.1016/j.gsd.2018.02.005

Preetha PP, Al-Hamdan AZ (2019) Multi-level pedotransfer modification functions of the USLE-K factor for annual soil erodibility estimation of mixed landscapes. Model Earth Syst Environ 5:767–779. https://doi.org/10.1007/s40808-018-0563-5

Preetha PP, Al-Hamdan AZ (2020a) Developing nitrate-nitrogen transport models using remotely-sensed geospatial data of soil moisture profiles and wet depositions. J Environ Sci Health Part A 55(5):615–628. https://doi.org/10.1080/10934529.2020.1724503

Preetha PP, Al-Hamdan AZ (2020b) Integrating finite-element-model and remote-sensing data into SWAT to estimate transit times of nitrate in groundwater. Hydrogeol J 28:2187–2205. https://doi.org/10.1007/s10040-020-02171-5

Preetha PP, Al-Hamdan AZ (2022a) A union of dynamic hydrological modeling and satellite remotely-sensed data for spatiotemporal assessment of sediment yields. Remote Sens 14:400. https://doi.org/10.3390/rs14020400

Preetha PP, Al-Hamdan AZ (2022b) Synergy of remotely sensed data in spatiotemporal dynamic modeling of the crop and cover management factor. Pedosphere 32(3):381–392. https://doi.org/10.1016/S1002-0160(21)60081-4

Preetha PP, Al-Hamdan AZ, Anderson MD (2019) Assessment of climate variability and short-term land use land cover change effects on water quality of Cahaba river basin. Int J Hydrol Sci Technol 11(1):54–75. https://www.inderscience.com/info/inarticle.php?artid=112656

Preetha PP, Johns M (2022) A review of recent water quality assessments in watersheds of south-eastern United States using continuous time models. Global J Eng Sci 9(4):1–4. https://doi.org/10.33552/GJES.2022.09.000717

Preetha PP, Joseph N, Narasimhan B (2021a) Quantifying surface water and groundwater interactions using a coupled SWAT_FEM model: implications of management practices on hydrological processes in irrigated river basins. Water Resour Manage 35:2781–2797. https://doi.org/10.1007/s11269-021-02867-7

Preetha PP, Shirani-bidabadi N, Al-Hamdan AZ, Anderson MD (2021b) A methodical assessment of floodplains in mixed land covers encompassing bridges in Alabama state: implications of spatial land cover characteristics on flood vulnerability. Water Resour Manage 35:1603–1618. https://doi.org/10.1007/s11269-021-02805-7

Simunek J, Genuchten MT, and Sejna M (2005) The HYDRUS-1D software package for simulating the one-dimensional movement of water, heat, and multiple solutes in variably-saturated media, Version 3.0, HYDRUS software series 1. Department of Environmental Sciences, University of California, Riverside, CA, p 270. https://www.ars.usda.gov/arsuserfiles/20360500/pdf_pubs/P2119.pdf

Sivaraman KR, Thillaigovidarajan S (2016). Chennai River Basin micro level report. https://studylib.net/doc/7449535/chennai-river-basin-micro-level-report

Sophocleous M, Perkins SP (2000) Methodology and application of combined watershed and ground-water models in Kansas. J Hydrol 236(3–4):185–201. https://doi.org/10.1016/S0022-1694(00)00293-6

Sridhar V, Thanthoni S (2004) A pipe dream? Frontline. https://frontline.thehindu.com/other/article30222555.ece

TNAU (2018) TNAU agritech portal: downloads. Tamil Nadu Agricultural University, Coimbatore. http://agritech.tnau.ac.in/downloads.html

Wood EF, Roundy JK, Troy TJ, Van Beek LPH, Bierkens MFP, Blyth E, Roo A, Doll P, Ek M, Famiglietti J, Gochis D, Giesen N, Houser P, Jaffe PR, Kollet S, Lehner B, Lettenmaier DP, Peters-Lidard C, Sivapalan M, Sheffield, Wade A, Whitehead P (2011) Hyperresolution global land surface modeling: meeting a grand challenge for monitoring Earth's terrestrial water. Water Resourc Res 47(5). https://doi.org/10.1029/2010WR010090

Yang ZL, Niu GY (2003) The versatile integrator of surface and atmosphere processes: part 1. Model description. Glob Planet Change 38(1–2):175–189. https://doi.org/10.1016/S0921-8181(03)00028-6

Chapter 13
Integrated Water Resources Management: Perspective for State of Uttarakhand, India

Epari Ritesh Patro, Pooran Singh Patwal, and Shahid Ul Islam

Abstract Himalayan areas are the water bucket of the world and contribute one of the world's greatest freshwater resources. The Himalayan system provides plentiful services to the downstream towns and population in terms of water for household purposes and ecosystems services, etc. More than 1.4 billion people directly depend on water from the rivers of the Himalaya. So, water resources and its management for providing clean water and sanitation are already a challenge in the Himalayan region. All the mitigation measures adopted under Ganga Action Plan (for cleaning of all tributaries of river Ganga started by ministry of water resource in 14 Jan 1986) focus primarily on the big cities for construction of sewage treatment plants, interceptor sewers, and sewage diversion mechanisms. But always questions are raising about the sustainability, maintenance and cost-efficiency of these mitigation measures, and its effect on water quality of the river. For small areas and towns of Uttarakhand, natural, sustainable, efficient, natural, and long-life mitigation measures are required for reducing the pollution level in the river system.

Keywords Himalaya · IWRM · Uttarakhand · Ganga · Sustainability

Abbreviations

GIS	Geographical information system
S	River meandering sinuosity value
IWRM	Integrated water resources management

E. R. Patro (✉)
Water, Energy and Environmental Engineering Research Unit, Faculty of Technology, University of Oulu, 90014 Oulu, Finland
e-mail: ritesh.patro@oulu.fi

P. S. Patwal
Hydrology and Natural Resource Management, Haridwar, India

S. U. Islam
Department of Civil Engineering, Baba Ghulam Shah Badshah University, Rajouri, Jammu and Kashmir, India

P. Shukla et al. (eds.), *Environmental Processes and Management*, Water Science and Technology Library 120, https://doi.org/10.1007/978-3-031-20208-7_13

RS	Remote sensing
RBF	Riverbank filtration
DEM	Digital elevation model
SOMA	Switch Organic Micro-Pollutant Assessment Tool
STP	Sewage treatment plants
LPCD	Litre per capita per day
MPN	Most probable numbe
MLD	Million litres per day

13.1 Introduction

Freshwater availability in India is 1545 m^3/person/year (according 2011 census), and it will decrease to 1140 m^3/person/year in year 2050 (UNICEF, FAO, and SaciWATERs 2013). It is reported that the water supply and demand gap in 2030 will be 94 billion liters/day (UNICEF, FAO, and SaciWATERs 2013). India will experience water stress in 2050 and will face water shortages when the availability of clean water falls below 1000 m^3/person/year (Ernest and Young 2011).

Water scarcity issue is not just linked to the availability of freshwater because there are places facing water scarcity in spite of abundance of freshwater. Uttarakhand is a Himalayan state situated in Northern India and one of the most rapidly developing states in India. Most part of the state is covered by hilly areas, having a demographic and geographic privilege of high surface water availability; however, the state often faces drinking water scarcity. Being a part of a Himalayan state, it has problems related to floods, earthquakes, and other natural disasters. In the past years, several floods took place in the state; the last being in June 2013 when the Alaknanda River rose up to more than 10 m at some places (Chevuturi and Dimri 2016). As a result, there were severe damages to drinking water schemes, irrigational water structure, buildings, roads, agricultural land, and other infrastructures.

At present, drinking water demand of Uttarakhand is 1035 MLD. It is expected to rise to 1237 MLD in 2021 with increase in the population and reach 1473 MLD in 2031. Drinking water availability in some parts of Uttarakhand is less than 12 LPCD (Kimothi et al. 2012). The primary cause of lower per capita availability is the dependence of water production and supply on rainfall. In monsoon, high flow velocity of the river damages the water abstraction structures frequently. In non-monsoon season, most of the springs go dry. Due to seasonal variation in water availability, currently existing water production systems for agricultural and domestic use are not able to cater the water demand. Constant drinking and irrigation water shortage is also due to the improper techniques of water harvesting and bad practices of water management. The rising population and increasing pollution in the water bodies further exert the pressure on rising water demands. Groundwater availability is limited, and many springs are drying. Additionally, there is a large quantity of surface water and rainwater runoff which is not utilized efficiently for development in these areas.

Riverbanks in the state are densely populated and fulfill the need of agricultural and drinking water of hundreds of towns and thousands of the villages. These river systems also take back all the untreated and treated sewage from these populated areas. In addition to pressures of population, there is lack of proper investment in wastewater treatment and rainwater collection infrastructures. A study conducted under Saph Pani (2013) project shows that one of the Himalayan rivers named Alaknanda River, a tributary of river Ganga at Srinagar, has total coli-form level reached more than 7500 MPN/100 ml. E. coli levels more than 6500 MPN/100 ml, which is greater than the required limit of 5000 MPN/100 ml set by the Central Pollution Control Board of India (CPCB) for usage of source for drinking water. On the basis of this report, it could be inferred that Himalayan river water of the state is not suitable for direct drinking purposes. To overcome these problems, the Indian Ministry of Water Resources came up with the Clean Ganga Mission with the aim to reduce the pollution level in the Himalayan rivers by locating and reducing major sources of wastewater and other point source discharges into the river.

Therefore, a suitable technology and integrated management system is required for these hilly (Himalayan) areas to utilize the water resource to meet the growing drinking and agricultural water demand while coping with these vast geological and climatic variations.

13.1.1 Integrated Water Resources Management

The Integrated Water Resources Management (IWRM) is a method for monitoring water resource and helps to develop, manage water resources in a sustainable and balanced way, taking account of economic, social, and environmental interests. In the Himalayan mountains, glacier melt water and rainfall are the major flow components of the river systems. As discussed in the first chapter, the major riverine towns in the Himalayan areas face frequent occurrence of water scarcity. Thus, there is a critical need for these towns to get an assessment of existing and identification of new potential water bearing zones to cater the population and control the contamination in the river water. In recent years, combination of surface information with subsurface information with the help of groundwater modeling and geographical information system (GIS) is emerging as a potential tool for the sustainable management of water resources (Michl 1996).

The coupling of these two technologies for river management and water resource management can come under the umbrella of IWRM which can form a balance between the environment and human water demands of these towns. The term IWRM emerged in the year 1980, and it is defined by the Global Water Partnership as a "process which promotes the coordinated development and management of water, land and related resources, in order to maximize the resultant economic and social welfare in an equitable manner without compromising the sustainability of vital ecosystems".

Declining per capita water availability due to consumption patterns, climate change, and water pollution always putting pressure on limited water resources, which come into focus of Integrated Water Resource Management (Gleick 1998; Bonato et al. 2019). Well-prepared and economically viable approaches to implement IWRM in the Himalayan region are not yet widely available (Nischalke 2014). IWRM of the river stretch should contain the following elements: water availability and uses, water demand, water deficits, water quality, and minimum environmental flow from the hydro-electricity generation dam to the downstream.

13.2 Water Issues of Uttarakhand

The availability of water in the Himalayan area and its quantity, quality, and scarcity depend upon the climatic conditions of the area. River water is highly seasonal and varies across the monsoon to non-monsoon. The river discharges are minimum in winters and maximum in rainy season. Changes in seasonal stream-flow have significant impacts on the local populations due to altered water availability patterns and become a main reason of water scarcity in the Himalayan towns. Other reason for non-portability of surface water is turbidity and bacterial populations in it. The growth of human population and human activities near the bank of river are further deteriorating the water quality of the river gradually.

In the recent years, the hilly area of the Uttarakhand state is facing many problems regarding the water supply and sanitation, continuous power supply cuts, collection of water from surface sources which are unsustainable and often far away from habitation and agricultural fields, direct abstraction of surface water for drinking purposes causing filter media chock, drying up of natural water sources, decline in the groundwater level, freezing of water supply pipelines in winter, damages of the pipelines and irrigation canals and damages of natural sources due to landslides, and frequent damages of water abstraction structures due to the high velocity of the river (Patro et al. 2020). Generally, all these problems are grouped into the following categories based on water production and supply for the local water demand.

i. **Low LPCD and bacteriological contamination**: Supply of drinking water is not sufficient (<12 LPCD) and not following the Indian drinking water standard (155 LPCD) in quantity and quality (bacteriological contamination) and becoming the main reason of health problems. Especially Himalayan women are always affected and facing these problems in their daily life, because they often have to carry water containers from a spring to their home.

ii. **High maintenance cost**: The current working conventional water supply methods which meet the local drinking water and agricultural demand are facing functional and operational problems of treatment, failure of pumping stations, huge maintenance cost after every monsoon, etc.

iii. **Increasing pollution and population level**: The pressure from increased urbanization, population growth, and improved standard of living results in a continuous depletion of local water sources and increasing pollution in the river system. People use the river water for cleaning, bathing, household use, rituals, and for funeral.

iv. **Undeveloped wastewater system**: Sustainability with respect to quality and quantity of drinking water is always a billion-dollar question of water supply organization. Water supply and wastewater services in the Himalayan towns are often underdeveloped.

v. **Increasing trends of pilgrims and opening of new education centers**: Due to increasing trends of pilgrims and opening of new education centers in peaceful environment of the Himalayan area, the urban population has increased. This had led to increase in municipal withdrawals of drinking water.

vi. **High variation of discharge in different seasons**: The alteration of water availability in different seasons and growing sewage pollution causes severe problem in direct abstraction from the river, which always become a cause of disturbance of the daily production.

vii. **Changing of river course seasonally**: In dry seasons (non-monsoon), river changes its course and increases the distance between riverbank and the water tapping structures. During the monsoon seasons, high velocity of river often damages these surface waters tapping structures. Most of the irrigation schemes are silted during monsoon, which affects the agricultural water supply.

viii. **Uneven rainfall pattern**: Uneven rainfall is affecting most of the rain-fed agricultural land via water shortage and becoming the main reason of drought in Himalayan areas. In summer (May–July), most of the springs and streams become dry due to a climatic effect, resulting in a shortage of water availability.

ix. **Migration of youth**: In the Himalayan region, many towns and villages are situated on the banks of rivers, but the unavailability of clean drinking water and enough agricultural water due to lack of application of proper technology results in great dissatisfaction of the people. Sometime it becomes a cause of the migration of people from the village area to the city area to access safe water, sanitation, and public service. Most of the migrants are younger and better educated than those who do not move. These non-movers are poor and the most vulnerable to the water scarcity and health problems in this region.

x. **Lack of advanced surface water treatment structures**: Lack of advanced surface water treatment structures causing insufficient filtration adversely impacts the quality of potable water and causes water-borne disease and also affects agricultural surface water pumping stations. The rural poor and urban people who do not have good social conditions and least capacity to adapt available home drinking water purification systems are most likely to be affected by the diseases.

xi. **Disputes in tapping the water sources**: Disputes often arise in tapping the sources of water in the most densely populated areas. Sometime one spring water feeds many villages, towns, or different parts of the towns and their agricultural land.

All these above problems display the link between Himalayan people and their environment in the context of water availability and scarcity, uncertainty in rainfall, climate, hydrology, and river behavior as well as demographics and water use patterns. A catchment or drainage basin is a unit geographical area of landform which drains all the water to a single outlet. Generally, watersheds are formed into many forms and sizes according to its geography and geology (Frissell 1986). The health of a river or lake is a direct indication of how its watershed is treated and handled (Wang et al. 2006). Due to inadequate and inappropriate technological intervention, many of the Himalayan areas have not been able to harness their unique resources.

Floodplains are adjacent to rivers, help maintain the health of the river and are very useful for temporarily storing water, filtering nutrients and contaminants, allow for infiltration, provide habitat to several species, and create recreational opportunities. Floodplains store flood waters and cause a reduction in flow velocity. They also improve water quality with the help of plants within the floodplain which filter sediments and pollutants. Water-related disaster management, including proper risk assessment, should not be considered in isolation, but rather as an essential component of IWRM. Following studies have been conducted on IWRM and its watershed management.

(a) In some parts of the world, land availability is becoming a big issue for urban development. The riverbank space is getting further attention of urban planner to use this space for development. Controlling development in river space is necessary to avoid illegal invasion and to create a better environment to support the river basin community (Patro et al. 2020, 2022).
(b) In planning and management, preservation of ecosystem and satisfaction of human needs must be prioritized. Thus, water resource planning system is always becoming flexible to the change due to the uncertainty issue in developmental framework (Kirby and White 1994).
(c) Riparian buffer maintains healthy aquatic ecosystems and provides a series of other environmental and social benefits. It helps for removing and trapping sediment from runoff and able to stabilize riverbanks. Some activities like construction of impermeable surfaces, mining of riverbed, construction of septic tank, application of pesticides, construction waste disposal sites are not suitable for river floodplain (Seth and Lawrie 2000).
(d) For IWRM, along hydrological boundaries, it is important to involve the local communities more actively in the management, planning, and operation of their water resources. With the help of community's involvement in management of water resources, we can compare the past and present water scenario of the watershed boundary (Amakali and Shixwameni 2003).
(e) Many problems associated to flooding in the river basin can be resolved by making corridor along the river to avoid the encroachment. River corridor defined as a buffer around the river usually based on the width of the river helps to preserve pollution and riverbank stabilization (Lee and Low 2004).
(f) In order to address water demand issues rising from population increase and agricultural pollutions, IWRM approach has been introduced and used. IWRM

includes the coordinated development and management of water resource usage toward environmental conservation, protection, and sustainability. There is a need for studying the holistic coordination of IWRM and GIS technology to mitigate the environmental problems in aquatic ecosystems (Eda and Higa 2010).

(g) With the help of GIS, a dynamic water balance and erosion model were developed for the catchment studied and assessing water demand and usage of water. Different strategies were developed to solve water allocation conflicts. IWRM was a new and modern computer-based toolset which was tested, validated, and sound documented procedures for decision support and implementation of water management strategies (Staudenrausch and Fliigel 2001).

13.3 River Morphology and Its Effects

13.3.1 River Morphology

In the Himalayan area, rivers are utilized for the supply of water for drinking and irrigation, hydropower generation, adventure sports like river rafting, habitats furnishing, and cleaning of wastewater from towns by self-purification ability. For these performances of the river, it is essential to identify the functional and environmental situation of a river with its channel pattern. Himalayan rivers are perennial rivers and make an alluvial flood by a different river process, like erosion, transportation, and sedimentation (Bridge 2009). Mostly, erosion occurs in the upper catchment area of drainage due to high slope and weathering of the rocks. V and U-shaped valleys are formed during this erosion and weathering process (Benn and Evans 2014). The eroded materials consist of rock fragments, including mud, silt, and sand. During large floods, the channels often change their course in the floodplain till to next flood (Cook et al. 2014). The formation of channels is explained by river patterns and river configurations and is determined by such factors as discharge, water surface slope, velocity of river, depth and width of the river and river bed materials (Church 1992). The basic forms of mountain river system are braided, meandering, and straight and were categorized by Leopold and Wolman (1957). The river's channel pattern formed under different flow conditions and its boundary condition is based on their sinuosity ratio, given by the channel length by valley length. Sinuosity is depending on the bed load, slope, and velocity of the rivers.

Studies conducted by Xu (1996), Lewin (1984), and Edgar (1984) show that alluvial rivers meandering patterns with channel sinuosity $S = 1.4–1.6$ and try to stable by self-adjustment under different flow boundary condition. An alluvial river has 39% occurrence frequency of $S = 1.4–1.6$, 20.0% of $S = 1.5–1.6$, and remaining 18.8% of $S = 1.4–1.5$. It is resolved that all alluvial rivers have similar intrinsic mechanisms that try to make the similar channel patterns with sinuosity 1.4–1.6. Besides, the field investigation done by Winkley (1982, 1983) shows that the river channel with $S = 1.4–1.6$ has minimum flood profiles and low maintenance cost.

13.3.2 Theoretical Value for Sinuosity

In mountain river system, stream has its maximum power (in terms of flow and velocity) at the origin of the river, and toward downstream, river channel tries to minimize this power to get the dynamic equilibrium for stabilization. That is the main reason of consistent changes in the river slope toward downstream, which is called minimum stream power theory (Yang 1986). According to this theory, an alluvial channel gets the dynamic equilibrium condition when river stream power of the river channel is minimum to its unit length. Let P be the stream power of the channel, then

$$P = Q * S * Y \text{ (for Minimum } P,\ S \to 0) \tag{13.1}$$

where Q = discharge, S = slope, and Y = specific weight of water.

Valley axis of a channel is always perpendicular to contour line. Let us assume that river meander bend is a uniform curve and arc of the circle is a channel centerline (Fig. 13.1). Then, the mean channel slope is

$$S = 2\Delta s/\,\mathrm{Ls} \tag{13.2}$$

where Δs = elevation difference of one meander, Lm = meander wavelength (distance between points A–C), and Ls = meander arc length.

The local channel slope $S(s)$ varies with the position in the bend. It is minimum at valley axis and maximum in farthest point in the valley axis. The minimum value of S is $(s) > 0$. Then,

$$S = 2 * \Delta s/\,\mathrm{Ls} = \text{ minimum 1st condition} \tag{13.3}$$

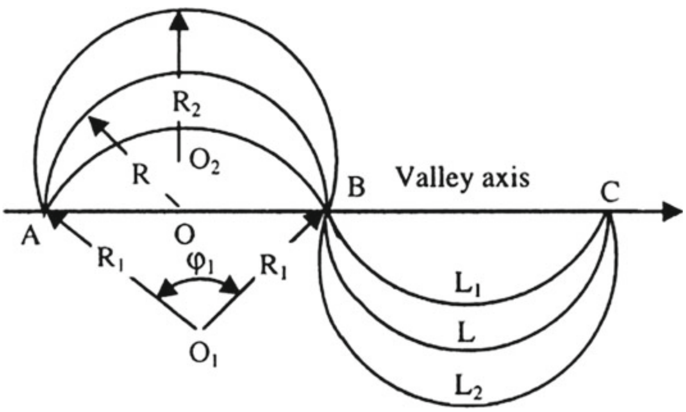

Fig. 13.1 Development of a meander loop (modified and adapted from, Deng and Singh, 2002)

$$S(s) > 0 \text{ 2nd condition} \quad (13.4)$$

$L1$, L, and $L2$ are the three different meander development stages of a river. $L2$ has the longest Ls which satisfy the first condition, but $S(s)$ is maximum and not satisfies the second condition, and $L1$ has minimum $S(s)$ which satisfies the second condition, but Ls are minimum and not satisfy the first condition. Only L is satisfying both conditions of minimum energy. From Fig. 13.1, it is clear that

$$\text{Lm} = 4R, \ \text{Ls} = 2 * \Pi * R \quad (13.5)$$

A field study conducted by Chang (1992) shows that the radius of alluvial river channel curvature is approx. 3 times to the channel width. Let us assume the river width is B and radius of curvature is R. Then from Eq. 13.5, it can be inferred that

$$R = 3 * B \,\&\, \text{Lm} = 12 * B \quad (13.6)$$

And it shows the river sinuosity S= Ls/Lm = $2\Pi R/4R$ from Eq. 13.6.

$$S = \Pi/2 = 1.57 \quad (13.7)$$

Therefore, on the basis of above calculation, it is clear that the sinuosity S=1.57 range of 1.4–1.6) with meander wavelength Lm = 12*B signifies alluvial rivers optimal channel pattern. For the low cost of maintenance and perfect management of the river channel, S = 1.4–1.6 and Lm close to 12*B should be maintained.

13.3.3 Relationship Between Purification Capacity and Sinuosity

It is important to calculate and enhance the self-purification capacity of the riverbank, to lessen the cost of wastewater treatment. Purification capacity depends on the lateral, longitudinal, and vertical mixing ability of river flow as well as filtration capacity of alluvial deposits (Peavy et al. 1985). The dispersion coefficient K, which represents the mixing ability of the river, is higher in longitudinal direction than in other directions (Deng et al. 2001), and the filtration capacity, represented by the hydraulic conductivity k, in the horizontal direction is 10 times greater than the vertical direction. It depends on the depth, area, and type of deposit soil, which plays a main role for adsorption, decomposition, and dilution. To calculate the purification capacity and its influence in river pattern, a study was conducted by Nordin and Sabol (1980) in the USA on 30 streams where 70 longitudinal dispersion coefficients were plotted against the channel sinuosity. On the basis of the results, it is clear that high values of self-purification capacity occur with S ranging from 1.35 to 1.57. Lower sinuosity values make straight rivers which generally made the wide channel with uniform and low velocity gradient which causes a weak self-purification capacity or dispersion coefficient (Fischer 1979).

High sinuosity leads to enhance the river channel resistance and reduced flow velocity of the river, which reduce the self-purification capacity. Consequently, rivers with sinuosity value 1.35–1.57 exhibit the strongest self-purification capacity. The sinuosity of *S* value 1.4–1.6 with a meander wavelength of twelve times the channel width is perfect for the sound management of alluvial rivers (Deng and Singh 2002). So the aim is to ultimately calculate the purification capacity of alluvial soil with a suitable sinuosity (higher value of *S* increases the clogging in the river, and lower value of *S* increases the erosion and decreases the contact time of water and alluvial soil) in the river stretch.

13.3.4 Riverbank Filtration as an Element of IWRM

Watershed area of a river stretch is large, highly sloped, less stable, and newly formed which is the primary reason of the high turbidity in the river water. Due to this watershed area, the river stretches facing the frequent landslides in monsoon season, and landslide mass is fleshed out by the river from upstream to downstream. This landslide mass is deposited in the bank of the river, and after long-time deposition of mass, these riverbanks are now becoming a good water potential zone for the Himalayan area (Fort 2000).

The areas near to the adjacent of rivers, streams, and lakes which are vulnerable to flooding are called floodplains. But in mountain area, floodplains cannot develop due to limit horizontal extent and steep slopes. In plain areas, floodplains can extend >1 mile from the source of water, but in Himalayan areas, riverbanks cannot extend 50 m, except in some parts of the foothill area and less steeps area, like Haridwar, Rishikesh, Dehradun, etc. These riverbanks are usually flooded during the whole monsoon periods. The main reason of the floods is increasing intense rainfall in a large catchment area. But the trend of rainfall is decreasing with increasing intensity in a short time (Basistha et al. 2009). Many surveys have shown that floodplain size is immediately associated with the overall health of a river (Postel and Richter 2003). Floodplains are really useful for temporarily storing water (they reduce the flow speed of the river and suck up and store flood waters), filtering pollutants and contaminants, allow water for infiltration in the soil, purify the river water through alluvial soil, provide the habitat for different type of species, and create recreational opportunities (Postel and Richter 2003).

These floodplains can act as a reservoir of water for these towns. In a floodplain, the recharge comes from both surface water and groundwater. Their water can be easily utilized by the drilling of shallow wells in unconfined aquifers and confined aquifer. In this process, lowering of the water table of unconfined aquifer relative to the adjoining surface water level causes surface water movement through the permeable riverbed into the unconfined aquifers. This water level difference provides a natural path to this subterranean flow, which provides the raw water for drinking purposes.

This process is called riverbank filtration (RBF) (Hiscock and Grischek 2002). These floodplains can become a part of IWRM in the following way:

(a) Floodplains can be used by natural technique RBF, to improve aquifer recharge by constructing the abstraction wells in the vicinity of natural open water bodies and can serve to manage the complete development of groundwater resources for Himalayan areas where groundwater is the limited resource for water supply (Sandhu et al. 2011).
(b) Floodplain acts as a natural filter, mixing the groundwater and bank filtrate water, can dilute the degree of concentration, and biochemically reduces contaminants present through RBF, especially suitable for Himalayan towns which are facing high sewerage pollution, high turbidity in surface water bodies, and high concentration of iron, arsenic, and nitrate in groundwater (Kumar and Mehrotra 2009).
(c) Floodplains can be used for the pre-treatment of surface water (during monsoon) for artificial recharge of groundwater through infiltration basins.
(d) Floodplains have a large capacity to purify the surface water through the alluvial deposition (good hydraulic conductive material) close to the meanders. Floodplains can enhance the sanitation of surface water bodies due to efficient biodegradation and sorption process in hyporheic zone, and it is a sustainable technique for water improvement production and management during the heavy pollution load in the river (Grischek et al. 2011).

13.4 Role of Geographical Information System (GIS) in IWRM

GIS application can play crucial role for the IWRM in the Himalayan region due to unavailability of detailed spatial data and the inaccessibility of many areas. With the help of remote sensing (RS), one can generate valid input data for hydrological models and calculate the water balance. By the combination of different spectral, temporal, and spatial information as well as with land measurements, one can extract valuable information for the IWRM process. GIS can be coupled with any modeling system and serve as a go-data management and pre-processing unit for the hydrological analysis. GIS is also employed as a post-processing component, mixing the various model results and serving as a platform for visualizing them (Michl 1996). Other relevant studies have been carried on GIS, and it is used in IWRM.

a. GIS and RS coupled the eco-hydrological modeling have a significant role in development of a series of indicators of water catchment and its health which is a part of a geographical audit of a river basin (Aspinall and Pearson 2000).
b. GIS and RS data were used for modeling sediment yield by generating and organizing spatial data (Pandey et al. 2007).

c. GIS techniques provide an efficient and useful tool for prediction of future erosion potential and also in understanding the impact of different cropping pattern and conservation support practices (Leidig 2008).
d. Detailed morphological mapping has been done for river shape and size mapping. It integrates with multidisciplinary information which was collected with field survey cartographic map and remote sensing data (Michael et al. 2012).
e. Non-point pollution source co-relates with watershed-scale conditions and its influence in ambient water quality. GIS and RS data evaluate concentration stream and its impacts in the river watershed and could help to optimizing the design of stream monitoring network. So GIS and RS are a promising tool for better management and controlling non-point source pollution (Yang 2010).
f. GIS and RS data help to derived information in terms of natural resources and their spatial distribution for the integration with socio-economic condition. It helps to develop resources action plans which are extremely useful for well-organized and sustainable management of water and natural resources (Shanwad et al. 2012).
g. Remotely sensed multispectral digital image can be conjunct with field data to classify hydro-geomorphic stream at fine scales. GIS is an effective tool for stream order and its concentration if accurate ground controls point was taken for image rectification (Wright et al. 2000).

In recent years, IWRM has been recognized globally as the crucial means in treating with many matters relating to the management of water (Martínez et al. 2014). From that point of view, GIS and RS are really useful to make the goals of the IWRM in the long term.

13.4.1 Use of GIS and RS in Land Suitability Analysis

Use of GIS and RS in land suitability analysis has become an emerging and favorable tool among the scientists, engineers, and managers due to its efficient, reliable, and fast output results, following other studies carried out by researcher for site suitability analysis with the help of GIS and remote sensing.

a. GIS and its analysis tool have been used for optimizing the locations of the sewage treatment plants (STP) and outfalls on the basis of eco-sensitivity areas. The key elements of site selection were encompassing 10 criteria and 15 indices that were established to generate the eco-suitability map and determine possible locations for STP and sewage outfalls (Zhao et al. 2009).
b. For identification of suitable site for solid waste management, a hydro-morpho-geological study was carried on the basis of hydrology, geomorphology, and geology with the help of digital elevation model and LANDSAT-TM satellite imagery. Results show that the site suitability analysis using remote sensing and GIS 17 favorable locations were identified with the help of GIS and RS data which can be used for solid waste management (Sumathi et al. 2008).

c. RS and GIS technologies have been used for study of urban–rural planning land suitability and its comprehensive evaluation. For the suitability analysis, data about limiting factors like terrain, landscapes, traffic, farmland protection, nature reserve and scenic area, and drinking water source protection were acquired from remote sensing techniques and GIS domain. Through analyzing all various factors which impact on land suitability and the distribution of population, the weight of the various factors was determine for evaluation of the land-use suitability (Luo et al. 2008).
d. Proper location of wastewater treatment plant helps to protect the groundwater pollution and soil degradation. Selection and identification of possible sites for the wastewater treatment facilities were assessed using suitability score which depends on land-use pattern, ground slope, and its distance from riverbank and roads. Finally, ideal location for wastewater treatment plant was designated on the basis of weightage value (Benujah and Devi 2009).

In the Himalaya, due to rough terrain, vast, and unapproachable catchment area, examining the drainage network to collect flow data through field visits is difficult. A study conducted by El-Magd et al. (2010) shows that digital elevation models (DEM) are fit for catchment area analysis, and its comparison with existing topographic maps of the area gives good results. DEM data within GIS domain have a potential to extract the drainage network of the river in fastest way, and it can be carried out by using an ASTER DEM data with a 30 $\times$ 30 m grid cell size. For the water modeling purposes, evaluation and slope in the streams are needed for starting with the end point of the river stretch. DEM data can delineate automatically streams in the presence of a river as a sink. With this sink, we can calculate the flow direction of the streams. On the basis of flow direction, we can calculate the flow accumulation of the river at any point. After that, stream network is generated within the catchment (Macka 2001).

13.4.2 Groundwater Flow Modeling for Purification Capacity Analysis

River water levels and its interaction with groundwater in the river stretch can be simulated with groundwater flow modeling, e.g., using MODFLOW. Inside the groundwater flow model, building the conceptual model, its design, calibration, and validation/simulation are the usual steps (Anderson and Woessner 1992). For the calculation of filtration capacity of the alluvial aquifer, hydraulic conductivity, river water level, meandering ratio, slope, the width of the alluvial plain, and discharge of the river are the main input parameters. River discharge and levels can be taken from secondary sources, the geo-hydraulic properties from pumping tests at some sites near the river stretch and other remaining parameters can be determined from remote sensing data. By using GIS and remote sensing techniques, the process of conceptualization and the selection of site can be added to make the best results and sites for exploration and purification of the river stretch. For the river stretch, the following methodology was adopted by different researcher: The geo-hydrological data were collected for the site including groundwater observation near the river stretch, discharge measurements of the river are used to calibrate the model, and a digital elevation model (DEM) of 30 $\times$ 30 m grid size is used for slope analysis. The purification capacity of the river is calculated with the help of numerical tools. To overcome the issue of water quality and availability and reduce the dependence on groundwater, the alluvial deposits near the riverbanks can play a big role for sustainable water sources and it can be a part of Integrated Water Resources Management of the Himalayan area (Grischek et al. 2011).

13.5 Conclusion

On the basis of literature review, following research gaps are identified for the mountain areas.

I. In India, IWRM approach has been developed only in some part, and only few papers are available on IWRM practices applied in the Himalayas focusing on small towns of Uttarakhand.
II. In 2013 flood in Himalaya, IWRM practices even in small way failed due to the glacier retreats and consequent disasters.
III. Studies on River Ganga have concerned only big cities and did not take into account its main tributary and population.
IV. Limited preliminary works have been done by scientists in development of bank filtration.
V. GIS and RS are used frequently by researchers for land cover analysis and management in India, but in Himalayan mountain area, many parts are untouched by researcher for IWRM with the help of GIS and RS technologies.
VI. Non-point source pollution in the Himalayan rivers has been the focus of several studies conducted by scientists and researchers in many government agencies. Projects have been implemented to correct and prevent related problems. But result shows that there is not much considerable improvement in water quality of the River Ganga.
VII. There has been lack of coordination among organizations and no attention toward integrated resource management in the river basin.
VIII. Few preliminary works have been done by scientists in development of indirect surface water abstraction schemes (bank filtration), which is a sustainable technology in mountain region. These preliminary studies show that mountain regions have a great potential of RBF system for sustainable potable water supply.

These riverbanks of the Himalayan state of India can produce safe and sustainable drinking and agriculture water. Indirect abstractions of surface water through the alluvial medium near the bank of a river can minimize river pollution level. The indirect abstraction of surface water can meet the water demand of the area in a sustainable manner. Thus, the purpose of the management plan should be aimed at a sustainable utilization of these water resources (alluvial plains) as well as of the natural environment. It is need of the present times, to estimate the water availability and demand, to determine suitable sites near a river stretch for drinking water exploration, suitable river meandering sites for calculation of the water purification capacity of the river stretch by inducing recharge, and to calculate the water purification and filtration capacity of these identified sites with the help of groundwater modeling and Switch Organic Micro-Pollutant Assessment Tool (SOMA).

References

Amakali M, Shixwameni L (2003) River basin management in Namibia. Phys Chem Earth 28:1055–1062

Anderson MP, Woessner WW (1992) Applied groundwater modeling: simulation of flow and advective transport (4). Gulf Professional Publishing, United states of America

Aspinall R, Pearson D (2000) Integrated geographical assessment of environmental condition in water catchments: Linking landscape ecology, environmental modelling and GIS. Environ Manage (J) 59:299–319

Bassist A, Arya DS, Goel NK (2009) Analysis of historical changes in rainfall in the Indian Himalayas. Int J Climatol 29:555–572

Benn D, Evans DJ (2014) Glaciers and glaciation. Routledge, New York, USA

Benujah BR, Devi G (2009) Site suitability evaluation for sewage treatment plant in Nagercoil Municipality, Tamil Nadu using remote sensing techniques

Bonato M, Ranzani A, Patro ER, Gaudard L, De Michele C (2019) Water-energy Nexus for an Italian storage hydropower plant under multiple drivers. Water 11:1838. https://doi.org/10.3390/w11091838

Bridge JS (2009) Rivers and floodplains: forms, processes, and sedimentary record. John Wiley & Sons, Hong kong

Chang HH (1992) Fluvial processes in river engineering. Melbourne, USA

Chevuturi A, Dimri AP (2016) Investigation of Uttarakhand (India) disaster-2013 using weather research and forecasting model. Nat Hazards 82:1703–1726. https://doi.org/10.1007/s11069-016-2264-6

Church M (1992) Channel morphology and typology. In: Calow P, Petts GE (eds) The rivers handbook: hydrological and ecological principles, vol 1. Oxford, Blackwell, pp 126–143

Cook KL, Turowski JM, Hovius N (2014) River gorge eradication by downstream sweep erosion. Nat Geosci 7(9):682–686

Deng ZQ, Singh VP, Bengtsson L (2001) Longitudinal dispersion coefficient in straight rivers. J Hydraul Eng 127(11):919–927. https://doi.org/10.1061/(ASCE)0733-9429(2001)127:11(919)

Deng ZQ, Singh VP (2002) Optimum channel pattern for environmentally sound training and management of alluvial rivers. Ecol Model 154(1):61–74

Eda LE, Higa WC (2010) Integrated water resources management in Peru. Procedia Environ Sci 2:340–348

Edgar DE (1984) The role of geomorphic thresholds in determining alluvial channel morphology. In: Elliot CM (eds) River meandering. ASCE, pp 44–54

El-Magd IA, Hermas E, Bastawesy ME (2010) GIS-modelling of the spatial variability of flash flood hazard in Abu Dabbab catchment, Red Sea Region, Egypt. Egypt J Remote Sens Space Sci 13(1):81–88

Ernest and Young (2011) Water sector in India, emerging investment opportunities. Available: http://www.ey.com/Publication/vwLUAssets/Water_sector_in_India. Accessed 1 Mar 2020

Fischer HB (1979) Mixing in inland and coastal waters. Academic press, USA
Fort M (2000) Glaciers and mass wasting processes: their influence on the shaping of the Kali Gandaki valley (higher Himalaya of Nepal). Quat Int Palaeodemography Southern South America 65:101–119
Frissell CA, Liss WJ, Warren CE, Hurley MD (1986) A hierarchical framework for stream habitat classification: viewing streams in a watershed context. Environ Manage 10(2):199–214
Gleick PH (1998) Water in crisis: paths to sustainable water use. Ecol Appl 8(3):571–579
Grischek T, Schoenheinz D, Sandhu C (2011) Water resource management and riverbank filtration. Drinking water source, treatment and distribution. Dehradun, India. Source: HTW library
Hiscock MK, Grischek T (2002) Attenuation of groundwater pollution by bank filtration. J Hydrol 266(3):139–144
Kimothi PC, Dimri DD, Adlakha LK, Kumar S, Rawat OP, Patwal PS, Grischek T, Sandhu C, Ebermanun J, Ruppert M, Dobhal R, Ronghang M, Kumar P, Mehrotra I, Uniyal HP (2012) Development of river bank filtration in Uttarakhand. J Indian Water Works Assoc (Special Issue), pp 13–18
Kirby C, White WR (1994) Integrated river basin development, England. John Wiley & Sons Ltd. Institution of Hydrology
Kumar P, Mehrotra I (2009) Riverbank filtration for water supply: Indian experience. In: Proceeding 2009 world environmental and water resources Congress, Missouri, May 17–21
Lee CM, Low KS (2004) An integrated approach towards management of River Basin Malaysian Water Partnership
Leidig M (2008) Estimation of erosion on a large scale–an approach for Tibet. Environ Sci Technol 2:260
Leopold LB, Wolman MG (1957) River channel patterns: braided, meandering and straight. US Geol Surv Prof Pap 282:39–85
Lewin J (1984) British meandering rivers: the human impact. In: Elliot CM (ed) River meandering. ASCE, p 369
Luo L, He Z, Hu Y (2008) Study on land use suitability assessment of urban-rural planning based on remote sensing—a case study of Liangping in Chongqing. Int Archives Photogram, Remote Sens Spatial Inform Sci, Beijing
Macka Z (2001) Determination of texture of topography from large scale contour maps. Geografski vestnik 73(2):53–62
Martinez-Santos P, Aldaya MM, Llamas MR (2014) Integrated water resources management in the 21st century: revisiting the paradigm. B. CRC Press, London
Michael BP, Allan LJ, Shroder FJ, Stephen JW (2012) Geospatial technologies and digital geomorphological mapping: concepts, issues and research. Geomorphology 137(1):5–26
Michl C (1996) Using GIS, MODFLOW and MODPATH for groundwater management of an alluvial aquifer of the River Sieg, Germany, vol 235. IAHS Publications-Series, IAHS, pp 551–558
Nischalke SM (2014) Adaptation options to improve food security in a changing climate in the Hindu Kush-Himalayan Region. Springer
Nordin CF, Troutman BM (1980) Longitudinal dispersion in rivers: the persistence of skewness in observed data. Water Resour Res 16(1):123–128
Pandey A, Chowdary VA, Mal BC (2007) Identification of critical erosion prone areas in the small agricultural watershed using USLE, GIS and remote sensing. Water Resour Manage 21(4):729–746
Patro ER, Voltz TJ, Kumar A, Grischek T (2020) Micro-hydropower in drinking water gravity pipelines: a case study in Uttarakhand, India. ISH J Hydraul Eng 26(3):332–342. https://doi.org/10.1080/09715010.2018.1492977
Patro ER, Kishore TS, Haghighi AT (2022) Levelized cost of electricity generation by small hydropower projects under clean development mechanism in India. Energies 15:1473. https://doi.org/10.3390/en15041473
Peavy HS, Rowe DR, Tchobanoglous G (1985) Environmental engineering. McGraw-Hill Book Company, McGraw-Hill Interamericana, pp 63–99

Postel S, Richter B (2003) Rivers for life: managing water for people and nature. Island Press
Sandhu C, Grischek T, Kumar P, Ray C (2011) Potential for riverbank filtration in India. Clean Technol Environ Policy 13(2):295–316
Saph Pani D1.2 (2013) Guidelines for flood-risk management of bank filtration schemes during monsoon in India. Saph Pani Project Deliverable D1.2. http://www.saphpani.eu/downloads. Accessed 1 Mar 2020
Seth JW, Lawrie F (2000) Protecting streams and river corridors: creating effective Local Riparian buffer ordinances. University of Georgia, United States of America Carl Vinson institute of Government
Shanwad UK, Patil VC, Gowda HH, Shashidhar KC (2012) Remote sensing and GIS for integrated resource management policy-a case study in Medak Nala Watershed, Karnataka, India. American-Eurasian J Agric Environ Sci 12:790–806
Staudenrausch H, Fliigel WA (2001) Development of an integrated water African catchments. Phys Chem Earth 26:561–564
Sumathi VR, Natesan U, Sarkar C (2008) GIS-based approach for optimized siting of municipal solid waste landfill. Waste Manage 28(11):2146–2160
UNICEF, FAO, SaciWATERs (2013) Water in India situation and prospects. Available: http://www.unicef.org/india/Final_Report.pdf. Accessed 1 Mar 2020
Wang QG, Gu G, Higano Y (2006) Toward integrated environmental management for challenges in water, environmental protection of Lake Taihu Basin in China. J Environ Manage 37(5):579–588
Winkley BR (1982) Response of the Lower Mississippi to river training and realignment. Gravel-bed Rivers. John Wiley & Sons, Chichester, pp 652–681
Winkley B.R. (1983). Stable river alignment. In: Elliot CM (ed) River meandering. ASCE, pp 370–383
Wright A, Marcus WA, Aspinall R (2000) Evaluation of multispectral, fine scale digital imagery as tool for mapping stream morphology. Geomorphology 33:107–120
Xu JX (1996) Fluvial processes in different natural zones in China. Science Press in Chinese, China
Yang YH, Zhou F, Guo HC, Sheng H, Liu H, Dao X, He CJ (2010) Analysis of spatial and temporal water pollution patterns in Lake Dianchi using multivariate statistical methods. Environ Monit Assess 170(1–4):407–416
Yang CT (1986) Dynamic adjustment of rivers. In: Wang SY, Shen HW, Ding LZ (eds) Proceeding Third Symposium River Sedimentation, Mississippi, Mar 31–Apr 4. The University of Mississippi, pp 118–132
Zhao YW, Qin Y, Chen B, Zhao X, Li Y, Yin XA, Chen GQ (2009) GIS-based optimization for the locations of sewage treatment plants and sewage outfalls–a case study of Nansha District in Guangzhou City, China. Commun Nonlinear Sci Numer Simul 14(4):1746–1757

Chapter 14
Water Resource Estimation and Management: Case Study of the Alaknanda River Basin

Pooran Singh Patwal, Epari Ritesh Patro, and Shahid Ul Islam

Abstract The Himalayan areas face frequent occurrence of water scarcity. There is a need for an assessment of water resources of the region. To meet the population's water needs, existing water resources and new potential water bearing zones must be investigated. Due to high seasonal variability in river flows and very high sediment transport and monsoonal turbidity in river water in mountainous areas, indirect surface water abstraction from riverbank for drinking water production is becoming a cost-effective and sustainable alternative to the direct abstraction of river water and associated conventional treatment. However, the identification of suitable sites for indirect surface water abstraction is problematic due to limited vertical and horizontal extent of alluvial deposits. For an economical identification of potential sites, an approach combining various noninvasive techniques using geographical information system (GIS), remote sensing and groundwater flow modeling (PMWin) software has been suggested for a study area comprising a 100-km-long mountainous stretch of the Alaknanda River in the state of Uttarakhand, India, having a catchment area of 10,577 km^2.

Keywords Himalaya · Uttarakhand · Ganga · Groundwater · Water demand · Climate change

---

P. S. Patwal
Independent Consultant (Hydrology and Natural Resource Management), Haridwar, India

E. R. Patro (✉)
Water, Energy and Environmental Engineering Research Unit, Faculty of Technology, University of Oulu, 90014 Oulu, Finland
e-mail: ritesh.patro@oulu.fi

S. U. Islam
Department of Civil Engineering, Baba Ghulam Shah Badshah University, Rajouri, Jammu and Kashmir, India

P. Shukla et al. (eds.), *Environmental Processes and Management*, Water Science and Technology Library 120, https://doi.org/10.1007/978-3-031-20208-7_14

14.1 Study Area: Alaknanda River Basin

The study area is situated in the northwest part of the Himalayan state Uttarakhand and located between 30.22° N to 30.27° N and 78.78° E to 79.25° E. The stretch is situated along the main pilgrim route Badrinath, Kedarnath and Hemkund Sahib with rapidly developing towns on the bank of river Alaknanda (Fig. 14.1). The length of the river stretch is approximately 100 km. The total catchment area of the river Alaknanda is 10.57×10^3 km^2 including the study area of 714 km^2 and exceeding heights of 496 masl to 775 masl. This river stretch receives a vast quantity of water from main tributaries such as Pinder and Mandakini River and rainfall over the catchment area.

Administratively, the starting point of the river stretch, Karnaprayag, comes under the Chamoli district and the midpoint, Rudraprayag, fall into Rudraprayag district, while the end point of the study area, Srinagar, is located in Pauri district. The study area is present in the Survey of India Toposheet Nos. 53 J/15, J/16, N/07 and K/09 on a scale of 1:50,000. The river stretch starts from medium slope of hills and moves southward to join with river Bhagirathi which make the river Ganga at Devprayag.

A new dam has been constructed on the lower river stretch of study area at Srinagar. This stretch comes under the main focus of the state and central government due to the Ganga Action Plan and construction of a new dam. The Ganga Action Plan is running for the protection of river from pollution. Other state departments like a state pollution control board, watershed management department and central pollution control boards are also working in the management of the river basin. They suggested some sewage treatment plant at riverbank sites of the river stretch like Devprayag, Srinagar, Rudraprayag and Karnaprayag under the Ganga Action Plan.

14.1.1 Geography and Geology

The study area represents highly rocky and undeveloped topography by steep slopes and triangular facets at many places. The areas have very high gradient hills, low

Fig. 14.1 Location of the study area showing the Alaknanda River between Karanprayag and Srinagar towns

permeability with low groundwater transmission and storage. Such areas do not have aquifers with promising groundwater potential. Alluvium occurs along the river courses and in their floodplains. Alluvial deposits present along the river stretch are suitable sites for water production and purification of polluted river water. The moderately sloping terrains are covered with a thin layer of weathered rocks. The entire study area presents a landscape of moderate to steep slopes intervening into a narrow valley. Generally, 'U', 'V' and 'S'-shaped compressed meanders, deep and narrow gorges are present along the river stretch. Many perennial rivers originate from the nearby area of the river stretch. The water of the entire river stretch is contributed by three rivers: Alaknanda, Pinder and Mandakini. The river stretch called "Alaknanda River stretch" due to its amount of discharge, length and non-crossing nature of the river, is the main cause of nomination of the river system.

Figure 14.2 shows the geological details of the study area. The Quaternary or alluvial deposits or terraces have been developed all along the Alaknanda valley and mostly present left side of the river, especially in Srinagar, Kaleshwar, Gaucher and Chauras. The alluvial terraces are generally composed of boulders, gravels, cobbles, pebbles, sand, silt and clay. The rock is composed of quartzite, granites, schists, gneisses and metaphysics. These terraces are either depositional or erosive in nature and are composed of gravels, sand, silt and clay. Generally, the oldest terraces are erosive in nature, while others are deposited. Along such portions where terraces were developed sinuosity, braiding and meandering is noticed which can be used for river water purification. At some places along the river, floodplains are also observed. The terraces are actually abandoned floodplains. Around Srikot, Srinagar and Gaucher developed floodplains are present, which are formed during over bank flow conditions. These terraces have provided flat land for the human settlement. The point bars were also developed adjacent to the floodplains, which contain mainly sand and silt.

14.1.2 Hydrology

The Alaknanda River originates from the glaciers Satopanth, and its basin covers an area of 11.8×10^3 km^2. During its flow, it drains through carbonates, massive quartzites, slates, phyllites and greywackes. River average discharge was measured by the dam construction authority in Srinagar. Figure 14.3 shows the minimum (January to February) and maximum (August to October) river discharge which was measured by ten daily measurements at Srinagar from 1972 to 1994.

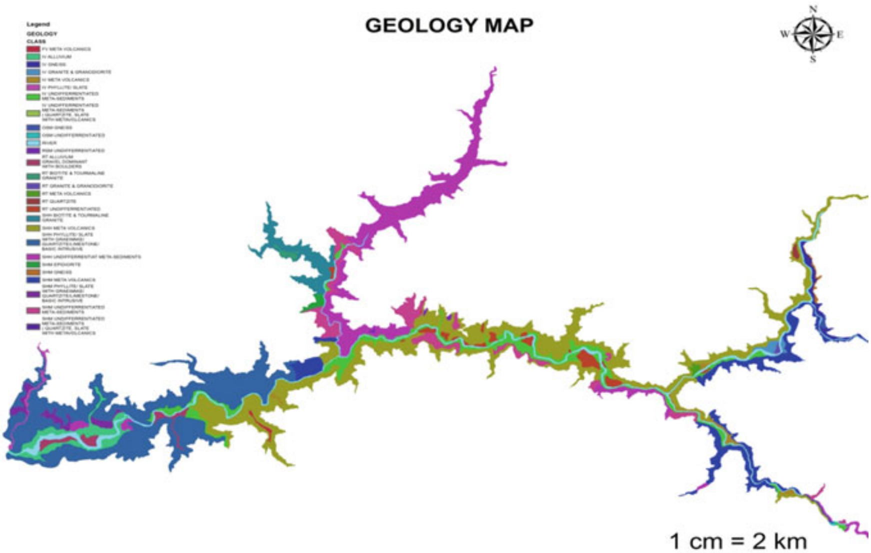

Fig. 14.2 Geological map of the study area showing the Alaknanda River between Karanprayag and Srinagar (based on Groundwater prospects map, 2008)

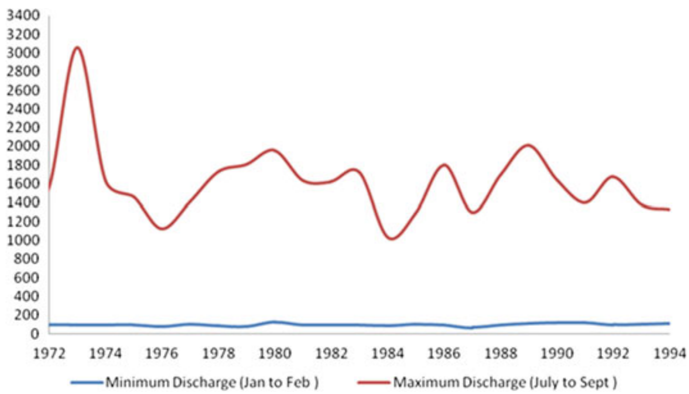

Fig. 14.3 River discharge m^3/s of Alaknanda River at Srinagar (*Source* DPR Srinagar dam, 1994)

14.1.3 River Morphology

On entering the Lesser Himalaya near Helang, the Alaknanda River flows in a wide valley. It takes a westerly swing at Karanprayag and is subsequent to the Alaknanda Fault. At Rudraprayag, it joins the river Mandakini and form a 'V'-shaped valley. After traveling 35 km, it reaches Srinagar town and flows in a wide valley. At Devprayag, it joins the river Bhagirathi to form the holy river Ganga. During the course upstream to Devprayag, it is joined by major rivers and forming the Punch Paryag (five junctions). Downstream to Devprayag at Vyasghat, the river meets Nayar River and flows westward up to Rishikesh where it takes a swing to the south. Downstream to Rishikesh, it cuts through the Sub-Himalaya and enters the Gangetic plain at Haridwar.

14.1.4 Demography

The permanent population of this river stretch includes the population of towns Srinagar, Rudraparyag, Gaucher and Karnaprayag. These towns have 200,353 persons, out of which 70,468 (including Pauri) persons permanently reside in the main or core area of these towns (Census of India 2011). Being in the way of three most important Hindu pilgrimage sites in the world, Badrinath, Kedarnath and Hemkund Sahib, these towns have a "floating" population of around 20,000 persons who reside temporarily within the main towns in religious retreat locations ("ashrams") and hotels. The growth rate of Srinagar town is 23%, Rudraprayag is 15.27%, Gaucher is 1.9%, and Karnaprayag is 1.75%. The geographical area of these towns is 9 km^2, 1 km^2, 2.5 km^2 and 25 km^2, respectively. The population density of these towns is 2235 people/km^2, 9313 people/km^2, 6000 people/km^2 and 332 people/km^2, respectively. Besides for these towns, the river stretch also provides water for population of many small villages.

14.1.5 Climate Condition

The climate of the Himalayan towns is largely influenced by their location on the different height of the Himalayan range. The climate varies greatly with altitude, from the glaciers at the highest altitude to the subtropical at the lower altitude. The climatic condition area in general depends on the summer monsoon currents and western disturbances and local orographic effect that occur in after during pre- and post-monsoon. The yearly seasonal cycle of nearby the study area can be classified into five different seasons. In the study area, winter starts from November and mid-March, spring lies between March and April, summer months are May and June, rainy season lies between July and September, and late September to end November is autumn season (Fig. 14.4). Maximum and minimum temperatures for the year 2013 were obtained for the river stretch as 36 °C to 6 °C, respectively.

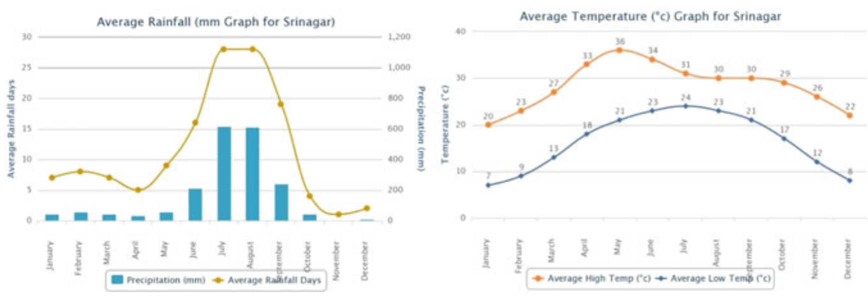

Fig. 14.4 Rainfall and temperature profile of the study area (*Source* www.worldweatheronline.com)

14.1.6 Rainfall, Temperature and Humidity

Rainfall, in the river stretch, occurs almost throughout the year. Maximum rainfall is 373–390 mm/month recorded during the monsoon period, i.e., from July to September. During the non-monsoon season, rainfall is 10–11 mm, quite low in November and increases from December onward till March (Fig. 14.4). Temperature and humidity increase in the river stretch between the months of March and September with a maximum rise between the months of April and July. In summers, the river stretches face different climate from nearby areas. Pauri, which is 25 km from the Srinagar town, faces temperatures of 25 °C but at the same time Srinagar faces 35 °C. The locations of these towns near the valley make it warm temperate conditions in summers. Figure 14.4 gives the details about yearly temperatures in the study area. However, in the higher part of the area temperature is around 15–18 °C. In winter, these valley towns are cold with temperatures going below 6 °C. Throughout the river stretches, the temperature ranges from 6 to 36 °C, and in the monsoon seasons, the temperature is approx. 30 °C from July to September.

14.1.7 The Main Towns and Features of the River Stretch

14.1.7.1 Srinagar

The town of Srinagar is located on the road to the important Hindu and Sikh shrines of Kedarnath, Badrinath and Hemkund Sahib. Srinagar was the ancient capital of Garhwal state and the cultural and educational center of Garhwal region of Uttarakhand. The area of a wide valley with the development of the Quaternary terraces intermontane valley and structural hills which are highly dissected. Along the side of the river channel, two youngest river terraces widely developed, get thinner and finally merge into each other. The main rock types are phyllite, slate with greywacke, quartzite and limestone present in the valley (based on groundwater prospects map, 2008). Srinagar is a middle-sized town categorized as urban area. The soil of the area is basically the product of fluvial processes of the river Alaknanda. The alluvial soil of the town is fine, coarse and medium with gravels. The drinking water supply of the Srinagar town was addressed through the supply created from the water of the river which was abstracted, purified and further spread. The entire population of the area is 150,000 as per the 2011 population census. The floating population of the area becomes 11,847 persons due to it being on the highly volatile pilgrim route of Badrinath, Kedarnath and Hemkund Sahib.

14.1.7.2 Karnaprayag

Karnaprayag town is located in Srinagar–Badrinath National Highway, 80 km from Srinagar. The town is located at the confluence of the rivers Alaknanda and Pinder. The town is situated in the Lesser Himalaya and is covered by quartzite of Berinag Formation. The territory of the town is basically the product of fluvial processes of the river Alaknanda and its deposits. The alluvial soil of Karnaprayag is dry, porous, sandy, brownish and clayey and consists of organic matter (Sandhu et al. 2011). The water needs of the Karnaprayag town were addressed through the supply created from the four streams which was tapped, purified and further spread. The entire population of the area is 8297 as per the 2011 census, and the floating population of the town becomes 1738 during the tourist season in summers. The yield of water from the streams was 600 m^3/day (Patwal 2015).

14.1.7.3 Gaucher

The town Gaucher is located between the towns Karnaprayag and Srinagar at the Alaknanda River. It is also situated along the main route to the major pilgrimage site of Badrinath. The town is located on undifferentiated sediments, quartzite and slate with Meta volcanic type of stain with the hard rock of Garhwal group. The geographical unit of the area comes under the intermediate valley, and aquifer is loose sediments, fissured rock with good recharge conditions. Drinking water supply in the town is mainly through tapping springs, perennial nasal, rivers and hand pumps. The town represents a wide valley with the development of Quaternary terraces. The town is situated in Lesser Himalaya and is covered quartzite of Berinag Formation. The alluvial soil of the town is dry, porous, sandy, brownish and clayey and consists of organic matter. This is a town with a population of approximately 15,500 people as per 2011 census, and the floating population of the town becomes 1738 during the tourist season in summers. The output of water from the three different sources is 264 m^3/day ((Patwal 2015).

14.1.7.4 Rudraprayag

Rudraprayag town is situated on the route of Srinagar–Karnaprayag, 35 km from Srinagar town. It is situated on the confluence of the rivers Alaknanda and Mandakini. Rudraprayag area is located on quartzite rock. Due to hard rock terrain, viz. quartzite and absence of alluvial deposit, the groundwater prospects are negligible. Geomorphologically, it is situated on the intermontane valley, and the rock type is undifferentiated metasedimentary (quartzite and slate with metabasics). Aquifer material is loose sediment and fissured rock. The town has a population of 9313 (as per Census of India 2011), and the floating population of the town becomes 4539 during the tourist season in summers. The outputs of water from the different sources are 500 m^3/day (Patwal 2015).

14.1.8 Hydroelectric Dam

The Srinagar hydroelectric dam is located on the river Alaknanda about 5 km upstream from the main town area of Srinagar on the route of Srinagar–Karnaprayag highway (Patro et al. 2020). The Srinagar hydroelectric project was authorized by the Environment Ministry in 1984 with 200 MW, and its capacity was increased to 330 MW in 1995. The total height of the dam diversion is 90 m with a storage capacity of 8 million cubic meters. The river minimum average discharge was 102 m^3/s in the mid of February, and average maximum discharge was 1326 m^3/s in the mid of August which was measured and analyzed by the dam authority and the central groundwater board on the basis of 22 years (1971–1994) discharge data and based on the 10 days observed discharge data on the river at dam site Srinagar. The total catchment area of the dam is 8460 km^2 (DPR Srinagar dam, 1994).

14.2 Existing Water Sources of Study Area

In the current study area within the 100 km stretch, four types of water resources are available: rain water, which is precipitated within the catchments; groundwater, which is available in local zone deep and tapped by hand pumps and wells; surface water, in the form of river water and spring water; impermeable strata intersection with the groundwater table and easily tapped by pipeline and water tanks. Relative ease of availability and quality and quantity of these waters varies in different watersheds. In mountain ecosystems, especially in Himalayan systems, limitations and advantages of the utilization of water resources are different and given in Table 14.1.

Table 14.1 Water source in a river catchment for IWRM

S. No.	Activity	Ground water	Rainwater	Surface water	Spring water
1	Cost of collection	High (deep well)	Medium (need structure)	High (pumping)	High (pipeline)
2	Cost of exploration	High (deep pumping)	Low	Low	Low
3	Cost of distribution	Low (less contaminated)	Low	High (need big structure)	Low
4	Water availability	Low	Low	High	Low
5	Water quality	Less contaminated by pathogen	Chance of contamination of pathogen	Highly contaminated by pathogen	Chance of contamination of pathogen
6	Storage time	High	Low	High	High
7	Need of chemical for disinfection	Low	Medium	High	Medium

14.2.1 Ground Water

In the Himalayan areas, hand pumps and wells are the main sources of groundwater abstraction. Due to geological limitations, it is not feasible to drill large diameter well everywhere in mountain area. Thus hand pumps are the only reliable source of groundwater abstraction in the mountains. Data collected during Patwal (2015), show that there are 201 hand pumps drilled in the study area.

Figure 14.5 shows the location of all hand pumps and all wells (at Srinagar) within the catchment of river stretch. The average discharge of the one hand pump is 12–18 LPM in the study area (CGWB 2012). If these hand pumps operate 24 h by small electrical pumps, total yield will be 4.34 MLD. Total yield is calculated using Eq. 14.1:

$$\begin{aligned}&\text{Total maximum groundwater yield (MLD)}\\&= \left[\text{No of hand pumps} * \text{average discharge (LPM)}/(60\,\text{min/h} * 24\,\text{h/day})\right]\end{aligned} \tag{14.1}$$

14.2.2 Spring Water

Within the selected river stretch, there are eight main perennial springs which contribute to meet the water demand of nearby towns and villages. Some springs are

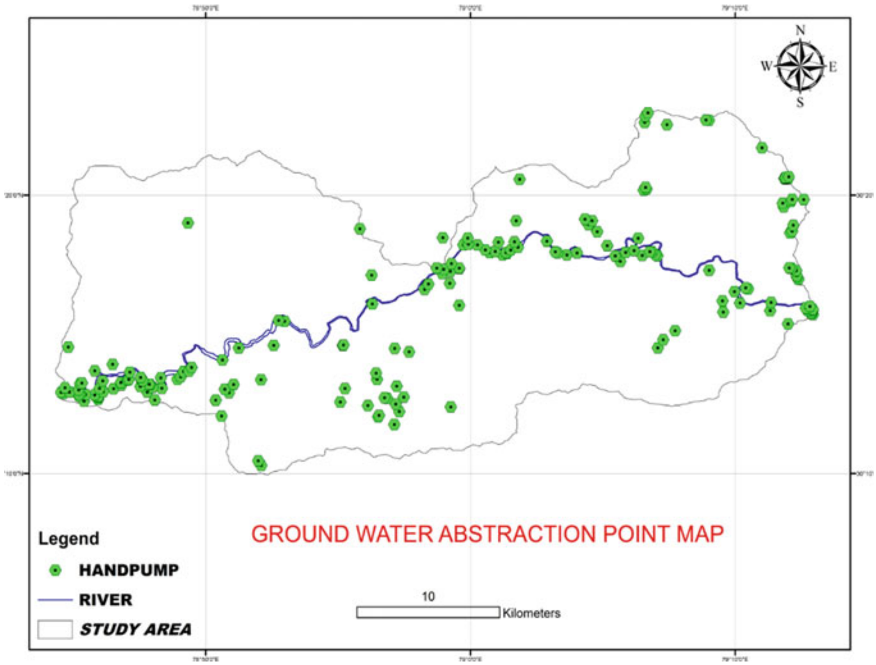

Fig. 14.5 Groundwater production location map (Patwal 2015) at the river stretch

far away from the habitation and not able to tap for drinking purposes. The approximate minimum and maximum discharge of the springs is given in Table 14.2. Total yearly discharge of all perennial springs is 691.4 million liter/year or maximum 1.75 million liter/day is calculated. Most of the other springs in the area are recharged by rainwater and only contribute water for drinking and agricultural purposes in rainy seasons. Total tapped water from these springs is 1.18 MLD (220 LPM at Gaucher and 600 LPM at Karnaprayag) around 67.47% spring water is tapped for drinking purposes. There is not much further scope for tapping the remaining spring water due to seepage of water from soil, seasonal variation and losses during tapping.

14.2.3 Rainwater

Rainfall in the river stretch occurs almost throughout the year (Table 14.3). Maximum rainfall is 549–586 mm/month recorded during the monsoon period, i.e., from July to August. During the non-monsoon season, rainfall is 0.1–81 mm, quite low from November onward till April. Winter rainfall is associated with the passage of the western turbulence. The annual rainfall ranges from 1570 to 2712.6 mm with an average of 1888.6 mm. About 80% of the rainfall occurs during the monsoon months, i.e., between June and August. The total rainfall availability at the river stretch area

Table 14.2 Springs discharge (Patwal 2015)

S. No.	Name	Discharge (MLD)		
		Max	Min	Yearly
1	Gulabrai Spring	0.17	0.05	18.7
2	Chatwapipal Spring	0.17	0.09	131.7
3	Kamera Spring	0.09	0.01	89.9
4	Panai Spring	0.14	0.09	51.1
5	Thali Gadh Spring	0.12	0.08	43.8
6	Kothar Spring	0.03	0.01	12.9
7	Ghat Gadh Spring	0.86	0.72	313.9
8	Bhaktiyana Spring	0.17	0.02	29.4
	Total	1.75	1.07	691.4

of 740 km^2 is 1.4×10^6 million liter/year and can meet the water demand of the area. But due to limited rainwater collection structures and technology, the maximum percentage of rainwater goes to the river. Due to heavy runoff through catchment area, there is always flooding and siltation in river during monsoon season.

14.2.4 Surface Water

The total average discharge of river Alaknanda in the upper stretch (Karnaprayag) is 445.5 m^3/s and in the lower stretch (Srinagar) 534.8 m^3/s, approx. 46,205.3 MLD after meeting the river Mandakini at Rudraprayag. Total direct abstract water from the river for drinking water purposes is 8.9 MLD at Srinagar and from indirect abstraction is 1.5 MLD. Due to limited technological intervention, geological conditions and space for a water purification plant near to the river no future scope are available for direct surface abstraction of water. The direct abstracted drinking water from the river was only 0.02% of the total available surface water. Huge amount of water just passes from towns without meeting the water demand of the river stretch. River discharge data shows (Table 14.4 and Fig. 14.6) that the surface water availability is higher at the time of monsoon due to a large catchment area of the river. The river has a lower discharge in February due to snow melting. The discharge of the river suddenly increases from June to August and slowly decreases from October to February.

14.3 River Water Quality

The water quality index (WQI) of Alaknanda River within the river stretch from Srinagar to Karnaprayag at two locations was calculated. The water quality data was collected from Uttarakhand Jal Sansthan, State Drinking water and sewerage

Table 14.3 Rainfall data from 2004 to 2010 at the river stretch (Patwal 2015)

S. No.	Rainfall data (mm)													
	Year	January	February	March	April	May	June	July	August	September	October	November	December	Annual
1	2004	80.4	0	0	68.3	66.8	155.6	680.6	632.2	367.6	212.8	0	0	2264.3
2	2005	70.7	85.6	38.9	0	7.4	180.5	1131.5	457	712.1	28.9	0	0	2712.6
3	2006	12	0	11.1	16.5	267.5	212.4	572.6	632.6	121.1	0	0	11.3	1857.1
4	2007	0	231.2	87.4	6.5	24	387	601.7	1115.5	245.6	22	N.A.	N.A.	N.A.
5	2008	N.A.	N.A.	N.A.	N.A.	N.A.	N.A.	324.6	276.6	47	79	0.4	0	N.A.
6	2009	N.A.	N.A.	N.A.	N.A.	N.A.	44.2	300.7	245	101	15.1	0.1	12.6	N.A.
7	2010	1.2	35.1	0	2.2	41.4	92	496.3	484	382.9	11.5	0	24	1570.6
Avg. Rainfall		32.9	70.4	27.5	18.7	81.4	178.6	586.9	549.0	282.5	52.8	0.1	8.0	1888.6

N.A. = Not measured

Table 14.4 River water discharge at different points at river stretches

S. No.	Location	Monthly river discharge in m/s											
		Jun	Jul	Aug	Sept	Oct	Nov	Dec	Jan	Feb	Mar	Apr	May
1	Alaknanda Rudraprayag	480.5	944	1083	677.2	267.1	156	109.2	89.9	82.5	92.4	128.9	248
2	Pinder Karanprayag	68.1	182.8	257.7	182.6	79.5	43.5	30.2	24.3	22	24.5	29.7	42
3	Mandakini Rudraprayag	84.9	234.6	303.2	178.5	75.1	41.7	25.7	20.6	19,6	25.5	35.6	46.4
4	Alaknanda Srinagar	633.5	1361.4	1643.9	1038.3	421.7	241.2	165.1	134.8	104.5	142.4	194.2	336.4
5	Alaknanda Karanprayag	548.6	1126.8	1340.7	859.8	346.6	199.5	139.4	114.2	104.5	116.9	158.6	290

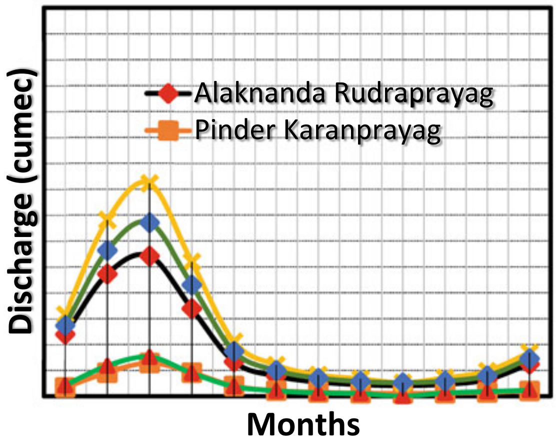

Fig. 14.6 Surface water discharge in different seasons at river stretch (*Source* DPR Srinagar dam, 1994)

department from May 2010 to December 2012. The river water quality data (Patwal 2015) shows that turbidity values in river water were found much higher than the desirable and permissible limits during monsoon. The highest value was recorded as 5000 NTU in river water. Other values such as pH, hardness and alkalinity, TDS, nitrate and fluoride concentration were found quite low and within the permissible limits. Concentration of major ion and metal ions was also quite low compared to their desirable and permissible limits except iron in some cases.

The water quality index was calculated on the basis of 11 water quality parameters which are listed in Table 14.5 with its standard values. Three steps are needed for calculation of WQI. First, the weightage of each parameter is calculated using Eq. 14.2:

$$W_i = K/S_i \tag{14.2}$$

where W_i = unit weightage of parameter; S_i = standard permissible values of each parameter (BIS); K = proportionally constant calculated unit weightage.

Secondly, each parameter is assigned with quality rating by dividing its concentration in sample by its permissible limit (BIS). Individual quality rating (Q_i) is than given by Eq. 14.3:

$$Q_i = (C_i/S_i) \times 100 \tag{14.3}$$

where Q_i = individual quality rating and C_i = parameter concentration. Finally, the sum of these all subindices gives the overall WQI from Eq. 14.4.

$$\text{WQI} = \sum_{i=1}^{n}(Q_i W_i) / \sum_{i=1}^{n}(W_i) \tag{14.4}$$

Table 14.5 Water quality parameters and its standard values

Water quality	Standard value (BIS 10500:1991)	Unit weight (W_i)
		Parameter
pH	8.5	0.09321
Total hardness, mg/l	600	0.00132
Turbidity, NTU	10	0.07923
Sulfate, mg/l	400	0.00198
Alkalinity, mg/l	600	0.00132
Calcium, mg/l	200	0.00396
Iron, mg/l	1	0.79227
Magnesium, mg/l	100	0.00792
Chloride, mg/l	1000	0.00079
Nitrate, mg/l	45	0.01761
Total dissolved solids, mg/l	2000	0.00040

Table 14.6 Water quality status values

S. No.	WQI scale	0–25	26–50	51–75	76–100	>100
1	WQI status	Excellent	Good	Poor	Suitable	Unsuitable
2	Grade	A	B	C	D	E

where n = number of parameters. The status of water quality for determining suitability for drinking purposes according to the WQI scale has been defined on the basis of criteria given in Table 14.6. The values of WQI determined for two locations of the river water within whole stretch are given in Table 14.7.

Figure 14.7 demonstrates that the river water is not suitable during monsoon and just after monsoon due to higher WQI and found unsuitable with grade 'E', whereas the post-monsoon and the pre-monsoon showed excellent to good water quality with grade 'A' and 'B' except January 2012. The main reason of higher WQI values in river water was found due to higher turbidity, alkalinity and iron concentrations. From above water quality index, it seems that the water quality of the Alaknanda River is overall good. But the main problem is that the presence of coliform population indicates the presence of pathogenic organisms in the river water.

The presence of coliform in drinking water creates health problems. Surface water quality data of two locations at Karanprayag and Srinagar shows that the river water is slightly alkaline, with pH values ranging from 8 to 8.2 and only coliform and turbidity recorded more than the desirable limits. The highest recorded value of coliform was 12,033 MPN/100 mL and highest value of turbidity 5368 NTU at the time of monsoon (June–October) (UJS). Figure 14.8 shows the fluctuation in turbidity and coliform in the time of monsoon in river water.

Table 14.7 Calculated water WQI vale of river water at lower stretch

S. No.	Season and year	WQI	Grading	Description of water quality	WQI	Grading	Description of water quality
		Srinagar			Karanprayag		
1	Pre-monsoon–May 2010	43.69	B	Good	60.33	C	Poor
2	Post-monsoon–August 2010	522.56	E	Unsuitable	299.62	E	Unsuitable
3	Post-monsoon–November 2011	28.55	B	Good	26.06	B	Good
4	Pre-monsoon–January 2012	541.49	E	Unsuitable	1115.12	E	Unsuitable
5	Pre-monsoon–February 2012	29.93	B	Good	46.59	B	Good
6	Pre-monsoon–March 2012	35.84	B	Good	21.02	A	Excellent
7	Pre-monsoon–April 2012	45.96	B	Good	38.33	B	Good
8	Pre-monsoon–May 2012	21.23	A	Excellent	16.15	A	Excellent
9	Monsoon–September 2012	1067.55	E	Unsuitable	758.35	E	Unsuitable
10	Post-monsoon–November 2012	18.14	A	Excellent	22.63	A	Excellent
11	Post-monsoon–December 2012	16.89	A	Excellent	15.36	A	Excellent

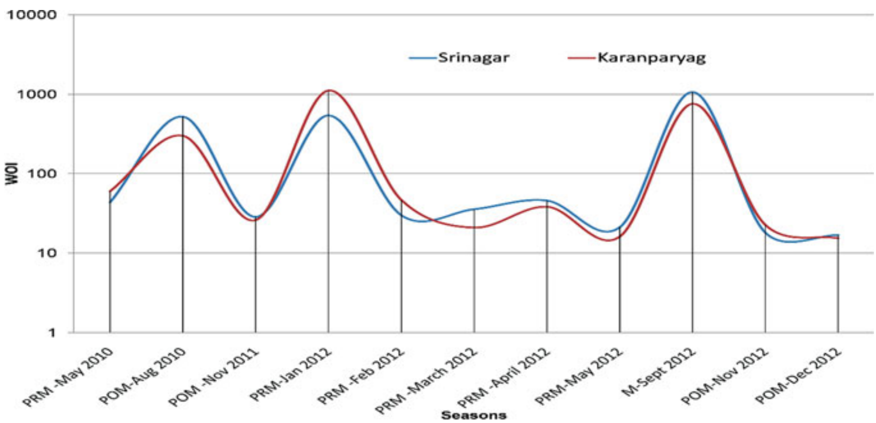

Fig. 14.7 Water quality index at upstream (Karanprayag) and downstream (Srinagar) (PRM = pre-monsoon and POM = post-monsoon)

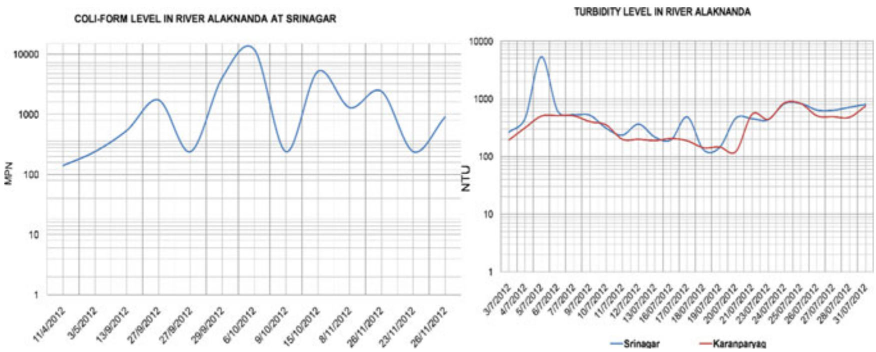

Fig. 14.8 Coliform and turbidity in the river stretch (based on Ronghang et al. 2011)

14.4 Water Demand

Mainly, two types of water demand were calculated for the study: domestic and agricultural water demand. The study area comes under the hilly part of Uttarakhand, and currently, there is no big industry developed. So industrial, fire, public space, institutional and building water demand is not calculated in this study.

14.4.1 Domestic Water Demand

Present water production for five major towns in the river stretch is 15 MLD which is not sufficient to fulfill the present and future demands of water supply. Town Pauri, which is 25 km far away from the river, is included in this river stretch because the drinking water supply system of Pauri is depending on the Alaknanda River. Drinking water for Pauri is pumped out from Srinagar. The total water demand of these five major towns, included Pauri, is 31 MLD, which was calculated on the basis of 135 LPCD (Patro et al. 2020) plus 15% water distribution losses for permanent population and 40 LPCD (30% of the permanent water demand, Economic Survey of Delhi 2005, 2006) for floating population. Table 14.8 shows the major demand–supply gap of different towns in the river stretch. Total water demand was calculated by following formula:

$$\begin{aligned}&\text{Domestic water demand (liter/capita/day)}\\&\quad=\left[\text{permanent population} * (135 + 15\% \text{ of } 135) + \text{floating population} * 40.5\right]\end{aligned} \tag{14.5}$$

In above equation, 135 L is the amount of water require for one person in one day, 15% is distribution losses, and 40 is amount of water require for one non-residential person (tourist and outside worker).

Table 14.8 Drinking water status on the river stretch

S. No.	Data	Srinagar + Pauri	Rudraprayag	Gaucher	Karanprayag
1	Population (Census of India 2011)	175,440	9313	7303	8297
2	Floating population	11,847	4539	1738	1738
3	Drinking water production (m^3/day)	13.4	0.5	0.3	0.6
4	Drinking water demand (floating demand 30% of domestic demand) (m^3/day)	27.4	1.5	1.1	1.3
5	Water deficit (m^3/day)	14.0	1.0	0.8	0.7
6	Per capita availability (l/capita/day)	76	46	39	72

Source Patwal (2015)

14.4.2 Agriculture Water Demand

Involvement of 80% population in agricultural activities in the Alaknanda catchment makes it a main source of livelihood of the local people within the study area. Horticultural practices are just negligible concerning productivity and land availability. River stretch catchment has a land area of 718 km^2. About 82% area comes under the more than 10% slope which is unsuitable for agriculture activity. According to the land use/land cover map, around 8.8% (2282 ha) of the total area comes under the agricultural land. The landscape of whole watershed is undulating, fragile and prone to high soil erosion, making it not feasible for canal irrigation. Out of 8.8%, only 8.8–11% of the cropped area is irrigated by small canals locally called Gools (Sati 2008) and the rest of agriculture area being rain fed. In mountains, farmers often grow rice and wheat one times in one year. The agriculture water demand is based on the growth of rice crop or Kharif (July to October months) season and wheat crop or Rabi (December to April) season.

According to study conducted by Kumar and Rajwar (2011) on grain production of wheat and rice on six villages in Garhwal Himalaya, Uttarakhand, in the subtropical zone (900–1300 m elevation), the average production of wheat in irrigated area was 2600 kg/ha and rice is 1200 kg/ha. Another study conducted by Mahajan and Gupta (2009) shows that for water demand for production, wheat needs 1000–1200 L /kg and rice needs 5000 L/kg. On the basis of studies, total water demand can be calculated by following equation:

$$\begin{aligned}&\text{Agricultural water demand}\\&= \text{Total agriculture area in hectare}\\&\quad * \{(\text{per kg water demand for rice crop} * \text{per hectare rice production in kg})\\&\quad + (\text{per kg water demand of wheat} * \text{per hectare wheat production in kg})\end{aligned} \tag{14.6}$$

Form the above formula, the total water demand for rice crop will be 13,692 million liter/ year and for wheat crop will be 7120 million liters/ year. If all the agricultural land comes under the irrigated area and used for only rice and wheat production, total agricultural water demand will be 20,812 million liter/year or 57 MLD.

14.4.3 Options to Meet the Agricultural Water Demand

14.4.3.1 Using Domestic Wastewater

As we discussed, agricultural is the main source of livelihood of the 80% local people. The water demand of the can be met by two ways: from wastewater and use of contaminated water. Around 80% of the total supplied domestic water is converted into wastewater containing phosphorus and nitrogen, which is very good for agricultural activities. Currently, only 2 MLD wastewater is collected and treated in whole river stretch. Currently, the total 11.2 MLD wastewater generated within the river stretch can meet the 20% of the agricultural water demand of the area. In future, 25.1 MLD wastewater will be generated within the river stretch that can meet the 44% of agricultural water demand. The total wastewater generation is calculated from the given equation:

$$\text{Total wastewater generation} = \left[(\text{Total population}) * (\text{liter/capita/day water demand}) * 80\right]/100] \quad (14.7)$$

14.4.3.2 Using Unfit Drinking Water

Some percentage of agricultural water demand can be supplied form the unfit drinking ground water. The water quality of the river stretch has many problems related to concentration of the water parameter. Figure 14.9 shows the number of water parameter existing higher than the permissible limits in different type of water resource at different locations in river stretch catchment. Many studies show that the water from wells and hand pumps containing the high percentage of nitrate can be utilized for agriculture purposes. Higher value of nitrate in water works as a fertilizer for crop and enhances the productivity of the field.

This type of integrated practices in the study area helps the people to increase their financial and economic status as well as reduce their health problems.

(a) **Using nitrate contaminated water**: Fig. 14.10 shows that the nitrate level in hand pumps water at one site Srinagar and maximum concentration of nitrate was recorded 377 mg/l in the hand pumps.

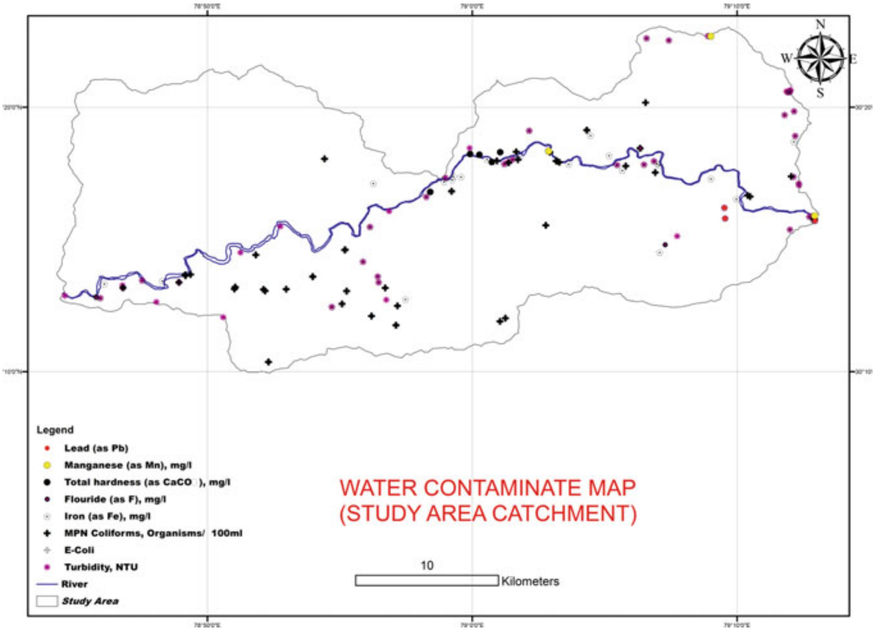

Fig. 14.9 Locations of the contaminated water sources in the study area (Patwal 2015)

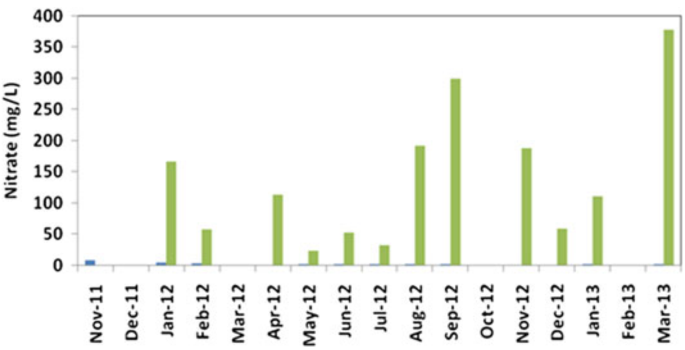

Fig. 14.10 Nitrate concentration in groundwater (*Source* Patwal 2015)

(b) **Using iron contaminated water**: Water quality map (Fig. 14.11) of iron shows that half of the area of the river stretch comes under the permissible limit of 0.15–0.3 (blue area) and half of the area comes under the 0.3–0.6 mg/l limit.

(c) **Using pathogenic contaminated water**: Water quality map of the area in Fig. 14.12 shows that the maximum water sources are contaminated with pathogenic contamination which leads to poor health and high medical warden to the local people. Contaminated water can be used of other non-drinking purpose, and other source of water should be identified in river stretch.

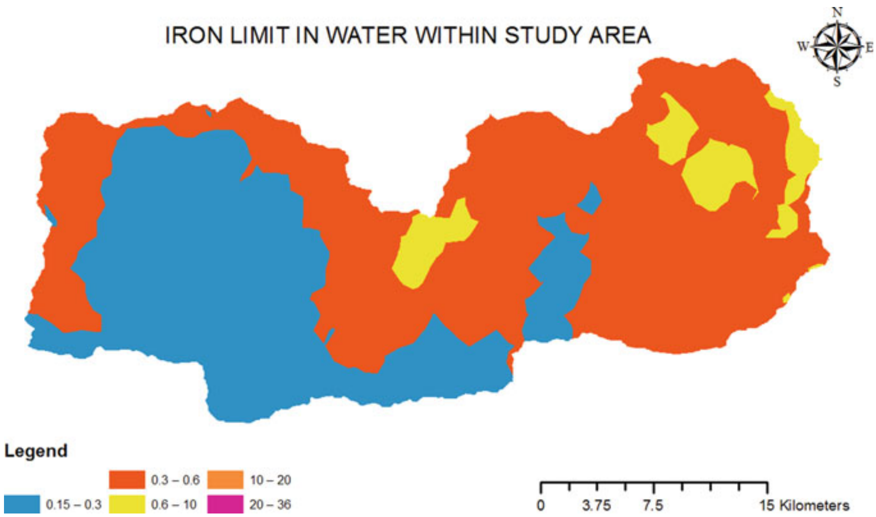

Fig. 14.11 Limit of iron content in different water sources map within study area (*Source* Patwal 2015)

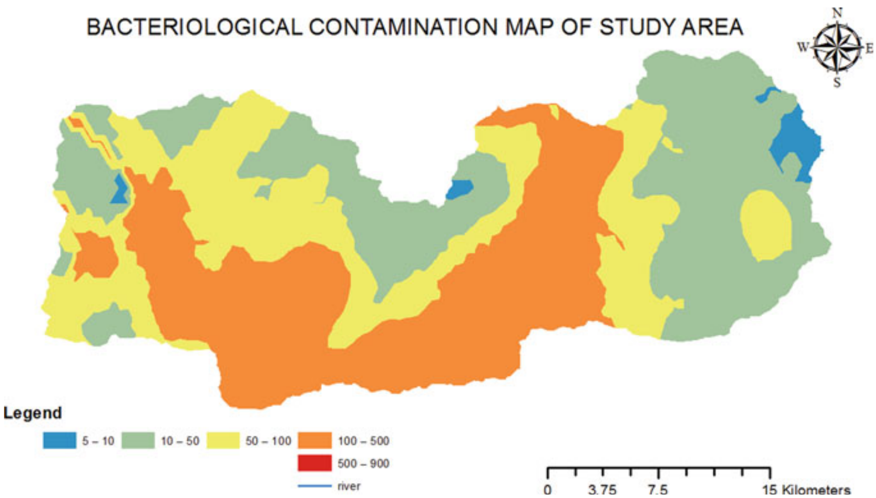

Fig. 14.12 Bacteriological contamination map of water sources within study area (*Source* Patwal 2015)

14.4.3.3 Using Rainwater

On the basis of Patro et al. (2018), about 50–60% of the annual rainwater is lost through runoff in the area. The total rainwater availability in the catchment area of the river stretch was 1.4×10^6 million liter/year calculated on the basis of the

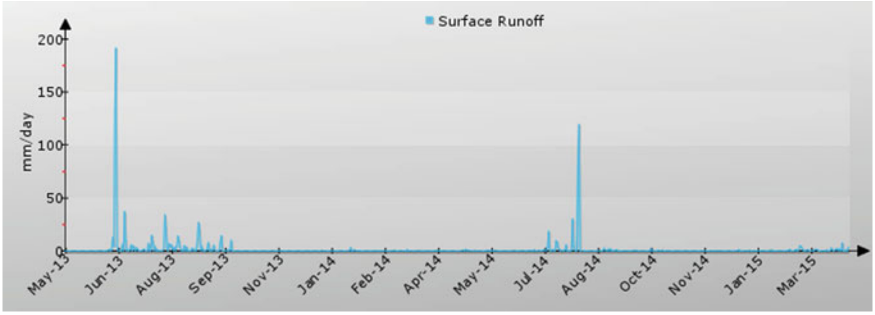

Fig. 14.13 Surface runoff of rain fall mm/day at study area (*Source* Patwal 2015)

average yearly rainfall data of seven years. If we save 60% (runoff) of the annual rainfall in the study area, it will be 8.4×10^5 million liter/year or 2301.4 MLD and can meet all agricultural water needs. This amount of water can fulfill 100% of the remaining agricultural water demand of the area. Figure 14.13 shows the surface runoff of rainwater yearly at the study area.

14.4.4 Gaps in Water Supply and Demand

The total drinking water availability from groundwater and spring water is 5 MLD, and there is a huge potential to tap the river and rainwater in the river stretch. This amount of water can meet the drinking water demand of 37,032 people at the rate of 135 L/capita/day + 15% distribution losses. Table 14.9 shows that the current total water demand gap is approx. 16.6 MLD. The main reason of this is insufficient water production, poor water management, improper tapping techniques of water sources and old leaking distribution system.

Table 14.9 Total water availability at river stretch

S. No.	Water source	Water production	
		MLD	MLY (yearly)
1	Ground water	4.3	1587.7
2	Rain water	3835.0	1.4×10^6
3	Spring water	1.1	691.4
4	Surface water	46,205.3	1.69×10^7

14.5 Existing Water Abstraction and Treatment Schemes

Currently in the study area, direct abstraction or conventional treatment systems (flocculation–sedimentation–rapid sand filtration–disinfection) are used for meeting the water demand. Groundwater hand pumps and springs also serve as drinking and agricultural water source. Currently, indirect surface water abstraction schemes called riverbank filtration are also used at locations at Srinagar and Gaucher for drinking water purposes.

14.5.1 Management Issues in Water Abstraction and Supply

There are many problems in directly abstracted river water followed by conventional treatment. Water quality, high operational and maintenance cost, abstraction of water directly influenced by climatic condition are the main problems which interrupt the water supply of the area. In terms of water quality, river water has pathogenic contamination, which increases in the monsoon and is often silted-up by sediments during monsoon. In monsoon time, coagulation and filtration which are commonly used in direct abstraction conventional water treatment units are inadequate to remove the turbidity. The water quality index of the river water also shows the detail overview of Alaknanda River water.

Another problem of direct surface water abstraction schemes, especially those relying on springs and streams that are recharged mainly during the monsoon, is that they are drought prone in the event of insufficient monsoon and winter precipitation. This particularly becomes evident in the months of April–June (pre-monsoon) when numerous springs and rain-fed streams dried up due to insufficient recharge from precipitation in the winters (December–February). Decreasing level and availability of groundwater lead to drying up of hand pumps in the mountain areas. The groundwater development in the Himalayan area is leaving very little scope for further development of drinking water wells because of typical hard geology and steep slope of the mountain area. Daily increasing cost of deep pumping well water also has limiting scope in groundwater development.

14.5.2 Sewage Water Management

Towns located near the river stretch are not provided with sewerage facilities at present except Srinagar town, which is also not fully covered by sewage facilities. Most of the population of these towns is settled in a scattered manner in different slope of hills. There are many wastewater drains which meet in Alaknanda River polluting it. Discharge of some of these drains has been calculated by field visit and

Table 14.10 Location of sewage water drains in river stretch

S. No.	Location	Name of Darin	Discharge in MLD
1	Karanprayag	Gurudwara Drain	0.03
2		Bus Stand Drain	0.01
3		Shanti Nagar Drains with spring water drain	0.9
4		BRO Drain	0.04
5		Ward No. 4 Drain	0.04
6	Rudraprayag	Belni Drain	0.01
7		Steel Bridge Drain	0.04
8		Jait Mandi Drain	0.03
9		Punar Nala (Gadhera) + Spring water	4.13
10	Gaucher	Panai (Gadhera) with spring water drain	0.3
11	Srinagar	Balmiki Mandir Drain	3.5
12		Purana Jain Mandir Drain	
13		Kotwali Drain	
14		Mahila Kotwali Drain	
15		Tiwari Mohalla Drain	
16		Agency Mohalla Drain	
Total			9.03

some measured under Ganga Action Plan. The detail discharge of each drain is given in Table 14.10.

Discharges of drains depend upon seasonal variation and floating population. The drainage systems of these towns are very poor and cover only some part of sewage water. In addition to above, newly developing areas do not have any disposal drain, and presently, water seems to be soaked by the soak pits (a pit which is made by mixture of stones and soil so that all the water absorbed by earth). Presently, only 3.5 MLD sewage water is treated within the whole river stretch at Srinagar. Remaining percentage of total 14.8 MLD sewage water is just flowing from drains and soaked by individual soak pits. The system is inadequate to carry the storm water resulting flooding of streets. The solid waste from these towns is collected and carted manually and is dumped at the bank of river, which results in serious health risks and aggravates the pollution load of Alaknanda River. Thus, the sewage of the city is either polluting river or creating health hazard to the community directly.

14.5.3 Higher Capital Costs

Higher cost of construction, operation and maintenance of water production schemes creates a management and functional problems in Himalaya areas. In Table 14.11, the capital costs, which are fixed, and one-time expenses incurred on the purchase of land and equipment are shown (UJS 2013). Surface water abstraction system with a production capacity of 2000 m^3/day at lower part of study area was constructed with total capital cost of INR 28.9 million. The average construction cost of 1 m^3 water production INR 14,450 is calculated. A summary of the construction cost for direct abstraction scheme of water production is presented in Table 14.11.

To overcome higher expenses of construction, operation and maintenance cost, indirect water abstraction water schemes were introduced in the Himalayan area in 2010. The indirect water abstraction schemes abstract around 2040 m^3/day in 20 h was constructed with construction cost INR 4.3 million at study area. The average construction cost of 1 m^3 water is INR 2110 calculated (UJS 2013). After abstraction, the water from indirect water abstraction is disinfected by sodium hypo-chloride at the well for safe delivery of drinking water. A summary of the construction cost for this type of water production is presented in Table 14.12.

Table 14.11 Construction cost of water production capacity 2000 m^3/day surface water-based conventional treatment system in towns

S. No.	Name of component	Cost (million, INR)
1	Treatment plant 2 MLD for 16 h	5.0
2	Clear water sumps MPS 400 KL	0.9
3	Pumps house (8 m*8 m)	1.0
4	Clear water pumping plant 2100 LPM	5.0
5	Transformer for pumping station	2.0
6	Internal electrification	0.2
7	Clear water pumping plant 1500 LPM 480 m head	2.4
8	Raw water pumping plant for surface water abstraction	1.8
9	Electricity line	8.0
10	Centage	2.6
Total		28.9

Table 14.12 Construction costs of two wells of water production capacity 2040 m^3/day riverbank purification methods

S. No.	Capital cost of indirect surface water production system	Cost (million, INR)
1	Drilling and development of monitoring well 125 mm, production well of 300 mm and 200 mm	1.4
2	Boundary wall	0.2
3	Pumping plant and DG set accessories	1.9
4	Chlorine analyzer and automation panel & accessories	0.6
5	Misc. works, resistivity survey, water testing, etc	0.1
6	Electrical connection for pump set	0.2
	Total	4.3

14.5.4 Higher Operation and Maintenance Costs

Operation and maintenance (O&M) costs or operating expenditures are the costs which are associated with the maintenance and operation of a water abstraction schemes, or to the operation of a schemes, component, and piece of equipment or facility. O&M are the total cost of resources used by an institution or organization just to maintain its existence. Based on an average daily direct surface water abstraction and subsequent conventional treatment capacity of around 2000 m^3/day, the average operating cost of drinking water production is calculated at 12.7 INR/m^3 by dividing the total O&M costs by the average daily drinking water production system (Table 14.13).

Based on an average abstraction of around 2040 m^3/day from the indirect surface water abstraction well, the average operating cost of drinking water production is calculated at 1.57 INR/m^3 or by dividing the total O&M costs by the average daily drinking water production (Table 14.14).

Construction, operation and maintenance (O&M) cost analysis shows that riverbank water purification systems are about 10–14 times less expensive than surface water abstraction schemes in the region (Fig. 14.14). In big towns, the construction cost of the bank purification system was 6.8 times less, and operation and maintenance cost were 8.1 times less than the currently operation surface water abstraction schemes.

Table 14.13 O&M cost of water production capacity 2000 m^3/day surface water-based conventional treatment system (UJS 2013)

S. No.	Component of water production system	Annual cost (million, INR)
1	Electricity power	3.8
2	Chemicals for water purification	2.9
3	Operation and maintenance (material)	1.4
4	Office and administration and Personnel costs	1.1
	Total	9.3

Table 14.14 O&M cost of two wells of water production capacity 2040 m^3/day indirect water abstraction methods

S. No.	Component of water production system	Annual cost (million, INR)
1	Electrical power	0.64
2	Chemicals for disinfection	0.20
3	Operation and maintenance (material)	0.04
4	Office and administration and personnel costs	0.30
	Total	1.20

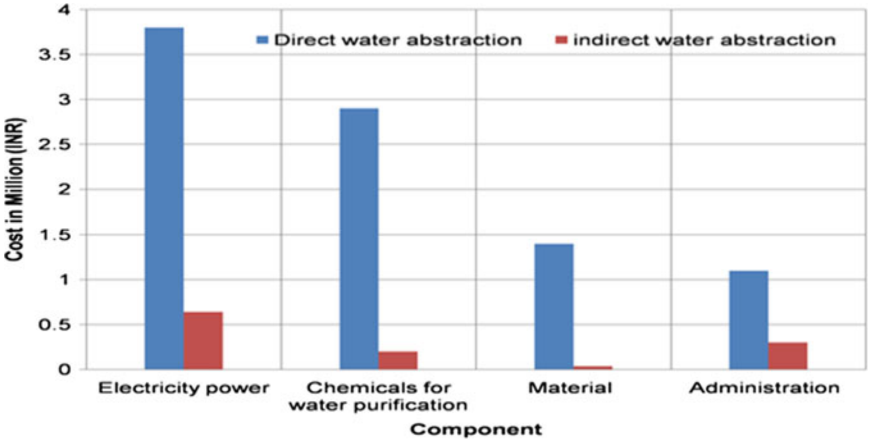

Fig. 14.14 Comparison of O&M cost between direct and indirect surface water abstraction schemes

14.6 Summary

In the river stretch, four types of water resources are available like groundwater, surface water, rainwater and springs water. The total water availability is 50,045 MLD, and total water demand is 88.7 MLD within the Alaknanda River stretch. Out of total water demand, agricultural water demand is 57.5 MLD calculated if all the agricultural land was used for rice and wheat seasonally. Total drinking water demand is 31.4 MLD, and gap is 16.6 MLD calculated for river stretch area. From surface water, 8.4 MLD water is abstracted from directed surface water scheme. In future, 25.1 MLD wastewater can meet the 43.4% agricultural water demand of the area. Currently, only 3.5 MLD wastewater is collected for treatment at Srinagar. Averagely, total rainwater 3538 MLD precipitated at watershed can be utilized by properly making rainwater structures and rainwater harvesting technology for drinking and agricultural purposes. Some hand pumps and wells contaminated by nitrate, pH, iron, etc., can be utilized for agricultural purposes. Due to higher construction, operation and maintenance cost of direct surface water abstraction schemes comparison to indirect surface abstraction schemes, it is required to identify the new water bearing zones for indirect water abstraction to meet the water demand of the local people. Figure 14.15 shows the detail overview of available and demand of water in the river stretch.

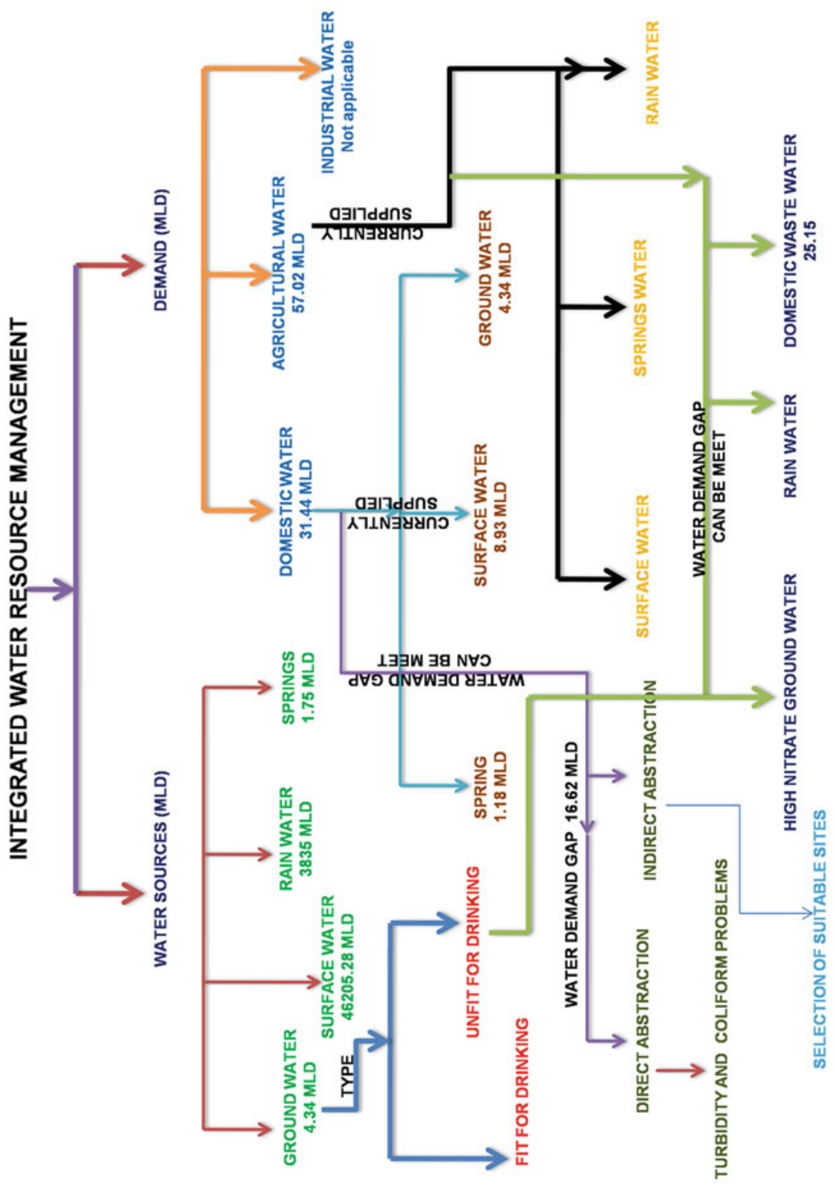

Fig. 14.15 Flowchart of IWRM of the Alaknanda River stretch study area

References

Census of India (2011) Office of the Registrar General and Census Commissioner, India, Ministry of Home Affairs, Government of India. Source: http://censusindia.gov.in and http://www.citypopulation.de/php/india-uttarakhand.php. Accessed 1 Mar 2020

Climate data: www.worldweatheronline.com.Accessed 1 Mar 2020

CGWB, (2012). Bhu-JAl News. Volume 27, No. 1 to 4, Jan to Dec 2012 www.cgwb.gov.in/INCGW/GC%20Negi%20Report.pdf. Accessed 4 Apr 2020

Detail Project report (1994) Srinagar Dam. Source: library IIT Roorkee

Economic Survey of Delhi (2005–2006) Water supply and sewerage. Available. http://delhiplanning.nic.in/Economic%20Survey/ES%202005-06/Chpt/13.pdf

Ground Water Prospects Map (2008) Uttarakhand Space Application Centre. NRSC (ISRO), Department of space, Government of India

Kumar M, Rajwar GS (2011) Grain production of wheat (*Triticum aestivum* L.) and rice (*Oryza sativa* L.) at different altitudes in Garhwal Himalaya, India. Agricultura (Slovenia) 8(1):11–16

Mahajan A, Gupta RD (2009) Integrated nutrient management (INM) in a sustainable rice-wheat cropping system. Springer Science & Business Media

Patro ER, Voltz TJ, Kumar A, Grischek T (2020) Micro-hydropower in drinking water gravity pipelines: a case study in Uttarakhand, India. ISH J Hydraulic Eng 26(3):332–342. https://doi.org/10.1080/09715010.2018.1492977

Patro ER, De Michele C, Avanzi F (2018) Future perspectives of run-of-the-river hydropower and the impact of glaciers' shrinkage: the case of Italian Alps. Appl Energy 231:699–713

Patwal PS (2015) Integrated water resources management of a river stretch using GIS & ground water flow modeling. M.Tech Thesis, Indian Institute of Technology Roorkee (IITR), India

Ronghang M, Kumar P, Mehrotra I (2011) Water quality investigations at four new RBF sites in Uttarakhand. CCRBF-HTWD internal report for phase 2 of DST-WTI project—Development of River Bank Filtration in Hill Regions for Sustainable Solution for Quality and Quantity Problems of Drinking Water in Uttarakhand

Sandhu C, Grischek T, Kumar P, Ray C (2011) Potential for riverbank filtration in India. Clean Technol Environ Policy 13(2):295–316

Sati VP (2008) Natural resource management and food security in the Alaknanda Basin of Garhwal Himalaya, India. ENVIS Bull: Himalayan Ecol 16(2):1–11

UJS (2013) Development of river bank filtration in hill regions for sustainable solutions for quality and quantity problems of drinking water in Uttarakhand. R&D project, internal report, Uttarakhand Jal Sansthan

Chapter 15
Impact of Flooding on Agricultural Crops—An Overview

Shabana Aslam and Saima Aslam

Abstract Water is an important ecological factor for plants and the soil water is a critical factor determining the distributional pattern of plant species on earth. Different plant species are adapted to different degrees of water or moisture availability prevailing in their habitats and are categorized either as xerophytes, mesophytes or hydrophytes. Majority of the wild and crop plants belong to the ecological group mesophytes and are adapted to moderate soil water content. This group of plants performs better under this moderate availability of soil water. Whenever the soil water availability increases to higher degrees during water logging, such plants face the water stress with consequences of decreased growth and survival. Flooding is an environmental stress which negatively influences the growth and biomass production in crop plants. The impact of flooding on growth and survival may be direct on the plant, or it may modify the habitat conditions of the plant and thus bring about its impact on the plants indirectly. Some plants are tolerant to water logging, and in them, the impact of flooding is significantly little as compared to the nontolerant species. The flooding is known to affect and modify the conditions and habitat features of plants as well as directly impacting their survival, growth and reproduction.

Keywords Flooding · Phytotoxins · Crops · Water logging

15.1 Impact of Flooding on Soil Properties

Soil redox potential and Elemental profile: In waterlogged soils, soil pores get completely filled with water, and consequently, the movement of gases through these soil pores is immensely inhibited by their water content, making the path of oxygen diffusion resistant by ten thousand times as that in air (Armstrong et al. 2002).

S. Aslam
Department of Botany, S.P. College, Cluster University, Srinagar, Jammu and Kashmir, India

S. Aslam (✉)
Department of Biotechnology, Baba Ghulam Shah Badshah University, Rajouri, Jammu and Kashmir, India
e-mail: saima@bgsbu.ac.in

P. Shukla et al. (eds.), *Environmental Processes and Management*, Water Science and Technology Library 120, https://doi.org/10.1007/978-3-031-20208-7_15

Under such circumstances, the little and slow influx of oxygen to roots does not match the demand or need of the growing roots, resulting in insufficient and limited availability of oxygen to the submerged roots. This inadequate or slowing oxygen supply to roots is the primary cause of root injury as well as of shoots which rely on roots (Vartapetian and Jackson 1997). The dissolved oxygen concentration in flood water is little, and this little amount gets consumed rapidly during the initial event of flooding by both plant roots and aerobic microorganisms. This way roots are exposed to complete absence of oxygen and thus suffer from anoxia (Gambrell and Patrick 1978). Besides anoxia, the flooding also hampers the outward diffusion as well as oxidative breakdown of important gases like ethylene (Arshad and Frankenberger 1990) and carbon dioxide that are produced by microorganisms and roots. These accumulated gases are known to inhibit the growth or damage the roots of many crop plants such as soyabean (Boru et al. 2003).

Since oxygen molecule acts as the ultimate acceptor of electrons in cellular respiration (Gibbs and Greenway 2003), its absence shuts off the oxidative phosphorylation in plant root cells (Moller 2001) causing huge reduction in ATP content of root cells. This inactivation of oxidative phosphorylation owing to anoxia results in reduced ATP: ADP ratio (Drew et al. 2000) as roots switch to anaerobic or fermentative pathways for energy generation. The low generation and supply of ATP in root cells do not match their ATP demand resulting in arrest of vital processes and eventually causing the death of root cells, root tips and root. The low supply of ATP also negatively impacts membrane integrity (Rawyler et al. 1999), and when this membrane organization is compromised, it causes irrecoverable damage to cells leading to their death (Zhang and Davies 1987). Absence of oxygen in root cells for non-respiratory reactions such as synthesis of important structural lipids used in membrane formation is also accounted as reason leading to cell death (Vartapetian et al. 1978). Roots in anoxia, which are commonly referred to as anaerobic roots, may also die because of accumulation of products of their fermentation metabolism (Gerendás et al. 2002). The acidification of cytoplasm and vacuole owing to accumulation of protons, acetaldehydes, etc., as a result of fermentative metabolism are thought to trigger early death of root cells and root tips. Long-standing water logging damages crops and incurs huge economic losses as it initially results in root death which in most crops is followed by shoot death and thus destruction of the whole crop.

Water logging causes phytotoxin mediated root death: It has been seen that even if root tips may survive anoxia of their own, it is the surrounding soil biochemistry which may injure or kill them (Ponnamperuma 1972). Flooding or water logging causes the conversion of an oxidizing soil environment into a reducing environment, with soil redox potential values sharply decreasing from +800 mV which can go up to −300 mV. A soil with positive redox potential of 800 mV has an aerobic environment with oxygen available for aerobic respiration. Once water logging sets in, the availability of oxygen decreases, and as soon as free oxygen depletes completely, facultative anaerobic microorganisms start using nutrient ions such as nitrates as electron acceptors in respiration as alternatives to oxygen. This way nitrates are reduced to nitrite and nitrous oxides, leading to release of molecular nitrogen, process referred to as denitrification. This way nitrates are made unavailable for roots. As the soil environment becomes more strongly reducing, obligate anaerobes use oxides of manganese MnO^{4+} and iron Fe^{3+} as electron acceptors reducing them to more soluble Mn^{2+} and Fe^{2+} ions (Laanbroek 1990). This causes a build up of these soluble Mn and Fe cations in the soil often to toxic concentrations (Marschner 1990), which enter the roots and impact the activity of the enzymes and also damage the membrane systems in root cells. With persistence of water logging stress and further reduction in the value of soil redox potential, anaerobes use sulphates and reduce them to hydrogen sulphide (Ponnamperuma 1972) which is a very toxic for respiratory enzymes and non-respiratory oxidases. The formation of methane from carbon dioxide and organic acids occurs on further depletion of soil redox potential by the activity of methanogenic bacteria.

Uptake of nutrients: Flooding is known to impact plant nutrient uptake negatively. The reduced or non-availability of oxygen for roots tremendously reduces the uptake of nutrients. The endogenous concentrations of nutrients drop to low concentrations in different parts of the plant, thereby drastically affecting the plant growth (Ashraf et al. 2011). Because of water logging, crop plants are known to witness acute deficiencies of many essential nutrients vital for plant growth and development (Smethurst et al. 2005). Hypoxia in the rhizosphere is known to cause a significant reduction in ion selectivity, viz. K+ /Na+ uptake, hampering the flux of K+ to the shoots (Armstrong et al. 2002) besides making membranes less permeable to Na^{+} ions (Barrett-Lennard et al. 1999). In canola, Boem et al. (1996) found that water logging results in reduced ability of roots to absorb elements such as N, P, K and calcium. In maize also, the reduced endogenous levels of critical elements (N, P, K, Ca and Mg) were found to be associated with water logging (Atwell and Steer 1990); the latter is known to bring about adverse effects in crops through reduced elemental concentrations (Sharma and Swarup 1989; Smethurst et al. 2005). In wheat also, water logging brought about decline in tissue levels of P, K and Mg in the shoots (Stieger and Feller 1994). Studies on flooding stress of *Medicago sativa* showed that in leaf and root, there is a significant decrease in the nutrient composition of P, K, B, Cu, Ca, Mg and Zn (Smethurst et al. 2005). The reduced concentrations of N, P, K, Ca and Mg hamper many metabolic processes including efficiency of PSII, which impair plant growth and crop yield (Smethurst et al. 2005). The impeded nutrient uptake in crop plants results in deficiency symptoms such as chlorosis, early senescence and retarded growth which are the adverse effects of elemental efficiencies such as that of N, Mg, Ca, P and K (Kaur et al. 2017).

Water logging affects soil pH: Flooding or water logging is also found to be associated with change in soil pH which influences solubility and availability of plant nutrients. Because of water logging, the pH of soils changes towards neutrality, that limits the solubility and hence availability of many nutrients for plant uptake, thereby impacting plant life negatively. This changed soil chemical property also contributes to diminished plant growth and performance. In flooded soils, changes in redox potential values are also found to be associated with change in soil pH (Kögel-Knabner et al. 2010). In acidic soils, pH increases after flooding on account of consumption of protons while as in alkali soils, flooding causes a decrease in pH because of carbon dioxide build up which is known to reduce the alkalinity (Sahrawat 2005). In response to flooding, the change in soil reaction or soil pH may take place in days to weeks, the duration of change being dictated by an array of factors such as soil microbial population, temperature and other allied physical and chemical properties of soil (Kongchum 2005). According to the Nernst equation, a change of 59 mV in the redox potential of soil is accompanied by one-unit change in pH (Kögel-Knabner et al. 2010). Some studies have shown an increase in pH near soil surface after water logging (Kaur 2016). Besides redox potential and soil pH, water logging also brings a change in the soil temperature. Some studies have shown that water logging brings about an increase in soil temperatures (Kaur 2016; Unger et al. 2009). Soil temperature is an important soil property which besides rate of reactions influences many processes in the roots and rhizosphere. The change in soil pH, soil redox potential and soil temperature is known to influence solubility and availability of plant nutrients, making many nutrients non-available for uptake such as nitrogen which then hampers plant metabolism, chlorophyll synthesis, carbon assimilation, crop growth, yield and survival of plants negatively.

Plant metabolism-shift to anaerobiosis: Soil water logging causes hypoxia which progressively and ultimately leads to anoxia. Under these circumstances, aerobic respiration is compromised, oxidative phosphorylation is drastically reduced, and the plants switch over to anaerobic mode of respiration for energy needs. The plants first switch over to lactic acid formation and then to alcohol formation. The activation of alcohol dehydrogenase enzyme comes in the backdrop of increased formation of lactic acid which acidifies the cell protoplasm. Thus, in order to prevent acidosis which causes necrosis or cell death, the acid fermentation shifts to alcoholic fermentation which helps maintain cell pH and allows cell survival. Under anoxia, the respiratory rate of roots is very low and the availability of energy or ATP is very little; this decreases the metabolic activity of roots leading to reduced root and plant growth.

Water logging induces change in morphological and anatomical features: Flooding or water stress has also been known to bring about many anatomical and morphological changes in the plants. These include development of aerenchyma, suberized epidermis, adventitious roots, hypertrophied lenticels, etc. (Yamamoto et al. 1995). An important change induced in root cortex of plants due to water logging is the development of aerenchyma in it (Arber 1920; Armstrong 1979; Crawford 1982; Jackson 1984; Justin and Armstrong 1987; Konings and Verschuren 1980; Sculthorpe 1967). The formation of aerenchyma is conceived to be an important anatomical modification which helps plants adapt to flooding or water stress (Laan et al. 1989). Under flooding stress in many woody species, an important anatomical change is hypertrophied lenticels. Although lenticels are believed to have role in gaseous exchange, downward diffusion of oxygen during flooding, but, a renewed insight considers them linked to water logging tolerance highlighting their role in water uptake in circumstances of a nonfunctional root system and thus maintenance of water homeostasis of the plant during flooding. They do take over the function of water intake for shoots when roots are decaying and not in action. Furthermore, hypertrophied lenticels occur in more numbers in underwater part of the plant than above water which strengthens the view of their involvement in water uptake and maintenance of plant water homeostasis under waterlogged conditions.

Formation of adventitious roots is conceived to be one more important response of plants to water logging. This is a very important morphological adaptation of plants to water logging as these specialized roots with good amount of aerenchyma help the plant to absorb water and minerals when the absorptive ability of the main root is drastically compromised. The formation of adventitious roots is commonly believed to lend water logging tolerance to plants which bear them (Kozlowski 1997; Malik et al. 2001; Parelle et al. 2006; Dat et al. 2006).

Flooding stress and Diseases: In addition to inducing metabolic stress, flooding may also enhance the occurrence of soil-borne pathogens and thus increases the susceptibility of plants to diseases (Yanar et al. 1997). The poor metabolic or energy status of roots renders them less resistant to pathogen attacks. Water-borne pests such as insects, fungi and bacteria easily damage roots of stressed plants (Urban et al. 2015). Pathogens such as *Pythium* (damping off), *Phytophthora* (wilting) and *Pseudomonas putida* are known for their damaging effects on roots of vegetable crops, trees and other plants under waterlogged conditions (Walker 1991). The symptoms of diseased roots include their discoloration and rotting which causes premature death of the plants. The diseased roots also are not able to uptake nutrients efficiently and perform other functions normally. Pathogens such as *Sclerophthora macrospora* causing crazy top or downy mildew, *Cercospora zeae-maydis* causing grey leaf spot in maize, *Ustilago maydis* causing common smut in corn, *Fusarium graminearum* causing blight in wheat and *Fusarium virguliforme* causing sudden death syndrome in soybeans are also known to damage crops during flooding.

Water logging affects plant photosynthesis: Water logging is known to affect plant photosynthesis negatively, decreasing photosynthetic capacity of plants. There are multiple effects associated with flooding which bring about decrease in photosynthesis. Water logging induces stomatal closure, reduction in transpiration, which impacts gaseous exchange, reduction in internal carbon dioxide concentration for carboxylation reaction and thus reduction in photosynthesis. The water logging is also known to decrease leaf area and chlorophyll content of leaves, both of which affect photosynthesis negatively, reducing photosynthesis and rate of photosynthesis. Water logging is also known to damage the PSII which results in consequent drastic decrease and inhibition of photosynthesis. Water logging also causes a change in the chloroplast form, damage to thylakoid membranes and destruction of chloroplast structure. This is the reason why water logging results in bringing down the photosynthetic capacity of leaves, with consequent decrease in overall growth, survival and yield of plants. In many studies, it has been found that water logging results in damage to the integrity of membrane systems of mesophyll cells, damage to mitochondria, with resultant death of mesophyll cells and reduction of photosynthetic capacity of leaves.

Flooding and Phytotoxins: In waterlogged soils with depleted oxygen or lack of oxygen, anaerobic bacterial activity results in increased concentrations of elemental phytotoxins such as Fe, Mn and H2S and organic phytotoxins like butyric acid, acetic acid and propionic acid especially in acidic soils. These phytotoxins are very harmful and impede root growth as well as cause root death. This way also flooding or water logging modifies plant environment parameters which eventually reduces plant growth, plant productivity and survival.

Submergence reduces plant survival: Most of the terrestrial plants, both wild and crop plants, are highly sensitive or intolerant to submergence. The submergence of aerial parts of the plant severely influences and reduces plant photosynthesis and respiration as the diffusion rates of gases and plant gas exchange are drastically reduced. The muddy or turbid waters with little or no transparency further block the light availability which further adds to the reduction in photosynthesis (Vervuren et al. 2003). These impaired physiological processes result in carbon and energy crisis with resultant reduction in growth and survival of the plant.

Submergence and Oxidative stress in plants: One more negative impact of inundation on crop plants is the generation of reactive oxygen species (ROS) that are known to perturb numerous metabolic processes in cells (Ashraf 2009; Ashraf et al. 2010). Hydrogen peroxide (H_2O_2), superoxide (O^2-) and hydroxyl radicals (OH) are some of the lethal reactive oxygen species generated in plants, and these reactive oxygen species (ROS) being highly reactive trigger damage to a number of biochemical components in cells such as lipids, proteins, DNA and pigments (Ashraf 2009; Ashraf and Akram 2009). In plants, reactive oxygen species are produced under non-stressed conditions as well but their rates of production are much less and are thus easily neutralized by the antioxidant enzyme system of the plants. But under stress full conditions such as flooding, their rate of generation is much higher than rate of their neutralization with resultant elevated concentration levels that prove damaging to the cellular components and cellular processes such as photosynthesis and PSII. Elevated levels of H_2O_2 in plants are known to inhibit Calvin cycle (Kaiser 1976). As water levels after submergence come down, the plant tissues are again exposed to high light environment and oxygen levels which compound the submergence mediated damage. This exposure to high oxygen concentration and high light intensity results in elevation of oxidative stress through a surge in the production of reactive oxygen species. This post-submergence ROS burst causes damage to the photosynthetic apparatus, membranes, DNA and PSII, thereby causing leaf senescence and cell death.

Flooding tolerance: Although majority of plants are sensitive to water logging and submergence, there are many plants which have adaptations to survive water logging or submergence. These plants are either having constitutive adaptations or they can develop these features once they are flooded. There is an array of biochemical, molecular, morphological and anatomical adaptations which lend tolerance to flood tolerant species. It is the outcome of these adaptations that there are plant species which grow and can occupy wetlands. These adaptations include formation of aerenchyma, avoidance of oxygen deficiency, anoxia tolerance, pressurized gas transport from shoot to root, ability to inhibit or reduce oxidative damage during re-aeration, formation of adventitious roots, etc. In plants like rice, submergence is avoided by elongation of stem, leaves and internodes, and this elongation is mediated by hormones such as ethylene and Gibberellic acid. This is commonly referred to as escape strategy for submergence tolerance. The other strategy is called as quiescent strategy where in a submerged plant species is able to tolerate submergence by cutting down energy consumptions, saving energy and remaining quiescent under water (Bailey-Serres and Voesenek 2008). The formation of leaf gas films is yet another important feature that attracts attention owing to its marked role in submergence tolerance in rice (Colmer and Voesenek 2009). The gas films help improve gaseous exchange between submerged shoots and the surrounding water by widening the water–gas interface around the leaves. This way both photosynthesis and internal aeration of roots are maintained. If these gas films are disturbed or removed, both photosynthesis and internal aeration of roots are compromised (Pedersen et al. 2009).

Flooding which includes water logging and submergence is the abiotic stress that is also known to affect species distribution and composition in many plant communities globally (Jackson and Colmer 2005). Species with adaptations for such stresses thrive well in wetlands and flood-prone areas worldwide.

References

Arber A, Arber AR (1920) Water plants: a study of aquatic angiosperms. University Press

Armstrong VV (1979) Aeration in higher plants. Adv Bot Res 7:225–332

Armstrong W, Drew MC (2002) Root growth and metabolism under oxygen deficiency. In: Waisel Y, Eshel A, Kafkafi U (eds) Plant roots: the hidden half, 3rd edn. Marcel Dekker, New York, pp 729–761

Arshad M, Frankenberger WT (1990) Production and stability of ethylene in soil. Biol Fertil Soils 10:29–34

Ashraf M (2009) Biotechnological approach of improving plant salt tolerance using antioxidants as markers. Biotechnol Adv 27(1):84–93

Ashraf MA, Ahmad MSA, Ashraf M, Al-Qurainy F, Ashraf MY (2011) Alleviation of waterlogging stress in upland cotton (Gossypium hirsutum L.) by exogenous application of potassium in soil and as a foliar spray. Crop Pasture Sci 62(1):25–38

Ashraf M, Akram NA (2009) Improving salinity tolerance of plants through conventional breeding and genetic engineering: an analytical comparison. Biotechnol Adv 27(6):744–752

Ashraf MA, Ashraf MUHAMMAD, Ali Q (2010) Response of two genetically diverse wheat cultivars to salt stress at different growth stages: leaf lipid peroxidation and phenolic contents. Pak J Bot 42(1):559–565

Atwell BJ, Steer BT (1990) The effect of oxygen deficiency on uptake and distribution of nutrients in maize plants. Plant and Soil 122(1):1–8

Bailey-Serres J, Voesenek LACJ (2008) Flooding stress: acclimations and genetic diversity. Annu Rev Plant Biol 59:313–319

Barrett-Lennard EG, Van Ratingen P, Mathie MH (1999) The developing pattern of damage in wheat (Triticum aestivum L.) due to the combined stresses of salinity and hypoxia: experiments under controlled conditions suggest a methodology for plant selection. Aust J Agric Res 50(2):129–136

Boem FHG, Lavado RS, Porcelli CA (1996) Note on the effects of winter and spring waterlogging on growth, chemical composition and yield of rapeseed. Field Crops Res 47(2-3):175–179

Boru G, van Ginkel M, Trethowan RM, Boersma L, Kronstad WE (2003) Oxygen use from solution by wheat genotypes differing in tolerance to waterlogging. Euphytica 132:151–158

Colmer TD, Voesenek LACJ (2009) Flooding tolerance: suites of plant traits in variable environments. Funct Plant Biol 36(8):665–681

Crawford RMM (1982) Physiological responses to flooding. In: Lange OL, Nobel PS, Osmond CB, Ziegler H (eds) Encyclopedia of plant physiology, vol J2B. Springer, Berlin, pp 453–477
Dat J, Folzer H, Parent C et al (2006) Hypoxia stress: current understanding and perspectives. In: Teixeira da Silva JA (ed) Floriculture, ornamental and plant biotechnology. Advances and tropical issues, vol 3. Global science books. Isleworth, United Kingdom, p 664–674
Drew MC, He CJ, Morgan PW (2000) Programmed cell death and aerenchyma formation in roots. Trends Plant Sci 5:123–127
Gambrell RP, Patrick WH (1978) Chemical and microbiological properties of anaerobic soils and sediments. In: Hook DD, Crawford RMM (eds) Plant life in Anaerobic environments, Ann Arbor Sci. Publ., Ann Arbor, MI, U.S.A, pp 375–423
Gerendás J, Ratcliffe RG (2002) Root pH control. In: Waisel Y, Eshel A, Kafkafi U (eds) Plant roots the hidden half. Marcel Deker Inc., New York, pp 553–570
Gibbs J, Greenway H (2003) Review: Mechanisms of anoxia tolerance in plants. I. Growth, survival and anaerobic catabolism. Funct Plant Biol 30:1–47
Jackson MB (1984) Effects of flooding on growth and metabolism of herbaceous plants. Flooding and plant growth 47–128
Jackson MB, Colmer TD (2005) Response and adaptation by plants to flooding stress. Annals Botany 96(4): 501–5. https://doi.org/10.1093/aob/mci205
Justin SHFW, Armstrong W (1987) The anatomical characteristics of roots and plant response to soil flooding. New Phvtologist 106:465–495
Kaiser W (1976) The effect of hydrogen peroxide on CO2 fixation of isolated intact chloroplasts. Biochim Biophys Acta 440(3):476–482
Kaur G (2016) Use of nitrogen fertilizer sources to enhance tolerance and recovery of corn hybrids to excessive soil moisture (Doctoral dissertation). University of Missouri-Columbia, Columbia, MS
Kaur G, Zurweller BA, Nelson KA, Motavalli PP, Dudenhoeffer CJ (2017) Soil waterlogging and nitrogen fertilizer management effects on corn and soybean yields. Agron J 109:1–10
Kögel-Knabner I, Amelung W, Cao Z, Fiedler S, Frenzel P, Jahn R, Kalbitz K, Kölbl A, Schloter M (2010) Biogeochemistry of paddy soils. Geoderma 157: 1–14
Kongchum M (2005) Effect of plant residue and water management practices on soil redox chemistry, methane emission, and rice productivity (Doctoral dissertation). Khon Kaen University, Khon Kaen, Thailand
Konings H, Verschuren G (1980) Form ation of aerenchyma in roots of Zea mays in aerated solutions, and its relation to nutrient supply. Physiol Plant 49:265–270
Kozlowski TT (1997) Responses to woody plants to flooding and salinity. In: Tree physiology, Monograph No. 1, Victoria. Heron Publishing, Canada, p 29
Laan P, Smolders A, Blom CWPM, Armstrong VV (1989) The relative roles of internal aeration, radial oxygen losses, iron exclusion and nutrient balance in flood-tolerance of Rumex species. Acta Botanica Neerlandica 38:131–145
Laanbroek HJ (1990) Bacterial cycling of minerals that affect plant growth in waterlogged soils: a review. Aquat Bot 38(1):109–125
Malik AI, Colmer TD, Lamber H et al (2001) Changes in physiological and morphological traits of roots and shoots of wheat in response to different depths of waterlogging. Aust J Plant Physiol 28(11):1121–1131
Marschner H (1991) Mechanisms of adaptation of plants to acid soils. In: Wright RJ et al (eds) Plant–soil interactions at low pH. Proceedings of the second international symposium on plant–soil interactions at low pH. Kluwer Academic Publisher, Beckley, West Virginia, USA, p 683–702
Moller IM (2001) Plant mitochondria and oxidative stress: Electron transport, NADPH turnover, and metabolism of reactive oxygen species. Annu Rev Plant Physiol Plant Mol Biol 52:561–591
Parelle J, Brendel O, Bodenes C et al (2006) Differences in morphological and physiological responses to waterlogging between two sympatric oak species (Quercus petraea [Matt.] Liebl., Quercus robur L.). Ann Forest Sci 63(8):849–859

Pedersen O, Rich SM, Colmer TD (2009) Surviving floods: leaf gas films improve O_2 and CO_2 exchange, root aeration, and growth of completely submerged rice. Plant J 58:147–156
Ponnamperuma FN (1972) The chemistry of submerged soil. Adv Agron 24:29–95
Rawyler A, Pavelic D, Gianinazzi C, Oberson J, Braendle R (1999) Membrane lipid integrity relies on a threshold of ATP production rate in potato cell cultures submitted to anoxia. Plant Physiol 120(1):293–300
Sahrawat KÁ (2005) Iron toxicity in wetland rice and the role of other nutrients. J Plant Nutr 27(8):1471–1504
Sculthorpe CD (1967) Biology of aquatic vascular plants
Sharma DP, Swarup A (1989) Effect of short-term waterlogging on growth, yield and nutrient composition of wheat in alkaline soils. J Agric Sci 112(2):191–197
Smethurst CF, Garnett T, Shabala S (2005) Nutritional and chlorophyll fluorescence responses of lucerne (Medicago sativa) to waterlogging and subsequent recovery. Plant and Soil 270(1):31–45
Stieger PA, Feller U (1994) Nutrient accumulation and translocation in maturing wheat plants grown on waterlogged soil. Plant and Soil 160(1):87–95
Unger IM, Motavalli PP, Muzika R (2009) Changes in soil chemical properties with flooding: a field laboratory approach. Agr Ecosyst Environ 131:105–110
Urban DW, Roberts MJ, Schlenker W, Lobell DB (2015) The effects of extremely wet planting conditions on maize and soybean yields. Climatic Change 130
Vartapetian BB, Jackson MB (1997) Plant adaptations to anaerobic stress. Ann Bot 79:3–20
Vartapetian BB, Mazliak P, Lance C (1978) Lipid biosynthesis in rice coleoptiles grown in the presence or the absence of oxygen. Plant Sci Lett 13:321–328
Vervuren PJA, Blom CWPM, De Kroon H (2003) Extreme flooding events on the Rhine and the survival and distribution of riparian plant species. J Ecol 91:135–146
Walker GE (1991) Chemical, physical and biological-control of carrot seedling diseases. Plant Soil 136:31–39
Yamamoto F, Sakata T, Terazawa K (1995) Physiological, morphological and anatomical response of Fraxin mandshurica seedlings to flooding. Tree Physiol 15(11):713–719
Yanar Y, Lipps PE, Deep IW (1997) Effect of soil saturation, duration and water content on root rot of maize caused by Pythium arrhenomanes. Plant Dis 81:475–480
Zhang J, Davies WJ (1987) ABA in roots and leaves of flooded pea plants. J Exp Bot 38(4):649–659

Chapter 16
Study of Rising Surface Water Levels on Land Submergence and Groundwater

Praveen Kumar, Prabhakar Shukla, and Raj Mohan Singh

Abstract Floods are most commonly caused by severe rains when natural water-courses fail to handle the excess water. They are not necessarily produced by excessive rainfall. There are many factors that can lead to floods, including storm surges associated with tropical cyclones, tsunamis, or high tides associated with higher-than-normal river levels, and especially in coastal areas, floods can occur due to a storm surge from a tropical cyclone, a tsunami, or a high tide and high river levels. Even in dry weather, dam failure, such as that induced by an earthquake, will result in downstream flooding. Other elements that might cause flooding include rainfall volume, intensity, and duration, spatial distribution; the capacity of a stream network to convey runoff; and catchment and weather conditions previous to a rainfall event, terrain, ground cover, and tidal forces. So for potential flooding sites, drainage network information must be known. The rivers, canals, water streams, etc., make a great network of drainage system. For any site, drainage network can be extracted with the elevation information. The elevation information is contained in DEM (Digital Elevation Data) data which you different sources and applying hydrological analysis, we can extract drainage network. Using a digital elevation model, a hydrological analysis was performed to determine the slope, flow direction, flow accumulation, and drainage network. The purpose of this study is to examine the boundaries of the Lucknow Municipal Corporation (LMC) in order to construct and test a GIS-based flood inundation map. DEM and drainage network information is further employed to assess the potential flooding sites in the Lucknow city, and the potential flooding sites are investigated starting from 107 to 122 m with an increment at 1 m interval. The results of this study show that at 110 msl total potential flooding area is approximately 23.75 km^2 and at 122 msl total potential flooding area is 133.35 km^2 are estimated.

P. Kumar (✉) · R. M. Singh
Motilal Nehru National Institute of Technology Allahabad, Prayagraj, India
e-mail: praveenkr@mnnit.ac.in

R. M. Singh
e-mail: rajm@mnnit.ac.in

P. Shukla
GIS and Water Resources Management, Department of Civil Engineering, IIT Delhi, Delhi, India

P. Shukla et al. (eds.), *Environmental Processes and Management*, Water Science and Technology Library 120, https://doi.org/10.1007/978-3-031-20208-7_16

Keywords Lucknow municipal corporation (LMC) · Flood inundation map · GIS

Abbreviations

DEM	Digital Elevation Model
LMC	Lucknow Municipal Corporation
UNDRO	United Nations Disaster Relief Co-ordinator
USGS	United State Geological Survey
GIS	Geographic Information System
CDP	City Development Plan
ASTER	Advance Spaceborne Thermal Emission and Reflection Radiometer
ESRI	Environmental Systems Research Institute
km^2	Square Kilometre
GWRA	Groundwater Resources Assessment
IMD	Indian Meteorological Department
INDIA-WARIS	Web-based Water Resources Information System

16.1 Introduction

In metropolitan area, where impermeable materials represent a huge portion of the ground surface, rapid runoff and reduced infiltration result in flooding that is not related to a floodplain. Riverine floods and flash flooding along floodplains have always attracted people's interest, while flooding in cities has not (e.g. UNDRO 1978; Ward 1978). As the severity and frequency of flood disasters have increased, an increasing global awareness of the need to minimize flood-related casualties and economic losses has emerged. One of the most crucial aspects of flood mitigation is the identification of flood-prone regions. Authorities can better design flood mitigation strategies by predicting vulnerable floodplains and high-risk flash flood-prone areas (Sarhadi et al. 2012). In order for modelling to be accurate, comprehensive elevation data is required; however, high-resolution elevation data is often difficult to obtain and is rarely available, and thus, only publicly available data sources (such as USGS DEMs and contour maps) can be utilized (Chen et al. 2009). During the monsoon season in India, major rivers overflow causing floods in various regions of the country. Collecting adequate flood inundation extent information is a time-consuming and difficult task, emphasizing the need for an automatic flood inundation mapping methodology.

Bates and De Roo (2000) developed a model for simulating flood inundation. The model is used to reproduce a significant flood incident that occurred in January 1995 over a 35 km stretch of Meuse River in the Netherlands using only available information. The best fit simulation of the model created in this study performs both the simpler and more advanced process visualizations, accurately predicting 81.9% of inundated and non-inundated regions.

In a GIS environment, Sun et al. (2018) and Sahoo and Sreeja (2015) developed strategic flood risk assessment. In their study, they make predictions on how floods caused by tides will wreak havoc on the area. As in the first case, GIS allowed them to create flood inundation maps, helping to build embankments at strategic locations near the sea to mitigate the effects of flooding.

Jian et al. (2009) created a GIS-based urban flood inundation model that consists of two parts: storm–runoff model and an inundation model. The outcome of the storm–runoff model, which comprised cumulative surface runoff, was fed into the inundation model.

Fosu et al. (2012) discussed river inundation and hazard mapping using GIS and HEC-RAS model. By superimposing the flooded region onto topographic maps, the affected buildings were identified. They arrived at the conclusion that high water depths occur along the main channel and gradually extend to the floodplain.

The goal of this study is to create a GIS-based flood inundation mapping model for the LMC region. DEM and drainage network information is further employed to assess the potential flooding sites in the Lucknow city, and the potential flooding sites are investigated.

16.2 Study Area

The study area comprises Lucknow city in Uttar Pradesh. This is the second largest city of the state after Kanpur. The city is located at a height of 123 m (404 feet) above sea level. The district of Lucknow is 2528 km^2 in size and is located at (26.8467°N, 80.9462°E). It is situated on the northwestern side of the Gomti River, with Barabanki and Unnao on the east, Raebareli on the south, and Sitapur on the north. Figure 16.1 depicts the study area geographical location (Lucknow city).

The city is divided into the Trans-Gomti and Cis-Gomti regions by the Gomti River, which meanders through the city. Trans-Gomti part includes the zone numbers 3 and 4, and the Cis-Gomti parts include the zone numbers 1, 2, 5, and 6. Lucknow city lies in the seismic zone III. The climate of Lucknow is subtropical humid. The rainy season occurs usually from June to September, when the south-west monsoon winds bring an average rainfall of 896.2 mm (35.28 in). The maximum temperature in the winter is around 25 °C (77 °F), while the minimum is between 2 and 3 °C. From late December to late January, fog is extremely common. Summers are extremely hot, with temperatures reaching at 40–45 °C. In Fig. 16.2, zones are identified in the LMC boundary map.

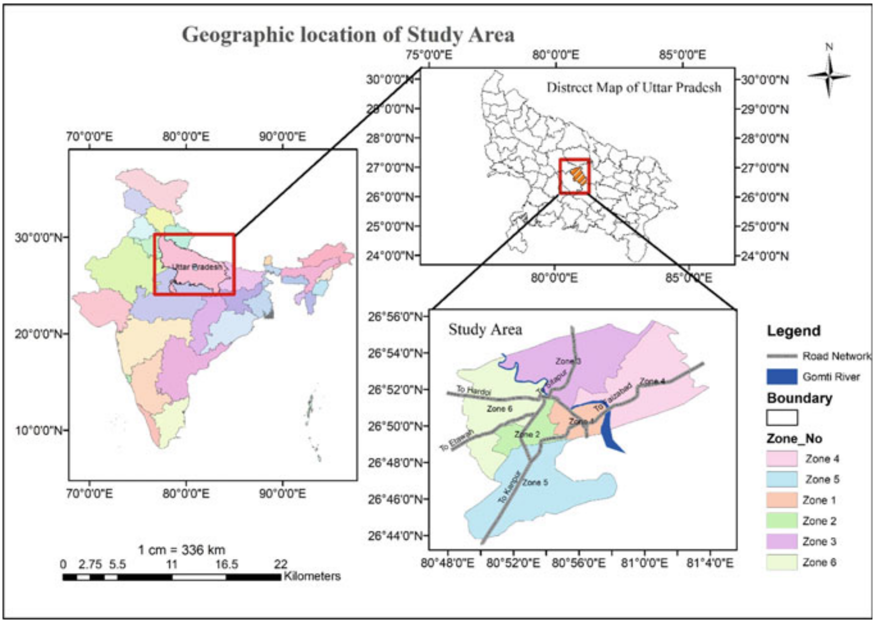

Fig. 16.1 Geographical location of the study area

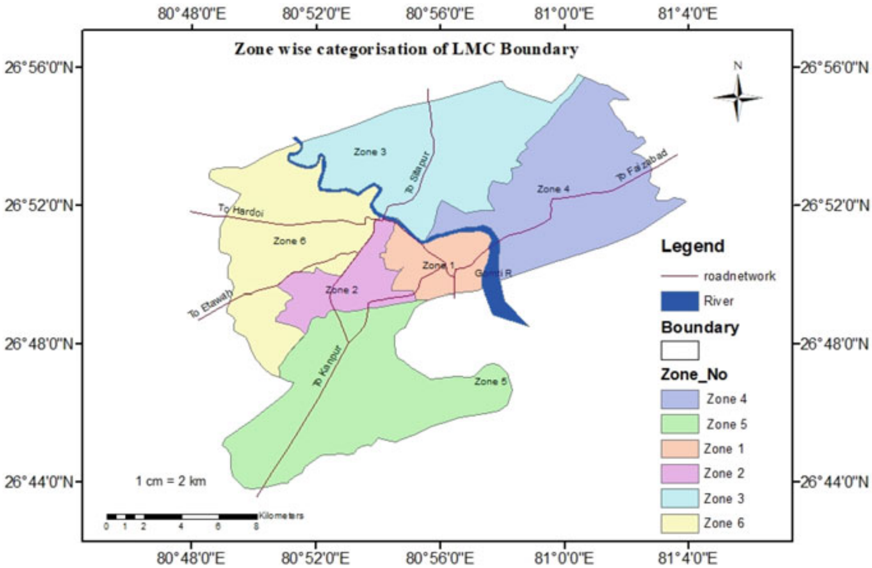

Fig. 16.2 Zone-wise categorization of LMC boundary

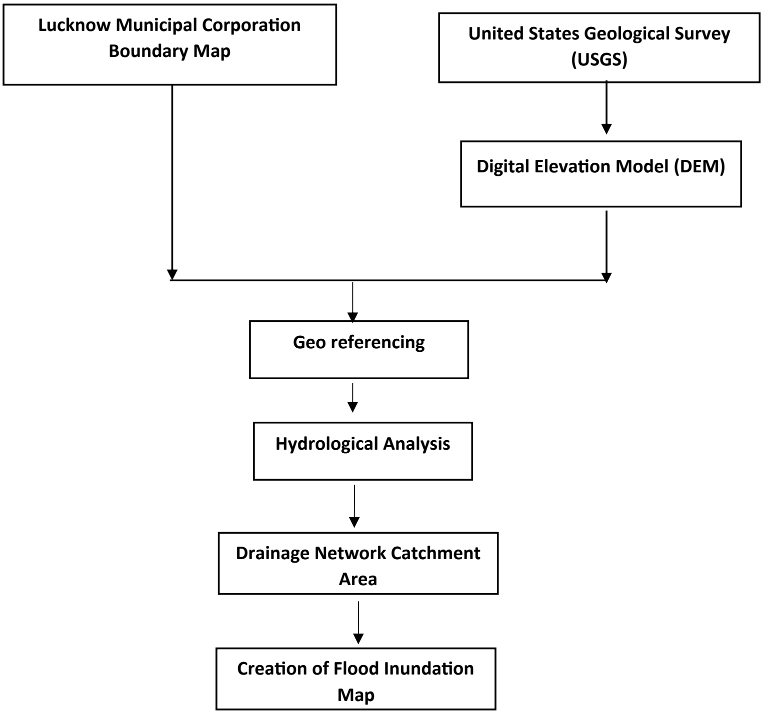

Fig. 16.3 Flow chart of the methodology adopted

16.3 Methodology

The flow diagram of developed methods for extracting the drainage network and drainage point is shown in Fig. 16.3. It consists of data gathering, data preparation, and data analysis. A variety of digital information was collected from several sources, including the LMC boundary map and USGS ASTER data at 30 m resolution (*United States Geological Survey*).

16.4 Hydrological Analysis

16.4.1 About Terrain Preprocessing

Terrain preprocessing is used to do a preliminary study of the terrain and prepare the data for future processing. For terrain preprocessing, a digital elevation model (DEM) of the research region is required: A DEM is a grid in which each cell is given the average elevation for the area it represents. ESRI GRID format is required for the DEM.

Potential difficulties with the terrain representation can be discovered throughout the processing, avoiding DEM mistakes from spreading to later stages of the research. An effective preprocessing signifies that the underlying DEM is free of significant problems that will obstruct further analysis.

16.4.2 Data Management—Terrain Preprocessing

The input/output to the tools is managed by Arc Hydro using tags that are automatically assigned to the selected inputs and outputs by the functions. A tag can be used as both an input and an output by different functions. The "Flow Direction Grid" tag, for example, is a Flow Direction output and a Flow Accumulation input.

A global view of tags assignments for each menu in the current Data Frame is provided by the Data Management function in the Terrain Preprocessing menu. The tags can also be assigned, reassigned, or reset using this function. By selecting "Null" as the matching layer, a tag can be reset. When a reset tag is used as an output, the function displays the tag's default layer name to the user. The XML file specifies the default name, which can be changed.

There is a list of different Hydrological Analysis Processes that all done here for hydrological analysis.

Operation name	File name	File needed
Fill sink	Fil (GRID format)	DEM (USGS DEM data)
Flow direction	Fdr (GRID format)	Fil (GRID format)
Flow accumulation	Fac (GRID format)	Fdr (GRID format)
Stream definition	Str (GRID format)	Fac (GRID format)
Stream segmentation	StrLink (GRID format)	Fdr (GRID format) Str (GRID format)
Catchment grid delineation	Cat (GRID format)	Fdr (GRID format) StrLnk (GRID format)
Catchment polygon processing	Catchment (feature class)	Cat (GRID format)
Drainage line processing	DrainageLine (feature class)	Cat (GRID format) Fdr (GRID format)
Adjustment catchment processing	Adjust catchment (feature class)	Drainage line (feature class) Catchment (feature class)
Longest flow for catchment	Longest flow path adj cat (feature class)	Catchment (feature class) Fdr (GRID format)
Drainage point processing	Drainage point (feature class)	Fdr (GRID format) Catchment (feature class) StrLnk (GRID format)

16.4.3 Drainage Network

It is possible to collect information about the hydrological structure of the rocks within a river basin by morphometrically assessing the characteristics of the drainage pattern (Kattimani et al. 2016 and Pakhmode et al. 2003). A drainage map of a watershed gives a realistic indication of the permeability of the geological structure as well as information on basin outflow (Wisler and Brater 1959). The study area's drainage map depicts the network of primary streams in the catchments, followed by tributaries in that order. The drainage network represents the major river Gomti includes a number of minor streams that flow through the research area. The city north-eastern corner is associated with high drainage density. As a result of the lower infiltration and faster movement of surface runoff in areas with increased drainage density, there is a greater risk of flooding (Fig. 16.5d).

16.5 Creation of Potential Flooding Sites

After extraction of the drainage network from the DEM data and elevation data of each sub-watershed, the potential flood inundation mapping has been created.

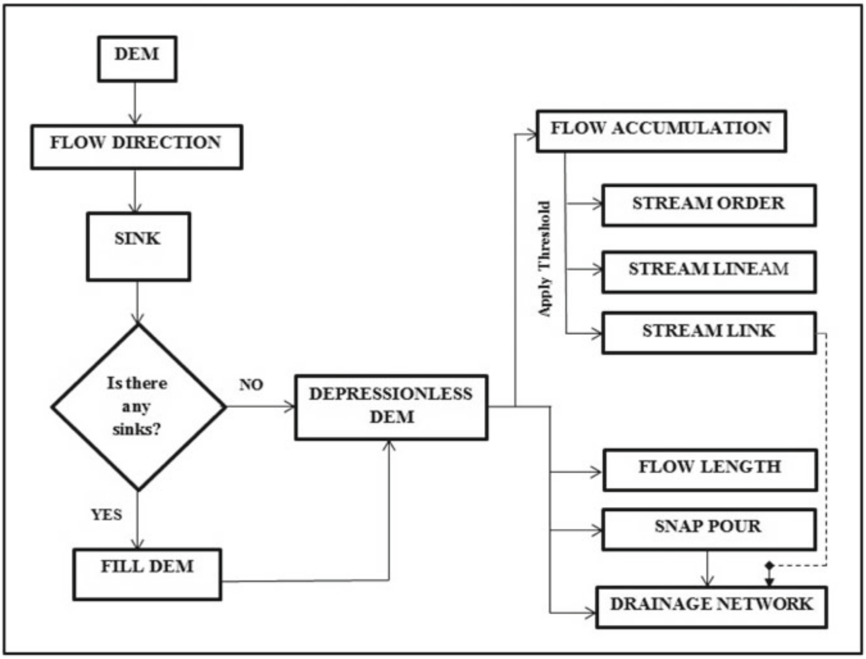

Fig. 16.4 Flow chart used in drainage network extraction

The flood inundation map shows that the area of potential flooding sites is more of Trans-Gomti region as compared to Cis-Gomti region of the LMC boundary. A flood inundation maps have been generated with 1 m increment at various elevations and the inundation area as shown red in colour in the depicted Fig. 16.5.

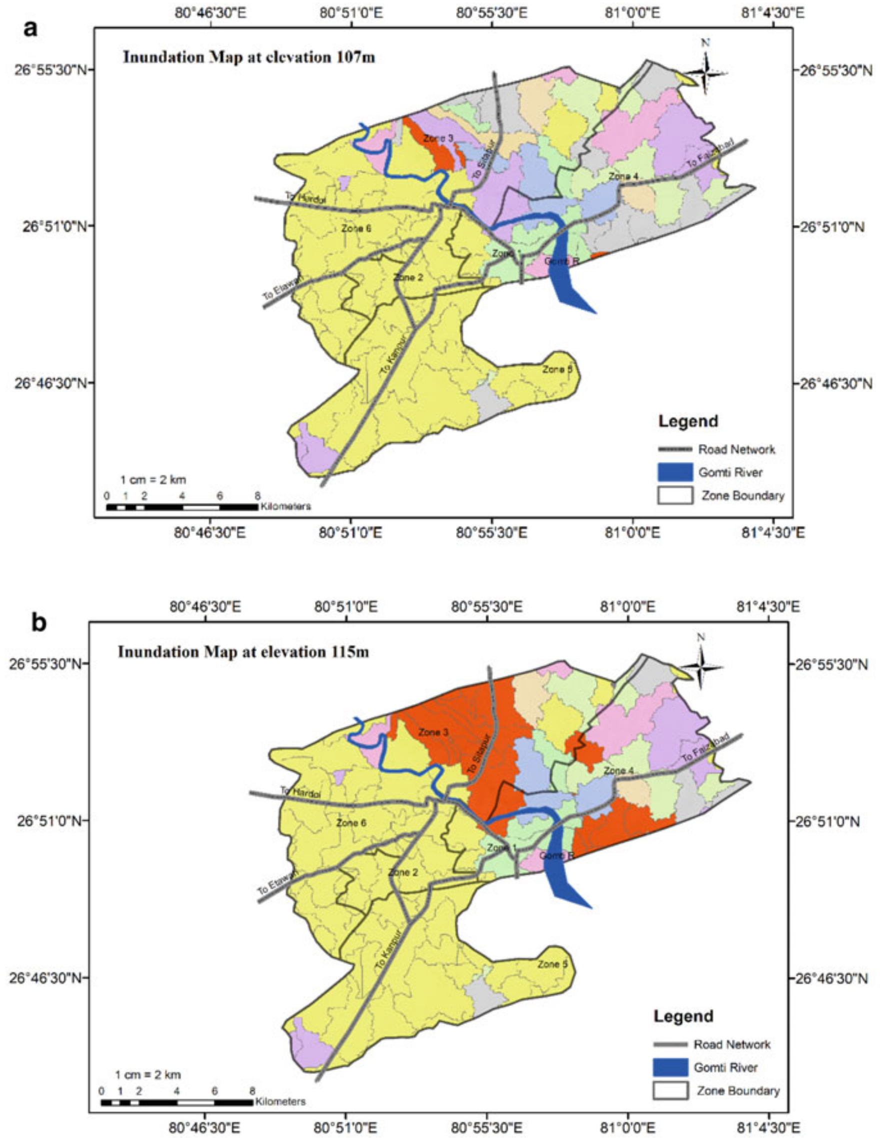

Fig. 16.5 **a** Map showing the inundation area at elevation 107 m. **b** Inundation map at elevation 115 m of the study area. **c** Inundation map at elevation 120 m of the study area. **d** Inundation map at elevation 122 m of the study area

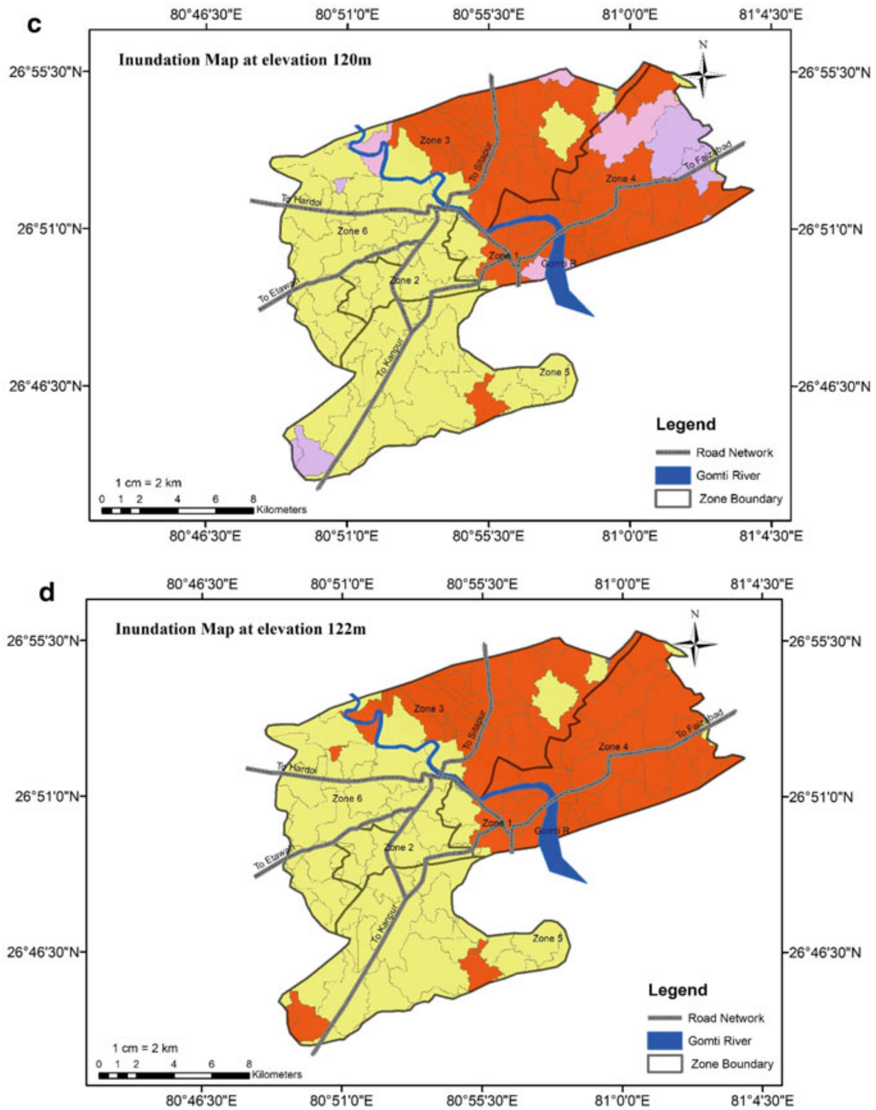

Fig. 16.5 (continued)

16.6 Evaluation of Submergence Area

The inundation areas 3.11, 42.83, 103.65, and 133.35 km^2 at the elevation of 107, 115, 120, and 122 m have been estimated, respectively. The relative submergence area corresponding to different elevation is listed in Table 16.1.

Table 16.1 Relative potential submergence areas

S. No.	Elevation (m)	Inundation area (km^2)	S. No.	Elevation (m)	Inundation area (km^2)
1	107	3.11	9	115	42.83
2	108	5.38	10	116	54.08
3	109	19.66	11	117	64.31
4	110	23.75	12	118	78.79
5	111	26.03	13	119	85.72
6	112	28.51	14	120	103.65
7	113	30.73	15	121	118.79
8	114	30.73	16	122	133.35
Total LMC area (km^2)			290		

In this study, a GIS-based flood inundation map was created by combining all weighted layers in a GIS environment. DEM and drainage network information is further employed to assess the potential flooding sites in the Lucknow city, and the potential flooding sites are investigated starting from 107 to 122 m with an increment at 1 m interval. At 110 msl, total potential flooding area is approximately 23.75 km^2 (8%, approx.), and at 122 msl, total potential flooding area is 133.35 km^2 (46%, approx.) which have been estimated.

This study shows beyond a possible doubt that a detailed feasibility analysis of the area utilizing remote sensing and GIS is required if unexpected adverse impacts of such a massive undertaking are to be avoided and the full advantages of this significant initiative to be realized. Spatial modelling, with the use of remote sensing and the GIS environment, for identifying consequences in impacted regions, can prove to be a vital instrument in such feasibility studies and help us attain an environmentally conscious approach to socio-economic problems. The flood inundation maps can also be used to quickly identify probable flood sites in order to reduce flood losses.

16.7 Impacts of Urbanization on Groundwater Systems and Recharge

The development of cities increases paved surfaces, roofs, and storm drains. The installation of an extensive subsurface network, including utilities, is another important part of urbanization, which affects both surface and groundwater. Cities require measures to deal with urban floods caused by the spread of low-lying area and the absence of stormwater drainage system. The study assessed the topography of Lucknow which is a cause for concern because they play a significant role in attenuating rainfall during storm events.

Various maps, such as drainage pattern maps of urban areas, flood inundation maps, and land use and land cover maps, are required to assess for effective drainage methods to minimize urban floods. In India, there are currently over 400 million people residing in metropolitan areas, with 52 cities having populations greater than one million (Kundu 2014). Green cover has reduced in cities as built-up regions have increased (Jim 2013).

In the last decade, India has experienced major flooding in Mumbai on July 26, 2005, with total rainfall of 994 mm in 24 h, Srinagar in September 2014, and Chennai in December 2015, with total rainfall of 400 mm in 24 h (Wamiq Ali et al. 2021). Flooding in cities occurs when rainfall exceeds 150 mm/day; this is known as phenomenal rainfall, and heavy rainfall occurs when rainfall exceeds 125 mm per day (De et al. 2013).

A range of anthropogenic activities from heavy vehicle movement, pavement development, and continuous digging activity along footpaths and pavements were found to reduce infiltration rates due to low porosities within soil profiles regardless of the soil composition comprising primarily fine sand and gravels. Despite short periods of flooding, urban green spaces are not managed properly, resulting in water logging. There is no proper information available for urban topography. Consequently, an alternative approach has been developed to identify areas at greatest risk of inundation that does not require extensive computation and hydrological observations.

As a result, an alternate method for determining where inundation and risk are greatest has been created that does not involve extensive computation or hydrological observations.

16.8 Outlook for Groundwater in Urban Area

Urban groundwater resource testing is similar to rural groundwater resource testing However, following factors are need to be considered.

Although data of existing underground drainage structures is available, their accuracy is questionable, and people in urban areas cannot even count the population census. As a result, it is recommended that the discrepancy between realistic water availability and demand is considered as the extraction from groundwater resources.

Unless particular efforts are taken to develop roads and pavement, urban areas can become concrete forests, and rainwater infiltration is not equivalent to that of rural areas. Temporarily, 30% rainfall is being used as a rainfall factor in urban areas until field investigations are completed and recorded studies are available.

Due to the water supply scheme, several pipelines are laid in the urban areas, and seepages are widespread in some places. Consequently, recharge estimation must also consider these other resources. The groundwater system can be recharged by collecting and using half of the per cent losses from water supply facilities. (GWRA India Report 2020).

In most Indian cities, there is no distinct drainage system for drainage or flash floods, either open or subsurface. These drains also help to recharge the groundwater reservoir to some extent. There is currently no confirmed field study that can be used to estimate the recharge. The nitrates from sewerage seepages are generally contaminating groundwater resources, which contribute to the quantity of resources when there is an underground drainage network. Therefore, the % for water supply drains may be used as the norm for the recharge of sewerage. Even if the drainage system has open channels, the same technique might be used until more recorded field studies are completed.

A separate groundwater assessment is recommended for urban areas with populations greater than 10 lakhs.

16.8.1 Rainfall Recharge

As per the GWRA India Report (2020), groundwater levels fluctuate with groundwater inputs and outputs, so it is important to consider groundwater level fluctuations and specific yields as measures of groundwater recharge. This, however, needs a succession of representative water level measurements over a sufficiently extended duration. It is proposed that the assessment unit has at least three observation wells that are spatially well distributed, or one observation well every 100 km^2. Water level data, as well as matching rainfall data, should be accessible for at least 5 years (preferably 10 years). The frequency of collecting data on water level should be at least two during the pre- and post-monsoon seasons.

16.8.2 Method of Fluctuation of Groundwater Levels

During the monsoon season, the groundwater level fluctuation approach will be used to estimate rainfall recharge. In non-command areas, the groundwater balance equation is defined by.

$$\Delta S = R_{\mathrm{SI}} + R_{\mathrm{GI}} + R_{\mathrm{R}} + R_{\mathrm{FC}} + R_{\mathrm{TP}} + R_{\mathrm{WS}} \pm V_{\mathrm{F}} \pm L_{\mathrm{F}} - G_{\mathrm{Ext}} - E - T - B \quad (16.1)$$

where

ΔS—Storage Change
R_{SI}—Recharge by surface water irrigation
R_{GI}—Recharge by groundwater irrigation
R_{R}—Recharge from rainfall
R_{FC}—Recharge due to flow channels
R_{TP}—Recharge due to tanks and ponds
R_{WS}—Recharge by water conservation structures
V_{F}—Vertical flow through the aquifer system
L_{F}—Lateral flow within the aquifer system (through flow)
G_{Ext}—Groundwater extraction
E—Evaporation

T—Transpiration

B—Base flow.

Whereas the water balance equation in command area will be written in another term, i.e. Recharge from canals (R_C) and the equation will be as follows:

$$\Delta S = R_C + R_{SI} + R_{GI} + R_R + R_{FC} + R_{TP} + R_{WS} \pm V_F \pm L_F - G_{Ext} - E - T - B \quad (16.2)$$

16.9 Assessment of Groundwater in Water Level Depletion Zones

Even during the monsoon season, there may be locations where groundwater levels decline. One or more of the following factors may be at this scenario; (a) A depletion of groundwater regime is observed, with natural groundwater discharge exceeding recharge during the monsoon season. (b) Water level data may be incorrect due to insufficiency of observation wells.

As per the GWRA India Report (2020), if the water level data is found to be erroneous, a recharge evaluation utilizing the rainfall infiltration factor approach may be undertaken. Alternatively, groundwater level fluctuations may be employed as a way of estimating recharge if water level data is considered accurate. The estimated recharge during the monsoon season will be lesser than the gross groundwater extraction because ΔS in Eqs. (16.1) and (16.2) is negative. This hydrological recharge can be estimated by subtracting the natural monsoon discharge from the gross recharge. This assessment will immediately indicate that the area has been overexploited, requiring further assessment at a micro-level.

16.10 Groundwater Status in Lucknow City

The yearly rainfall trends for Lucknow from January 2015 to December 2020 are given in Table 16.2. This gridded data is taken from IMD (Indian Meteorological Department). It is important to remember that the maximum rainfall of 1039.39 mm was recorded in 2019, while the lowest rainfall of 507.21 mm was recorded in 2015 in Lucknow. However, while comparing current water levels in 2020, 2019, and 2018, it can be found that the water level in 2020 has increased by 0.80 m and 3.67 m, respectively. The Trans-Gomtis region of the study area falls into the low elevation corresponding to the Cis-Gomti region. Because high elevation produces low infiltration and faster surface runoff movement, there is a greater possibility of flooding in the Trans-Gomti region. The yearly groundwater trends for Lucknow from January 2015 to December 2020 are given in Table 16.3.

Table 16.2 Yearly rainfall trends for Lucknow from January 2015 to December 2020

Year	Normal (mm)	Actual (mm)
2015	927	507.21
2016	927	671.37
2017	927	669.64
2018	927	971.62
2019	927	1039.49
2020	927	707.69

Source India WRIS

Table 16.3 Yearly groundwater trends for Lucknow from January 2015 to December 2020

Year	Last 10 year avg (m bgl)	Last year (m bgl)	Current level (m bgl)
2015	11.64	11.71	13.83
2016	11.99	13.83	14.68
2017	12.23	14.67	14.39
2018	12.60	14.39	14.91
2019	12.67	14.91	12.04
2020	12.58	12.04	11.24

Source India WRIS

16.11 Conclusions

Although it is generally said that urbanization reduces groundwater recharge due to increased impervious cover, this is not the case. According to the groundwater level data for 2019 and 2020, the groundwater level is decreasing in contrast to past years, which might be regarded as a significant decline. This could be because the growth of urban areas and impermeable surfaces has resulted in an increase in surface runoff because less water is lost through soil infiltration. The infiltration capacity of the soil and an inadequate drainage network may also play a role in the establishment of flooding sites within the city limits. The present study may be useful for planning and management in the following manners:

1. To forecast foods and inundation phenomenon,
2. To assess the consequences of decisions aimed at decreasing economic, social, and environmental damage based on planned or real-time anticipated scenarios,
3. To identify risk area's and estimation of expected damages,
4. To assess groundwater recharge from the available spatial and temporal information.

References

Ali QSW, Pandey S, Chaudhuri RR, Behera S, Jayakumar L (2021) Development of rainfall-infiltration measurement system and recharge strategies for urban flooding areas: a case study of Delhi, India. Model Earth Syst Environ. https://doi.org/10.1007/s40808-020-01050-y

A report on National Compilation on Dynamic Ground Water Resources of India (2020)

Bates PD, De Roo APJ (2000) A simple raster-based model for flood inundation simulation 236(1–2):0–77. https://doi.org/10.1016/s0022-1694(00)00278-x

Chen J, Hill AA, Urbano LD (2009) A GIS-based model for urban flood inundation 373(1–2):184–192. https://doi.org/10.1016/j.jhydrol.2009.04.021

De US, Singh GP, Ras DM (2013) Urban fooding in recent decades in the four mega cities of India. J Indian Geophys Union 17(2):153–165

Fosu C, Forkuo EK, Asare MY (2012) River inundation and hazard mapping—a case study of Susan River—Kumasi. In: Proceedings of global geospatial conference 2012 Québec City, Canada, 14–17 May 2012

Inception Report for Revised City Development Plan of Lucknow City under JnNURM, vol I, January 2015

Jim CY (2013) Sustainable urban greening strategies for compact cities in developing and developed economies. Urban Ecosyst 16(4):741–761. https://doi.org/10.1007/s11252-012-0268-x

Kattimani JM, Renuka Prasad TJ (2016) Cartosat digital elevation model (DEM) to drainage extraction techniques of Vrushabhavati basin of Karnataka, India using remote sensing and GIS techniques. Int J Adv Res 4(7):2008–2013

Kundu D (2014) Cities for all, XI metropolis world congress. https://www.niua.org/sites/all/fles/cites_for_all.pdf. Accessed 12 Sep 2019

Pakhmode V, Kulkarni H, Deolankar SB (2003) Hydrological-drainage analysis in watershed-programme planning: a case from the Deccan basalt, India 11(5):595–604. https://doi.org/10.1007/s10040-003-0279-z

Sahoo SN, Sreeja P (2015) Development of flood inundation maps and quantification of flood risk in an urban catchment of Brahmaputra river. ASCE-ASME J Risk Uncertainty Eng Syst Part A: Civ Eng A4015001. https://doi.org/10.1061/AJRUA6.0000822

Sarhadi A, Soltani S, Modarres R (2012) Probabilistic flood inundation mapping of ungauged rivers: linking GIS techniques and frequency analysis. J Hydrol 458–459:68–86. https://doi.org/10.1016/j.jhydrol.2012.06.039

Sun P, Wen Q, Zhang Q, Singh VP, Sun Y, Li J (2018) Nonstationary evaluation of flood frequency and flood risk in the Huai River basin, China. J Hydrol S0022169418307935. https://doi.org/10.1016/j.jhydrol.2018.10.031

UNDRO (1978) Disaster prevention and mitigation—compendium of current knowledge—United-Nations 2(2–3):176–178

Ward RC (1978) Floods: a geographical perspective. Macmillan, London

Wisler CO, Brater BF (1959) Hydrology. Wiley, New York, p 408

Chapter 17
Impact of Climatic Changes on Groundwater Regime: A Case Study of Tinsukia District, Assam, India

Alka Dash

Abstract Hydro-climatic changes can significantly disturb the balance between natural parameters, leading to difficulty predicting trends in groundwater system. Rainfall and temperature variations can affect all other climatic elements; therefore, identification of trends of these two elements becomes relevant to studying the globally increasing effect of climate change. In the past decades, scientific research on the impact of climate change on the various hydro-climatic parameters has identified trends in the extreme seasonal and annual values. The most accepted statistical tool for examining trends was the Mann–Kendall test, Sen's slope and linear regression. The whole planet is struggling with water crises due to climate change, so groundwater is the only resource to lie on to fulfill fresh water needs. Thus, studying trends in groundwater levels becomes the necessity of the coming era. This research's main objective is applying the Mann–Kendall test and Sen's slope method to identify the trends and magnitude of groundwater levels under the climate conditions in Tinsukia District, Assam, India. This objective is important in analyzing groundwater resources in close connection with their efficient management. The study is based on the secondary data of the monthly groundwater level (mbgl) obtained from the Central Water Commission, India and climatic data (average annual rainfall, maximum and minimum temperature) for the period 2012–2021 from India Meteorological Department (IMD). The findings suggested that the average yearly rainfall, maximum temperature and minimum temperature have an increasing trend along with the groundwater levels in the study area. This leads to saturation in the recharge system and storage capacity. The higher intensity of rainfall and greater saturation level in the groundwater system may lead to a higher runoff rate, thereby initiating a major flood-like situation in the study area.

Keywords Groundwater · Trend analysis · Mann–Kendall · Sen's slope · Climate change

A. Dash (✉)
Department of Geography, Central University of Haryana, Mahendragarh, India
e-mail: dashalka07@gmail.com

P. Shukla et al. (eds.), *Environmental Processes and Management*, Water Science and Technology Library 120, https://doi.org/10.1007/978-3-031-20208-7_17

17.1 Introduction

Throughout history and throughout the world, the ubiquitous resource of groundwater has played a central part in ecosystem sustainability and helping human adaptation to climate change. Variability in the major climatic parameters (precipitation, soil moisture and surface water) will aggravate the risk of climate extremities (droughts and floods), thereby intensifying the strategic importance of groundwater (Taylor et al. 2012). Rapid population growth along with surface water pollution escalates groundwater demand (Wu et al. 2020) which results in the lowering of groundwater levels. The groundwater crisis in the coming years shows the global concern as its vulnerability increases with the substantial extraction of groundwater for various purposes (Halder et al. 2020). In Tinsukia, Assam, India, according to District Irrigation Plan, 2016–2020 by NABARD Consultancy Services, the water budget shows a negative gap between water availability and requirement that indicates sufficient water resources available for various purposes (irrigation, domestic and industrial) with no deficit in the water potential. Meanwhile, the poor domestic wastewater management paints a situation of looming water crises in Tinsukia. Around 97% of household wastewater is untreated and discharged to the environment with no proper secondary and tertiary treatment facility arrangement (CSE-2020, SFD Lite Report—Tinsukia, India). Therefore, examining how trends in groundwater level change in response to the changing trends in rainfall and temperature becomes crucial. Fluctuations in an area's annual and seasonal rainfall patterns may lead to stress on groundwater levels with consequent implications in strategizing groundwater development and management for sustainable water use in the region (Goswami and Radha 2020). Out of all methods applied to identify hydro-meteorological time series (Duhan and Pandey 2013), trend analysis of rainfall and temperature (by parametric and non-parametric tools) shows the direction and magnitude of the trend and its statistical significance (Jain and Kumar 2012). Researchers confirmed the Mann–Kendall test (Mann 1945; Kendall 1975) and Sen's slope (Sen 1968) as one of the best methods used to analyze the temporal change in an area (Aditya et al. 2021). Pathak and Dodamani (2018) applied cluster analysis on long-term monthly groundwater levels and opted Standardized Groundwater Level Index (SGI) for evaluating groundwater drought along with Mann–Kendall tests to investigate annual and seasonal trends of groundwater levels in the groundwater drought-prone Ghataprabha River basin of India. Le Brocque et al. (2018) applied a modified Mann–Kendall test and Sen's slope estimator to data of 381 groundwater bores in southern Queensland in Australia for 26 years (1989–2015). They found a significant overall decline in groundwater levels due to highly irrigated areas. Patle et al. (2015) recognized pre- and post-monsoon groundwater level trends using the Mann–Kendall test and Sen's slope estimator in the Karnal district of Haryana in India from 1974 to 2010. Fenelon and Moreo (2002) used Locally Weighted Scatterplot Smooths for graphical representation and Mann–Kendall trend tests on groundwater levels and spring discharge for statistical purposes from 1960 to 2000 in the Yucca Mountain Region, USA. Jain and Kumar (2012) studied trends in rainfall from 1950 to 2000 and temperature for the period of 1900–2000 in the context of various river basins of India, addressing the need for a baseline station network for climatic studies. Aswad et al. (2020) also applied the Mann–Kendall test and Sen's slope estimator to study the annual and monthly rainfall trend in the Sinjar district of Nineveh, Iraq, for a 70-year period (1940–2010). Thakur and Thomas (2011) applied Kendall's rank correlation test to identify trends in groundwater level data and a linear regression test to identify the significance of the slope in the Sagar district of Madhya Pradesh in India. Engelenburg et al. (2018) applied the AZURE hydrological model to assess the effect of climate change and extensive groundwater extraction in the Veluwe aquifer of the Netherland to analyze the groundwater level in the nearby dependent ecosystem. Sishodia et al. (2016) analyzed the bi-decadal groundwater level trend in three administrative districts of semi-arid South India. They briefed it through variability in rainfall, irrigation and agricultural power subsidy. Tiwari et al. (2011) utilized GRACE satellite and in-situ groundwater and Gravity Recovery data to study groundwater levels and compare them to Cumulative Rainfall Departure (CRD) and Standardized Precipitation Index (SPI) in Andhra Pradesh. They found a net increase on account of variability in rainfall. Patra et al. (2018) performed Kendall's Tau to examine the relation of hydro-climatic parameters (e.g., rainfall, temperature) with hydrological components (e.g., groundwater level). Normalized Built-up Index was used to evaluate land cover and use change and the inverse distance weighting (IDW) interpolation method for the spatial distribution of temperature, rainfall and groundwater level analysis. These tools identified the effects of urban sprawl on groundwater recharge, and the study suggested clustering wells for effective groundwater level and recharge patterns. Salem et al. (2018) focused on the result of climate change on irrigational cost for a region in North-West Bangladesh by using a hydrological and general circulation model, which requires analysis of present and future trends to replicate the groundwater level from climatic variables. Bora et al. (2022) analyzed the changes in annual and seasonal rainfall patterns in seven North-East Indian states for the period 1901–2020, using non-parametric tests like Mann–Kendall, trend-free pre-whitening Mann–Kendall, modified Mann–Kendall (MMK) and innovative trend analysis (ITA) revealing almost identical results for all the tests with. The study revealed the variable cities in annual and seasonal rainfall in these seven states. In most cases, the tests' results were almost identical, which helps policymakers frame crucial climatic and water resource management decisions. Bahadur et al. (2017) conducted a study to assess the significance of three hydro-climatic variables, viz., temperature, rainfall and runoff over the Rangoon watershed in the Dadeldhura, Nepal. Monthly, seasonal and annual data were evaluated using the Mann–Kendall test and Sen's slope estimate for rainfall and temperature (1979–2010) and 1967–1996 for runoff. The study's main objective is to apply the Mann–Kendall test to predict the existing trend direction and Sen's slope method to detect the trend direction and the magnitude of change over time in groundwater levels under varying rainfall and temperature conditions in Tinsukia District, Assam, India. This cardinal objective is necessary for interpreting the growing effect of climate change on groundwater resources and is considered an opening move to analyze groundwater resources in close connection to well-structured management.

17.2 Study Area

Study area Tinsukia is an administrative district in the eastern parts of Assam, India. The spatial stretch is 27° 14′03″–27° 48′05″ N latitude and 95° 13′03″–96° 00′00″ E longitude covering 3790 km^2 in Brahmaputra Basin. It comprises three sub-divisions, seven blocks and 88 g Panchayats for transparent and smooth governance. The great river the Brahmaputra is the major drainage source feeding the study area along with Dibru and Burhi-Dihing. Being a huge water resource for Tinsukia, all these drainage systems also prove to be the misery of Tinsukians carrying loads of sediments and voluminous water during monsoons to the low-lying area and creating a flood-like situation. The area enjoys a humid subtropical climate with high humidity in the rainy season. The mercury ranges from 21 to 35 °C in summers and falls to as low as 13 °C in winters. A high rainfall pattern also accounts for around 65% of rainfall during monsoons. The spectacular geomorphic landforms in the area are Brahmaputra plains, structural hills in the southern part and young and old alluvium plains. Paddy, the major crop in the area, has now been accompanied by other cash crops, which ultimately grow at the cost of irrigation and groundwater utilization. As per CGWB, the groundwater level in 2021 is 3.546 mbgl, decreasing compared to 2020, which stands at 3.802. The water quality of Tinsukia is fresh and portable on average, but iron (Fe) is found in some areas more than permissible. The groundwater development in Tinsukia is low-key, which may gain pace with coming management strategies (Fig. 17.1).

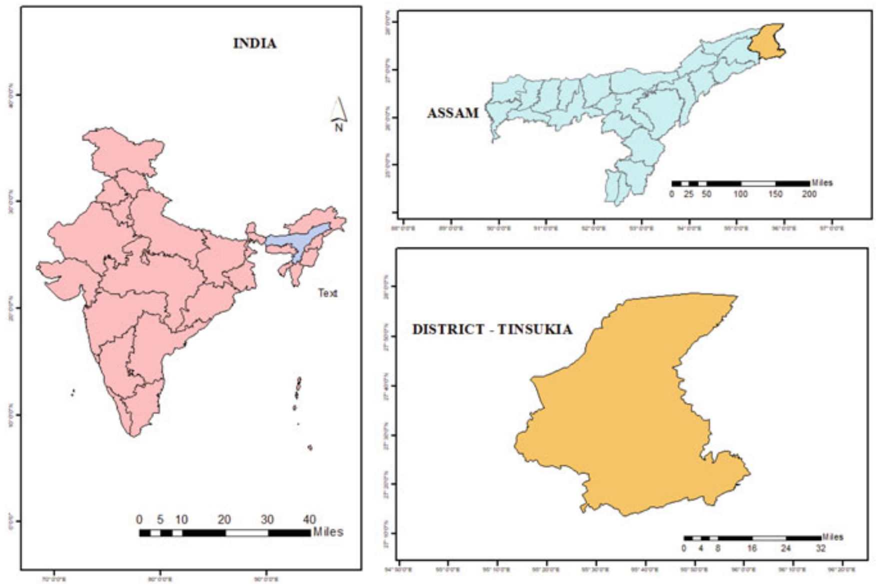

Fig. 17.1 Study area (Tinsukia district)

17.3 Data Source

Yearly meteorological parameter temperature and rainfall of the Tinsukia district in Assam were collected from the India Meteorological Department for a decade, i.e., from 2012 to 2021. The maximum, minimum and average temperatures were considered for temperature. The rainfall data were collected from three different IMD stations in Tinsukia situated at Udaipur, Dholabazar and Margherita. Trend analysis for groundwater includes data from the Central Ground Water Board, Govt. of India for the same study area and period.

17.4 Data Processing

The major climatic variables, temperature and rainfall, along with a significant hydrological parameter groundwater level, were assessed for trend analysis in the current study. The most widely accepted time series analysis in climatic and hydrological trends includes the Mann–Kendall test and Sen's slope estimator. The calculations have been done in the coming sections to establish a relationship between the testing parameters. For ease of calculation, the MS-Excel program MAKESENS 1.0 is used.

17.4.1 MK Test

MK test or Mann–Kendall test (Mann 1945; Kendall 1975; Gilbert 1987) is a widely recognized non-parametric test to detect monotonic trends in a series of climate and hydrological data. Data following a monotonic trend confirm the existence of a trend using an alternative hypothesis (H_1). Independently and identically distributed data are given by the null hypothesis (H_0) for this statistical test. H_0 represents the non-existence of any trend. The presence of a significant trend is identified using the values of a test statistic Z, the positive and negative values indicating an upward and downward trend, respectively. "Mann–Kendall test does not require that datasets to follow a normal distribution and show homogeneity in variance; transformations are not required if data already follow a normal distribution, and in skewed distribution, greater power is achieved" (Duhan and Pandey 2013). The test helps evaluate the slope's nature in a trend, coefficient of variation and type of probability distribution. "Mann–Kendall test is used for trend analysis as it eliminates the effect of serial dependence on auto-correlated data which modifies the variance in datasets" (Hamed and Rao 1998). The mathematical explanation can be read from various literature mentioned in the reference section.

17.4.2 *Sen's Slope Estimation*

Sen's (1968) slope estimator is a significant statistical tool to establish linear relationships having the advantage over the slope of regression. "This method assumes the trend line is a linear function in the time series. In Sen's slope model, the slope value shows the rise and fall of the variable" (Jain and Kumar 2012). "Another advantage of using Sen's slope is that it is not affected when outliers and single data errors are present in the dataset" (Salmi et al. 2002). For mathematical understanding, literature from the reference section can be read.

17.5 Result and Discussion

Trend analysis of annual temperature, rainfall and groundwater level was carried out using the MK test and Sen's slope for ten years (2012–2021) in the Tinsukia district of Assam. Results are discussed separately for each parameter in this section to establish a legit relationship.

17.5.1 *Trend Analysis for Temperature*

17.5.1.1 Minimum Temperature

The result of the annual minimum temperature during 2012–2021 is given in Table 17.1. From the table, the *Z*-value of 0.36 and *Q*-value of 0.02 indicate the existence of the H_1 hypothesis. A positive value reveals a significant upward trend which implies an increasing trend over time in the annual minimum temperature pattern. The trend is not so strong as the *Q*-value indicates a weak magnitude of a movement.

Table 17.1 Tinsukia district—trend result of temperature, rainfall and groundwater level by Mann–Kendall test and Sen's slope estimator from 2012 to 2021

Parameters	*n*	*Z*-value	*Q*-value	Significance	*B* value
Temperature_Max (°C)	10	0.64	0.021	–	29.48
Temperature_Min (°C)	10	0.36	0.020	–	16.53
Temperature_Avg (°C)	10	0.00	0.003	–	24.47
Rainfall_Dholabazar (mm)	10	1.97	110.728	*	1771.37
Rainfall_Udaipur (mm)	10	0.54	17.644	–	978.89
Rainfall_Margherita (mm)	10	1.43	39.844	–	2063.03
Groundwater level (mbgl)	10	−0.18	−0.025	–	3.72

"*" represents a significant trend at 0.05 level of significance

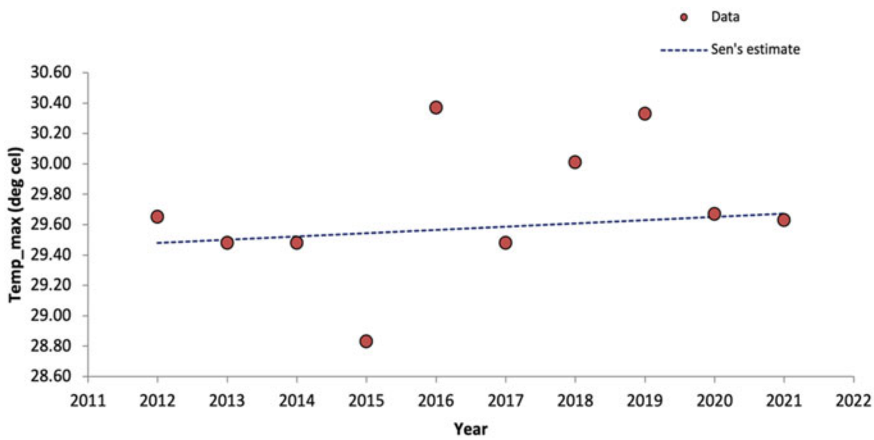

Fig. 17.2 Linear maximum temperature trends for the period 2012–2021

17.5.1.2 Maximum Temperature

The result of the MK test and Sen's slope of annual maximum temperature during 2012–2021 is given in Table 17.1. From the table, the *Z*-value of 0.64 and *Q*-value of 0.021 indicate the existence of the H_1 hypothesis. A positive value reveals a significant upward trend which implies an increasing trend over time in the annual maximum temperature pattern. The trend is not so strong as the *Q*-value indicates a weak magnitude of a trend. The maximum temperature variation is shown in Fig. 17.2.

17.5.1.3 Average Temperature

The result of MK test and Sen's slope of annual average temperature during 2012–2021 is given in Table 17.1. From the table, the *Z*-value of 0.00 and *Q*-value of 0.003 indicate no trend in the annual average temperature pattern. Here, the H_0 hypothesis is valid.

17.5.2 Trend Analysis for Rainfall

The total rainfall for ten years (2012–2021) for three specific station—Dholabazar, Udaipur and Margherita is shown in Table 17.1. The *Z*-value and *Q*-value for Dholabazar are 1.97 and 110.728, respectively, marking a significant positive trend at 0.05 level of significance having 95% significance interval of *Q*. For Margherita, the *Z*-value and *Q*-value are 1.43 and 39.844, respectively, signifying a positive trend in the rainfall distribution. Similarly, a positive trend exists for Udaipur station as the *Z*-value and *Q*-value are 0.54 and 17.644, respectively. Here also, the null hypothesis (H_0) rules out, indicating the presence of a trend in the rainfall pattern in Tinsukia, Assam. Rainfall variations in these stations are shown in Figs. 17.3, 17.4 and 17.5.

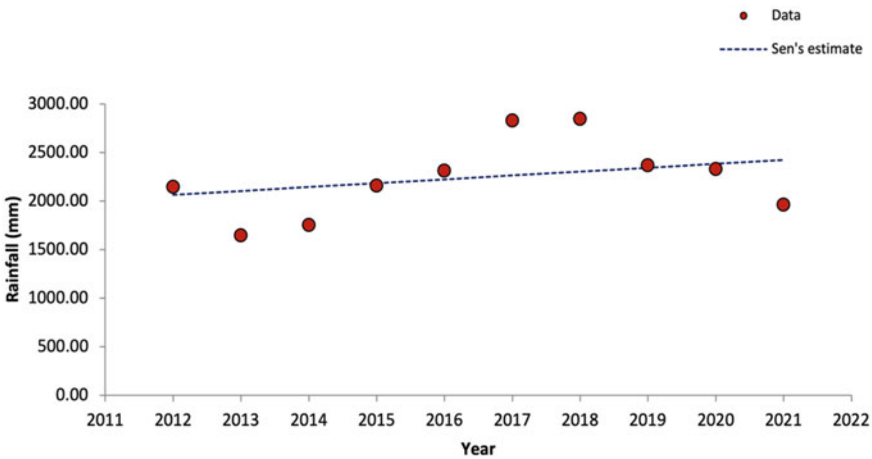

Fig. 17.3 Linear rainfall trends for the period 2012–2021, Dholabazar

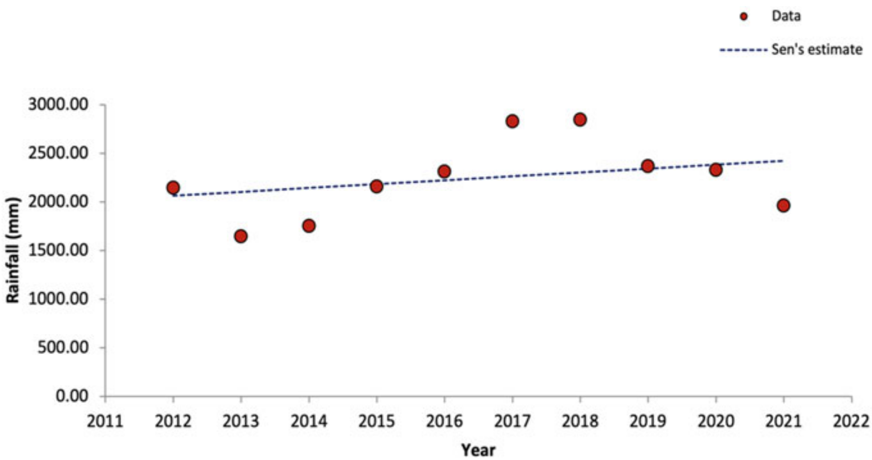

Fig. 17.4 Linear rainfall trends for the period 2012–2021, Margherita

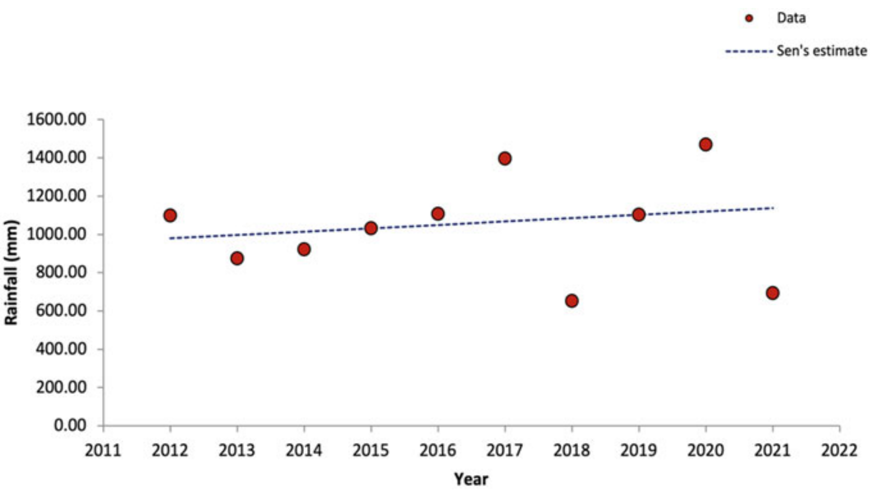

Fig. 17.5 Linear rainfall trends for the period 2012–2021, Udaipur

17.5.3 Trend Analysis for Groundwater Level

The result of the annual groundwater level in Tinsukia studied for ten years (2012–2021) using the MK test and Sen's slope is summarized in Table 17.1. As for groundwater level in mgbl, a negative value of Z and Q indicates an increasing trend in water availability from the ground level. The Z-value and Q-value are -0.18 and -0.025, respectively, which means the groundwater level is increasing at a higher rate in Tinsukia, Assam. Variations in groundwater level are shown in Fig. 17.6.

Positive Z- and Q-value for maximum and minimum temperature shows an increasing trend for an annual temperature rise in Tinsukia. The increase in temperature bears witness to a growing rainfall trend for the period of 2012–2021. The groundwater level is also increasing at a higher rate, leading to saturation in the recharge system and storage capacity. The higher intensity of rainfall and greater saturation level in the groundwater system may lead to a higher runoff rate, thereby initiating a major flood-like situation in the study area. The vast network of river Brahmaputra, along with its tributaries, supplements the devastating floods in Assam. The recent 2022 flood in Assam testifies to the statement enhancing high alerts for the Tinsukia inhabitants.

17.6 Conclusion

The work incorporated in this chapter was a mere study to analyze the effect of climate change on groundwater levels in Tinsukia district of Assam which lies on the banks of the river Brahmaputra. Verifying unattempted study of climate change

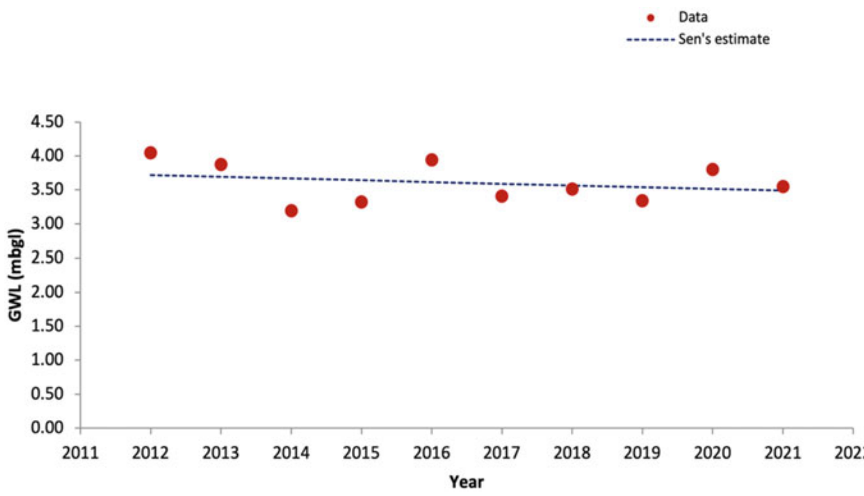

Fig. 17.6 Linear groundwater level trends for the period 2012–2021

in the area with respect to temperature and rainfall, trends for a time period of 2012–2022 were studied using the above suitable non-parametric methods. Following this, to establish a robust relationship between climate change and groundwater, trend analysis for groundwater levels was also computed. The obtained results show an increasing trend in all the calculated variables which should not be a matter of concern. But increasing rainfall and groundwater levels can also be a noteworthy reason for frequent flood events in Assam. So further study may take up to assess the trends in sedimentation, runoff and land use patterns to study the realistic viewpoint of such catastrophic events. Increasing surface water contamination in the area also endangers groundwater levels. Thus, the study caters to the need for effective water management along with the adoption of necessary policies and implementations for sustainable development.

References

Aditya F, Gusmayanti E, Sudrajat J (2021) Rainfall trend analysis using Mann-Kendall and Sen's slope estimator test in West Kalimantan. IOP Conf Ser Earth Environ Sci 893:012006. https://doi.org/10.1088/1755-1315/893/1/012006

Aswad F, Yousif A, Ibrahim S (2020) Trend analysis using Mann–Kendall and Sen's slope estimator test for annual and monthly rainfall for Sinjar district, Iraq

Bahadur A, Khare D, Mishra P, Singh L (2017) Trend analysis of rainfall, temperature and runoff data: a case study of Rangoon watershed in Nepal. Int J Stud Res Technol Manage 5:21. https://doi.org/10.18510/ijsrtm.2017.535

Bora S, Bhuyan K, Hazarika P, Gogoi J, Goswami K (2022) Analysis of rainfall trend using non-parametric methods and innovative trend analysis during 1901–2020 in seven states of North East India. Curr Sci 122:801. https://doi.org/10.18520/cs/v122/i7/801-811

Brocque AF, Kath J, Reardon-Smith K (2018) Chronic groundwater decline: a multi-decadal analysis of groundwater trends under extreme climate cycles. J Hydrol
(CSE-2020, SFD Lite Report, Tinsukia, India)
Duhan D, Pandey A (2013) Statistical analysis of long term spatial and temporal trends of precipitation during 1901–2002 at Madhya Pradesh, India. Atmos Res 122:136–149. https://doi.org/10.1016/j.atmosres.2012.10.010
Fenelon JM, Moreo MT (2002) Trend analysis of ground-water levels and spring discharge in the Yucca Mountain region, Nevada and California, 1960–2000. Water-Resources Investigations Report 02-4178, US Geological Survey. https://doi.org/10.3133/wri024178
Ganguly A, Ray Chaudhuri R, Sharma P (2015) Analysis of trend of the precipitation data: a case study of Kangra district, Himachal Pradesh. Int J Res Granthaalayah 3(9):87–95. https://doi.org/10.29121/granthaalayah.v3.i9.2015.2948
Gilbert RO (1987) Statistical methods for environmental pollution monitoring. John Wiley and Sons, New York
Goswami M, Rabha D (2020) Trend analysis of ground-water levels and rainfall to assess sustainability of groundwater in Kamrup metropolitan district of Assam in Northeast India
Halder S, Roy MB, Roy PK (2020) Analysis of groundwater level trend and groundwater drought using standard groundwater level index: a case study of an eastern river basin of West Bengal, India. SN Appl Sci 2(3). https://doi.org/10.1007/s42452-020-2302-6
Hamed KH, Rao AR (1998) A modified Mann-Kendall trend test for autocorrelated data. J Hydrol 204:182–196
Jain S and Kumar V (2012) Trend analysis of rainfall and temperature data for India. Current Science (Bangalore) 102(1):37–49
Kendall MG (1975) Rank correlation methods, 4th edition, Charles Griffin, London
Kumar S, Rathnam E (2019) Analysis and prediction of groundwater level trends using four variations of Mann Kendall tests and ARIMA modelling. J Geol Soc India 94:281–289. https://doi.org/10.1007/s12594-019-1308-4
Mann HB (1945) Nonparametric tests against trend. Econometrica 13(3):245–259. https://doi.org/10.2307/1907187
Pathak A, Dodamani B (2018) Trend analysis of groundwater levels and assessment of regional groundwater drought: Ghataprabha River Basin, India. Nat Resour Res 28. https://doi.org/10.1007/s11053-018-9417-0
Patle GT, Singh DK, Sarangi A, Rai A, Khanna M, Sahoo RN (2015) Time series analysis of groundwater levels and projection of future trend. J Geol Soc India 85(2):232–242. https://doi.org/10.1007/s12594-015-0209-4
Patra S, Sahoo S, Mishra P, Mahapatra SC (2018) Impacts of urbanization on land use/cover changes and its probable implications on local climate and groundwater level. J Urban Manage 7(2):70–84. https://doi.org/10.1016/j.jum.201
Salem GSA, Kazama S, Shahid S, Dey NC (2018). Impacts of climate change on groundwater level and irrigation cost in a groundwater dependent irrigated region. Agric Water Manage 208:33–42. https://doi.org/10.1016/j.agwat.2018.0
Salmi T, Määttä A, Anttila P, Ruoho-Airola T, Amnell T (2002) Detecting trends of annual values of atmospheric pollutants by the Mann-Kendall test and Sen's solpe estimates the excel template application MAKESENS. Publications on Air Quality 31
Sen PK (1968) Estimates of the regression coefficient based on Kendall's Tau. J Am Stat Assoc 63:1379–1389. https://doi.org/10.1080/01621459.1968.10480934
Sishodia RP, Shukla S, Graham WD, Wani SP, Garg KK (2016) Bi-decadal groundwater level trends in a semi-arid south Indian region: declines, causes and management. J Hydrol Reg Stud 8:43–58. ISSN 2214-5818
Taylor RG, Scanlon B, Döll P, Rodell M, van Beek R, Wada Y, Longuevergne L, Leblanc M, Famiglietti JS, Edmunds M, Konikow L, Green TR, Chen J, Taniguchi M, Bierkens MF, MacDonald A, Fan Y, Maxwell RM, Yechieli Y, Treidel H et al (2012) Ground water and climate change. Nat Clim Change 3(4):322–329. https://doi.org/10.1038/nclimate1744

Thakur G, Thomas T (2011) Analysis of groundwater levels for detection of trend in Sagar district, Madhya Pradesh. J Geol Soc India 77:303–308. https://doi.org/10.1007/s12594-011-0038-z

Tiwari V, Wahr JM, Swenson S, Singh B (2011) Land water storage variation over Southern India from space gravimetry. Curr Sci 101:536–540

Van Engelenburg J, Hueting R, Rijpkema S, Teuling A, Uijlenhoet R, Ludwig F (2018) Impact of changes in groundwater extractions and climate change on groundwater-dependent ecosystems in a complex hydrogeological setting. Water Resour Manage 32. https://doi.org/10.1007/s11269-017-1808-1

Wu W-Y, Lo M-H, Wada Y, Famiglietti JS, Reager JT, Yeh PJF, Ducharne A, Yang ZL (2020) Divergent effects of climate change on future groundwater availability in key mid-latitude aquifers. Nat Commun 11(1)

Chapter 18
Evaluation of Groundwater Contamination Due to Solid Waste Management

Isha Burman

Abstract It is essential to monitor the quality of the groundwater since it is a vital resource utilised to satisfy the demands of various sectors, including agricultural, industrial, and residential. Due to the leachates, solid waste disposal also has an impact on the quality of surface and groundwater in addition to overusing groundwater. The study's goal is to comprehend how the disposal of solid waste causes land and groundwater to become contaminated. Around urban areas, enormous amounts of solid trash are deposited. This municipal solid waste, which is commonly referred to as "garbage", is a natural by-product of anthropological activity and is dumped. The most typical way of disposing of solid waste is landfilling. The garbage collection facilities are open dumpsites because they have cheap running expenses and no equipment or knowledge to provide leachate collection systems. Dumping in the open is unattractive, unhealthy, and generally unpleasant. They draw pigs, rodents, insects, scavenger animals, and other pests. Hazardous chemicals that are dissolved or leached out of dumpsites by surface or subsurface runoff can be moved away from the dumpsites by surface or subsurface water percolating through the rubbish. Heavy metals are among these substances that are particularly pernicious and can cause bioaccumulation and biomagnifications. If the leachate migrates into groundwater, these heavy metals could pose a threat to the environment. The groundwater is at risk of contamination due to bore wells that are present at dump sites. The results of this study showed that poor solid waste management has a significant impact on a region's groundwater system.

Keywords Leachate · Solid waste · Landfills · Contamination · Groundwater

I. Burman (✉)
Department of Environmental Science and Engineering, Indian Institute of Technology (ISM) Dhanbad, Dhanbad, India
e-mail: ishaburmanjsr@gmail.com

P. Shukla et al. (eds.), *Environmental Processes and Management*, Water Science and Technology Library 120, https://doi.org/10.1007/978-3-031-20208-7_18

Abbreviations

SW	Solid waste
MSW	Municipal solid waste
WQI	Water quality index
GIS	Geographic information system
CO_2	Carbon dioxide
BIS	Bureau of Indian Standards
WHO	World Health Organization
GVMC	Greater Visakhapatnam Municipal Corporation
CPHEEO	Central Public Health and Environmental Engineering Organisation
DO	Dissolved oxygen
BOD	Biochemical oxygen demand
COD	Chemical oxygen demand
CH_4	Methane
CO	Carbon monoxide
H_2S	Hydrogen sulphide

18.1 Introduction

When there is irregular garbage disposal, which occurs in many nations across the world, we are required to take the solid waste that is generated nearby (Kumar and Prakash 2020). Due to constrained municipal resources, a deficiency of knowledge, and a deficiency of data available, waste management concerns frequently represent significant environmental challenges in many developing nations like India (Abdel-Shafy and Mansour 2018). In India, the dilemma of illegal dumping of solid waste is triggering water pollution. Environmental contamination, however, has started to have an impact on human health and welfare more recently. Although these contaminants are compounds that organically exist in the ecosystem, they become harmful when emitted in large quantities by humans. Due to the growing population expansion, urbanisation, and industrialisation, solid waste has turned out to be a comprehensive challenge at local, regional, and national level (Hoornweg and Perinaz 2012) In most regions in developing nations, the management of solid waste causes issues that harm human and mammal wellbeing and in the long run result in losses in terms of the economy, the environment, and biological diversity (Sharholy et al. 2008). Impact of garbage is influenced by illegal disposal methods and waste mix. Both immediate and long-term effects of garbage dumping on the environment have an impact on health (8, 9).

18.2 Scenario of Solid Waste in India

Due to the dense population, solid waste (SW) is a significant problem in Indian cities. Numerous aspects have been carried out in order to pinpoint this issue and assess the current situation (Sharholy et al. 2008). Municipal solid trash generation per capita grew significantly in Indian cities with increasing social standing and way of life for the populace. Estimates from the Ministry of Urban Affairs, Government of India, state that India produces about 1,000,000 Quintals of solid garbage every day, of which 90% is abandoned in the open (MoUD 2000). The challenges surrounding disposal have gotten much more difficult since more land is required for the final disposition of these SWs (Idris et al. 2004). The SW management systems in India have not evolved all that much, despite major social, economic, and environmental advancements (Narayan 2008). Leachate from undeveloped municipal SW landfill sites, which contains heavy metals, xenobiotics, aromatic hydrocarbons, phenols, and other contaminants, as well as landfill gas, which includes CO_2, CH_4, CO, H_2S, and other pollutants, poses serious environmental risks (Ubavin et al. 2018). The community health, the ecosystem, and the economy are all negatively impacted by the ineffective SW management systems currently in use (Biswas et al. 2010). The Ministry of Environment and Forests in India introduced the waste management and handling regulations (MoEF 2015). According to reports, India's urban centres generate 120,000 tonnes of solid trash every day, and the improper disposal of this material has polluted the environment in almost all of the cities.

18.3 Impact of Solid Waste on Groundwater Quality

The groundwater is used by the locals near the landfill for drinking water and other domestic needs. Leachate percolates into the aquifer system as a result of unconditional open dumping of trash without protective liners underneath. A number of biological and physico-chemical reactions begin right away following the landfilling of the MSW. One tonne of solid trash is thought to produce 0.2 m^3 of landfill leachate throughout the breakdown processes (Christensen 2005).

Inorganic compounds (heavy metals, chlorides, sulphates, etc.), organic matter, and xenobiotics are all present in landfill leachate, a highly contaminated thick liquid mixture that seeps out of decomposing solid wastes (Kjeldsen et al. 2002). Additionally, if unchecked or untreated, it seeps into the soil of the next receiver and interacts with it before reaching the groundwater table, diminishing their quality and upsetting the hydrological cycle. Because groundwater is a crucial resource for agriculture and drinking (Kamble et al. 2020), its contamination by MSW leachate causes a major menace to biotic ecosystems. It also has a negative impact on populated biodiversity (Oztürk et al. 2009). Therefore, it is crucial that landfill leachate is properly collected and treated.

18.4 Assessment and Monitoring of Groundwater

The necessity of the hour is also for routine groundwater well monitoring and quality assessment near the dumpsites. On a global scale, a number of scientific research (Christensen et al. 2005) are being conducted to determine how MSW leachate pollution affects aquatic bodies. The geological structure through which groundwater streams and anthropogenetic events in the groundwater both affect the spatial variance of groundwater quality (Sharholy et al. 2007). The best environmental criterion and one of the most useful instruments for describing the water quality state for drinking purposes is the water quality index (WQI). One number, the WQI, reflects the inclusive water quality at a particular place. It simplifies complex data on water quality into evidence that the general public can use and comprehend, and it aids in the creation of environmental management plans to reduce groundwater pollution.

Other approaches, such as heavy metal pollution indices like the degree of contamination and the heavy metal evaluation index, have a substantial influence on regulating the level of pollution in groundwater resources.

A powerful combination for evaluating and routinely monitoring the quality of groundwater is the geographic information system (GIS) in conjunction with the IDW interpolation technique. Huge data sets are converted into geographical projections using a less time-consuming and more affordable approach, allowing for the observation of pollution patterns and relationships. Additionally, it aids in locating potential sources and origins of pollutants. The best approach is to carry out a GIS-based learning to track the water quality's tendency to change over time. For environmental managers and decision-makers, this contemporary technique greatly facilitates precise monitoring and prompt decision-making.

A research was conducted at the Ghazipur landfill site by Banerjee (2021) on municipal SW management, disposal, and effects. In this study, the authors looked at the economic impacts of noise, air, soil, and groundwater pollution on the local population. The Guwahati waste disposal facility Boragaon was used for the analysis of the aforementioned variables. They deduced from the analysis that the environmental impact of the MSW on these sites is negative. Additionally, they discovered that both sites had a detrimental impact on locals' quality of life and that an increase in the volume of MSW in the near future would make them even more of an environmental danger. In the Pathardi area of Nashik, Maharashtra, India, researchers Borawake et al. (2015) assessed the quality parameters of groundwater for household and agricultural use. The study was conducted at ten distinct sites around the Pathardi district, close to the municipal corporation's composting initiative in Nashik City. During the pre-monsoon season (May month), they collected water samples from wells and bore wells and examined them for parameters including Ca^{2+}, Mg^{2+}, Cl, and NO_3 presence. The outcomes were contrasted with IS 10500 criteria from 2012. (BIS). The groundwater quality at the study location was found to be degraded as a result of this study. This was brought on by an overabundance of TH, HCO^{3-}, Ca^{+}, Mg^{2+}, Total coliforms, and *E. coli*. In certain regions, the groundwater is unfit for human consumption because of an excess of these factors. The effect of landfill leachate on the groundwater in Kolkata, India, was studied by De et al. (2017). In the 2014 pre-monsoon, monsoon, and post-monsoon seasons, they examined groundwater samples for twenty-two physico-chemical parameters. They evaluated the effects of the leachate and discovered that nearly all of its physico-chemical properties altered with time. The researchers discovered that groundwater samples were contaminated with Hg and Mn, demonstrating the negligible influence of redox regulation on the presence and movement of heavy metals. They also found that most groundwater samples were unsafe for drinking when they compared the physico-chemical parameters to those recommended by the World Health Organization (WHO) and the Bureau of Indian Standards (BIS). An overview study on the dangers that dump sites pose to groundwater and their effects on human health was engraved by Kumari et al. (2017). They looked at numerous studies on the negative impacts on human health of groundwater contamination at landfill sites, largely owing to open dumping or improper landfills in India and other countries. They discovered from the investigation that numerous studies have proven that there is a risk of adverse health impacts in inhabitants. These contaminants pose a greater threat to youngsters and pregnant women, and new-born babies are more likely to be at risk. A case study on the evaluation of groundwater quality parameters in the Andhra Pradesh, India, was conducted by Satyanarayana et al. (2013). The outcomes of the samples were compared to the water quality requirements set forth by the WHO, BIS, and CPHEEO. In the vicinity of the GVMC, they have taken water samples from bore wells. By modifying established methodologies, they examined a number of physico-chemical parameters in this study, including pH, EC, and Manganese. Researchers Pandey et al. (2013) studied how municipal SW affected the quality of subsurface water near the dump site. In order to determine the effects of MSW on the groundwater resources at that area, groundwater samples were taken in and around the Khermai Road dump. The study's goal was to examine how landfills in residential areas closer to Satna city, a landfill site, pollute underground water. To determine the quality of the underground water, they evaluated the physical and chemical characteristics of the samples. According to the study, a few indicators, including TDS, and magnesium concentration, should be over the recommended limits of the WHO and Indian Measures for Drinking Water (BIS-10500:1991). The investigation came to the additional conclusion that the MSW now has little influence on the subsurface water quality.

18.5 Effects of Decomposition of Waste Products on Groundwater Quality

Most current methods of disposal for rubbish result in the transfer of breakdown products following their creation inside the waste. In addition to any created leachate, gas rises into the atmosphere and seeps into the earth. The nature and amount of the pollutants produced in the fill as well as the closeness of the groundwater to the landfill are the main determinants of the degree of groundwater quality damage. Leaching may be used to remove some of the organic and inorganic material from the waste before it decomposes. As the substance decomposes, more will eventually be released. The kind of waste, the rate of leaching, and the quantity of leachable material available will all affect how much the water quality is impaired. The fulfilment of the biochemical oxygen requirement is necessary for the bacterial breakdown of organic substances leached from the trash. The free oxygen present in the incoming water satisfies this oxygen need. A significant organic load will reduce the available free oxygen and DO, resulting in anaerobic conditions. Mineral leachate is virtually always permanent, in contrast to organic leachate, which will stabilise with time. However, dispersion and mixing with fluids of greater quality might minimise the severity of the damage. Groundwater extraction may also reduce and potentially even eliminate the degree of damage. In general, leachate's impacts on receiving water include increases in mineral concentrations, which lead to a decline in quality and a reduction in the water's appropriateness for beneficial uses.

18.6 Effects of Gas on Groundwater

The presence of free carbon dioxide may contribute to the acidity of groundwater. The aggressiveness of water is increased by excessive acidity (excess free carbon dioxide), which speeds up the corrosion of iron and steel and the solvent action on calcium carbonate in concrete. Over 20 ppm of free carbon dioxide can quickly corrode iron, steel, and concrete, necessitating preventative measures. The existence of carbonates, bicarbonates, and hydroxides is the main source of alkalinity. Alkalinity mostly takes the form of bicarbonates. Waters that are very alkaline are unpleasant. Several instances of carbon dioxide affecting groundwater quality have been reported by different researchers.

18.7 Conclusions

More research is urgently needed to determine the amount, quality, and impact of landfill leachates and gas on the quality of groundwater. By aerobic and anaerobic organisms, the organic components in waste are reduced to simple substances that cannot further breakdown. Gases and soluble organic and inorganic chemicals are some of these decompositional by-products. Decomposition by-products may dissolve in water if there is enough of it, creating leachate, an aqueous solution. Organic matter, chloride, sulphate, potassium, calcium, and salt are the main substances that are leached from garbage. Temperature, moisture content, waste content, and aeration all directly affect how much gas is produced. When water is permitted to travel through the decomposed material in sufficient quantities to ultimately reach the local groundwaters, waste decomposition products are often a problem. Inadequately managed landfills, where leachate produced by the fill is allowed to escape and seep into the surrounding and underlying earth, pose the biggest hazard to groundwater. Adequate laws must be passed and put into practice in order to manage the rising amounts of trash in emerging nations and avoid environmental degradation. It is necessary to implement an integrated waste management strategy that consists of a hierarchical and coordinated series of measures to cut down on pollution. Leachate collection and treatment facilities should be included when building a new dumping site to ensure that the produced leachate has the least possible effect on water sources.

References

Abdel-Shafy HI, Mansour MSM (2018) Solid waste issue: sources, composition, disposal, recycling, and valorization. Egypt J Pet 27:1275–129

Banerjee A (2021) Impact of municipal solid waste landfill on surrounding environment: a case study. In: Patel S, Solanki CH, Reddy KR, Shukla SK (eds) Proceedings of the Indian geotechnical conference 2019. Lecture notes in civil engineering, vol 134. Springer, Singapore. https://doi.org/10.1007/978-981-33-6370-0_23

Biswas AK, Kumar S, Babu SS, Bhattacharyya JK, Chakrabarti T (2010) Studies on environmental quality in and around municipal solid waste dumpsite. Resour Conserv Recycl 55:129–134

Borawake A, Gaikwad VB, Patil S, Anjana K (2015) Assessment of groundwater quality of Pathardi Region of Nashik, Maharashtra, India. 4(7). July 2015, www.ijsr.net

Christensen HA (2005) Generalized water-level contours, September–October 2000 and March–April 2001, and Long-term water-level changes, at the U.S. Air Force Plant 42 and Vicinity, Palmdale, California. U.S. GEOLOGICAL SURVEY, Scientific investigations report 2005–5074, Sacramento, California

Christensen TH, Cossu R, Stegmann R (2005) Landfilling of waste: leachate. CRC Press

De S, Maiti SK, Hazra T, Dutta A (2017) evaluation of the impact of landfill leachate on groundwater quality in Kolkata, India. Pollution 3(3):443–452. Summer 2017, https://doi.org/10.7508/pj.2017.03.009, ISSN 2383-451X, Online ISSN 2383-4501, Web page: https://jpoll.ut.ac.ir, Email: jpoll@ut.ac.ir, March 2017

Gautam SP, Bundela PS, Pandey AK, Jamaluddin Awasthi MK, Sarsaiya S (2012) Diversity of cellulolytic microbes and the biodegradation of municipal solid waste by a potential strain. Hind Pub Corp Int J Microbiol 325907:1–12

Han Z, Ma H, Shi G, He L, Wei L, Shi Q (2016) A review of groundwater contamination near municipal solid waste landfill sites in China. Sci Total Environ 569–570:1255–1264

Hoornweg D, Perinaz BT (2012) What a waste: a global review of solid waste management. Urban development series, knowledge papers no. 15. World Bank, Washington, DC. © World Bank, 2012

Idris A, Inane B, Hassan MN (2004) Overview of waste disposal and landfills/dumps in Asian countries. Mater Cycles Waste Manag 16:104–110

Kamble SB, Saxena PR, Kurakalva RM, Shankar K (2020) Evaluation of seasonal and temporal variations of groundwater quality around Jawaharnagar municipal solid waste dumpsite of Hyderabad city, India. SN Appl Sci 2(3):1–22

Kjeldsen P, Barlaz MA, Rooker AP, Baun A, Ledin A, Christensen TH (2002) Present and long-term composition of MSW landfill leachate: a review. Crit Rev Environ Sci Technol 32(4):297–336

Kumar S, Bhattacharyya JK, Vaidya AN, Chakrabarti T, Devotta S et al (2009) Assessment of the status of municipal solid waste management in metro cities, state capitals, class I cities, and class II towns in India: an insight. Waste Manag 29(2):883–895

Kumari P, Gupta NC, Kaur A (2017) A review of groundwater pollution potential threats from municipal solid waste landfill sites: assessing the impact on human health. Avicenna J Environ Health Eng 4(1):e11525

Kumar M, Prakash V (2020) A review on solid waste: its impact on air and water quality. J Pollut Eff Cont 8:252. https://doi.org/10.35248/2375-4397.20.8.252

Mattiello A, Chiodini P, Bianco E, Forgione N, Flammia I et al (2013) Health effects associated with the disposal of solid waste in landfills and incinerators in populations living in surrounding areas: a systematic review. Int J Public Health 58:725–735

Ministry of Environment and Forests (MoEF) (2015) The gazette of India. Municipal solid waste (Management and Handling) rules, New Delhi, India

MoUD (2000) Manual on municipal solid waste management, the expert committee constituted by Ministry of Urban Development, Government of India

Narayan T (2008) Municipal solid waste management in India: from waste disposal to recovery of resources? Waste Manage 29:1163–1166

Oztürk G, Ozozen O, Minareci E (2009) Determination of heavy metals in fish, water and sediments of Avsar Dam Lake in Turkey. Iran J Environ Health Sci Eng 6(2):73–80

Pandey RK, Tiwari RP, Kirloskar SG (2013) Impact of municipal solid waste on subsurface water quality near the landfill site. Int J Eng Res Technol (IJERT) 2(11). ISSN 2278-0181

Raman N, Narayanan DS (2008) Impact of solid waste effect on ground water and soil quality nearer to pallavaram solid waste landfill site in Chennai. Rasayan J Chem 4:828–836

Satyanarayana P, Appala Raju N, Harikrishna K, Viswanath K (2013) Urban groundwater quality assessment: a case study of greater Visakhapatnam municipal corporation area (GVMC), Andhra Pradesh, India. Int J Eng Sci Invention 2(5):20–31. ISSN (Online) 2319-6734, ISSN (Print) 2319-6726. www.ijesi.org

Sharholy M, Ahmad K, Vaishya R, Gupta R (2007) Municipal solid waste characteristics and management in Allahabad, India. Waste Manag 27(4):490–496

Sharholy M, Ahmad K, Mahmood G, Trivedi RC (2008) Municipal solid waste management in Indian cities—a review. Wast Manag 28(2):459–467

Singh CR, Dey M (2014) Surface water quality with respect to municipal solid waste disposal within the imphal municipality area. Int J Sci Res Pub 4(2)

Ubavin D, Agarski B, Maodus N, Stanisavljevic N, Budak I (2018) A model for prioritizing landfills for remediation and closure: a case study in Serbia. Integr Environ Assess Manag 14(1):105–119

Youcai Z, Ziyang L (2017) Chapter Five——Pollution control and resource recovery for landfill gas. In: Pollution control and resource recovery. Municipal Solid Wastes Landfill, pp 227–319

Chapter 19
Groundwater Toxicity Link to Epidemiology of Parkinson's Disease

Poonam Yadav, Akchhara Pandey, Anusha Ramdoss, Mounika Aradala, Bishal Pokharel, M. D. Deepthi Nair, Tamanna Tazin, Farzaneh Dadvar, Farima Fakhri, Rukhsana Miraj Uddin, Nermeen Kolta, and Nirupama Nayudu

Abstract *Background* Groundwater is described as an unsaturated liquid that exists out of sight and below land surface. It appears as a layer of water that accumulates at depths between 5 and 500 feet below the land surface and often contains halogens in concentration hazardous to humans. The most common source of halogens, chlorine and bromine, are found in local groundwater at levels which exceed EPA drinking

P. Yadav
Department of Neurology, Apex Hospital, Jaipur, Rajasthan, India

A. Pandey (✉)
Department of Pharmacology, Institute of Medical Sciences, BHU, Varanasi, Uttar Pradesh, India
e-mail: akchharaa@gmail.com

A. Ramdoss
PSG Institute of Medical Science and Research, Coimbatore, India

M. Aradala
University of Soochow, New Taipei, China

B. Pokharel
Department of Neurosurgery, Bhaktapur Cancer Hospital, Bhaktapur, Nepal

M. D. Deepthi Nair
Department of Child Neurology, Seattle Children's Research Institute, Seattle, USA

T. Tazin
Department of Internal Medicine, Greenville Community Shelter Clinic, Greenville, NC, USA

F. Dadvar
University of Toronto, Kensington Eye Institute, Toronto, Canada
e-mail: fdadvar@kensingtonhealth.org

F. Fakhri
Department of Neuroscience, Kerman University of Medical Science, Kerman, Iran

R. M. Uddin
Women Medical College, Peshawar, Pakistan

N. Kolta
Department of Internal Medicine, MM Jersey City Breathing Center, Jersey, USA

N. Nayudu
Zhengzhou University, Zhengzhou, China

P. Shukla et al. (eds.), *Environmental Processes and Management*, Water Science and Technology Library 120, https://doi.org/10.1007/978-3-031-20208-7_19

water guidelines for lifetime exposure. When present in high concentration over long periods of time, these contaminants can cause multisystem disorders. *Objective* This chapter's purpose is to contextualize the fundamental mechanism of organic molecules found in groundwater over the period of time due to use of pesticides and insecticides. As a result of conditioning, molecules incorporate into physiology of human body and its effects on neurobiology. *Discussion* The covering knowledge on increment of environmental pH and risks of nutrient deficiencies identifies a problematic model of groundwater and its chemistry. Lack of nutrient uptake or loss from digestive system of animal and human body mounts for exploration of metal biology of soil and water. Over the time period, groundwater became an important source for domestic and irrigation purpose. However, rapid increase in population growth led to rapid industrial and economic growth, hence tremendous use of groundwater. The largest natural groundwater calamities in recorded history have been caused by metal poisoning of groundwater in the vast plain built by Ganga and Brahmaputra River in India and also fluvial plains of Padma and Meghna in Bangladesh. According to data from the Parkinson Environment and Gene Study, those who drank pesticide-tainted well water that has been around for a while in California's central valley possess high potential for development of Parkinson's disease than people who did not (Chen in J Parkinsons Dis 8:1–12, 2018). The epidemiological studies on progression of non-familial form of PD emphasize on prodromal period of toxin exposure. Access point of pesticides is via eating, drinking, nose, and skin contact. Various animal studies showed these entry points for pesticides initiate pathogenesis of synucleinopathy via olfactory-gut-brain axis. The objective is to discuss effects of environmental geochemistry on neurological well-being of human health in developing countries. *Conclusion* Analysis of exposure is easy to quantify through advanced experimental methods versus adequately measuring the organic molecule along with its persistence use affecting the neurobiological system. Overall exposure and monitoring over a very long period can align our understanding of gene-environmental etiology causing neurodegenerative diseases.

Abbreviations

PD	Parkinson's disease
SN	Substantia nigra
DDT	Dichlorodiphenyltrichloroethane
EPA	Environmental Protection Agency
WHO	World Health Organization
Na	Sodium
Ca	Calcium
K	Potassium
IMA	Indian Medical Association
ROS	Reactive oxidation species
TCA	Tricarboxylic Acid

DAT	Dopamine transporter
BBB	Blood-Brain Barrier
NITI	National Institute of Technology
HQ	Head Quarter
TR	Targeted Risk
HI	Hazard index
CA	Correlation analysis
FA	Factorial Analysis

19.1 Introduction

India makes up 15% of the global population, but it only possesses 2.5% of the world's land and just 6% of its water resources. Based on April 2015, the country's potential annual river water availability is 1869 BCM/year; however, its actual useable water availability is 1123 BCM/year. 433 BCM/year is the portion of groundwater that is useable. The yearly contribution of rainfall to groundwater is 68% (Suhag 2016).

According to Flora SJS study, 63 samples were taken during the southwest monsoon from sedimentary formations. The hard rock aquifers were examined for the presence of heavy metals such as lithium, beryllium, aluminum, Rb, strontium, cesium, barium, lead, manganese, iron, chromium, zinc, gallium, copper, arsenic, nickel, and cobalt. While Zn predominated in sedimentary formations, Ba predominated in hard rock aquifers, with concentrations ranging from 441 to 42,638 g/l to 44 to 118,281 g/l. In both formations, the Fe, Ni, Cr, Al, and Ni contents were higher than allowed. To prevent the potential health risks connected with intake, statutory limitations of these concentrations of contact zone and long-term monitoring for the threshold value are necessary. According to WHO, arsenic safe limit is 0.01 mg l^{-1}, but in India due to poor availability of potable drinking water, the acceptable level is 0.05 mg l^{-1} (Flora 2022). Multiple studies have been conducted on the quality of potable water and the effect it has on the population consuming it. These studies have assessed the risk associated with utilization of poor quality of water for drinking and cooking purposes.

Interference and exposure of organic molecules such as mercury, drug molecule, and alcohol prenatally cause metabolic changes in neuronal development and its neurotransmitters. Likewise, these heavy metals and organic molecule inhibit the nerve cells from communicating through electrical signals. With the help of ion channel, these nerve cells generate signals. These ion channels are voltage dependent and get activated through potential difference generated by ion (Na, Ca, K) concentration. These changes across membranes contribute to further alteration in biochemical mechanism and affect processes of cognition, memory circuit and behavior.

Due to the simplicity of use and capacity for large-scale data comparisons, the multivariate method models are used for extremely challenging data to accomplish number tables with information (Bingo 2013). The most commonly used statistical methods are factor analysis, cluster analysis, and correlation analysis for identifying what is causing the increasing poor quality of groundwater, among multivariate approaches. The correlations between hydro-chemical variables are analyzed using correlation in order to pinpoint their possible causes. Comparison and dissimilarities among the samples are assessed by CA. FA is used to identify probable significant natural and man-made elements (such as hydrogeochemical processes) that affect groundwater quality without prior information on number of sources or the pollutants' source characteristics. There have been numerous studies conducted throughout the world using multivariate statistics to pinpoint the groundwater trace element sources. These investigations demonstrated that hydrogeochemical processes and possible sources of contaminants in water could both be found using multivariate techniques. For instance, use of multivariate statistical analysis helped to evaluate likely source of toxins in few chosen areas of Northwest Iran's groundwater of shabestar region. The results demonstrated that effects of weathering and dissolution of rocks formed into silicates and its evaporites, causing groundwater toxicity. Furthermore, through ion exchange the salinity of water increased and the pH skewed towards alkalinity. 10% of the total variation in groundwater quality was caused by the effects of nitrate and zinc in fertilizers and agrochemicals.

Sodium (Na) channel gates are the primary site for the action of pesticides such as pyrethroid, aldrin, dieldrin, and dichlorodiphenyltrichloroethane (DDT). During rising phase of action potential, these organic molecules keep the gate open for extended period of time causing depolarization and hyperexcitation of cell. This state of sodium channel causes behavioral changes in rodents such as hypersensitivity, tremor, convulsions, choreoathetosis, and excessive salivation. Though human cells are not very sensitive to these kind of changes in sodium channel, some percentage of mammals shows sensitivity to pyrethroids. The pyrethroids cause two kinds of behavior: 1st is aggression, hypersensitivity, tremor, and convulsions, and 2nd is choreoathetosis and hypersalivation.

19.2 Overview of Groundwater and Usage

The groundwater layering on hydrogeological setting has a vulnerable position. The layering starts with land surface, unsaturated zone, and surface water, followed by saturated zone with groundwater. The lowest layer beneath are the fracture rocks and gravel which is sandwiched with soil (Shrikant and Limaye 2013). The groundwater fills spaces between soil and fracture rocks below the unsaturated zone (Suhag 2016). Water travels through the rocks and fills in aquifers. The large spaces between the graveled stones, sand, and sandstone are connected which defines the permeability of surface hence called saturated zone. The hydrogeological setting in India is divided into two categories:

1. Hard rock aquifers of central peninsular India: It contains 65% of overall aquifer area. The hard rock formation is complex, which creates low water storage space.

Due to low water storage, in order to reach the water table, one must dig farther. Once the water table which is a boundary between soil surface and sediments of rocks, fall more than 2–6 meter, then the level of water drops too. This means one has to dig deeper to reach the water table. Moreover, due to poor permeability, there is limitation in recharge from rainfall and hence aquifer dry out with continuous usage.

2. Alluvial aquifers of indigo gangetic plains: It is found in northern India with significant storage in gangetic and Indus plains. Combination of water resource vulnerability along with excessive exploitation significantly reduces the recharge rates and makes the process irreversible (Suhag 2016).

Majority of groundwater, i.e., approx. 89%, is used in irrigation sector, remaining 9% for domestic use and 2% by industrial use. With Green revolution, extensive use of groundwater increased exponentially. Government provided incentives and subsidies with credits for equipment to boost farm production. These low power tariffs worsened the situation of water tables. This also led to overuse of fertilizers and pesticides which contaminated the groundwater with bacteria, heavy metals, and pollutants, leading to chronic multisystem disorder.

19.3 Overview of Groundwater Toxicity

The landowners have substantial power over groundwater. Water requirements by urban population are 50% versus rural domestic usage, which is 85% of groundwater. Usage of private wells is most risk for contamination with pesticides, as pesticide travels through soil. It can easily affect more than 100 m of nearby area. The monitoring of private well is not done unlike municipal water supplies. These exogenous contaminants have shown to be linked with Parkinson's disease; the research is backed up by animal studies. Various epidemiological studies showed relatively consistent relationship between people using private well water for a very long time who have 15–57% likely chances of getting Parkinson's disease than control. Stronger association was found with use of paraquat, trichloroethylene and tetrachlorethylene, rotenone and organochlorines, and much consistent with women (Goldman 2013). Heavy metal exposure (lead, cadmium, mercury, arsenic) in groundwater is characteristic of non-biodegradable products which can contaminate living system and damage the molecular level of living organisms.

Small towns in India, including Sukinda in Orissa and Vapi in Gujarat, are among the top 10 most polluted places in the world, according to Leading US Business magazine. Sukinda water contains high concentrations of chromium affecting more than 2.6 million people. Vapi seen to have high industrial pollution especially high mercury level, which is said to be 96 times higher than standards set by WHO. Also stated, West Bengal has that highest arsenic concentration than acceptable standards, in turn affecting a population of more than 50 million population. According to IMA (Indian Medical Association) report, the major causality of contamination in drinking water is due to poor disposal of industrial wastes. Based on the Indian toxicology report, there is enough awareness for the matter on groundwater contamination and ground radiation from nuclear testing but India lacks in decisive plans and program to aid with the development of preventive programs (Flora 2022).

Additionally, many organizations came to the conclusion that these heavy metals also contribute to fluorosis, chemical dermatitis, skin, lung, and throat malignancies, high incidence of abortions, infertility, and abnormal fetuses. Additionally, these heavy metals lessen energy at multisystem level. The metalloids cause the molecular damage of muscles and neurons causing imbalance of antioxidant and free radical production. These changes detoxify the protective reactive intermediates. As a result, ROS (reactive oxygen species) increases and causes cell death by apoptosis and other enzymatic reactions at cellular level also affecting release of neurotransmitter such as dopamine and also its regulation simultaneously. Neurological disease like Parkinson, Alzheimer's, metal deposition like disease such as Wilson disease, muscular dystrophy, and multiple sclerosis are all examples of degenerative neurological and muscular diseases caused by chronic oxidative stress.

According to several studies, human health can suffer significantly from exposure to potentially harmful chemicals, such as trace elements in water, and these impacts include a range of malignancies and multiple system involvement such as kidney, cardiac events, and neurological and generalized neurological impairment. Human health can suffer significantly from exposure to potentially harmful chemicals, such as trace elements in water, and these impacts include a range of malignancies, intellectual impairments, neurological, cardiovascular, kidney, and bone problems. An evaluation of the health risks can be used to estimate the likelihood of source, which release risk agents into the environment, how many risk agents will come into contact with human-environment boundaries, and the potential health effects of exposure to a mixture of trace elements. Numerous researchers have written about the risks posed to human health, are caused by these trace elements in groundwater (Esmaeili et al. 2018; Barzegar et al. 2017) used the two factors such as hazard quotient and target risk factor to assess the health risk of as pollution in drinking groundwater in southern Taiwan. Results indicated that TR levels exceeded the threshold value of 10E-6 and that HQ values for the 95th percentile were above the value of 1. They came to the conclusion that 0.01–7.5% of the population had HQ levels higher than 1, and 77.7–93.3% of people had TR values of 10E-6, placing them in the high cancer risk category. The results of the TR exposure estimates, implied that drinking groundwater put people at risk. In a rural part of Thailand's Ubon Ratchathani province, looked into the risks on human health caused by consuming water from shallow groundwater wells. They found that few of the wells with arsenic, copper, zinc, and lead had unsatisfactory non-carcinogenic health risk levels with HQs ranging from 0.004 to 2.901, 0.053 to 54.818, 0.003 to 6.399, and 0.007 to 26.80, respectively. In 58% of the wells, the hazard index (HI) values (range from 0.10 to 88.21) were higher than permitted (Liang et al. 2016).

19.4 Overview of Parkinson's Disease

In general, a syndrome of bradykinesia (slow voluntary movement) with rigidity or tremor is referred to as Parkinsonism in general. Idiopathic Parkinsonism, or Parkinson's disease, is Parkinsonism with a limited neurological manifestation. A disease that gradually destroys the brain's nerve cells which make the neurotransmitter, called Dopamine. Dopamine sends signals to the brain that regulate coordination and movement. Dopamine deficiency causes the following hallmark motor signs of Parkinson's disease: tremor during rest, bradykinesia, rigidity of the limbs (cogwheel rigidity), along with small handwriting, decreased facial expression, difficulty swallowing, and soft speech. With the progression of the disease, patient experiences postural instability and imbalanced shuffling gate, leading to falls causing more injuries.

19.4.1 Overall Disease Burden

In India, with a population of more than one billion, the population of PD is approx. 7 million (Behari et al. 2002), i.e., 70 per 100,000. 70% population is rural resident, of which a large number of populations live under the poverty line with an average income of $250. A total number of trained neurologists in India are about 1200, of which 400 work in major metro cities. Therefore, the burden of disease depicts the misery of the country. Due to lack of social security in India, drugs are expensive for low-income population. On comparison of cheaper living cost, treatment is expensive and increases exponentially as the disease progresses. On the face of odd circumstances, the resilience and ability to remain in balance of mind are praiseworthy.

19.4.2 Identifying Etiology

Identifying triggering factor for Parkinson's disease pathogenesis is multifactorial, and hence, it is complex. The methods for early identification of disease are elusive. Population of Parkinson's disease is growing exponentially with growing age, i.e., between 60 and 65 years. Based on epidemiological data, the experimental database is wide and inconsistent; thus, the plausible biological causes vary too. According to the database, Parkinson's disease has two main causes: environmental factors (which can be reversed) and hereditary factors. However, the experimental data observation demonstrated opposite causality, such as smoking, coffee consumption, intense exercise, ibuprofen use, plasma urate, and pesticide use which have an inverse connection with Parkinson's disease. Consequently, thorough monitoring in the upcoming years will aid in identifying the most prevalent etiological causes producing PD.

A history of using pesticides, herbicides, insecticides showed link to heightened potential for Parkinson's disease with respect to particular age. Pesticides showed high risk for Parkinson's disease between ages of 26 and 35, herbicides between ages 26 and 55, whereas insecticides usage demonstrated between the ages of 46 and 55 (Semchuk et al. 1992).

Tyrosine hydroxylase activity is upregulated in response to effects on the striatal dopaminergic system, which may result in a short-term rise in dopamine turnover or a temporary fall in dopamine levels as a short-term compensatory mechanism. This is crucial to consider in analyzing the mechanistic evidence of pesticide's impact of novel compound on development, of Parkinson's disease. This is important to take into account in epidemiological or experimental investigations.

19.4.3 Understanding Pathogenesis of Organic Molecule

The significant loss of pigmented neurons, particularly in the pars compacta of the substantia nigra (SN), is the primary pathologic characteristic of PD. The loss of pigmented neurons is accompanied by the appearance of Lewy bodies, which are substantial eosinophilic inclusions made of a variety of proteins, including neuro-filaments, alpha-synuclein fibrils, ubiquitin, parkin, and proteasomal components. The probable underlying cellular mechanisms of Parkinson's disease (PD) and the presence of external agents are outlined in Fig. 19.4.

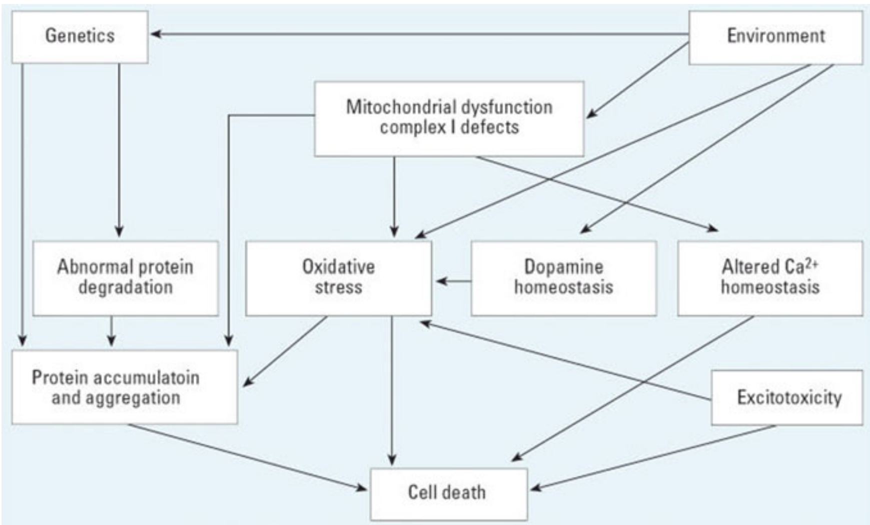

Fig. 19.4 Picture is inspired from (Betarbet et al. 2000)

The wide observational contribution of epidemiologic studies suggests association of pesticides and environmental toxins with PD implies defect in mitochondria complex 1. The prolonged chronic use of pesticides systemically inhibits the complex 1 during prodromal stage. This damage to complex 1 degenerates the selective nigrostriatal dopaminergic pathway located in substantia nigra (an area of the brain associated with voluntary movement) responsible for debilitating motor symptoms such as tremors, bradykinesia, and muscle rigidity. Rotenone is known potent inhibitor of mitochondrial TCA cycle enzymes; furthermore, it causes degenerative effect on nigral neurons damaging axons and accumulation of fibrillar cytoplasmic inclusion containing ubiquitin and alpha-synuclein.

19.4.4 Toxicological Evidence of Pesticides

The monitoring of data over decades at different point in time shows late-onset Parkinson's disease is triggered due to environmental factors, which is modifiable.

Rotenone: Naturally occurring pesticide easily penetrates biological membranes, inhibiting complex 1 systemically without needing dopamine transporter (DAT) to enter cytoplasm (Betarbet et al. 2000). At a low free rotenone concentrations of 20–30 nmol/L in the brain shows that rotenone affects striatal nerve ends more severely than nigral bodies. There were cytoplasmic inclusions containing synuclein that resembled pale bodies, which are progenitors to the Lewy bodies observed in individuals with Parkinson's disease, in the nigral neurons of rats with these lesions. Even when the rotenone therapy is stopped, rotenone-treated rats continued to exhibit anomalies in movement and posture that are typical of PD, whose severity was correlated with the number of pathologic lesions.

Rotenone and the inflammatory substance lipopolysaccharide jointly caused dopaminergic degeneration in mouse and rat neuron-glial cell cultures (Gao et al. 2002). According to Niehaus and Lange 2003, environmental and inflammatory agents such as lipopolysaccharide may influence in causing neurological disease PD. The formation of ROS, the free radical, and inflammatory mediators produced by microglia of the brain have been linked to toxicity caused by rotenone (Naylor 1995).

Paraquat: It is a potential neurotoxin which does not easily cross BBB. It causes severe pulmonary toxicity as per study by (Corsaniti et al. 1998). But majority of molecular structure changes by paraquat are formed outside BBB (Naylor 1995). In contrast to the mechanism of increased activity of four dopaminergic pathways in Parkinson's disease, when a neonatal mice dosed with paraquet on days 10–11 of gestation, it shows slowness and reduction in input model of striatum with release of DA (dopamine) and its metabolite. Although it causes neuronal cell death, it just does not depend upon common dopaminergic pathway of human brain to cause neurotoxicity (Bagetta etal. 1992; Calò et al. 1990; Corsaniti 1998).

Pyrethroid: It is not a dose-dependent insecticides. This insecticide inhibits dopamine and related metabolite in region of the brain causing marked damage to both dopaminergic and cholinergic pathways.

Mixture of pesticide (Paraquat and Maneb): Maneb is also an herbicide like paraquat and contains manganese dithiocarbonate, used widely geographically. Combined exposure causes decreased dopaminergic levels triggering reduced motor activity, also as central nervous depressant, proving relevant pathophysiology. This means mixtures of pesticides enhance the nigrostriatal dopaminergic pathway and cause significant neurotoxicity (Thiruchelvam et al. 2002).

Role of neuronal protein: According to (Uversky et al. 2001) study, he demonstrated Lewy body formation is an integral part of the disease and reactive system conditions for change in α-synuclein (neuronal protein), exaggerating formation of fibrils. Majority of these pesticides have a similar mechanism of action and hence increase risk for development of Parkinson's disease.

19.5 Conclusion

Based on the epidemiological studies, along with aging, exposure of environmental toxins showed significant multifactorial association with Parkinson's disease. However, because of inconsistent finding with the confounding variables like residents of rural area, farmers, and well water consumption, it is yet to be explored more for causal nature of pesticides use in relation to Parkinson's disease. Combined exposure of pesticides developed exaggerative effects and susceptibility in adults. Selective collection of all ages and reporting for extended period of time can provide appropriate sample size for adequate information on exposure and causes.

Identification of physiological mutation in voltage-gated channels also added significant amount of knowledge to pharmacological properties in mammals and insects. The distinct pharmacology exhibited by sodium channels in insects can serve as a source of inspiration for the research and development of novel insecticides. Additionally, research on the effects of new neurotoxins should advance our fundamental knowledge of sodium channel gating and pharmacological traits specific to insects. Numerous neurotoxins, including the present crop of pesticides, target sodium channels. Some peptides only affect sodium channels in insects and do not affect sodium channels in mammals (Bosmans et al. 2005).

The abrupt decrease in rainfall needed to replenish the city's aquifers is what is causing Bengaluru's impending disaster. A city that was formerly known for its thousand lakes has completely changed how much water is available due to population increase, droughts, and inefficient water use. The groundwater supply in New Delhi was also examined by NITI, and it was discovered to be equally severely depleted. Researchers from the National Institute of Technology (NITI) cautioned more than 20 million residents of New Delhi, the capital of the country, on a collision course with rising demand and declining moisture that is so uncompromising that it could run out of groundwater in two years. Critical groundwater supplies, which supply 40% of India's water, are depleting at unsustainable rates, according to NITI analysts.

References

Bagetta G, Corasaniti MT, Iannone M, Nisticò G, Stephenson JD (1992) Production of limbic motor seizures and brain damage by systemic and intracerebral injections of paraquat in rats. Pharmacol Toxicol 71:443–448

Barzegar R, Asghari Moghaddam A, Tziritis E, Fakhri MS, Soltani S (2017) Identification of hydrogeochemical processes and pollution sources of groundwater resources in the Marand plain, northwest of Iran. Environ Earth Sci 76(7):297

Behari M, Bhatnagar S, Muthane U, Deo D (2002) Experiences of Parkinson's disease in India. Lancet Neurol 1(4):258–262. https://doi.org/10.1016/S1474-4422(02)00105-9

Betarbet R, Sherer TB, MacKenzie G, Garcia-Osuna M, Panov AV, Greenamyre JT (2000) Chronic systemic pesticide exposure reproduces features of Parkinson's disease. Nat Neurosci 3(12):1301–1306. https://doi.org/10.1038/81834 PMID: 11100151

Bingöl D, Ay Ü, Bozbaş SK, Uzgören N (2013) Chemometric evaluation of the heavy metals distribution in waters from the Dilovası region in Kocaeli, Turkey. Mar Pollut Bull 68(1–2):134–139

Bosmans F, Martin-Eauclaire MF, Tytgat J (2005) The depressant scorpion neurotoxin LqqIT2 selectively modulates the insect voltage-gated sodium channel. Toxicon 45:501–507

Calò M, Iannone M, Passafaro M, Nisticò G (1990) Selective vulnerability of hippocampal CA3 neurones after micro-infusion of paraquat into the rat substantia nigra or into the ventral tegmental area. J Comp Pathol 103:73–78

Chen H (2018) The changing landscape of Parkinson epidemiologic research. J Parkinsons Dis 8:1–12

Corasaniti MT, Strongoli MC, Rotiroti D, Bagetta G, Nisticò G (1998) Paraquat: a useful tool for the in vivo study of mechanisms of neuronal cell death. Pharmacol Toxicol 83(1):1–7. https://doi.org/10.1111/j.1600-0773.1998.tb01434.x PMID: 9764419

Esmaeili S, Asghari Moghaddam A, Barzegar R, Tziritis E (2018) Multivariate statistics and hydrogeochemical modeling for source identification of major elements and heavy metals in the groundwater of Qareh-Ziaeddin plain NW Iran. Arab J Geosci 11:5

Flora SJS (2022) Challenges in the field of toxicity of metals in India including the development of new treatment. J Environ Biol 43(4):III–V. https://doi.org/10.22438/jeb/43/4/Editorial

Gao H-M, Hong J-S, Zhang W, Liu B (2002) Distinct role for microglia in rotenone-induced degeneration of dopaminergic neurons. J Neurosci 22:782–790

Goldman (2013) Parkinson's disease. In: Effects of persistent and bioactive organic pollutants on human health. Wiley, pp 471–513. https://doi.org/10.1002/9781118679654.ch18

Liang CP, Wang SW, Kao YH, Chen JS (2016) Health risk assessment of groundwater arsenic pollution in southern Taiwan. Environ GeoChem Health 38:1271–1281

Naylor JL, Widdowson PS, Simpson MG, Farnworth M, Ellis MK, Lock EA (1995) Further evidence that the blood/brain barrier impedes paraquat entry into the brain. Hum Exp Toxicol 14:587–594

Semchuk KM, Love EJ, Lee RG (1992) Parkinson's disease and exposure to agricultural work and pesticide chemicals. Neurology 42:1328–1335

Suhag R (2016) Overview of ground water in India. Working Papers [Internet]. Available from: https://ideas.repec.org/p/ess/wpaper/id9504.html

Shrikant D, Limaye D (2013) A brief history of Indian hydrogeology. In: Howden N, Mather J (eds) History of hydrogeology. IAH, Goring, UK, pp 127–133

Thiruchelvam M, Richfield EK, Goodman BM, Baggs RB, Cory-Slechta DA (2002) Developmental exposure to the pesticides paraquat and maneb and the Parkinson's disease phenotype. Neurotoxicology 23:621–633

Uversky VN, Li J, Fink AL (2001) Evidence for a partially folded intermediate in alpha-synuclein fibril formation. J Biol Chem 276(14):10737–10744. https://doi.org/10.1074/jbc.M010907200 Epub 2001 Jan 10 PMID: 11152691

Chapter 20
GIS for Groundwater Resources and Contamination Risk Assessment

Shahid Ul Islam and Sumedha Chakma

Abstract Natural resources are gradually becoming insufficient, and the results of human actions are omnipresent. In such a case, the focus should be on how to reduce impacts and improve sustainability using the best available tools for environmental characterization, impact assessment, and plan development. A clear understanding of the process, how water is collected and stored, and an understanding of how runoff changes in mountainous areas is useful for developing water resource use and planning. Groundwater is mainly used for drinking and irrigation purpose. Pollution in groundwater can lead to unsafe drinking water, water supply loss, excessive cleaning cost, and increase in cost of other water supply sources and/or potential health risks. With the Geographic Information Systems (GIS) application, better and innovative methods can be developed to process the huge amount of data and information related to groundwater. This chapter provides a comprehensive review of GIS applications for groundwater resource assessment, exploration, groundwater contamination risk assessment, and protection planning. In this chapter, the relevant literature in different locations and in various ways has been collected to provide a comprehensive review. Conclusions are drawn based on identified gaps and on research prospectus in groundwater assessment of groundwater resources and pollution risk using GIS.

Keywords GIS · Groundwater · Modeling · Contamination · Water quality

S. U. Islam (✉) · S. Chakma
Department of Civil Engineering, Indian Institute of Technology (IIT) Delhi, Hauz Khas, New Delhi 110016, India
e-mail: shahid@bgsbu.ac.in

S. Chakma
e-mail: Sumedha.Chakma@civil.iitd.ac.in

S. U. Islam
Department of Civil Engineering, Baba Ghulam Shah Badshah University, Rajouri, Jammu and Kashmir, India

P. Shukla et al. (eds.), *Environmental Processes and Management*, Water Science and Technology Library 120, https://doi.org/10.1007/978-3-031-20208-7_22

Abbreviations

GIS	Geographic Information Systems
WQI	Water quality index
WHPA	Wellhead protection areas
GWQI	Groundwater quality index
RS	Remote sensing
AVI	Aquifer vulnerability index
MCET	Multi-criteria evaluation technique
AHP	Analytical hierarchy process
CT	Catastrophe theory

20.1 Introduction

The modern era of industrialization has led to increasing scarcity of natural resources, and human actions have consequences everywhere (Marín-Beltrán et al. 2022). Due to global warming, climate change, population growth, urbanization, and industrialization, managing water resources is a difficult challenge (Salem et al. 2022). In such a condition, focus should be on how to reduce the impacts and improve sustainability by using the best available tools for environment characterization, impact assessment, and plan development (Olabi et al. 2022) because safe drinking water is not available to one by third of global population (WHO 2019). The groundwater can fulfill the water requirements of two-third of earth's total population (Adimalla 2019). Groundwater management includes evaluating the importance of the groundwater system in hydrological balance, predicting long-term pumping capability and effects, and assessing conditions of water quality (Johnson 2016). Large quantities of good quality data should be available for reliable groundwater analysis and for validation (Tiyasha et al. 2020). For hydrogeological studies, data should be rational and in logical structure in a commuting nature available (Gogu et al. 2001). Placing all data in a consistent logical structure supported by a computer environment provides an important tool for study of hydrogeological features and helps to ensure accuracy and accessibility (Gogu et al. 2001). GIS has found widespread use for groundwater assessments because of large amounts of data (Pinder 2002; Jha et al. 2007). GIS technologies, tools, and practices provide significant advantages for reserve inventory, modeling, and communication of options to participating agencies and interested people (Tomlinson 2007). With the digital representation of maps and other spatial information, connections can be established between different activities based on their geographic proximity (Elwood 2009). The geographic view of the data provides new insights and explanations which are not recognized without GIS but are critical for understanding and managing different activities and resources (Franch-Pardo 2020). GIS has completely modified our approach for dealing with environmental reserves and particularly hydro-resources (Jha et al. 2007). Better methods can be developed and innovative approaches to process huge amounts of data and information related to groundwater by using GIS (Thakur et al. 2017).

A GIS is a spatial data model, together with a set of operators for the model. GIS is used for conceptualization and modeling of geographic reality (Morehouse 1992). A Geographic Information System is a computerized system utilized to collect, store, retrieve, evaluate, and display spatial data (Clarke 1995). GIS is “an information system that is designed to work with data referenced by spatial or geographical coordinates” (Star and Estes 1990). GIS “manipulates data about points, lines, and areas to retrieve data for ad hoc queries and analyses” (Duecker 1987). Five basic components of GIS are “data, hardware, software, procedure, and people” (Dangermond 1988). GIS is “an institutional entity, reflecting an organizational structure that integrates technology with a database, expertise, and continuing financial support over time” (Carter 1989). GIS can store, organize, extract, categorize, handle, evaluate, and represent large spatial data and information in a clear manner (Howari et al. 2007). GIS is ideal for the continuous updating and recalculation of different scenarios which are typically important in water resource projects (Warwick and Haness 1994). GIS stores, evaluates, and visualizes a huge amount of different electronic data and displays them on a map (Rifai et al. 1993). An internal as well as external information exchange of GIS in an organization is shown in Fig. 20.1.

GIS is considered crucial and productive tool for advanced and complicated groundwater systems (Machiwal et al. 2018). The uses and capabilities of GIS in hydrogeology and hydrological modeling are just emerging, and many applications have already been developed (Bhasker et al. 1992; Gossel et al. 2004). Contamination of groundwater with nitrates is a global hazard and is primarily caused by application of excessive fertilizers. (World Health Organization 1985). GIS and water quality index are used to estimate groundwater resources (Adimalla and Taloor 2020). Many researchers use geospatial techniques to spatially estimate groundwater parameters (Mehrjardi et al. 2008; Taghizadeh et al. 2008; Gorai and Kumar 2013; Abbasnia

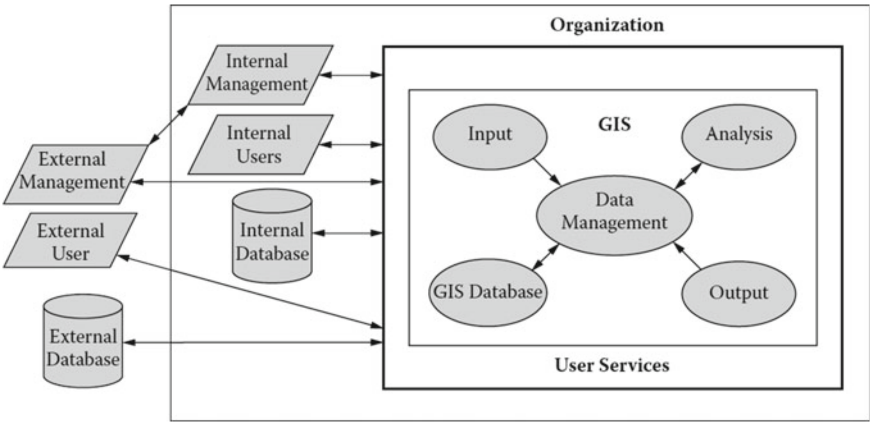

Fig. 20.1 Internal and external information exchange of GIS in an organization (Aronoff 1991)

et al. 2019; Ugochukwu et al. 2019). The DRASTIC approach is widely used to evaluate internal exposure and is commonly used to assess an aquifer's vulnerability (Aller et al. 1987; Lasserrea et al. 1999; Baalousha 2006; Nobre et al. 2007; Assaf and Saadeh 2009). Horton (1965) developed the numerical tool water quality index (WQI) which provides a complete model for groundwater quality analysis (Deshmukh et al. 2016).

There are only a few good reviews of GIS applications for groundwater assessment and evaluation (Engman and Gurney 1991; Tsihrintzis et al. 1996; Watkins et al. 1996; Pinder 2002; Jha et al. 2007). The primary purpose of this chapter is to highlight GIS techniques and provide a comprehensive overview of their applications in groundwater hydrology. Comprehensive description of the previous literature on GIS applications for exploration and assessment of groundwater resource has been provided. Also, review of GIS application for groundwater pollution risk evaluation and protection planning is discussed, and literature related to GIS application for groundwater is collected and presented it in a comprehensive manner.

20.2 Applications of GIS in Water Resources

GIS technology has significant applications in groundwater for assessing groundwater pollution risks, planning and detection of hazards, and for protection assessment (Chen et al. 2004; Jha et al. 2007). Tsihrintzis et al. (1996) gave an outline of GIS applications for water resources. In order to identify likely causes of pollution along with the socioeconomic value of groundwater wells, a risk map was provided based on the risk and vulnerability map (Ducci 1999). Integration of conventional hydrochemical assessment with statistical component assessment can be a reliable tool for finding causes that affect groundwater chemistry (El-Rawy et al. 2019).

The combination of GIS and neural ambiguity methods involved assessing the sensitivity of the models which helps to present in a three-dimensional framework the results (Dixon 2005a). GIS provides excellent opportunities for mapping and modeling groundwater pollution (Roy et al. 2022). However, the results or simulations presented should not replace an empirical interpretation. Appropriate field data results should be used to evaluate planned maps (Dixon 2005b). Gebru and Tesfahunegn (2020) analyzed GIS-assisted WetSpass model and a powerful tool for estimating spatial variables. These conclusions are important for predicting the effective consumption of water resources for meeting different needs of the population for selected area. The procedure applied by the researchers to identify potential groundwater zones and selecting suitable locations for groundwater recharge is shown in Fig. 20.2. The dashed arrows as shown in the figure represent the possible step as it is not followed always due to field data unavailability.

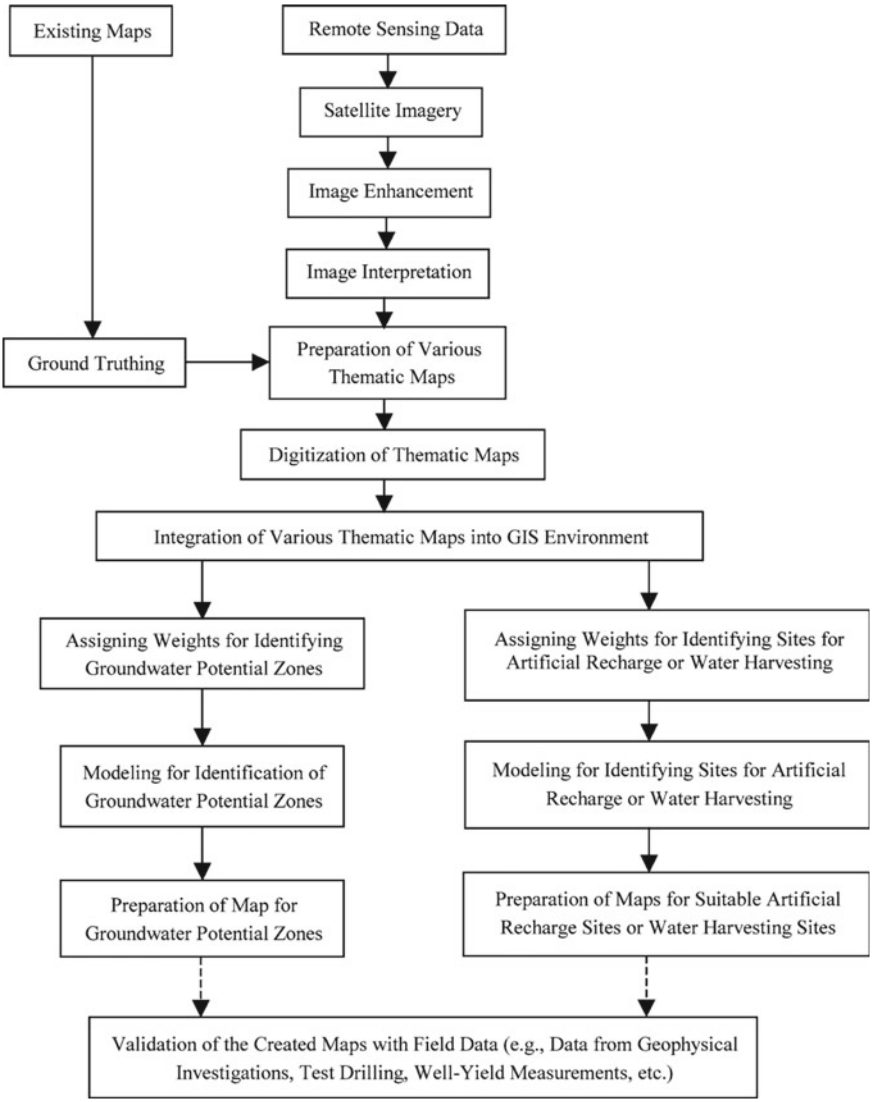

Fig. 20.2 Flow chart showing combination of GIS and remote sensing (RS) techniques for groundwater resource management (Jha et al. 2007)

20.3 Applications of GIS in Groundwater Hydrology

GIS has proved to be very beneficial for managing of natural resources including groundwater (Abebrese et al. 2022). GIS has demonstrated to be an important tool for analysis of the appropriateness of the locations, management of the location inventory data, groundwater susceptibility assessment to the pollution potential due to non-selective pollution sources, modeling of the groundwater movement, modeling, transport, and washing out of dissolved substances as well as for creation of spatial decision support systems by integrating groundwater quality assessment models with geodata (Engel et al. 1999). For most of the earth's population, protection of groundwater quality is a very important issue; GIS has proven to be effective means for assessing groundwater pollution threats (Merchant 1994). GIS has several advantages and can be utilized for groundwater protection, resource assessment, and for designing different underground structures as is useful in collecting and storing subsurface data (Adams and Bosscher 1992). GIS technology is often used to encode, store, extract, evaluate, and modeling of groundwater (Baker et al. 1993). GIS provide excellent opportunities for screening and mapping of potential sources of pollution (Hall and Zidar 1993). The method to measure groundwater using GIS is that thematic layers of different characteristics of groundwater are created and reclassified according to their hydrogeological importance. Weight factors are allocated to topics and their correspondent categories according to the groundwater outlook. The composite map for contamination risk is to be prepared for the site selected by integrating the reclassified layers based on weighted factors into a GIS environment. Potential areas of the generated groundwater are validated with existing field and groundwater data. The flow chart showing the method is shown in Fig. 20.3.

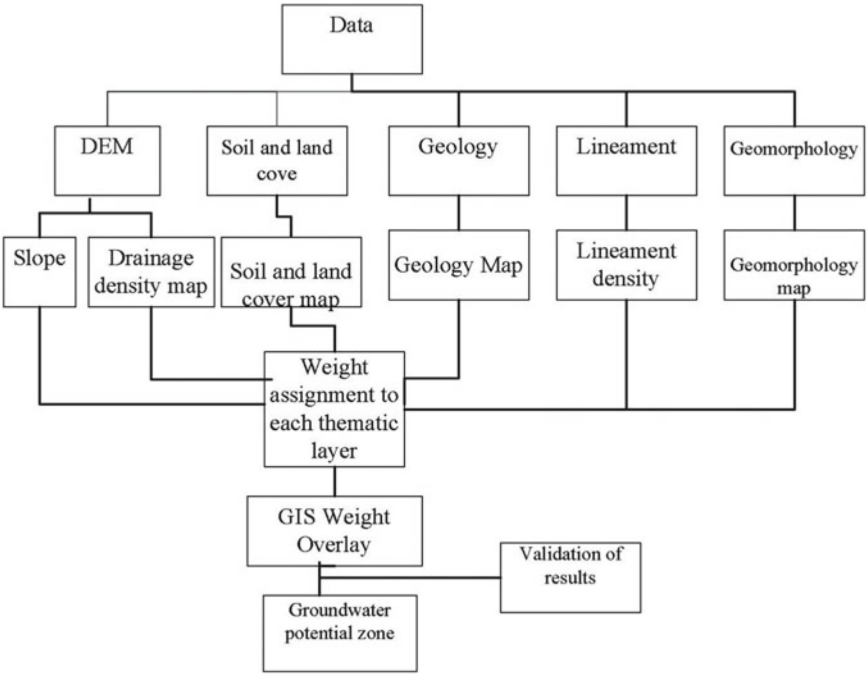

Fig. 20.3 Flow chart showing groundwater potential map development using GIS

20.4 Application of GIS for Assessment and Exploration of Groundwater Resources

Rifai (1993) built an interface for GIS modeling that defines wellhead protection areas (WHPA) around public water wells. The users can automatically retrieve selected data from a GIS database by using this modeling interface. For assessment of potential for groundwater contamination of nitrogen fertilizers on arable land in Texas, a GIS (GRASS 3.1) was created. By combining DRASTIC data in planted area of nine harvests with recommended amount of nitrogen fertilizer, an index of the contamination potential of nitrogen fertilizers was generated (Halliday and Wolfe 1991). The PI method is a GIS-oriented approach of plotting the exposure of groundwater to pollution with observable consideration of karst aquifers (Ghadimi et al. 2022). The PI includes two parts of the protective cover (the P factor) along with the infiltration conditions (I factor). (Goldscheider et al. 2000).

Adams et al. (1993) illustrated the use of a GIS called wellhead, which can be utilized by hydrological scientists, geologists, and hydrological chemists to show land information as well as to reconstruct it in an interactive and graphical way. A simple model for the transport of nitrates from groundwater in the GIS IDRISI environment was developed by Lasserre et al. (1999). Lee et al. (2003) integrated the statistical models with GIS for characteristic analysis of groundwater. Well location in the city, intensive agricultural activities, increasing industrial activities, variations in weather conditions, particularly precipitation, changes in groundwater quantity that is taken from wells, groundwater conditions, and fluctuations in the water table are different factors that lead to increase in nitrate concentration (Nas and Berktay 2006; Brunner et al. 2007; Asadi et al. 2007). Discussion on previous studies of application of GIS for assessment and evaluation of groundwater resources is given in Table 20.1.

20.5 GIS Application for Groundwater Pollution Hazard Assessment and Protection Planning

The water quality index (WQI) is analyzed to evaluate the drinking water feasibility of groundwater in areas with environmental stress in relation to water quality and appropriate corrective actions are proposed. Distributed input data is required for regional groundwater models (Wondzell et al. 2009). Chenini and Mammou (2010) demonstrated numerical modeling for groundwater resource using GIS. Integration of MODFLOW and GIS was developed by Gaur et al. (2011). Baalousha (2011) suggests a different methodology for contamination risk assessment of groundwater by taking into consideration hydrogeology factors, land use, and water catchment areas of public wells potential impact of contamination. This implementation of this method is easy, and to suit different local conditions, it can be modified accordingly. GIS has proved to be an important tool for preparation of final maps. Rawy et al.

Table 20.1 Application of GIS for assessment and exploration of groundwater resources

Objective	Methodology	Study Area	References
Groundwater potential zones	Landsat data was used, and computer programs were developed to enhance images	Doddaguni area in Karnataka, India West Godavari District of Andhra Pradesh, India	Rampal and Rao (1989), Kamaraju et al. (1995)
Rhode Island GIS (RIGIS) for groundwater protection planning	RIGIS aimed to prepare classification map of groundwater	Southern Arizona	Baker and Panciera (1990)
GIS compatible groundwater vulnerability mapping method Aquifer vulnerability index (AVI)	To define groundwater protection zones and to review locations for land use selection, AVI maps were used	Salt River System, Western Australia	Stempvoort et al. (1993)
Identifying recharge and discharge zones	Aerial photographs and Landsat data were used for identifying recharge and discharge zones	Saskatchewan-Alberta boundary	Salama et al. (1994)
RS and GIS integrated for improving the site selection of borehole drilling	An affordable GIS software package "IDRISI" and Landsat TM satellite image	Volta basin, Northern Ghana	Teeuw (1995)
Demarcating groundwater potential areas	A model with logical conditions was developed	Marudaiyar basin, Tamil Nadu, India	Krishnamurthy et al. (1996)
Developing better well-siting strategies	RS, GPS, and GIS were used	Sedimentary basin, Central Ghana	Sander et al. (1996)
Potential groundwater development resource delineation	Radar imagery and aerial photographs	Cross River State of southeastern Nigeria	Edet et al. (1998)
Groundwater storage and transmission	Integration of GIS and RS data with traditionally collected data	Syrian Arab Republic	Travaglia and Ammar (1998)
Assessment of dependencies between layers and maps to estimate groundwater	Multi-criteria evaluation technique (MCET)	Rawasen and Pili watersheds, Uttar Pradesh, India	Goyal et al. (1999)
Groundwater potential zone classification	Integrated RS and GIS system	Langat Basin, Malaysia	Musa et al. (2000)
Mapping potential groundwater resources	GIS multi-criteria analysis	Truyàre River catchment, France	Lachassagne et al. (2001)

(continued)

Table 20.1 (continued)

Objective	Methodology	Study Area	References
Groundwater potential zones	Integration of weighted maps with GIS-based aggregation method	Midnapore District, West Bengal, India	Shahid and Nath (2002)
Delineate groundwater potential areas	Combined RS, geophysics, and GIS methods to delineate	Ojhala sub-watershed, Mirjapur district, Uttar Pradesh, India	Singh and Prakash (2002)
Groundwater potential and exploration	RS, geoelectrical, and GIS techniques	Sonebatra, Mirjapur, and Chaundali, Uttar Pradesh, India Ratmau-Pathri Rao watershed, Haridwar, India	Singh et al. (2002), Hadithi et al. (2003
Investigating underground features, aquifer geometry, and groundwater quality	RS data integrated with the hydrologic data	Ken Graben, Uttar Pradesh, India	Srivastava (2002)
Groundwater potential zone delineation and exploring the changes in land use and land cover	RS and GIS techniques	Bardhaman District, West Bengal, India	Sikdar et al. (2004)
Mapping and assessing quality of groundwater	ArcGIS 9.0 and ArcGIS Geostatistical Analyst	Konya City, Turkey	Nas and Berktay (2010)
Spatial variations in groundwater quality	GIS spatial interpolation technique	Gulbarga, Karnataka, India	Balakrishnan et al. (2011)
Feasibility assessment of groundwater for drinking	Various multivariate statistical techniques	Northwest of Iran	Mosaferi et al. (2014)
Assessment of groundwater quality	Traditional hydrochemical analysis and GIS integration with factor analysis	Egyptian governorate of Qena	El-Rawy et al. (2019)
Groundwater quality assessment	GWQI was used for analysis of groundwater	Medak, Telangana, India	Adimalla and Taloor (2020)
Delineating the groundwater potential zones	Analytical hierarchy process (AHP) and catastrophe theory (CT)	Yamuna sub-basin (Panipat region), India	Kaur et al. (2020)

(continued)

Table 20.1 (continued)

Objective	Methodology	Study Area	References
Investigation of parameters of groundwater quality	Water quality index (WQI) and GIS	Madurai, Tamil Nadu, India	Kumar and Sangeetha (2020)
Drinking water feasibility assessment from groundwater	WQI model based on the GIS	Bokaro, Jharkhand, India	Verma (2020)
Estimate the components of the water balance	WetSpass model integrated with GIS	Dura sub-catchment, northern Ethiopia	Gebru (2020)

(2019) integrated the GIS, hydrochemistry, and factor assessment for groundwater quality due to increase in activities of agriculture in Qena Governorate, Egypt.

Adimalla et al. (2020) selected a collection of one hundred ninety-four hard rock groundwater samples from Medak (Telangana, India) for assessing groundwater quality using GIS and groundwater quality index (GWQI). Groundwater samples were tested for different parameters of water quality. The evaluation of groundwater was done using the spatial distribution and water quality index. Kumar and Sangeetha (2020) assessed the quality of groundwater in and around the city of Madurai using the analysis of parameters, WQI, and geodata. The study showed that integrating GIS techniques and RS with field data, we can accurately assess the groundwater quality. Previous studies of GIS application for groundwater pollution hazard assessment and protection planning are discussed in Table 20.2.

20.6 Limitations of GIS for Groundwater Resource Management

1. The high requirements of input parameters and, due to inherent complexities of groundwater, statistics tools integrated with GIS do not always produce desired results. Use of machine leaning and intelligence techniques integrated with GIS has many advantages, but they should be applied carefully and after proper evaluation.
2. The GIS-based GWQI which can be accepted universally is not available, and results depend on selected parameters as well as assigned weight of each parameter, thus making it subjective.
3. The WQI map is prepared based on water quality guidelines which are not universal; the WQI maps need to be updated with changing jurisdiction and change in water quality parameters.

Table 20.2 Application of GIS for groundwater pollution hazard assessment and protection planning

Objective	Methodology	Study Area	References
Groundwater protection planning	Rhode Island GIS (RIGIS)	Rhode Island	Baker and Panciera (1990)
Groundwater pollution potential	Hazard and risk assessment maps based on GIS	Columbia	Evans and Myers (1990)
Analyzing groundwater contamination problems	GRASS GIS linked with the DRASTIC model	Texas	Halliday and Wolfe (1991)
Groundwater protection planning	GIS	Northeast America	Flockhart et al. (1993)
Water supply protection model	Florida Water Management District's GIS	Southwest Florida Water Management District	Griner (1993),
Analyzing the possible sources of contamination inside the demarcated area	GIS database was developed using SYSTEM 9 software a wellhead. modeling user interface (WMUI)	Houston, Texas	Rifai et al. (1993)
Comprehensive wellhead protection scheme	GIS technology	North Dakota	Hammen and Gerla (1994)
Combining the groundwater simulation models and demographic databases	GIS technology	Groton, Massachusetts	Maslia et al. (1994)
Underground storage tank (UST) management system	GIS technology	Denton, Texas	Hudak et al. (1995)
Identification of site for solid waste management	GIS as screening tool	Golbasi region of Turkey	Basagaoglu et al. (1997)
Estimation of time of travel to river/well from any point inside the catchment	GIS integrated with spatial analysis tools	Massif Central, France	Laurent et al. (1998)
Vulnerability assessments	Regional GIS-driven integrated evaluation approach	Fresno, California,	Loague and Corwin (1998)
Pesticide contamination vulnerability evaluation of groundwater	GIS-based attenuation factor (AF) model	Louisa County, Virginia	Shukla et al. (1998)

(continued)

Table 20.2 (continued)

Objective	Methodology	Study Area	References
Model for nitrate transport in groundwater	Simulations were carried out with MT3D-MODFLOW. The combination of GIS and transport model was developed	Poitou–Charentes region, France	Lasserre (1999)
Mapping contamination vulnerability of groundwater	GIS-based approach PI method	Karst aquifers	Goldscheider et al. (2000)
Evaluation of groundwater pollution potential (GWPP)	RS, GIS, and other data	Haridwar, India	Dubey and Sharma (2002)
Predictive groundwater model	GIS utilizing RS and auxiliary data	Murray Valley Irrigation Region of New South Wales, Australia	Lamble and Fraser (2002)
Assessment of the vulnerability of aquifers	An AHP-DRASTIC software package integrated into ArcView GIS	North Arcot, Tamil Nadu, India,	Thirumalaivasan et al. (2003)
Prediction of groundwater vulnerability	Neuro-fuzzy techniques, GIS, GPS and RS	Northwest Arkansas	Dixon (2004)
Location of contamination risk zones	A process-based model for the flow transport system was integrated with GIS	Cortland, New York	Sinkevich et al. (2005)
Spatially distributed nitrate concentrations for groundwater wells	ArcView GIS 3.2 was utilized for groundwater contamination assessment	Konya city (Turkey)	Nas and Berktay (2006)
Spatial distribution of the selected water quality parameters	AutoCad and Arc/Info GIS software	Warangal, Andhra Pradesh	Asadi (2007)
Contamination risk assessment of groundwater	GIS technology	Urban and periurban areas, Italy	Corniello et al. (2007)
Evaluation of risk for groundwater contamination	GIS by taking into consideration hydrogeological factors, land use, public well catchment areas, and the potential effect of contamination	Gaza Strip, Palestine	Baalousha (2011)

(continued)

Table 20.2 (continued)

Objective	Methodology	Study Area	References
New integrated GIS modeling method to assess groundwater contamination risk was proposed	Statistical methods have been used within the framework of GIS	Crete, Greece	Kourgialas and Karatzas (2015)
Evaluation of risk for contamination of groundwater	The integration layers of hydrogeological parameters by overlaying the DRASTIC index	Selangor River Basin, Malaysia	Ariffin et al. (2016)
To investigate the susceptibility of groundwater	Regression based on DRASTIC	Buncombe County, North Carolina	Adu Agyemang (2017)
Spatial distribution of GWQI	Combination of GIS and geochemical approaches	Assam, India	Nath (2018)
Determining the susceptibility of groundwater to contamination	DRASTIC and GOD method	Asadabad alluvial aquifer, western Iran	Oroji (2018)
Characterization of water quality of groundwater samples by developing a reliable multi-statistical method	ArcGIS	Agra, India	Yadav (2018)
Groundwater contamination model	GIS and WQI	Pavagada, Karnataka, India	Nandeesha et al. (2020)

20.7 Conclusions and Discussions

With the growing necessity for mathematical and quantitative assessment of the environmental effects due to release of contaminated substances into the environment, GIS provides solution for problems associated with large data in time-efficient and convenient way. After comprehensive literature review on GIS applications for examination and assessment of groundwater resource and for groundwater pollution hazard evaluation and protection planning, the following conclusions are drawn.

1. GIS is an effective tool for exploration as well as assessment of groundwater resources. Moreover, groundwater pollution hazard assessment and protection planning can also be done by continuous monitoring.
2. By integrating GIS with various ground and surface water models, modeling of water resources can be done, and this can change a complex task into a simple one.

3. Further research is essential for evaluation existing GIS software packages and their design along with their limitations to provide specifications to GIS operators that will play a critical role in the advanced application of newly developed techniques in machine learning and artificial intelligence for groundwater assessment.
4. Research should be continued to solve integration problems for comprehensive evaluation of land use maps, soil properties, sewer pipes, and water well construction data.
5. The integration of expert techniques, machine learning, artificial intelligence, numerical analysis, and GIS is not widespread in assessment of groundwater resource and groundwater pollution hazard assessment. This is a prospective research area to explore and enhance the modeling development.

References

Abbasnia A, Yousefi N, Mahvi AH, Nabizadeh R, Radfard M, Yousefi M, Alimohammadi M (2019) Evaluation of groundwater quality using water quality index and its suitability for assessing water for drinking and irrigation purposes: case study of Sistan and Baluchistan province (Iran). Appl Water Sci 9–12

Abebrese S, Anornu GK, Kabo-Bah AT, Dekongmen BW, Sunkari ED (2022) Assessment of groundwater potential zones using GIS and remote sensing techniques in the Bole District, Savannah Region, Ghana. Int J Energy Water Res 1–12

Adams TM, Bosscher PJ (1992) Management of subsurface data using spatial analysis. In: Computing in civil engineering and geographic information systems symposium. ASCE, pp 582–589

Adams TM, Tang AY, Wiegand N (1993) Spatial data models for managing subsurface data. J Comput Civ Eng 7(3):260–277

Adimalla N, Taloor AK (2020) Hydrogeochemical investigation of groundwater quality in the hard rock terrain of South India using geographic information system (GIS) and groundwater quality index (GWQI) techniques. Groundw Sustain Dev 10:100288

Adimalla N (2019) Spatial distribution, exposure, and potential health risk assessment from nitrate in drinking water from semi-arid region of South India. Hum Ecol Risk Assess Int J 1–25

Adu Agyemang AB (2017) Vulnerability assessment of groundwater to NO_3 contamination using GIS, DRASTIC model and geostatistical analysis

Aller L, Bennett T, Lehr J, Petty RJ, Hackett G (1987) DRASTIC: A standardized system for evaluating ground water pollution potential using hydrogeologic settings. US Environmental Protection Agency, Washington, DC, p 455

Ariffin SM, Zawawi MAM, Man HC (2016) Evaluation of groundwater pollution risk (GPR) from agricultural activities using DRASTIC model and GIS. In: IOP conference series: earth and environmental science, vol 37, no 1. IOP Publishing, p 012078

Aronoff S (1991) GIS: a management perspective. WDL Publications, Ottawa

Asadi SS, Rajani G, Reddy MA (2007) Analysis and interpretation of groundwater contamination using remote sensing and GIS: a case study. Current World Environ 2(2):115

Assaf H, Saadeh M (2009) Geostatistical assessment of groundwater nitrate contamination with reflection on DRASTIC vulnerability assessment: the case of the Upper Litani Basin, Lebanon. Water Resour Manage 23(4):775–796

Baalousha H (2006) Vulnerability assessment for the gaza strip, palestine using DRASTIC. Environ Geol 50:405–414

Baalousha HM (2011) Mapping groundwater contamination risk using GIS and groundwater modelling. A case study from the Gaza Strip, Palestine. Arab J Geoscis 4(3–4):483–494
Baker CP, Panciera EC (1990) A geographic information system for groundwater protection planning. J Soil Water Conserv 45:246–248
Baker CP, Bradley MD, Bobiak SMK (1993) Wellhead protection area delineation: linking flow model with GIS. J Water Resour Plan Manag 119(2):275–287
Balakrishnan P, Saleem A, Mallikarjun ND (2011) Groundwater quality mapping using geographic information system (GIS): a case study of Gulbarga City, Karnataka, India. Afr J Environ Sci Technol 5(12):1069–1084
Basagaoglu H, Celenk E, Marino MA, Usul N (1997) Selection of waste disposal sites using GIS. J Am Water Resour Assoc 33(2):455–464
Bhasker NR, Wesely PJ, Devulapalli RS (1992) Hydrologic parameter estimation using geographic information systems. J Water Res Plan Manage 118:492–512
Brunner P, Franssen HJH, Kgotlhang L, Bauer-Gottwein P, Kinzelbach W (2007) How can remote sensing contribute in groundwater modeling? Hydrogeol J 15(1):5–18
Carter JR (1989) On defining the geographic information system. Fundamentals of geographic information systems: a compendium, pp 3–7
Chen Y, Takara K, Cluckie ID, Smedt FHD (eds) (2004) GIS and remote sensing in hydrology, water resources and environment. IAHS Publication No. 289. IAHS Press, Wallingford, p 422
Chenini I, Mammou AB (2010) Groundwater recharge study in arid region: an approach using GIS techniques and numerical modeling. ComputGeosci 36(6):801–817
Clarke KC (1995) Analytical and computer cartography, 2nd edn. Prentice-Hall, Englewood Cliffs, N.J.
Corniello A, Ducci D, Ruggieri G (2007) Areal identification of groundwater nitrate contamination sources in periurban areas. J Soils Sediments 7(3):159–166
Dangermond J (1988) Introduction and overview of GIS. Paper presented at geographic information systems seminar: data sharing—Myth or reality. Ministry of Natural Resources, Ontario
Deshmukh KK, Aher SP (2016) Assessment of the impact of municipal solid waste on groundwater quality near the Sangamner City using GIS approach. Water Resour Manage 30(7):2425–2443
Dixon B (2004) Prediction of ground water vulnerability using an integrated GIS-based Neuro-Fuzzy techniques. J Spat Hydrol 4(2):1–38
Dixon B (2005a) Applicability of neuro-fuzzy techniques in predicting ground-water vulnerability: a GIS-based sensitivity analysis. J Hydrol 309(1–4):17–38
Dixon B (2005b) Groundwater vulnerability mapping: a GIS and fuzzy rule based integrated tool. Appl Geogr 25(4):327–347
Dubey OP, Sharma DC (2002) Integrated remote sensing and factor analytic GIS model for evaluating groundwater pollution potential
Ducci D (1999) GIS techniques for mapping groundwater contamination risk. Natural Hazards 20(2–3):279–294
Duecker KJ (1987) Geographic information systems and computer-aided mapping. J Am Plann Assoc 53:383–390
Edet AE, Okereke CS, Teme SC, Esu EO (1998) Application of remote sensing data to groundwater exploration: a case study of the cross-river state, Southeastern Nigeria. Hydrogeol J 6:394–404
El-Rawy M, Ismail E, Abdalla O (2019) Assessment of groundwater quality using GIS, hydrogeochemistry, and factor statistical analysis in Qena Governorate, Egypt. Desalin Water Treat
Elwood S (2009) Geographic Information Science: new geovisualization technologies—emerging questions and linkages with GIScience research. Prog Hum Geogr 33(2):256–263
Engel BA, Navulur KCS (1999) The role of geographical information systems in groundwater engineering. In Delleur JW (ed) The handbook of groundwater engineering. CRC, Boca Raton, pp 21, 1–16
Engman ET, Gurney RJ (1991) Remote sensing in hydrology. Chapman and Hall Ltd.

Evans BM, Myers WL (1990) A GIS-based approach to evaluating regional groundwater pollution potential with DRASTIC. J Soil Water Conserv 45:242–245
Flockhart DE, Sham CH, Xiao Y (1993) Maximizing the value of information for ground-water protection: three test cases. Water Res Bulletin AWRA 29(6):957–964
Franch-Pardo I, Napoletano BM, Rosete-Verges F, Billa L (2020) Spatial analysis and GIS in the study of COVID-19. A review. Sci Total Environ 739:140033
Gaur S, Chahar BR, Graillot D (2011) Combined use of groundwater modeling and potential zone analysis for management of groundwater. Int J Appl Earth Obs Geoinf 13(1):127–139
Gebru TA, Tesfahunegn GB (2020) GIS based water balance components estimation in northern Ethiopia catchment. Soil Tillage Res 197:104514
Ghadimi M, Zangenehtabar S, Malekian A, Kiani M (2022) Groundwater vulnerability assessment in a karst aquifer: a case study of western Iran. Int J Environ Sci Technol 1–14
Gogu R, Carabin G, Hallet V, Peters V, Dassargues A (2001) GIS-based hydrogeological databases and groundwater modelling. Hydrogeol J 9(6):555–569
Goldscheider NICO, Klute M, Sturm S, Hötzl H (2000) The PI method–a GIS-based approach to mapping groundwater vulnerability with special consideration of karst aquifers. Z AngewGeol 46(3):157–166
Gorai AK, Kumar S (2013) Spatial distribution analysis of groundwater quality index using GIS: a case study of Ranchi municipal corporation area. Geoinf Geostatist Overview 1:1–11
Gossel W, Ebraheem AM, Wyeisk P (2004) A very large-scale GIS based groundwater flow model for Nubian sandstone aquifer in Eastern Sahara (Egypt, northern Sudan and Eastern Libya). Hydrogeol J 12:698–713
Goyal S, Bharawadaj RS, Jugran DK (1999) Multicriteria analysis using GIS for groundwater resource evaluation in Rawasen and Pilli watershed. UP Proc Map India 99
Griner AJ (1993) Development of awater-supply protection model in a GIS. Water Resources Bulletin, AWRA 29(6):965–971
Hadithi MA, Shukla DC, Israil M (2003) Evaluation of groundwater resources potential in Ratmau-Pathri Rao watershed Haridwar district, Uttaranchal, India using geo-electrical, remote sensing and GIS techniques. In: Proceedings of the international conference on water and environment (WE-2003), Bhopal, India, Ground Water Pollution, pp 123–125
Hall P, Zidar M (1993) The use of geographic information systems and models on personal computer and workstation platforms, in the development of a wellhead protection program, Salinas Valley, California. In Engineering Hydrology. ASCE, pp 377–382
Halliday SL, Wolfe ML (1991) Assessing ground water pollution potential from nitrogen fertilizer using a geographic information system 1. JAWRA J Am Water Res Assoc 27(2):237–245
Hammen JL, Gerla PJ (1994) A geographic information-systems approach to wellhead protection. Water Res Bullet AWRA 30(5):833–840
Horton RK (1965) An index number system for rating water quality. J Water Pollut Control Fed 37(3):300–306
Howari MF, Sherif MM, Singh PV, Al Asam SM (2007) Application of GIS and remote sensing techniques in identification, assessment and development of groundwater resources. In: Thangarajan M (ed) Groundwater resource evaluation, augmentation, contamination, restoration, modeling and management. Springer, Netherlands, pp 1–25
Hudak PF, Speas RK, Schoolmaster FA (1995) Managing underground-storage tanks in urban environments—a geographic information-systems approach. Water Res Bulletin, AWRA 31(3):439–445
Jha MK, Chowdhury A, Chowdary VM, Peiffer S (2007) Groundwater management and development by integrated remote sensing and geographic information systems: prospects and constraints. Water Resour Manage 21(2):427–467
Johnson LE (2016) Geographic information systems in water resources engineering. CRC Press
Kamaraju MVV, Bhattacharya A, Reddy GS, Rao GC, Murthy GS, Rao TCM (1995) Groundwater potential evaluation of West Godavari District, Andhra Pradesh State, India—a GIS approach. Ground Water 34(2):318–325

Kaur L, Rishi MS, Singh G, Thakur SN (2020) Groundwater potential assessment of an alluvial aquifer in Yamuna sub-basin (Panipat region) using remote sensing and GIS techniques in conjunction with analytical hierarchy process (AHP) and catastrophe theory (CT). Ecol Ind 110:105850

Kourgialas NN, Karatzas GP (2015) Groundwater contamination risk assessment in Crete, Greece, using numerical tools within a GIS framework. Hydrol Sci J 60(1):111–132

Krishnamurthy J, Kumar NV, Jayaraman V, Manivel M (1996) Anapproach to demarcate groundwater potential zones through remote sensing and a geographic information system. Int J Remote Sens 17(10):1867–1884

Kumar S, Sangeetha B (2020) Assessment of ground water quality in Madurai city by using geospatial techniques. Groundw Sustain Dev 10:100297

Lachassagne P, Wyns R, B´erard P, Bruel T, Ch´ery L, Coutand T, Desprats J-F, Strat PL (2001) Exploitation of high-yields in hard-rock aquifers: downscaling methodology combining GIS and multicriteria analysis to delineate field prospecting zones. Ground Water 39(4):568–581

Lamble P, Fraser D (2002) Creation of a GIS-based predictive model for groundwater in the Murray Valley Irrigation Region (NSW) Cartography 31(1):234–242

Lasserre F, Razack M, Banton O (1999) A GIS-linked model for the assessment of nitrate contamination in groundwater. J Hydrol 224(3–4):81–90

Laurent F, Anker W, Graillot D (1998) Spatial modelling with geographic information systems for determination of water resources vulnerability application to an area in Massif Central (France). J Am Water Res Assoc 34(1):123–134

Lee SM, Min KD, Woo NC, Kim YJ, Ahn CH (2003) Statistical models for the assessment of nitrate contamination in urban groundwater using GIS. Environ Geol 44:210–221

Loague K, Corwin DL (1998) Regional-scale assessment of non-point source groundwater contamination. Hydrol Process 12(6):957–966

Machiwal D, Cloutier V, Güler C et al (2018) A review of GIS-integrated statistical techniques for groundwater quality evaluation and protection. Environ Earth Sci 77:681. https://doi.org/10.1007/s12665-018-7872-x

Marín-Beltrán I, Demaria F, Ofelio C, Serra LM, Turiel A, Ripple WJ, Mukul SA, Costa MC (2022) Scientists' warning against the society of waste. Sci Total Environ 811:151359

Maslia ML, Aral MM,Williams RC, Susten AS, Heitgerd JL (1994) Exposure assessment of populations using environmental modeling. Demographic-analysis, and GIS. Water Res Bulletin. AWRA 30(6):1025–1041

Mehrjardi TR, Jahromi ZM, Mahmodi S, Heidari A (2008) Spatial distribution of groundwater quality with Geostatistics, case study: Yazd-Ardakan Plain. World Appl Sci J 4:9–17

Merchant JW (1994) GIS-based groundwater pollution hazard assessment: a critical review of the DRASTIC model. Photogramm Eng Remote Sens 60:1117–1117

Morehouse S (1992) The ARC/INFO geographic information system. Comput Geosci 18(4):435–441

Mosaferi M, Pourakbar M, Shakerkhatibi M, Fatehifar E, Belvasi M (2014) Quality modeling of drinking groundwater using GIS in rural communities, northwest of Iran. J Environ Health Sci Eng 12(1):99

Musa KA, Akhir JM, Abdullah I (2000) Groundwater prediction potential zone in Langat Basin using the integration of remote sensing and GIS. In The 21st Asian Conference on Remote Sensing (pp. 4–8)

Nandeesha Khandagale VR, Mahesh VB, Suman AK, Velagapudi MT (2020) Assessment of groundwater quality by integration of water quality index and GIS techniques. In AIP Conference Proceedings (Vol. 2204, No. 1, p. 020026). AIP Publishing LLC

Nas B, Berktay A (2006) Groundwater contamination by nitrates in the city of Konya, (Turkey): a GIS perspective. J Environ Manage 79(1):30–37

Nas B, Berktay A (2010) Groundwater quality mapping in urban groundwater using GIS. Environ Monit Assess 160(1–4):215–227

Nath BK, Chaliha C, Bhuyan B, Kalita E, Baruah DC, Bhagabati AK (2018) GIS mapping-based impact assessment of groundwater contamination by arsenic and other heavy metal contaminants in the Brahmaputra River valley: a water quality assessment study. J Clean Prod 201:1001–1011
Nobre R, Filho O, Mansur W, Nobre M, Cosenza C (2007) Groundwater vulnerability and risk mapping using GIS, modelling and a fuzzy logic tool. J Contam Hydrol 94:277–292
Olabi AG, Obaideen K, Elsaid K, Wilberforce T, Sayed ET, Maghrabie HM, Abdelkareem MA (2022) Assessment of the pre-combustion carbon capture contribution into sustainable development goals SDGs using novel indicators. Renew Sustain Energy Rev 153:111710
Oroji B (2018) Groundwater vulnerability assessment using GIS-based DRASTIC and GOD in the Asadabad plain. J Mater Environ Sci 9(6):1809–1816
Pinder GF (2002) Groundwater modeling using geographical information systems. Wiley, New York, p 248
Rampal KK, Rao VVG (1989) Groundwater targeting using digital enhanced imagery. In: Proceedings of the 10th Asian conference on remote sensing, Kuala Lumpur, Malaysia, pp 23–29
Rifai HS, Hendricks LA, Kilborn K, Bedient PB (1993) A geographic information system (GIS) user interface for delineating wellhead protection areas. Groundwater 31(3):480–488
Roy S, Bose A, Mandal G (2022) Modeling and mapping geospatial distribution of groundwater potential zones in Darjeeling Himalayan region of India using analytical hierarchy process and GIS technique. Modeling Earth Syst Environ 8(2):1563–1584
Salama RB, Tapley I, Ishii T, Hawkes G (1994) Identification of areas of recharge and discharge using Landsat-TM satellite imagery and aerial photography mapping techniques. J Hydrol 162(1–2):119–141
Salem HS, Pudza MY, Yihdego Y (2022) Water strategies and water–food Nexus: challenges and opportunities towards sustainable development in various regions of the World. Sustain Water Resour Manag 8:114. https://doi.org/10.1007/s40899-022-00676-3
Sander P, Chesley MM, Minor TB (1996) Groundwater assessment using remote sensing and GIS in a rural groundwater project in Ghana: lessons learned. Hydrogeol J 4(3):40–49
Shahid S, Nath SK (2002) GIS integration of remote sensing and electrical sounding data for hydrogeological exploration. J Spat Hydrol 2(1):1–10
Shukla S, Mostaghimi S, Shanholtz VO, Collins MC (1998) A GIS-based modeling approach for evaluating groundwater vulnerability to pesticides. J Am Water Resour Assoc 34(6):1275–1293
Sikdar PK, Chakraborty S, Adhya E, Paul PK (2004) Land use/land cover changes and groundwater potential zoning in and around Raniganj coal mining area, Bardhaman District, West Bengal: a GIS and remote sensing approach. J Spat Hydrol 4(2):1–24
Singh AK, Prakash SR (2002) An integrated approach of remote sensing, geophysics and GIS to evaluation of groundwater potentiality of Ojhala sub-watershed, Mirjapur district, UP, India. In: Asian conference on GIS, GPS, aerial photography and remote sensing, Bangkok-Thailand
Sinkevich MG Jr, Walter MT, Lembo AJ Jr, Richards BK, Peranginangin N, Aburime SA, Steenhuis TS (2005) A GIS-based ground water contamination risk assessment tool for pesticides. Ground Monitor Remed 25(4):82–91
Srivastava A (2002) Aquifer geometry, basement topography and groundwater quality around Ken Graben India. J Spat Hydrol 2(2):1–8
Star J, Estes J (1990) Geographic information systems: an introduction. Prentice Hall, Englewood Cliffs, N.J.
Stempvoort DV, Ewert L, Wassenaar L (1993) Aquifer vulnerability index: a GIS-compatible method for groundwater vulnerability mapping. Canad Water Res J 18(1):25–37
Taghizadeh RF, Zare'ian M, Mahmoudi S, Heidari A, Sarmadian F (2008) Evaluation of spatial interpolation methods for determining spatial changes in groundwater quality, Rafsanjan plain. Iran Water Sci Eng 2:932–941
Teeuw RM (1995) Groundwater exploration using remote sensing and a low-cost geographical information system. Hydrogeol J 3(3):21–30

Thakur JK, Singh SK, Ekanthalu VS (2017) Integrating remote sensing, geographic information systems and global positioning system techniques with hydrological modeling. Appl Water Sci 7(4):1595–1608

Thirumalaivasan D, Karmegam M, Venugopal K (2003) AHP-DRASTIC: software for specific aquifer vulnerability assessment using DRASTIC model and GIS. Environ Model Softw 18(7):645–656

Tiyasha Tung TM, Yaseen ZM (2020) A survey on river water quality modelling using artificial intelligence models: 2000e2020. J Hydrol 585:124670. https://doi.org/10.1016/j.jhydrol.2020,124670

Tomlinson RF (2007) Thinking about GIS: geographic information system planning for managers, vol 1. ESRI, Inc

Travaglia C, Ammar O (1998) Groundwater exploration by satellite remote sensing in the Syrian Arab Republic. RSC Series (FAO)

Tsihrintzis VA, Hamid R, Fuentes HR (1996) Use of geographic information systems (GIS) in water resources: a review. Water Resour Manage 10(4):251–277

Ugochukwu UC, Onuora OH, Onuorah AL (2019) Water quality evaluation of Ekulu river using water quality index (WQI). J Environ Stud 4(1):4

Verma P, Singh PK, Sinha RR, Tiwari AK (2020) Assessment of groundwater quality status by using water quality index (WQI) and geographic information system (GIS) approaches: a case study of the Bokaro district India. Appl Water Sci 10(1):27

Warwick JJ, Haness SJ (1994) Efficacy of ARC/INFO GIS application to hydrologic modeling. J Water Resour Plan Manag 120(3):366–381

Watkins DW, McKinney DC, Maidment DR, Lin MD (1996) Use of geographic information systems in groundwater flow modeling. J Water Res Plann Manage ASCE 122(2):88–96

WHO (World Health Organization) (2019) 1 in 3 people globally do not have access to safe drinking water—UNICEF, WHO. June 18, 2019. https://www.who.int/news/item/18-06-2019-1-in-3-people-globally-do-not-have-access-to-safe-drinking-water-unicef-who. Retrieved 7 Aug 2022

Wondzell SM, LaNier J, Haggerty R (2009) Evaluation of alternative groundwater flowmodels for simulating hyporheic exchange in a smallmountain stream. J Hydrol 364(1–2):142–151

World Health Organization (WHO) 1985 Anon (1985) Health Hazards from Nitrates in Drinking Water. WHO, Regional office for Europe

Yadav KK, Gupta N, Kumar V, Choudhary P, Khan SA (2018) GIS-based evaluation of groundwater geochemistry and statistical determination of the fate of contaminants in shallow aquifers from different functional areas of Agra city, India: levels and spatial distributions. RSC Adv 8(29):15876–15889

Chapter 21
Water Quality Modelling and Parameter Assessment Using Machine Learning Algorithms: A Case Study of Ganga and Yamuna Rivers in Prayagraj, Uttar Pradesh, India

A. K. Shukla, R. Singh, Raj Mohan Singh, and R. P. Singh

Abstract Due to the rapid growth in population, industrialization and agricultural outputs, the stress on groundwater and surface water has increased exponentially. The water quality depends on the interaction of both the groundwater and surface water; therefore, management and monitoring of the surface water are the need of the hour. River water management is a major environmental challenge worldwide. Because of the nonlinear behaviour of various water quality parameters, estimating the water quality of a surface water at any point of its flow is a time-consuming task. River quality monitoring is a difficult, cumbersome, and costly process that can lead to many analytical errors. Therefore, the main objective of this work is to create a reliable model for assessing and forecasting changes in water quality in Prayagraj (earlier know as Allahabad), Uttar Pradesh, India at three separate places, including the Ganga River, Yamuna River, and confluence of both rivers (also known as Sangam) using artifical neural network (ANN) and genetic algorithm (GA) models. The developed model was used to statistically compare the results by analysing samples collected from the selected stations fortnightly. Based on the correlation matrix of the water quality for three stations, general prediction models for the selected parameters, namely DO, hardness, turbidity, and BOD, were developed. The prediction model was developed for DO, hardness, and turbidity for station 1 (Ganga River). The results showed that the correlation coefficient (R) for the ANN prediction model is 0.97, the average absolute relative error (AARE) is 0.002, and the model efficiency (ME) is 0.95 for the hardness prediction model. Similarly, the BOD-ANN prediction

A. K. Shukla · R. Singh · R. P. Singh
Department of Civil Engineering, Motilal Nehru National Institute of Technology, Allahabad 211002, India

A. K. Shukla (✉)
Department of Civil Engineering, Indian Institute of Technology Kanpur, Kanpur, India
e-mail: ashutoshshukla904@gmail.com

R. Singh
Department of Civil Engineering, Indian Institute of Technology Delhi, New Delhi, India

R. M. Singh
Motilal Nehru National Institute of Technology Allahabad, Prayagraj, India

P. Shukla et al. (eds.), *Environmental Processes and Management*, Water Science and Technology Library 120, https://doi.org/10.1007/978-3-031-20208-7_20

model performed well at station 2 (Yamuna River) and station 3 (Sangam), with $R = 0.99$, AARE = 0.006, root mean square error (RMSE) = 0.06, and ME = 0.99 at station 2. Overall, ANN outperforms all other modelling techniques for all four prediction models.

21.1 Introduction

Surface water bodies have the ability to replenish groundwater or receive water from it. Therefore, drawing water from rivers and streams can deplete groundwater and vice versa, pumping groundwater can decrease water in lakes, marshes, springs, rivers, and streams. Due to socio-economic advancements and the need to ensure that water resources remain accessible and secure for future generations, groundwater management is crucial. The stress on groundwater has expanded enormously as a result of the population boom, industrialization, and especially agriculture. It is crucial to regulate and keep an eye on the quality of the surface water since groundwater and surface water interact to determine the water quality. Globally, managing river water quality presents a significant environmental challenge.

Rivers are the most important source of water, but their water quality is deteriorating as a result of increased demand of water for domestic, municipal, agricultural, and industrial purposes. Pollution in rivers first affects the physicochemical quality of the water before systematically destroying the community and disrupting the delicate food web. River water quality is a major concern these days because many major cities are built along its banks. As a result, if its water becomes polluted, a large population is affected due to poor water quality. India's rivers have a very high significance due to its religious sentiments among its people and cover a large area of 0.329 billion ha. Because of their wider significance in cultural, economical, and geographical development, India's rivers are extremely valuable. Therefore, its proper management is highly significant and require various advance technical support to make it safe and secure.

Artificial neural network (ANN) modelling is being used in this process to manage water quality, conduct financial analysis, plan for water-related resources, and estimate hydrologic graphs, according to various publications (Chakraborty et al. 1992; Lachtermacher and Fuller 1994; Schizas et al. 1994; Wen and Lee 1998).

ANNs have been used extensively in recent years for modelling in several water-related fields, including oceanography (Makarynskyy 2004), river water quality (Grubert 2003), and mapping of the landslide events (Liong and Sivapragasam 2002; Muttil and Chau 2006; El-Shafie et al. 2008; Vahidnia et al. 2010). Broadhursta and Cipolla (1999) concluded that pyrolysis mass spectrometry can benefit from the use of genetic algorithms (GA) model as a strategy for selection of parameters in various linear regression models as well as partial least square regression models. GA is a potent tool that allowing the search for solutions when no other practical method is available (Lubna et al. 2015). The most physically fit members of this new generation become parents to the next and so on. With this process, bad family lines and worse solutions are eliminated. The algorithm is simple to create, easy to comprehend, and straightforward to add improvements. As a result, the algorithm is quite flexible. After scanning only, a small section of the search space, the GA uncovers results that are close to ideal quickly. Various modelling outcomes indicate that the evolutionary algorithm can discover the best solution to a linear problem.

Therefore, the present study aims to identify the possible relations among the physical, chemical, and biological indicators of the water quality sampled from three different locations including Ganga River, Yamuna River, and confluence of both the rivers (Sangam) in Prayagraj, Uttar Pradesh, and India. Further, prediction models of water quality variables were developed using ANN and GA. Furthermore, the comparative analyses of developed were performed with linear regression model.

21.2 Methodology

21.2.1 Details of Sampling Sites

Prayagraj is among the ancient religious cities of India. Prayagraj is located at 25.45° N, 81.84° E in the extreme south part of one of the largest states of India, Uttar Pradesh. For monitoring of river water, three stations were selected in the flow area of rivers Ganga and Yamuna at Sangam Prayagraj, Uttar Pradesh, India. The Sangam is at the meeting point of three rivers, Ganga, Yamuna, and Saraswati (invisible). A brief description of the monitoring stations is as follows; (i) *station-1 Ramghat*: It is located approximately 0.5 km upstream of Sangam. About 0.1 km ahead of this station, a major sewage outfall of Ganga pollution control unit joins the river, (ii) *station-2 Quila Ghat*: it is 0.4 km upstream of Sangam in Yamuna River near Prayagraj fort, and (iii) *station 3 Sangam*: this station is at the Sangam around 150 m from the right bank of river Ganges. These three stations are important with respect to both the spiritual and pollution perspective as many people use this water for bathing on many religious occasions such as *"Kumbh."* Therefore, poor water quality of these places could affect the human health and ecology drastically.

Eighteen parameters were selected for monitoring for this study, i.e. pH, dissolved solids, dissolved oxygen (DO), temperature, fixed solids, MPN, iron, volatile solids (VS), nitrate nitrogen, biological oxygen demand (BOD), chlorides, sulphate, total solids (TS), hardness, turbidity, suspended solids (SS), fluoride, and alkalinity. The samples of river water were collected during eight-month time period between August 2016 and March 2017 in every fifteen days interval at the three stations. According to the protocols outlined in conventional methodologies, water samples were taken simultaneously from each of the three locations across the breadth of the river, roughly one-third of the way from the riverbank, and 30–40 cm beneath the water's surface following the standard protocol, i.e., APHA 2000. The water samples for the bacteriological analysis were collected in 300 mL sterilized "*borosil*" BOD bottles. The samples for determination of DO were fixed at the sight and then brought to the laboratory for the analysis. The temperature was monitored at the time of collection using thermometer. The apparatus used to measure the water quality variables mainly include (i) pH metre (Orion 420 A+) standardized with buffer solutions at pH 4.0 and pH 7.0, (ii) digital turbidity meter-331E, (iii) UV-spectrophotometer (Genesys 20, Thermo Spectronic, USA), (iv) BOD incubator, (v) electric oven, and (vi) hot air oven and many other supporting instruments. Standard analytical methods (APHA 2000) were followed for the testing of water and wastewater for the analysis of water quality parameters.

21.2.2 Correlation Matrix

The performance of the water quality models based on predictive modelling relies on the characteristics of the input parameters. Therefore, choosing appropriate inputs and outputs is crucial for getting the models to function well. The correlation matrix of the various water quality measures and the environmental link between the various water quality parameters are used in the current study to choose the input and output for the water quality prediction model. The correlation coefficient assesses how strongly two variables are associated, i.e., whether one normally rises as the other rises, whether it falls as the other rises, or whether their patterns of variation are completely unrelated. Pearson's r is the most often used as correlation metrix. Because 'r' quantifies the linear relationship between two variables, it is also known as the linear correlation coefficient. If X and Y are the two variables, then Eq. 21.1 provides the correlation coefficient (r) between X and Y.

$$R = \frac{\sum (X_i - X_m)(Y_i - Y_m)}{\sqrt{\sum (X_i - X_m)^2}\sqrt{\sum (Y_i - Y_m)^2}} \tag{21.1}$$

21.2.3 ANN

Weights (synapses) that fluctuate in strength with experience are firmly connected to slow, basic processing elements (neurons). The method offers associative distributed memory and integrates a number of limitations. The brain's performance of a task or function is modelled by ANN. For optimal performance, neural networks connect a large number of "neurons" or "processing units." It is similar to the brain in two ways: first, the network learns, and second, knowledge is stored using synaptic weights. Speech recognition and pattern categorization are predicted by ANN. It is an approach to information processing that is motivated by the brain. The design, learning or training algorithm, and activation function of an ANN are what define it.

In supervised learning, the outside world serves as the "teacher," providing the desired outcome for each training input vector. In unsupervised learning, network output is neither provided by or classified by the outside world. The learning rule modifies the network weights based on the correlation of the input vector to classify it into "clusters". Similar network outputs will result from comparable input vectors since they are members of the same cluster. This is self-directed education. Using (error) backpropagation (BP), which modifies the layer weights, ANN is trained. ANN is continuously updated till the performance goal is met. With error detection and linking weight updates in between, the ANN is trained in two passes: a forward pass and a backward pass. Because batch training expedites training and MSE convergence, it is employed.

21.2.4 GA

The travelling salesperson problem (TSP), for example, has practical applications in path finding and VLSI design. Imagine for a moment that you are using GPS navigation and it takes a while (or even a few hours) to calculate the "best" route from the source to the destination. Delay in these real-world applications is unacceptable, so what is needed is a "good enough" solution that is delivered "quickly", and GA is able to provide that quick solution. The terms in GA are:

- Population—It is a subset of all potential (encoded) answers to the questions posed. The population of a GA is similar to the population of humans, with the exception that we have candidate solutions that indicate humans instead of actual humans.
- Chromosomes—One such solution to the stated issue is a chromosome.
- Gene—A gene is one of a chromosome's element positions.
- Genotype—The population in the computing space is called the genotype. The solutions are represented in the computation space in a form that makes them simple to comprehend and manipulate with a computing system.
- Phenotype—The population of solutions that are represented in the same way they are in actual real-world situations is known as a phenotype.
- Fitness Function—Simply explained, a fitness function is a function that accepts a solution as an input and outputs if the answer is suitable. Depending on the challenge, the fitness function and the objective function could be the same in some instances and different in others.
- Genetic Operators—These change the genetic make-up of the progeny. These include selection, mutation, and crossover.

A few GA's practise elitism. Simply said, it indicates that the population always propagates its fittest members to the following generation. The fittest member of the existing population cannot, therefore, ever be replaced. The simplest strategy is to remove random individuals from the population, but this approach frequently has convergence problems; hence, the following tactics are frequently employed.

21.2.5 Linear Correlation

A method for modelling the connection between a scalar dependent variable y and one or more independent variables represented by X is known as linear regression in statistics. Simple linear regression is used when there is only one explanatory variable. In the current study, linear regression was performed using SPSS, and the obtained coefficients were used to predict the corresponding water quality parameter. Based on some performance statistics computed using the linear regression equation, the coefficients were then used for comparison with other predictive models.

21.3 Results and Discussion

A correlation matrix is developed by using the data collected by the analysis of the sampled data from Sangam, Prayagraj. The correlation matrix is shown in Table 21.1.

Table 21.1 Correlation matrix for different water quality parameters

	pH	Temp	Turbidity	Sulphate	Chloride	DO	BOD	MPN/100 ml	TS
pH	1.0								
Temp	−0.2	1.0							
Turbidity	−0.4	**0.4**	1.0						
Sulphate	−0.5	0.5	0.8	1.0					
Chloride	0.4	−0.3	−0.2	−0.2	1.0				
DO	0.6	**−0.8**	−0.4	−0.4	0.5	1.0			
BOD	**0.2**	**−0.3**	0.0	−0.2	−0.2	**0.3**	1.0		
MPN/100 mL	−0.1	0.2	0.3	0.3	0.3	0.0	−0.2	1.0	
TS	−0.2	0.3	−0.2	−0.1	0.5	−0.1	−0.3	0.2	1.0
TSS	−0.4	0.4	0.0	0.1	0.3	−0.1	−0.3	0.3	0.9
TDS	0.2	0.0	−0.2	−0.2	0.6	0.1	−0.2	0.0	0.7
FS	−0.2	0.3	0.0	0.0	0.5	−0.2	−0.4	0.3	0.9
VS	−0.2	0.2	−0.2	−0.1	0.3	0.1	−0.2	0.0	0.8
Hardness	0.5	**−0.5**	−0.2	−0.2	0.6	0.5	−0.2	0.0	0.0
Alkalinity	0.4	−0.4	−0.4	−0.3	0.9	**0.5**	−0.3	0.1	0.5
Iron	−0.3	0.1	0.8	0.7	−0.1	−0.2	0.1	0.1	−0.3
Fluoride	0.5	−0.6	−0.3	−0.1	0.6	0.5	−0.1	0.2	0.0
NO_3–N	−0.2	0.1	0.7	0.5	0.3	0.0	−0.2	0.4	0.1

21.3.1 Selection of Modelling Parameters

Based on the results of correlation matrix, four parameters are selected for modelling.

21.3.1.1 DO

The DO water quality prediction model has DO parameter as output with temperature and alkalinity parameter as input. The DO of a water body is highly influenced by the temperature of the water body; as the temperature rises, the dissolution of gas in liquid decreases according to the Henry's law. Therefore, the DO decreases with the rise in temperature at 0 °C; it is 14.6, and at 30 °C, it is 9.2 mg/l approximately. DO of a liquid is highly negatively correlated with the temperature which can be seen from the correlation matrix (−0.8). The DO of a water body is also correlated with the alkalinity present in the water. The alkalinity of a given water sample has bicarbonates ions (HCO_3^-) which contain oxygen in the dissolved form. Hence, the alkalinity of the water body is positively correlated with the DO of that water body which can also be seen by the correlation matrix.

21.3.1.2 Hardness

The hardness water quality prediction model has hardness parameter as output with temperature and alkalinity parameter as input. The hardness of a water body is negatively related with temperature because when the temperature of the water body is raised the temporary hardness of the water is removed which can be shown by Eq. 21.2.

$$Ca(HCO_3)_2 = CaCO_3 + H_2O + CO_2 \tag{21.2}$$

The negative correlation between the hardness and temperature of the water sample can also be seen in the correlation matrix. The hardness is also affected by the alkalinity present in the water body. The alkalinity of a given water sample represents the presence of bicarbonates ions (HCO_3^-) in which it corresponds to the temporary hardness of that body. Hence, the alkalinity of the water body is positively correlated with the hardness of that water body which can also be seen by correlation matrix. Therefore, one can predict the hardness of water body taking both temperature and alkalinity as an input parameter.

21.3.1.3 Turbidity

The turbidity water quality prediction model has turbidity parameter as output with temperature and hardness parameter as input. From the environmental point of view, the surface water generally contains temporary hardness and with increase in temporary hardness of the water body increases the divalent cations in the water sample and consequently decreases the turbidity of the water sample which can also be seen in the correlation matrix. Temperature also affects the turbidity of a given water sample as the rise in the temperature causes dissolution of some settled solids into the water imparts more turbidity to the water body. It can also be seen in the correlation matrix.

21.3.1.4 BOD

The BOD water quality prediction model has turbidity parameter as output with temperature, pH, and DO parameter as input. The BOD, decomposition of the organic matter present in the given water sample and in presence of air, is influenced by pH, temperature, and DO of the given water body. The microbial activity is highest at optimum temperature and at optimum pH. Therefore, any deviation from the optimum value of pH or temperature, either less or more will affect the BOD satisfied of the water sample. The activity of the microbes too is affected by the amount of dissolved oxygen present in the given sample, as aerobic microbe degrades the organic matter more rapidly in the presence of air. Hence, if more and more oxygen is dissolved in the water sample, then microbial disintegration of organic matter becomes faster, and BOD satisfies very fast. As a result, using temperature, pH, and DO as input factors, one may forecast the BOD water quality parameter of a given water body.

21.3.2 Simulation of Prediction Models Based on Selected Parameters

The four prediction models used for the prediction of the above parameters are following.

21.3.2.1 ANN

On the basis of the correlation analysis and environmental relationship between the various water quality variables, the three-layer feedforward backpropagation neural network-based ANN architecture is being used. ANN model is developed for the selected output parameters on the basis of correlation coefficient. SPSS software is used for the ANN modelling of the water quality variables. Result of different water quality ANN models is given. The R value shows the predicted value has good correlation with the observed value with maximum of 0.99 for station 2, Yamuna training set. For station 2, RMSE and AARE values are also very less and ME value is close to 1, but it showed poor result for training set and for other stations. For station 1 Ganga, the hardness–ANN model gives good result as compared to other two stations.

21.3.2.2 GA Linear and Nonlinear

Genetic algorithm models are developed for the selected water quality models using MATLAB 7.0. A programme has been written in the MATLAB command window to minimize the least square error value, and the coefficients are obtained. Then predicted values are calculated based on the coefficients obtained after optimization of objective function. The programme developed for the application of GA to the four water quality models. To simulate and anticipate the hardness, sophisticated predictive models based on GA were created. The programme is such that it optimizes the linear and nonlinear least square regression value for hardness with temperature and alkalinity as input parameters.

21.3.2.3 Linear Regression

The model using linear regression is developed for the four selected water quality model to compare with the other general predictive models. The linear regression is done using SPSS. The performance of these models is evaluated by computing *R*, AARE, and RMSE, and ME.

21.3.3 Comparison for Results from the General Predictive Models

For station 1 (Ramghat at river Ganga), the DO, hardness, and turbidity prediction only ANN modelling techniques show better result than other modelling techniques with correlation coefficient of 0.92, AARE value of 0.004, and ME value is 0.60. For the BOD prediction, the ANN modelling techniques show good result than other modelling techniques with correlation coefficient of 0.96, AARE value of −0.001, and ME value of 0.99. All the model details are shown in Table 21.2.

For station 2 (Quillaghat at river Yamuna), the DO prediction model GA nonlinear shows good result with correlation coefficient of 0.50, AARE value of 0.03, but ANN is the best modelling techniques for the prediction of DO. For turbidity prediction model, ANN modelling technique shows good performance with correlation coefficient of 0.88 and ME of 0.95. For the prediction of BOD, ANN model shows good performance statistics with correlation coefficient of 0.91 and ME value is 0.99 which indicates a better statistic. All the required model details of station 2 are shown in Table 21.3.

Table 21.2 Summary of performance evaluation statistics of different models developed for the station 1

Station 1: Ramghat at Ganga River								
Error	*R*		RMSE		AARE		ME	
	Training	Testing	Training	Testing	Training	Testing	Training	Testing
DO prediction models								
GA linear	0.35	0.34	2.02	0.52	−0.03	−0.06	−15.2	−2.03
GA NL	0.6	0.61	0.66	0.54	0.02	0.07	−0.72	−2.3
ANN	0.46	0.51	0.45	0.18	−0.005	0.008	0.2	0.64
linear	0.6	0.62	0.4	0.22	−0.0027	0.0007	0.4	0.5
Hardness prediction models								
GA linear	0.01	−0.12	22.6	27.6	0.05	−0.21	−12.2	−2.9
GA NL	−0.06	0.09	7.7	22.8	0.01	−0.15	−0.6	−1.7
ANN	0.97	0.7	1.42	20	0.002	−0.12	0.95	−1.05
Linear	0.02	0.13	7.9	21.4	0.03	−0.14	−0.62	−1.34
Turbidity prediction models								
GA linear	0.37	0.47	93.7	96.2	−0.77	−6.2	0.02	−2314.1
GA NL	−0.49	−0.54	95.9	121.1	−1	−7.7	−0.02	−3667.1
ANN	0.71	0.78	69.7	49.3	−0.6	−1.95	1	1.49
Linear	0.52	0.62	82.66	65.31	−0.76	−3.4	1	1.86
BOD prediction models								
GA linear	0.59	0.57	1.5	1.3	−0.21	−0.26	−0.44	−104.8
GA NL	−0.44	−0.45	4.96	4.7	0.99	0.99	−61.3	−22.4
ANN	0.72	0.71	0.51	0.05	0.01	−0.003	0.33	0.79
Linear	0.71	0.69	0.44	0.2	−0.003	−0.015	0.52	−2.93

For station 3 (Sangam), the DO prediction model, all the modelling techniques show good performance results with highest value of correlation coefficient of 0.91, AARE value of 0.004, and ME value 0.6 for ANN modelling technique. For the prediction of BOD, GA linear and GA nonlinear show good performance than other three water quality models with maximum correlation coefficient of 0.65 and ME value 0.99 for GA linear modelling techniques, while ANN is the best modelling technique for the prediction of BOD with correlation coefficient of 0.95 and ME value is 0.99. For turbidity and hardness prediction, the ANN model performance is satisfactory with correlation coefficient of 0.94. All the required model details of station 3 are shown in Table 21.4.

Table 21.3 Summary of performance evaluation statistics of different models developed for the station 2

Station 2: Quillaghat at Yamuna River								
Error	R		RMSE		AARE		ME	
	Training	Testing	Training	Testing	Training	Testing	Training	Testing
DO prediction models								
GA linear	0.95	0.85	1.3	1.9	−1.2	−0.3	−1.2	−2.8
GA NL	0.98	0.97	1.03	0.5	0.005	−0.06	−0.5	0.8
ANN	0.99	0.96	0.11	0.6	0.001	−0.8	0.98	−32.9
Linear	0.96	0.86	0.32	0.69	0.02	−0.1	0.9	−46.2
Hardness prediction models								
GA linear	−0.71	−0.57	17.7	29.6	0.0002	−0.06	−1.02	−0.2
GA NL	0.67	0.39	11.2	29.1	0.01	−0.04	0.2	−0.2
ANN	0.97	0.65	2.9	27	−0.001	−0.02	0.95	0.77
Linear	0.68	0.58	9.5	23.3	0.005	−0.05	0.4	−183.8
Turbidity prediction models								
GA linear	0.62	0.51	61.1	67.5	−0.6	−1.9	0.32	−181.5
GA NL	0.5	0.55	72.5	67.9	−0.9	−1.9	0.04	−183.8
ANN	0.97	0.97	17.9	13.9	−0.2	−0.4	0.94	−6.8
Linear	0.68	0.59	57	62.4	−0.4	−1.55	0.4	−154.7
BOD prediction models								
GA linear	0.37	0.19	0.94	0.81	−0.07	−0.2	0.12	−41.2
GA NL	0.1	0.07	1.1	0.2	−0.2	0.04	−0.3	−0.8
ANN	0.99	0.99	0.06	0.04	0.001	−0.01	0.99	0.9
Linear	0.47	0.36	0.92	0.4	−0.06	−0.09	0.2	−8.2

21.4 Conclusions

The important conclusions derived from the present study following water quality assessment and water quality forecasting models of rivers at Sangam in Prayagraj are outlined below:

- The present study is based upon analysis of eighteen water quality variables at confluence of the river Ganga and Yamuna, i.e. Sangam, with two other sites, one each at upstream of Sangam, i.e. at rivers Ganga and Yamuna.
- General prediction models have been developed using ANN and GA. Utilizing RMSE, R, AARE, and ME, the effectiveness of ANN was evaluated. It was discovered that the ANN methodology proved to be a successful method for modelling water quality. A further benefit of ANN is that no assumptions regarding the range of flow discharge, temperature, BOD, or DO are needed. However, both

Table 21.4 Summary of performance evaluation statistics of different models developed for the station 3

Station 3: Sangam								
Error	R		RMSE		AARE		ME	
	Training	Testing	Training	Testing	Training	Testing	Training	Testing
DO prediction models								
GA linear	−0.33	−0.39	1.4	0.6	0.2	0.1	−8.6	−18.7
GA NL	0.1	0.18	0.5	0.4	−0.02	0.04	−0.05	−7.7
ANN	0.7	0.69	0.42	0.33	0.001	0.04	0.2	−5.5
Linear	0.41	0.46	0.42	0.3	−0.02	−0.04	0.2	−4
Hardness prediction models								
GA linear	−0.41	0.38	25.3	30.3	−0.05	0.02	−0.46	0.38
GA NL	0.81	0.59	19.5	42.8	−0.06	0.06	0.13	−0.23
ANN	0.75	0.61	14.1	0.39	−0.005	−0.013	0.55	−0.02
Linear	0.63	0.64	16.4	34.1	−0.007	−0.06	0.4	0.22
Turbidity prediction models								
GA linear	0.14	0.43	103.3	95.5	−5.9	−4.1	−0.1	−852
GA NL	0.13	0.59	128.4	79.2	−0.03	−3.4	−0.7	−586
ANN	0.24	0.39	101.7	105.8	−5	−4	−0.05	10.1
Linear	0.16	0.44	106.2	78.8	−5.8	−3.3	−0.14	−579.6
BOD prediction models								
GA linear	−0.37	−0.39	2.03	0.91	−0.35	0.08	−4.4	−1
GA NL	0.1	0.19	1.2	0.5	−0.1	0.03	−0.7	0.5
ANN	0.7	0.7	0.6	0.64	−0.02	−0.014	0.5	−2E−07
Linear	0.71	0.47	0.8	0.7	−0.03	−0.02	0.2	−0.04

the training and test sets of data should have the same controlling variables and consistent input data.

- The findings of the ANN model exhibit a lower AARE, a lower RMSE value, and a higher ME value. By using ANN-based water quality models, river water quality monitoring has been made simpler. These models are able to calculate characteristics like DO, BOD, turbidity, and hardness using simple inputs.
- It was discovered that the ANN methodology proved to be a successful method for modelling water quality. A further benefit of ANN is that no assumptions regarding the range of flow discharge, temperature, BOD, or DO are needed. However, both the training and test sets of data should have the same controlling variables and consistent input data.

References

Broadhurst A, Cipolla R (1999) The applications of uncalibrated occlusion junctions. In: BMVC, pp 1–10

Chakraborty K, Mehrotra K, Mohan CK, Ranka S (1992) Forecasting the behavior of multivariate time series using neural networks. Neural Netw 5(6):961–970

El-Shafie A, Noureldin AE, Taha MR, Basri H (2008) Neural network model for Nile River inflow forecasting based on correlation analysis of historical inflow data

Grubert JP (2003) Acid deposition in the eastern United States and neural network predictions for the future. J Environ Eng Sci 2(2):99–109

Lachtermacher G, Fuller JD (1994) Backpropagation in hydrological time series forecasting. In: Stochastic and statistical methods in hydrology and environmental engineering. Springer, Dordrecht, pp 229–242

Li S, Wunsch DC, O'Hair E, Giesselmann MG (2001) Comparative analysis of regression and artificial neural network models for wind turbine power curve estimation. J Sol Energ Eng 123(4):327–332

Liong SY, Sivapragasam C (2002) Flood stage forecasting with support vector machines 1. J Am Water Resour Assoc 38(1):173–186

Lubna H, Masoom MR (2015) Hydro-dissection—a simple solution in difficult laparoscopic cholecystectomy. Mymensingh Med J MMJ 24(3):592–595

Makarynskyy O (2004) Improving wave predictions with artificial neural networks. Ocean Eng 31(5–6):709–724

Muttil N, Chau KW (2006) Neural network and genetic programming for modelling coastal algal blooms. Int J Environ Pollut 28(3/4):223

Schizas CN, Pattichis CS, Michaelides SC (1994) Forecasting, minimum temperature vvith short time-length data using. Neural Netw World 2(94):219–230

Vahidnia MH, Alesheikh AA, Alimohammadi A, Hosseinali F (2010) A GIS-based neuro-fuzzy procedure for integrating knowledge and data in landslide susceptibility mapping. Comput Geosci 36(9):1101–1114

Wen CG, Lee CS (1998) A neural network approach to multiobjective optimization for water quality management in a river basin. Water Resour Res 34(3):427–436

Chapter 22
Response of Groundwater Level to Climate Variability: A Case Study of Mirzapur, Uttar Pradesh, India

Swati Dwivedi

Abstract This paper presents the trend analysis of two climatic variables: annual average rainfall and annual average temperature and fluctuating groundwater levels (GWL) for the pre-monsoon and post-monsoon season at ten different stations of Mirzapur district of Uttar Pradesh, India, using the decadal data ranging from 2011 to 2021 using nonparametric Mann–Kendall (MK) test. The trend magnitude for each of the parameter is studied using Sen's slope estimate. The result of the decadal study showed that there has been a strong negative trend reflecting the general consistent decline in the annual average rainfall pattern temporally. On the other hand, a non-significant negative trend was witnessed in the case of annual average temperature showing the overall decline in temperature over the last ten years but with varying yearly fluctuations. The groundwater levels trend analysis shows an overall negative trend of falling groundwater level during the pre-monsoon period. However, a locally varied trend was observed in the post-monsoon season where certain stations showed the rise in GWL. Decline in the annual average rainfall and temperature were associated with the gradual impact of climate change on the northern Gangetic plains of India. Declining groundwater levels during pre-monsoon season was attributed to the delayed and declining rainfall pattern, resulting in groundwater extraction during the sowing season of kharif crops. On the other hand, variability in the groundwater level trends during post-monsoon was attributed to the possible role of concretisation in urban areas, increasing surface runoff and its extraction for household and agricultural activities during lean season. Since this area has been limited studied in the context of impact of climate change on climatic variables and groundwater levels, this study would further aid the future researches, policy making and agricultural management.

Keywords Groundwater levels · Mirzapur district · Rainfall · Temperature · Climate change · Mann–Kendall · Sen's slope

S. Dwivedi (✉)
Department of Urban Studies, Indira Gandhi National Open University, New Delhi 110028, India
e-mail: swatidw241@gmail.com

P. Shukla et al. (eds.), *Environmental Processes and Management*, Water Science and Technology Library 120, https://doi.org/10.1007/978-3-031-20208-7_21

22.1 Introduction

For a variety of tasks, such as watershed management, hydrological modeling, flood forecasting, global warming research, hydrologic calculations, relative humidity modeling for agricultural production, irrigation management, etc., quantitative estimation of the temporal distribution of precipitation and temperature is necessary. The unpredictability of rainfall distribution and temperature change both geographically and dynamically would be among the foremost important effects of global warming caused by an increase in greenhouse gases. It is important to find out whether the shift is perceptible in the Indian setting while discussing climate change. Rainfall in India has a significant impact on the nation's economy, and understanding its tendencies is helpful for the country's hydrologic plans, emergency response and productivity expansion. With the advent of the phenomenon of climate change, global attention has been shifted upon studying the most important climatic variables, temperature and precipitation. The study includes their spatiotemporal variability from global to local levels and their direct or indirect impact on several other phenomena existing on the earth. One such phenomenon is the groundwater which is a significant part of hydrosphere of the earth. It is a vital resource for humanity and environment. More than one-third of the world's water is underground. More than 85% of rural and 50% urban population is dependent upon groundwater. India's usage consists of 25% of global annual groundwater use. More than 60% of groundwater is utilized in irrigating the Indian agriculture. Moreover, 85% of domestic water use in India is sourced from its groundwater. Although several researches have been conducted to study the changing trends of climatic variables, which are important to understand the phenomenon of climate change, only few attempts have been made to study the impact of climate change on groundwater in the mid-northern plains of India. Thus examining the trends in groundwaterlevel change in response to the changing trends in rainfall and temperature in this region becomes crucial. Fluctuations in an area's annual and seasonal rainfall patterns may lead to stress on groundwater levels with consequent implications in strategizing groundwater development and management for sustainable water use in the region. Understanding rainfall variability and the dynamics of climatic changes requires shift and trend analysis. However, owing to many non-climatic elements (such as station surroundings, site of stations, equipment, monitoring practices, rapid climate variability and computation technique) impacting the time series data, long-term time series may not be consistent or homogenous. According to Gajbhiye et al. (2016), one of the most important elements that affects crop yields is essential to economic growth and way of life is rainfall patterns and intensity (Kumar and Gautam 2014). In light of the aforementioned, several researches have made an effort to look into the country's climactic variables pattern. These studies have examined trends at various scales, including the national level (Kumar et al. 2010; Athar 2015; Fan and Chen 2016; Szabó et al. 2019); regional level (Bhutiyani et al. 2007; Elnesr et al. 2010; Karpouzos and Kavalieratau 2010; Duhan and Pandey 2013; Duan et al. 2017). In essence, the local and regional magnitude assessment seems to be more pertinent to developing tailored growth and adaptation strategies to lessen the consequences of climate change (Fischer and Ceppi 2012; Babar and Ramesh 2013).

Even in usually water-rich regions, such as the Indo-Gangetic plain, the climatic variability and its impact on groundwater are visible at the microlevels due to its varied physiography and increasing role of humans in changing demography, cropping patterns, urbanization levels and associated change in groundwater use. Hence, the attempt has been made to study the changing annual rainfall and temperature pattern and its impact upon the groundwaterlevel variability in the Mirzapur district of Eastern Uttar Pradesh, India lying in the mid Indo-Gangetic plain region. Mann–Kendall test and Sen's slope estimate is used to find the magnitude of the trend to better understand the impact of climate change at the local level.

22.2 Methodology

The trend analysis and estimation of Sen's slope are accomplished using nonparametric Mann–Kendall test and Sen's slope estimator method, respectively, for the given data sets. Mann–Kendall test is a nonparametric test for finding the monotonic increasing or decreasing linear trends in time series. Along with that, the trend magnitude for each of the parameter is studied using Sen's slope estimate. The detailed mechanism is discussed in Kendall (1975) and Sen (1968), respectively.

22.3 Study Area

Mirzapur district lies between the latitude of 24°59'−25°28' N and longitude of 82°08'−83°18' E. The Indian Standard Meridian Line which is located at the longitude of 82°30' E passes through Mirzapur district based on which Indian standard time is calculated. It is surrounded by Varanasi district from the North and northwest, (Allahabad) Prayagraj district from the southeast and Sonbhadra district from the northeast, as shown in Fig. 22.1. The city occupies 4,405 km^2 of area and has population of 2,496,970 (Census 2011). Out of the total population of Mirzapur, Urban population consists of 13.9% while Rural population consists of 86.1%. The district is divided into four tehsils, namely Lalganj, Madihan, Mirzapur city and Chunar. Like most of the eastern Uttar Pradesh region, Mirzapur receives rainfall from the Bay of Bengal branch of southwest monsoon during the month of June–July–August–September. The district experiences three seasons, Summer, Monsoon and Winter. The average annual rainfall of Mirzapur district during the period 2011 and 2021 is 1015.08 mm per year, and the average annual temperature during the same period is 31.76 °C. Mirzapur has a diverse physiography as its northern part is cut across by the river Ganga experiencing a strong meandering. It majorly divides the district into two halves; the left bank consists of low-lying flood plains, i.e., Khaddar, which gets flooded, and the soil is rejuvenated with the fresh alluvium

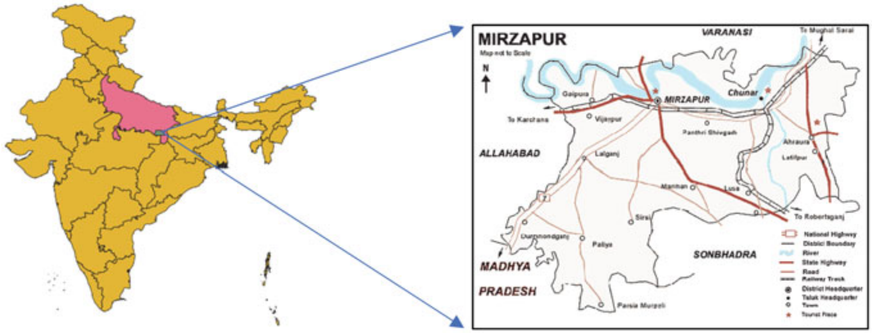

Fig. 22.1 Site map of study area (i) India, Uttar Pradesh, (ii) Mirzapur. *Source:* Modified after Centre for Rural Education and Development Action, Mirzapur

during every monsoon season. The right bank of river Ganga that is the Southern Mirzapur has comparatively higher average elevation of 128 m which rises to more than 220 m as one moves southwards toward the elevated Vindhyan escarpments with rugged topography and hard rocks. The interplay of varied topography, soil texture, proximity to the river channel, changing cropping patterns and intensity of agricultural activities, changing land use land cover due to urbanization, changing demography and the phenomenon of climate change altogether play an imperative role in the variable trends of changing groundwater levels at the local scale.

22.4 Data Set

The rainfall data of the duration 2011 and 2021 was acquired from India Meteorological Department (IMD). The groundwaterlevel data was acquired from Central Groundwater Board (CGWB), Water Resources Information System (WRIS). The temperature data was obtained from the Climatic Research Unit (CRU), National Centre for Atmospheric Science (NCAS), University of East Anglia, UK.

22.5 Results and Discussion

22.5.1 Nonparametric Test Results of Two Climatic Variables—Annual Average Rainfall and Temperature

Annual average rainfall and the annual average temperature of Mirzapur district is 1015.08 mm per year and 31.76 °C, respectively. The Mann–Kendall test and Sen slope estimate are the most frequently used nonparametric statistics test for

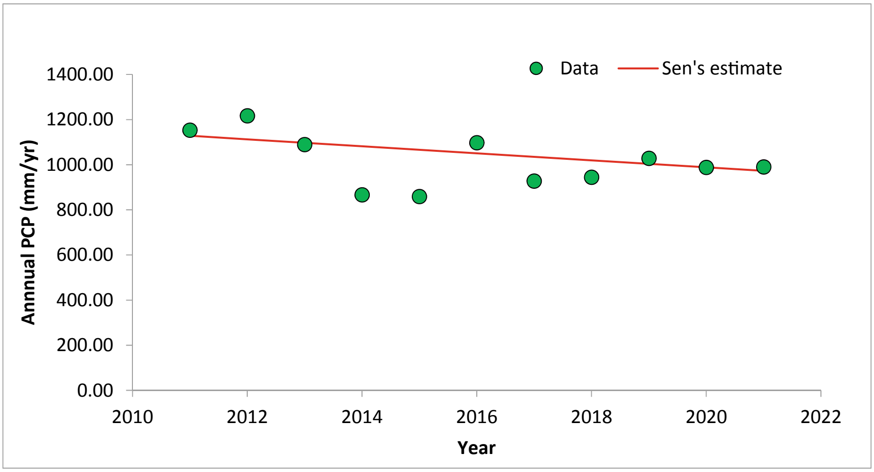

Fig. 22.2 Trend of changing annual average rainfall in Mirzapur district between 2011–2021 ($Z = -0.78$, $Q = -15.538$)

identifying trends in hydrological variables to observe the trend of annual rainfall and temperature of Mirzapur district. Here, the negative trend of annual rainfall and temperature indicates decline in the overall rainfall and temperature in the district over a period of 10 years (2011–2021). The following trends were observed with respect to the rainfall and temperature parameters.

22.5.1.1 Trend Analysis of Annual Average Rainfall of Mirzapur District

Figure 22.2 shows the decadal change in the annual rainfall pattern of Mirzapur District for the short-term period of 2011–2021. The Mann-Kendall test and Sen slope estimate shown below with Q = −15.538 depicts the strong negative trend indicating the temporal decline in the general rainfall levels. The highest rainfall is recorded in the year 2012 (1217.4 mm/yr.). The lowest rainfall falls outside the general negative trend depicting the 2014–2016 years being the El-Nino years. The trend indicates a strong correlation between the climate change and its impact on falling annual rainfall.

22.5.1.2 Trend Analysis of Annual Average Temperature of Mirzapur District

Figure 22.3 shows the decadal change in annual temperature pattern of Mirzapur district for the short-term period of 2011–2021. The Mann-Kendall test and Sen slope estimate shown below with Z = −0.60 and Q = −0.05 depict the general negative

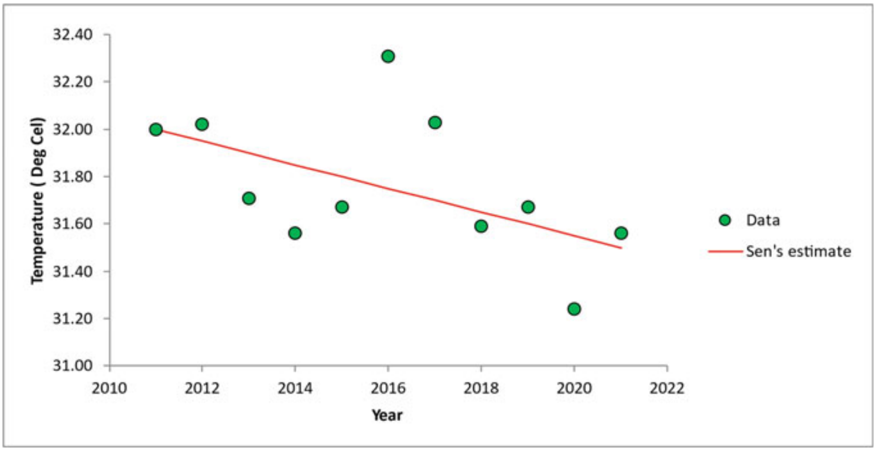

Fig. 22.3 Trend of changing annual average Temperature in Mirzapur district between 2011−2021 ($Z = -1.64$, $Q = -0.05$)

trend indicating the temporal decline in general temperature levels. However, the strong correlation could not be developed between climate change and changing annual temperature.

22.5.2 Nonparametric Test Results of GroundWater Level (GWL)

The deployed statistical approaches are the nonparametric Mann–Kendall test for accessing the existence of the monotonic increasing or decreasing trend and the nonparametric Sen's method for assessing the slope of a linear trend of the changing groundwater levels (GWL) at different stations.

Contrary to the positive correlation between rainfall and temperature change and their Z and Q values, there is a negative correlation with respect to groundwater-level data and their Z and Q values since the GWL data is recorded from surface level to the GWL depth below the earth's surface.

Hence, in the above study, negative trend denotes rise in groundwater level (as reduction of distance between earth's surface and GWL reflects rise in GWL) at a particular station, whereas positive trend indicates decline in groundwater level. The values of Z and Q statistics obtained through Sen slope test and MK test for the change in groundwater levels at the several stations of Mirzapur district during the pre-monsoon and post-monsoon period are presented in Table 22.1. The increase or decrease in GWL at each station is represented through upward and downward arrow respectively.

Table 22.1 Mann Kendall test (Z) and Sen's slope (Q) values for Pre-monsoon and Post-monsoon groundwater level GWL at different stations of Mirzapur district (Uttar Pradesh)

S. NO	STATIONS	PRE-MONSOON			POST-MONSOON		
		Z	Q	GWL	Z	Q	GWL
1	Bakiyabad	0.99	0.23	↓	-0.99	-0.069	↑
2	Chunar	-0.09	-0.014	↑	-0.99	-0.081	↑
3	GIC Hostel Campus	0.00	0.00	-	-	0.125	↓
4	Gosaipur Kantit	-	0.264	↓	-	-0.113	↑
5	Nagarpalika Ahrora, Jamalpur	1.97	0.267	↓	0.00	0.00	-
6	Jubilee Inter college, Police Lines	-	0.025	↓	0.000	0.006	↓
7	Polytechnic Campus, Bathua	-0.11	-	↑	-	0.517	↓
8	R R Vidyalaya, Chandradeepa	1.17	0.12	↓	1.79	0.258	↓
9	Rajkiya Paudhshala	0.72	0.04	↓	-1.25	-0.138	↑
10	Van Vibhag, Jalalpur	2.07	0.17	↓	0.63	0.063	↓

(↑)—Rising Groundwater level (↓)—Declining groundwater level

22.5.2.1 Sen's Slope Estimate Graph of Groundwater Level (GWL) Trends for Different Stations in Mirzapur District (Pre-monsoon and Post-monsoon)

MK test was conducted for all the ten stations spread across the Mirzapur district of Uttar Pradesh for the pre-monsoon and post-monsoon seasons over a short-term period of 2011–2021. The trend detection was achieved using MK test-statistics Z along with trend magnitude Q using Sen's slope estimate. The graphical representation of the statistical tests of groundwater level (GWL) for pre-monsoon and post-monsoon season for each of the ten stations over a short-term period of 2011–2021 are presented in the graphs below (Figs. 22.4, 22.5, 22.6, 22.7, 22.8, 22.9, 22.10, 22.11, 22.12 and 22.13).

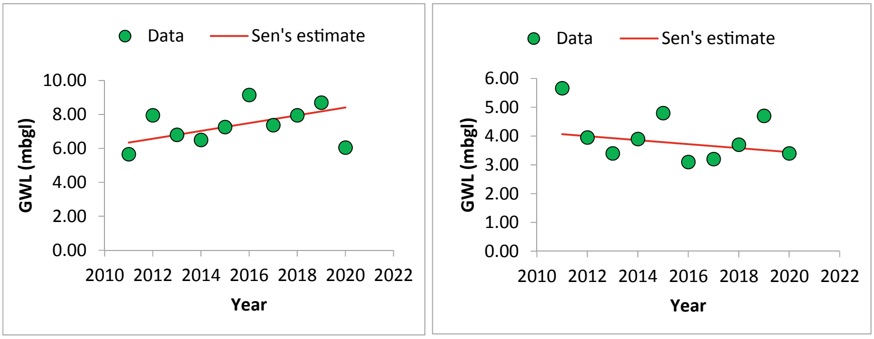

a). Pre-monsoon (Z= 0.99 Q= 0.23) b). Post-monsoon (Z= -0.99 Q= -0.069)

Fig. 22.4 Groundwaterlevel fluctuation at Bakiyabad

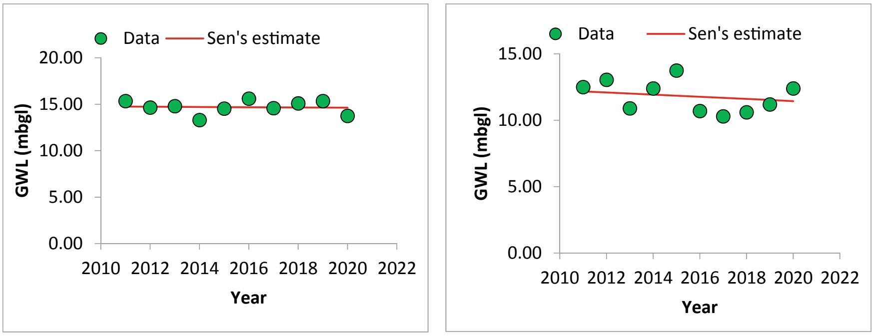

a). Pre-monsoon (Z= -0.09, Q= -0.014) b). Post-monsoon (Z= -0.99, Q= -0.081)

Fig. 22.5 Groundwaterlevel fluctuation at Chunar

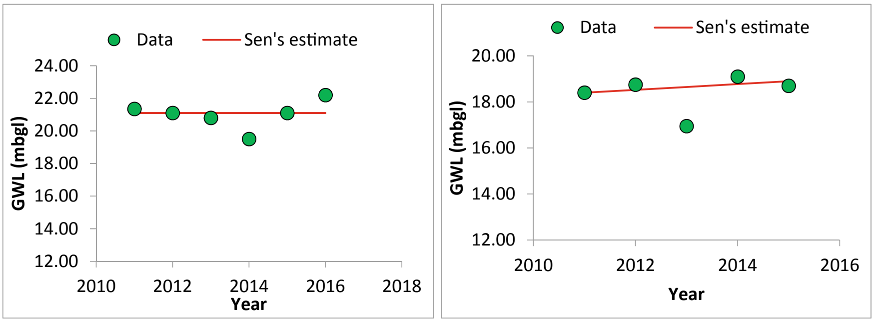

a). Pre-monsoon (Z= 0.00) b). Post-monsoon (Q=0.125)

Fig. 22.6 Groundwaterlevel fluctuation at GIC Hostel Campus

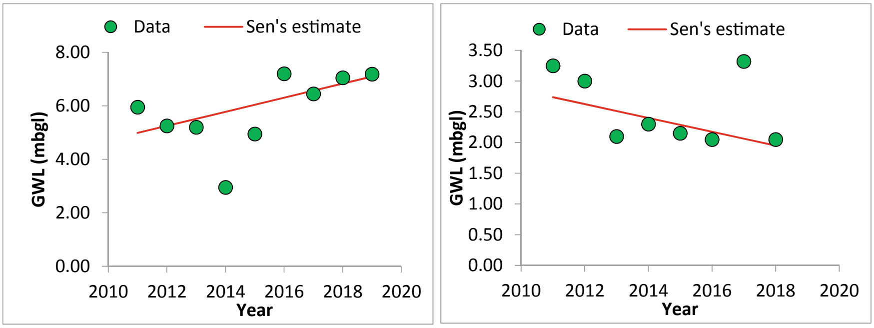

a). Pre-monsoon (Q= 0.264) b). Post-monsoon (Q= -0.113)

Fig. 22.7 Groundwaterlevel fluctuation at Gosaipur Kantit

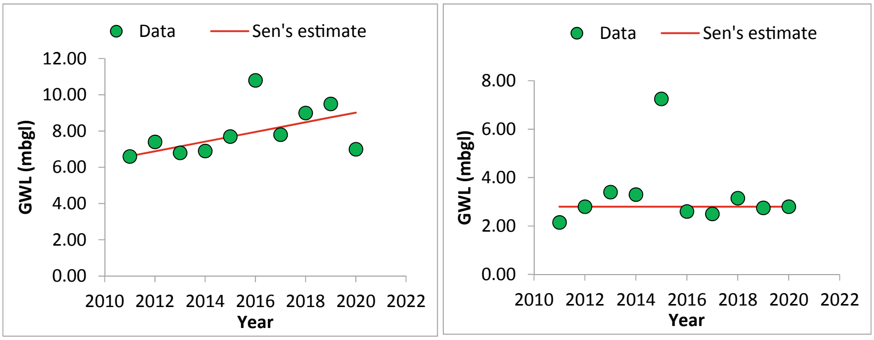

a). Pre-monsoon (Z= 1.97, Q= 0.267) b). Post-monsoon (Z= 0.00, Q= 0.00)

Fig. 22.8 Groundwaterlevel fluctuation at Nagarpalika Ahrora, Jamalpur

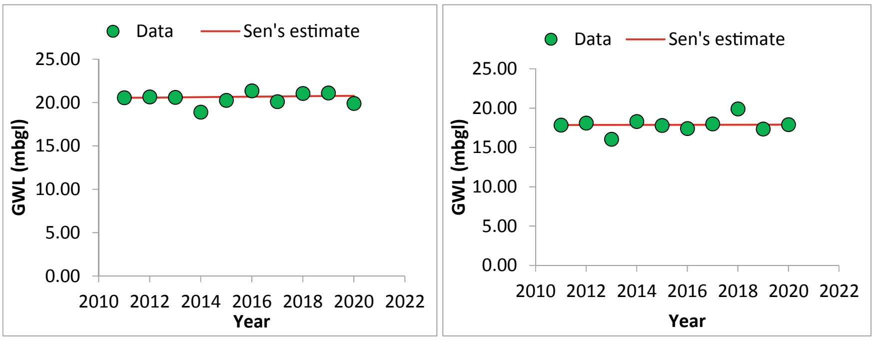

a). Pre-monsoon (Z= 0.00, Q= 0.025) b). Post-monsoon (Z= 0.00, Q= 0.006)

Fig. 22.9 Groundwaterlevel fluctuation at Jubilee Inter College, Police Lines

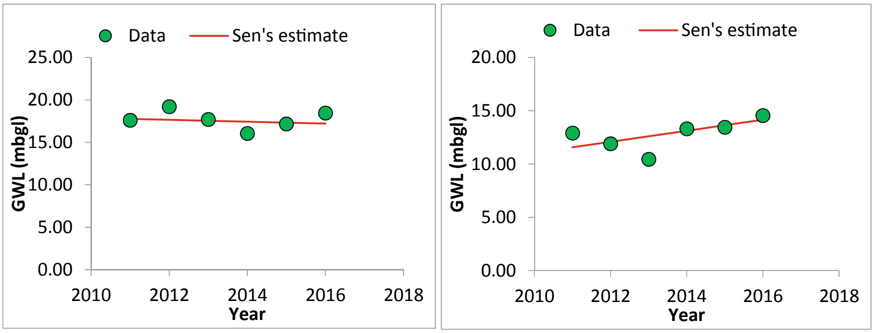

a). Pre-monsoon (Q= -0.11) b). Post-monsoon (Q= 0.517)

Fig. 22.10 Groundwaterlevel fluctuation at Polytechnic Campus, Bathua

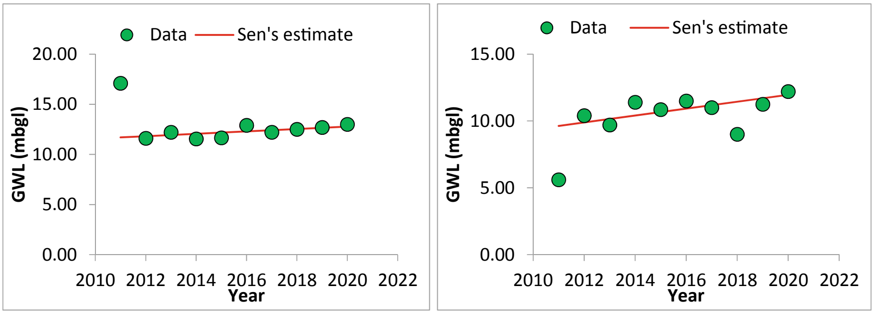

a). Pre-monsoon (Z= 1.17, Q= 0.12) b). Post-monsoon (Z= 1.79, Q= 0.258)

Fig. 22.11 Groundwaterlevel fluctuation at R R Vidyalaya, Chandradeepa

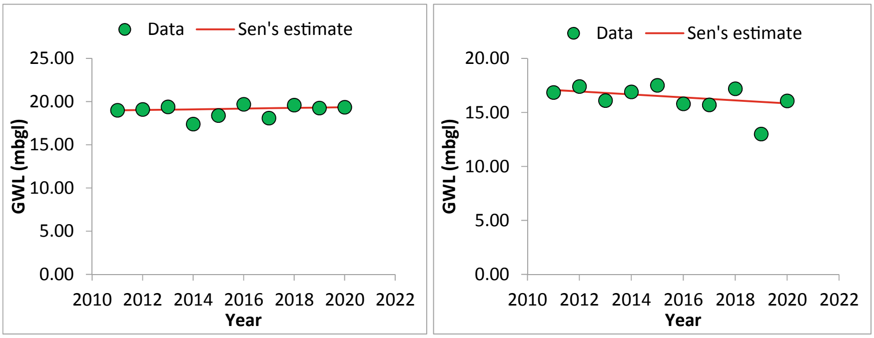

a). Pre-monsoon (Z= 0.72, Q= 0.040) b). Post-monsoon (Z= -1.25, Q= -0.138)

Fig. 22.12 Groundwaterlevel fluctuation at Rajkiya Paudhshala

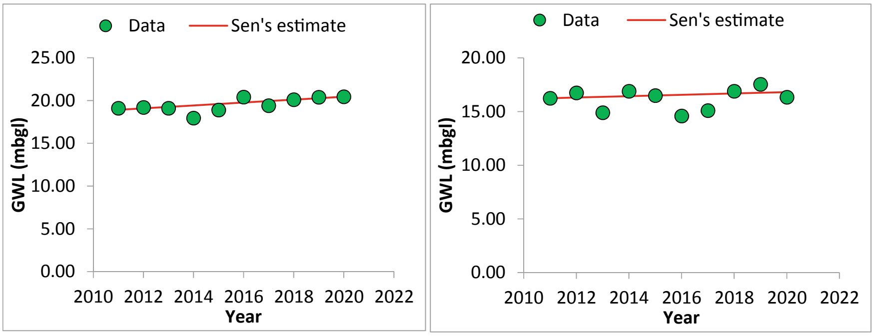

a). Pre-monsoon (Z=2.07, Q= 0.17) b). Post-monsoon (Z= 0.63, Q= 0.063)

Fig. 22.13 Groundwaterlevel fluctuation at Van Vibhag, Jalalpur

22.5.2.2 Trend Analysis of Seasonal Fluctuations in Groundwater Level (GWL) at Different Stations of Mirzapur District

a) Pre-monsoon Trend

Among ten stations, Chunar and Polytechnic campus, Bathua have shown the trend of rising groundwater levels over the past 10 years. Rest of the seven stations have shown the trend of declining GWL excluding one station showing no change. The dominating fall in GWL during pre-monsoon period can be attributed to changing rainfall pattern and delayed monsoon, resulting in extraction of groundwater for irrigation during the sowing season of kharif crops.

b) Post-monsoon Trend

In the post-monsoon period, a locally varied trend was observed where four out of ten stations, Bakiyabad, Chunar, Gosaipur Kantit and Rajkiya Paudhshala have shown the rise in groundwater levels. The rest five stations have shown the fall in groundwater levels. Nagarpalika Ahrora, Jamalpur did not show either negative or positive trend during post-monsoon period. There seems to be the positive impact on GWL on the stations residing close to the river Ganga banks post-monsoon season, aiding in groundwater recharge. Other stations located in the city region have shown neutral or declining trend in their GWL post-monsoon. One of the probable reasons can be concretisation and high surface runoff and groundwater extraction for household and agricultural purposes during the lean season.

22.6 Conclusion

In the framework of global climate change, the climatic variables such as rainfall and temperature play a crucial role in understanding the changing groundwater levels. In the study, Mann–Kendall test and Sen's slope estimate were performed to understand the impact of changing rainfall and temperature on the groundwater levels of one of the least studied regions of India, Mirzapur district located in the eastern Uttar Pradesh region with a complex physiography varying from the low-lying flood plains of the river Ganga in the North to the rugged topography of Vindhyan escarpments in the South.

The trend analysis of rainfall of the last 10 years indicates the strong negative trend with >10% significance level reflecting the general consistent decline in the overall annual rainfall in the last 10 years. Similarly, the temperature trend for the last 10 years also depicted a non-significant general decline but with varying yearly fluctuations. The MK test and Sen's estimate test indicate the strong negative trend of falling groundwater level in the pre-monsoon period with eight out of ten stations showing annual decline. It can be attributed to changing rainfall pattern and delayed monsoon, resulting in extraction of groundwater during the sowing season of kharif crops. However, a locally varied trend was observed in the post-monsoon season where four out of ten stations have shown the rise in GWL. There seems to be a positive impact on GWL on the stations residing close to the river Ganga banks post-monsoon season, aiding in groundwater recharge. Other stations located in the city region have shown neutral or declining trend in their GWL post-monsoon. One of the probable reasons can be concretisation and high surface runoff and groundwater extraction for household and agricultural purposes during the lean season.

Thus, from the above results, it can be concluded that the phenomenon of Climate Change and its impact on the changing spatiotemporal pattern of two climatic variables, Rainfall and Temperature has direct correlation with the falling Groundwater level (GWL) during the water scarce period of pre-monsoon season. However, the locally varied correlation between Rainfall-Temperature trend and GWL at the micro scale (station level) has been witnessed during the water sufficient post-monsoon season. It can probably be attributed to the increasing role of humans in changing demography, cropping patterns, urbanization, land use land cover change and the associated change in groundwater levels.

The findings of the study help in understanding the changing trends in groundwater levels in the backdrop of climate change and its manifestation in the form of changing spatial and temporal patterns of rainfall and temperature along with other anthropogenic factors. The study of GWL trends of Mirzapur district in the eastern region of Uttar Pradesh also aims to understand the otherwise less studied area. The trend analysis of rainfall, temperature and groundwater levels would help policy makers, district administration and farmers at the local level in taking informed decisions and in their effort toward adaptation and mitigation to climate change.

References

Athar H (2015) Teleconnections and variability in observed rainfall over Saudi Arabia during 1978–2010. Atmospheric Sci Lett 16:373–379. https://doi.org/10.1002/asl2.570

Babar SF, Ramesh H (2013) Analysis of south west monsoon rainfall trend using statistical techniques over Nethravathi basin. Int J Adv Technol Civ Eng 2(1):2231–5721

Bhutiyani MR, Kale VS, Pawar NJ (2007) Long-term trends in maximum, minimum and mean annual air temperatures across the Northwestern Himalaya during the twentieth century. Clim Change 85:159–177

Duan W, Bin H, Sahu N, Pingping L, Daniel N, Maochuan H, Kaoru T (2017) Spatiotemporal variability of Hokkaido's seasonal precipitation in recent decades and connection to water vapor flux. Int J Climatol 37(9):3660–3673. https://doi.org/10.1002/joc.4946

Duhan D, Pandey A (2013) Statistical analysis of long term spatial and temporal trends of precipitation during 1901–2002 at Madhya Pradesh, India. Atmos Res 122:136–149

Elnesr MN, Abu-Zreig MM, Alazba AA (2010) Temperature trends and distribution in the Arabian Peninsula. American J Environ Sci 6:191–203

Fan L, Chen D (2016) Trends in extreme precipitation indices across China detected using quantile regression. Atmospheric Sci Lett 17:400–406. https://doi.org/10.1002/asl.671

Fischer AM, Ceppi P (2012) Revisiting Swiss temperature trends 1959–2008. Int J Climatol 32(2):203–213

Gajbhiye S, Meshram C, Singh SK, Srivastava PK, Islam T (2016) Precipitation trend analysis of Sindh River basin, India, from 102-year record (1901–2002). Atmospheric Sci Lett 17:71–77

https://www.censusindia.co.in/district/mirzapur-district-uttar-pradesh-199

IPCC 2007 Climate change (2007) climate change impacts, adaptation and vulnerability. Working group II contribution to the intergovernmental panel on climate change, Fourth Assessment Report, Summary for Policymakers, pp. 23

Karpouzos DK, Kavalieratau S (2010) Trend analysis of precipitation data in Piera region (Greece). European Water 30(30):30–40

Kendall MG (1975) Rank correlation methods, 4th edn. Charles Griffin, London, UK

Kumar R, Gautam HR (2014) Climate change and its impact on agricultural productivity in India. J Climatol Weather Forecasting 2:109. https://doi.org/10.4172/2332-2594.1000109

Kumar V, Jain SK, Singh Y (2010) Analysis of long term rainfall trends in India. Hydrol Sci J 55(4):484–496

Mann HB (1945) Non-parametric tests against trend. Econometrica 13:163–171

Sen PK (1968) Estimates of the regression coefficient based on Kendall's tau. J Am Stat Assoc 39:1379–1389

Szabó S, Elemér L, Kovács Z, Püspöki Z, Kertész A, Singh SK, Balázs B (2019) NDVI dynamics as reflected in climatic variables: spatial and temporal trends—a case study of Hungary. GIScience & Remote Sensing 56:624–644. 10. 1080/15481603.2018.1560686